THE UNIVERSITY
of EDINBURGH

Generating Novel Molecular Tools to Manipulate Gene Regulation in Cyanobacteria

Grant Arthur Ronald Gale

Thesis presented for the degree of Doctor of Philosophy

School of Biological Sciences

The University of Edinburgh

2021

Declaration

I declare that this thesis was composed by myself, that the work contained herein is my own except where explicitly stated otherwise in the text, and that this work has not been submitted for any other degree or professional qualification.

Grant Gale

30/03/2021

Acknowledgements

I would first like to thank my PhD supervisors Alistair McCormick and Baojun Wang, who not only gave me this opportunity, but taught me, mentored me, encouraged me, and at times consoled me. Without their kindness, guidance, and substantial patience, for me this project would not have been achievable. I am extremely lucky to have been part of two lab groups. Having two pools of talented scientists and friends to give me advice and help has been a blessing.

My thanks also to Scotbio, their collaboration with the University of Edinburgh making the project possible.

I must give special thanks to my fellow cyanobacteria people. Ale, Anton and Anja. The three of you have been so generous and helped me so much, more than you will probably ever know. Something that may have seemed small to you, made the world of difference to me. Thank you also to Trevor, Filipe, Yang and Xinyi, for your guidance and help with technical matters, cloning advice, flow cytometry instruction and discussion and trouble shooting help. Thank you also to PK, Sophie, Nicky, Aranzazú, Liat, Yuwei, for being good friends and good lab mates. Thank you to my bubble mate Marcos, who helped keep me sane, not just during the difficult times of lockdown, but thesis writing as well.

To my mum Gerd, dad Neil, brother Bjørn, Uncle Eugen and Fong, without your love and support, I may very well have given up a long time ago.

Lay Summary

Cyanobacteria (also known as blue-green algae), are a very special type of bacteria that can photosynthesise in a similar way to plants. The process of photosynthesis allows cyanobacteria to absorb light energy, which is then used to convert carbon dioxide from the air into food for themselves, in the form of sugars. Cyanobacteria then use these sugars as fuel to generate energy to live and as building blocks for the synthesis of more complex molecules, some of which are used by the cell to grow and replicate.

The instructions for all cellular processes are encoded within DNA. With modern advances in synthetic biology, it is now possible, and in a relatively cheap way, to synthesise and manipulate DNA. DNA is made up of several different functional sequence types, some of which encode proteins (e.g. genes), and some special sequence types that facilitate the reading and expression of these genes. Cyanobacteria have been engineered to produce a wide variety of molecules that they do not produce in nature, through the uptake of synthetic DNA. Currently, the quantities of these chemicals produced in the lab are not yet high enough for large scale production. For cyanobacteria to reach their potential as a tool for green biotechnology applications, more strategies for the control of gene expression are needed so that better instructions for the cell can be written in the form of synthetic DNA.

This thesis has focused on the design and testing of new DNA (molecular) tools. We have designed and tested a molecular engineering toolkit for use in cyanobacteria, called CyanoGate. It is based on a type of DNA assembly called Golden Gate. Golden Gate allows DNA sequences to be modified and treated like ‘Lego’, and can be assembled efficiently and easily in a modular way. This allows large DNA constructs to be assembled quickly, reducing the time and cost required. The CyanoGate kit includes a large suite of molecular tools and several different strategies for inserting the synthetic DNA into the cyanobacterial cell.

The reading of DNA consists of two main steps; the ‘start’, which is performed by a DNA sequence called a promoter, and ‘stop’, which is performed by a sequence called a terminator. The termination step is important, as if the reading of the DNA is not stopped efficiently, regions of DNA may be expressed that were not intended. Using the modular assembly standards of the CyanoGate kit, I constructed a molecular tool to test terminator efficiency. I used this tool to test the efficiency of a library of terminators in two different cyanobacterial species, as well as *Escherichia coli*. This comparison is important, as the cellular machinery for reading DNA is different in cyanobacteria compared to other types of bacteria, meaning that molecular tools tend to behave differently between species.

Lastly, I tested a series of inducible promoters. Most promoters are what is termed ‘constitutive’, which means that they are always on so that the DNA associated with them is continuously being read and expressed. An inducible promoter does not drive gene expression unless a certain condition is met e.g. presence of a small molecule. There are very few inducible promoters tested in cyanobacteria that have proved very useful thus far. These inducible systems are typically ported from other organisms, that have naturally evolved the ability to respond to or ‘sense’ certain environmental cues. Inducible promoters are important tools and required for design of more complex synthetic gene circuits in cyanobacteria.

Abstract

Cyanobacteria are unique among prokaryotes in that they can conduct oxygenic photosynthesis. With just the addition of light, water and some trace minerals, cyanobacteria utilise carbon dioxide to synthesise the simple carbohydrates required to produce the chemical energy that drives all cellular processes. Cyanobacteria have a complex metabolism when compared to other model heterotrophs (e.g. *Escherichia coli*) and therefore can produce a wide variety of complex biomolecules not possible in other prokaryotes. Although cyanobacteria show great potential for green biotechnology applications, availability of molecular tools and strategies required to drive forward basic research and the engineering of new strains alike, has been quite limited.

To address the lack of a unified strategy for the engineering of cyanobacteria, we developed a molecular cloning system called CyanoGate that unifies cyanobacteria and plants. This system is based on the widely adopted modular and high throughput Golden Gate cloning syntax. CyanoGate contains a suite of well characterised modular parts and acceptors for episomal and chromosomal gene expression, genome engineering applications, and CRISPR interference and sRNA tools for gene repression studies.

Building on the CyanoGate platform, I adapted a strategy for the evaluation of transcription terminators. Transcription terminators are important control elements for the regulation of gene expression, and there have been relatively few studies limited only to the model species *Synechocystis* sp. PCC 6803 thus far. Here, I have constructed and validated a high throughput molecular tool that can be used in any organism where the broad host range RSF1010 origin of replication is functional. With this tool, a library of transcription terminators was characterised and compared between *Escherichia coli*, *Synechocystis* sp. PCC 6803 and *Synechococcus elongatus* UTEX 2973. Surprisingly, our findings showed that transcription termination efficiency was not only different between *E. coli* and cyanobacteria, but the library also performed differently between cyanobacterial species.

Lastly, I investigated several heterologous inducible and repressible expression systems in *Synechocystis.* I developed a rhamnose-responsive genetic inverter with a range of output strengths using a transcription factor repressor new to cyanobacteria. There are very few inducible and repressible systems thus far reported as functional in cyanobacteria, and this new repressor will be a useful addition for the construction of more complex gene circuits in cyanobacteria.

Contents

List of Figures

List of Tables and Supplementary Information

Abbreviations

AB^R	Antibiotic resistance gene
AHL	N-acyl-homoserine lactones
asRNA	Antisense RNA
aTc	anhydrotetracycline
Cas	CRISPR associated system
CRISPR	Clustered regularly interspaced short palindromic repeats
DAPG	2,4-diacetylphloroglucinol
DMF	N,N-dimethylformamide
DMSO	Dimethyl sulfoxide
DNA	Deoxyribonucleic acid
eYFP	Enhanced yellow fluorescent protein
IPTG	Isopropyl β- d-1-thiogalactopyranoside
mRNA	Messenger RNA
PTasRNA	Paired termini antisense RNA
ori	Origin of replication
PCC 7942	*Synechococcus elongatus* PCC 7942
PCR	Polymerase chain reaction
RBS	Ribosomal binding site
RNA	Ribonucleic acid
RNAP	RNA polymerase

ssRNA	single stranded RNA
sgRNA	single guide RNA
Synechocystis	*Synechocystis* sp. PCC 6803
TA	Transcriptional activator
TF	Transcription factor
TR	Transcriptional repressor
TIR	Translation initiation rate
UTEX 2973	*Synechococcus elongatus* UTEX 2973
WT	Wild-type

Chapter 1 Introduction

1.1 The need for green biotechnology

Since the industrial revolution, ever increasing quantities of greenhouse gasses have been released into the Earth's atmosphere. This has resulted in major disasters, including the destruction of the ozone layer by CFCs (chlorofluorocarbons), and global warming where greenhouse gasses trap heat within the Earth's atmosphere. Global warming has been implicated in numerous deleterious environmental effects including extreme weather events, droughts and deoxygenation of the world's oceans (Skeie et al., 2021). CO_2 (carbon dioxide) is a major greenhouse gas and contributor to global warming. If the Earth is to survive as we know it, we must develop new approaches to environmentally responsible industrial processes and production, and new strategies for carbon mitigation.

1.2 Cyanobacteria as solar powered cell factories

Cyanobacteria are an ancient and diverse phylum containing photosynthetic Gram-negative bacteria. The oldest fossil records discovered have identified what are believed to be predecessors of modern-day cyanobacteria and have been dated to approximately 3.5 billion years ago (Schopf & Packer, 1987). Cyanobacteria have evolved to occupy many ecological niches, from the arctic to hot water springs, and are found in a wide variety of marine and freshwater habitats (Seckbach, 2007; Flombaum et al., 2013; Pedersen & Miller, 2017; Puente-Sánchez et al., 2018). Cyanobacteria are unique amongst prokaryotes in that they have evolved to conduct oxygenic photosynthesis, where light energy is absorbed by pigments and transduced into chemical energy by way of a complex set of redox reactions. These redox reactions lead to the oxidation of H_2O, the release of O_2 as a by-product, and the subsequent reduction of atmospheric inorganic carbon in the form of CO_2 to generate simple carbohydrates (sugars). These sugars are utilised for generation of biochemical energy (e.g. ATP) that drive cellular metabolic processes. These sugars are also utilised as a carbon source for the synthesis of a wide array of different compounds including low value (biofuels, feedstocks/biomass)

(Möllers et al., 2014; Sarsekeyeva et al., 2015), high value products (e.g. nutraceuticals, pigments) (Glazer, 1994; Fernández-Rojas et al., 2014; Nicoletti, 2016) and a vast number of secondary metabolites (Jones et al., 2021). The carbon fixation is catalysed by the enzyme Rubisco (Ribulose-1,5-bisphosphate carboxylase-oxygenase), which is localised within the carboxysome, a microcompartment unique to cyanobacteria (Kerfeld & Melnicki, 2016). The carboxysome is a core component of the cyanobacterial carbon concentrating mechanism, which facilitates concentration of CO_2 up to 1,000 times that of atmospheric levels (Rae et al., 2013a), contributing to higher photosynthetic efficiencies when compared to plants (Long et al., 2018). Cyanobacteria are estimated to be responsible for up to 30% of net global carbon fixation (Rae et al., 2013b).

Compared to model heterotrophs such as *Escherichia coli*, cyanobacteria offer several advantages for biotechnological applications, including 1) greater metabolic versatility (e.g. presence of P450 cytochromes (Liu et al., 2020b)), 2) cheaper to culture needing only CO_2, light, water and trace minerals, 3) culturing without a fixed carbon source reduces contamination risk and provides the additional incentive of CO_2 mitigation, 4) many strains can grow under hostile environments (e.g. high pH and temperature) (Rampelotto, 2013; Pedersen & Miller, 2017; Puente-Sánchez et al., 2018), further minimising contamination risk, 5) the carbon sources required for heterotroph cultivation typically are of plant origin (e.g. beet molasses), growth of which directly completes for land resources with arable crops. However, it is important to note that many cyanobacterial species have been identified that naturally produce toxins; therefore, appropriate care must be taken when choosing new non-model cyanobacterial species for use in biotechnology applications (Lee et al., 2017; Henao et al., 2019; Kubickova et al., 2019).

New cyanobacterial strains are increasingly being developed to take advantage of this capacity to convert CO_2 and H_2O into valuable products using solar energy. Some examples of compounds that have been produced in cyanobacteria include: bulk chemicals e.g. sucrose (Lin et al., 2020a),

chemicals used as fuel precursors e.g. butanol and isobutyraldehyde (Atsumi et al., 2009; Jazmin et al., 2017; Miao et al., 2017), high-value chemicals used in manufacturing and pharmaceuticals e.g. ethylene (Carbonell et al., 2019; Durall et al., 2020), isoprene (Lindberg et al., 2010; Gao et al., 2016), L-lysine (Korosh et al., 2017; Lin et al., 2020b), poly-β-Hydroxybutyrate (Zhang et al., 2015; Singh et al., 2019), mycosporine-like amino acids (e.g. natural sunscreen) (Yang et al., 2018) and terpenoids (Wang et al., 2016; Englund et al., 2018; Pattanaik et al., 2020). Nevertheless, despite the diversity of heterologous products that have so far been produced in cyanobacteria, titres are generally too low at lab scale and thus not economically viable for larger scale industrial applications.

1.3 The rise of synthetic biology

Synthetic biology is a relatively recent paradigm, taking a multidisciplinary approach to the rational re-design and engineering of biology, with the goal of generating living systems with new-to-nature capabilities (Cheng & Lu, 2012). The central tenet of synthetic biology revolves around the 'design-build-test-learn' cycle. Using engineering principles, the process typically starts with rational design, which takes into consideration factors such as chassis choice and molecular tool availability. Other sources of information, including genomics, metabolomics, and transcriptomics, where available, can be incorporated at the design stage. Additional information will help to make better informed decisions to determine the genetic modifications required to achieve the desired outcome. The 'build' stage seeks to assemble the DNA required to introduce the desired genetic modifications to the host organism. Despite the cost reduction in DNA synthesis in recent years, most DNA assembly is still undertaken in the lab, using various cloning strategies (Gibson et al., 2009; Werner et al., 2012; Patron et al., 2015; Moore et al., 2016; Kim et al., 2017; Andreou & Nakayama, 2018; Taylor et al., 2019; Vasudevan et al., 2019; Stukenberg et al., 2021; Valenzuela-Ortega & French, 2021). The build step has typically been a bottleneck when conducting high-throughput experiments. However, the introduction of modular cloning strategies, such as Golden Gate, the capacity for 'Lego-like' 'plug and play', and compatibility with

automation, have resulted in high-throughput experiments becoming more accessible (Engler et al., 2014; Chambers et al., 2016).

A key requirement at both the design and build stages, is access to large libraries of well characterised molecular parts. Despite recent advances, the availability of genetic tools to engineer cyanobacteria still lagged those available in *E. coli*. For the synthetic biology paradigm to progress cyanobacterial research, more well characterised genetic tools are needed, for example, for metabolic pathway manipulation to engineer new strains that produce titres that are economically viable for industrial applications. Therefore, an increase in availability and type of molecular tools and the uptake of the synthetic biology paradigm would be beneficial to drive forward the development of this promising green biotechnology platform.

1.4 Thesis Aims and Outline

The aim of my PhD thesis was to design, generate and characterise new molecular tools that could be used in the furtherment of cyanobacterial synthetic biology research.

We developed and tested CyanoGate, a molecular toolkit for the engineering of cyanobacteria. CyanoGate contains a large number of modular genetic parts including promoters, transcription terminators, vectors for integration and self-replication, and tools for gene repression. CyanoGate is built on the Golden Gate cloning standard, thus DNA can be quickly and efficiently assembled, and easily shared.

I adapted an established strategy for characterisation of transcription terminator efficiency. The system was designed to be compatible with CyanoGate, to facilitate easy part reuse and high-throughput assembly and screening. I used this new tool to evaluate the efficiency of 34 heterologous and synthetic intrinsic transcription terminators and compared the efficiency in *E. coli* *Synechocystis* sp. PCC 6803 and *Synechococcus elongatus* UTEX 2973.

Lastly to address the shortage of conditional gene expression systems in cyanobacteria, I tested four new and four existing promoters that are regulated by heterologous transcription factors. These were then evaluated for the potential for further synthetic gene circuit design. Subsequently several variants of a genetic inverter circuit were built and tested based on a promoter/repressor pair new to cyanobacteria.

Chapter 2 Emerging Species and Genome Editing Tools: Future Prospects in Cyanobacterial Synthetic Biology

2.1 Chapter Preface

The following review was published in the journal *Microorganisms*[1]. This review was written in collaboration between Alejandra A. Schiavon and I from the McCormick Lab, and Lauren A Mills and David Lea-Smith from the Lea-Smith Lab.

In this review, we highlighted a potential limitation in current cyanobacterial research, which has focused primarily on a small subset of model species. We discuss some recently discovered non-model species that demonstrate attributes that may make them promising chassis for biotechnology applications. We reviewed the current state of CRISPR (Clustered Regularly Interspaced Short Palindromic Repeats/CRISPR associated protein (CRISPR/Cas)) and CRISPR interference (CRISPRi) in cyanobacteria. We critically evaluated some drawbacks with current CRISPR technologies in cyanobacteria and highlighted several new Cas enzymes that show promise. For the existing and new Cas enzymes, we discussed the PAM recognition sites and the relative abundance in 17 published cyanobacterial genomes. We discussed several new tools and strategies for genome modification and gene regulation in common use in other model organisms, yet to be ported to cyanobacteria, that could prove useful additions to the synthetic biology toolbox in cyanobacteria. Lastly, we gave some details on the then upcoming CyanoSource: A Barcoded Mutant Library for *Synechocystis* sp. PCC 6803.

I co-wrote the introduction and conclusion with Alejandra A. Schiavon, and the following sections: '*3.1:CRISPR/Cas Genome Editing in Cyanobacteria'*, '*4.1:Gene Regulation with CRISPRi and Synthetic Small Regulatory RNAs*', '*4.2: Sigma Factors and RNA Polymerase as Regulatory Tools for Gene Transcription*' and '*4.4 Using Inteins to Progress Genetic Circuit Research in*

[1] Gale GAR, Schiavon Osorio AA, Mills LA, Wang B, Lea-Smith DJ, McCormick AJ. Emerging Species and Genome Editing Tools: Future Prospects in Cyanobacterial Synthetic Biology. Microorganisms. 2019 Sep 29;7(10):409. doi: 10.3390/microorganisms7100409.

Cyanobacteria‘. Alejandra A. Schiavon, Alistair McCormick, and I prepared the final draft for publication and wrote the rebuttal to the reviewers’ comments.

2.2 Main Text

microorganisms

MDPI

Review

Emerging Species and Genome Editing Tools: Future Prospects in Cyanobacterial Synthetic Biology

Grant A. R. Gale [1,2,3,†], Alejandra A. Schiavon Osorio [1,2,†], Lauren A. Mills [4], Baojun Wang [2,3], David J. Lea-Smith [4] and Alistair J. McCormick [1,2,*]

1 Institute of Molecular Plant Sciences, School of Biological Sciences, University of Edinburgh, Edinburgh EH9 3BF, UK; grant.gale@ed.ac.uk (G.A.R.G.); alejandra.schiavon@ed.ac.uk (A.A.S.O.)
2 Centre for Synthetic and Systems Biology, University of Edinburgh, Edinburgh EH9 3BF, UK; baojun.wang@ed.ac.uk
3 Institute of Quantitative Biology, Biochemistry and Biotechnology, School of Biological Sciences, University of Edinburgh, Edinburgh EH9 3FF, UK
4 School of Biological Sciences, University of East Anglia, Norwich NR4 7TJ, UK; l.mills@uea.ac.uk (L.A.M.); d.lea-smith@uea.ac.uk (D.J.L.-S.)
* Correspondence: alistair.mccormick@ed.ac.uk
† These authors contributed equally to this work.

Received: 1 September 2019; Accepted: 24 September 2019; Published: 29 September 2019

Abstract: Recent advances in synthetic biology and an emerging algal biotechnology market have spurred a prolific increase in the availability of molecular tools for cyanobacterial research. Nevertheless, work to date has focused primarily on only a small subset of model species, which arguably limits fundamental discovery and applied research towards wider commercialisation. Here, we review the requirements for uptake of new strains, including several recently characterised fast-growing species and promising non-model species. Furthermore, we discuss the potential applications of new techniques available for transformation, genetic engineering and regulation, including an up-to-date appraisal of current Clustered Regularly Interspaced Short Palindromic Repeats/CRISPR associated protein (CRISPR/Cas) and CRISPR interference (CRISPRi) research in cyanobacteria. We also provide an overview of several exciting molecular tools that could be ported to cyanobacteria for more advanced metabolic engineering approaches (e.g., genetic circuit design). Lastly, we introduce a forthcoming mutant library for the model species *Synechocystis* sp. PCC 6803 that promises to provide a further powerful resource for the cyanobacterial research community.

Keywords: CRISPR/Cas; CRISPRi; genetic circuits; genome engineering; inteins; genome-scale models; mutant library; optogenetics; serine integrase; sigma factors; synthetic biology

1. Introduction

Cyanobacteria are a diverse phylum of photosynthetic prokaryotes that are found in a wide variety of marine and freshwater habitats [1–4]. Oxygenic photosynthesis evolved approximately 2.5 billion years ago in the predecessors to modern-day cyanobacteria [5]. Their early success led to a significant increase in free oxygen (O_2) in the Earth's atmosphere and the subsequent evolution of most aerobic organisms [6–8]. Today, cyanobacteria account for 20%–30% of global carbon dioxide (CO_2) fixation [9].

The ability of cyanobacteria to convert captured carbon into a wide variety of complex organic molecules makes them promising platforms for the sustainable production of biofuels and high-value chemicals [10–12]. Compared to plants, cyanobacteria offer several advantages for biotechnological applications, including (1) higher photosynthetic efficiencies [13,14], (2) capacity to grow in hostile living environments (e.g., in extremes of temperature, salinity and pH) [1,3,4], (3) the ability to be cultured on

non-arable land with minimal nutrients [15], and (4) the relatively rapid and inexpensive generation of mutants (predominantly in model species) [16]. Moreover, chloroplasts descend from an internalised cyanobacterium [17], thus certain physiological and biochemical features are conserved in eukaryotic photosynthetic organisms, making cyanobacteria excellent chassis for production of plant-derived natural products, such as terpenes [18,19]. Currently, several companies are investigating the use of cyanobacteria for producing biochemicals, including biofuels (Algenol), inks (Living Ink Technologies) and pigments for food and cosmetics (DIC Corp., Lumen Bioscience, ScotBio). Nevertheless, several hurdles still need to be overcome for more widespread industrial adoption.

One key issue has been the relatively slow growth rates of cyanobacterial species, including those developed as models such as *Synechocystis* sp. PCC 6803 (PCC 6803) and *Synechococcus elongatus* PCC 7942 (PCC 7942). For example, PCC 6803 has a doubling-time of *ca*. 7 h under standard growth conditions [20], compared to 20 min for *Escherichia coli* and 2 h for *Saccharomyces cerevisiae* [21,22]. Recently, several genetically tractable cyanobacterial species have been characterised with faster growth rates that are comparable with *S. cerevisiae* [20,23,24]. In this review, we will discuss these strains and other non-model species that demonstrate the potential for cyanobacteria to close the gap between industrially viable heterotrophic and phototrophic bio-platforms or are useful organisms for investigating unique aspects of cyanobacterial biology and how they adapt to different environments.

A further significant challenge limitation has been the limited availability of molecular tools to engineer cyanobacteria. However, the past few years have seen a rapid proliferation of characterised tools and parts for cyanobacteria, including CRISPR/Cas-based systems [25–28]. This has driven the widespread adoption of the synthetic biology paradigm for the design of biological tools based on the bottom-up approach of recombining standardised parts or modules (e.g., promoters, ribosome binding sites (RBS), coding sequences and terminators) [29–35]. Many of those tools were initially developed in *E. coli* or *S. cerevisiae* and have been adapted and modified for use in cyanobacteria [36,37]. A significant drawback is that they may behave differently in cyanobacteria and between different cyanobacterial species. Thus, the functionality of all new tools ported for cyanobacterial applications must first be validated [35,38]. Here, we will outline several recent developments in genome engineering using CRISPR/Cas and recombinase approaches, as well as the opportunities and limitation of recent tools developed in *E. coli* that show promise for cyanobacterial research and biotechnology applications.

To date, 290 draft genomes and 85 full genomes are available online in the CyanoBase database (http://genome.microbedb.jp/cyanobase [39]). The growing availability of cyanobacterial genome sequencing data has helped to foster the development of genome-scale models (GSMs) for a variety of species, ranging from model species (e.g., PCC 6803) to the industrial relevant strain *Arthrospira* (Spirulina) *platensis* NIES-39 [40–43]. As with *E. coli* [44], GSMs have allowed cyanobacterial researchers to adopt a systems biology approach to propose and predict the outcomes of engineering strategies. Here, we will also highlight examples where GSMs have successfully guided efforts to modify metabolism to improve production in cyanobacteria and how GSMs could drive an increase in available cyanobacterial omics data.

Finally, we will introduce a forthcoming barcoded mutant library in PCC 6803 called CyanoSource. CyanoSource will be a powerful tool to develop a deeper understanding of metabolism in PCC 6803, guide work in other species (including new fast-growing strains) and will set a benchmark for high-throughput research in the cyanobacterial field.

2. "Non-Model" Species: Requirements for Uptake and Genetic Manipulation

Cyanobacterial research has focused primarily on model organisms that are straightforward to culture under laboratory conditions, amenable to genetic modification and can be frozen for long-term storage [16,45–47]. The uptake of more recalcitrant, non-model species for laboratory research can present significant challenges. Table 1 outlines some basic features that are desirable for culturing and engineering. Below, we have highlighted several new or known "non-model" cyanobacteria, including

Microorganisms **2019**, *7*, 409

their potential benefits, challenges for widespread uptake and industrial usage, and where applicable, progress towards efficient genetic manipulation (Table 2).

Table 1. Desirable features required for culturing and genetically engineering cyanobacterial strains.

(1)	Capacity to grow on agar plates and generate isolated colonies.
(2)	Amenability to heterologous DNA uptake, either naturally using native DNA import systems [33,48], or via conjugation (i.e., tri- or bi-parental mating) or electroporation.
(3)	Sensitivity to antibiotics for selection following DNA uptake [49].
(4)	Lack of native endonucleases that digest heterologous DNA. If present, the efficiency of DNA uptake can be improved by selecting for strains where endonucleases have been inactivated [48]. Otherwise specific methylases, restriction inhibitors and liposomes could be employed during delivery [50–53].
(5)	Ability to take up broad-host-range self-replicating plasmids (e.g., RSF1010-based) for heterologous gene expression.
(6)	Capacity for genomic integration via allelic exchange (e.g., homologous recombination (HR) to facilitate the generation of gene knockouts or genomic integration of gene expression cassettes. Ideally, species will be amenable to the generation of unmarked mutants, which is important for industrial applications. Unmarked mutants can be generated using negative selection markers (e.g., *sacB*) [16,54] or by CRISPR/Cas [25].

2.1. The Emergence of Fast-Growing and Stress-Tolerant Synechococcus Strains

Cyanobacterial strains that can achieve growth rates comparable with heterotrophic microbes could be of significant value to basic research and the biotechnology industry. Recently, three new *Synechococcus* strains have been reported with high growth rates: *Synechococcus elongatus* UTEX 2973 (UTEX 2973), *Synechococcus elongatus* PCC 11801 (PCC 11801) and *Synechococcus* sp. PCC 11901 (PCC 11901). UTEX 2973 was first described in 2015 as a fast-growing, stress-tolerant strain that was re-isolated from a previously characterised fast-growing strain that had lost the ability for fast growth [20,55]. Under high light (>500 µmol photons m^{-2} s^{-1}) and high temperatures (38–42 °C), UTEX 2973 can achieve doubling times similar to that of *S. cerevisiae* (*ca.* 2 h) during the early growth phase [20,24,56]. Under those conditions, UTEX 2973 can produce biomass twice as fast as its close relative PCC 7942, despite only a small number of nucleotide differences between the two genomes [57]. However, growth was not examined for longer periods of time (i.e., >24 h). At lower temperatures (30 °C), growth of UTEX 2973 is slower than PCC 7942 or PCC 6803 at 300 or 500 µmol photons m^{-2} s^{-1} [35], and slower than 6803 when cultured for longer periods (up to 10 days) under high light (750 µmol photons m^{-2} s^{-1}) [24]. UTEX 2973 is not naturally competent, but is amenable to conjugation and genome editing by CRISPR/Cas [20,58]. Furthermore, naturally transformable mutants of UTEX 2973 have been described [33], while three point mutations in PCC 7942 can reportedly lead to growth rates similar to that of UTEX 2973 [57]. The latter finding could have a significant impact on cyanobacterial research as PCC 7942 is a naturally transformable and widely used model species.

PCC 11801 was isolated from India and first described in 2018 [23]. Similarly to UTEX 2973, PCC 11801 is tolerant to high light and temperatures and exhibits fast growth rates (i.e., a doubling time of 2.3 h). Furthermore, PCC 11801 is tolerant of high levels of NaCl (i.e., it can grow at sea salt concentrations (*ca.* 0.7 M), whereas PCC 7942 cannot) and it is naturally transformable. The genome sequence of PCC 11801 is highly similar to PCC 7942 and UTEX 2973 (*ca.* 83%). Thus, existing plasmid vectors used for engineering PCC 7942 are widely compatible in PCC 11801.

One of the best-performing strains reported to date is PCC 11901, which was isolated in Singapore from an estuarine environment enriched with nitrogen and phosphorous compounds [24]. PCC 11901 is tolerant to high light levels, achieves fast growth rates comparable to UTEX 2973, and is tolerant to a wide range of salinities, similar to PCC 11801. Although UTEX 2973 grows faster than PCC 11901 during the early growth phase, PCC 11901 reportedly outperforms UTEX 2973 when grown for longer time periods (i.e., >24 h). PCC 11901 accumulated 2–3 times more biomass when grown alongside PCC

6803, PCC 7942, *Synechococcus* sp. PCC 7002 (PCC 7002) and UTEX 2973, achieving an OD_{730} = 101 and a biomass of 18.3 g dry weight per litre. PCC 11901 is naturally transformable with efficiencies similar to that of PCC 7002, as demonstrated by the generation of markerless mutants using methods previously described in PCC 7002 [59].

2.2. *Nostoc punctiforme ATCC 29133*

Nostoc punctiforme ATCC 29133 (ATCC 29133) is a nitrogen (N_2)-fixing, heterocyst-forming cyanobacterium which forms a symbiotic relationship within the coralloid roots of plants. ATCC 29133 is a useful organism for investigating symbiotic relationships between plants and N_2-fixing cyanobacteria [60]. It has also been key to understanding the biosynthetic pathway of scytonemin, a natural sunscreen against UV damage produced by many cyanobacterial species [61]. Transformation of ATCC 29133 was first described in 1994 [62] and has since been further developed to generate scytonemin-deficient mutants [63]. Mutants were obtained via conjugation, either by random transposon insertion into the open reading frame of the scytonemin biosynthesis operon or by allelic exchange. ATCC 29133 appears amenable to selection using chloramphenicol, neomycin, streptomycin and *sacB* markers.

2.3. *Cyanothece sp.*

Cyanothece species are a group of unicellular cyanobacteria that can perform photosynthesis and fix N_2 within the same cell via temporal separation of the two processes. N_2 fixation occurs during the dark period when O_2 levels are low. They are natural contributors to N_2 fixation in rice paddies, and, therefore, could play an important role in reducing agricultural fertiliser use [64,65]. A genetic transformation protocol for producing targeted gene knockouts in *Cyanothece* sp. PCC 7822 was developed in 2010 [66], where a single-stranded DNA fragment encoding a spectinomycin resistance cassette was electroporated into cells, leading to integration of the cassette at random points in the genome via non-homologous recombination. Despite testing *Cyanothece* sp. ATCC 51142, PCC 7424, PCC 7425, PCC 8801 and PCC 8802, mutants could only be generated in PCC 7822 via this technique. More recently, Liberton et al. [67] reported a method for generating targeted mutations in *Cyanothece* sp. ATCC 51142 using triparental mating. A plasmid encoding two methylases was required in order to make the cargo plasmid more resistant to digestion. Using this system, a kanamycin resistance cassette was inserted into a targeted chromosomal site.

2.4. *Arthrospira sp.*

Arthrospira species are the source of high-value nutraceuticals (e.g., Spirulina) and natural blue pigments in food (e.g., the phycobiliprotein, *C*-phycocyanin) [68,69]. They tolerate high levels of alkalinity and can be cultured in a variety of closed or open (e.g., race way pond) environments. Nevertheless, *Arthrospira* sp. are highly resistant to genetic modification due to an abundance of native restriction–modification systems that can rapidly degrade heterologous DNA [70]. The most efficient transformation system reported to date used a Tn5 transposase expression cassette to generate random integration events in the genome of *Arthrospira platensis* C1 and selection via a spectinomycin resistance cassette [53]. DNA degradation was minimised by encapsulation in liposomes and mixing with a type 1 restriction inhibitor prior to electroporation. Transformed cells resistant to spectinomycin were reportedly stable for several months. It is tempting to speculate that delivery of a CRISPR/Cas system with this approach could enable targeted genome editing in *Arthrospira* sp.

2.5. *Leptolyngbya sp.*

Leptolyngbya species are widely distributed in terrestrial and freshwater environments [71], and are, therefore, of great ecological interest. *Leptolyngbya* sp. BL0902 is also used for the production of biomass and bioproducts, as it can grow at a range of industrially viable temperatures, tolerate high salt concentrations, pH extremes and variable light conditions. Growth rates in the laboratory and in

outdoor ponds are similar to those of *Arthrospira* species [72]. Conjugal transformation of *Leptolyngbya* sp. BL0902 (BL0902) with broad host range vectors based on RSF1010 was successfully carried out in 2012 [72,73], although two antibiotics were required to limit the appearance of spontaneous resistant mutants. Conjugation was used for generation of a transposon library and introduction of an expression plasmid.

2.6. Fremyella diplosiphon

Fremyella diplosiphon is a filamentous, heterocyst-forming, freshwater species that can adjust its photosynthetic receptors and antenna to differences in light intensity and quality. Detailed methods for genetic manipulation are available that allow for the generation of unmarked mutants [74]. First, the plasmid of interest is methylated to protect it from digestion in *F. diplosiphon*. The plasmid is then introduced via triparental mating and transconjugates selected on plates containing neomycin [75]. Unmarked mutants can then be generated using *sacB*.

2.7. Marine Synechococcus sp. and Prochlorococcus sp.

Marine *Synechococcus* and *Prochlorococcus* genera are responsible for approximately a quarter of ocean primary productivity [2], and are, therefore, of great academic interest. Genetic manipulation of *Prochlorococcus* sp. (including the introduction of a heterologous plasmid) has not been reported. However, *Prochlorococcus* strains can be cultured on semi-solid agar plates in the presence of specific 'helper' heterotrophic bacteria [76], fulfilling the initial requirement for genetic manipulation. Gene deletion has been reported in the marine *Synechococcus* species WH7803, WH8102 and WH8103 [77,78]. Plasmids were introduced into cells via biparental mating or electroporation. Transformants were plated on semi-solid (0.3% *w/v*) agar plates and kanamycin was used as the selectable marker. Via this method, self-replicating and suicide plasmids were introduced, which facilitated targeted mutations.

2.8. Thermosynechococcus elongatus

Thermosynechococcus elongatus BP-1 is a thermophilic cyanobacterium with optimal growth at 55 °C, making it ideal for biotechnology applications that require high temperatures [79]. *T. elongatus* BP-1 proteins are also ideal for purification and crystallographic studies, due to their increased stability at high temperatures [80]. A natural transformation method for chromosomal integration has been developed for *T. elongatus* BP-1, with either kanamycin or chloramphenicol used for selection of transformants [81]. More recently, *T. elongatus* PKUAC-SCTE542 has been highlighted as a naturally transformable strain with high growth rates that is sensitive to spectinomycin [82].

2.9. Chlorogloeopsis fritschii and Fischerella muscicola

Chlorogloeopsis fristchii sp. PCC 6912 and *Fischerella muscicola* PCC 7414 are two of the most complex species of cyanobacteria, in that they are filamentous, heterocyst-forming strains able to undergo multiplanar cell division and thereby create multiseriate filaments [83]. Introduction of expression plasmids via conjugation and biolistic DNA transfer methods has been reported in both species. Conjugation was made possible by the partial removal of the exopolysaccharide sheath by introducing a salt washing step.

2.10. Chroococcidiopsis thermalis

Chroococcidiopsis thermalis is found in environments with extremes of temperature (both hot and cold) [84]. Furthermore, these extremophile cyanobacteria can survive long periods of desiccation and high levels of solar radiation that few other organisms can tolerate. *C. thermalis* incorporates chlorophyll *f* in its photosystems, allowing absorption of far-red light not available to other photosynthetic organisms [85]. *Chroococcidiopsis* species have been suggested as possible candidates for terraforming

other planets [86]. Expression plasmids have been introduced into several strains of *C. thermalis* via conjugation [84].

2.11. Gloeobacter violaceus PCC 7421

Gloeobacter violaceus PCC 7421 (PCC 7421) is a primordial cyanobacterium that lacks thylakoid membranes [87]. PCC 7421 localises proteins involved in photosynthesis and respiration to specific regions of the cytoplasmic membrane [88]. Despite its very slow growth, a method of transforming PCC 7421 with an expression vector via conjugation has been developed [89].

Microorganisms **2019**, *7*, 409

Table 2. Summary of genetic manipulations carried out in model and non-model cyanobacterial species discussed in Section 2.

Species	Strain	Desirable Features from Table 1	Transformation Method	Reported Selection Markers	Agar Medium	References
Synechococcus sp.	UTEX 2973	1), 2), 3), 4), 5), 6)	Conjugation CRISPR/Cas *pilN* mutants are naturally transformable	Apramycin Chloramphenicol Kanamycin Spectinomycin Streptomycin	BG-11	[20,33,35,58]
	PCC 11801	1), 2), 3), 5), 6)	Naturally transformable	Spectinomycin	BG-11	[23]
	PCC 11901	1), 2), 3), 5), 6)	Naturally transformable	Acrylic acid Spectinomycin	AD7	[24]
Nostoc punctiforme	ATCC 29133	1), 2), 3), 4), 5), 6)	Conjugation	Chloramphenicol Neomycin *sacB* markers Streptomycin	Allen and Arnon	[62,63,90]
Cyanothece sp.	PCC 7822	1), 2), 3), 5)	Electroporation	Spectinomycin	BG-11	[66]
	ATCC 51142	1), 2), 3), 4), 6)	Conjugation	Kanamycin	BG-11 ASP2	[67]
Arthrospira platensis	C1	1), 2), 3), 4), 5)	Electroporation	Spectinomycin	Zarrouk	[53]
Leptolyngbya sp.	BL0902	1), 2), 3), 4), 5), 6)	Conjugation	Chloramphenicol Erythromycin Neomycin Spectinomycin Streptomycin	BG-11	[72,73]
Fremyella diplosiphon	SF33	1), 2), 3), 4), 6)	Conjugation	Kanamycin Neomycin *sacB* markers	BG-11/HEPES	[74,75,91]
Marine *Synechococcus* sp.	WH7803 WH8102 WH8103	1), 2), 3), 6)	Conjugation Electroporation	Kanamycin	SN	[76,77,92]
Marine *Prochlorococcus* sp.		1), 3)	-	Spectinomycin	Pro99	[76,93]

Table 2. *Cont.*

Species	Strain	Desirable Features from Table 1	Transformation Method	Reported Selection Markers	Agar Medium	References
Thermosynechococcus elongatus	BP-1	1), 2), 3), 4), 5), 6)	Naturally transformable	Chloramphenicol Kanamycin	BG-11	[81]
	PKUAC-SCTE542	1), 2), 3), 6)	Naturally transformable	Spectinomycn	BG-11	[82]
Chlorogloeopsis fritschii	PCC 6912	1), 2), 3), 4), 5)	Biolistic Conjugation	Kanamycin Neomycin	Allen and Arnon	[83,90]
Fischerella muscicola	PCC 7414	1), 2), 3), 4), 5)	Biolistic Conjugation	Kanamycin Neomycin	Allen and Arnon	[83,90]
Chroococcidiopsis thermalis		1), 2), 3), 4), 5)	Conjugation	Neomycin	BG-11	[84]
Gloeobacter violaceus	PCC 7421	1), 2), 3), 4), 5)	Conjugation	Streptomycin	BG-11	[89]

Microorganisms **2019**, *7*, 409

3. Current and Future Strategies for Genome Engineering in Cyanobacteria

3.1. CRISPR/Cas Genome Editing in Cyanobacteria

The RNA-guided CRISPR/Cas family of enzymes has been the driving force for a revolutionary step change in precision genome editing capacity in almost every field of biology, including photosynthetic biology [94–96]. Briefly, all CRISPR/Cas genome editing systems exploit the Class II family of CRISPR-associated endonuclease (Cas) enzymes (comprising types II, V and VI Cas) [97,98]. The type II-A Cas of *Streptococcus pyogenes* (SpCas9) was first demonstrated as a site-specific RNA-guided DNA cleavage tool by Jinek et al. [99]. Since then, a vast array of CRISPR/Cas technologies have been produced and continue to be developed at a rapid pace [100–105]. Genome editing studies using CRISPR/Cas have now been reported in several cyanobacterial species, including PCC 6803, PCC 7942, UTEX 2973 and the filamentous strain *Nostoc* (*Anabaena*) PCC 7120, from four separate labs (for recent reviews, see [25,27,106]).

We will not cover the specific mechanisms of all the available CRISPR/Cas tools here (for reviews, see [94,96]). We will focus on Cas9, which confers a blunt-ended double-stranded break (DSB) in DNA (Figure 1A), and type V-A Cas (Cas12a, or previously Cpf1), which produces a staggered DSB (Figure 1B) [107]. Use of CRISPR/Cas systems for gene editing relies on a synthetic single-guide RNA (sgRNA or gRNA), which, for Cas9, is a fusion of a crRNA (CRISPR-RNA) and a tracrRNA (trans-activating crRNA). For CRISPR/Cas9 systems, gRNAs are commonly expressed from a DNA template, with each gRNA transcribed from a single expression cassette. The crRNA component is customised for targeting a specific genomic locus and the tracrRNA acts as a scaffold for recruitment of Cas9. In contrast, Cas12a enzymes possess an intrinsic RNase activity that facilitates autoprocessing of gRNAs that can be expressed from 'spacer arrays' (Figure 1C) and a tracrRNA fusion is not required. Spacer arrays are comprised of spacers that code for gRNAs, which are each separated by a direct repeat (DR). The DR facilitates recognition and cleavage of the precursor RNA by Cas12a to form mature gRNAs. To date, all Cas isoforms that target DNA require a 2–6 nucleotide sequence called a protospacer-adjacent motif (PAM) site for Cas to bind DNA and generate a DSB. Depending on the type of Cas used, PAM sites are situated immediately upstream or downstream of the gRNA target locus. As PAM sites are sequence-specific, the choice of Cas enzyme used can impact on the gRNA loci available.

Microorganisms **2019**, *7*, 409

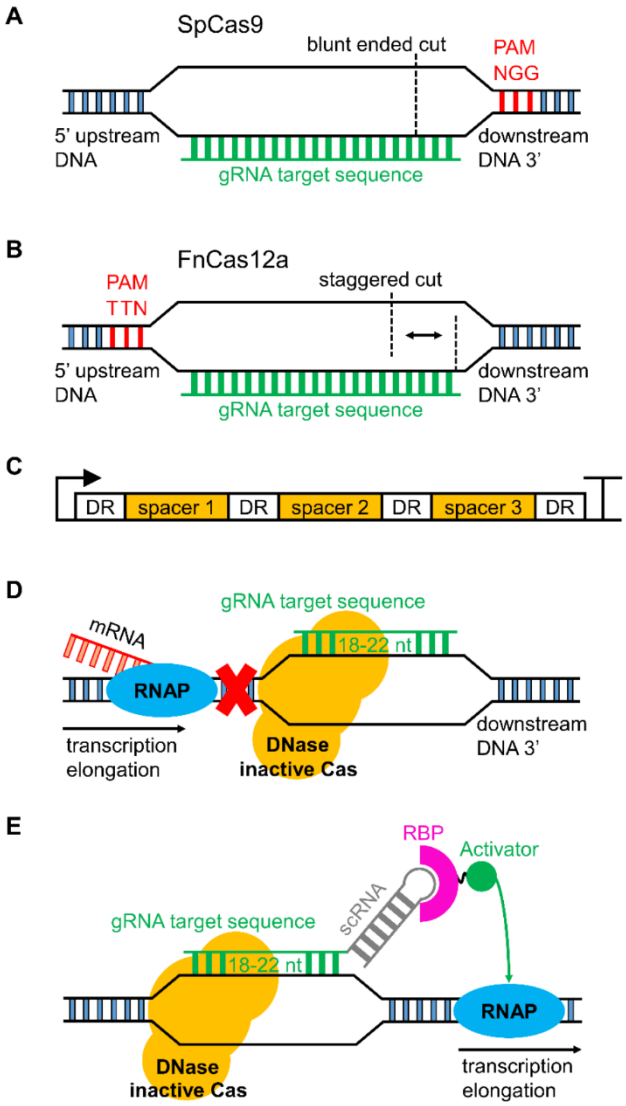

Figure 1. Basic overview of CRISPR/Cas-based genome editing and CRISPR interference in cyanobacteria. (**A**) The type II-A CRISPR/Cas system comprising SpCas9 that is targeted by a guide RNA (gRNA, green) upstream of an NGG protospacer adjacent motif (PAM) (red). SpCas9 generates a blunt-ended double-stranded break (DSB) in DNA (black dashed line). (**B**) The type II-V CRISPR/Cas system comprising FnCas12a that is targeted by a gRNA downstream of a TTN PAM. Cas12a confers a staggered DSB in DNA that results in a five-nucleotide overhang. (**C**) Illustration of a single expression cassette containing three spacers (i.e., a spacer array, orange) that are flanked by direct repeat regions (DRs, white). Cas12a recognises and cleaves spacers in response to a DR to generate a mature gRNA from each spacer. (**D**) Overview of transcriptional inhibition by CRISPRi. DNase inactive Cas enzymes (e.g., dCas9 or ddCas12a) are targeted to a DNA locus by a gRNA (typical length indicated as 18–22 nucleotides), which blocks RNA polymerase (RNAP, blue) to prevent mRNA (red) synthesis. (**E**) Example of transcriptional activation by CRISPRa. DNase inactive Cas enzymes (e.g., dCas9 or ddCas12a) are targeted by a gRNA fused to a scaffold RNA (scRNA, grey). The scRNA recruits an RNA binding protein (RBP, pink) fused to a transcriptional activator (green) (e.g., [108]), which subsequently leads to activation of RNAP and transcription elongation.

Microorganisms **2019**, *7*, 409

In cyanobacteria (as in other prokaryotes that lack an endogenous non-homologous end joining (NHEJ) pathway) [109,110]), CRISPR/Cas has been used as an enhancement tool to improve the frequency of targeted mutation by HR [58,111–113]. In brief, expression of Cas and a gRNA mediates cleavage at a specific DNA target site. The co-expressed editing template contains homology flanks (*ca*. 1 kb in length) and subsequent repair modifies the locus and mutates the PAM site to avoid repeated cleavage. The potential advantages of CRISPR/Cas over established HR strategies in model cyanobacteria such as PCC 6803 [16] are that 1) a markerless mutation is induced at the DNA target site in a single event; 2) multiple sites could be modified simultaneously, provided the appropriate gRNAs and editing templates are co-expressed; and 3) CRISPR/Cas systems could be more efficient for engineering species that are not naturally transformable (e.g., by conjugation or electroporation). Potential drawbacks include toxicity of the Cas enzyme and the time required to cure new mutants of the CRISPR/Cas vector following editing. One approach to accelerate the latter issue is the inclusion of a negative selection marker (e.g., *sacB*) on the CRISPR/Cas vector [113]. Thus far, SpCas9 is the only Cas9 reported to have been expressed in cyanobacterial strains, including PCC 6803, PCC 7942 and UTEX 2973 (Table 3) [58,111,112]. Expression of SpCas9 has been linked to toxicity and failure to recover colonies following transformation or conjugation in all three species, even at low expression levels. It remains unclear why SpCas9 appears toxic in cyanobacteria, or whether other Cas9 enzymes may be more compatible.

Table 3. Cyanobacterial species where CRISPR/Cas has been used for gene editing.

Species and Strain	Cas Type	Expression System	Reference
Synechococcus elongatus PCC 7942	SpCas9	episomal	[111]
Synechocystis sp. PCC 6803 *Synechococcus elongatus* UTEX 2973 *Nostoc* sp. PCC 7120	FnCas12a	episomal	[114]
Synechococcus elongatus UTEX 2973	SpCas9	episomal	[58]
Synechocystis sp. PCC 6803	SpCas9	chromosomal	[112]
Synechococcus elongatus PCC 7942 *Synechococcus elongatus* UTEX 2973	FnCas12a	episomal	[57]
Nostoc sp. PCC 7120	FnCas12a	episomal	[113]

In contrast to Cas9, expression of Cas12a in the cyanobacterial strains examined so far does not appear to result in toxicity [57,113,114]. Gene editing using Cas12a from *Francisella novicida* (FnCas12a) has been demonstrated in PCC 6803, PCC 7942, UTEX 2973 and *Nostoc* PCC 7120. An additional advantage of Cas12a is that the intrinsic RNase activity allows for the design of a single expression cassette containing multiple gRNAs to target several DNA loci simultaneously (Figure 1C) [115–117]. A recent multiplexing study with Cas12a designed an array of 25 gRNAs on a single plasmid that simultaneously edited multiple genomic target sites in mammalian cells [105].

Previously, reports of gene editing with FnCas12a in cyanobacteria have been limited to a single lab [57,114]. However, Niu et al. [113] have recently also demonstrated that *Nostoc* PCC 7120 can be edited by FnCas12a. A high efficacy was demonstrated for FnCas12a-mediated gene editing of single target sites (83%) by attempting to generate knockout mutants in 26 different genes using 52 gRNAs (two per gene) [113]. In addition, a markerless double-knockout mutant was generated for two genes required for heterocyst formation (*hetR* (alr2339) and *hetN* (alr5358)) in a single step following co-conjugation with two CRISPR/FnCas12a editing vectors carrying different antibiotic selection markers. Lastly, a conditional knockout was generated for the essential gene *polA* (alr1254; DNA polymerase I) by replacing the RBS of the *polA* promoter with a theophylline-induced riboswitch [118,119]. Successfully transconjugated lines were only viable when grown with theophylline. Transconjugates were then cured of the self-replicating CRISPR/FnCas12a vector by withdrawing antibiotics and using *sacB* counter selection on sucrose plates.

Microorganisms **2019**, *7*, 409

Table 4. The available PAM sequences for cyanobacterial species highlighted in this study for different Cas variants. Only species with full genomes available are shown. The Cas variants indicated are *Streptococcus pyogenes* Cas9 (SpCas9), *Francisella novicida* Cas12a (FnCas12a), *Acidaminococcus* sp. Cas12a (AcCas12a, and variants AsCas12a-RR and ASCas12a-RVR), *Lachnospiraceae bacterium* Cas12a (LbCas12a) and *Deltaproteobacteria bacterium* CasX (CasX). The average number of PAM sites (in brackets) per kb of genome are shown (N = A, T, C, G; V = A, C, G; Y = C, T). Genome data was sourced from The European Nucleotide Archive (https://www.ebi.ac.uk/ena) and The National Centre for Biotechnology Information (https://www.ncbi.nlm.nih.gov/genome).

Cyanobacteria	Genome Size (bp)	SpCas9 (NGG)	FnCas12a (TTN)	AsCas12a and LbCas12a (TTTV)	AsCas12a-RR (TYCV)	ASCas12a-RVR (TATV)	CasX (TTCN)
Arthrospira platensis C1	6,089,210	134	168	24	46	21	33
Arthospira plantensis NIES 39	6,788,435	114	171	37	46	22	33
Chroococcidiopsis thermalis PCC 7203	6,315,792	89	175	38	41	17	34
Cyanothece sp. ATCC 51142	4,934,271	118	221	35	40	23	39
Cyanothece sp. PCC 7822	6,091,620	114	210	33	39	21	36
Gleobacter violaceus PCC 7421	4,659,019	170	89	17	42	6	26
Nostoc punctiforme strain ATCC 29133	8,234,322	114	194	43	40	20	35
Nostoc sp. PCC 7120	6,413,771	119	191	27	39	39	34
Synechococcus elongatus PCC 6301	2,696,255	142	113	10	41	7	28
Synechococcus elongatus PCC 7942	2,695,903	141	113	10	41	6	28
Synechococcus elongatus PCC 11801	2,691,022	139	115	10	41	7	29
Synechococcus sp. PCC 7002	3,008,047	153	163	22	48	11	33
Synechococcus sp. PCC 11901	3,081,514	152	163	22	47	11	33
Synechococcus sp. UTEX 2973	2,690,418	142	113	10	41	6	28
Synechococcus sp. WH 8102	2,434,428	173	86	7	49	4	28
Synechocystis sp. PCC 6803	3,569,561	161	174	23	51	12	32
Thermosynechococcus elongatus BP-1	2,593,857	176	126	13	42	10	27

Thus far, FnCas12a is the only reported Cas12a used in cyanobacteria genome editing studies. One general constraint of CRISPR/Cas editing is the specificity of the PAM site required for DNA cleavage. Of potential interest to cyanobacterial researchers is the growing availability of different Cas12a isoforms (e.g., AsCas12a and LbCas12a from *Acidaminococcus* sp. and *Lachnospiraceae bacterium*, respectively) and those engineered to recognise alternative PAM sequences (Table 4) [96,120]. Increased flexibility in PAM recognition will allow for more choice when targeting loci for genome editing [120,121]. New Cas enzymes continue to be identified but remain to be evaluated in cyanobacteria, such as CasX, which also produces a staggered DSB but is smaller than Cas12a [122]. If CasX is less toxic than Cas9, it may provide a useful new set of tools for genome-editing in cyanobacterial species.

3.2. Serine Integrases for Generating Multiple Knock-ins

The most commonly used methods for genome engineering in cyanobacteria still rely on HR and the use of selective markers. For example, to generate a gene knockout or a knock-in mutant, heterologous DNA must be integrated with a selective marker (e.g., an antibiotic resistance cassette). Thus, the ability to generate mutants in a given species with multiple insertional mutations is limited by the availability and efficacy of selective markers. To overcome this limitation, several methods have been developed for generating markerless mutants, which allows mutant strains to undergo further genetic modifications. One of the most widely used markerless techniques in PCC 6803 uses a two-step HR approach with the negative selection marker *sacB*, which produces levansucrase, an enzyme conferring sensitivity to sucrose [16]. Nevertheless, generating a fully segregated markerless mutant for a single locus takes *ca.* 4 weeks to several months, depending on the target locus, while sequential engineering for multi-mutant strains can be very time consuming. Tsujimoto et al. [123] demonstrated an insertion of 20.8 kb in PCC 6803, but this was achieved by a laborious five-step HR process using *ca.* 4 kb at a time. Therefore, new methods need to be developed to allow large DNA insertions and/or multiple loci engineering in a more efficient timeframe.

Serine integrases are a subfamily of the site-specific recombinases that catalyse DNA rearrangement through small DNA sequences (<50 bp) called attachments (*att*) (commonly used for GateWay cloning) [124]. Serine integrases catalyse recombination between the *att* sites from linear or circular DNA that can result in excision, integration or inversion of DNA sequences, depending on the position and orientation of the *att* sites. Temperate bacteriophages encode serine integrases to catalyse integration of their DNA into bacterial genomes through recombination of *att*P (phage) and *att*B (bacteria) attachment sites, generating *att*L (left) and *att*R (right) sites (Figure 2A). Serine integrases bind to the *att*P and *att*B sites to make a staggered cut in the central region, generating halves with a two base-pair 3′ overhang. Then, rotation takes place to swap the *att*P and *att*B half-sites and finally, the two bp complementary overhangs religate to generate *att*R and *att*L sites that cannot recombine again unless a recombination directionality factor (RDF) is present (Figure 2B). Six pairs of nonpalindromic central overlap sequences (TT, CT, GT, CA, CC, and TC) can be used to create orthogonal sites and allows multiple *att* sites to be used simultaneously (e.g., *att*P^{TT} will only recombine with *att*B^{TT} in a specific orientation) [125]. The control of directionality and orthogonality have made serine integrases attractive tools for genome engineering and genetic logic gate design [126,127]. In contrast to CRISPR/Cas-based approaches, site-specific recombination using serine integrases does not rely on endogenous DNA repair pathways, such as NHEJ or HR. Although CRISPR/Cas knock-in approaches are able to generate small insertions in a single step, the size of the insertion remains limited by the efficiency of HR. In addition, unlike Cas9, no toxicity has been reported with the usage of serine integrases in several organisms [124,126,128].

Serine integrases have been used for genome engineering in a variety of organisms, including mice [129], *Drosophila melanogaster* [130], *S. cerevisiae*, *E. coli* [126] and *Clostridium ljungdahlii* [128]. A recent strategy outlined a portable method to simplify the introduction of multiple genomic insertions using the orthogonal *att* sites of the PhiC31 serine integrase [126]. Firstly, one or more selective markers flanked by two orthogonal *att*B sites were integrated into the genome of *E. coli* as

Microorganisms **2019**, *7*, 409

"landing pads". Although Snoeck et al. [126] used HR to introduce the landing pads, other techniques such as CRISPR/Cas have been used for *att* site integration [128]. Secondly, a donor vector carrying an expression cassette for PhiC31 integrase and the DNA fragment(s) to be inserted flanked by *att*P orthogonal sites was introduced to generate insertions specific for each corresponding landing pad by *att*B × *att*P recombination (Figure 2C).

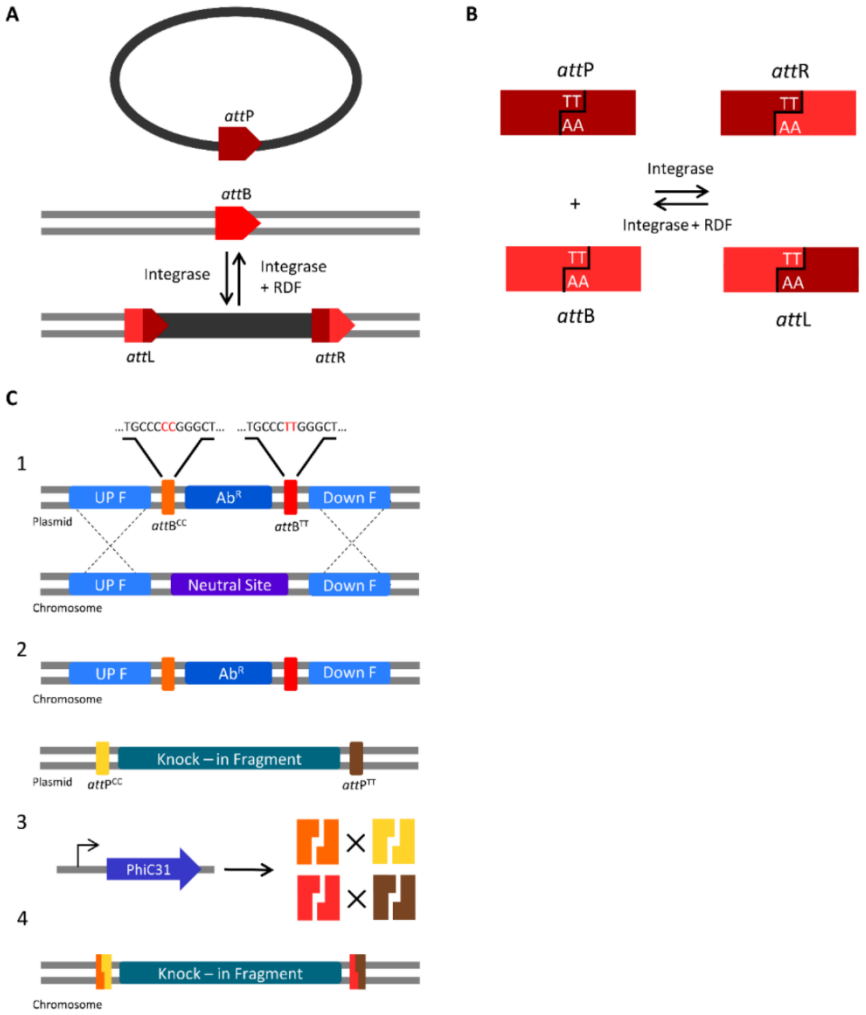

Figure 2. Mechanism of action of serine integrases and knock-in strategies. (**A**) DNA rearrangement with serine integrases: *att*B and *att*P sites recombine to make *att*L and *att*R sites. In the presence of the cognate recombination directionality factor (RDF), the reaction is reversed [124]. (**B**) The serine integrases bind to the *att*P and *att*B sites, generate a staggered 2 bp cut to produce two halves at each site, and then rotate to swap the two halves from each site. If the halves are complementary, relegation occurs to generate *att*L and *att*R sites. (**C**) A serine integrase-mediated knock-in strategy for cyanobacteria. Integration of a landing pad (the landing pad shown carries orthogonal *att*B^{CC} and *att*B^{TT} sites) occurs by homologous recombination (HR) at a neutral site in the cyanobacterial chromosome (C1). A self-replicating vector carrying the donor DNA fragment flanked by *att*P^{CC} and *att*P^{TT} sites and a PhiC31 integrase expression cassette is introduced into the cyanobacterial strain (C2). Expression of PhiC31 integrase results in the recombination of the orthogonal *att*B and *att*P pairs (C3), replacing the "landing pad" with the donor DNA to generate an unmarked knock-in mutant (C4).

Using a single landing pad, a 10.3 kb DNA fragment was inserted with 100% efficiency. Simultaneous recombination with three landing pads generated a triple-knock-in mutant (all fragments were *ca.* 2.5 kb in size), with an efficiency of 75%.

In cyanobacteria, integration of one or more landing pads at a given locus could proceed either by a two-step HR approach if the species is naturally transformable [16], or by CRISPR/Cas-mediated HR [114]. CRISPR/Cas could also be used to insert landing pads at multiple loci in a single step [113], Broad host range vectors able to self-replicate in cyanobacteria (e.g., pPMQAK1) could be used to construct the donor vector [35]. To generate a markerless knock-in mutant following serine intergrase-mediated recombination, the donor vector could be cured from the strain by inclusion of the negative selection marker *sacB* on the vector backbone. Thus, serine integrases could emerge as a useful tool for the generation of multi-knock-in markerless mutants for large DNA fragments in cyanobacteria. Generating a library of strains with *att* "landing pads" in combination with high-throughput assembly methods, such as Golden Gate MoClo for the assembly of the donor vectors [35], could significantly speed up the design-build-test cycle.

4. Known and Novel Tools for Regulating Gene Expression in Cyanobacteria

4.1. Gene Regulation with CRISPRi and Synthetic Small Regulatory RNAs

The emergence of CRISPR interference (CRISPRi) and synthetic small regulatory RNA (sRNA) tools in cyanobacterial research has allowed for fine modulation of gene expression at both the transcriptional and translational levels. For translational repression, sRNA tools employ an antisense RNA to bind a specific mRNA transcript target and generate an RNA duplex [131,132]. The RNA duplex suppresses translation and subsequently targets the mRNA transcript for degradation. sRNA-based approaches have been demonstrated in PCC 6803 and PCC 7002, including a paired termini antisense RNA approach and an Hfq-mediated system using sRNAs fused to a MicC scaffold [132–134]. Both approaches demonstrated up to 90% reduction in protein expression.

For transcriptional repression, CRISPRi approaches make use of DNase-inactive variants of Cas, called "dead" Cas9 (dCas9) or DNase "dead" Cas12a (ddCas12a; also known as ddCpf1) (Figure 1D) [100,117]. To date, SpdCas9 is the only reported DNase-inactive Cas used in cyanobacterial research, but it has been used successfully to repress gene expression in PCC 6803, PCC 7002, PCC 7942 and *Nostoc* PCC 7120 [35,133,135–138]. Unlike SpCas9, SpdCas9 does not appear to be toxic. However, in our lab, we have observed a reduction in growth rates in PCC 6803 when SpdCas9 was expressed at high levels, suggesting that low/medium strength promoters should be used when designing SpdCas9 expression cassettes. Decreased growth rates and changes in cell morphology and division have been observed in *E. coli* when expressing SpdCas9 at high levels [139].

Multiplexing of gRNAs to target several genes simultaneously with SpdCas9 has been demonstrated in PCC 6803 [137,140]. Kaczmarzyk et al. [137] demonstrated simultaneous repression of six native genes. However, a potential limitation to multiplexing using dCas9 is the need for individual expression cassettes for each gRNA. Kaczmarzyk et al. [137] reported issues with vector recombination in PCC 6803 due to repeated use of common promoters and terminators for each gRNA cassette. ddCas12a may provide an improvement over SpdCas9 in cyanobacteria for multiplexing gRNAs and repression of multiple loci, as demonstrated in *E. coli* [117]. Cas12a requires a DR length of 19 base pair (bp) to generate mature gRNAs from spacer arrays [141], which is significantly less than that of most promoters and terminators; this may help to reduce plasmid vector size requirements and mitigate recombination issues when multiplexing is required. However, cloning spacer arrays can be challenging due to the multiple repeated sequences, and is not always achievable even using commercial DNA synthesis companies.

CRISPRi using SpdCas9 has been reported to reduce protein expression of heterologous reporter genes (e.g., YFP) between 40% and 99%, depending on the gRNA(s) used [35,140]. Native gene repression has been shown to vary, with a maximum reduction of 94% achieved for *glgC* in PCC

7942 [136,140]. Yao et al. [136,140] targeted a range of native genes with CRISPRi in PCC 6803 and observed reductions of <90% for *slr0942*, *sll0990*, and *slr1192*, but more modest knock down of 50% for *slr0091*. Thus, validation of gRNA(s) is important to ensure effective transcriptional repression, which can be time consuming. To achieve more robust and consistent down regulation, it may be advantageous to combine CRISPRi and sRNA to simultaneously modulate transcription and translation. Furthermore, CRISPR/Cas variants have been characterised that target RNA, and thus also can modulate expression at the translational level. For example, Cas13 cleaves single-stranded RNA [142], and in its deactivated form (dCas13), can bind mRNA and suppress translation [143]. Cas13 may provide additional tools for RNA manipulation and additional strategies for gene and multigene repression studies.

Finally, dCas9 has also been used to drive gene expression by so called CRISPR activation (CRISPRa). CRISPRa relies on gRNA(s) modified to include an extended hairpin sequence (termed a scaffold RNA, scRNA) that function, for example, to recruit an RNA binding protein (RBP) fused to a transcriptional activator [108]. Thus, when the dCas9-scRNA complex binds to a target locus, the scRNA recruits the appropriate machinery to drive transcription (Figure 1E). As the dCas9 is unmodified, CRISPRi and CRISPRa could be achieved concurrently with the expression of multiple gRNAs and scRNAs for simultaneous gene repression and activation [108,144]. In *E. coli*, effective gene activation by CRISPRa does require appropriately positioned PAM sites situated at specific locations upstream of the transcription start site. Recent work shows that shifting the gRNA target site by as little as two nucleotides can lead to a significant loss in activation [145]. Nevertheless, these approaches could improve on current strategies in cyanobacteria to both express heterologous pathways and repress native gene expression for the redirection of metabolic flux towards desired products [137].

4.2. Sigma Factors and RNA Polymerase as Regulatory Tools for Gene Transcription

The highlighted serine integrase recombination and CRISPR-based approaches are examples of promising tools for genome engineering and gene regulation in cyanobacteria. However, applying these approaches often requires careful regulation of the composite parts by inducible and, ideally, orthogonal gene expression systems to generate predictable outputs [146–148].

Sigma factors are critical components required for transcription initiation in bacteria that interact with the core RNA polymerase (RNAP) complex to facilitate binding to specific DNA promoter regions [149]. Thus, different sigma factors are involved in driving the transcription of different subsets of genes, and are themselves expressed by different environmental or stress inputs [150,151]. All cyanobacterial sigma factors belong to the sigma 70 family [152], although several others exist in bacteria [153].

Recent reports have provided good evidence that sigma factors may be compatible with RNAP complexes from different bacterial species, paving the way for a potential novel orthogonal expression system in cyanobacteria. *Nostoc* PCC 7120 contains twelve sigma factors that regulate gene expression according to environmental conditions [154]. In a recent study, Wells et al. [155] tested the sigma factors from *Nostoc* PCC 7120 in *E. coli* and observed that several cyanobacterial promoters were able to drive transcription in *E. coli* only when sigma factors from *Nostoc* PCC 7120 were co-expressed. Similarly, sigma factors from *Bacillus subtilis* can be co-expressed in *E. coli* to construct an orthogonal expression system [156]. Thus, testing non-sigma 70 factors in cyanobacteria may help to identify novel tools for orthogonal transcriptional regulation [157]. For example, *E. coli* have a sigma 54 factor [158,159], which if functional in cyanobacteria, could allow for transcription from sigma 54-dependant promoters as a novel orthogonal trans-acting expression system [152]. Liu et al. [160] have recently demonstrated in *E. coli* that sigma 54-dependent promoters can be combined with CRISPRa and have a higher dynamic range compared to sigma 70-dependent promoters.

Similarly, heterologous RNAP systems could be employed. For example, the T7 RNAP is a single subunit RNA polymerase of viral origin that is commonly used as an expression tool in *E. coli* due to its orthogonality to bacterial transcription machinery [161–163]. Use of T7 RNAP has also recently been

demonstrated in PCC 6803 and PCC 7942 [164,165]. As in *E. coli*, native sigma factors in cyanobacteria do not interact with the T7 promoter sequence (P_{T7}), so genes driven by P_{T7} are transcribed only if the cognate T7 RNAP is expressed. Directed evolution approaches have produced new variants of T7 RNAP with altered promoter recognition characteristics [161,166]. P_{T7} has also undergone substantial analysis, with Komura et al. [167] testing transcriptional activity of 7847 P_{T7} variants. T7 RNAP has also been adapted to act as a photoactivatable genetic switch in *E. coli* with dark-off/light-on properties [168]. The latter system could be of use in cyanobacterial biotechnology; for example, light- or dark-dependent control of protein production (e.g., for light-sensitive bioproducts) with a variety of different promoter strengths.

4.3. The Potential of Optogenetic Systems

Several small-molecule inducible/repressible systems have been characterised in *E. coli* [169–171]. However, only a small number have been characterised in cyanobacteria, and thus far, only in model species [31,37,164,172–174]. The commonly used lac operon induction system, which uses isopropyl β–D-1 thiogalactopyranoside (IPTG), has been shown to be leaky and have low induction levels, possibly due to the limited capacity of IPTG to diffuse into cyanobacterial cells [119,175,176]. Metal ion inducible promoters have been tested in several cyanobacterial strains [177–179], but these are sometimes not practical as many metals ions are present in standard growth media (e.g., BG11 [180]) and toxicity can be an issue. More recently, an arabinose inducible and a rhamnose inducible promoter were characterised in PCC 6803, which showed tight regulation, linear response and sustained expression [31,37]. However, the relatively low availability of inducible/repressible systems in cyanobacterial species compared to model heterotrophs still limits the progress and development of more advanced synthetic circuits for dynamic control of cellular behaviour [108,181].

In the last decade, optogenetics (i.e., light-controlled regulation) has emerged as a promising tool for tuning synthetic circuits in mammalian and bacterial cell systems [182–186]. Compared with chemical induction systems, optogenetic systems allow for more targeted, rapid and precise control of genetic elements with increased spatial and temporal control, while being minimally invasive and reversible [187–190]. Optogenetic systems can be classified broadly into two-component systems (TCSs) or one-component systems (OCSs).

An optogenetic TCS requires two elements: a light-sensing module and a light-responsive module that is activated by the light-sensing module. For example, the green light-inducible CcaS/CcaR TCS in PCC 6803 relies on the membrane-bound histidine kinase CcaS (i.e., the light-sensing module), which is phosphorylated in green light (Figure 3A) [191]. Phosphorylated CcaS subsequently phosphorylates the cytosolic response regulator protein CcaR (i.e., the light-responsive module) that, in turn, activates the expression of the phycobilisome linker gene *cpcG2*. TCSs have been identified in plants [192], bacteria [191] and fungi that specifically sense UV [193], blue [194,195], green [196–198], red [199] or near-infrared light [200]. In contrast, optogenetic OCSs act as both the sensing and responsive modules and are found in the cytosol. So far, only the blue light-activated OCSs that belong to the LOV (Light–Oxygen–Voltage) family of proteins have been characterised in heterotrophic bacteria [187,201], *S. cerevisiae* [186,202] and *Arabidopsis thaliana* [203] (Figure 3B,C). Both systems have been used in the control of genetic circuits at multiple levels, such as transcription and protein activity.

Microorganisms **2019**, *7*, 409

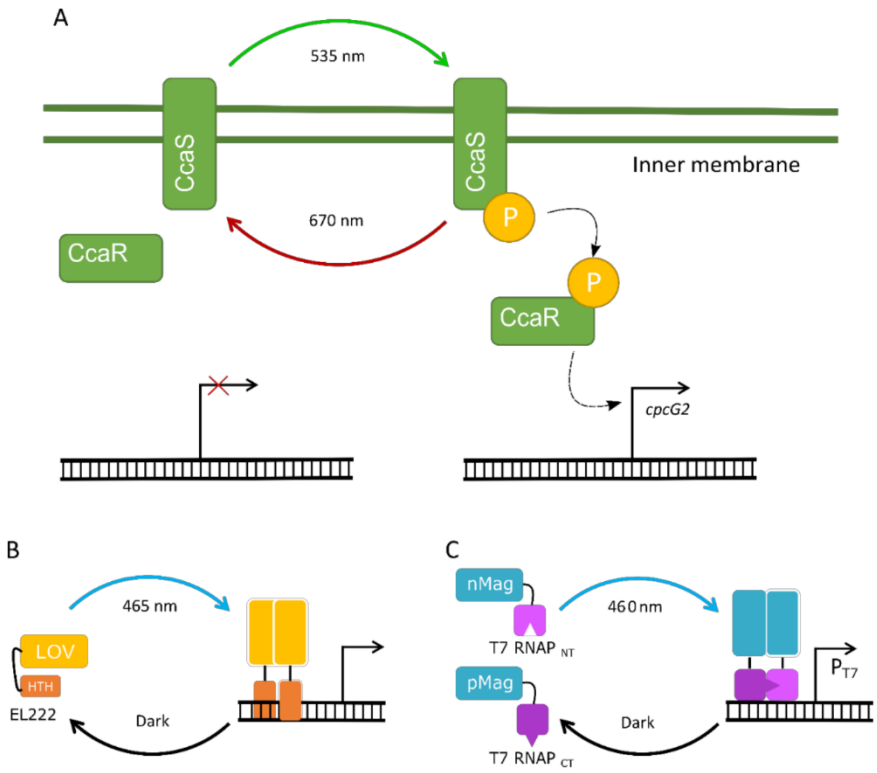

Figure 3. Examples of optogenetic two-component and one-component systems. (**A**) The two-component green light-inducible CcaS/CcaR system native to *Synechocystis* sp. PCC 6803. In the presence of green light (535 nm), the histidine kinase CcaS is phosphorylated and, in turn, phosphorylates the response activator CcaR, which results in expression of cpcG2 [191,196]. (**B**) The EL222 transcription factor from *Erythrobacter litoralis* HTCC2594 is a one-component system. Blue light induces a conformational change between the LOV and the Helix-Turn-Helix (HTH) DNA binding domain, allowing dimerisation and DNA binding [187]. (**C**) Split T7 RNA polymerase (RNAP) fused to the Vivid (VVD) photoreceptor from *Neurospora crassa* is a one-component system. In blue light, the two subunits of VVD (nMag and pMag) interact to assemble the split T7 RNAP (T7 $RNAP_{NT}$ and T7 $RNAP_{CT}$) as a functional RNA polymerase [204].

Apart from the green light-inducible CcaS/CcaR system, only one other optogenetic TCS has been characterised in PCC 6803, the near-UV activated UirS/UirR system that regulates phototaxis [205]. The latter has not yet been exploited in cyanobacterial research, but the CcaS/CcaR system has been used in PCC 6803 to regulate GFP expression [196], and drive expression of two T4 phage-derived lysis genes to generate a green light-induced cell membrane lytic system [197]. The CcaS/CcaR system has also been used to modulate GFP in a marine species where the CcaS/CcaR system is absent (*Synechococcus* sp. NKBG 15041c), and demonstrated tight repression under red light and a 20-fold induction of GFP under green light [206]. Thus, cyanobacterial TCSs show promise as tools for transcriptional control in species where those TCSs are not present.

There are also several optogenetic systems characterised in *E. coli* that could be used in cyanobacterial research. For example, the near-infrared (760 nm) TCS BphP1/PpsR2 from *Rhodopseudomonas palustris* showed rapid response dynamics and a 2.5-fold dynamic range [200]. Recently, an OCS based on the Vivid (VVD) photoreceptor from the filamentous fungus *Neurospora crassa* was used to generate a blue-light-inducible T7 RNAP system (Figure 3B) [204]. In the dark, only low levels of gene expression were observed, while high levels of expression were achieved in blue light (460 nm), with an inducible range of >300-fold. Optogenetic systems responsive to different

light wavelengths can also be combined to achieve multichromatic gene control [199]. For example, a red–green–blue (RGB) system was constructed in *E. coli* for production of three different pigments to generate colour biophotographs [188]. The RGB system used a fragmented T7 RNAP that could bind to specific promotors depending on the light input, and demonstrated little crosstalk, high dynamic range and fast responses when induced.

Currently, the main challenge for porting optogenetic systems into cyanobacteria is ensuring compatibility with native light-responsive components. Cyanobacteria naturally produce many of the cofactors required for light-sensing and light-responsive modules [207], which could provide an advantage when porting heterologous optogenetic systems. However, growing cyanobacteria in specific wavelengths (e.g., blue, green, orange, red) will affect photosynthetic efficiencies and growth [208]. Therefore, optimising optogenetic systems might require testing several sources of light to limit any impacts on photosynthesis and achieve the desired outputs.

4.4. Using Inteins to Progress Genetic Circuit Research in Cyanobacteria

Genetic circuits occur in nature and form the basis by which living cells respond and adapt to the surrounding environment [146]. A key goal in synthetic biology is the generation of synthetic genetic circuits that operate as Boolean logic functions to give digital-like control over gene expression in response to environmental stimuli [146,209,210]. Basic Boolean logic functions include 'AND' and 'NOT' gates: AND gates will give an output signal if all inputs are 'ON', while NOT gates will give an output signal only if all inputs are 'OFF' [147,211,212]. To date, relatively few synthetic genetic circuits have been constructed in cyanobacteria [213]. These include an oxygen-responsive AND gate in PCC 6803 [214] and four NOT gate variants in PCC 6803, PCC 7942, *Nostoc* PCC 7120, *Synechocystis* sp. WHSyn, and *Leptolyngbya* sp. BL0902 [73]. Currently, two key constraints for making more complex synthetic genetic circuits in cyanobacteria are the relatively small number of characterised inducible expression systems available, and the limited means to integrate multiple input signals (i.e., from different inducible systems) into a single output [215]. Thus, new tools (such as those highlighted in this review) will be required.

Inteins are naturally occurring polypeptides (100–150 amino acids) within a larger precursor protein that can excise themselves spontaneously from flanking protein regions (exteins (external proteins)) [216]. Inteins have been identified in several cyanobacteria [217], and a variety of other organisms, including other bacterial species, archaea, viruses and eukaryotes [218,219]. Intein excision involves the cleavage of two peptide bonds, resulting in the formation of a new peptide bond, which ligates the flanking exteins together, forming a newly rearranged protein. This auto-catalytic posttranslational modification is referred to as protein splicing and it exists in two forms, cis- and trans-splicing [220]. In the former, the intein coding sequence is embedded in frame with the gene, such that the precursor protein is produced from a single mRNA transcript and translated as two exteins flanking the intein. Upon cis-splicing, the intein is excised from the precursor protein and the flanking exteins are ligated seamlessly to form a new protein. In contrast, trans-splicing events are facilitated by two precursor proteins translated from separate mRNAs, where each encodes a "split intein" fragment (i.e., an *N*-intein half and a *C*-intein half) fused to an extein (Figure 4). When the precursor proteins are brought into close proximity, the split inteins re-assemble non-covalently [221]. Trans-splicing then occurs, resulting in excision of the split inteins and ligation of the exteins via a covalent bond to generate an intact protein [221,222].

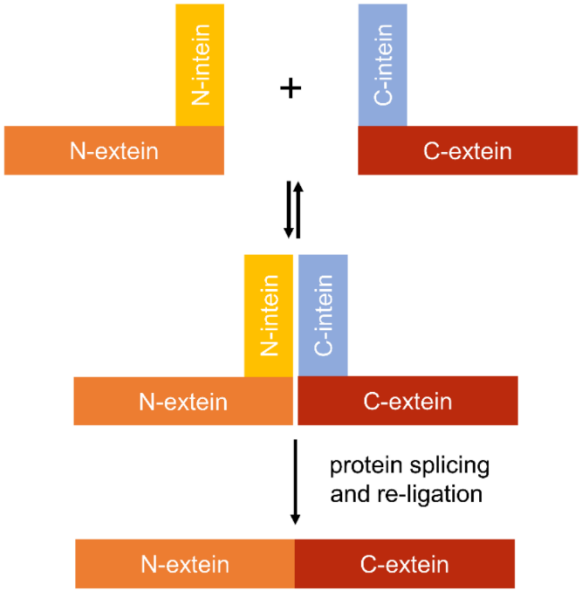

Figure 4. Overview of protein trans-splicing with split inteins. Each precursor protein is composed of a split intein (an *N*-intein half or a *C*-intein half) fused to an extein (an *N*-extein half and a *C*-extein half). When the split inteins are brought into close proximity, they undergo an autocatalytic trans-splicing reaction. During this process, each split intein fragment is cleaved and the extein halves are spliced together to generate an intact protein via a covalent bond.

Split inteins have been used in *E. coli* to construct a functional two input transcriptional AND gate system using a split T7 RNAP approach [222]. T7 RNAP was separated into two domains, each fused to an *N*- or a *C*-intein half, and expressed from two different inducible promoters. Schaerli et al. [222] showed that expression of both T7 RNAP domain-intein fusions was required to reconstitute a functional T7 RNAP and drive transcription of GFP from P_{T7}. Using a similar trans-splicing approach, split inteins have also been used to facilitate re-assembly of split variants of the more complex multidomain transcriptional regulator TetR [223]. Like T7 RNAP, TetR repressible systems have been used in PCC 6803 and PCC 7942 [164]. Thus, these split intein-based gate systems may be straightforward to port into cyanobacteria, provided that the inteins used are orthogonal (i.e., not of cyanobacterial origin) [224]. Split intein strategies could also be used for other transcription factors successfully trailed in cyanobacterial species (e.g., LacI, AraC and RhaS [37,176,214,225]) to construct larger synthetic genetic circuits.

5. Genome-Scale Models

Manipulating cyanobacteria for biotechnology applications is dependent not just on developing better genetic tools but also improving our understanding of cellular metabolism. Genome-scale models (GSMs) are large-scale simulation tools that comprise a global description of the metabolic reactions and pathways of an organism using stoichiometric coefficients and mass balances of the participating metabolites [226]. GSMs are receiving increasing interest due to their predictive power in metabolome and flux changes, thereby making them a valuable tool in metabolic engineering approaches and optimisation for enhanced production of target metabolites [227,228].

Currently, 290 draft genomes and 85 full genomes are available for cyanobacterial species [39]. However, GSMs have only been developed for a small number of these, primarily models such as PCC 6803 [42], PCC 7942 [41] and more recently, UTEX 2973 [43] (Table 5). GSMs from model species can be used as a scaffold to draft GSMs for other cyanobacterial species, as many pathways are conserved [229]. Generating robust and accurate GSMs is an iterative and bottom-up process

dependent on the expansion and updating of draft models with available experimental data. Thus, GSM models are continually being improved due to the growing availability of sequencing and omics information.

Table 5. Genome-scale models currently available for different cyanobacterial strains.

Cyanobacteria	GSM Name	Reference
Synechocystis sp. PCC 6803	iSynCJ816 imSyn716	[230] [42]
Synechococcus sp. PCC 7942	iSyf715	[231]
	iJB785 iJB792	[41] [232]
Synechococcus sp. UTEX 2973	iSyu683 imSyu593	[233] [43]
Synechococcus sp. PCC 7002	iSpy708 iSpy821	[234] [235]
Arthrospira platensis NIES-39 *Nostoc* sp. PCC 7120	n/a n/a	[40] [236]

Recent cyanobacterial GSMs have attempted to include algorithms to model components of the photosynthetic electron transport chain [41,230,232,235]. However, representing the mechanisms of light capture and electron flow in stoichiometric coefficients is challenging as fluxes cannot be determined experimentally by standard methods (e.g., ^{13}C metabolic flux analysis) [41,237,238]. The model iJB785 for PCC 7942 incorporates the impact of light availability on metabolic flux [41]. When used to estimate whether genes were essential or non-essential for survival, the model achieved an accuracy of 78% based on previous experimental data [239]. Recently, the PCC 7942 model was updated (i.e., iJB792) to include whole-cell light absorbance and the rate of photosynthetic O_2 evolution to predict metabolic reaction fluxes [232]. The updated model demonstrated a 98% correlation between simulated and experimental metabolic fluxes under low- (60 µmol photons $m^{-2} \cdot s^{-1}$) and high-light (600 µmol photons $m^{-2} \cdot s^{-1}$) conditions. Similarly, the model iSynCJ816 for PCC 6803 can account for changes in energy absorption for different light qualities [230], and achieved a 77% accuracy when compared with experimental results from online databases and literature searches. In comparison, the latest GSM for *E. coli* (iML1515) can predict gene essentiality in minimal media with 16 different carbon sources with an average accuracy of 94% [44]. The relatively higher accuracy of iML1515 relies on the integration of biochemical, physiological, localisation, genetic, transcriptomic, proteomic and fluxomic data. Currently, protein localisation and transcriptomic data are not included in GSMs for cyanobacteria.

Cyanobacterial GSMs have been used to detect key metabolic differences between species [240] and to identify bottlenecks for the biosynthesis of relevant metabolites [241]. These include a composite GSM for the closely related strains, PCC 7942 and UTEX 2973, based on the model inSyn617 for PCC 6803. The resulting model (iSyu683) identified pathways where resources were allocated differently between PCC 7942 and UTEX 2973, the most prominent difference being carbon uptake rates [233]. An improved model for UTEX 2973 (imSyu593) was recently developed using transient ^{13}C-labeling. The flux elucidation revealed nearly complete conversion (>96%) of the assimilated carbon into biomass compared with only 86% conversion in PCC 6803. Comparison of the UTEX 2973 flux map with that of PCC 6803 revealed differences in the synthesis of key Calvin cycle metabolites, fructose-6-phosphate and sedoheptulose-7-phosphate, and production of amino acids, glycine and serine, from the photorespiratory salvage pathway [43].

GSMs can be used in cyanobacteria to improve bioproduction. Recently, the model iBJ792 for PCC 7942 was used to determine an optimal solution *in silico* to maximise the production of 2,3-butanediol [232]. GSMs can be also be combined with other computational tools for production

optimisation. For example, OptFlux and OptForce are software tools that identify all possible engineering interventions by determining what genes to knock out, or which reaction fluxes in a model need to increase, decrease or fall to zero, to overproduce specific metabolites [242,243]. OptFlux has been combined with GSMs in PCC 6803 to improve the production of *n*-butanol [138]. OptFlux confirmed that genes targeted for manipulation based on previous experimental data were essential for growth. Subsequent repression of the gene targets arrested growth and redirected carbon flux towards the production of *n*-butanol, resulting in a 5-fold yield increase compared to the non-repressed strain. Similarly, OptForce was used to increase the production of limonene [244]. Overexpressing three predicted gene targets (two involved in the pentose phosphate pathway and geranyl diphosphate synthase) resulted in a 2.3-fold improvement in limonene production in vivo.

Further improvements in the accuracy of GSMs in cyanobacteria are constrained by the lack of available omics data. For example, a large percentage of the predicted proteins in most cyanobacterial genomes are still annotated as unknown or hypothetical [245]. In addition, transcriptomic data and transcriptional regulatory mechanisms are not integrated in current cyanobacterial GSM models, unlike those for other species such as *E. coli* (iML1515) [44,246]. Lastly, incorporation of more accurate models for photosynthesis, light-harvesting and electron transport is required [232]. The current expansion of high-throughput omics technologies and automated cloning facilities (e.g., genome foundries) can be used to generate large amounts of experimental data under different growth conditions, which promises to help overcome current limitations for cyanobacterial GSMs.

6. Development of CyanoSource: A Barcoded Mutant Library for *Synechocystis* sp. PCC 6803

Mutant generation is a key tool in bacterial research and for altering species for biotechnology applications. Individual research laboratories currently generate mutants of interest via a variety of different experimental methods, using a range of plasmid systems in sub-strains that can vary significantly at both the phenotypic and genotypic level (e.g., in PCC 6803 [247–249]). This raises the issue of whether studies are directly comparable, a key concern given the growing emphasis on reproducibility within the scientific community. The construction of mutant libraries is a consistent and efficient method for the study of protein properties, regulation and function. Mutant libraries have been generated for model photosynthetic eukaryotes, such as *Chlamydomonas reinhardtii* [250] and *Arabidopsis thaliana* [251], and model microbial species including *E. coli* [252] and *S. cerevisiae* [253]. The existence of mutant libraries accelerates the pace of research, avoids unnecessary replication between research groups and helps to improve experimental designs. Targeted mutant libraries also provide knowledge on the essential gene set required for survival, further avoiding wasteful laboratory replication [239]. In addition, many research groups, particularly in developing countries, lack the expertise and resources to generate cyanobacterial mutants.

Cyanobacteria remain underdeveloped for fundamental research and viable biotechnological exploitation. Nevertheless, cyanobacterial research is a rapidly growing field with approximately 13,000 new papers published in the last 5 years, making it the third most studied group of autotrophs behind plants and algae. In PCC 6803, only *ca.* 1050 coding sequences (~30%) have assigned functions, compared to ~80% in *E. coli* and *S. cerevisiae* [226]. Of these, only a small proportion have been characterised in a cyanobacterium [39]. The majority have been assigned functions based on studies of homologues in other bacteria, even though the function and importance of characterised genes may differ significantly between phototrophic and heterotrophic bacteria. Transposon libraries have been reported for two model cyanobacterial species [239,254], but these suffer from common issues associated with transposon mutagenesis, including random large insertions, pleiotropic effects, incomplete saturation of the genome and difficulty in recovering individual mutants of interest. A publicly available genome-wide collection of gene knockout mutants would generate a much-needed step change in resource availability and significantly accelerate research in functional genomics and cellular processes in cyanobacteria. It would also supplement existing algal and plant resources, allowing researchers to further examine genes conserved across the photosynthetic lineage.

Microorganisms **2019**, *7*, 409

Gene characterisation studies remain challenging and time-consuming but recent developments in automation [255] can streamline and shorten the process of one of the major experimental hurdles: generation of targeted mutants in which the gene of interest has been deleted. DNA assembly and bacterial transformation are complex manual tasks that are time consuming and can suffer from high error rates. Investment by the UK Research and Innovation councils in automated DNA Foundry technologies has provided an opportunity to overcome these challenges [255]. In collaboration with the Earlham DNA Foundry (EDF) and the Edinburgh Genome Foundry (EGF) we will carry out the generation of the plasmids and mutants for this library by using a recently established MoClo system for cyanobacteria [35]. This resource, termed CyanoSource, will target 3456 genes in PCC 6803 (Figure 5). Conditional mutants (i.e., specialised mutants that require an external stimulus to repress a gene) will be constructed for essential genes that cannot be removed. Here, where appropriate, we will use a copper-sensitive promoter that switches off the gene when copper is present [256–258]. For the cyanobacterial community, a genome-wide library of mutants and genetic parts generated via automation will guarantee a standard of quality control not otherwise achievable.

In addition to automation, this library will be barcoded to allow for the tracking of individual strains within a pooled mutant library. This powerful approach has been described in *S. cerevisiae* [253] and *C. reinhardtii* [250], where barcoded libraries can be subjected to different conditions and the relative fitness of individual mutants in a population can be determined via deep sequencing. Construction of this library will begin in November 2019. All plasmids and mutants will be made available to UK and international researchers via a public database, which will be updated throughout the project.

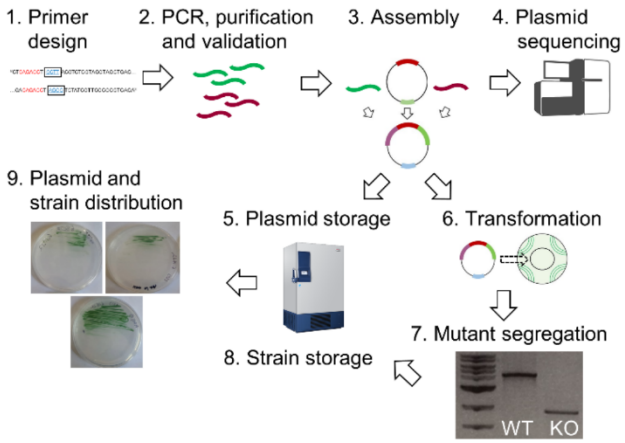

Figure 5. Workflow for the automated production of the CyanoSource resource at two UK DNA Foundry facilities. Primers (**1**) will be used to generate amplicons carrying BsaI sites (red) and appropriate four-nucleotide overhangs (blue, boxed) for MoClo assembly. PCR products will then be purified and validated (**2**) and used to assemble suicide vectors (**3**) for natural transformation of *Synechocystis* sp. PCC 6803. Vectors will be sequenced by MiSeq (**4**) and glycerol stocks made for long-term storage (**5**). PCC 6803 mutants will be generated (**6**), followed by several rounds of re-streaking to produce segregated mutants that will be confirmed by colony PCR (**7**), and stored as glycerol stocks (**8**). For distribution, plasmid stocks are planned to be supplied by Addgene and mutants supplied by the University of East Anglia CyanoSource Hub as streaked plates from glycerol stocks (**9**).

7. Conclusions

Given the ongoing advances in complex synthetic biology tools to finely modulate metabolism in microbes, the future looks bright for progressing both fundamental and applied cyanobacterial research. The topics outlined in this review highlight just some of the current exciting methods that could be used to generate a step change for cyanobacteria researchers by improving transformation

efficiencies, gene regulation and capacity for metabolic engineering. Development of the techniques and resources outlined in this review should significantly improve our knowledge of this environmentally important phylum, especially for poorly characterised species. Moreover, their application towards the development of cyanobacteria as a renewable biotechnology platform could have immense implications, not just commercially but also in replacing polluting fossil fuels usage for chemical production and reducing carbon emissions.

Author Contributions: Conceptualization, G.A.R.G., A.A.S.O., A.J.M.; Writing–Original Draft Preparation, G.A.R.G., A.A.S.O., L.A.M., D.J.L.-S., A.J.M.; Writing–Review & Editing, all authors; Supervision, D.J.L.-S., B.W., A.J.M.

Acknowledgments: G.A.R.G., A.A.S.O., and L.A.M. acknowledge funding support from the BBSRC EASTBIO CASE PhD programme [BB/M010996/1], the Consejo Nacional de Ciencia y Tecnología (CONACYT) PhD programme, and the BBSRC Norwich Research Park Doctoral Training Partnership programme [BB/S507404/1], respectively. A.J.M and D.J.L.-S. acknowledge funding from the UK Biotechnology and Biological Sciences Research Council (BBSRC) grants [BB/S020128/1] and [BB/S020365/1], respectively. B.W. acknowledges funding support by the UK BBSRC grant [BB/N007212/1], and UK Research and Innovation grant [MR/S018875/1].

Conflicts of Interest: The authors declare no conflict of interest.

References

1. Seckbach, J. *Algae and Cyanobacteria in Extreme Environments*; Cellular Origin, Life in Extreme Habitats and Astrobiology; Springer: Dordrecht, The Netherlands, 2007; ISBN 978-1-4020-6111-0.
2. Flombaum, P.; Gallegos, J.L.; Gordillo, R.A.; Rincón, J.; Zabala, L.L.; Jiao, N.; Karl, D.M.; Li, W.K.W.; Lomas, M.W.; Veneziano, D.; et al. Present and future global distributions of the marine Cyanobacteria *Prochlorococcus* and *Synechococcus*. *Proc. Natl. Acad. Sci. USA* **2013**, *110*, 9824–9829. [CrossRef] [PubMed]
3. Pedersen, D.; Miller, S.R. Photosynthetic temperature adaptation during niche diversification of the thermophilic cyanobacterium *Synechococcus* A/B clade. *ISME J.* **2017**, *11*, 1053–1057. [CrossRef] [PubMed]
4. Puente-Sánchez, F.; Arce-Rodríguez, A.; Oggerin, M.; García-Villadangos, M.; Moreno-Paz, M.; Blanco, Y.; Rodríguez, N.; Bird, L.; Lincoln, S.A.; Tornos, F.; et al. Viable cyanobacteria in the deep continental subsurface. *Proc. Natl. Acad. Sci. USA* **2018**, *115*, 10702–10707. [CrossRef] [PubMed]
5. Schirrmeister, B.E.; Gugger, M.; Donoghue, P.C.J. Cyanobacteria and the great oxidation event: Evidence from genes and fossils. *Palaeontology* **2015**, *58*, 769–785. [CrossRef] [PubMed]
6. Knoll, A.H. Paleobiological perspectives on early microbial evolution. *Cold Spring Harb. Perspect. Biol.* **2015**, *7*, 1–17. [CrossRef] [PubMed]
7. Nutman, A.P.; Bennett, V.C.; Friend, C.R.L.; Van Kranendonk, M.J.; Chivas, A.R. Rapid emergence of life shown by discovery of 3700-million-year-old microbial structures. *Nature* **2016**, *537*, 535–538. [CrossRef] [PubMed]
8. Dick, G.J.; Grim, S.L.; Klatt, J.M. Controls on O_2 production in cyanobacterial mats and implications for Earth's oxygenation. *Annu. Rev. Earth Planet. Sci.* **2018**, *46*, 123–147. [CrossRef]
9. Pisciotta, J.M.; Zou, Y.; Baskakov, I.V. Light-dependent electrogenic activity of cyanobacteria. *PLoS ONE* **2010**, *5*, e10821. [CrossRef]
10. Lea-Smith, D.J.; Howe, C.J. The use of cyanobacteria for biofuel production. In *Biofuels and Bioenergy*; Love, J., Bryant, J.A., Eds.; John Wiley & Sons, Ltd.: Chichester, UK, 2017; pp. 143–155. ISBN 9781118350553.
11. Singh, R.; Parihar, P.; Singh, M.; Bajguz, A.; Kumar, J.; Singh, S.; Singh, V.P.; Prasad, S.M. Uncovering potential applications of cyanobacteria and algal metabolites in biology, agriculture and medicine: Current status and future prospects. *Front. Microbiol.* **2017**, *8*, 1–37. [CrossRef]
12. Carroll, A.L.; Case, A.E.; Zhang, A.; Atsumi, S. Metabolic engineering tools in model cyanobacteria. *Metab. Eng.* **2018**, *50*, 47–56. [CrossRef]
13. Dismukes, G.C.; Carrieri, D.; Bennette, N.; Ananyev, G.M.; Posewitz, M.C. Aquatic phototrophs: Efficient alternatives to land-based crops for biofuels. *Curr. Opin. Biotechnol.* **2008**, *19*, 235–240. [CrossRef] [PubMed]
14. Long, B.M.; Hee, W.Y.; Sharwood, R.E.; Rae, B.D.; Kaines, S.; Lim, Y.L.; Nguyen, N.D.; Massey, B.; Bala, S.; von Caemmerer, S.; et al. Carboxysome encapsulation of the CO_2-fixing enzyme Rubisco in tobacco chloroplasts. *Nat. Commun.* **2018**, *9*, 3570. [CrossRef] [PubMed]

15. Lau, N.S.; Matsui, M.; Abdullah, A.A.A. Cyanobacteria: Photoautotrophic microbial factories for the sustainable synthesis of industrial products. *BioMed Res. Int.* **2015**, *2015*, 754934. [CrossRef] [PubMed]
16. Lea-Smith, D.J.; Vasudevan, R.; Howe, C.J. Generation of marked and markerless mutants in model cyanobacterial species. *J. Vis. Exp.* **2016**, *2016*, e54001. [CrossRef] [PubMed]
17. Keeling, P.J. Diversity and evolutionary history of plastids and their hosts. *Am. J. Bot.* **2004**, *91*, 1481–1493. [CrossRef] [PubMed]
18. Nielsen, A.Z.; Mellor, S.B.; Vavitsas, K.; Wlodarczyk, A.J.; Gnanasekaran, T.; Perestrello Ramos H de Jesus, M.; King, B.C.; Bakowski, K.; Jensen, P.E. Extending the biosynthetic repertoires of cyanobacteria and chloroplasts. *Plant J.* **2016**, *87*, 87–102. [CrossRef] [PubMed]
19. Lin, P.C.; Pakrasi, H.B. Engineering cyanobacteria for production of terpenoids. *Planta* **2019**, *249*, 145–154. [CrossRef]
20. Yu, J.; Liberton, M.; Cliften, P.F.; Head, R.D.; Jacobs, J.M.; Smith, R.D.; Koppenaal, D.W.; Brand, J.J.; Pakrasi, H.B. *Synechococcus elongatus* UTEX 2973, a fast growing cyanobacterial chassis for biosynthesis using light and CO_2. *Sci. Rep.* **2015**, *5*, 8132. [CrossRef]
21. Sezonov, G.; Joseleau-Petit, D.; D'Ari, R. *Escherichia coli* physiology in Luria-Bertani broth. *J. Bacteriol.* **2007**, *189*, 8746–8749. [CrossRef]
22. Snoep, J.L.; Mrwebi, M.; Schuurmans, J.M.; Rohwer, J.M.; Teixeira de Mattos, M.J. Control of specific growth rate in *Saccharomyces cerevisiae*. *Microbiology* **2009**, *155*, 1699–1707. [CrossRef]
23. Jaiswal, D.; Sengupta, A.; Sohoni, S.; Sengupta, S.; Phadnavis, A.G.; Pakrasi, H.B.; Wangikar, P.P. Genome features and biochemical characteristics of a robust, fast growing and naturally transformable cyanobacterium *Synechococcus elongatus* PCC 11801 isolated from India. *Sci. Rep.* **2018**, *8*, 16632. [CrossRef] [PubMed]
24. Włodarczyk, A.; Selão, T.T.; Norling, B.; Nixon, P.J. Unprecedented biomass and fatty acid production by the newly discovered cyanobacterium *Synechococcus* sp. PCC 11901. *bioRxiv* **2019**, 684944. [CrossRef]
25. Behler, J.; Vijay, D.; Hess, W.R.; Akhtar, M.K. CRISPR-based technologies for metabolic engineering in cyanobacteria. *Trends Biotechnol.* **2018**, *36*, 996–1010. [CrossRef] [PubMed]
26. Sun, T.; Li, S.; Song, X.; Diao, J.; Chen, L.; Zhang, W. Toolboxes for cyanobacteria: Recent advances and future direction. *Biotechnol. Adv.* **2018**, *36*, 1293–1307. [CrossRef] [PubMed]
27. Santos-Merino, M.; Singh, A.K.; Ducat, D.C. New applications of synthetic biology tools for cyanobacterial metabolic engineering. *Front. Bioeng. Biotechnol.* **2019**, *7*, 1–24. [CrossRef] [PubMed]
28. Vijay, D.; Akhtar, M.K.; Hess, W.R. Genetic and metabolic advances in the engineering of cyanobacteria. *Curr. Opin. Biotechnol.* **2019**, *59*, 150–156. [CrossRef] [PubMed]
29. Markley, A.L.; Begemann, M.B.; Clarke, R.E.; Gordon, G.C.; Pfleger, B.F. Synthetic biology toolbox for controlling gene expression in the cyanobacterium *Synechococcus* sp. strain PCC 7002. *ACS Synth. Biol.* **2015**, *4*, 595–603. [CrossRef]
30. Nielsen, J.; Keasling, J.D. Engineering cellular metabolism. *Cell* **2016**, *164*, 1185–1197. [CrossRef]
31. Immethun, C.M.; DeLorenzo, D.M.; Focht, C.M.; Gupta, D.; Johnson, C.B.; Moon, T.S. Physical, chemical, and metabolic state sensors expand the synthetic biology toolbox for *Synechocystis* sp. PCC 6803. *Biotechnol. Bioeng.* **2017**, *114*, 1561–1569. [CrossRef]
32. Ferreira, E.A.; Pacheco, C.C.; Pinto, F.; Pereira, J.; Lamosa, P.; Oliveira, P.; Kirov, B.; Jaramillo, A.; Tamagnini, P. Expanding the toolbox for *Synechocystis* sp. PCC 6803: Validation of replicative vectors and characterization of a novel set of promoters. *Synth. Biol.* **2018**, *3*, 1–15. [CrossRef]
33. Li, S.; Sun, T.; Xu, C.; Chen, L.; Zhang, W. Development and optimization of genetic toolboxes for a fast-growing cyanobacterium *Synechococcus elongatus* UTEX 2973. *Metab. Eng.* **2018**, *48*, 163–174. [CrossRef] [PubMed]
34. Roulet, J.; Taton, A.; Golden, J.W.; Arabolaza, A.; Burkart, M.D.; Gramajo, H. Development of a cyanobacterial heterologous polyketide production platform. *Metab. Eng.* **2018**, *49*, 94–104. [CrossRef] [PubMed]
35. Vasudevan, R.; Gale, G.A.R.; Schiavon, A.A.; Puzorjov, A.; Malin, J.; Gillespie, M.D.; Vavitsas, K.; Zulkower, V.; Wang, B.; Howe, C.J.; et al. CyanoGate: A modular cloning suite for engineering cyanobacteria based on the plant MoClo syntax. *Plant Physiol.* **2019**, *180*, 39–55. [CrossRef] [PubMed]
36. Wang, B.; Eckert, C.; Maness, P.C.; Yu, J. A Genetic toolbox for modulating the expression of heterologous genes in the cyanobacterium *Synechocystis* sp. PCC 6803. *ACS Synth. Biol.* **2018**, *7*, 276–286. [CrossRef] [PubMed]

37. Kelly, C.L.; Taylor, G.M.; Hitchcock, A.; Torres-Méndez, A.; Heap, J.T. A rhamnose-inducible system for precise and temporal control of gene expression in cyanobacteria. *ACS Synth. Biol.* **2018**, *7*, 1056–1066. [CrossRef] [PubMed]
38. Heidorn, T.; Camsund, D.; Huang, H.H.; Lindberg, P.; Oliveira, P.; Stensjö, K.; Lindblad, P. Synthetic biology in cyanobacteria. In *Methods in Enzymology*; Voigt, C., Ed.; Elsevier: Boston, MA, USA, 2011; Volume 497, pp. 539–579. ISBN 9780123850751.
39. Fujisawa, T.; Narikawa, R.; Maeda, S.I.; Watanabe, S.; Kanesaki, Y.; Kobayashi, K.; Nomata, J.; Hanaoka, M.; Watanabe, M.; Ehira, S.; et al. CyanoBase: A large-scale update on its 20th anniversary. *Nucleic Acids Res.* **2017**, *45*, 551–554. [CrossRef] [PubMed]
40. Yoshikawa, K.; Aikawa, S.; Kojima, Y.; Toya, Y.; Furusawa, C.; Kondo, A.; Shimizu, H. Construction of a genome-scale metabolic model of *Arthrospira platensis* NIES-39 and metabolic design for cyanobacterial bioproduction. *PLoS ONE* **2015**, *10*, e0144430. [CrossRef]
41. Broddrick, J.T.; Rubin, B.E.; Welkie, D.G.; Du, N.; Mih, N.; Diamond, S.; Lee, J.J.; Golden, S.S.; Palsson, B.O. Unique attributes of cyanobacterial metabolism revealed by improved genome-scale metabolic modeling and essential gene analysis. *Proc. Natl. Acad. Sci. USA* **2016**, *113*, E8344–E8353. [CrossRef]
42. Gopalakrishnan, S.; Pakrasi, H.B.; Maranas, C.D. Elucidation of photoautotrophic carbon flux topology in *Synechocystis* PCC 6803 using genome-scale carbon mapping models. *Metab. Eng.* **2018**, *47*, 190–199. [CrossRef]
43. Hendry, J.I.; Gopalakrishnan, S.; Ungerer, J.; Pakrasi, H.B.; Tang, Y.J.; Maranas, C.D. Genome-scale fluxome of *Synechococcus elongatus* UTEX 2973 using transient 13 C-labeling data. *Plant Physiol.* **2019**, *179*, 761–769. [CrossRef]
44. Monk, J.M.; Lloyd, C.J.; Brunk, E.; Mih, N.; Sastry, A.; King, Z.; Takeuchi, R.; Nomura, W.; Zhang, Z.; Mori, H.; et al. iML1515, a knowledgebase that computes *Escherichia coli* traits. *Nat. Biotechnol.* **2017**, *35*, 904–908. [CrossRef] [PubMed]
45. Shestakov, S.V.; Khyen, N.T. Evidence for genetic transformation in blue-green alga *Anacystis nidulans*. *MGG Mol. Gen. Genet.* **1970**, *107*, 372–375. [CrossRef] [PubMed]
46. Stevens, S.E.; Porter, R.D. Transformation in *Agmenellum quadruplicatum*. *Proc. Natl. Acad. Sci. USA* **1980**, *77*, 6052–6056. [CrossRef] [PubMed]
47. Elhai, J. Strong and regulated promoters in the cyanobacterium *Anabaena* PCC 7120. *FEMS Microbiol. Lett.* **1993**, *114*, 179–184. [CrossRef] [PubMed]
48. Wendt, K.E.; Pakrasi, H.B. Genomics approaches to deciphering natural transformation in cyanobacteria. *Front. Microbiol.* **2019**, *10*, 1259. [CrossRef] [PubMed]
49. Taton, A.; Unglaub, F.; Wright, N.E.; Zeng, W.Y.; Paz-Yepes, J.; Brahamsha, B.; Palenik, B.; Peterson, T.C.; Haerizadeh, F.; Golden, S.S.; et al. Broad-host-range vector system for synthetic biology and biotechnology in cyanobacteria. *Nucleic Acids Res.* **2014**, *42*, e136. [CrossRef] [PubMed]
50. Elhai, J.; Wolk, C.P. Conjugal transfer of DNA to cyanobacteria. In *Methods in Enzymology*; Packer, L., Glazer, A.N., Eds.; Academic Press: Cambridge, MA, USA, 1988; Volume 167, pp. 747–754. ISBN 9780121820688.
51. Masukawa, H.; Inoue, K.; Sakurai, H.; Wolk, C.P.; Hausinger, R.P. Site-directed mutagenesis of the *Anabaena* sp. strain PCC 7120 nitrogenase active site to increase photobiological hydrogen production. *Appl. Environ. Microbiol.* **2010**, *76*, 6741–6750. [CrossRef]
52. Mandakovic, D.; Trigo, C.; Andrade, D.; Riquelme, B.; Gómez-Lillo, G.; Soto-Liebe, K.; Díez, B.; Vásquez, M. CyDiv, a conserved and novel filamentous cyanobacterial cell division protein involved in septum localization. *Front. Microbiol.* **2016**, *7*, 94. [CrossRef]
53. Jeamton, W.; Dulsawat, S.; Tanticharoen, M.; Vonshak, A.; Cheevadhanarak, S. Overcoming intrinsic restriction enzyme barriers enhances transformation efficiency in *Arthrospira platensis* C1. *Plant Cell Physiol.* **2017**, *58*, 822–830. [CrossRef]
54. Ried, J.L.; Collmer, A. An nptI-sacB-sacR cartridge for constructing directed, unmarked mutations in gram-negative bacteria by marker exchange-eviction mutagenesis. *Gene* **1987**, *57*, 239–246. [CrossRef]
55. Kratz, W.A.; Myers, J. Nutrition and growth of several blue-green algae. *Am. J. Bot.* **1955**, *42*, 282–287. [CrossRef]

56. Ungerer, J.; Lin, P.C.; Chen, H.Y.; Pakrasi, H.B. Adjustments to photosystem stoichiometry and electron transfer proteins are key to the remarkably fast growth of the cyanobacterium *Synechococcus elongatus* UTEX 2973. *MBio* **2018**, *9*, e02327-17. [CrossRef] [PubMed]
57. Ungerer, J.; Wendt, K.E.; Hendry, J.I.; Maranas, C.D.; Pakrasi, H.B. Comparative genomics reveals the molecular determinants of rapid growth of the cyanobacterium *Synechococcus elongatus* UTEX 2973. *Proc. Natl. Acad. Sci. USA* **2018**, *115*, E11761–E11770. [CrossRef] [PubMed]
58. Wendt, K.E.; Ungerer, J.; Cobb, R.E.; Zhao, H.; Pakrasi, H.B. CRISPR/Cas9 mediated targeted mutagenesis of the fast growing cyanobacterium *Synechococcus elongatus* UTEX 2973. *Microb. Cell Fact.* **2016**, *15*, 115. [CrossRef]
59. Begemann, M.B.; Zess, E.K.; Walters, E.M.; Schmitt, E.F.; Markley, A.L.; Pfleger, B.F. An organic acid based counter selection system for cyanobacteria. *PLoS ONE* **2013**, *8*, e76594. [CrossRef] [PubMed]
60. Meeks, J.C. Symbiosis between nitrogen-fixing cyanobacteria and plants. *Bioscience* **1998**, *48*, 266–276. [CrossRef]
61. Gao, Q.; Garcia-Pichel, F. Microbial ultraviolet sunscreens. *Nat. Rev. Microbiol.* **2011**, *9*, 791–802. [CrossRef]
62. Cohen, M.F.; Wallis, J.G.; Campbell, E.L.; Meeks, J.C. Transposon mutagenesis of *Nostoc* sp. strain ATCC 29133, a filamentous cyanobacterium with multiple cellular differentiation alternatives. *Microbiology* **1994**, *140*, 3233–3240. [CrossRef] [PubMed]
63. Soule, T.; Stout, V.; Swingley, W.D.; Meeks, J.C.; Garcia-Pichel, F. Molecular genetics and genomic analysis of scytonemin biosynthesis in *Nostoc punctiforme* ATCC 29133. *J. Bacteriol.* **2007**, *189*, 4465–4472. [CrossRef]
64. Reddy, K.J.; Haskell, J.B.; Sherman, D.M.; Sherman, L.A. Unicellular, aerobic nitrogen-fixing cyanobacteria of the genus *Cyanothece*. *J. Bacteriol.* **1993**, *175*, 1284–1292. [CrossRef] [PubMed]
65. Bandyopadhyay, A.; Elvitigala, T.; Welsh, E.; Stöckel, J.; Liberton, M.; Min, H.; Sherman, L.A.; Pakrasi, H.B. Novel metabolic attributes of the genus *Cyanothece*, comprising a group of unicellular nitrogen-fixing cyanobacteria. *MBio* **2011**, *2*, e00214-11. [CrossRef] [PubMed]
66. Min, H.; Sherman, L.A. Genetic transformation and mutagenesis via single-stranded DNA in the unicellular, diazotrophic cyanobacteria of the genus *Cyanothece*. *Appl. Environ. Microbiol.* **2010**, *76*, 7641–7645. [CrossRef] [PubMed]
67. Liberton, M.; Bandyopadhyay, A.; Pakrasi, H.B. Enhanced nitrogen fixation in a glgX -deficient strain of *Cyanothece* sp. strain ATCC 51142, a unicellular nitrogen-fixing cyanobacterium. *Appl. Environ. Microbiol.* **2019**, *85*, e02887-18. [CrossRef] [PubMed]
68. Ohmori, M.; Ehira, S. Spirulina: An example of cyanobacteria as nutraceuticals. In *Cyanobacteria*; Sharma, N.K., Rai, A.K., Stal, L.J., Eds.; John Wiley & Sons, Ltd.: Chichester, UK, 2013; pp. 103–118. ISBN 9781118402238.
69. Adir, N.; Bar-Zvi, S.; Harris, D. The amazing phycobilisome. *Biochim. Biophys. Acta Bioenerg.* **2019**. [CrossRef] [PubMed]
70. Fujisawa, T.; Narikawa, R.; Okamoto, S.; Ehira, S.; Yoshimura, H.; Suzuki, I.; Masuda, T.; Mochimaru, M.; Takaichi, S.; Awai, K.; et al. Genomic structure of an economically important cyanobacterium, *Arthrospira* (Spirulina) platensis NIES-39. *DNA Res.* **2010**, *17*, 85–103. [CrossRef]
71. Shimura, Y.; Hirose, Y.; Misawa, N.; Osana, Y.; Katoh, H.; Yamaguchi, H.; Kawachi, M. Comparison of the terrestrial cyanobacterium *Leptolyngbya* sp. NIES-2104 and the freshwater *Leptolyngbya boryana* PCC 6306 genomes. *DNA Res.* **2015**, *22*, 403–412. [CrossRef]
72. Taton, A.; Lis, E.; Adin, D.M.; Dong, G.; Cookson, S.; Kay, S.A.; Golden, S.S.; Golden, J.W. Gene Transfer in *Leptolyngbya* sp. strain BL0902, a cyanobacterium suitable for production of biomass and bioproducts. *PLoS ONE* **2012**, *7*, e30901. [CrossRef]
73. Taton, A.; Ma, A.T.; Ota, M.; Golden, S.S.; Golden, J.W. NOT gate genetic circuits to control gene expression in cyanobacteria. *ACS Synth. Biol.* **2017**, *6*, 2175–2182. [CrossRef] [PubMed]
74. Busch, A.W.U.; Montgomery, B.L. The Tryptophan-Rich Sensory Protein (TSPO) is involved in stress-related and light-dependent processes in the cyanobacterium *Fremyella diplosiphon*. *Front. Microbiol.* **2015**, *6*, 1393. [CrossRef]
75. Pattanaik, B.; Montgomery, B.L. FdTonB is involved in the photoregulation of cellular morphology during complementary chromatic adaptation in *Fremyella diplosiphon*. *Microbiology* **2010**, *156*, 731–741. [CrossRef]
76. Morris, J.J.; Kirkegaard, R.; Szul, M.J.; Johnson, Z.I.; Zinser, E.R. Facilitation of robust growth of *Prochlorococcus* colonies and dilute liquid cultures by "helper" heterotrophic bacteria. *Appl. Environ. Microbiol.* **2008**, *74*, 4530–4534. [CrossRef] [PubMed]

77. Brahamsha, B. A genetic manipulation system for oceanic cyanobacteria of the genus *Synechococcus*. *Appl. Environ. Microbiol.* **1996**, *62*, 1747–1751. [PubMed]
78. Ostrowski, M.; Mazard, S.; Tetu, S.G.; Phillippy, K.; Johnson, A.; Palenik, B.; Paulsen, I.T.; Scanlan, D.J. PtrA is required for coordinate regulation of gene expression during phosphate stress in a marine *Synechococcus*. *ISME J.* **2010**, *4*, 908–921. [CrossRef]
79. Yamaoka, T.; Satoh, K.; Katoh, S. Photosynthetic activities of a thermophilic blue-green alga. *Plant Cell Physiol.* **1978**, *19*, 943–954. [CrossRef]
80. Liang, Y.; Kaczmarek, M.B.; Kasprzak, A.K.; Tang, J.; Shah, M.M.R.; Jin, P.; Klepacz-Smółka, A.; Cheng, J.J.; Ledakowicz, S.; Daroch, M. *Thermosynechococcaceae* as a source of thermostable C-phycocyanins: Properties and molecular insights. *Algal Res.* **2018**, *35*, 223–235. [CrossRef]
81. Onai, K.; Tabata, S.; Ishiura, M.; Kaneko, T.; Morishita, M. Natural transformation of the thermophilic cyanobacterium *Thermosynechococcus elongatus* BP-1: A simple and efficient method for gene transfer. *Mol. Genet. Genom.* **2004**, *271*, 50–59. [CrossRef]
82. Liang, Y.; Tang, J.; Luo, Y.; Kaczmarek, M.B.; Li, X.; Daroch, M. *Thermosynechococcus* as a thermophilic photosynthetic microbial cell factory for CO2 utilisation. *Bioresour. Technol.* **2019**, *278*, 255–265. [CrossRef]
83. Stucken, K.; Ilhan, J.; Roettger, M.; Dagan, T.; Martin, W.F. Transformation and Conjugal Transfer of Foreign Genes into the Filamentous Multicellular Cyanobacteria (Subsection V) *Fischerella* and *Chlorogloeopsis*. *Curr. Microbiol.* **2012**, *65*, 552–560. [CrossRef]
84. Billi, D.; Friedmann, E.I.; Helm, R.F.; Potts, M. Gene transfer to the desiccation-tolerant Cyanobacterium *Chroococcidiopsis*. *J. Bacteriol.* **2001**, *183*, 2298–2305. [CrossRef]
85. Nürnberg, D.J.; Morton, J.; Santabarbara, S.; Telfer, A.; Joliot, P.; Antonaru, L.A.; Ruban, A.V.; Cardona, T.; Krausz, E.; Boussac, A.; et al. Photochemistry beyond the red limit in chlorophyll f–containing photosystems. *Science* **2018**, *360*, 1210–1213. [CrossRef]
86. Verseux, C.; Baqué, M.; Lehto, K.; De Vera, J.P.P.; Rothschild, L.J.; Billi, D. Sustainable life support on Mars—The potential roles of cyanobacteria. *Int. J. Astrobiol.* **2016**, *15*, 65–92. [CrossRef]
87. Rippka, R.; Waterbury, J.; Cohen-Bazire, G. A cyanobacterium which lacks thylakoids. *Arch. Microbiol.* **1974**, *100*, 419–436. [CrossRef]
88. Rexroth, S.; Mullineaux, C.W.; Ellinger, D.; Sendtko, E.; Rögner, M.; Koenig, F. The plasma membrane of the cyanobacterium *Gloeobacter violaceus* contains segregated bioenergetic domains. *Plant Cell* **2011**, *23*, 2379–2390. [CrossRef] [PubMed]
89. Araki, M.; Shimada, Y.; Mimuro, M.; Tsuchiya, T. Establishment of the reporter system for a thylakoid-lacking cyanobacterium, *Gloeobacter violaceus* PCC 7421. *FEBS Open Bio* **2013**, *3*, 11–15. [CrossRef] [PubMed]
90. Allen, M.B.; Arnon, D.I. Studies on nitrogen-fixing blue-algae. I. Growth and nitrogen fixation by *Anabaena cylindrica* Lemm. *Plant Physiol.* **1955**, *27*, 366–372. [CrossRef] [PubMed]
91. Bordowitz, J.R.; Montgomery, B.L. Photoregulation of cellular morphology during complementary chromatic adaptation requires sensor-kinase-class protein RcaE in *Fremyella diplosiphon*. *J. Bacteriol.* **2008**, *190*, 4069–4074. [CrossRef] [PubMed]
92. Waterbury, J.B.; Willey, J.M. Isolation and growth of marine planktonic cyanobacteria. *Methods Enzymol.* **1988**, *167*, 100–105.
93. Moore, L.R.; Coe, A.; Zinser, E.R.; Saito, M.A.; Sullivan, M.B.; Lindell, D.; Frois-Moniz, K.; Waterbury, J.; Chisholm, S.W. Culturing the marine cyanobacterium *Prochlorococcus*. *Limnol. Oceanogr. Methods* **2007**, *5*, 353–362. [CrossRef]
94. Naduthodi, M.I.S.; Barbosa, M.J.; van der Oost, J. Progress of CRISPR-Cas Based Genome Editing in Photosynthetic Microbes. *Biotechnol. J.* **2018**, *13*, 1700591. [CrossRef]
95. Khumsupan, P.; Donovan, S.; McCormick, A.J. CRISPR/Cas in *Arabidopsis*: Overcoming challenges to accelerate improvements in crop photosynthetic efficiencies. *Physiol. Plant.* **2019**, *166*, 428–437. [CrossRef]
96. Zhang, Y.T.; Jiang, J.Y.; Shi, T.Q.; Sun, X.M.; Zhao, Q.Y.; Huang, H.; Ren, L.J. Application of the CRISPR/Cas system for genome editing in microalgae. *Appl. Microbiol. Biotechnol.* **2019**, *103*, 3239–3248. [CrossRef] [PubMed]
97. Makarova, K.S.; Wolf, Y.I.; Alkhnbashi, O.S.; Costa, F.; Shah, S.A.; Saunders, S.J.; Barrangou, R.; Brouns, S.J.J.; Charpentier, E.; Haft, D.H.; et al. An updated evolutionary classification of CRISPR-Cas systems. *Nat. Rev. Microbiol.* **2015**, *13*, 722–736. [CrossRef] [PubMed]

98. Koonin, E.V.; Makarova, K.S. Origins and evolution of CRISPR-Cas systems. *Philos. Trans. R. Soc. B Biol. Sci.* **2019**, *374*, 20180087. [CrossRef] [PubMed]
99. Jinek, M.; Chylinski, K.; Fonfara, I.; Hauer, M.; Doudna, J.A.; Charpentier, E. A programmable dual-RNA-guided DNA endonuclease in adaptive bacterial immunity. *Science* **2012**, *337*, 816–821. [CrossRef] [PubMed]
100. Qi, L.S.; Larson, M.H.; Gilbert, L.A.; Doudna, J.A.; Weissman, J.S.; Arkin, A.P.; Lim, W.A. Repurposing CRISPR as an RNA-guided platform for sequence-specific control of gene expression. *Cell* **2013**, *152*, 1173–1183. [CrossRef] [PubMed]
101. Murovec, J.; Pirc, Ž.; Yang, B. New variants of CRISPR RNA-guided genome editing enzymes. *Plant Biotechnol. J.* **2017**, *15*, 917–926. [CrossRef] [PubMed]
102. Abudayyeh, O.O.; Gootenberg, J.S.; Essletzbichler, P.; Han, S.; Joung, J.; Belanto, J.J.; Verdine, V.; Cox, D.B.T.; Kellner, M.J.; Regev, A.; et al. RNA targeting with CRISPR-Cas13. *Nature* **2017**, *550*, 280–284. [CrossRef] [PubMed]
103. Eid, A.; Alshareef, S.; Mahfouz, M.M. CRISPR base editors: Genome editing without double-stranded breaks. *Biochem. J.* **2018**, *475*, 1955–1964. [CrossRef] [PubMed]
104. Abudayyeh, O.O.; Gootenberg, J.S.; Kellner, M.J.; Zhang, F. Nucleic acid detection of plant genes using CRISPR-Cas13. *CRISPR J.* **2019**, *2*, 165–171. [CrossRef] [PubMed]
105. Campa, C.C.; Weisbach, N.R.; Santinha, A.J.; Incarnato, D.; Platt, R.J. Multiplexed genome engineering by Cas12a and CRISPR arrays encoded on single transcripts. *Nat. Methods* **2019**, *6*, 887–893. [CrossRef]
106. Zhang, Y.; Malzahn, A.A.; Sretenovic, S.; Qi, Y. The emerging and uncultivated potential of CRISPR technology in plant science. *Nat. Plants* **2019**, *5*, 778–794. [CrossRef]
107. Swarts, D.C.; van der Oost, J.; Jinek, M. Structural basis for guide RNA processing and seed-dependent DNA targeting by CRISPR-Cas12a. *Mol. Cell* **2017**, *66*, 221–233.e4. [CrossRef] [PubMed]
108. Dong, C.; Fontana, J.; Patel, A.; Carothers, J.M.; Zalatan, J.G. Synthetic CRISPR-Cas gene activators for transcriptional reprogramming in bacteria. *Nat. Commun.* **2018**, *9*, 2489. [CrossRef]
109. Jiang, W.; Bikard, D.; Cox, D.; Zhang, F.; Marraffini, L.A. RNA-guided editing of bacterial genomes using CRISPR-Cas systems. *Nat. Biotechnol.* **2013**, *31*, 233–239. [CrossRef] [PubMed]
110. Vento, J.M.; Crook, N.; Beisel, C.L. Barriers to genome editing with CRISPR in bacteria. *J. Ind. Microbiol. Biotechnol.* **2019**, 1–15. [CrossRef]
111. Li, H.; Shen, C.R.; Huang, C.H.; Sung, L.Y.; Wu, M.Y.; Hu, Y.C. CRISPR-Cas9 for the genome engineering of cyanobacteria and succinate production. *Metab. Eng.* **2016**, *38*, 293–302. [CrossRef] [PubMed]
112. Xiao, Y.; Wang, S.; Rommelfanger, S.; Balassy, A.; Barba-Ostria, C.; Gu, P.; Galazka, J.M.; Zhang, F. Developing a Cas9-based tool to engineer native plasmids in *Synechocystis* sp. PCC 6803. *Biotechnol. Bioeng.* **2018**, *115*, 2305–2314. [CrossRef]
113. Niu, T.C.; Lin, G.M.; Xie, L.R.; Wang, Z.Q.; Xing, W.Y.; Zhang, J.Y.; Zhang, C.C. Expanding the potential of CRISPR-Cpf1-based genome editing technology in the cyanobacterium *Anabaena* PCC 7120. *ACS Synth. Biol.* **2019**, *8*, 170–180. [CrossRef] [PubMed]
114. Ungerer, J.; Pakrasi, H.B. Cpf1 Is A versatile tool for CRISPR genome editing ccross diverse species of cyanobacteria. *Sci. Rep.* **2016**, *6*, 39681. [CrossRef]
115. Zetsche, B.; Gootenberg, J.S.; Abudayyeh, O.O.; Slaymaker, I.M.; Makarova, K.S.; Essletzbichler, P.; Volz, S.E.; Joung, J.; van der Oost, J.; Regev, A.; et al. Cpf1 Is a Single RNA-guided endonuclease of a class 2 CRISPR-Cas system. *Cell* **2015**, *163*, 759–771. [CrossRef]
116. Fonfara, I.; Richter, H.; BratoviÄ, M.; Le Rhun, A.; Charpentier, E. The CRISPR-associated DNA-cleaving enzyme Cpf1 also processes precursor CRISPR RNA. *Nature* **2016**, *532*, 517–521. [CrossRef] [PubMed]
117. Zhang, X.; Wang, J.; Cheng, Q.; Zheng, X.; Zhao, G.; Wang, J. Multiplex gene regulation by CRISPR-ddCpf1. *Cell Discov.* **2017**, *3*, 17018. [CrossRef] [PubMed]
118. Nakahira, Y.; Ogawa, A.; Asano, H.; Oyama, T.; Tozawa, Y. Theophylline-dependent riboswitch as a novel genetic tool for strict regulation of protein expression in cyanobacterium *Synechococcus elongatus* PCC 7942. *Plant Cell Physiol.* **2013**, *54*, 1724–1735. [CrossRef] [PubMed]
119. Ma, A.T.; Schmidt, C.M.; Golden, J.W. Regulation of gene expression in diverse cyanobacterial species by using theophylline-responsive riboswitches. *Appl. Environ. Microbiol.* **2014**, *80*, 6704–6713. [CrossRef] [PubMed]

120. Gao, L.; Cox, D.B.T.; Yan, W.X.; Manteiga, J.C.; Schneider, M.W.; Yamano, T.; Nishimasu, H.; Nureki, O.; Crosetto, N.; Zhang, F. Engineered Cpf1 variants with altered PAM specificities. *Nat. Biotechnol.* **2017**, *35*, 789–792. [CrossRef] [PubMed]
121. Kleinstiver, B.P.; Prew, M.S.; Tsai, S.Q.; Topkar, V.V.; Nguyen, N.T.; Zheng, Z.; Gonzales, A.P.W.; Li, Z.; Peterson, R.T.; Yeh, J.R.J.; et al. Engineered CRISPR-Cas9 nucleases with altered PAM specificities. *Nature* **2015**, *523*, 481–485. [CrossRef] [PubMed]
122. Liu, J.J.; Orlova, N.; Oakes, B.L.; Ma, E.; Spinner, H.B.; Baney, K.L.M.; Chuck, J.; Tan, D.; Knott, G.J.; Harrington, L.B.; et al. CasX enzymes comprise a distinct family of RNA-guided genome editors. *Nature* **2019**, *566*, 218–223. [CrossRef]
123. Tsujimoto, R.; Kotani, H.; Yokomizo, K.; Yamakawa, H.; Nonaka, A.; Fujita, Y. Functional expression of an oxygen-labile nitrogenase in an oxygenic photosynthetic organism. *Sci. Rep.* **2018**, *8*, 7380. [CrossRef]
124. Merrick, C.A.; Zhao, J.; Rosser, S.J. Serine integrases: Advancing synthetic biology. *ACS Synth. Biol.* **2018**, *7*, 299–310. [CrossRef]
125. Colloms, S.D.; Merrick, C.A.; Olorunniji, F.J.; Stark, W.M.; Smith, M.C.M.; Osbourn, A.; Keasling, J.D.; Rosser, S.J. Rapid metabolic pathway assembly and modification using serine integrase site-specific recombination. *Nucleic Acids Res.* **2014**, *42*, e23. [CrossRef]
126. Snoeck, N.; De Mol, M.L.; Van Herpe, D.; Goormans, A.; Maryns, I.; Coussement, P.; Peters, G.; Beauprez, J.; De Maeseneire, S.L.; Soetaert, W. Serine integrase recombinational engineering (SIRE): A versatile toolbox for genome editing. *Biotechnol. Bioeng.* **2019**, *116*, 364–374. [CrossRef] [PubMed]
127. Guiziou, S.; Mayonove, P.; Bonnet, J. Hierarchical composition of reliable recombinase logic devices. *Nat. Commun.* **2019**, *10*, 456. [CrossRef] [PubMed]
128. Huang, H.; Chai, C.; Yang, S.; Jiang, W.; Gu, Y. Phage serine integrase-mediated genome engineering for efficient expression of chemical biosynthetic pathway in gas-fermenting *Clostridium ljungdahlii*. *Metab. Eng.* **2019**, *52*, 293–302. [CrossRef] [PubMed]
129. Andreas, S.; Schwenk, F.; Küter-Luks, B.; Faust, N.; Kühn, R. Enhanced efficiency through nuclear localization signal fusion on phage phiC31-integrase: Activity comparison with Cre and FLPe recombinase in mammalian cells. *Nucleic Acids Res.* **2002**, *30*, 2299–2306. [CrossRef] [PubMed]
130. Groth, A.C.; Fish, M.; Nusse, R.; Calos, M.P. Construction of transgenic *Drosophila* by using the site-specific integrase from phage φC31. *Genetics* **2004**, *166*, 1775–1782. [CrossRef] [PubMed]
131. Na, D.; Yoo, S.M.; Chung, H.; Park, H.; Park, J.H.; Lee, S.Y. Metabolic engineering of *Escherichia coli* using synthetic small regulatory RNAs. *Nat. Biotechnol.* **2013**, *31*, 170–174. [CrossRef] [PubMed]
132. Sun, T.; Li, S.; Song, X.; Pei, G.; Diao, J.; Cui, J.; Shi, M.; Chen, L.; Zhang, W. Re-direction of carbon flux to key precursor malonyl-CoA via artificial small RNAs in photosynthetic *Synechocystis* sp. PCC 6803. *Biotechnol. Biofuels* **2018**, *11*, 26. [CrossRef]
133. Higo, A.; Isu, A.; Fukaya, Y.; Ehira, S.; Hisabori, T. Application of CRISPR interference for metabolic engineering of the heterocyst-forming multicellular cyanobacterium *Anabaena* sp. PCC 7120. *Plant Cell Physiol.* **2018**, *59*, 119–127. [CrossRef]
134. Zess, E.K.; Begemann, M.B.; Pfleger, B.F. Construction of new synthetic biology tools for the control of gene expression in the cyanobacterium *Synechococcus* sp. strain PCC 7002. *Biotechnol. Bioeng.* **2016**, *113*, 424–432. [CrossRef]
135. Gordon, G.C.; Korosh, T.C.; Cameron, J.C.; Markley, A.L.; Begemann, M.B.; Pfleger, B.F. CRISPR interference as a titratable, trans-acting regulatory tool for metabolic engineering in the cyanobacterium *Synechococcus* sp. strain PCC 7002. *Metab. Eng.* **2016**, *38*, 170–179. [CrossRef]
136. Huang, C.H.; Shen, C.R.; Li, H.; Sung, L.Y.; Wu, M.Y.; Hu, Y.C. CRISPR interference (CRISPRi) for gene regulation and succinate production in cyanobacterium *S. elongatus* PCC 7942. *Microb. Cell Fact.* **2016**, *15*, 196. [CrossRef] [PubMed]
137. Kaczmarzyk, D.; Cengic, I.; Yao, L.; Hudson, E.P. Diversion of the long-chain acyl-ACP pool in *Synechocystis* to fatty alcohols through CRISPRi repression of the essential phosphate acyltransferase PlsX. *Metab. Eng.* **2018**, *45*, 59–66. [CrossRef] [PubMed]
138. Shabestary, K.; Anfelt, J.; Ljungqvist, E.; Jahn, M.; Yao, L.; Hudson, E.P. Targeted repression of essential genes to arrest growth and increase carbon partitioning and biofuel titers in cyanobacteria. *ACS Synth. Biol.* **2018**, *7*, 1669–1675. [CrossRef] [PubMed]

139. Cho, S.; Choe, D.; Lee, E.; Kim, S.C.; Palsson, B.; Cho, B.K. High-Level dCas9 Expression induces abnormal cell morphology in *Escherichia coli*. *ACS Synth. Biol.* **2018**, *7*, 1085–1094. [CrossRef] [PubMed]
140. Yao, L.; Cengic, I.; Anfelt, J.; Hudson, E.P. Multiple Gene Repression in Cyanobacteria Using CRISPRi. *ACS Synth. Biol.* **2016**, *5*, 207–212. [CrossRef]
141. Miao, C.; Zhao, H.; Qian, L.; Lou, C. Systematically investigating the key features of the DNase deactivated Cpf1 for tunable transcription regulation in prokaryotic cells. *Synth. Syst. Biotechnol.* **2019**, *4*, 1–9. [CrossRef] [PubMed]
142. Abudayyeh, O.O.; Gootenberg, J.S.; Konermann, S.; Joung, J.; Slaymaker, I.M.; Cox, D.B.T.; Shmakov, S.; Makarova, K.S.; Semenova, E.; Minakhin, L.; et al. C2c2 is a single-component programmable RNA-guided RNA-targeting CRISPR effector. *Science* **2016**, *353*, aaf5573. [CrossRef]
143. Cox, D.B.T.; Gootenberg, J.S.; Abudayyeh, O.O.; Franklin, B.; Kellner, M.J.; Joung, J.; Zhang, F. RNA editing with CRISPR-Cas13. *Science* **2017**, *358*, 1019–1027. [CrossRef]
144. Martella, A.; Firth, M.A.; Taylor, B.J.M.; Goeppert, A.U.; Cuomo, E.M.; Roth, R.G.; Dickson, A.J.; Fisher, D.I. Systematic evaluation of CRISPRa and CRISPRi modalities enables development of a multiplexed, orthogonal gene activation and repression system. *ACS Synth. Biol.* **2019**, *8*, 1998–2006. [CrossRef]
145. Fontana, J.; Dong, C.; Kiattisewee, C.; Chavali, V.P.; Tickman, B.I.; Carothers, J.M.; Zalatan, J.G. Effective CRISPRa-mediated control of gene expression in bacteria must overcome strict target site requirements. *bioRxiv* **2019**, 770891. [CrossRef]
146. Bradley, R.W.; Buck, M.; Wang, B. Tools and principles for microbial gene circuit engineering. *J. Mol. Biol.* **2016**, *428*, 862–888. [CrossRef] [PubMed]
147. Nielsen, A.A.K.; Der, B.S.; Shin, J.; Vaidyanathan, P.; Paralanov, V.; Strychalski, E.A.; Ross, D.; Densmore, D.; Voigt, C.A. Genetic circuit design automation. *Science* **2016**, *352*, aac7341. [CrossRef] [PubMed]
148. Lalwani, M.A.; Zhao, E.M.; Avalos, J.L. Current and future modalities of dynamic control in metabolic engineering. *Curr. Opin. Biotechnol.* **2018**, *52*, 56–65. [CrossRef] [PubMed]
149. Buck, M.; Cannon, W. Specific binding of the transcription factor sigma-54 to promoter DNA. *Nature* **1992**, *358*, 19–21. [CrossRef] [PubMed]
150. Feklístov, A.; Sharon, B.D.; Darst, S.A.; Gross, C.A. Bacterial sigma factors: A historical, structural, and genomic perspective. *Annu. Rev. Microbiol.* **2014**, *68*, 357–376. [CrossRef] [PubMed]
151. Davis, M.C.; Kesthely, C.A.; Franklin, E.A.; MacLellan, S.R. The essential activities of the bacterial sigma factor. *Can. J. Microbiol.* **2017**, *63*, 89–99. [CrossRef]
152. Stensjö, K.; Vavitsas, K.; Tyystjärvi, T. Harnessing transcription for bioproduction in cyanobacteria. *Physiol. Plant.* **2018**, *162*, 148–155. [CrossRef] [PubMed]
153. Helmann, J.D. Where to begin? Sigma factors and the selectivity of transcription initiation in bacteria. *Mol. Microbiol.* **2019**, *112*, 335–347. [CrossRef]
154. Imamura, S.; Asayama, M. Sigma factors for cyanobacterial transcription. *Gene Regul. Syst. Biol.* **2009**, *3*, 65–87. [CrossRef]
155. Wells, K.N.; Videau, P.; Nelson, D.; Eiting, J.E.; Philmus, B. The influence of sigma factors and ribosomal recognition elements on heterologous expression of cyanobacterial gene clusters in *Escherichia coli*. *FEMS Microbiol. Lett.* **2018**, *365*, fny164. [CrossRef]
156. Bervoets, I.; Van Brempt, M.; Van Nerom, K.; Van Hove, B.; Maertens, J.; De Mey, M.; Charlier, D. A sigma factor toolbox for orthogonal gene expression in *Escherichia coli*. *Nucleic Acids Res.* **2018**, *46*, 2133–2144. [CrossRef] [PubMed]
157. Tripathi, L.; Zhang, Y.; Lin, Z. Bacterial sigma factors as targets for engineered or synthetic transcriptional control. *Front. Bioeng. Biotechnol.* **2014**, *2*, 33. [CrossRef]
158. Iyer, L.M.; Koonin, E.V.; Aravind, L. Evolution of bacterial RNA polymerase: Implications for large-scale bacterial phylogeny, domain accretion, and horizontal gene transfer. *Gene* **2004**, *335*, 73–88. [CrossRef] [PubMed]
159. Zhao, K.; Liu, M.; Burgess, R.R. Promoter and regulon analysis of nitrogen assimilation factor, σ54, reveal alternative strategy for *E. coli* MG1655 flagellar biosynthesis. *Nucleic Acids Res.* **2010**, *38*, 1273–1283. [CrossRef]
160. Liu, Y.; Wan, X.; Wang, B. Engineered CRISPRa enables programmable eukaryote-like gene activation in bacteria. *Nat. Commun.* **2019**, *10*, 3693. [CrossRef]
161. Meyer, A.J.; Ellefson, J.W.; Ellington, A.D. Directed evolution of a panel of orthogonal T7 RNA polymerase variants for in vivo or in vitro synthetic circuitry. *ACS Synth. Biol.* **2015**, *4*, 1070–1076. [CrossRef] [PubMed]

162. Hussey, B.J.; McMillen, D.R. Programmable T7-based synthetic transcription factors. *Nucleic Acids Res.* **2018**, *46*, 9842–9854. [CrossRef]
163. Temme, K.; Hill, R.; Segall-Shapiro, T.H.; Moser, F.; Voigt, C.A. Modular control of multiple pathways using engineered orthogonal T7 polymerases. *Nucleic Acids Res.* **2012**, *40*, 8773–8781. [CrossRef]
164. Kim, W.J.; Lee, S.M.; Um, Y.; Sim, S.J.; Woo, H.M. Development of SyneBrick vectors as a synthetic biology platform for gene expression in *Synechococcus elongatus* PCC 7942. *Front. Plant Sci.* **2017**, *8*, 293. [CrossRef]
165. Jin, H.; Lindblad, P.; Bhaya, D. Building an inducible T7 RNA polymerase/T7 promoter circuit in *Synechocystis* sp. PCC6803. *ACS Synth. Biol.* **2019**, *8*, 655–660. [CrossRef]
166. Pu, J.; Zinkus-Boltz, J.; Dickinson, B.C. Evolution of a split RNA polymerase as a versatile biosensor platform. *Nat. Chem. Biol.* **2017**, *13*, 432–438. [CrossRef] [PubMed]
167. Komura, R.; Aoki, W.; Motone, K.; Satomura, A.; Ueda, M. High-throughput evaluation of T7 promoter variants using biased randomization and DNA barcoding. *PLoS ONE* **2018**, *13*, e0196905. [CrossRef] [PubMed]
168. Han, T.; Chen, Q.; Liu, H. Engineered photoactivatable genetic switches based on the bacterium phage T7 RNA Polymerase. *ACS Synth. Biol.* **2017**, *6*, 357–366. [CrossRef] [PubMed]
169. Meyer, A.J.; Segall-Shapiro, T.H.; Glassey, E.; Zhang, J.; Voigt, C.A. *Escherichia coli* "Marionette" strains with 12 highly optimized small-molecule sensors. *Nat. Chem. Biol.* **2019**, *15*, 196–204. [CrossRef] [PubMed]
170. Miyazaki, K. Molecular engineering of the salicylate-inducible transcription factor Sal7AR for orthogonal and high gene expression in *Escherichia coli*. *PLoS ONE* **2018**, *13*, e0194090. [CrossRef]
171. Kelly, C.L.; Liu, Z.; Yoshihara, A.; Jenkinson, S.F.; Wormald, M.R.; Otero, J.; Estévez, A.; Kato, A.; Marqvorsen, M.H.S.; Fleet, G.W.J.; et al. Synthetic chemical inducers and genetic decoupling enable orthogonal control of the rhaBAD Promoter. *ACS Synth. Biol.* **2016**, *5*, 1136–1145. [CrossRef] [PubMed]
172. Huang, H.H.; Lindblad, P. Wide-dynamic-range promoters engineered for cyanobacteria. *J. Biol. Eng.* **2013**, *7*, 10. [CrossRef]
173. Albers, S.C.; Gallegos, V.A.; Peebles, C.A.M. Engineering of genetic control tools in *Synechocystis* sp. PCC 6803 using rational design techniques. *J. Biotechnol.* **2015**, *216*, 36–46. [CrossRef]
174. Cao, Y.Q.; Li, Q.; Xia, P.F.; Wei, L.J.; Guo, N.; Li, J.W.; Wang, S.G. AraBAD based toolkit for gene expression and metabolic robustness improvement in *Synechococcus elongatus*. *Sci. Rep.* **2017**, *7*, 18059. [CrossRef]
175. Huang, H.H.; Camsund, D.; Lindblad, P.; Heidorn, T. Design and characterization of molecular tools for a Synthetic Biology approach towards developing cyanobacterial biotechnology. *Nucleic Acids Res.* **2010**, *38*, 2577–2593. [CrossRef]
176. Camsund, D.; Heidorn, T.; Lindblad, P. Design and analysis of LacI-repressed promoters and DNA-looping in a cyanobacterium. *J. Biol. Eng.* **2014**, *8*, 4. [CrossRef] [PubMed]
177. Blasi, B.; Peca, L.; Vass, I.; Kós, P.B. Characterization of stress responses of heavy metal and metalloid inducible promoters in *Synechocystis* PCC6803. *J. Microbiol. Biotechnol.* **2012**, *22*, 166–169. [CrossRef] [PubMed]
178. Pérez, A.A.; Gajewski, J.P.; Ferlez, B.H.; Ludwig, M.; Baker, C.S.; Golbeck, J.H.; Bryant, D.A. Zn^{2+} -inducible expression platform for *Synechococcus* sp. strain PCC 7002 based on the smtA promoter/operator and smtB repressor. *Appl. Environ. Microbiol.* **2017**, *83*, 1–14. [CrossRef] [PubMed]
179. Englund, E.; Liang, F.; Lindberg, P. Evaluation of promoters and ribosome binding sites for biotechnological applications in the unicellular cyanobacterium *Synechocystis* sp. PCC 6803. *Sci. Rep.* **2016**, *6*, 36640. [CrossRef] [PubMed]
180. Rippka, R.; Deruelles, J.; Waterbury, J.B. Generic assignments, strain histories and properties of pure cultures of cyanobacteria. *J. Gen. Microbiol.* **1979**, *111*, 1–61. [CrossRef]
181. Gao, C.; Hou, J.; Xu, P.; Guo, L.; Chen, X.; Hu, G.; Ye, C.; Edwards, H.; Chen, J.; Chen, W.; et al. Programmable biomolecular switches for rewiring flux in *Escherichia coli*. *Nat. Commun.* **2019**, *10*, 3751. [CrossRef]
182. Polstein, L.R.; Gersbach, C.A. A light-inducible CRISPR-Cas9 system for control of endogenous gene activation. *Nat. Chem. Biol.* **2015**, *11*, 198–200. [CrossRef]
183. Lee, D.; Hyun, J.H.; Jung, K.; Hannan, P.; Kwon, H.B. A calcium- and light-gated switch to induce gene expression in activated neurons. *Nat. Biotechnol.* **2017**, *35*, 858–863. [CrossRef]
184. Mansouri, M.; Strittmatter, T.; Fussenegger, M. Light-controlled mammalian cells and their therapeutic applications in synthetic biology. *Adv. Sci.* **2019**, *6*, 1800952. [CrossRef]
185. Tandar, S.T.; Senoo, S.; Toya, Y.; Shimizu, H. Optogenetic switch for controlling the central metabolic flux of *Escherichia coli*. *Metab. Eng.* **2019**, *55*, 68–75. [CrossRef]

186. Zhao, E.M.; Suek, N.; Wilson, M.Z.; Dine, E.; Pannucci, N.L.; Gitai, Z.; Avalos, J.L.; Toettcher, J.E. Light-based control of metabolic flux through assembly of synthetic organelles. *Nat. Chem. Biol.* **2019**, *15*, 589–597. [CrossRef] [PubMed]
187. Jayaraman, P.; Devarajan, K.; Chua, T.K.; Zhang, H.; Gunawan, E.; Poh, C.L. Blue light-mediated transcriptional activation and repression of gene expression in bacteria. *Nucleic Acids Res.* **2016**, *44*, 6994–7005. [CrossRef] [PubMed]
188. Fernandez-Rodriguez, J.; Moser, F.; Song, M.; Voigt, C.A. Engineering RGB color vision into *Escherichia coli*. *Nat. Chem. Biol.* **2017**, *13*, 706–708. [CrossRef] [PubMed]
189. Rost, B.R.; Schneider-Warme, F.; Schmitz, D.; Hegemann, P. Optogenetic tools for subcellular applications in neuroscience. *Neuron* **2017**, *96*, 572–603. [CrossRef] [PubMed]
190. Yu, Q.; Wang, Y.; Zhao, S.; Ren, Y. Photocontrolled reversible self-assembly of dodecamer nitrilase. *Bioresour. Bioprocess.* **2017**, *4*, 36. [CrossRef] [PubMed]
191. Hirose, Y.; Shimada, T.; Narikawa, R.; Katayama, M.; Ikeuchi, M. Cyanobacteriochrome CcaS is the green light receptor that induces the expression of phycobilisome linker protein. *Proc. Natl. Acad. Sci. USA* **2008**, *105*, 9528–9533. [CrossRef] [PubMed]
192. Tilbrook, K.; Arongaus, A.B.; Binkert, M.; Heijde, M.; Yin, R.; Ulm, R. The UVR8 UV-B Photoreceptor: Perception, signaling and response. *Arab. Book* **2013**, *11*, e0164. [CrossRef] [PubMed]
193. Ramakrishnan, P.; Tabor, J.J. Repurposing synechocystis PCC6803 UirS-UirR as a UV-violet/green photoreversible transcriptional regulatory tool in *E. coli*. *ACS Synth. Biol.* **2016**, *5*, 733–740. [CrossRef] [PubMed]
194. Möglich, A.; Ayers, R.A.; Moffat, K. Design and signaling mechanism of light-regulated histidine kinases. *J. Mol. Biol.* **2009**, *385*, 1433–1444. [CrossRef]
195. Jin, X.; Riedel-Kruse, I.H. Biofilm Lithography enables high-resolution cell patterning via optogenetic adhesin expression. *Proc. Natl. Acad. Sci. USA* **2018**, *115*, 3698–3703. [CrossRef]
196. Abe, K.; Miyake, K.; Nakamura, M.; Kojima, K.; Ferri, S.; Ikebukuro, K.; Sode, K. Engineering of a green-light inducible gene expression system in *Synechocystis* sp. PCC6803. *Microb. Biotechnol.* **2014**, *7*, 177–183. [CrossRef] [PubMed]
197. Miyake, K.; Abe, K.; Ferri, S.; Nakajima, M.; Nakamura, M.; Yoshida, W.; Kojima, K.; Ikebukuro, K.; Sode, K. A green-light inducible lytic system for cyanobacterial cells. *Biotechnol. Biofuels* **2014**, *7*, 56. [CrossRef] [PubMed]
198. Ong, N.T.; Tabor, J.J. A miniaturized *Escherichia coli* green light sensor with high dynamic range. *ChemBioChem* **2018**, *19*, 1255–1258. [CrossRef] [PubMed]
199. Tabor, J.J.; Levskaya, A.; Voigt, C.A. Multichromatic control of gene expression in *Escherichia coli*. *J. Mol. Biol.* **2011**, *405*, 315–324. [CrossRef] [PubMed]
200. Ong, N.T.; Olson, E.J.; Tabor, J.J. Engineering an *E. coli* near-infrared light sensor. *ACS Synth. Biol.* **2018**, *7*, 240–248. [CrossRef] [PubMed]
201. Takakado, A.; Nakasone, Y.; Terazima, M. Sequential DNA binding and dimerization processes of the photosensory protein EL222. *Biochemistry* **2018**, *57*, 1603–1610. [CrossRef] [PubMed]
202. Xu, X.; Du, Z.; Liu, R.; Li, T.; Zhao, Y.; Chen, X.; Yang, Y. A single-component optogenetic system allows stringent switch of gene expression in yeast cells. *ACS Synth. Biol.* **2018**, *7*, 2045–2053. [CrossRef] [PubMed]
203. Papanatsiou, M.; Petersen, J.; Henderson, L.; Wang, Y.; Christie, J.M.; Blatt, M.R. Optogenetic manipulation of stomatal kinetics improves carbon assimilation, water use, and growth. *Science* **2019**, *363*, 1456–1459. [CrossRef]
204. Baumschlager, A.; Aoki, S.K.; Khammash, M. Dynamic blue light-inducible T7 RNA Polymerases (Opto-T7RNAPs) for precise spatiotemporal gene expression control. *ACS Synth. Biol.* **2017**, *6*, 2157–2167. [CrossRef] [PubMed]
205. Song, J.Y.; Cho, H.S.; Cho, J.I.; Jeon, J.S.; Lagarias, J.C.; Park, Y.I. Near-UV cyanobacteriochrome signaling system elicits negative phototaxis in the cyanobacterium Synechocystis sp. PCC 6803. *Proc. Natl. Acad. Sci. USA* **2011**, *108*, 10780–10785. [CrossRef]
206. Badary, A.; Abe, K.; Ferri, S.; Kojima, K.; Sode, K. The Development and characterization of an exogenous green-light-regulated gene expression system in marine cyanobacteria. *Mar. Biotechnol.* **2015**, *17*, 245–251. [CrossRef] [PubMed]

207. Wiltbank, L.B.; Kehoe, D.M. Diverse light responses of cyanobacteria mediated by phytochrome superfamily photoreceptors. *Nat. Rev. Microbiol.* **2019**, *17*, 37–50. [CrossRef] [PubMed]
208. Luimstra, V.M.; Schuurmans, J.M.; Verschoor, A.M.; Hellingwerf, K.J.; Huisman, J.; Matthijs, H.C.P. Blue light reduces photosynthetic efficiency of cyanobacteria through an imbalance between photosystems I and II. *Photosynth. Res.* **2018**, *138*, 177–189. [CrossRef] [PubMed]
209. Wan, X.; Volpetti, F.; Petrova, E.; French, C.; Maerkl, S.J.; Wang, B. Cascaded amplifying circuits enable ultrasensitive cellular sensors for toxic metals. *Nat. Chem. Biol.* **2019**, *15*, 540–548. [CrossRef] [PubMed]
210. Wang, B.; Buck, M. Rapid engineering of versatile molecular logic gates using heterologous genetic transcriptional modules. *Chem. Commun.* **2014**, *50*, 11642–11644. [CrossRef] [PubMed]
211. Brophy, J.A.N.; Voigt, C.A. Principles of genetic circuit design. *Nat. Methods* **2014**, *11*, 508–520. [CrossRef] [PubMed]
212. Xiang, Y.; Dalchau, N.; Wang, B. Scaling up genetic circuit design for cellular computing: Advances and prospects. *Nat. Comput.* **2018**, *17*, 833–853. [CrossRef]
213. Xia, P.; Ling, H.; Foo, J.L.; Chang, M.W. Synthetic biology toolkits for metabolic engineering of cyanobacteria. *Biotechnol. J.* **2019**, *14*, 1800496. [CrossRef]
214. Immethun, C.M.; Ng, K.M.; Delorenzo, D.M.; Waldron-Feinstein, B.; Lee, Y.C.; Moon, T.S. Oxygen-responsive genetic circuits constructed in *Synechocystis* sp. PCC 6803. *Biotechnol. Bioeng.* **2016**, *113*, 433–442. [CrossRef]
215. Wang, B.; Barahona, M.; Buck, M. A modular cell-based biosensor using engineered genetic logic circuits to detect and integrate multiple environmental signals. *Biosens. Bioelectron.* **2013**, *40*, 368–376. [CrossRef]
216. Noren, C.J.; Wang, J.; Perler, F.B. Dissecting the chemistry of protein splicing and its applications. *Angew. Chem. Int. Ed.* **2000**, *39*, 450–466. [CrossRef]
217. Caspi, J.; Amitai, G.; Belenkiy, O.; Pietrokovski, S. Distribution of split DnaE inteins in cyanobacteria. *Mol. Microbiol.* **2003**, *50*, 1569–1577. [CrossRef] [PubMed]
218. Perler, F.B. InBase: The intein database. *Nucleic Acids Res.* **2002**, *30*, 383–384. [CrossRef] [PubMed]
219. Novikova, O.; Topilina, N.; Belfort, M. Enigmatic distribution, evolution, and function of inteins. *J. Biol. Chem.* **2014**, *289*, 14490–14497. [CrossRef] [PubMed]
220. Saleh, L.; Perler, F.B. Protein splicing in cis and in trans. *Chem. Rec.* **2006**, *6*, 183–193. [CrossRef] [PubMed]
221. Lockless, S.W.; Muir, T.W. Traceless protein splicing utilizing evolved split inteins. *Proc. Natl. Acad. Sci. USA* **2009**, *106*, 10999–11004. [CrossRef] [PubMed]
222. Schaerli, Y.; Gili, M.; Isalan, M. A split intein T7 RNA polymerase for transcriptional AND-logic. *Nucleic Acids Res.* **2014**, *42*, 12322–12328. [CrossRef]
223. Zeng, Y.; Jones, A.M.; Thomas, E.E.; Nassif, B.; Silberg, J.J.; Segatori, L. A split transcriptional repressor that links protein solubility to an orthogonal genetic circuit. *ACS Synth. Biol.* **2018**, *7*, 2126–2138. [CrossRef]
224. Carvajal-Vallejos, P.; Pallissé, R.; Mootz, H.D.; Schmidt, S.R. Unprecedented rates and efficiencies revealed for new natural split inteins from metagenomic sources. *J. Biol. Chem.* **2012**, *287*, 28686–28696. [CrossRef]
225. Huang, H.H.; Seeger, C.; Helena Danielson, U.; Lindblad, P. Analysis of the leakage of gene repression by an artificial TetR-regulated promoter in cyanobacteria. *BMC Res. Notes* **2015**, *8*, 459. [CrossRef]
226. Goodall, E.C.A.; Robinson, A.; Johnston, I.G.; Jabbari, S.; Turner, K.A.; Cunningham, A.F.; Lund, P.A.; Cole, J.A.; Henderson, I.R. The Essential Genome of *Escherichia coli* K-12. *MBio* **2018**, *9*, e02096-17. [CrossRef] [PubMed]
227. Lee, S.Y.; Kim, H.U. Systems strategies for developing industrial microbial strains. *Nat. Biotechnol.* **2015**, *33*, 1061–1072. [CrossRef] [PubMed]
228. Gu, C.; Kim, G.B.; Kim, W.J.; Kim, H.U.; Lee, S.Y. Current status and applications of genome-scale metabolic models. *Genome Biol.* **2019**, *20*, 1–18. [CrossRef] [PubMed]
229. Baroukh, C.; Muñoz-Tamayo, R.; Bernard, O.; Steyer, J.P. Mathematical modeling of unicellular microalgae and cyanobacteria metabolism for biofuel production. *Curr. Opin. Biotechnol.* **2015**, *33*, 198–205. [CrossRef] [PubMed]
230. Joshi, C.J.; Peebles, C.A.M.; Prasad, A. Modeling and analysis of flux distribution and bioproduct formation in *Synechocystis* sp. PCC 6803 using a new genome-scale metabolic reconstruction. *Algal Res.* **2017**, *27*, 295–310. [CrossRef]
231. Triana, J.; Montagud, A.; Siurana, M.; Fuente, D.; Urchueguía, A.; Gamermann, D.; Torres, J.; Tena, J.; de Córdoba, P.; Urchueguía, J. Generation and evaluation of a genome-scale metabolic network model of *Synechococcus elongatus* PCC7942. *Metabolites* **2014**, *4*, 680–698. [CrossRef] [PubMed]

232. Broddrick, J.T.; Welkie, D.G.; Jallet, D.; Golden, S.S.; Peers, G.; Palsson, B.O. Predicting the metabolic capabilities of *Synechococcus elongatus* PCC 7942 adapted to different light regimes. *Metab. Eng.* **2019**, *52*, 42–56. [CrossRef]
233. Mueller, T.J.; Ungerer, J.L.; Pakrasi, H.B.; Maranas, C.D. Identifying the metabolic differences of a fast-growth phenotype in *Synechococcus* UTEX 2973. *Sci. Rep.* **2017**, *7*, 41569. [CrossRef]
234. Vu, T.T.; Hill, E.A.; Kucek, L.A.; Konopka, A.E.; Beliaev, A.S.; Reed, J.L. Computational evaluation of *Synechococcus* sp. PCC 7002 metabolism for chemical production. *Biotechnol. J.* **2013**, *8*, 619–630. [CrossRef]
235. Qian, X.; Kim, M.K.; Kumaraswamy, G.K.; Agarwal, A.; Lun, D.S.; Dismukes, G.C. Flux balance analysis of photoautotrophic metabolism: Uncovering new biological details of subsystems involved in cyanobacterial photosynthesis. *Biochim. Biophys. Acta Bioenerg.* **2017**, *1858*, 276–287. [CrossRef]
236. Malatinszky, D.; Steuer, R.; Jones, P.R. A comprehensively curated genome-scale two-cell model for the heterocystous cyanobacterium *Anabaena* sp. PCC 7120. *Plant Physiol.* **2017**, *173*, 509–523. [CrossRef] [PubMed]
237. Nogales, J.; Gudmundsson, S.; Knight, E.M.; Palsson, B.O.; Thiele, I. Detailing the optimality of photosynthesis in cyanobacteria through systems biology analysis. *Proc. Natl. Acad. Sci. USA* **2012**, *109*, 2678–2683. [CrossRef] [PubMed]
238. Knoop, H.; Gründel, M.; Zilliges, Y.; Lehmann, R.; Hoffmann, S.; Lockau, W.; Steuer, R. Flux balance analysis of cyanobacterial metabolism: The metabolic network of *Synechocystis* sp. PCC 6803. *PLoS Comput. Biol.* **2013**, *9*, e1003081. [CrossRef] [PubMed]
239. Rubin, B.E.; Wetmore, K.M.; Price, M.N.; Diamond, S.; Shultzaberger, R.K.; Lowe, L.C.; Curtin, G.; Arkin, A.P.; Deutschbauer, A.; Golden, S.S. The essential gene set of a photosynthetic organism. *Proc. Natl. Acad. Sci. USA* **2015**, *112*, E6634–E6643. [CrossRef] [PubMed]
240. Abernathy, M.H.; Yu, J.; Ma, F.; Liberton, M.; Ungerer, J.; Hollinshead, W.D.; Gopalakrishnan, S.; He, L.; Maranas, C.D.; Pakrasi, H.B.; et al. Deciphering cyanobacterial phenotypes for fast photoautotrophic growth via isotopically nonstationary metabolic flux analysis. *Biotechnol. Biofuels* **2017**, *10*, 273. [CrossRef] [PubMed]
241. Shabestary, K.; Hudson, E.P. Computational metabolic engineering strategies for growth-coupled biofuel production by *Synechocystis*. *Metab. Eng. Commun.* **2016**, *3*, 216–226. [CrossRef] [PubMed]
242. Ranganathan, S.; Suthers, P.F.; Maranas, C.D. OptForce: An optimization procedure for identifying All genetic manipulations leading to targeted overproductions. *PLoS Comput. Biol.* **2010**, *6*, e1000744. [CrossRef] [PubMed]
243. Rocha, I.; Maia, P.; Evangelista, P.; Vilaça, P.; Soares, S.; Pinto, J.P.; Nielsen, J.; Patil, K.R.; Ferreira, E.C.; Rocha, M. OptFlux: An open-source software platform for in silico metabolic engineering. *BMC Syst. Biol.* **2010**, *4*, 45. [CrossRef] [PubMed]
244. Lin, P.C.; Saha, R.; Zhang, F.; Pakrasi, H.B. Metabolic engineering of the pentose phosphate pathway for enhanced limonene production in the cyanobacterium *Synechocystis* sp. PCC 6803. *Sci. Rep.* **2017**, *7*, 17503. [CrossRef]
245. Lv, Q.; Ma, W.; Liu, H.; Li, J.; Wang, H.; Lu, F.; Zhao, C.; Shi, T. Genome-wide protein-protein interactions and protein function exploration in cyanobacteria. *Sci. Rep.* **2015**, *5*, 15519. [CrossRef]
246. Vivek-Ananth, R.P.; Samal, A. Advances in the integration of transcriptional regulatory information into genome-scale metabolic models. *Biosystems* **2016**, *147*, 1–10. [CrossRef] [PubMed]
247. Zavřel, T.; Očenášová, P.; Červený, J. Phenotypic characterization of *Synechocystis* sp. PCC 6803 substrains reveals differences in sensitivity to abiotic stress. *PLoS ONE* **2017**, *12*, e0189130. [CrossRef] [PubMed]
248. Soppa, J.; Ludt, K.; Zerulla, K. The ploidy level of *Synechocystis* sp. PCC 6803 is highly variable and is influenced by growth phase and by chemical and physical external parameters. *Microbiology* **2016**, *162*, 730–739.
249. Morris, J.N.; Eaton-Rye, J.J.; Summerfield, T.C. Phenotypic variation in wild-type substrains of the model cyanobacterium *Synechocystis* sp. PCC 6803. *N. Z. J. Bot.* **2017**, *55*, 25–35. [CrossRef]
250. Li, X.; Patena, W.; Fauser, F.; Jinkerson, R.E.; Saroussi, S.; Meyer, M.T.; Ivanova, N.; Robertson, J.M.; Yue, R.; Zhang, R.; et al. A genome-wide algal mutant library and functional screen identifies genes required for eukaryotic photosynthesis. *Nat. Genet.* **2019**, *51*, 627–635. [CrossRef] [PubMed]
251. Alonso, J.M.; Stepanova, A.N.; Leisse, T.J.; Kim, C.J.; Chen, H.; Shinn, P.; Stevenson, D.K.; Zimmerman, J.; Barajas, P.; Cheuk, R.; et al. Genome-wide insertional mutagenesis of *Arabidopsis thaliana*. *Science* **2003**, *301*, 653–657. [CrossRef] [PubMed]

252. Baba, T.; Ara, T.; Hasegawa, M.; Takai, Y.; Okumura, Y.; Baba, M.; Datsenko, K.A.; Tomita, M.; Wanner, B.L.; Mori, H. Construction of *Escherichia coli* K-12 in-frame, single-gene knockout mutants: The Keio collection. *Mol. Syst. Biol.* **2006**, *2*. [CrossRef]
253. Giaever, G.; Chu, A.M.; Ni, L.; Connelly, C.; Riles, L.; Véronneau, S.; Dow, S.; Lucau-Danila, A.; Anderson, K.; André, B.; et al. Functional profiling of the *Saccharomyces cerevisiae* genome. *Nature* **2002**, *418*, 387–391. [CrossRef] [PubMed]
254. Watabe, K.; Mimuro, M.; Tsuchiya, T. Development of a high-frequency in vivo transposon mutagenesis system for *Synechocystis* sp. PCC 6803 and *Synechococcus elongatus* PCC 7942. *Plant Cell Physiol.* **2014**, *55*, 2017–2026. [CrossRef]
255. Chambers, S.; Kitney, R.; Freemont, P. The Foundry: The DNA synthesis and construction Foundry at Imperial College. *Biochem. Soc. Trans.* **2016**, *44*, 687–688. [CrossRef]
256. Kuchmina, E.; Wallner, T.; Kryazhov, S.; Zinchenko, V.V.; Wilde, A. An expression system for regulated protein production in *Synechocystis* sp. PCC 6803 and its application for construction of a conditional knockout of the ferrochelatase enzyme. *J. Biotechnol.* **2012**, *162*, 75–80. [CrossRef] [PubMed]
257. Krynická, V.; Tichý, M.; Krafl, J.; Yu, J.; Kaňa, R.; Boehm, M.; Nixon, P.J.; Komenda, J. Two essential FtsH proteases control the level of the Fur repressor during iron deficiency in the cyanobacterium *Synechocystis* sp. PCC 6803. *Mol. Microbiol.* **2014**, *94*, 609–624. [CrossRef] [PubMed]
258. Schuergers, N.; Nürnberg, D.J.; Wallner, T.; Mullineaux, C.W.; Wilde, A. PilB localization correlates with the direction of twitching motility in the cyanobacterium *Synechocystis* sp. PCC 6803. *Microbiology* **2015**, *161*, 960–966. [CrossRef] [PubMed]

2.3 Conclusion

In this review, we discussed the potential of cyanobacteria for use in the green biotechnology revolution. We described new molecular tools, currently not used in cyanobacteria, that may help this potential to be realised.

The critical review of the current state of CRISPR and CRISPRi in cyanobacteria, highlighting the toxicity issues of Cas9, and the calculation of the available PAM sequences relative to the specific Cas enzyme, did inform my decision making when planning the ddCas12a work (**See section 3.4.6.2**). I chose ddCas12a from *Francisella novicida*, owing to the relatively greater number of PAM sites in *Synechocystis* sp. PCC 6803 genome when compared to the commonly used isoforms from either *Acidaminococcus* sp. or *Lachnospiraceae bacterium*.

Chapter 3 CyanoGate: A modular cloning suite for engineering cyanobacteria based on the plant MoClo syntax

3.1 Chapter Preface

The following work, except for section '***3.4.6.2 ddCas12a and paired termini antisense RNA'***, has been published in the journal *Plant Physiology*[2] (**Appendix III - Publications**). This was a collaborative project where I took the lead for most of the work relating to *Synechocystis* sp. PCC 6803 (hereafter *Synechocystis*). I verified the integration system worked as intended in *Synechocystis* by making both the unmarked *eYFP* knock in and the unmarked knockout strains and associated genome modification vectors. I planned and executed the promoter characterisation in *Synechocystis*, including cloning of level 1 and level T vectors, cyanobacterial conjugations, strain maintenance, and flow cytometry and plate reader data analysis. I assembled and tested the vectors with new origins of replication (RK2, pBBR1 and pRO1600/ColE1), executed the associated experiments determining differential eYFP expression of vectors harbouring either RK2 or RSF1010, plasmid copy number and *Synechocystis* genome copy number determination by qPCR and associated data analysis. For the gene repression systems, I cloned all the required level 1 and T vectors, performed all cyanobacterial conjugations, experiment execution and data analysis. Ravendran Vasudevan designed the CyanoGate system and cloned all new acceptor vectors except for the vectors harbouring RK2, pBBR1 and pRO1600/ColE1 (as above). Alejandra A. Schiavon cloned all level 0 promoter parts used in the promoter study and submitted all vectors to Addgene.

[2]Vasudevan, R., Gale, G. A. R., Schiavon, A. A., Puzorjov, A., Malin, J., Gillespie, M. D., Vavitsas K., Zulkower V., Wang B., Howe C.J., Lea-Smith D.J., McCormick A.J. (2019). Cyanogate: A modular cloning suite for engineering cyanobacteria based on the plant moclo syntax. Plant Physiology, 180(1), 39–55. https://doi.org/10.1104/pp.18.01401

3.2 Introduction

Much work is focused on expanding synthetic biology approaches to engineer photosynthetic organisms, including cyanobacteria. Cyanobacteria are an evolutionarily ancient and diverse phylum of photosynthetic prokaryotic organisms that are ecologically important, and are thought to contribute *ca*. 25% to oceanic net primary productivity (Castenholz et al., 2001; Flombaum et al., 2013). The chloroplasts of all photosynthetic eukaryotes, including plants, resulted from the endosymbiotic uptake of a cyanobacterium by a eukaryotic ancestor (Keeling, 2004). Therefore, cyanobacteria have proved useful as model organisms for the study of photosynthesis, electron transport and associated biochemical pathways, many of which are conserved in eukaryotic algae and higher plants. Several unique aspects of cyanobacterial photosynthesis, such as the biophysical carbon concentrating mechanism, also show promise as a means for enhancing productivity in crop plants (Rae et al., 2017). Furthermore, cyanobacteria are increasingly recognized as valuable platforms for industrial biotechnology to convert CO_2 and H_2O into valuable products using solar energy (Ducat et al., 2011; Tan et al., 2011; Ramey et al., 2015). They are metabolically diverse and encode many components (e.g. P450 cytochromes) necessary for generating high-value pharmaceutical products that can be challenging to produce in other systems (Nielsen et al., 2016b; Wlodarczyk et al., 2016; Pye et al., 2017; Stensjö et al., 2018). Furthermore, cyanobacteria show significant promise in biophotovoltaic devices for generating electrical energy (McCormick et al., 2015; Saar et al., 2018).

Based on morphological complexity, cyanobacteria are classified into five sub-sections (I–V) (Castenholz et al., 2001). Several members of the five sub-sections have been reportedly transformed (Vioque, 2007; Stucken et al., 2012), suggesting that many cyanobacterial species are amenable to genetic manipulation. Exogenous DNA can be integrated into or removed from the genome through homologous recombination-based approaches using natural transformation, conjugation (tri-parental mating), or electroporation (Heidorn et al., 2011). Exogenous DNA can also be propagated by replicative vectors,

although the latter are currently restricted to a single vector type based on the broad-host range RSF1010 origin (Mermet-Bouvier et al., 1993; Huang et al., 2010; Taton et al., 2014). Transformation tools have been developed for generating “unmarked” mutant strains (lacking an antibiotic resistance marker cassette) in several model species, such as *Synechocystis* sp. PCC 6803 (*Synechocystis* hereafter) (Lea-Smith et al., 2016). More recently, markerless genome editing using CRISPR-based approaches has been demonstrated to function in both unicellular and filamentous strains (Ungerer & Pakrasi, 2016; Wendt et al., 2016).

Although exciting progress is being made in developing effective transformation systems, cyanobacteria still lag behind in the field of synthetic biology compared to bacterial (heterotrophic), yeast and mammalian systems. Relatively few broad host-range genetic parts have been characterised, but many libraries of parts for constructing regulatory modules and circuits are starting to become available, albeit using different standards, which makes them difficult to combine (Huang & Lindblad, 2013; Camsund et al., 2014; Albers et al., 2015; Markley et al., 2015; Englund et al., 2016; Taton et al., 2017; Immethun et al., 2017; Kim et al., 2017; Wang et al., 2018; Ferreira et al., 2018; Li et al., 2018; Liu & Pakrasi, 2018). One key challenge is clear: parts that are widely used in *Escherichia coli* behave very differently in model cyanobacterial species, such as *Synechocystis* (Heidorn et al., 2011). Furthermore, different cyanobacterial strains generally show a wide variation regarding functionality and performance of different genetic parts (e.g. promoters, reporter genes and antibiotic resistance markers) (Taton et al., 2014, 2017; Englund et al., 2016; Kim et al., 2017). This suggests that parts need to be validated, calibrated, and perhaps modified for individual strains, including model species and strains that may be more commercially relevant. Rapid cloning and assembly methods are essential for accelerating the ‘design, build, test and learn’ cycle, which is a central tenet of synthetic biology (Nielsen & Keasling, 2016).

The adoption of new cloning and vector assembly methods (e.g. Isothermal (Gibson) Assembly and MoClo), assembly standards and part libraries has greatly enhanced the scalability of synthetic biology-based approaches in a range of biological systems (Moore et al., 2016; Vazquez-Vilar et al., 2018). Recent advances in synthetic biology have led to the development of standards for Type IIS restriction endonuclease-mediated assembly (commonly known as Golden Gate cloning) for several model systems, including plants (Sarrion-Perdigones et al., 2013; Engler et al., 2014; Andreou & Nakayama, 2018). Based on a common Golden Gate Modular Cloning (MoClo) syntax, large libraries are now available for fusion of different genetic parts to assemble complex vectors cheaply and easily without proprietary tools and reagents (Patron et al., 2015). High-throughput and automated assembly are projected to be widely available soon through DNA synthesis and construction facilities, such as the UK DNA Synthesis Foundries, where MoClo is seen as the most suitable assembly standard (Chambers et al., 2016).

Here, we describe the development of an easy-to-use system called CyanoGate that unites cyanobacteria with plant and algal systems. This system builds on the established Golden Gate MoClo syntax and assembly library for plants (Engler et al., 2014) that has been adopted by the OpenPlant consortium (www.openplant.org), iGEM competitions as “Phytobricks” and the MoClo kit for the microalga *Chlamydomonas reinhardtii* (Crozet et al., 2018). Firstly, we constructed and characterised a suite of known and new genetic parts (level 0) for use in cyanobacterial research, including promoters, terminators, antibiotic resistant markers, neutral sites and gene repression systems (Na et al., 2013; Yao et al., 2016; Sun et al., 2018a). Secondly, we designed an additional level of acceptor vectors (level T) to facilitate integrative or replicative transformation. We characterised assembled level T vectors in *Synechocystis* and in *Synechococcus elongatus* UTEX 2973 (UTEX 2973 hereafter), which has a reported doubling time similar to that of *Saccharomyces cerevisiae* under specific growth conditions (Yu et al., 2015; Ungerer et al., 2018a, 2018b). Lastly, we developed an online tool for

assembly of CyanoGate and Plant MoClo vectors to assist with the adoption of the CyanoGate system.

3.3 Materials and Methods

3.3.1 Cyanobacterial culture conditions

Cyanobacterial strains of *Synechocystis* were maintained on 1.5% (w/v) agar plates containing BG11 medium. Liquid cultures were grown in Erlenmeyer flasks (100 ml) containing BG11 medium (Rippka et al., 1979) supplemented with 10 mM $NaHCO_3$, shaken at 100 rpm and aerated with filter-sterilised water-saturated atmospheric air. *Synechocystis* was grown at 30°C with continuous light (100 µmol photons m^{-2} s^{-1}) in an Infors Multitron-Pro supplied with warm white LED lighting (Infors HT).

3.3.2 Vector construction

3.3.2.1 Level 0 vectors

Native cyanobacterial genetic parts were amplified from genomic DNA using NEB Q5 High-Fidelity DNA Polymerase (New England Biolabs) (**Figure 3-1; Appendix Table 8-1**). Where necessary, native genetic parts were domesticated (i.e. BsaI and BpiI sites were removed) using specific primers. Alternatively, parts were synthesised as Gblocks® DNA fragments (Integrated DNA Technology) and cloned directly into an appropriate level 0 acceptor (see Vasudevan et al. (2019) for vector maps) (Engler et al., 2014).

Golden Gate assembly reactions were performed with restriction enzymes *Bsa*I (New England Biolabs) or *Bpi*I (Thermofisher), and T4 DNA ligase (Thermofisher) (see **Appendix Information 8-2; Appendix Information 8-3** for detailed protocols). Vectors were transformed into One Shot TOP10 chemically competent *Escherichia coli* (Thermofisher) as per the manufacturer's instructions. Transformed cultures were grown at 37°C on [1.5% (w/v)] LB agar plates or in liquid LB medium shaking at 260 rpm, with appropriate antibiotic selection for level 0, 1, M and P vectors as outlined in Engler et al. (2014).

3.3.2.2 Level T acceptor vectors and new level 0 acceptors

A new level T vector system was designed that provides MoClo-compatible replicative vectors or integrative vectors for genomic modifications in cyanobacteria (Heidorn et al., 2011) (**Figure 3-2; Appendix Table 8-1**). For replicative vectors, we modified the pPMQAK1 carrying an RSF1010 replicative origin (Huang et al., 2010) to make pPMQAK1-T, and vector pSEVA421 from the Standard European Vector Architecture (SEVA) 2.0 database (seva.cnb.csic.es) carrying the RK2 replicative origin to make pSEVA421-T (Silva-Rocha et al., 2013). Replicative vector backbones were domesticated to remove native BsaI and BpiI sites where appropriate. The region between the BioBrick's prefix and suffix was then replaced by a lacZ expression cassette flanked by two BpiI sites that produce overhangs TGCC and GGGA, which are compatible with the plant Golden Gate MoClo assembly syntax for level 2 acceptors (e.g. pAGM4673) (Engler et al., 2014). For integrative vectors, we domesticated a pUC19 vector backbone and introduced two BpiI sites compatible with a level 2 acceptor (as above) to make pUC19A-T and pUC19S-T. In addition, we made a new low copy level 0 acceptor (pSC101 origin of replication) for promoter parts based on the BioBrick standard vector pSB4K5 (Liu et al., 2018). DNA was amplified using NEB Q5 High-Fidelity DNA Polymerase (New England Biolabs). All vectors were sequenced following assembly to confirm domestication and the integrity of the MoClo cloning site.

3.3.2.3 Level 0 parts for CRISPRi and srRNA

A nuclease deficient Cas9 gene sequence sourced from Addgene (www.addgene.org/44249/) was domesticated and assembled as a level 0 CDS part (**Appendix Table 8-1; Appendix Table 8-2**) (Qi et al., 2013). Five promoters of different strengths were truncated to the transcriptional start site (TSS) and cloned into a new level 0 acceptor vector with the unique overhangs GGAG and TAGC (**Figure 3-1**). Two new level 0 parts with the unique overhangs GTTT and CGCT were generated for the sgRNA scaffold and srRNA HFQ handle (based on MicC) (Na et al., 2013), respectively. Assembly

of level 1 expression cassettes proceeded by combining appropriate level 0 parts with a PCR product for either a srRNA or sgRNA (**Figure 3-1**).

3.3.3 Cyanobacterial transformation and conjugation

Transformation with integrative level T vectors was performed as in Lea-Smith et al. (2016). For transformation by electroporation, cultures were harvested during the 'exponential' growth phase (OD_{750} of ~0.6) by centrifugation at 4,000 *g* for 10 min. The cell pellet was washed 3 times with 2 ml of sterile 1 mM HEPES buffer (pH 7.5), re-suspended in water with 3–5 µg of level T vector DNA and transferred into a 0.1-cm electroporation cuvette (Scientific Laboratory Suppliers). Re-suspended cells were electroporated using an Eppendorf 2510 electroporator (Eppendorf) set to 1200 V. Sterile BG-11 (1 ml) was immediately added to the electroporated cells. Following a 1-hr incubation at RT, the cells were plated on 1.5% (w/v) agar plates containing BG-11 with antibiotics at standard working concentrations to select for transformed colonies. The plates were sealed with parafilm and placed under 15 µmol photons m^{-2} s^{-1} light at 30°C for 1 day. The plates were then moved to 30 µmol photons m^{-2} s^{-1} light until colonies appeared. After 15–20 days, putative transformants were recovered and streaked onto new plates with appropriate antibiotics for further study.

Genetic modification by conjugation in *Synechocystis* was facilitated by an *E. coli* strain (HB101) carrying both mobilizer and helper vectors pRK2013 (ATCC® 37159™) and pRL528 (www.addgene.org/58495/), respectively (Tsinoremas et al., 1994). Cultures of HB101 and OneShot TOP10 *E. coli* strains carrying level T cargo vectors were grown for approximately 15 hr with appropriate antibiotics. Cyanobacterial strains were grown to an OD_{750} of ~1. All bacterial cultures were washed three times with either fresh LB medium for *E. coli* or BG11 for cyanobacteria prior to use. *Synechocystis* cultures (100 µl, OD_{750} of 0.5–0.8) were conjugated by combining appropriate HB101 and the cargo strains (100 µl each) and plating onto HATF 0.45-µm transfer membranes (Merck Millipore) placed on LB: BG11 (1: 19) agar plates. *Synechocystis* transconjugates were grown under culturing conditions outlined

above. Following growth on non-selective media for 24 hr, the membranes were transferred to BG11 agar plates supplemented with appropriate antibiotics. Colonies were observed within a week. Chlorophyll content of wild-type (WT) and mutant strains was calculated as in Lea-Smith et al. (2013).

3.3.4 Fluorescence assays

Transgenic strains maintained on agar plates containing appropriate antibiotics were used to inoculate 10-ml seed cultures that were grown to an optical density at 750 nm (OD_{750}) of approximately 1.0, as measured with a WPA Biowave II spectrometer (Biochrom). Seed cultures were diluted to an OD_{750} of 0.2, and 2-ml starting cultures were transferred to 24-well plates (Costar® Corning Incorporated) for experiments. *Synechocystis* was grown in an Infors Multitron-Pro in the same culturing conditions described above. OD_{750} was measured using a FLUOstar OMEGA microplate reader (BMG Labtech). Fluorescence of eYFP for individual cells (10,000 cells per culture) was measured by flow cytometry using an Attune NxT Flow Cytometer (Thermofisher). Cells were gated using forward and side scatter, and median eYFP fluorescence was calculated from excitation/emission wavelengths 488 nm/515–545 nm (Kelly et al., 2018) and reported at 48 hr unless otherwise stated.

3.3.5 Plasmid vector and genome copy number determination

The genome copy number and copy number of heterologous self-replicating plasmid vectors in *Synechocystis* was estimated using a quantitative real-time PCR (qPCR) approach adapted from Zerulla et al. (2016). Cytoplasmic extracts containing total cellular DNA were harvested from *Synechocystis* cultures after 48 hr growth (OD_{750} = *ca*. 5) according to Zerulla et al. (2016). Cells in 10 ml of culture were pelleted by centrifugation at 4,000 *g* for 15 min, disrupted by shaking at 30 Hz for 10 min in a TissueLyser II with a mixture of 0.2-mm and 0.5-mm acid washed glass beads (0.35 g each), and then resuspended in dH_2O. The culture cell count was determined prior to harvest using a haemocytometer and checked again after cell disruption to calculate the efficiency of cell disruption. A standard curve based on a dilution series of

vector DNA was generated and used for qPCR analysis in parallel with extracts carrying the same vector. Two DNA fragments (*ca*. 1 kb) targeting two separate loci (*petB* and *secA*) were amplified from isolated genomic DNA from *Synechocystis* using standard PCR (Pinto et al., 2012). DNA mass concentrations were determined photometrically and the concentrations of DNA molecules were calculated from the known molecular mass. As above, a standard curve based on a dilution series of the two fragments was generated to estimate genome copy number in the extracts (Zerulla et al., 2016). The Ct of the extracts were then plotted against the linear portion of the standard curves to estimate plasmid vector copy number and genome copy number per cell. Oligonucleotides used are summarised in **Appendix Table 8-3**.

3.4 Results and Discussion

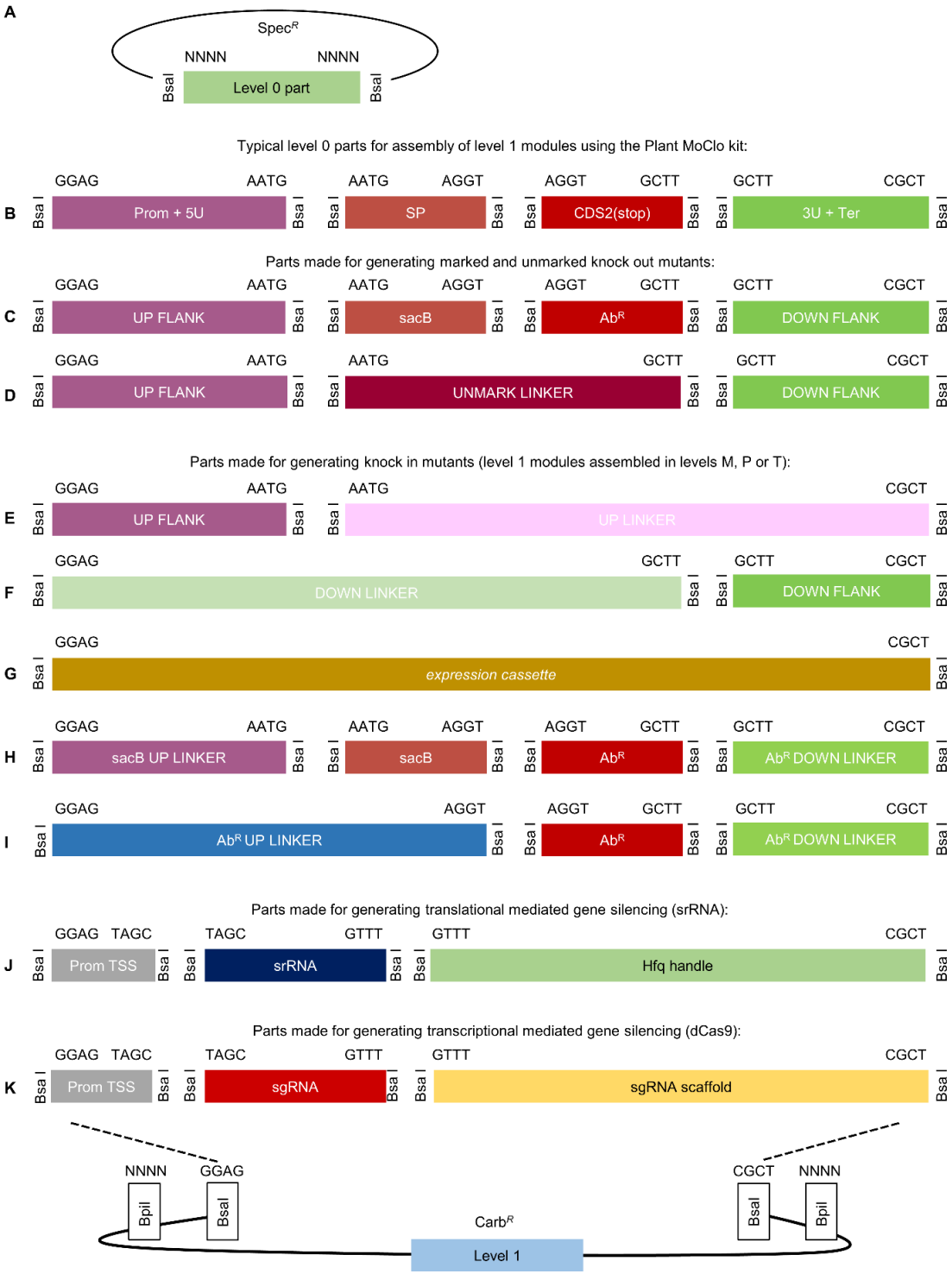

Figure 3-1: Adaptation of the Plant Golden Gate MoClo level 0 syntax for generating level 1 assemblies for transfer to Level T

(A) The format for a level 0 MoClo acceptor vector with the part bordered by two BsaI sites. (B) Typical level 0 parts from the Plant MoClo kit, where parts of the same type are bordered by the same pair of fusion sites (for each fusion site, only the sequence of the top strand is shown). Note that the parts are not drawn to scale. (C) and (D), The syntax of the Plant MoClo kit was adapted to generate level 0 parts for engineering marked and unmarked cyanobacterial mutant strains. (E) to (I), To generate knock-in mutants, short linker parts (30 bp) were constructed to allow assembly of individual flanking sequences, or marker cassettes (Ab^R or *sacB*) in level 1 vectors for subsequent assembly in level T. (J) and (K), Parts required for generating synthetic srRNA or CRISPRi level 1 constructs. See **Appendix Information 8-2; Appendix Information 8-3** for workflows. Abbreviations: 3U+Ter, 3'UTR and terminator; Ab^R, antibiotic resistance cassette; Ab^R DOWN LINKER, short sequence (~30 bp) to provide CGCT overhang; Ab^R UP LINKER, short sequence (~30 bp) to provide GAGG overhang; CDS2(stop), coding sequence with a stop codon; DOWN FLANK, flanking sequence downstream of target site; DOWN FLANK LINKER, short sequence (~30 bp) to provide GGAG overhang; Prom+5U, promoter and 5' UTR; Prom TSS, promoter transcription start site; *sacB*, levansucrase expression cassette; *sacB* UP LINKER, short sequence (~30 bp) to provide GAGG overhang; sgRNA, single guide RNA; SP, signal peptide; srRNA, small regulatory RNA; UP FLANK, flanking sequence upstream of target site; UP FLANK LINKER, short sequence (~30 bp) to provide CGCT overhang; UNMARK LINKER, short sequence to bridge UP FLANK and DOWN FLANK. (Figure by Ravendran Vasudevan, (Vasudevan et al., 2019) [(www.plantphysiol.org) Copyright American Society of Plant Biologists. ASPB further grants to authors the permission to make digital or hard copies of part or all of a work published in Plant Physiology® without fee for personal or classroom use].

3.4.1 Construction of the CyanoGate system

The CyanoGate system integrates with the two-part Golden Gate MoClo Plant Tool Kit, which can be acquired from Addgene [standardised parts (Kit #1000000047) and backbone acceptor vectors (Kit # 1000000044), (www.addgene.org)] (Engler et al., 2014). A comparison of the benefits of MoClo- and Gibson assembly-based cloning strategies is shown in Appendix **Information 8-1**. The syntax for level 0 parts was adapted for prokaryotic cyanobacteria to address typical cloning requirements for cyanobacterial research (**Figure 3-1**). New level 0 parts were assembled from a variety of sources (**Appendix Table 8-1**). Level 1, M and P acceptor vectors were adopted from the MoClo Plant Tool Kit, which facilitates assembly of level 0 parts in a level 1 vector, and subsequently up to seven level 1 modules in level M. Level M assemblies can be combined further into level P and cycled back

into level M to produce larger multi-module vectors if required (**Appendix Information 8-2**). Vectors >50 kb in size assembled by MoClo have been reported (Werner et al., 2012). Modules from level 1 or level P can be assembled in new level T vectors designed for cyanobacterial transformation (**Figure 3-2**). We found that *Synechocystis* produced recombinants following electroporation or conjugation methods with level T vectors. For the majority of the work outlined below, we relied on the conjugation approach.

3.4.2 Integration

3.4.3 Generating marked and unmarked knockout mutants

A common method for engineering stable genomic knock-out and knock-in mutants in several cyanobacteria relies on homologous recombination via integrative (suicide) vectors using a two-step marked-unmarked strategy (Lea-Smith et al., 2016) (**Appendix Information 8-3**). Saar et al. (2018) used this approach to introduce up to five genomic alterations into a single *Synechocystis* strain. To make an unmarked mutant, firstly marked mutants are generated with an integrative vector carrying two sequences (approximately 1 kb each) identical to the regions of the cyanobacterial chromosome flanking the deletion/insertion site. Two gene cassettes are inserted between these flanking sequences: a levansucrase expression cassette (*sacB*) that confers sensitivity to transgenic colonies grown on sucrose and an antibiotic resistance cassette (Ab^R) of choice. Secondly, unmarked mutants (carrying no selection markers) are generated from fully segregated marked lines using a separate integrative vector carrying only the flanking sequences and selection is on plates containing sucrose.

This approach was adapted for the CyanoGate system (**Figure 3-1**). To generate level 1 vectors for making knock-out mutants, sequences flanking the upstream (UP FLANK) and downstream (DOWN FLANK) site of recombination were ligated into the plant MoClo Prom+5U (with overhangs GGAG-AATG), and 3U+Ter (GCTT-CGCT) positions, respectively, to generate new level 0 parts (**Figure 3-1B**). In addition, full expression cassettes were made for sucrose selection (*sacB*) and antibiotic resistance (Ab^RSpec, Ab^RKan and

Ab^{R}Ery) in level 0 that ligate into positions SP (AATG-AGGT) and CDS2 (stop) (AGGT-GCTT), respectively. Marked level 1 modules can be assembled using UP FLANK, DOWN FLANK, *sacB* and the required Ab^R level 0 part. For generating the corresponding unmarked level 1 module, a short 59-bp linker (UNMARK LINKER) can be ligated into the CDS1ns (AATG-GCTT) position for assembly with an UP FLANK and DOWN FLANK (**Figure 3-1D**). Unmarked and marked level 1 modules can then be assembled into level T integrative vectors, with the potential capacity to include multiple knock-out modules in a single level T vector (**Figure 3-2**).

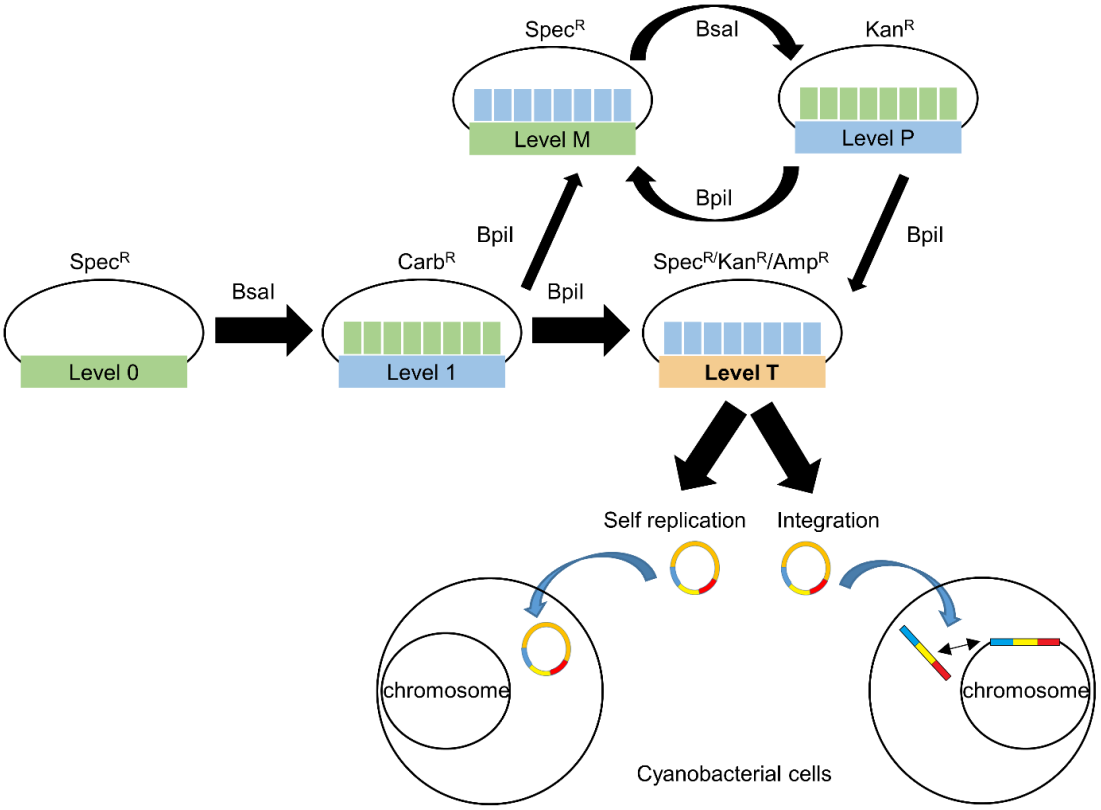

Figure 3-2: Extension of the Plant Golden Gate MoClo Assembly Standard for cyanobacterial transformation.

Assembly relies on one of two Type IIS restriction endonuclease enzymes (*Bsa*I or *Bpi*I). Domesticated level 0 parts are assembled into level 1 vectors. Up to seven level 1 modules can be assembled directly into a level T cyanobacterial transformation vector, which consists of two sub-types (either a replicative or an integrative vector). Alternatively, larger vectors with more modules can be built by assembling level 1 modules into level M, and then cycling assembly between level M and level P, and finally transferring from Level P to level T. Antibiotic selection markers are shown for each level. Level T vectors are supplied with internal antibiotic selection markers (shown), but additional selection markers could be included from level 1 modules as required. See Appendix Table 8-1 and Vasudevan et al. (2019) for the full list and maps of level T acceptor vectors. (Figure by Ravendran Vasudevan, (Vasudevan et al., 2019) [(www.plantphysiol.org) Copyright American Society of Plant Biologists. ASPB further grants to authors the permission to make digital or hard copies of part or all of a work published in Plant Physiology® without fee for personal or classroom use].

To validate the approach, Ravendran Vasudevan first constructed the level 0 flanking vectors pC0.024 and pC0.025 and assembled the level T integrative vector *cpcBA*-M using pUC19-T containing *sacB* and Ab^R. I then assembled *cpcBA*-UM with the *sacB* and Ab^R cassettes replaced with the unmark linker to remove the *cpcBA* promoter and operon in *Synechocystis* and generate an "Olive" mutant unable to produce the phycobiliprotein C-phycocyanin (Kirst et al., 2014; Lea-Smith et al., 2014) (**Figure 3-3;** Appendix Table 8-1). Following transformation with *cpcBA*-M, we successfully generated a marked Δ*cpcBA* mutant carrying the *sacB* and the Ab^RKan cassettes after selective segregation (*ca*. 3 months) (**Figure 3-3A**). Following my transformation of the marked Δ*cpcBA* mutant with *cpcBA*-UM, the unmarked Δ*cpcBA* mutant was then isolated following selection on sucrose (*ca*. 2 weeks) (**Figure 3-3B**). Absence of C-phycocyanin in the Olive mutant resulted in a characteristic change in colour and drop in absorbance at 625 nm (**Figure 3-3C, D**) and a significant reduction in chlorophyll content compared to that in WT cells (28.4 ± 0.2 and 48.3 ± 0.2 amol chl $cell^{-1}$, respectively) (Kirst et al., 2014; Lea-Smith et al., 2014).

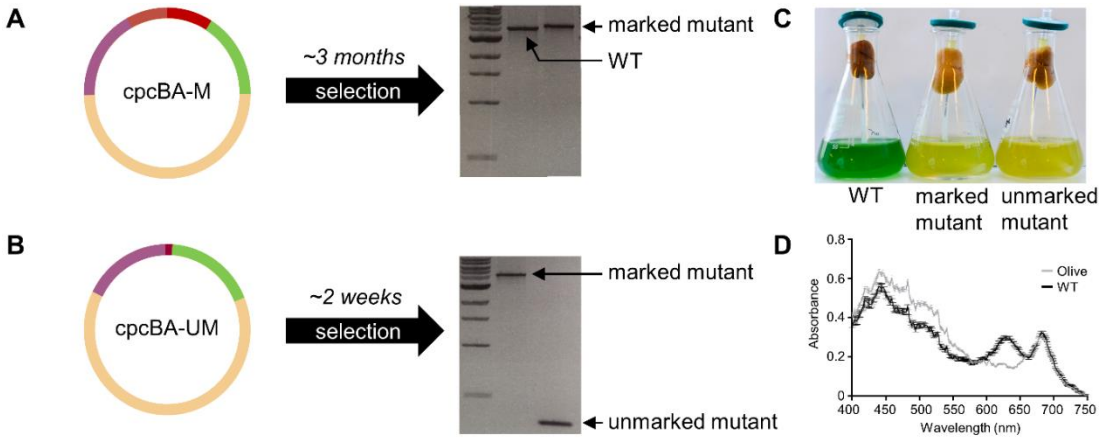

Figure 3-3: Generating knock-out mutants in cyanobacteria.

(A) Assembled level T vector *cpcBA*-M (see Figure 3-1C) targeting the *cpcBA* promoter and operon (3,563 bp) to generate a marked Δ*cpcBA* "Olive" mutant in *Synechocystis* sp. PCC 6803. Following transformation and segregation on kanamycin (*ca*. 3 months), a segregated marked mutant was isolated (WT band is 3,925 bp, marked mutant band is 5,503 bp, 1-kb DNA ladder (NEB) is shown). (B) Assembled level T vector *cpcBA*-UM (see Figure 3-1D) for generating an unmarked Δ*cpcBA* mutant. Following transformation and segregation on sucrose (*ca*. 2 weeks), an unmarked mutant was isolated (unmarked band is 425 bp). (C) Liquid cultures of WT, marked and unmarked Olive mutants. (D) Spectrum showing the absorbance of the unmarked Olive mutant and WT cultures after 72 hr of growth. Values are the average of four biological replicates ± SE and are standardised to 750 nm (Vasudevan et al., 2019). [(www.plantphysiol.org) Copyright American Society of Plant Biologists. ASPB further grants to authors the permission to make digital or hard copies of part or all of a work published in Plant Physiology® without fee for personal or classroom use].

3.4.3.1 Generating knock-in mutants

Flexibility in designing level 1 insertion cassettes is needed when making knock-in mutants. Thus, for knock-in mutants the upstream and downstream sequences flanking the insertion site, and any required expression or marker cassettes, are first assembled into separate level 1 modules from UP FLANK and DOWN FLANK level 0 parts (**Figure 3-1E, F**). Seven level 1 modules can be assembled directly into Level T (**Figure 3-2**). Therefore, with a single pair of flanking sequences, up to five level 1 expression cassettes could be included in a Level T vector.

Linker parts (20 bp) UP FLANK LINKER and DOWN FLANK LINKER were generated by Ravendran Vasudevan, to allow assembly of level 0 UP FLANK

and DOWN FLANK parts into separate level 1 acceptor vectors. Similarly, level 0 linker parts were generated for *sacB* and Ab^R (**Figure 3-1H, I**). Level 1 vectors at different positions can then be assembled in level T (or M) containing one or more expression cassettes, an Ab^R of choice, or both *sacB* and Ab^R (**Figure 3-2**).

Using this approach, CyanoGate can facilitate the generation of knock-in mutants using a variety of strategies. For example, if curing of the resistance marker is not an experimental requirement (e.g. Liberton et al., (2017)), only a single antibiotic resistance cassette needs to be included in level T. Alternatively, a two-step marked-unmarked strategy could be followed, as for generating knock-out mutants above.

Whereas knock-out strategies can target particular loci, knock-in approaches often rely on recombination at designated 'neutral sites' within the genome of interest that can be disrupted with no or minimal impact on the growth phenotype (Ng et al., 2015; Pinto et al., 2015). Based on loci reported in the literature, we have assembled a suite of flanking regions including four that target neutral sites in *Synechocystis* (designated 6803 NS1-4) (Pinto et al., 2015) (**Appendix Table 8-1**). Pinto et al. (2015) have qualitatively compared the impact of these four *Synechocystis* neutral sites assembled here under several different growth conditions, and observed that insertions at 6803 NS3 and NS4 had no significant effect on growth compared to that of WT cultures, whereas insertions at NS2 and NS1 had small but significant effects depending on the growth conditions. Several studies have used 6803 NS3, for example, to engineer a *Synechocystis* strain for the bioremediation of microcystins (Dexter et al., 2018) and the development of T7 polymerase-based synthetic promoter systems (Ferreira et al., 2018).

To validate our system, I generated a level T vector carrying the flanking regions for the *cpcBA* operon and an eYFP expression cassette (*cpcBA*-eYFP) (**Figure 3-4A, B; Appendix Table 8-1**). I successfully transformed this vector into our marked "Olive" *Synechocystis* mutant, and generated a stable olive mutant with constitutive expression of eYFP (Olive-eYFP) (**Figure 3-4C**).

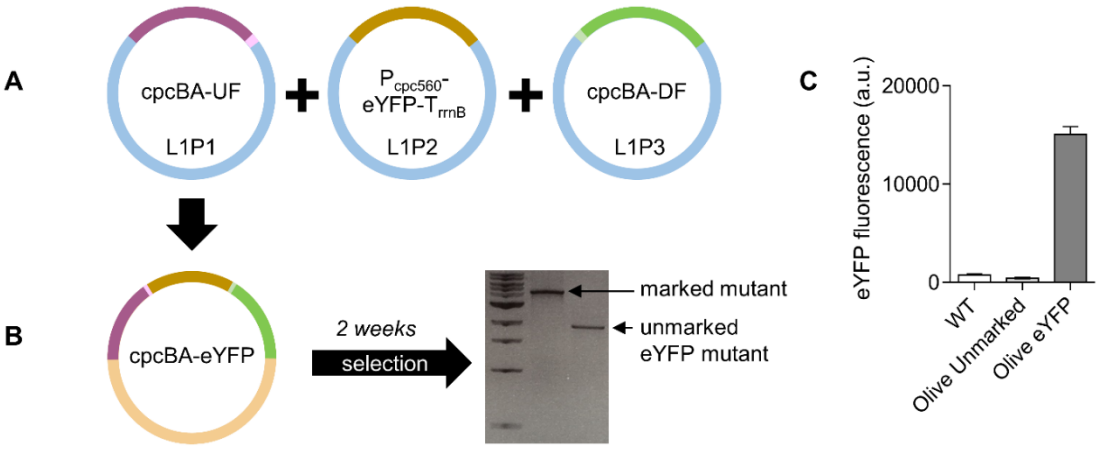

Figure 3-4: Generating an unmarked knock-in mutant in *Synechosystis* sp. PCC 6803. (A) Assembly of level 1 modules *cpcBA*-UF (see Figure 3-1E) in the level 1, position 1 acceptor (L1P1), P_{cpc560}-eYFP-T_{rrnB} (see Figure 3-1G) in L1P2 and *cpcBA*-DF (see Figure 3-1F) in L1P3. (B) Transfer of level 1 assemblies to level T vector *cpcBA*-eYFP for generating an unmarked Δ*cpcBA* mutant carrying an eYFP expression cassette. Following transformation and segregation on sucrose (ca. 3 weeks), an unmarked eYFP mutant was isolated (1,771 bp). (C) Fluorescence values are the means ± SE of four biological replicates, where each replicate represents the median measurements of 10,000 cells (Vasudevan et al., 2019). [(www.plantphysiol.org) Copyright American Society of Plant Biologists. ASPB further grants to authors the permission to make digital or hard copies of part or all of a work published in Plant Physiology® without fee for personal or classroom use].

3.4.4 Characterising promoter parts in *Synechocystis* sp. PCC 6803

A wide selection of level 0 promoter parts, both synthetic and native to *Synechocystis*, were included in CyanoGate. Promoters were assembled as expression cassettes driving eYFP in replicative level T vector pPMQAK1-T to test for relative expression levels when conjugated into *Synechocystis* or UTEX 2973. I will only discuss expression levels pertaining to *Synechocystis*, as I took responsibility for planning the experiments and analysing the data for this strain.

3.4.4.1 Promoters native to *Synechocystis* sp. PCC 6803

Included in the CyanoGate kit were several promoters native to *Synechocystis* including *rnpB* promoter, P_{rnpB}, from the Ribonuclease P gene (Huang et al., 2010), a long version of the *psbA2* promoter, P_{psbA2L}, from the Photosystem II

protein D1 gene (Lindberg et al., 2010; Englund et al., 2016) and the promoter of the C-phycocyanin operon, P_{cpc560} (also known as P_{cpcB} and P_{cpcBA}) (Zhou et al., 2014). P_{rnpB} and P_{psbA2L} were placed in front of RBS* (Heidorn et al., 2011) (**Figure 3-5A**). To build on a previous functional characterisation of P_{cpc560} (Zhou et al., 2014), John Malin assembled four variants of this strong promoter. Firstly, $P_{cpc560+A}$ consisted of the promoter and the 4-bp MoClo overhang AATG. Secondly, P_{cpc560} was truncated by one bp (A), so that that the start codon was aligned with the native P_{cpc560} RBS spacer region length. Zhou et al. (2014) identified 14 predicted transcription factor binding sites (TFBSs) in the upstream region of P_{cpc560} (-556 to -381 bp) and removal of this region resulted in a significant loss of promoter activity. However, alignment of the reported TFBSs showed their locations are in the downstream region of the promoter (-180 to -5 bp). John Malin identified 11 additional predicted TFBSs using Virtual Footprint (Münch et al., 2005) in the upstream region and hypothesised that the promoter activity may be modified by duplicating either of these regions. So thirdly, we generated P_{cpc560_Dx2} containing a duplicated downstream TFBS region. For P_{cpc560_Dx2}, only the region between -31 to -180 bp was duplicated to avoid repeating the Shine-Dalgarno (SD) sequence. Fourthly, we duplicated the upstream region to generate P_{cpc560_Ux2}. We then assembled P_{rnpB}, P_{psbA2L} and the four P_{cpc560} variants with eYFP and the *rrnB* terminator (T_{rrnB}) into a Level 1 expression cassette, and subsequently into a level T replicative vector (pPMQAK1-T) for expression analysis (**Appendix Table 8-2**).

In *Synechocystis* the highest expressing promoter was P_{cpc560} (**Figure 3-5B**), which indicated that maintaining the native RBS spacer region for P_{cpc560} is important for maximising expression. Neither P_{cpc560_Dx2} nor P_{cpc560_Ux2} resulted in higher expression levels compared to that of P_{cpc560}. P_{cpc560_Dx2}–driven expression was strongly decreased compared to that of P_{cpc560}, suggesting that promoter function is sensitive to modification of the downstream region and this region could be a useful target for modulating P_{cpc560} efficacy. Previous work in *Synechocystis* has suggested that modification of the middle region of P_{cpc560} (-380 to -181 bp) may also affect function (Lea-Smith et al., 2014).

P_{psbA2L} produced lower expression levels than any variant of P_{cpc560} in *Synechocystis*, whereas P_{rnpB} produced the lowest expression levels. The observed differences in expression levels are consistent with those in other studies with *Synechocystis* (Camsund et al., 2014; Englund et al., 2016; Liu & Pakrasi, 2018).

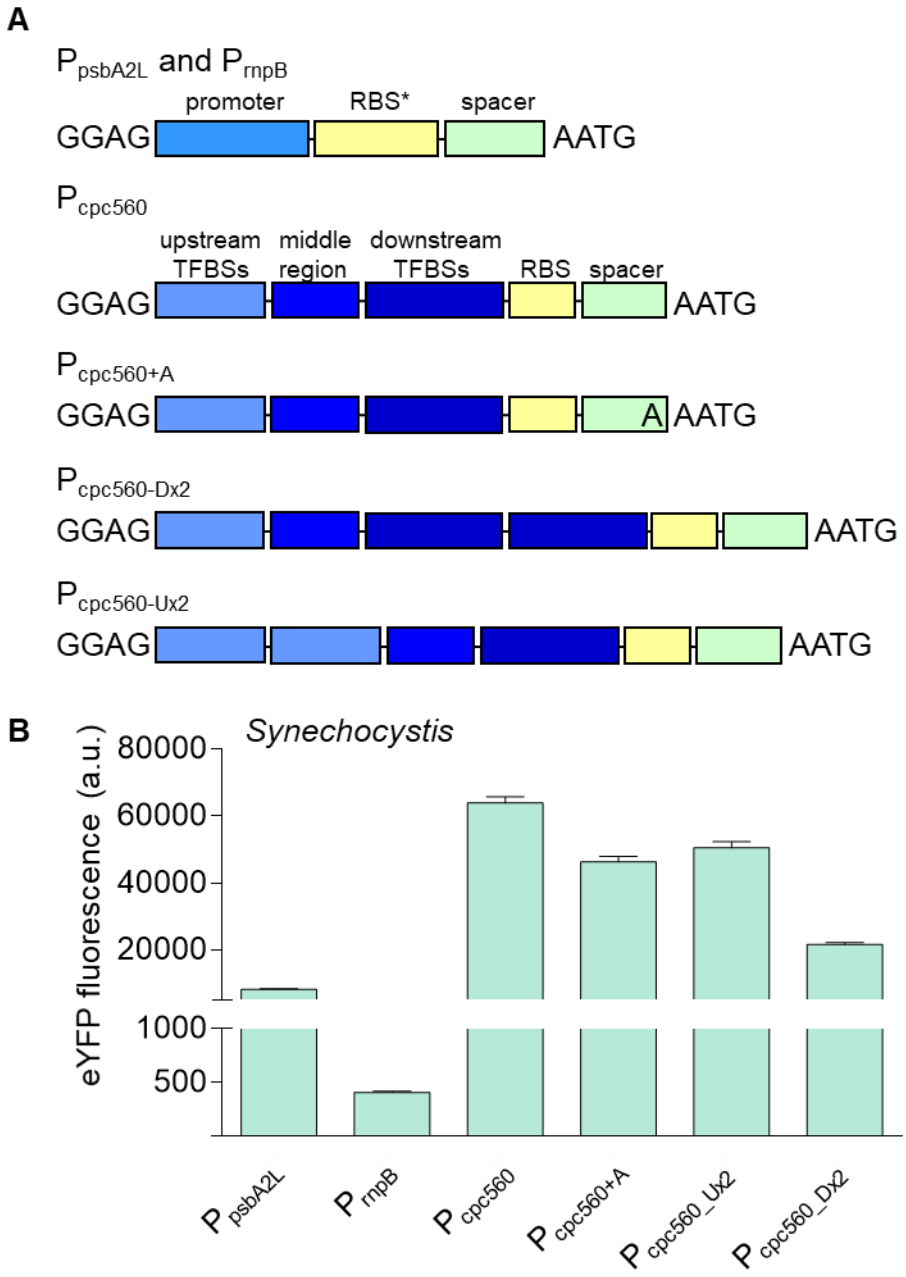

Figure 3-5: Expression levels of cyanobacterial promoters in *Synechocystis*

(A) Structure of the cyanobacterial promoters adapted for the CyanoGate kit. Regions of P_{cpc560} shown are the upstream transcription factor binding sites (TFBSs) (-556 to -381 bp), middle region (-380 to -181 bp), and the downstream TFBSs, ribosome binding site (RBS) and spacer (-180 to -5 bp). (B) Expression levels of eYFP driven by promoters in *Synechocystis* calculated from measurements taken from 10,000 individual cells. Values are the means ± SE from at least four biological replicates after 48 hr of growth (average OD_{750} values for *Synechocystis* cultures were 3.5 ± 0.2). See **Appendix Figure 8-2** for more info. (Figure adapted from Vasudevan et al. (2019) [(www.plantphysiol.org) Copyright American Society of Plant

3.4.4.2 Heterologous and synthetic promoters

Alejandra Schiavon assembled a suite of twenty constitutive synthetic promoters in level 0 based on the modified BioBricks BBa_J23119 library of promoters (Markley et al., 2015), and the synthetic P_{trc10}, P_{tic10} and P_{tac10} promoters (Huang et al., 2010; Albers et al., 2015) (**Appendix Table 8-1**). We retained the broad-range BBa_B0034 RBS (AAAGAGGAGAAA) and *lac* operator (*lacO*) from Huang et al. (2010), for future *lacI*-based repression experiments (*lacI* and the P_{lacIQ} promoter are included in the CyanoGate kit) (Bahl et al., 1977). We cloned eight new variants (J23119MH_V01-8) with mutations in the canonical BBa_J23119 promoter sequence (**Figure 3-6A**).

We then tested the expression levels of eYFP driven by the synthetic promoters in *Synechocystis* following assembly in pPMQAK1-T (**Figure 3-6B; Appendix Table 8-2**) where the promoters demonstrated a 120-fold dynamic range. The highest expression levels were observed for J23119 and P_{trc10}, but these were still approximately 50% lower than values for the native P_{cpc560} promoters (**Figure 3-5B**). The expression trends for the BBa_J23119 library were consistent with the subset reported by Camsund et al. (2014), whereas the observed differences between P_{trc10} and P_{cpc560} were similar to those reported by Liu and Pakrasi (2018).

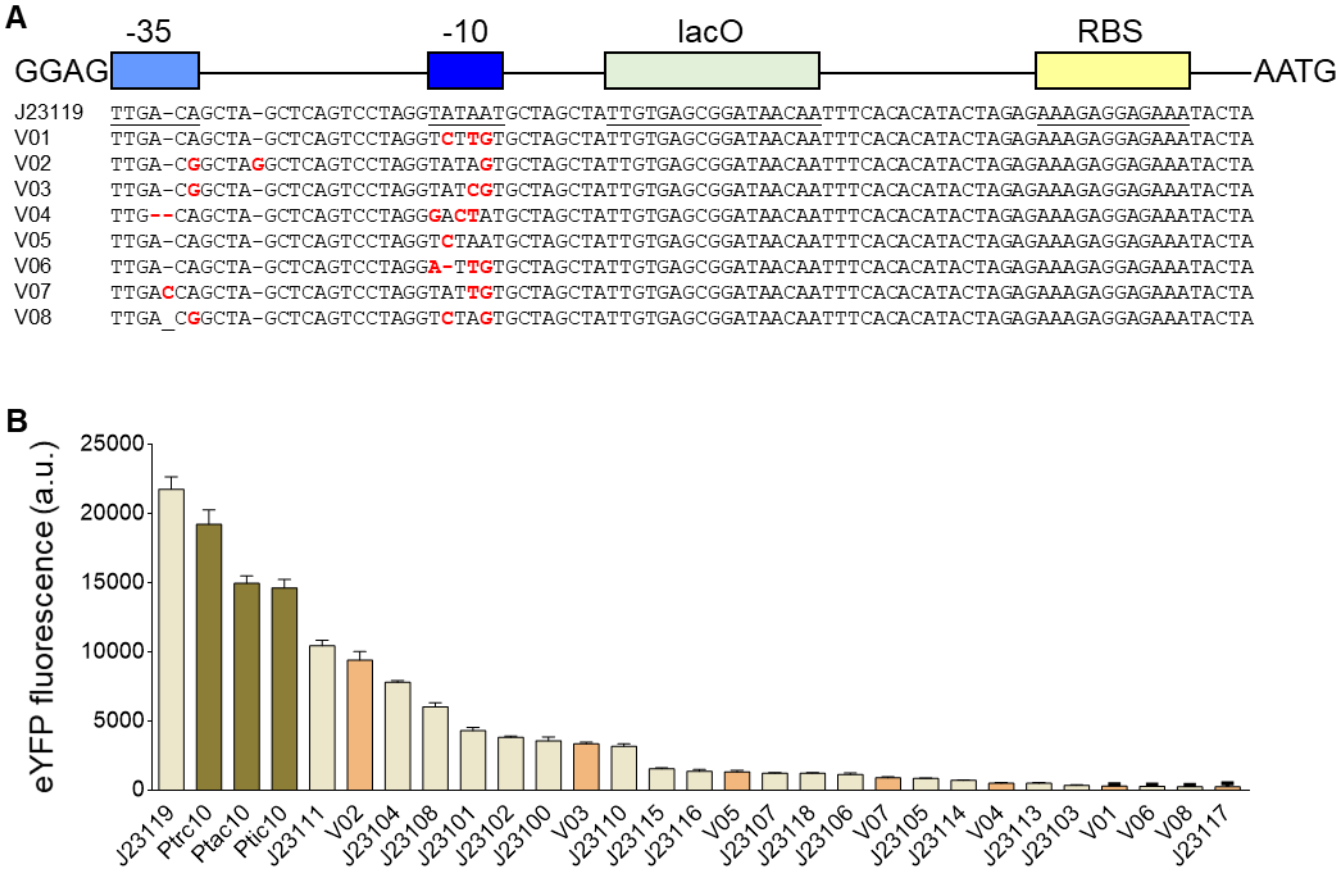

Figure 3-6: Expression levels of heterologous and synthetic promoters in *Synechocystis* sp. PCC 6803

(A) Structure and alignment of eight new synthetic promoters derived from the BioBricks BBa_J23119 library and P_{trc10} promoter design (18). (B) Expression levels of eYFP driven by promoters in *Synechocystis* calculated from measurements taken from 10,000 individual cells. Values are

the means ± SE from at least four biological replicates after 48 hr of growth (average OD_{750} values for *Synechocystis* cultures were 3.5 ± 0.2). See **Appendix Figure 8-2** for more info. (Figure adapted from Vasudevan et al. (2019) [(www.plantphysiol.org) Copyright American Society of Plant Biologists. ASPB further grants to authors the permission to make digital or hard copies of part or all of a work published in Plant Physiology® without fee for personal or classroom use].

3.4.5 The RK2 origin of replication is functional in *Synechocystis*

Synthetic biology tools (e.g. gene expression circuits, CRISPR/Cas-based systems) are often distributed between multiple plasmid vectors at different copy numbers in order to synthesise each component at the required concentration (Bradley et al., 2016). The large RSF1010 vector is able to replicate in a broad range of microbes including gram-negative bacteria such as *E. coli* and several cyanobacterial species. However, for 25 years it has remained the only non-native vector reported to be able to self-replicate in cyanobacteria (Mermet-Bouvier et al., 1993). Recently, two small plasmids native to *Synechocystis*, pCA2.4 and pCB2.4, have been engineered for gene expression (Armshaw et al., 2015; Ng et al., 2015; Liu & Pakrasi, 2018). The pANS plasmid (native to PCC 7942) has also been adapted as a replicative vector, but so far it has been only shown to function in PCC 7942 and *Anabaena* PCC 7120 (Chen et al., 2016). Similarly, the high copy number plasmid pAQ1 (native to PCC 7002) has been engineered for heterologous expression, but up to now it has only been used in PCC 7002 (Xu et al., 2011). To expand the replication origins available for cyanobacterial research further we tested the capacity for vectors from the SEVA library to replicate in *Synechocystis* (Silva-Rocha et al., 2013).

We acquired three vectors driven by three different replication origins [pSEVA421 (RK2), pSEVA431 (pBBR1) and pSEVA442 (pRO1600/ColE1)] and carrying a spectinomycin antibiotic resistance marker. These vectors were domesticated and modified as level T acceptor vectors, assembled and then transformed into *Synechocystis* by electroporation or conjugation. Only *Synechocystis* strains conjugated with vectors carrying RK2 (pSEVA421-T) grew on spectinomycin-containing plates (**Appendix Table 8-1**). To confirm that RSF1010 and RK2 replication origins can replicate autonomously in *Synechocystis*, we recovered the pPMQAK1-T or pSEVA421-T vector from lysates of axenic *Synechocystis* strains previously conjugated with each vector by transformation into *E. coli*. The identity and integrity of pPMQAK1-T and pSEVA421-T extracted from transformed *E. coli* colonies were confirmed by restriction digest and Sanger sequencing.

We then assembled two level T vectors with an eYFP expression cassette (P_{cpc560}-eYFP- T_{rrnB}) to produce pPMQAK1-T-eYFP and pSEVA421-T-eYFP, which were conjugated into *Synechocystis* (**Figure 3-7; Appendix Table 8-2**). Both pPMQAK1-T-eYFP and pSEVA421-T-eYFP transconjugates grew at similar rates in 50 µg ml^{-1} kanamycin and 5 µg ml^{-1} spectinomycin, respectively (**Figure 3-7A**). However, eYFP levels were 8-fold lower in pSEVA421-T-eYFP, suggesting that RK2 has a reduced copy number relative to RSF1010 in *Synechocystis* (**Figure 3-7B**). We measured the heterologous plasmid vector copy number in strains expressing pSEVA421-T or pPMQAK1-T and estimated an average copy number per cell of 9 ± 2 and 31 ± 5, respectively (**Figure 3-7C**). The copy number for pPMQAK1-T was similar to values reported previously for RSF1010-derived vectors in *Synechocystis* (*ca*. 30) (Ng et al., 2000). Our results are also consistent with the lower copy numbers in *E. coli* for vectors with RK2 (4–7 copies) compared to those with RSF1010 (10–12 copies) replication origins (Frey et al., 1992; Blasina et al., 1996). Furthermore, we compared the genome copies per cell between transformants and wild-type strains and found no significant differences - the average value was 11 ± 2, which is consistent with the typical range of genome copy numbers observed in *Synechocystis* cells (Zerulla et al., 2016).

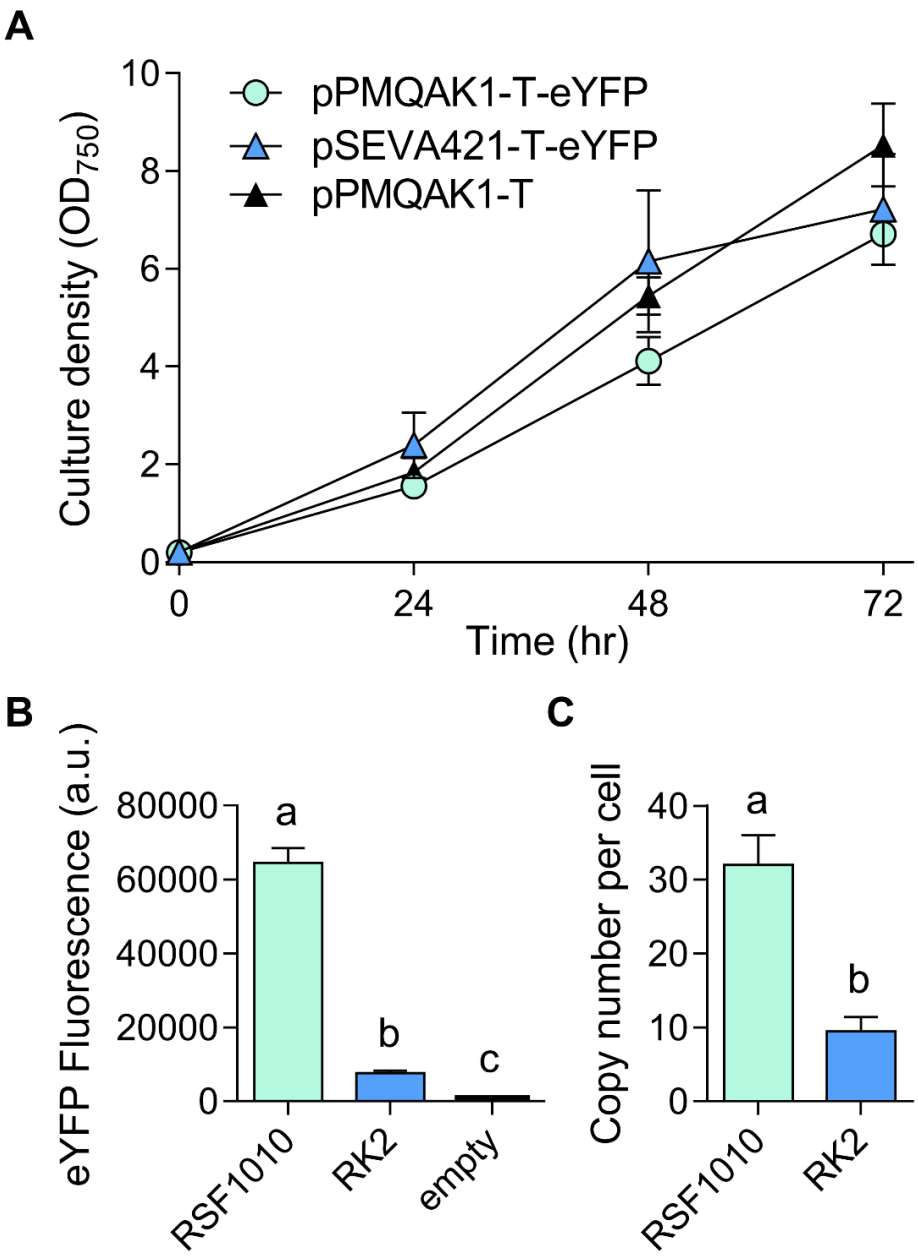

Figure 3-7: Cell growth and expression levels of eYFP with the RK2 replicative origin in *Synechocystis*.

(A) Growth of strains carrying RK2 (vector pSEVA421-T-eYFP), RSF1010 (pPMQAK1-T-eYFP) or empty pPMQAK1-T, with cultures containing appropriate antibiotic selection. Growth was measured as OD_{750} under a constant illumination of 100 µmol photons $m^{-2}s^{-1}$ at 30°C. (B) Expression levels of eYFP after 48 hr of growth calculated from measurements taken from 10,000 individual cells. (C) Plasmid copy numbers per cell after 48 hr of growth. Letters indicating significant difference ($P < 0.05$) are shown, as determined by ANOVA followed by Tukey's HSD tests. Values are the means ± SE of four biological replicates. (Figure adapted from Vasudevan et al. (2019) [(www.plantphysiol.org) Copyright American Society of Plant Biologists. ASPB further grants to authors the permission to make

3.4.6 Gene repression systems

CRISPR (clustered regularly interspaced short palindromic) interference (CRISPRi) is a relatively new but well characterised tool for modulating gene expression at the transcription stage in a sequence-specific manner (Qi et al., 2013; Behler et al., 2018). CRISPRi typically uses a nuclease deficient Cas9 from *Streptococcus pyogenes* (dCas9) and has been demonstrated to work in several cyanobacterial species, including *Synechocystis* (Yao et al., 2016), PCC 7002 (Gordon et al., 2016); PCC 7942 (Huang et al., 2016) and *Anabaena* sp. PCC 7120 (Higo et al., 2018). A second approach for gene repression uses rationally designed small regulatory RNAs (srRNAs) to regulate gene expression at the translation stage (Na et al., 2013; Higo et al., 2018). In one approach, the synthetic srRNA is attached to a scaffold to recruit the Hfq protein, an RNA chaperone that is conserved in a wide-range of bacteria and cyanobacteria, which facilitates the hybridization of srRNA and target mRNA, and directs mRNA for degradation. The role of cyanobacterial Hfq in interacting with synthetic srRNAs is still unclear (Zess et al., 2016). However, regulatory ability can be improved by introducing Hfq from *E. coli* into *Synechocystis* (Sakai et al., 2015). Both CRISPRi- and srRNA-based systems have potential advantages as they can be used to repress multiple genes simultaneously.

3.4.6.1 dCas9

To validate the CRISPRi system, we assembled an expression cassette for dCas9 (P_{cpc560}-dCas9-T_{rrnB}) on the Level 1 position 1 vector pICH47732, and four different sgRNA expression cassettes (P_{trc10_TSS}-sgRNA-sgRNA scaffold) targeting eYFP on the Level 1 position 2 vector pICH47742 (Engler et al., 2014) (**Appendix Table 8-2**). For assembly of CRISPRi sgRNA expression cassettes in level 1, we targeted four 18–22-bp regions of the eYFP non-template strand with an adjacent 3’ protospacer adjacent motif (PAM) of 5′-NGG-3′, as required by *S. pyogenes* dCas9 (**Figure 3-8**:**A**). The sgRNA sequences contained no off-target sites in the *Synechocystis* genome

(confirmed by CasOT; (Xiao et al., 2014)). The sgRNAs templates were made by PCR using two complementary primers carrying the required overhangs and *Bsa*I sites, and were assembled with P_{trc10}_TSS promoter (pC0.203) and the sgRNA scaffold (pC0.122) (**Figure 3-1K**). Level T vectors were assembled carrying dCas9 and a single sgRNA, or just the sgRNA alone. We subsequently conjugated the Olive-eYFP mutant and tracked eYFP expression.

Transconjugants carrying only the sgRNA showed no reduction in eYFP level compared to that in non-transconjugated Olive-eYFP (**Figure 3-8**:**B**). However, all strains carrying dCas9 and a sgRNA showed a decrease in eYFP that ranged from 40–90% depending on the sgRNA used. These reductions are similar to those observed previously in PCC 7002 and in *Synechocystis* (Gordon et al., 2016; Yao et al., 2016) and demonstrated that CRISPRi system is functional in the CyanoGate kit.

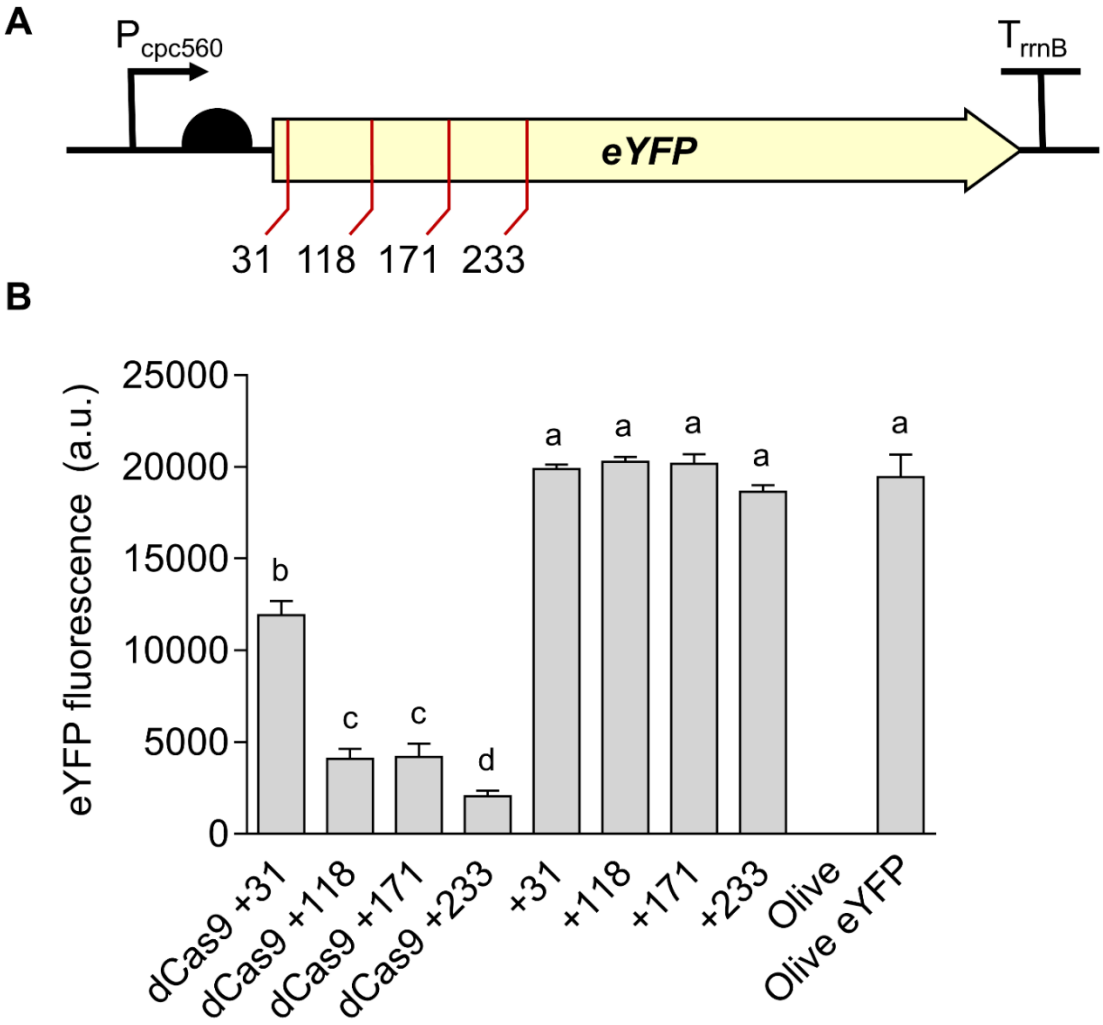

Figure 3-8: Gene regulation system using dCas9 CRISPRi in *Synechocystis*

(A) Four target regions were chosen as sgRNA protospacers to repress eYFP expression in Olive-eYFP (**Figure 3-4**): 'CCAGGATGGGCACCACCC' (+31), 'ACTTCAGGGTCAGCTTGCCGT' (+118), 'AGGTGGTCACGAGGGTGGGCCA' (+171) and 'AGAAGTCGTGCTGCTTCATG' (+233). (B) eYFP fluorescence of Olive-eYFP expressing constructs carrying sgRNAs with and without dCas9 (representative of 10,000 individual cells). Untransformed Olive-eYFP and the Olive mutant were used as controls. Letters indicating significant difference ($P < 0.05$) are shown, as determined by ANOVA followed by Tukey's HSD tests. Values are the means ± SE of four biological replicates. (Figure adapted from Vasudevan et al. (2019) [(www.plantphysiol.org) Copyright American Society of Plant Biologists. ASPB further grants to authors the permission to make digital or hard copies of part or all of a work published in Plant Physiology® without fee for personal or classroom use].

3.4.6.2 ddCas12a and paired termini antisense RNA

This section contains additional work that was not published with Vasudevan et al. (2019).

The more recently discovered Cas12a (formerly Cpf1), has some advantages over Cas9, including a smaller size and apparent reduced toxicity (Zetsche et al., 2015; Gale et al., 2019a). Similar to dCas9, ddCas12a is a mutated variant where the DNase activity has been eliminated to make it 'DNase dead'. ddCas12a has been used for CRISPRi applications in several organisms including the two cyanobacterial strains *Synechocystis* and UTEX 2973 (Knoot et al., 2020; Liu et al., 2020a). Unlike dCas9, ddCas12a possesses an RNase active catalytic site (RuvC-like domain), which enables ddCas12a to process its own guide strands (Zetsche et al., 2015; Fonfara et al., 2016). The enhanced abilities of ddCas12a conferred by the RNase activity have facilitated more elaborate gene repression studies, including the use of polycistronic guide strands that harbour sgRNAs for multiple target loci in a single expression cassette (Zhang et al., 2017). This potentially reduces the cloning complexity as fewer total expression cassettes are needed and thus fewer promoters and terminators are required (**Figure 3-10A, B**).

In addition to the Hfq-mediated sRNA gene repression discussed above, expression of an antisense RNA (asRNA) is another sRNA-based method used for gene repression. This relies solely on the expression of an asRNA, which through complementation binds to the nascent mRNA transcript making it unavailable for translation by the ribosome. However, sRNAs are prone to rapid degradation by endogenous RNase, which results in poor knockdown efficiency. asRNAs with a 'paired termini' design, that is a complementary region of ~38 bp at the 5' and 3' termini of the transcript, allows the sRNA to form a loop that confers some resistance to degradation thus results in higher knockdown efficiency (**Figure 3-10C**). The paired termini antisense RNA (PTasRNA) design has been demonstrated to increase knockdown efficiency in *E. coli* by ~60% over 'non-paired termini' asRNA (Nakashima et al., 2006)

and produce knockdown efficiencies of ~85% in *Synechocystis* (Sun et al., 2018b).

We have shown for dCas9 that choice of guide strand is important as repression can vary significantly (**Figure 3-8**:**B**), which has also been demonstrated previously (Yao et al., 2016). It can be laborious to test several different guide strands for the best repression. I hypothesised that using the RNase activity of ddCas12a to facilitate the processing of a polycistronic guide strand carrying several individual guide strands may lead to better repression when compared to the repression from a single guide strand alone. I also hypothesised that combining the transcription repression of ddCas12a, with the translational repression of PTasRNA, can also lead to increased repression and less reliance on the requirement to screen multiple sgRNAs.

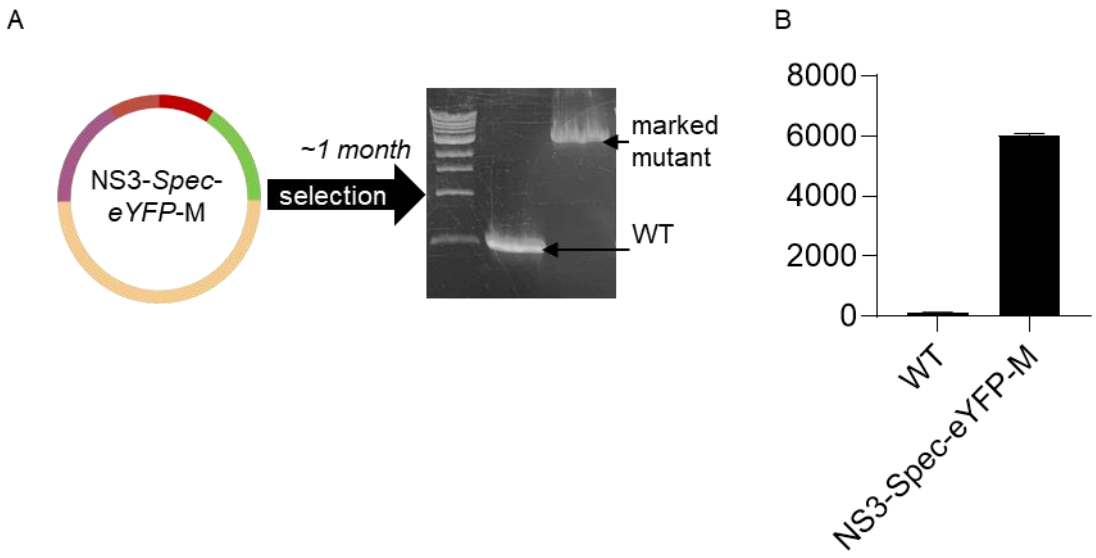

Figure 3-9: Generating a marked eYFP expressing mutant in *Synechocystis* sp. PCC 6803 in neutral site 3.

(A) Assembled level T vector NS3-*Spec*-*eYFP*-M (see Figure 3-1B) targeting neutral site 3 to insert Spec^R and P_{cpc560}-*eYFP* in *Synechocystis*. Following transformation and segregation on 50 µg/ml spectinomycin (*ca*. 1 month), a segregated marked mutant was isolated (WT band is 500 bp, marked mutant band is 3,313 bp, 1-kb DNA ladder (NEB) is shown). (B) Fluorescence values are the means ± SE of four biological replicates, where each replicate represents the median measurements of 10,000 cells.

To test the repression of ddCas12a and PTasRNA in *Synechocystis*, I constructed the new marked mutant NS3-*Spec-eYFP*. Using the strategy above (**Section 3.4.2**), I created the level T vector NS3-*Spec-eYFP*-M, containing $Spec^R$, P_{cpc560}-*eYFP*-T_{rrnB} and the flanking regions for NS3 (pC0.169 and pC0.170) (**Figure 3-1B, Figure 3-2, Supplementary Table S1**). On transformation and selection on 50 µg/ml spectinomycin, a fully segregated line was obtained after ~ 4 weeks and confirmed by PCR (**Figure 3-9**).

The ddCas12a mutant E917A from *Francisella novicida* was a gift from Liu Yang (Liu et al., 2019). I assembled the expression cassette for ddCas12a (P_{J23100}-ddCas12a-T_{rrnB}) into the Level 1 position 1 vector pICH47732 (Engler et al., 2014). Six expression cassettes were synthesised (Invitrogen GeneArt®), which included five containing either an individual sgRNA (P_{trc10_TSS}-sgRNA), or all four in a polycistronic array (P_{trc10_TSS}-sgRNA-Poly) as well as a PTasRNA expression cassette (P_{trc10_TSS}-PTasRNA). P_{trc10_TSS}-sgRNA and P_{trc10_TSS}-sgRNA-Poly were designed so that on *BpiI* digestion, Level 1 position 2 vector pICH47742 overhangs GCAA-ACTA would be generated, and P_{trc10_TSS}-PTasRNA was designed so that on *BpiI* digestion, Level 1 position 3 vector pICH47751 overhangs ACTA-TTAC would be generated (Engler et al., 2014). I designed the sgRNAs to target four loci within *eYFP* using Cas-Designer (http://www.rgenome.net/cas-designer/) adjacent to PAM 5′-TTN-3′ (Zetsche et al., 2015).

Transconjugants carrying only the sgRNA showed no reduction in eYFP expression compared to the NS3-*Spec-eYFP* mutant carrying an empty vector, which was as expected and commensurate with dCas9 (**Figure 3-8**:**B, Figure 3-10D**). For the strains carrying ddCas12a and a single sgRNA, the decrease in eYFP expression ranged from 0 – 85%. In contrast, the strain expressing all four sgRNA in the polycistronic array demonstrated only a 35% reduction (**Figure 3-10D**). A further unexpected result was the relative lack of reduction in eYFP expression from the strains carrying PTasRNA and the apparent attenuation in knockdown efficiency of ddCas12a-sgRNA when compared with the strains co-expressing PTasRNA in addition to ddCas12a-sgRNA.

Unfortunately I did not have further time to pursue these results. The next steps I would take to troubleshoot would be to test if the RNase activity of the ddCas12a is processing the guide strand RNA transcripts. I would have expected that the polycistronic guide array would have produced at least as good repression as ddCas12a-sgRNA +195. To do this, I would first use the 5' Rapid Amplification of cDNA Ends (RACE) method. The RACE method generates cDNA from mRNA, starting from a known internal site to an unknown sequence at either the 5' or 3' ends of the mRNA. The known internal sequence would be any of the four sgRNAs and once the length and sequence of the cDNA had been determined, it would be possible to confirm whether ddCas12a was cleaving at the DR. Another consideration is the composition of the guide strands, specifically the GC content. A very recent yet non-peer reviewed article, has proposed that high GC composition can affect the efficiency of the RNA cleavage (Magnusson et al., 2021). They report that the secondary structure produced by a GC rich guide sequence transcript may obscure the cleavage site, and therefore reduce efficiency of the guide strand processing by Cas12a. The GC content of my guide strands are all >60%, so it is possible that the secondary structure due to higher GC content is reducing processing efficiency.

The PTasRNA has also not worked as expected and no knockdown was demonstrated for any of these strains. My first approach would be to ascertain whether the PTasRNA is being expressed by performing an RNA extraction and reverse transcriptase reaction. On the cDNA, I would then do a regular PCR and electrophoresis gel to check for the presence of the asRNA.

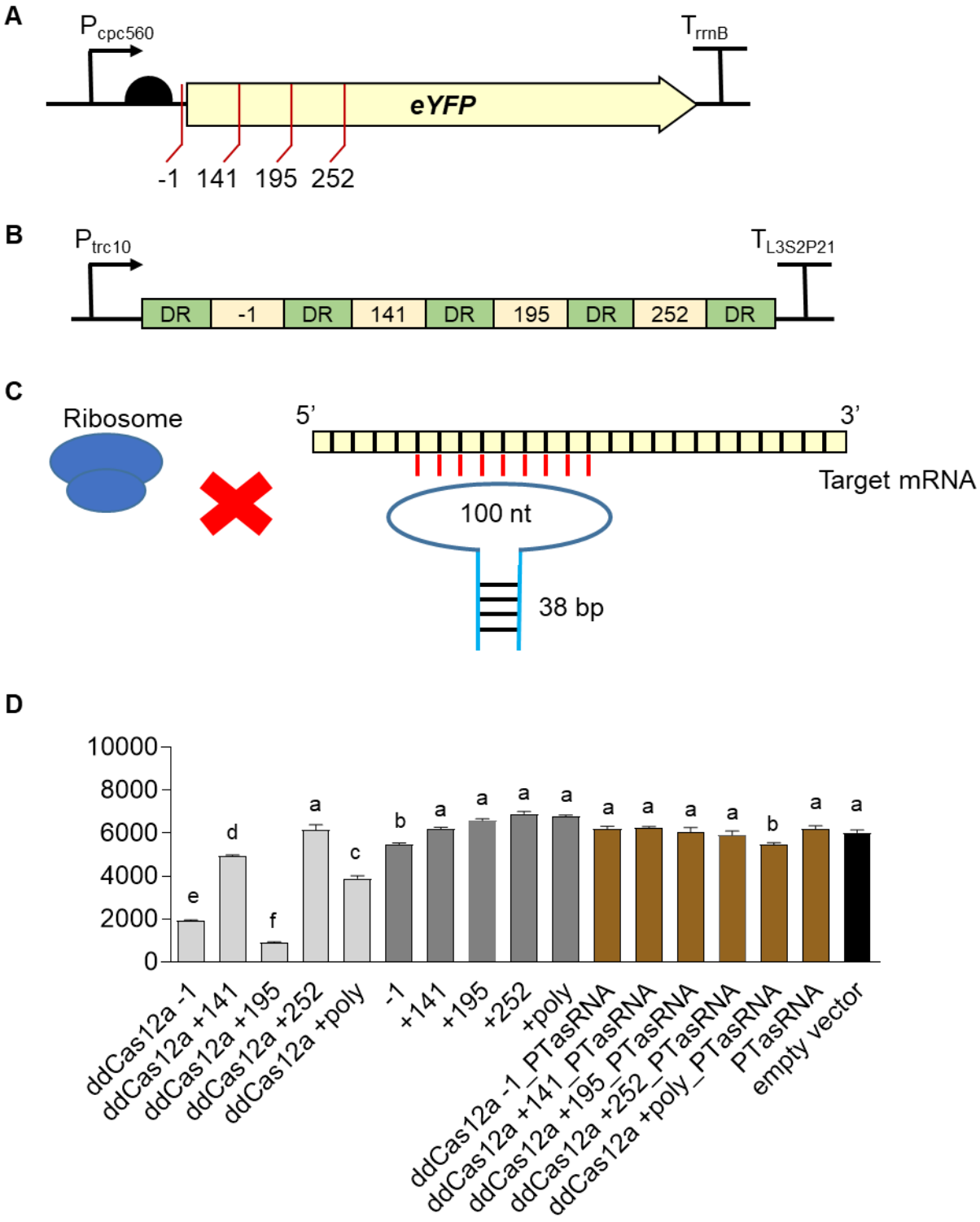

Figure 3-10: Gene regulation system using ddCas12a CRISPRi and paired termini antisense RNA in *Synechocystis*

Figure not to scale. (A) Four regions were chosen as sgRNA target loci to repress eYFP expression in NS3-*Spec-eYFP* (**Figure 3-9**): 'AATGGTGAGCAAGGGCGAGGAGC' (-1), 'ATCTGCACCACCGGCAAGCTGCC' (+141), 'GGCTACGGCCTGCAATGCTTCGC' (+195)

and 'TTCAAGTCCGCCATGCCCGAAGG' (+252). Each sgRNA sequence is flanked 5' and 3' by the 19bp direct repeat (DR) sequence 'AATTTCTACTGTTGTAGAT' (Fonfara et al., 2016) (B) Schematic of polycistronic guide strand harbouring all four sgRNAs, each flanked by a DR (see above). (C) Schematic of the paired termini antisense RNA (PTasRNA), where the region targeting the eYFP mRNA (100nt) 'GAACTTGTGGCCGTTTACGTCGCCGTCCAGCTCGACCAGGATGGGCACCACCCCGGT GAACAGCTCCTCGCCCTTGCTCACcattGAATTAATCTCCTAC' is flanked by 'AGGAGGAATTAACCATGCAGTGGTGGTGGTGGTGGTGC' at the 5' and the reverse compliment at the 3' end of the expression cassette (blue lines). The complementation of the PTasRNA with the mRNA transcript causes formation of double stranded RNA, which is inaccessible to the ribosome for translation. (D) eYFP fluorescence of NS3-*Spec-eYFP* expressing constructs. Light grey represents strains carrying ddCas12a with sgRNAs, dark grey sgRNAs alone, brown PTasRNA with and without ddCas12a with sgRNAs. (representative of 10,000 individual cells). NS3-*Spec-eYFP* carrying an empty vector (pPMQAK-T) was used as the control (black bar). Letters indicating significant difference ($P < 0.05$) are shown, as determined by ANOVA followed by Tukey's HSD tests. Values are the means ± SE of four biological replicates.

3.5 Conclusion

The CyanoGate kit was designed to increase the availability of well-characterised libraries and standardised modular parts in cyanobacteria (Sun et al., 2018a). We aimed to simplify and accelerate modular cloning methods in cyanobacterial research and allow integration with the growing number of labs that rely on the established common plant and algal syntax for multi-part DNA assembly (Patron et al., 2015; Crozet et al., 2018). Here, we have demonstrated the functionality of CyanoGate in sufficient detail to show that it is straightforward to adopt and functionally robust in *Synechocystis.* CyanoGate includes parts for usage in other cyanobacterial species and could likely be utilised also in non-cyanobacterial microbes amenable to transformation (e.g. *Rhodopseudomonas* spp.) and adapted for use in subcellular eukaryotic compartments of prokaryote origin (e.g. chloroplasts) (Economou et al., 2014; Doud et al., 2017; Leonard et al., 2018). In addition to the parts discussed, we have also assembled a suite of 21 terminators (**Appendix Table 8-1**). To increase the accessibility and usability of the CyanoGate, we have included the vector maps for all parts and new acceptors (see Vasudevan et al. (1019)), implemented support for CyanoGate

assemblies in the online DNA “Design and Build” portal of the Edinburgh Genome Foundry (dab.genomefoundry.org) (**Appendix Information 8-5**), and submitted all vectors as a toolkit for order from Addgene (Addgene Kit #1000000146; www.addgene.org/kits/mccormick-cyanogate).

Standardisation will help to accelerate the development of reliable synthetic biology tools for biotechnological applications and promote sharing and evaluation of genetic parts in different species and under different culturing conditions (Patron et al., 2015). Going forward, it will be important to test the performance of different parts with different components (e.g. gene expression cassettes) and in different assembly combinations. Several groups using plant MoClo assembly have reported differences in cassette expression and functionality depending on position and orientations (e.g. Ordon et al., (2017)), which highlights a key synthetic biology crux - the performance of a system is not simply the sum of its components (Mutalik et al., 2013; Heyduk & Heyduk, 2018).

Chapter 4 Genetic Modification of Cyanobacteria by Conjugation Using the CyanoGate Modular Cloning Toolkit

4.1 Chapter Preface

The following work was published in the *Journal of Visualised Experiments*[3]. As part of the CyanoGate project (**see Chapter 3**), we assembled and tested a suite of molecular parts and vectors for the engineering of cyanobacteria. To undertake this substantial work, there were several aspects including cyanobacterial conjugation, and growth and fluorescence experiments, that we had to optimise for this high throughput workflow to make the CyanoGate project possible. The Golden Gate cloning methodology does lend itself to high throughput testing owing to its 'Lego-like' modular assembly, thus we needed to develop new strategies to facilitate the growth and testing of many strains simultaneously. We were given the opportunity to publish our optimised protocols, which we felt was important to share with the community. If cyanobacterial synthetic biology is to progress at a reasonable pace, large scale parallel testing and characterisation is essential.

This was a collaborative project, and the protocols are based on the experience gained and optimisations performed by Alejandra A. Schiavon and I during the large-scale characterisation experiments that generated the data for CyanoGate. I wrote the introduction, all authors contributed to the writing of the protocols and discussion. All authors edited and proof-read the manuscript. Alejandra A. Schiavon performed the practical demonstration for the demonstration video[4].

[3] Gale, G. A. R., Schiavon Osorio, A. A., Puzorjov, A., Wang, B., McCormick, A. J. Genetic Modification of Cyanobacteria by Conjugation Using the CyanoGate Modular Cloning Toolkit. *J. Vis. Exp.* (152), e60451, doi:10.3791/60451 (2019).
[4] available at: https://www.jove.com/t/60451

4.2 Main Text

jove Journal of Visualized Experiments www.jove.com

Video Article

Genetic Modification of Cyanobacteria by Conjugation Using the CyanoGate Modular Cloning Toolkit

Grant A. R. Gale*[1,2,3], Alejandra A. Schiavon Osorio*[1,2], Anton Puzorjov*[1,2], Baojun Wang[2,3], Alistair J. McCormick[1,2]

[1]Institute of Molecular Plant Sciences, School of Biological Sciences, University of Edinburgh

[2]Centre for Synthetic and Systems Biology, University of Edinburgh

[3]Institute of Quantitative Biology, Biochemistry and Biotechnology, School of Biological Sciences, University of Edinburgh

*These authors contributed equally

Correspondence to: Alistair J. McCormick at alistair.mccormick@ed.ac.uk

URL: https://www.jove.com/video/60451
DOI: doi:10.3791/60451

Keywords: Biology, Issue 152, flow cytometry, fluorescence, Golden Gate, plate reader, *Synechocystis* sp. PCC 6803, *Synechococcus elongatus* UTEX 2973, toolkit, transient expression

Date Published: 10/31/2019

Citation: Gale, G.A., Schiavon Osorio, A.A., Puzorjov, A., Wang, B., McCormick, A.J. Genetic Modification of Cyanobacteria by Conjugation Using the CyanoGate Modular Cloning Toolkit. *J. Vis. Exp.* (152), e60451, doi:10.3791/60451 (2019).

Abstract

Cyanobacteria are a diverse group of prokaryotic photosynthetic organisms that can be genetically modified for the renewable production of useful industrial commodities. Recent advances in synthetic biology have led to development of several cloning toolkits such as CyanoGate, a standardized modular cloning system for building plasmid vectors for subsequent transformation or conjugal transfer into cyanobacteria. Here we outline a detailed method for assembling a self-replicating vector (e.g., carrying a fluorescent marker expression cassette) and conjugal transfer of the vector into the cyanobacterial strains *Synechocystis* sp. PCC 6803 or *Synechococcus elongatus* UTEX 2973. In addition, we outline how to characterize the performance of a genetic part (e.g., a promoter) using a plate reader or flow cytometry.

Video Link

The video component of this article can be found at https://www.jove.com/video/60451/

Introduction

Cyanobacteria are autotrophic bacteria that can be used for the biosynthesis of a wide variety of natural and heterologous high value metabolic products[1,2,3,4,5,6]. Several hurdles still need to be overcome to expand their commercial viability, most notably, the relatively poor yields compared to heterotrophic bio-platforms (e.g., *Escherichia coli* and yeast)[7]. The recent expansion of available genetic engineering tools and uptake of the synthetic biology paradigm in cyanobacterial research is helping to overcome such challenges and further develop cyanobacteria as efficient biofactories[8,9,10].

The main approaches for introducing DNA into cyanobacteria are transformation, conjugation and electroporation. The vectors transferred to cyanobacteria by transformation or electroporation are "suicide" vectors (i.e., integrative vectors that facilitate homologous recombination), while self-replicating vectors can be transferred to cyanobacteria by transformation, conjugation or electroporation. For the former, a protocol is available for engineering model species amenable to natural transformation[11]. More recently, a modular cloning (MoClo) toolkit for cyanobacteria called CyanoGate has been developed that employs a standardized Golden Gate vector assembly method for engineering using natural transformation, electroporation or conjugation[12].

Golden Gate-type assembly techniques have become increasingly popular in recent years, and assembly standards and part libraries are now available for a variety of organisms[13,14,15,16,17]. Golden Gate uses type IIS restriction enzymes (e.g., BsaI, BpiI, BsmBI, BtgZI and AarI) and a suit of acceptors and unique overhangs to facilitate directional hierarchical assembly of multiple sequences in a "one pot" assembly reaction. Type IIS restriction enzymes recognize a unique asymmetric sequence and cut a defined distance from their recognition sites to generate a staggered, "sticky end" cut (typically a 4 nucleotide [NT] overhang), which can be subsequently exploited to drive ordered DNA assembly reactions[15,18]. This has facilitated the development of large libraries of modular Level 0 parts (e.g., promoters, open reading frames and terminators) defined by a common syntax, such as the PhytoBricks standard[19]. Level 0 parts can then be readily assembled into Level 1 expression cassettes, following which more complex higher order assemblies (e.g., multigene expression constructs) can be built in an acceptor vector of choice[12,15]. A key advantage of Golden Gate-type assembly techniques is their amenability to automation at high-throughput facilities, such as DNA foundries[20,21], which can allow for the testing of complex experimental designs that cannot easily be achieved by manual labor.

CyanoGate builds on the established Plant MoClo system[12,15]. To incorporate a new part into CyanoGate, the part sequence must first be domesticated, i.e., "illegal" recognition sites for BsaI and BpiI must be removed. In the case of a part coding for an open reading frame (i.e., a coding sequence, CDS), recognition sites can be disrupted by generating synonymous mutations in the sequence (i.e., changing a codon to an alternative that encodes for the same amino acid residue). This can be achieved by a variety of approaches, ranging from DNA synthesis

jove Journal of Visualized Experiments www.jove.com

to polymerase chain reaction (PCR) amplification-based strategies such as Gibson assembly[22]. Depending on the expression host being used, care should be taken to avoid the introduction of rare codons that could inhibit the efficiency of translation[23]. Removing recognition sites in promoter and terminator sequences is typically a riskier endeavor, as modifications may affect function and the part might not perform as expected. For example, changes to putative transcription factor binding sites or the ribosome binding site within a promoter could alter strength and responsiveness to induction/repression. Likewise, modifications to key terminator structural features (e.g., the GC rich stem, loop and poly-U tail) may change termination efficiency and effect gene expression[24,25]. Although several online resources are available to predict the activity of promoter and terminator sequences, and inform whether a proposed mutation will impact performance[26,27], these tools are often poor predictors of performance in cyanobacteria[28,29,30]. As such, in vivo characterization of modified parts is still recommended to confirm activity. To assist with the cloning of recalcitrant sequences, CyanoGate includes a low copy cloning acceptor vector based on the BioBrick vector pSB4K5[12,16,31]. Furthermore, a "Design and Build" portal is available through the Edinburgh Genome Foundry to help with vector design (dab.genomefoundry.org). Lastly, and most importantly, CyanoGate includes two Level T acceptor vector designs (equivalent to Level 2 acceptor vectors)[15] for introducing DNA into cyanobacteria using suicide vectors, or broad host-range vectors capable of self-replication in several cyanobacterial species[32,33,34].

Here we will focus on describing a protocol for generating Level T self-replicating vectors and the genetic modification of *Synechocystis* PCC 6803 and *Synechococcus elongatus* UTEX 2973 (*Synechocystis* PCC 6803 and *S. elongatus* UTEX 2973 hereafter) by conjugation (also known as tri-parental mating). Conjugal transfer of DNA between bacterial cells is a well described process and has been previously used for engineering cyanobacterial species, in particular those that are not naturally competent, such as *S. elongatus* UTEX 2973[35,36,37,38,39,40,41]. In brief, cyanobacterial cultures are incubated with an *E. coli* strain carrying the vector to be transferred (the "cargo" vector) and vectors (either in the same *E. coli* strain or in additional strains) to enable conjugation ("mobilizer" and "helper" vectors). Four key conditions are required for conjugal transfer to occur: 1) direct contact between cells involved in DNA transfer, 2) the cargo vector must be compatible with the conjugation system (i.e., it must contain a suitable origin of transfer (*oriT*), also known as a *bom* (basis of mobility) site), 3) a DNA nicking protein (e.g., encoded by the *mob* gene) that nicks DNA at the *oriT* to initiate single-stranded transfer of the DNA into the cyanobacterium must be present and expressed from either the cargo or helper vectors, and 4) the transferred DNA must not be destroyed in the recipient cyanobacterium (i.e., must be resistant to degradation by, for example, restriction endonuclease activity)[35,42]. For the cargo vector to persist, the origin of replication must be compatible with the recipient cyanobacterium to allow for self-replication and proliferation into daughter cells post division. To aid with conditions 3 and 4, several helper vectors are available through Addgene and other commercial sources that encode for *mob* as well as several methylases to protect from native endonucleases in the host cyanobacterium[43]. In this protocol, conjugation was facilitated by an MC1061 *E. coli* strain carrying mobilizer and helper vectors pRK24 (www.addgeneorg/51950) and pRL528 (www.addgene.org/58495), respectively. Care must be taken when choosing the vectors to be used for conjugal transfer. For example, in the CyanoGate kit the self-replicating cargo vector pPMQAK1-T encodes for a Mob protein[12]. However, pSEVA421-T does not[44], and as such, *mob* must be expressed from a suitable helper vector. The vectors used should also be appropriate to the target organism. For example, efficient conjugal transfer in *Anabaena* sp. PCC 7120 requires a helper vector that protects the mobilizer vector against digestion (e.g., pRL623, which encodes for the three methylases AvaiM, Eco47iiM and Ecot22iM)[45,46].

In this protocol we further outline how to characterize the performance of parts (i.e., promoters) with a fluorescent marker using a plate reader or a flow cytometer. Flow cytometers are able to measure fluorescence on a single cell basis for a large population. Furthermore, flow cytometers allow users to "gate" the acquired data and remove background noise (e.g., from particulate matter in the culture or contamination). In contrast, plate readers acquire an aggregate fluorescence measurement of a given volume of culture, typically in several replicate wells. Key advantages of plate readers over cytometers include the lower cost, higher availability and typically no requirement for specialist software for downstream data analyses. The main drawbacks of plate readers are the relatively lower sensitivity compared to cytometers and potential issues with the optical density of measured cultures. For comparative analyses, plate reader samples must be normalised for each well (e.g., to a measurement of culture density, typically taken as the absorbance at the optical density at 750 nm [OD_{750}]), which can lead to inaccuracies for samples that are too dense and/or not well mixed (e.g., when prone to aggregation or flocculation).

As an overview, here we demonstrate in detail the principles of generating Level 0 parts, followed by hierarchical assembly using the CyanoGate kit and cloning into a vector suitable for conjugal transfer. We then demonstrate the conjugal transfer process, selection of axenic transconjugant strains expressing a fluorescent marker, and subsequent acquisition of fluorescence data using a flow cytometer or a plate reader.

Protocol

1. Vector assembly using the Plant MoClo and CyanoGate toolkits

NOTE: Before proceeding with vector assembly, it is strongly recommended that users familiarize themselves with the vector level structures of the Plant and CyanoGate MoClo systems[12,15].

1. Construction of Level 0 parts
   NOTE: Level 0 parts can be synthesized as complete vectors or as linear sequences for assembly with Level 0 acceptors (e.g., gBlocks, IDT). Alternatively, sequences can be amplified from a source template (e.g., a vector or purified genomic DNA). Here, how to generate a new Level 0 part from an amplified product is described. An overview of the Golden Gate assembly process from Level 0 to Level T is shown in **Figure 1**.
   1. Design the primers.
      1. Decide what Level 0 module to assemble and identify the appropriate 5′ and 3′ overhangs (**Table 1**)[12,15]. Check the DNA sequence to clone for the presence of BpiI or BsaI restriction sites.
         NOTE: A sequence containing one of these sites must be domesticated by modifying one or more NTs in the restriction site sequence. A strategy for doing this using Golden Gate assembly is outlined in **Figure 2**.
      2. To amplify a DNA sequence, design an appropriate forward and reverse primer pair. For the forward primer, select 18−30 bp complementary to the 5′ end of the DNA template sequence. For the reverse primer, select 18−30 bp reverse complementary to the 3′ end of the DNA template sequence.

jove Journal of Visualized Experiments www.jove.com

NOTE: Primers with melting temperatures (T_m) of 58−62 °C typically give the most consistent amplification results (**Figure 1A**).
3. Add the following to the 5′ end of the forward primer: 1) a random string of 4−6 NTs at the 5′ end of the BpiI site, 2) the BpiI restriction site (GAAGAC), 3) two random NTs, and 4) the 5′ overhang selected in step 1.1.1.1. Add the following to the 5′ end of the reverse primer: 1) a random string of 4−6 NTs at the 5′ end of the BpiI site, 2) the BpiI restriction site (GAAGAC), 3) two random NTs, and 4) the 3′ overhang selected in step 1.1.1.1. When finalized, order the primer pairs.
NOTE: See **Figure 1A** for an example of a forward and reverse primer pair.

2. Amplify a DNA sequence from genomic DNA.
1. Extract genomic DNA as described in section 5. Amplify products by PCR using a high-fidelity DNA polymerase (**Table of Materials**).
NOTE: As an example, set up PCR reactions (20−50 µL) according to manufacturer's instructions. Use ~100 ng of genomic DNA per reaction. Use a thermal cycling program consisting of an initial denaturation step of 98 °C for 30 s, followed by no more than 25 cycles of denaturation at 98 °C for 10 s, primer annealing at 58 °C for 15 s and product extension at 72 °C for 30 s (modify the latter depending on the size of the product/type of DNA polymerase used), followed by a final extension step of 72 °C for 2 min.
2. If the PCR product is to be gel purified, run the entire PCR reaction on an agarose gel as described in section 6. Cut the band of interest out of the agarose gel and purify it using a gel extraction kit (**Table of Materials**).
3. Alternative to step 1.1.2.2, if the PCR product is to be used without gel purification, verify the band size by running an aliquot of the PCR reaction sample (~5 µL) on an agarose gel. If the gel shows only the appropriate band and no evidence of primer dimers, purify the PCR product using a DNA purification kit (**Table of Materials**).
4. Elute purified DNA in a small volume of deionized water (e.g., 10 µL) to obtain a high DNA concentration (>20 ng/µL is typically sufficient).

3. Assemble the amplified DNA product (or products, see **Figure 2**) in Level 0. Prepare a 20 µL reaction mix with BpiI (**Figure 1B**) and set up the thermal cycler program as described in **Table 2**. Proceed to *E. coli* transformation using 5 µL of the assembled Level 0 reaction mix (as described in section 2).

2. Construction of Level 1 assemblies
1. Decide what Level 0 parts to assemble (**Figure 1C** and **Table 1**). Choose an appropriate Level 1 acceptor vector[15].
NOTE: At this stage it is important to know what the final vector design will be in Level T, as this will impact the choice of Level 1 acceptor vector. Level 1 position 1 (Forward) acceptor vector (pICH47732) can be used as a default if the goal is to have a single Level 1 assembly (e.g., a gene expression cassette) in Level T. However, if two or more Level 1 assemblies are to be assembled in Level T, the position and direction of each Level 1 assembly must be considered. Up to seven Level 1 assemblies can be assembled in a Level T acceptor vector by using Level 1 acceptor vectors with appropriate positions[12].
2. Assemble the Level 0 parts in Level 1. Prepare a 20 µL reaction mix with BsaI and set up the thermal cycler program as described in **Table 2**. Proceed to *E. coli* transformation using 5 µL of the assembled Level 1 reaction mix (as described in section 2).

3. Construction of Level T assemblies
1. Decide what Level 1 assemblies to assemble (**Figure 1D**). Choose an appropriate Level T acceptor vector.
NOTE: pUC19A-T (ampicillin resistance) and pUC19S-T (spectinomycin resistance) are high-copy number integrative vectors that are not able to replicate in cyanobacteria and are primarily used for genomic integration (i.e., knock-in or knock-out of genes) via homologous recombination[12]. Delivery of integrative vectors can proceed by natural transformation in amenable cyanobacterial species[11]. pPMQAK1-T is a broad host range, replicative vector that is delivered by conjugal transfer (section 3).
2. Choose an appropriate End-Link to ligate the 3′ end of the final Level 1 assembly to the Level T backbone[15].
NOTE: The End-Link required is the same number as the position of the final part. For example, a Level T vector with only one Level 1 position 1 (forward or reverse) part will require End-Link 1 (pICH50872) for ligation into the Level T backbone.
3. Assemble one or more Level 1 assemblies in Level T. Prepare a reaction mix with BpiI and the required End-Link vector and set up the thermal cycler program as described in **Table 2**. Proceed to *E. coli* transformation using 5 µL of the assembled Level T reaction mix (as described in section 2).

2. *E. coli* transformation and vector purification

1. *E. coli* transformation (day 1)
1. Defrost an aliquot (~25 µL) of chemically competent *E. coli* cells (**Table of Materials**) and gently pipette into a 1.5 mL tube on ice. Add 5 µL of the assembly mix (Level 0, 1 or T) and incubate the tube on ice for a further 30−60 min.
2. Heat-shock cells by incubating the tube in a water bath at 42 °C for 30 s, then place the tube back on ice for 2 min. Add room temperature (RT) super optimal broth with catabolite repression (S.O.C.) medium (250 µL) to the tube. Incubate the tube at 37 °C for 1 h at 225 rpm in a shaking incubator.
3. Plate 40 µL of the culture onto an LB agar plate containing the appropriate final concentration of antibiotics (100 µg/mL for spectinomycin dihydrochloride pentahydrate [Level 0], 100 µg/mL of carbenicillin disodium [Level 1], or 50 µg/mL of kanamycin sulphate [Level T]), 1 mM isopropyl-beta-D-thiogalactopyranoside (IPTG) and 40 µg/mL of 5-bromo-4-chloro-3-indolyl-β-D-galactopyranoside (X-Gal) for blue-white screening. Incubate the plate overnight at 37 °C.
NOTE: The amount of culture plated can be varied depending on the efficiency of the *E. coli* competent cells and the ligation reaction. Plate a larger volume if <10 colonies are observed after overnight incubation.

2. Selection of white colonies and preparation of liquid cultures (day 2)
NOTE: Depending on the efficiencies of the assembly reaction and subsequent transformation, LB agar plates may contain no colonies, blue colonies or white colonies (**Figure 3**). Blue colonies are indicative of acceptor vectors that have not undergone restriction (i.e., a functional copy of *lacZ* is still present). White colonies indicate that the *lacZ* expression cassette has been lost and replaced by a part/assembly.
1. Optionally, validate that white colonies contain the expected vector by performing PCR as described in section 7.

jove Journal of Visualized Experiments www.jove.com

2. Pick single white colonies (or PCR verified colonies) with a 10 µL tip and transfer to a 15 mL centrifuge tube containing LB medium (5 mL) and appropriate antibiotic concentrations (step 2.1.3). Incubate the tubes at 37 °C overnight at 225 rpm in a shaking incubator.

3. Plasmid vector purification (day 3)
   1. Optionally, prepare a glycerol stock of the overnight *E. coli* culture for long-term cryostorage of vectors. Add 500 µL of bacterial culture to 500 µL of 50% (v/v) glycerol in an appropriate 1.5−2.0 mL tube for cryostorage at -80 °C. Mix gently by inverting 5−10x. Flash-freeze samples in liquid nitrogen and store in a -80 °C freezer.
   2. Spin down cultures in 15 mL centrifuge tubes at 3,000 x *g* for 5−10 min. Discard the supernatant without disturbing the cell pellet. Purify the vector using a plasmid purification kit (**Table of Materials**). Elute purified vector in 35 µL of deionized water.
      NOTE: Use lower elution volumes to further increase the vector concentration. The same eluent can be put through a purification column twice for increased yields.
   3. Measure the concentration of the vector in the eluent using a spectrophotometer (**Table of Materials**).
      NOTE: High copy-number vectors in *E. coli*, such as pUC19, typically give yields of 50−300 ng/µL. Low copy-number vectors, such as pPMQAK1-T, typically give yields of 15−60 ng/µL.

4. Vector validation
   NOTE: Vectors can be verified by restriction digestion (step 2.4.1) and/or sequencing (step 2.4.2).
   1. Restrict 0.5−1 µg of vector with an appropriate restriction enzyme(s) and verify the expected band sizes as described in section 6 (**Figure 4**).
      NOTE: Incorrect band sizes typically indicate erroneous assembly, in which case more white colonies can be screened or assembly can be repeated. BsaI and BpiI can be used to validate the correct size of the insert for Level 0 and Level 1 assemblies, respectively. BsaI or BpiI can be used in conjunction with an additional, compatible restriction enzyme that cuts within the insert and/or the vector backbone to produce a distinct set of well-separated bands following digestion.
   2. Sequence the vector by Sanger sequencing using an appropriate primer upstream of the assembled region using commercial sequencing facility (**Table 3**).
      NOTE: All new Level 0 parts should be sequenced to confirm the expected sequence identity. Sequence validation of Level 1 and T vectors is not typically required if assembled from previously sequenced level 0 parts.

3. Generation of mutants by conjugation

NOTE: Here, a protocol for conjugal transfer of a self-replicating cargo vector into *Synechocystis* PCC 6803 or *S. elongatus* UTEX 2973[11,47] is described. This protocol is applicable to other model species (e.g., *S. elongatus* PCC 7942 and *Synechococcus* sp. PCC 7002). All work with cyanobacteria (and associated buffer preparations) should be done under sterile conditions in a laminar flow hood.

1. Growth of the cyanobacterial culture (day 1)
   1. Prepare BG11 medium according to Lea-Smith et al.[11], and agar plates with LB-BG11 and BG11+Kan50 (section 8).
   2. Set up a fresh culture of *Synechocystis* PCC 6803 or *S. elongatus* UTEX 2973 by inoculating a 100 mL conical flask of fresh BG11 medium (50 mL) with cells sourced from an axenic BG11 agar plate. Grow *Synechocystis* PCC 6803 cultures at 30 °C, 100 µmol photons $m^{-2}s^{-1}$ at 100 rpm and grow *S. elongatus* UTEX 2973 at 40 °C, 300 µmol photons $m^{-2}s^{-1}$ at 100 rpm. Grow cultures until OD_{750} = 0.5−1.5 (typically 1−2 days).
      NOTE: *S. elongatus* UTEX 2973 cultures can be grown at 40 °C in high light intensities (e.g., 2000 µmol photons $m^{-2}s^{-1}$)[48].

2. Growth of helper and cargo *E. coli* strains (day 2)
   1. Inoculate LB medium containing ampicillin (final concentration 100 µg/mL) and chloramphenicol (final concentration 25 µg/mL) with a MC1061 *E. coli* strain containing vectors pRK24 and pRL528 (i.e., the helper strain) and grow at 37 °C overnight at 225 rpm in a shaking incubator. Grow up a sufficient volume of helper strain culture, assuming 1 mL of culture is required per conjugation.
   2. Inoculate LB medium (5 mL) containing appropriate antibiotics with the *E. coli* culture carrying the cargo vector (i.e., a Level T vector). Grow the culture at 37 °C overnight at 225 rpm in a shaking incubator.

3. Conjugal transfer (tri-parental mating) (day 3)
   1. Prepare the *E. coli* helper and cargo strains. Centrifuge the helper and the cargo *E. coli* overnight cultures at 3,000 x *g* for 10 min at room temperature. Discard the supernatant without disturbing the cell pellet.
   2. Wash the pellet by adding fresh LB medium without antibiotics. Use the same volume as the initial culture. Resuspend the pellet by gently pipetting up and down. Do not vortex the culture. Repeat this step 3x to remove residual antibiotics from the overnight culture.
   3. Centrifuge the resuspended culture (as in step 3.3.1), discard the supernatant and resuspend in half the volume of LB medium of the initial culture volume (e.g., 2.5 mL if the overnight culture was 5 mL). Combine 450 µL of the helper strain with 450 µL of the cargo strain in a 2 mL tube and set aside (leave at RT) until step 3.3.6.
   4. Prepare the cyanobacterial culture. For each conjugation reaction, use 1 mL of cyanobacterial culture (OD_{750} = 0.5−1.5).
   5. Centrifuge the required total volume of cyanobacterial culture at 1,500 x *g* for 10 min at RT, then discard the supernatant carefully without disturbing the cell pellet. Wash the pellet by adding fresh BG11 medium of the same initial volume. Resuspend the pellet by gently pipetting up and down, do not vortex the culture. Repeat this step 3x and set the washed culture aside.
   6. Add an aliquot of washed cyanobacterial culture (900 µL) to the combined *E. coli* strains (helper and cargo) (900 µL) in a 2 mL tube. Mix the cultures by gently pipetting up and down. Do not vortex. Incubate the mixture at RT for 30 min for *Synechocystis* PCC 6803 or 2 h for *S. elongatus* UTEX 2973.
   7. Centrifuge the mixture at 1,500 x *g* for 10 min at RT. Remove 1.6 mL of the supernatant. Resuspend the pellet in the remaining ~200 µL of supernatant. Place one 0.45 µm membrane filter on an LB-BG11 agar plate lacking antibiotics (section 8). Carefully spread 200 µL of the *E. coli*/cyanobacterial culture mix on the membrane with a sterile spreader or a sterile bended tip and seal the plate with paraffin film.

jove Journal of Visualized Experiments www.jove.com

8. Incubate the LB-BG11 plate with the membrane for 24 h. Maintain membranes with *Synechocystis* PCC 6803 cultures at 30 °C, 100 µmol photons $m^{-2}s^{-1}$. Maintain membranes with *S. elongatus* UTEX 2973 cultures at 40 °C in 150 µmol photons $m^{-2}s^{-1}$.

4. Membrane transfer
   1. After 24 h, carefully transfer the membrane using flame-sterilized forceps to a fresh BG11 agar plate containing appropriate antibiotics (section 8) to select for the cargo vector. Seal the plate with paraffin film.
   2. Incubate the BG11 agar plate under appropriate growth conditions, as described above for *Synechocystis* PCC 6803 or *S. elongatus* UTEX 2973, until colonies appear.
      NOTE: Colonies typically appear after 7−14 days for *Synechocystis* PCC 6803 and 3−7 days for *S. elongatus* UTEX 2973.

5. Selection of conjugants
   NOTE: Only cyanobacterial colonies carrying the cargo vector will be able to grow on the membrane (**Figure 5**).
   1. Using a heat sterile loop, select at least two individual colonies from the membrane and streak onto a new BG11 agar plate containing appropriate antibiotics (**Figure 5C**).
      NOTE: Freshly streaked colonies may still be contaminated with *E. coli* carried over from conjugation (i.e., if small white colonies are evident on the plate), so two or three additional rounds of re-streaking onto fresh BG11 agar plates typically are needed to obtain an axenic cyanobacterial culture.
   2. Confirm absence of *E. coli* contamination by inoculating a streak of cyanobacterial culture into a 15 mL centrifuge tube containing 5 mL of LB medium and incubating at 37 °C overnight at 225 rpm in a shaking incubator. Following a sufficient growth period (~7 days), pick individual axenic colonies to set up liquid cultures for long-term cryostorage or subsequent experimentation.

6. Cryostorage of cyanobacterial strains
   1. Grow a cyanobacterial liquid culture in BG11 (as described in section 3.1) until OD_{750} = 1.5−3.0. Centrifuge 10 mL of culture for 10 min at 1,500 x *g*, remove the supernatant and resuspend the cells in 5 mL of fresh BG11 medium.
   2. Add 3.5 mL of autoclave sterilized 50% (v/v) glycerol for a final glycerol concentration of ~20% (v/v)[49]. This approach works well for *Synechocystis* PCC 6803. Alternatively, add 5 mL of filter sterilized BG11 containing 16% (v/v) dimethyl sulfoxide (DMSO) for a final DMSO concentration of ~8% (v/v)[50]. This approach is recommended for most strains, including *S. elongatus* UTEX 2973.
      CAUTION: DMSO is toxic and should be handled with appropriate protection.
   3. Mix gently by inverting 5−10x. Subaliquot ~1 mL of culture into separate cryostorage compatible 1.5 mL screw-cap tubes (**Table of Materials**). Place tubes in a -80 °C freezer for cryostorage. Do not flash freeze in liquid nitrogen.
      NOTE: At least three stocks per strain are recommended.
   4. For recovery, remove a tube from the -80 °C freezer and thaw the culture in a 35 °C water bath while gently mixing. Add the thawed culture to 50 mL of fresh BG11 medium and grow as a liquid culture (as described in section 3.1).
      NOTE: Alternatively, the culture can be streaked and grown on a fresh BG11 agar plate. Transgenic cultures carrying selection markers must be revived initially on BG11 agar plates without antibiotics and then restreaked onto BG11 agar plates with appropriate antibiotics.

4. Promoter characterization

NOTE: Here a standard approach is described for analyzing the strength of a promoter part by measuring the expression levels of a fluorescent marker (eYFP) following a 72 h growth period using either a plate reader or a flow cytometer[12].

1. Culture growth
   1. Set up seed cultures by inoculating 10 mL of BG11 medium containing appropriate antibiotics with a single colony of the transgenic cyanobacterial strain carrying the fluorescent marker expression cassette. Also prepare seed cultures for appropriate negative control strains (e.g., a wild type strain and/or a transgenic strain carrying the same vector backbone but lacking the fluorescent marker expression cassette).
      NOTE: At least four biological replicates are recommended.
   2. Grow the seed cultures for 48 h or until OD_{750} = 1−1.5 under growth conditions appropriate for the species strain.
   3. To track promoter expression over time, first measure the OD_{750} of each seed culture. Calculate the dilution requirements to bring each culture to a starting OD_{750} = 0.2. Set up diluted experimental culture samples (2 mL total volume) in a flat-bottom 24-well plate (**Table of Materials**).
   4. Incubate the plate in a shaking incubator with white LED lights (**Table of Materials**) under appropriate growth conditions. Measure culture growth density (OD_{750}) and enhanced yellow fluorescent protein (eYFP) fluorescence using either a plate reader (section 4.2) or a flow cytometer (section 4.3).
      NOTE: *Synechocystis* PCC 6803 and *S. elongatus* UTEX 2973 cultures can be grown as in step 3.1.2. It is highly recommended that the plate be maintained under a high humidity (95%) to avoid evaporation of the culture samples.

2. Plate reader
   1. Briefly mix the cultures in the 24-well plate (step 4.1.4) with gentle pipetting. Transfer a sub-sample of each culture to a black flat-bottom 96-well plate (**Table of Materials**). Dilute if necessary (100 µL final volume). Avoid the formation of bubbles as this can interfere with measurement accuracy.
      NOTE: It is recommended that all measurements be performed on samples in an OD_{750} range of 0.2−1.0. As the density of the cultures in the 24-well will increase over time, the following dilutions are recommended based on the expected increases in standard growth conditions: no dilution at 0 h, 1:4 at 24 h, 1:10 at 48 h and 1:10 at 72 h. So for example, at 24 h harvest 25 µL of culture and mix with 75 µL of BG11 medium.
   2. Include two blank wells in the 96-well plate (i.e., 100 µL of BG11 medium). Put the 96-well plate into a plate reader (**Table of Materials**). Shake the plate for 60 s at 500 rpm using the orbital shaker in the plate reader to mix the wells.
      NOTE: Cyanobacterial cultures can aggregate and/or flocculate, so good mixing is critical prior to reading for accurate measurements.
   3. Measure OD_{750} and eYFP fluorescence with excitation/emission wavelengths at 485 nm/520 nm.

jove Journal of Visualized Experiments www.jove.com

4. Subtract the average of the OD_{750} measurements of the two blank wells from the OD_{750} measurement of each sample well containing cyanobacteria culture.
5. Normalize the fluorescence values of each culture sample by dividing the eYFP fluorescence measurement (step 4.2.3) by the adjusted OD_{750} of the culture (step 4.2.4). Then, subtract the average normalized eYFP fluorescence value (eYFP fluorescence/OD_{750}) of the biological replicates of an appropriate negative control strain from the transgenic strains carrying the eYFP expression cassette.
   NOTE: Cyanobacteria naturally fluoresce due the presence of pigments, such as chlorophyll and phycobiliproteins.
6. Plot culture growth over time (**Figure 6A**) and the average normalized eYFP fluorescence values of each experimental culture at the desired time points (e.g., 72 h; **Figure 6B**).

3. Flow cytometer
   1. Choose a compatible plate for the flow cytometer liquid handling system. For example, use a round-bottom 96-well plate (**Table of Materials**) with the flow cytometer (**Table of Materials**) used in this protocol.
   2. Briefly mix the cultures in the 24-well plate (step 4.1.4) with gentle pipetting. Dilute cultures to OD_{750} = 0.1−0.2 to avoid nozzle blockages in the liquid handling system. Add an appropriate volume of culture sample to the 96-well plate and bring to a final volume of 250 µL with filter-sterilized 1x phosphate-buffered saline (PBS). Include a blank well for the medium solution on the plate containing 60 µL of BG11 and 190 µL of 1x PBS.
      NOTE: This volume is recommended in case there is a need to re-run samples. Volumes higher than 250 µL are not recommended as the maximum volume of each well is 300 µL.
   3. Once the flow cytometer is ready for use, place the 96-well plate with culture samples in the liquid handling station. Set up the software protocol for the flow cytometer to collect the measurements of 10,000 individual events (e.g., cells). Measure eYFP fluorescence with excitation/emission wavelengths of 488 nm/515−545 nm. First measure and check the reading from the blank well (**Figure 7A**), then run the samples.
   4. Gate the population of cyanobacteria cells within the forward and side scatter data sets, excluding regions common with the blank reading (**Figure 7B**). Subtract the average eYFP fluorescence values of the biological replicates of an appropriate negative control strain from the transgenic strains carrying the eYFP expression cassette (**Figure 7C,D**). Plot the average of the median fluorescence values per cell for each experimental culture at the desired time points (e.g., 72 h; **Figure 7E**).

5. Genomic DNA extraction from cyanobacteria

NOTE: The protocol below uses a commercial DNA extraction kit (**Table of Materials**).

1. Grow a cyanobacterial liquid culture in BG11 (as described in section 3.1) until OD_{750} = 1.5−3.0. Spin down 10 mL of culture at 3,000 x *g* for 10 min and discard the supernatant. Freeze the pellet by incubating the tubes at -20 °C for 30 min.
2. Add 400 µL of lysis buffer (buffer AP1) and 400 µL of ribonuclease solution (RNase A), and 50% (w/v) of glass beads (0.5 mm diameter). Disrupt samples using a bead mill (**Table of Materials**) at 30 Hz (i.e., equivalent to 1,800 oscillations/min) for 6 min.
3. Spin the sample at 17,000 x *g* for 5 min and carefully transfer the supernatant into a new tube and discard the pellet. Proceed according to the manufacturer's instructions (**Table of Materials**).

6. Agarose gel electrophoresis

1. Cast a 1% (w/v) agarose gel containing 0.02% (v/v) ethidium bromide. Load samples and an appropriate DNA ladder reference.
2. Run the samples for 50 min at 125 V. Check for band separation on an ultraviolet (UV) transilluminator.
   NOTE: The running time and agarose gel percentage can be modified to suit the expected band size. For example, a higher percentage agarose gel and longer running time may improve the band resolution and separation of DNA products <500 bp.

7. Colony PCR

1. Set up a PCR reaction mix using a standard kit (**Table of Materials**) and an appropriate combination of primers (e.g., primers that flank the assembly region or are specific to sequences within the assembly region (**Table 3**). Pipette 10 µL into a PCR tube.
2. Gently touch the top of a single white colony with a sterile toothpick or 10 µL pipette tip and inoculate a PCR tube containing PCR reaction mix. Take care to mark the colony and match with the specific PCR tube. Gently stir the reaction mix to ensure *E. coli* cells are shed into the solution.
3. Amplify products by PCR. Use a program consisting of an initial denaturation step of 95 °C for 60 s, 30 rounds of 95 °C for 15 s, 58 °C for 15 s (few degrees below the T_m values of the primers) , 72 °C for 30 s (30 s/kb of insert), followed by a final extension step of 72 °C for 5 min.

8. Preparation of BG11 medium and plates

1. Prepare stock solutions of 100x BG11 medium, iron (ammonium ferric citrate), trace elements, phosphate (K_2HPO_4), Na_2CO_3 and TES buffer according to Lea-Smith et al.[11]. Autoclave phosphate and Na_2CO_3 stocks. Use 0.2 µm filters to filter sterilize the TES buffer (pH 8.2) and $NaHCO_3$ stock solutions.
2. Prepare 1 L of BG11 medium. Mix 10 mL of 100x BG11, 1 mL of trace elements and 1 mL of iron stock and autoclave the solution with 976 mL of water. Once the solution has cooled down to RT, add 1 mL of phosphate stock, 1 mL of Na_2CO_3 stock and 10 mL of $NaHCO_3$, and adjust to pH 7.6−7.8 with 1 M HCl.
3. LB-BG11 agar plates (1.5% [w/v])
   1. Combine 700 mL of deionized water and 15 g of agar in a glass flask. In a second flask, add 186 mL of water, 10 mL of 100x BG11, 1 mL of trace elements and 1 mL of iron stock. Autoclave both solutions.

jove Journal of Visualized Experiments www.jove.com

2. Once the solutions have cooled down to around 60 °C, combine them and add 1 mL of phosphate stock, 1 mL of Na_2CO_3 stock, 10 mL of $NaHCO_3$ stock and 50 mL of LB sterile medium, which should give a final volume of 1 L. Cast Petri dishes with 25 mL of LB-BG11 agar medium.

4. BG11+Kan50 agar plates (1.5% [w/v])
    1. Combine 700 mL of deionized water and 15 g of agar in a glass flask. In a second flask, add 3 g of sodium thiosulphate ($Na_2S_2O_3$), 226 mL of water, 10 mL of 100x BG11 stock, 1 mL of trace elements and 1 mL of iron stock. Autoclave both solutions.
    2. Once the solutions have cooled down to around 60 °C, combine them and add 1 mL of phosphate stock, 1 mL of Na_2CO_3 stock, 10 mL of TES buffer stock, and 10 mL of $NaHCO_3$ stock, which should give a final volume of 1 L. Add kanamycin sulphate to a final concentration of 50 µg/mL and cast Petri dishes with 35 mL of medium.

Representative Results

To demonstrate the Golden Gate assembly workflow, an expression cassette was assembled in the Level 1 position 1 (Forward) acceptor vector (pICH47732) containing the following Level 0 parts: the promoter of the C-phycocyanin operon P_{cpc560} (pC0.005), the coding sequence for eYFP (pC0.008) and the double terminator T_{rrnB} (pC0.082)[12]. Following transformation of the assembly reaction, successful assemblies were identified using standard blue-white screening of *E. coli* colonies (**Figure 3**). The eYFP expression cassette in the Level 1 vector and the End-Link 1 vector (pICH50872) were then assembled into a Level T acceptor vector (pPMQAK1-T) to give the vector *cpcBA*-eYFP (**Figure 4A**). The assembled *cpcBA*-eYFP vector was verified by restriction digestion (**Figure 4B**).

Successful conjugal transfer of *cpcBA*-eYFP or the empty pPMQAK1-T vector (i.e., a negative control lacking the eYFP expression cassette) resulted in the growth of up to several hundred colonies on the membrane for *Synechocystis* PCC 6803 and *S. elongatus* UTEX 2973 after 7−14 days and 3−7 days, respectively (**Figure 5**). Individual colonies were picked and streaked onto fresh BG11+Kan50 agar plates; 2−3 re-streaks were required to generate axenic cultures.

As expected for the strong P_{cpc560} promoter[51], the values for normalised eYFP fluorescence from the plate reader and eYFP fluorescence per cell from the flow cytometer were high compared to the negative control (**Figure 6** and **Figure 7**). Fluorescence values were higher in *S. elongatus* UTEX 2973 than in *Synechocystis* PCC 6803[12].

jove Journal of Visualized Experiments www.jove.com

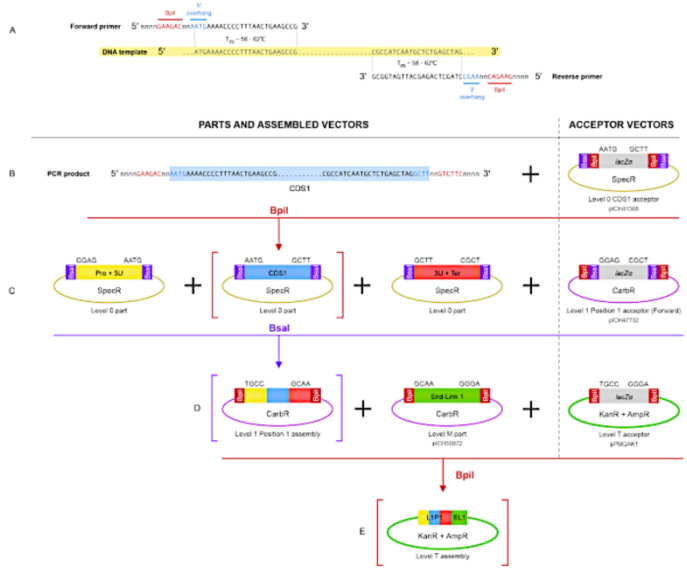

Figure 1: Overview of the Golden Gate assembly process in CyanoGate. Assembly of a gene expression cassette is shown, starting from amplification of a sequence of interest from template DNA to assembly in a Level T vector (parts are not drawn to scale). (**A**) Design of forward and reverse primers for amplification of a CDS1 part from template DNA (e.g., genomic or plasmid DNA). The locations of the BpiI restriction sites and overhangs required for insertion into the acceptor vector (i.e., 5′ and 3′ of the template sequence) are highlighted in red and blue, respectively. The letter "n" denotes that any NT can be used at this position. The annealing regions of the primers with the DNA template and their recommended melting temperatures (T_m) are indicated. (**B**) Level 0 assembly of the PCR product into the Level 0 CDS1 acceptor vector pICH41308. The sequence that will be excised by BpiI and ligated into the acceptor vector is highlighted in blue. (**C**) Level 1 assembly of a gene expression cassette containing three Level 0 parts (Pro + 5U, CDS1 and 3U + Ter) into the Level 1 position 1 (forward) acceptor vector pICH47732 using BsaI. (**D**) Level T assembly of the Level 1 assembly and End-Link 1 (pICH50872, called "Level M End-link 1" in Engler et al.[15]) into a Level T acceptor vector (e.g., pPMQAK1-T) using BpiI. (**E**) The final assembled Level T vector. Abbreviations: AmpR, ampicillin resistance cassette; CarbR, carbenicillin resistance cassette; CDS1, coding sequence in the Level 0 syntax[15]; EL1, End-Link 1 part; KanR, kanamycin resistance cassette; *lacZα*, β-galactosidase expression cassette; SpecR, spectinomycin resistance cassette. Please click here to view a larger version of this figure.

jove Journal of Visualized Experiments www.jove.com

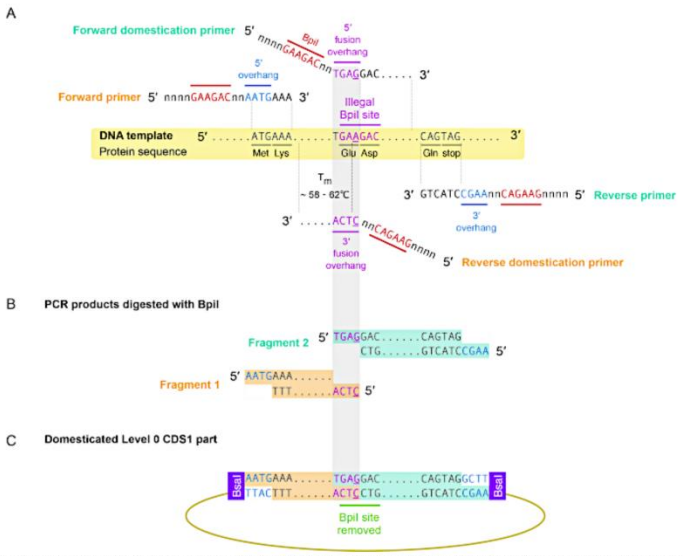

Figure 2: A PCR-based domestication strategy for removal of an illegal type IIS restriction site. (**A**) Schematic diagram showing two primer pairs (in green and orange, respectively) for modifying a BpiI site (GAAGAC) to GAGGAC in a protein coding DNA sequence intended for assembly into the CDS1 Level 0 acceptor vector (pICH41308). Note that modification preserves the codon for glutamic acid (Glu) (i.e., GAA to GAG). Although the BpiI site is shown in frame with the start codon, this approach will work even if the site is not in frame (i.e., as long as the site is disrupted, and the protein sequence preserved). The locations of the BpiI restriction sites and overhangs in the primers are highlighted in red and blue, respectively. The DNA template and the translated protein sequence is highlighted in yellow. The annealing regions of the primers with the DNA template and their recommended melting temperatures (T_m) are indicated. The orange pair is used to amplify the 5′ end of the sequence with overhangs AATG and TGAA (fragment 1), while the green pair is used to amplify the 3′ end with overhangs TGAA and GCTT (fragment 2). Before ordering the primers, the fidelity of the TGAA fusion overhang for Fragment 1 and 2 was carefully checked[52]. Poorly designed fusion overhangs can lead to assembly failure (i.e., no colonies following transformation; **Figure 5**) or false positives (e.g., truncated or erroneous assemblies). The latter can be resolved by screening a larger number of white colonies to identify a correctly assembled construct. (**B**) Amplicons of fragments 1 and 2 after restriction with BpiI during Golden Gate assembly. (**C**) The domesticated sequence assembled into the Level 0 CDS1 acceptor vector. Please click here to view a larger version of this figure.

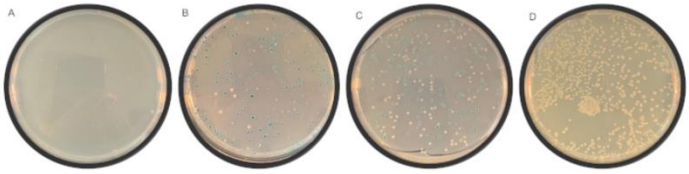

Figure 3: Blue-white colony screening of *E. coli* transformants following Golden Gate assembly. The plates shown contain LB agar (1% [w/v]) supplemented with X-Gal, IPTG and antibiotics at appropriate concentrations. (**A**) No colonies, suggesting a failed assembly reaction and/or *E. coli* transformation. (**B**) Mostly blue colonies, indicating a successful assembly, but that the efficiency of restriction enzyme used in the assembly reaction was low. (**C**) Mostly white colonies, indicative of a typical, successful assembly reaction. (**D**) No blue colonies, indicating very efficient assembly. Please click here to view a larger version of this figure.

jove Journal of Visualized Experiments www.jove.com

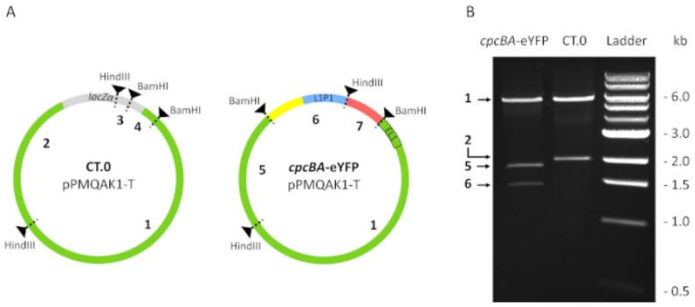

Figure 4: Verification of an assembled Level T vector by restriction digestion. The vectors were digested with HindIII and BamHI. (**A**) Sequence map of empty pPMQAK1-T acceptor vector (CT.0) and Level T assembly (*cpcBA*-eYFP) showing components of the eYFP expression cassette (P_{cpc560}-eYFP-T_{rrnB}). The positions of the restriction sites for HindIII and BamHI are indicated. Following double digestion, the predicted sizes of the DNA fragments are indicated: (1) 5,847 bp, (2) 2,004 bp, (3) 30 bp, (4) 374 bp, (5) 1,820 bp, (6) 1,289 bp, and (7) 156 bp. (**B**) An agarose gel (0.8% [w/v]) run at 125 V for 60 min loaded with the digested Level T assembly (*cpcBA*-eYFP) showing bands 1, 5 and 6, the digested empty pPMQAK1-T acceptor vector (CT.0) showing bands 1 and 2 and a DNA ladder (**Table of Materials**). Note that bands 3, 4 and 7 were too small to visualize on the gel. Please click here to view a larger version of this figure.

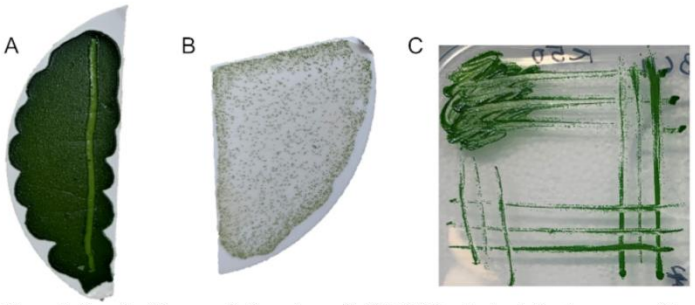

Figure 5: Growth of transgenic *Synechocystis* PCC 6803 colonies following successful conjugation. Examples of membranes following incubation on BG11+Kan50 agar plates are shown. (**A**) Overgrowth following very efficient conjugation-the *Synechocystis* PCC 6803 colonies have developed into a lawn with no individual colonies. (**B**) A good conjugation efficiency showing several hundred individual colonies after 12 days. (**C**) Growth of an axenic strain after 14 days following several rounds of re-streaking onto a fresh BG11+Kan50 agar plate. Absence of bacterial contamination indicated that the *Synechocystis* PCC 6803 transconjugant was axenic. Please click here to view a larger version of this figure.

jove Journal of Visualized Experiments www.jove.com

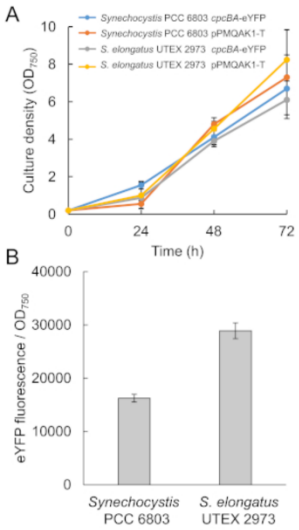

Figure 6: Representative growth data and normalized eYFP fluorescence values using a plate reader. (**A**) Growth comparison of strains carrying *cpcBA*-eYFP or the empty pPMQAK1-T vector (CT.0, negative control) in *Synechocystis* PCC 6803 and *S. elongatus* UTEX 2973. Values are the means ± SE from four biological replicates. *Synechocystis* PCC 6803 and *S. elongatus* UTEX 2973 were cultured for 72 h at 30 °C with continuous light (100 µmol photons $m^{-2}s^{-1}$) and 40 °C with 300 µmol photons $m^{-2}s^{-1}$, respectively. (**B**) Normalized eYFP fluorescence values for *Synechocystis PCC* 6803 or *S. elongatus* UTEX 2973 conjugated with *cpcBA*-eYFP at 72 h. Values are the means ± SE from four biological replicates. Please click here to view a larger version of this figure.

jove Journal of Visualized Experiments www.jove.com

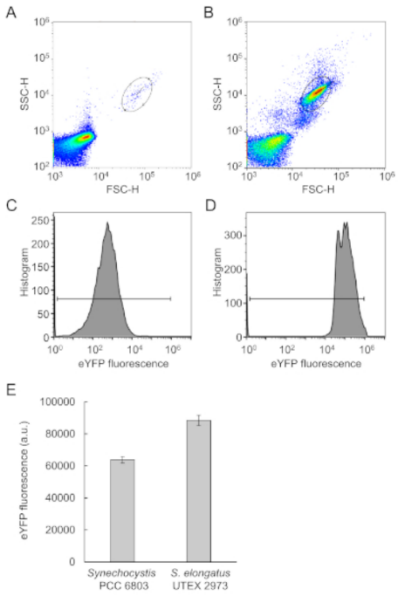

Figure 7: Representative eYFP fluorescence values using a flow cytometer. (**A**) Forward (FSC-H) and side (SSC-H) scatter plot from the "blank" medium solution (BG11 and PBS). (**B**) Scatter plot for a *Synechocystis PCC* 6803 sample (right). The circle indicates the selected region gating the cyanobacteria population from the remainder of the sample signal. (**C**) Histogram of the gated region for a strain carrying the empty pPMQAK1-T vector (CT.0, negative control). (**D**) Histogram of the gated region for a strain carrying *cpcBA*-eYFP. (**E**) eYFP fluorescence values per cell in *Synechocystis* PCC 6803 and *S. elongatus* UTEX 2973 at 72 h. Fluorescence from the negative control has been subtracted. Values are the means ± SE from four biological replicates. Please click here to view a larger version of this figure.

jove Journal of Visualized Experiments www.jove.com

No.	Vector ID	Name	Description	5' overhang	3' overhang
1	pICH41233	Pro	Promoter	GGAG	TACT
2	pICH41295	Pro + 5U	Promoter and 5' untranslated region	GGAG	AATG
3	pAGM1251	Pro + 5U (f)	Promoter and 5' untranslated sequence for N terminal fusions	GGAG	CCAT
4	pICH41246	5U	5' untranslated region	TACT	CCAT
5	pAGM1263	5U (f)	5' untranslated sequence for N terminal fusions	TACT	CCAT
6	pICH41246	5U + NT1	5' untranslated region and N terminal coding region	TACT	CCAT
7	pAGM1276	NT1	N terminal tag or localisation signal	CCAT	AATG
8	pICH41258	SP	Signal peptide	AATG	AGGT
9	pICH41258	NT2	N terminal tag or localisation signal	AATG	AGGT
10	pAGM1287	CDS1 ns	Coding region without stop codon	AATG	TTCG
11	pICH41308	CDS1 stop	Coding region with stop codon	AATG	GCTT
12	pAGM1299	CDS2 ns	Coding region - without start and stop codon	AGGT	TTCG
13	pICH41264	CDS2 stop	Coding region - without start and with stop codon	AGGT	GCTT
14	pAGM1301	CT	C terminal tag or localization signal	TTCG	GCTT
15	pICH53388	3U	3' untranslated region	GCTT	GGTA
16	pICH53399	Ter	Terminator	GGTA	CGCT
17	pICH41276	3U + Ter	3' untranslated region and terminator	GCTT	CGCT
18	pICH41331	CGM	Acceptor for complete gene cassettes	GGAG	CGCT
19	pCA0.002	Pro (low copy)	Promoter, low copy number acceptor (pSC101 ori)	GGAG	TACT
20	pCA0.001	Pro TSS	Promoter truncated to the transcription start site	GGAG	TAGC
21	*Direct to Level 1*	srRNA	Small regulatory RNA (for translational silencing)	TAGC	GTTT
22	*Direct to Level 1*	sgRNA	Single guide RNA (for CRISPRi)	TAGC	GTTT
23	pICH41295	UP FLANK	Flanking sequence upstream of target homologous recombination site	GGAG	AATG
24	pICH41276	DOWN FLANK	Flanking sequence downstream of	GCTT	CGCT

jove Journal of Visualized Experiments www.jove.com

			target homologous recombination site		

Table 1: A list of available Level 0 acceptor vectors and overhangs. Vectors 1−18 are from the Plant MoClo kit[15]. Vectors 19−22 are from the CyanoGate kit[12]. For srRNA and sgRNA parts, synthesized sequences or PCR products are assembled directly into Level 1 acceptor vectors. Vectors 23−24 are from the Plant MoClo kit that have been re-purposed for transformation by homologous recombination using the CyanoGate kit.

BpiI assembly components (Level 0, T)		**BsaI assembly components (Level 1)**	
50−100 ng of acceptor vector		50−100 ng of acceptor vector	
For each vector/part to insert, use a 2:1 ratio of insert: acceptor vector.		For each vector/part to insert, use a 2:1 ratio of insert: acceptor vector.	
2 µL 10 mM ATP (**Table of Materials**)		2 µL 10 mM ATP (**Table of Materials**)	
2 µL buffer G (buffer for BpiI/BsaI)		2 µL buffer G (buffer for BpiI/BsaI)	
2 µL BSA (10x) (**Table of Materials**)		2 µL BSA (10x) (**Table of Materials**)	
10 units BpiI (1 µL10 U/µL BpiI, **Table of Materials**)		10 units BsaI (1 µL 10 U/µL BsaI, **Table of Materials**)	
Bring to 20 µL with dH_2O.		Bring to 20 µL with dH_2O.	
200 units T4 DNA ligase (1 µL 200 U/µL, **Table of Materials**)		200 units T4 DNA ligase (1 µL 200 U/µL, **Table of Materials**)	
Thermocycler protocol (Level 0, T)		**Thermocycler protocol (Level 1)**	
37 °C for 10 min	cycle x 5	37 °C for 10 min	cycle x 5
16 °C for 10 min		16 °C for 10 min	
37 °C for 20 min		37 °C for 20 min	
65 °C for 10 min		65 °C for 10 min	
16 °C (hold)		16 °C (hold)	

Table 2: Protocols for Golden Gate assemblies in Levels 0, 1 and T. Assembly in Level 0 and Level T acceptor vectors uses restriction enzyme BpiI (left). Assembly in Level 1 acceptor vectors uses restriction enzyme BsaI (right). This table has been adapted from Vasudevan et al.[12].

Primer No.	**Sequence (5'-3')**	**Length (bp)**	**Description**
L0T forward	GTCTCATGAGCGGATACATA TTTGAATG	28	For amplification from Level 0 and Level T
L1 reverse	GAACCCTGTGGTTGGCATGC ACATAC	26	For amplification from Level 1
L1 forward	CTGGTGGCAGGATATATTGT GGTG	24	For amplification from Level 1
L0T reverse	TTGAGTGAGCTGATACCGCT	20	For amplification from Level 0 and Level T

Table 3: List of primers for PCR validation or sequencing of Level 0, 1 and T vectors.

Discussion

Golden Gate assembly has several advantages compared to other vector assembly methods, particularly in terms of scalability[20,21]. Nevertheless, setting up the Golden Gate system in a lab requires time to develop a familiarity with the various parts and acceptor vector libraries and overall assembly processes. Careful planning is often needed for more complex assemblies or when performing a large number of complex assemblies in parallel (e.g., making a suite of Level T vectors containing multiple gene expression cassettes). We recommend first listing all the gene expression cassette combinations required and then mapping the workflow from Level 0 to Level T in silico. During this process, users should consider the Level 1 "Dummy" parts available in the Plant MoClo kit that allow for the assembly of non-sequential Level 1 vectors in Level T (e.g., Level 1 position 1 and position 3 vectors can be assembled together with "Dummy" part Level 1 position 2), which can reduce the overall number of assembly reactions and cloning steps required[15].

jove Journal of Visualized Experiments www.jove.com

DNA synthesis is typically the simplest method for building new Level 0 parts. However, when cloning is required (e.g., from plasmids or genomic DNA), optimizing the design of the primers used for amplification is important for maximizing the efficiency of subsequent Level 0 vector assembly. The two most critical steps in primer design are: 1) checking that the correct overhangs are included and are in the appropriate orientation for the forward and reverse primers (**Figure 1** and **Table 1**), and 2) ensuring that the length of the primer sequence that anneals to the template is sufficiently long (18−30 bp) and that the T_m value for this sequence (ideally 58−62°C) is similar for the primer pair (**Figure 1A**). If a sequence requires domestication, several strategies are available. For short sequences (e.g., <200 bp), a pair of long forward and reverse primers can be designed in which the 3′ ends anneal to each other (i.e., an overlap of >20 bp) and form a double stranded sequence following amplification. For longer sequences, separate fragments of the sequence can be amplified that remove illegal restriction sites and then assembled using a Golden Gate assembly approach (**Figure 2**). If assembly efficiency with PCR products is poor, individual fragments of a Level 0 sequence can be cloned into the Level 1 universal acceptor vector (pAGM1311), validated, and then assembled together into the appropriate Level 0 acceptor vector[15]. A 2:1 insert:acceptor vector molar ratio is recommended for efficient Golden Gate assembly. However, for assemblies of only 2-3 vectors (e.g., two Level 0 parts and a Level 1 acceptor vector), combining ~100 ng of each regularly typically results in successful assemblies. The efficiency of assemblies does tend to decrease as the number of vectors used per reaction increases, resulting in a reduction in total numbers of white colonies following transformation (**Figure 3**).

Prior to conjugation, validation of finalized Level T vectors by restriction digest and PCR is recommended. Conjugal DNA transfer is a well stablished technique for cyanobacterial strains, including those that are not naturally transformable[41,45]. Important steps in the conjugation protocol include: 1) careful handling of the helper *E. coli* strain following overnight growth (e.g., avoid vortexing)[35], 2) taking care to completely remove traces of the antibiotics used to grow helper and cargo *E. coli* strains, 3) an appropriate incubation period for the mixture of cargo and helper strains and cyanobacteria (e.g., a longer incubation period was critical for *S. elongatus* UTEX 2973), and 4) the initial transfer period of the cell mixture on membranes in LB-BG11 agar plates lacking antibiotics for 24 h.

Isolated cyanobacterial colonies should develop on the membrane within two weeks for *Synechocystis* PCC 6803 and *S. elongatus* UTEX 2973, otherwise it is likely that conjugation has failed. Several modifications to the protocol could then be tested, including 1) using a cyanobacterial culture with a higher starting density (e.g., OD_{750} = 1.5−2); 2) increasing the incubation period before transfer to the membrane; and 3) extending the initial incubation period on the membrane from 24 h to 48 h (i.e., to allow more time for the expression of the antibiotic resistance gene on the transferred vector). If conjugation still fails, alternative methods such as electroporation could be tried[53]. Confirming a transgenic cyanobacterial strain is axenic is important prior to further experimentation. Finally, it is good practice to confirm the size of the heterologous vector in the transgenic cyanobacterial strain. The latter requires DNA extraction (section 5), transformation into *E. coli* and selection (section 2.1), and vector validation (section 2.4).

The outlined promoter characterization protocol uses small culture volumes (i.e., 2 mL) as a means of achieving a high throughput screening methodology. Larger volumes could be used depending on the photobioreactor space available, which would help to mitigate culture evaporation issues. If high throughput screening with small culture volumes is required, it is essential to have high humidity within the growth chamber to inhibit evaporation. Evaporation during a growth experiment can be detrimental to the accuracy and validity of sample measurements. Do check culture volumes during and after the experiment to confirm how much evaporation has occurred.

For plate reader measurements, it is important to measure cultures at low densities, ideally OD_{750} < 1, to ensure the acquisition of reliable and reproducible growth and fluorescence data. A linear relationship between cell number and OD_{750} is observed only within a specific range[54]. To establish this range, we recommend performing a serial dilution (e.g., from OD_{750} = 0.1−1.0) using a known transformant where eYFP fluorescence has been confirmed. Plotting absolute fluorescence against normalized fluorescence (eYFP fluorescence/OD_{750}) will help to identify the linear working range of culture densities. Several plate readers include a "gain" feature to modify the sensitivity of the fluorescence detector. In this case, the gain value should be set to an appropriate level before beginning the experiment and not changed between different experimental runs or the data will not be directly comparable.

Although the operation of different flow cytometers will vary between manufacturers, it is important to take a blank reading of the medium solution to facilitate the identification and gating of the target cyanobacterial population from any background signal in the medium (**Figure 7A,B**). Following this, subtraction of the fluorescence value of the negative control sample (e.g., a wild type strain) will help to remove native autofluorescence (**Figure 7C,D**). The photomultiplier tube (PMT) voltage parameter in a flow cytometer has a similar function to the gain in a plate reader, i.e., increasing or decreasing the sensitivity of the detector to the intensity of the fluorescence signal. As with the plate reader, PMT voltage should be set to an appropriate level before beginning the experiment[55]. Once set, the PMT voltage value should be maintained between different experimental runs or the data will not be directly comparable.

Disclosures

The authors have nothing to disclose.

Acknowledgments

The authors are grateful to the PHYCONET Biotechnology and Biological Sciences Research Council (BBSRC) Network in Industrial Biotechnology and Bioenergy (NIBB) and the Industrial Biotechnology Innovation Centre (IBioIC) for financial support. GARG, AASO and AP acknowledge funding support from the BBSRC EASTBIO CASE PhD program (grant number BB/M010996/1), the Consejo Nacional de Ciencia y Tecnología (CONACYT) PhD program, and the IBioIC-BBSRC Collaborative Training Partnership (CTP) PhD program, respectively. We thank Conrad Mullineaux (Queen Mary University of London), and Poul Eric Jensen and Julie Annemarie Zita Zedler (University of Copenhagen) for plasmid vector and protocol contributions and advice.

References

1. Luan, G., Lu, X. Tailoring cyanobacterial cell factory for improved industrial properties. *Biotechnology Advances.* **36** (2), 430-442 (2018).
2. Madsen, M.A., Semerdzhiev, S., Amtmann, A., Tonon, T. Engineering mannitol biosynthesis in Escherichia coli and Synechococcus sp. PCC 7002 using a green algal fusion protein. *ACS Synthetic Biology.* **7** (12), 2833-2840 (2018).
3. Menin, B. et al. Non-endogenous ketocarotenoid accumulation in engineered Synechocystis sp. PCC 6803. *Physiologia Plantarum.* **166** (1), 403-412 (2019).
4. Varman, A.M., Yu, Y., You, L., Tang, Y.J. Photoautotrophic production of D-lactic acid in an engineered cyanobacterium. *Microbial Cell Factories.* **12** (1), 1-8 (2013).
5. Vavitsas, K. et al. Responses of Synechocystis sp. PCC 6803 to heterologous biosynthetic pathways. *Microbial Cell Factories.* **16**, 140 (2017).
6. Yang, G. et al. Photosynthetic production of sunscreen shinorine using an engineered cyanobacterium. *ACS Synthetic Biology.* **7** (2), 664-671 (2018).
7. Nielsen, A.Z. et al. Extending the biosynthetic repertoires of cyanobacteria and chloroplasts. *Plant Journal.* **87** (1), 87-102 (2016).
8. Nielsen, J., Keasling, J.D. Engineering cellular metabolism. *Cell.* **164** (6), 1185-1197 (2016).
9. Stensjö, K., Vavitsas, K., Tyystjärvi, T. Harnessing transcription for bioproduction in cyanobacteria. *Physiologia Plantarum.* **162** (2), 148-155 (2018).
10. Santos-Merino, M., Singh, A.K., Ducat, D.C. New applications of synthetic biology tools for cyanobacterial metabolic engineering. *Frontiers in Bioengineering and Biotechnology.* **7**, 1-24 (2019).
11. Lea-Smith, D.J., Vasudevan, R., Howe, C.J. Generation of marked and markerless mutants in model cyanobacterial species. *Journal of Visualized Experiments.* **111**, e54001 (2016).
12. Vasudevan, R. et al. CyanoGate: A modular cloning suite for engineering cyanobacteria based on the plant MoClo syntax. *Plant Physiology.* **180** (1), 39-55 (2019).
13. Andreou, A.I., Nakayama, N. Mobius assembly: A versatile golden-gate framework towards universal DNA assembly. *PLoS ONE.* **13** (1), 1-18 (2018).
14. Crozet, P. et al. Birth of a Photosynthetic Chassis: A MoClo toolkit enabling synthetic biology in the microalga Chlamydomonas reinhardtii. *ACS Synthetic Biology.* **7** (9), 2074-2086 (2018).
15. Engler, C. et al. A Golden Gate modular cloning toolbox for plants. *ACS Synthetic Biology.* **3** (11), 839-843 (2014).
16. Moore, S.J. et al. EcoFlex: A multifunctional MoClo kit for E. coli synthetic biology. *ACS Synthetic Biology.* **5** (10), 1059-1069 (2016).
17. Pollak, B. et al. Loop assembly: a simple and open system for recursive fabrication of DNA circuits. *New Phytologist.* **222** (1), 628-640 (2019).
18. Werner, S., Engler, C., Weber, E., Gruetzner, R., Marillonnet, S. Fast track assembly of multigene constructs using golden gate cloning and the MoClo system. *Bioengineered Bugs.* **3** (1), 38-43 (2012).
19. Patron, N.J. et al. Standards for plant synthetic biology: a common syntax for exchange of DNA parts. *New Phytologist.* **208** (1), 13-19 (2015).
20. Chao, R., Mishra, S., Si, T., Zhao, H. Engineering biological systems using automated biofoundries. *Metabolic Engineering.* **42**, 98-108 (2017).
21. Chambers, S., Kitney, R., Freemont, P. The Foundry: the DNA synthesis and construction Foundry at Imperial College. *Biochemical Society Transactions.* **44** (3), 687-688. (2016).
22. Gibson, D.G. et al. Enzymatic assembly of DNA molecules up to several hundred kilobases. *Nature Methods.* **6** (5), 343-345 (2009).
23. Rosano, G.L., Ceccarelli, E.A. Rare codon content affects the solubility of recombinant proteins in a codon bias-adjusted *Escherichia coli* strain. *Microbial Cell Factories.* **8**, 1-9 (2009).
24. Cambray, G. et al. Measurement and modeling of intrinsic transcription terminators. *Nucleic Acids Research.* **41** (9), 5139-5148 (2013).
25. Chen, Y.J. et al. Characterization of 582 natural and synthetic terminators and quantification of their design constraints. *Nature Methods.* **10** (7), 659-664 (2013).
26. Münch, R. et al. Virtual Footprint and PRODORIC: An integrative framework for regulon prediction in prokaryotes. *Bioinformatics.* **21** (22), 4187-4189 (2005).
27. Salis, H.M., Mirsky, E.A., Voigt, C.A. Automated design of synthetic ribosome binding sites to control protein expression. *Nature Biotechnology.* **27** (10), 946-950 (2009).
28. Englund, E., Liang, F., Lindberg, P. Evaluation of promoters and ribosome binding sites for biotechnological applications in the unicellular cyanobacterium Synechocystis sp. PCC 6803. *Scientific Reports.* **6**, 36640 (2016).
29. Heidorn, T. et al. Synthetic biology in cyanobacteria engineering and analyzing novel functions. *Methods in Enzymology.* **497**, 539-579 (2011).
30. Thiel, K. et al. Translation efficiency of heterologous proteins is significantly affected by the genetic context of RBS sequences in engineered cyanobacterium Synechocystis sp. PCC 6803. *Microbial Cell Factories.* **17**., 34 (2018).
31. Liu, Q., Schumacher, J., Wan, X., Lou, C., Wang, B. Orthogonality and burdens of heterologous and gate gene circuits in E. coli. *ACS Synthetic Biology.* **7** (2), 553-564 (2018).
32. Ferreira, E.A. et al. Expanding the toolbox for Synechocystis sp. PCC 6803: Validation of replicative vectors and characterization of a novel set of promoters. *Synthetic Biology.* (August), 1-39 (2018).
33. Liang, F., Lindblad, P. Synechocystis PCC 6803 overexpressing RuBisCO grow faster with increased photosynthesis. *Metabolic Engineering Communications.* **4**, 29-36 (2017).
34. Taton, A. et al. Broad-host-range vector system for synthetic biology and biotechnology in cyanobacteria. *Nucleic Acids Research.* **42** (17), e136 (2014).
35. Elhai, J., Wolk, C.P. Conjugal transfer of DNA to cyanobacteria. *Methods in Enzymology.* **167** (1984), 747-754 (1988).
36. Gormley, E.P., Davies, J. Transfer of plasmid RSF1010 by conjugation from Escherichia coli to Streptomyces lividans and Mycobacterium smegmatis. *Journal of Bacteriology.* **173** (21), 6705-6708 (1991).
37. Huang, H.H., Camsund, D., Lindblad, P., Heidorn, T. Design and characterization of molecular tools for a synthetic biology approach towards developing cyanobacterial biotechnology. *Nucleic Acids Research.* **38** (8), 2577-2593 (2010).
38. Huang, H.-H., Lindblad, P. Wide-dynamic-range promoters engineered for cyanobacteria. *Journal of Biological Engineering.* **7**, 10 (2013).

39. Li, S., Sun, T., Xu, C., Chen, L., Zhang, W. Development and optimization of genetic toolboxes for a fast-growing cyanobacterium *Synechococcus elongatus* UTEX 2973. *Metabolic Engineering.* **48**, 163-174 (2018).
40. Pansegrau, W., Balzer, D., Kruft, V., Lurz, R., Lanka, E. In vitro assembly of relaxosomes at the transfer origin of plasmid RP4. *Proceedings of the National Academy of Sciences, USA.* **87** (17), 6555-6559 (1990).
41. Song, K., Tan, X., Liang, Y., Lu, X. The potential of Synechococcus elongatus UTEX 2973 for sugar feedstock production. *Applied Microbiology and Biotechnology.* **100** (18), 7865-7875 (2016).
42. Waters, V.L., Guiney, D.G. Processes at the nick region link conjugation, T-DNA transfer and rolling circle replication. *Molecular Microbiology.* **9** (6), 1123-1130 (1993).
43. Elhai, J., Vepritskiy, A., Muro-Pastor, A.M., Flores, E., Wolk, C.P. Reduction of conjugal transfer efficiency by three restriction activities of *Anabaena* sp. strain PCC 7120. *Journal of Bacteriology.* **179** (6), 1998-2005 (1997).
44. Silva-Rocha, R. et al. The Standard European Vector Architecture (SEVA): A coherent platform for the analysis and deployment of complex prokaryotic phenotypes. *Nucleic Acids Research.* **41** (D1), D666-D675, (2013).
45. Mandakovic, D. et al. CyDiv, a conserved and novel filamentous cyanobacterial cell division protein involved in septum localization. *Frontiers in Microbiology.* **7** (FEB), 1-11 (2016).
46. Masukawa, H., Inoue, K., Sakurai, H., Wolk, C.P., Hausinger, R.P. Site-directed mutagenesis of the Anabaena sp. strain PCC 7120 nitrogenase active site to increase photobiological hydrogen production. *Applied and Environmental Microbiology.* **76** (20), 6741-6750 (2010).
47. Yu, J. et al. Synechococcus elongatus UTEX 2973, a fast growing cyanobacterial chassis for biosynthesis using light and CO2. *Scientific Reports.* **5** (1), 8132 (2015).
48. Ungerer, J., Wendt, K.E., Hendry, J.I., Maranas, C.D., Pakrasi, H.B. Comparative genomics reveals the molecular determinants of rapid growth of the cyanobacterium *Synechococcus elongatus* UTEX 2973. *Proceedings of the National Academy of Sciences, USA.* **115** (50), E11761-E11770 (2018).
49. Lepesteur, M., Martin, J.M., Fleury, A. A comparative study of different preservation methods for phytoplankton cell analysis by flow cytometry. *Marine Ecology Progress Series.* **93** (1-2), 55-63 (1993).
50. Day, J.G. Cryopreservation of cyanobacteria. *Cyanobacteria: An Economic perspective*. Wiley Blackwell pubs. New York. 319-327 (2014).
51. Zhou, J. et al. Discovery of a super-strong promoter enables efficient production of heterologous proteins in cyanobacteria. *Scientific Reports.* **4**, 4500 (2014).
52. Potapov, V. et al. Comprehensive profiling of four base overhang ligation fidelity by T4 DNA ligase and application to DNA assembly. *ACS Synthetic Biology.* **7** (11), 2665-2674 (2018).
53. Ravindran, C.R.M, Suguna, S., Shanmugasundaram, S. Electroporation as a tool to transfer the plasmid pRL489 in Oscillatoria MKU 277. *Journal of Microbiological Methods.* **66**, 174-176 (2006).
54. Stevenson, K., McVey, A.F., Clark, I.B.N., Swain, P.S., Pilizota, T. General calibration of microbial growth in microplate readers. *Scientific Reports.* **6**, 38828 (2016).
55. Maecker, H.T., Trotter, J. Flow cytometry controls, instrument setup, and the determination of positivity. *Cytometry Part A.* **69** (9), 1037-1042 (2006).

4.3 Conclusion

Here we provide an in depth and detailed set of protocols for the use of Golden Gate cloning, transfer of DNA by conjugation, and how to perform high throughput growth and fluorescence characterisation experiments using plate reader and flow cytometry in cyanobacteria, respectively. This knowledge was gained, and optimisations conducted during the work constructing the CyanoGate kit (See **Chapter 3**).

Without strategies for conducting high throughput experiments, the synthetic biology paradigm may continue to lag in cyanobacteria with the 'test phase' causing a substantial bottle neck. This could result in this promising platform continuing to lag other model systems and failing to lead the way in the green biotechnology revolution. The optimised workflows detailed in this protocol are now standard practice in our lab, and these protocols have been applied to all subsequent work conducted in this thesis.

Chapter 5 Evaluation and Comparison of the Efficiency of Transcription Terminators in Different Cyanobacterial Species

5.1 Chapter Preface

The following work has been published in the journal *Frontiers in Microbiology*[5]. I conducted all cloning and performed all experiments.

In **Chapter 3**, we developed and validated the CyanoGate molecular toolkit. The suite of modular parts included some transcription terminators, that were not characterised as part of the study.

In this chapter, I adapted an established strategy for the characterisation of transcription terminators and generated a CyanoGate compatible molecular tool called pDUOTK1-L1. I validated pDUOTK1-L1 in *Escherichia coli* against published data and then characterised the behaviour of the library of transcription terminators in two different cyanobacterial species.

[5] Gale, G. A. R., Wang, B., & McCormick, A. J. (2021). Evaluation and Comparison of the Efficiency of Transcription Terminators in Different Cyanobacterial Species. Frontiers in Microbiology, 11, 3585. https://doi.org/10.3389/fmicb.2020.624011

5.2 Main text

frontiers in Microbiology

ORIGINAL RESEARCH
published: 15 January 2021
doi: 10.3389/fmicb.2020.624011

Evaluation and Comparison of the Efficiency of Transcription Terminators in Different Cyanobacterial Species

*Grant A. R. Gale[1,2,3], Baojun Wang[2,3] and Alistair J. McCormick[1,2]**

[1] School of Biological Sciences, Institute of Molecular Plant Sciences, University of Edinburgh, Edinburgh, United Kingdom, [2] Centre for Synthetic and Systems Biology, University of Edinburgh, Edinburgh, United Kingdom, [3] School of Biological Sciences, Institute of Quantitative Biology, Biochemistry and Biotechnology, University of Edinburgh, Edinburgh, United Kingdom

Cyanobacteria utilize sunlight to convert carbon dioxide into a wide variety of secondary metabolites and show great potential for green biotechnology applications. Although cyanobacterial synthetic biology is less mature than for other heterotrophic model organisms, there are now a range of molecular tools available to modulate and control gene expression. One area of gene regulation that still lags behind other model organisms is the modulation of gene transcription, particularly transcription termination. A vast number of intrinsic transcription terminators are now available in heterotrophs, but only a small number have been investigated in cyanobacteria. As artificial gene expression systems become larger and more complex, with short stretches of DNA harboring strong promoters and multiple gene expression cassettes, the need to stop transcription efficiently and insulate downstream regions from unwanted interference is becoming more important. In this study, we adapted a dual reporter tool for use with the CyanoGate MoClo Assembly system that can quantify and compare the efficiency of terminator sequences within and between different species. We characterized 34 intrinsic terminators in *Escherichia coli*, *Synechocystis* sp. PCC 6803, and *Synechococcus elongatus* UTEX 2973 and observed significant differences in termination efficiencies. However, we also identified five terminators with termination efficiencies of >96% in all three species, indicating that some terminators can behave consistently in both heterotrophic species and cyanobacteria.

Keywords: CyanoGate, *Escherichia coli*, Golden Gate, intrinsic terminator, MoClo, *Synechococcus elongatus* UTEX 2973, *Synechocystis* sp. PCC 6803, synthetic biology

OPEN ACCESS

Edited by:
Robert Kourist,
Graz University of Technology, Austria

Reviewed by:
Paul Hudson,
Royal Institute of Technology, Sweden
Ilka Maria Axmann,
Heinrich Heine University of Düsseldorf, Germany

***Correspondence:**
Alistair J. McCormick
alistair.mccormick@ed.ac.uk

Specialty section:
This article was submitted to Microbiotechnology, a section of the journal Frontiers in Microbiology

Received: *30 October 2020*
Accepted: *23 December 2020*
Published: *15 January 2021*

Citation:
Gale GAR, Wang B and McCormick AJ (2021) Evaluation and Comparison of the Efficiency of Transcription Terminators in Different Cyanobacterial Species. Front. Microbiol. 11:624011. doi: 10.3389/fmicb.2020.624011

INTRODUCTION

Cyanobacteria comprises a large and diverse phylum of photoautotrophic bacteria that can capture and convert inorganic carbon (e.g., CO_2) into a wide variety of secondary metabolites (Huang and Zimba, 2019). Many cyanobacterial species are genetically tractable and show great potential for green biotechnology applications, such as the sustainable production of biofuels and high value biomolecules (Lin et al., 2017; Knoot et al., 2018; Eungrasamee et al., 2019; Lin and Pakrasi, 2019; Włodarczyk et al., 2019). Much of the recent progress in engineering cyanobacteria has been driven by the uptake of synthetic biology approaches. One major aim of cyanobacterial synthetic biology is the development of new tools and strategies to facilitate stringent and precise control of gene

expression. A wide variety of new molecular tools and genetic parts to tune gene expression are now available for use by the research community (Englund et al., 2016; Kim et al., 2017; Ferreira et al., 2018; Kelly et al., 2018; Vasudevan et al., 2019; Yao et al., 2020). The increase in availability of well-characterized genetic parts has allowed rational design, a core process to the synthetic biology paradigm, to be more routinely employed in the engineering of new cyanobacterial strains. Nevertheless, the majority of synthetic biology work in cyanobacteria has thus far concentrated on characterizing genetic elements that control gene transcription (e.g., promoters, CRISPRi) or translation modulation (e.g., ribosomal binding sites (RBS), riboswitches, small RNAs) (Huang and Lindblad, 2013; Camsund et al., 2014; Ma et al., 2014; Immethun et al., 2017; Kelly et al., 2018; Sun et al., 2018; Behle et al., 2020; Yao et al., 2020). Transcription terminators are also key transcriptional control elements, but far fewer studies have examined their roles in regulating gene expression in cyanobacteria.

The rational design of efficient gene expression cassettes (and more advanced gene circuits) requires the use of genetic parts with well-characterized and predictable function (Moser et al., 2018). For instance, strong terminators attenuate transcription and isolate downstream genetic sequences, which can prevent interference and disruption of function from unwanted transcriptional readthrough (Kelly et al., 2019). This is particularly important when considering synthetic gene constructs, where several gene expression cassettes driven by strong promoters may occupy a short stretch of DNA. Furthermore, many prokaryotes (including cyanobacteria) are prone to homologous recombination. Homologous regions as small as 23–27 bp have been demonstrated to lead to recombination in *Escherichia coli*, so multiple distinct terminators are generally preferable for multi-gene expression systems and gene circuits (Shen and Huang, 1986; Sleight et al., 2010; Chen et al., 2013). As with other genetic parts, an understanding of terminator performance and robustness between species is also important. Promoters have been shown to drive gene expression differently in cyanobacteria compared to heterotrophic species (e.g., *Escherichia coli*) and between cyanobacterial species (Camsund et al., 2014; Vasudevan et al., 2019). In contrast, potential differences in behavior between cyanobacterial species has not yet been investigated for transcription terminators.

In prokaryotes, transcription is terminated by two distinct terminator types: (i) Rho-dependent terminators that rely on a Rho transcription factor, and (ii) Rho-independent, or intrinsic terminators, which do not require a transcription factor. In *E. coli*, approximately 20% of terminators are Rho-dependent (Peters et al., 2009). However, Rho transcription factors appear to be absent in cyanobacteria, such that all transcription termination events are thought to rely on intrinsic termination (Vijayan et al., 2011). Intrinsic terminators are defined by a sequence motif that forms a hairpin loop secondary structure in the nascent RNA transcript. The hairpin loop is comprised of a GC-rich stem (8–12 nucleotides) (nt) and a loop (3–6 nt). Upstream of the hairpin loop is an adenine-rich region (the A-tract) typically 6–8 nt in length, while downstream is a uracil-rich region of 7–12 nt in length (the U-tract). Intrinsic termination depends upon the differential binding affinities between nucleotides. The interaction between U and A is weak, such that transcription of the U-tract results in a pause in transcription that allows the hairpin loop to form. The presence of the hairpin loop in the RNA polymerase (RNAP) exit channel, causes a ratcheting action and subsequent disruption of RNA-DNA binding. This leads to dissociation of RNAP from the DNA template and the subsequent release of the nascent RNA transcript (Wilson and Von Hippel, 1995; Herbert et al., 2008; Peters et al., 2011). In *E. coli*, many terminators have been assessed for termination efficiency (TE), which is typically calculated as a percentage estimate of the RNAP transcription elongation complexes prevented from continuing transcription passed a given sequence (i.e., a terminator) (Cambray et al., 2013; Chen et al., 2013). Importantly, a "no terminator" control was included to determine a normalized value for TE in those studies.

Characterization studies of terminators in cyanobacteria are currently limited to the model species *Synechocystis* sp. PCC 6803 (PCC 6803). Liu and Pakrasi (2018) evaluated the relative strengths of seven native terminators using a dual fluorescent reporter system similar to that used by Chen et al. (2013). More recently, Kelly et al. (2019) evaluated 19 synthetic and heterologous intrinsic terminators ported from *E. coli*, with the aim of identifying terminators able to insulate a specific genomic locus in PCC 6803 from native promoter readthrough originating from upstream of the insertion site. Each terminator sequence was inserted between the transcription start site (TSS) and RBS of an inducible promoter driving *YFP*, and following induction, twelve terminators were shown to efficiently block transcription indicating a potential efficiency of nearly100%. These studies have provided valuable insights into terminator function in PCC 6803. But if comparisons in performance between different strains are to be achieved, a normalized quantitative parameter, such as TE, should be calculated.

In this study we assembled a set of 34 intrinsic terminators from PCC 6803, and *E. coli* and synthetic libraries that have previously demonstrated a wide range of TE values in *E. coli* (Chen et al., 2013). We re-designed an established dual fluorescent reporter system to be compatible with the CyanoGate MoClo Assembly system, which allowed for increased cloning throughput (Liu and Pakrasi, 2018; Vasudevan et al., 2019). Importantly, all assays included a "no terminator" control vector as a reference to calculate a normalized TE value for each terminator, such that the TE values could be compared between different experiments and species irrespective of the instrument or gain settings used. We first validated and benchmarked our testing system by comparing TE values from the literature with our results in *E. coli*. Then we tested the performance of the terminators in two different cyanobacterial species: PCC 6803 and the recently described high-light tolerant *Synechococcus elongatus* UTEX 2973 (UTEX 2973) (Williams, 1988; Yu et al., 2015).

MATERIALS AND METHODS

Cyanobacterial Culture Conditions

The *Synechocystis* sp. PCC 6803 glucose tolerant (GT) strain (obtained from the Lea-Smith lab at the University of East-Anglia, United Kingdom) (Zavøel et al., 2017) and UTEX 2973 were maintained on 1.5% (w/v) agar plates containing BG11 medium (Lea-Smith et al., 2016). Liquid cultures were grown in BG11 (supplemented with 10 mM $NaHCO_3$) in 100 ml Erlenmeyer flasks. Liquid cultures were shaken at 100 rpm and aerated with filter-sterilized, water-saturated air. PCC 6803 and UTEX 2973 transconjugants were cultured in BG11 medium and on BG11 agar plates, supplemented with 50 μg/ml kanamycin (BG11 + Kan50). Strains were grown under continuous light with PCC 6803 grown at 30°C, 100 μmol photons m^{-2} s^{-1} and UTEX 2973 at 40°C, 300 μmol photons m^{-2} s^{-1} in a Multitron Pro incubator supplied with warm white LED lighting (Infors HT).

Vector Construction and Parts Assembly

All cloning was performed in OneShot TOP10 *E. coli* cells. Transformed cells were cultured in LB medium and on 1.5% (w/v) LB agar plates supplemented with either 100 μg/ml spectinomycin or 50 μg/ml kanamycin as required. *E. coli* strain MC1061 was cultured in LB medium supplemented with 100 μg/ml ampicillin and 25 μg/ml chloramphenicol. All *E. coli* strains were grown at 37°C with shaking at 225 rpm.

pPMQAK1-T (pCAT.000) from the CyanoGate toolkit was modified to generate pDUOTK1-L1 (pCA1.332, Addgene vector ID 162351)[1] (**Supplementary Information S1**) (Vasudevan et al., 2019). To assemble pDUOTK1-L1, pPMQAK1-T was first digested with *Bpi*I and *Bsa*I (Thermo Fisher Scientific). The linearized backbone was gel purified using a Monarch DNA Gel Extraction Kit (NEB). Sequences encoding P_{trc10}-*eYFP* from the CyanoGate vector pCAT.262, the *LacZ* expression cassette from the Plant MoClo level 1 acceptor vector pICH47732 and *mTagBFP*-T_{rrnB} (from an available vector containing BBa_K592100)[2] fused at the 5′ end to the RBS-associated sequence used by Chen et al. (2013) (BBa_B0034) were amplified using Q5 High-Fidelity DNA Polymerase (NEB) (**Supplementary Table S1**). Finally, the three amplicons and the linearized pPMQAK1-T backbone were assembled together using Golden Gate assembly (Vasudevan et al., 2019). pDUOTK1-L1 contains *Bsa*I restriction sites flanking *LacZ* that generate overhangs GCTT-CGCT, such that level 0 terminator parts can be assembled directly and screened using blue-white selection.

Terminator parts were generated by overlap extension PCR using two synthesized oligonucleotides (Integrated DNA Technology) (**Supplementary Table S1**), and the resulting amplicons were assembled into the level 0 (3U + Ter) acceptor vector pICH41276 (**Supplementary Information S1**) (Engler et al., 2014). New level 0 terminator parts and existing parts from CyanoGate toolkit (Addgene Kit #1000000146)[3] were assembled into pDUOTK1-L1 to give vectors pC1.342 to pC1.375 (**Supplementary Table S2**).

Two "no terminator" control vectors were generated to determine 0% TE (i.e., the maximum ratio of mTagBFP relative to eYFP). pC1.376 was assembled as pDUOTK1-L1 above, but without inclusion of *LacZ* (**Supplementary Information S1**). For pC1.377, the spacer sequence rd1.2 (5′-cgccccggaggctttcccggggcaaatca-3′) from Cambray et al. (2013) was generated using overlap extension PCR (**Supplementary Table S1**), and the PCR product was assembled into pDUOTK1-L1 using Golden Gate assembly.

Cyanobacterial Conjugation

Genetic modification by conjugation in PCC 6803 and UTEX 2973 was facilitated by *E. coli* strain MC1061 carrying the mobilizer vector pRK24[4] and helper vector pRL528[5] (Tsinoremas et al., 1994; Gale et al., 2019). Conjugal transfer was performed as in Gale et al. (2019).

Fluorescence Assays

To measure fluorescence in *E. coli*, transformants were first inoculated into 5 ml LB medium supplemented with 50 μg/ml kanamycin and grown overnight at 37°C with constant shaking at 225 rpm. To initiate the assay, overnight cultures were diluted 1:1000 into a black 96 well flat bottom plate (F-Bottom (Chimney Well) μCLEAR®, Greiner Bio-One) containing fresh LB medium supplemented with 50 μg/ml kanamycin to a final volume of 200 μl. The plates were incubated at 37°C with constant shaking at 600 rpm and culture density (OD_{600}) was measured hourly using a FLUOstar OMEGA microplate reader (BMG Labtech). At early exponential phase (*ca*. 4.5 h following inoculation), eYFP and mTagBFP fluorescence levels were measured for individual cells by flow cytometry (minimum 10,000 cells per culture) with a FACSCanto II with HTS Flow Cytometer (Becton Dickinson). Cells were gated using forward and side scatter. Median eYFP and mTagBFP fluorescence levels were calculated from excitation/emission wavelengths 488 nm/530/30 nm and 407 nm/450/50 nm, respectively. An "empty" pPMQAK1-T vector (i.e., with no eYFP or mTagBFP expression cassettes) was included as a base line control. Fluorescence values for the latter control were subtracted from transconjugant strain measurements.

To measure fluorescence in cyanobacteria, PCC 6803 or UTEX 2973 transconjugants maintained on BG11 + Kan50 agar plates were first inoculated into 10 ml BG11 + Kan50 medium and grown for 2–3 days to OD_{750} ∼1.0. To initiate the assay, the seed cultures were diluted to a starting OD_{750} of 0.2 in 24-well plates (Costar Corning Incorporated) containing fresh BG11 + Kan50 medium to a final volume of 2 ml. Cultures were grown for three days under culturing conditions and high humidity (95%) to avoid evaporation. eYFP and mTagBFP fluorescence were measured by flow cytometry for individual cells (minimum 10,000 cells per culture) with an LSRFortessa SORP with HTS Flow Cytometer (Becton Dickinson). Cells were

[1] www.addgene.org

[2] http://parts.igem.org

[3] www.addgene.org/kits/mccormick-cyanogate

[4] www.addgene.org/51950

[5] www.addgene.org/58495

gated using forward and side scatter. Median eYFP and mTagBFP fluorescence levels were calculated from excitation/emission wavelengths 488 nm/515–545 nm and 407 nm/ 425–475 nm, respectively. As above, a base line control was included for each species.

Calculations for Termination Efficiency

TE was calculated as a percentage from the ratio of the mTagBFP fluorescence signal downstream of the terminator to the eYFP fluorescence signal upstream relative to a control containing no terminator between fluorescent reporters:

$$\Delta Term_0 = \frac{BFP_0}{YFP_0} \quad (1)$$

Where BFP_0 and YFP_0 are the mTagBFP and eYFP fluorescence signals, respectively, of the strain containing either pCA1.376 or pCA1.377.

$$TE = 100 - \left(\frac{BFP_{Term}}{YFP_{Term}} \times \frac{1}{\Delta Term_0} \times 100\right) \quad (2)$$

Where BFP_{Term} and YFP_{Term} are the mTagBFP and eYFP fluorescence signals, respectively, of a strain carrying a given level 1 terminator vector (**Supplementary Table S2**).

Statistical Analysis

Significant differences between sample groups were assessed by one-way ANOVA followed by Tukey's honest significant difference (HSD) *post-hoc* test using GraphPad Prism (version. 8.4.2).

Estimation of Gibbs Free Energy

Estimated Gibbs free energy values were generated using mFold v3.0[6] (Zuker, 2003). Free energy values were calculated without adjustment of the standard parameters, which included a fixed temperature of 37°C.

RESULTS

Generating a Screening System for Level 0 Terminator Parts

The RSF1010-based level T acceptor vector pPMQAK1-T from the CyanoGate toolkit was modified to generate the new level 1 acceptor vector pDUOTK1-L1 for terminator screening (**Figure 1A** and **Supplementary Information S1**) (Vasudevan et al., 2019). pDUOTK1-L1 comprises a dual fluorescent reporter system with eYFP and mTagBFP, similar to that in Liu and Pakrasi (2018). Terminators can be assembled as level 0 parts into pDUOTK1-L1 using Golden Gate assembly (**Figure 1B**), while the RSF1010 origin of replication allows for screening in a wide range of species (Mermet-Bouvier et al., 1993).

We compiled a library of 34 level 0 vectors containing intrinsic transcription terminators (**Table 1** and **Figure 1C**), and then assembled these into pDUOTK1-L1 (**Supplementary Table S2**). In order to maximize potential orthogonality with terminators in cyanobacterial genomes, we primarily targeted heterologous terminator sequences. The library included 22 native terminators from *E. coli* and eight synthetic terminators based on *E. coli* sequences that have been previously characterized in *E. coli* (Chen et al., 2013). We also included T_{rrnB} (i.e., T_{rrnB} from *E. coli* and the T7 viral terminator in tandem (Vasudevan et al., 2019)) and the pSB1AK3 terminator ($T_{pSB1AK3}$) that was derived from the *E. coli* ribosomal RNA rrnC operon and is used in several BioBricks vectors, including pPMQAK1, to flank the cloning site (Huang et al., 2010). From PCC 6803, the terminator of the highly expressed D1 subunit of photosystem II was included (T_{psbA2}), as we expected it to have a high efficiency of termination. In contrast, T_{psaB} was included as a potentially low efficiency terminator based on previous work (Liu and Pakrasi, 2018). Two "no terminator" control vectors, pC1.376 and pC1.377, were assembled based on sequences used in previous *E. coli* studies (Cambray et al., 2013; Chen et al., 2013). In pC1.376, eYFP and mTagBFP were separated only by an RBS-associated sequence, while pCA1.377 included a spacer sequence reported to be inert (i.e., free from promoter or terminator activity in *E. coli*) (**Supplementary Information S1**).

Validation of the Dual Reporter Testing System in *E. coli*

We first assessed the dual fluorescent reporter system in *E. coli* by generating TE values for each terminator and compared these to the data reported by Chen et al. (2013) (**Figure 2A**). Terminator strength (TS) values reported by Chen et al. (2013) were converted to a more commonly reported TE (**Supplementary Table S3**; Hess and Graham, 1990; Yager and von Hippel, 1991; Cambray et al., 2013; Mairhofer et al., 2015).

E. coli cultures measured at early exponential growth phase had similar levels of eYFP fluorescence across different strains with an average value of 7034 ± 134 arbitrary units (a.u.) (**Supplementary Figure S1**). In contrast, the strains showed a wide range of mTagBFP fluorescence values from 1.3 ± 3.4 a.u. to 9094 ± 446 a.u. Both eYFP and mTagBFP fluorescence values showed a unimodal and narrow distribution (**Supplementary Figure S2**). As expected, the two "no terminator" controls pC1.376 and pC1.377 produced the highest mTagBFP fluorescence values. Previous reports have indicated that translation efficiency is dependent on the length of the transcript (Lim et al., 2011), so we checked if eYFP levels might be decreased in the "no terminator" controls compared to plasmid with terminators. However, we observed no significant differences in eYFP levels between different plasmids, indicating that efficiency of eYFP translation was not reduced in either "no terminator" controls (**Supplementary Figure S1B**). The mTagBFP:eYFP ratio (i.e., Equation 1) for pC1.376 was 22% higher than for pC1.377, which indicated that pC1.376 produced more transcripts containing both mTagBFP and eYFP. Thus, we decided to use pC1.376 for all TE calculations in this study.

Sixteen terminators had TE values of >95% in *E. coli* (**Figure 2A** and **Supplementary Table S3**), with $T_{L3S2P21}$ and

[6]http://unafold.rna.albany.edu/?q=mfold

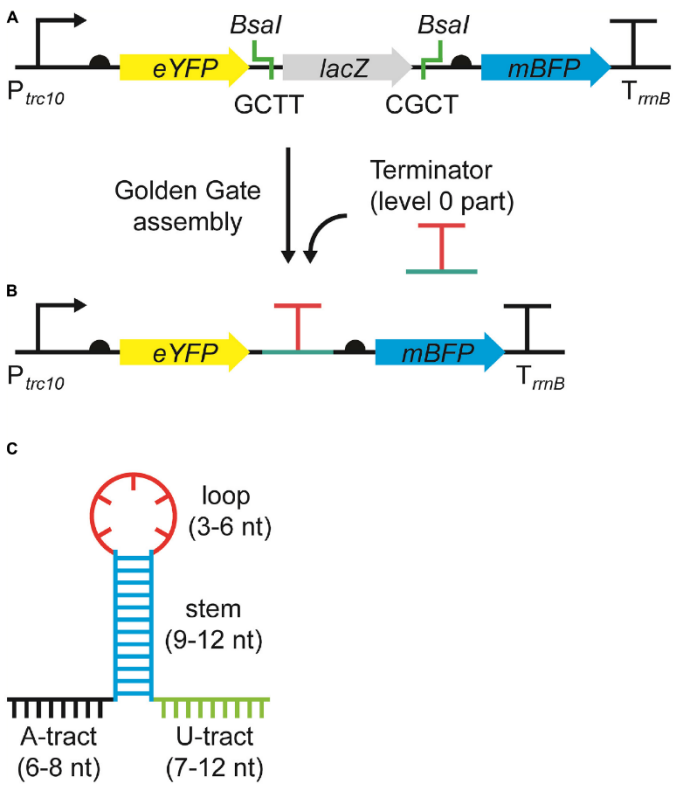

FIGURE 1 | The dual fluorescence reporter system for screening terminators. **(A)** The acceptor vector pDUOTK1-L1 contains two *Bsa*I sites that generate 4 nucleotide (nt) overhangs (i.e., GCTT and CGCT) following restriction, which are compatible with standard level 0 terminator parts (Engler et al., 2014). **(B)** Following a level 1 Golden Gate assembly reaction (Vasudevan et al., 2019), the level 0 terminator part is inserted between eYFP and mTagBFP and the dual fluorescent reporter system is formed, which can then be used to evaluate termination efficiency (TE). The reporter system is driven by the strong promoter P_{trc10} and is terminated by the terminator T_{rrnB}. Ribosome binding sites (half circles) are indicated (see **Supplementary Information S1** for sequence details). **(C)** Example of an intrinsic terminator structure and nt sequence, comprised of an adenine rich region (A-tract) (black), followed by a G-C rich stem (blue), a hairpin loop (red), and a uracil rich region (U-tract) (green).

T_{Bba_B0011} producing the highest (99.9%) and lowest values (40.8%), respectively. TE values for both PCC 6803 terminators were relatively low in *E. coli* (*ca.* 60%). Overall, the terminator library demonstrated a corresponding 10-fold change reduction in normalized downstream reporter expression (**Figure 2B**). We then compared the TE values for 30 native *E. coli* and synthetic terminators with those also reported in Chen et al. (2013) and observed a reasonable correlation (coefficient of determination (R^2) = 0.78), with 19 of the observed TE values differing by less than 5% (**Figure 2C**). The latter included 14 of the 16 strongest terminators with TE values of >95%. Similarly, the three weakest terminators (T_{Bba_B0011}, $T_{ECK120010842}$, and $T_{ECK120010820}$) were the same in both data sets. Six terminators showed a greater difference in TE values (i.e., 12–26%), which comprised four native *E. coli* terminators ($T_{ECK120030798}$, $T_{ECK120010820}$, T_{Bba_B0011}, and T_{Bba_B0061}) and two synthetic terminators ($T_{L3S1P22}$ and $T_{L3S1P13}$). These variations may have been due to differences in experimental setup (e.g., the vector, origin of replication (ori) and reporter genes) and the different strain of *E. coli* used, as significant differences in the behavior of some terminators has been reported between different *E. coli* strains (Kelly et al., 2019).

Performance of the Terminator Library in *Synechocystis* sp. PCC 6803

We next evaluated the terminator library in PCC 6803. Due to the slower growth rates of PCC 6803 compared to *E. coli* (**Supplementary Figure S3A**), we measured fluorescence levels at 24, 48, and 72 h (**Supplementary Figure S3B**). The cyanobacterial strains grew at comparable rates and the majority expressed eYFP at similar levels between strains at each time

TABLE 1 | List of terminators used in this study.

Vector ID	Part name	ΔG_A (kcal/mol)	Length (bp)	Terminator sequence	Origin	Reference
pC0.291	$T_{L3S2P21}$	−11.0	61	CTCGGTACCAAATTCCAGAAAAGAGGCCTCCCGAAAGGGGGGCCTTTTTTCGTTTTGGTCC		
pC0.292	$T_{L3S2P11}$	−11.0	57	CTCGGTACCAAATTCCAGAAAAGAGACGCTTTCGAGCGTCTTTTTTCGTTTTGGTCC		
pC0.293	$T_{L3S2P55}$	−2.8	57	CTCGGTACCAAAGACGAACAATAAGACGCTGAAAAGCGTCTTTTTTCGTTTTGGTCC		
pC0.294	$T_{L3S3P21}$	−4.1	53	CCAATTATTGAAGGCCTCCCTAACGGGGGGCCTTTTTTTGTTTCTGGTCTCCC	Synthetic	Chen et al., 2013
pC0.295	$T_{L3S1P13}$	−2.8	51	GACGAACAATAAGGCCTCCCTAACGGGGGGCCTTTTTTATTGATAACAAAA		
pC0.296	$T_{L3S3P11}$	−4.2	47	CCAATTATTGAACACCCTTCGGGGTGTTTTTTTGTTTCTGGTCTCCC		
pC0.306	$T_{L3S1P22}$	−2.8	48	GACGAACAATAAGGCCGCAAATCGCGGCCTTTTTTATTGATAACAAAA		
pC0.307	$T_{L3S1P47}$	−8.4	52	TTTTCGAAAAAAGGCCTCCCAAATCGGGGGGCCTTTTTTTATAGCAACAAAA		
pC0.066	T_{pheA-1}	−2.8	52	GACGAACAATAAGGCCTCCCAAATCGGGGGGCCTTTTTTATTGATAACAAAA		
pC0.068	$T_{ECK120010850}$	−4.4	45	AGTTAACCAAAAAGGGGGGATTTTATCTCCCCTTTAATTTTTCCT		
pC0.069	$T_{ECK120026481}$	−6.3	54	TACCACCGTCAAAAAAAACGGCGCTTTTTAGCGCCGTTTTTATTTTTCAACCTT		
pC0.072	$T_{ECK120010842}$	−2.5	47	CCGACGTAAAAAGACGGTAAGTATCGCTTTCAGTCTTATGAATATCG		
pC0.074	$T_{ECK120048902}$	−7.9	36	GCGTAAAAAAGCACCTTTTTAGGTGCTTTTTTGTGG		
pC0.062	T_{Bba_B0011}	−5.5	46	AGAGAATATAAAAAGCCAGATTATTAATCCGGCTTTTTTATTATTT	*E. coli*	Chen et al., 2013; Vasudevan et al., 2019
pC0.064	$T_{ECK120010820}$	−5.3	33	CTAAGCGTTGTCCCCAGTGGGGATGTGACGAAG		
pC0.070	T_{Bba_B0061}	−13.1	31	AAGTCAAAAGCCTCCGGTCGGAGGCTTTTGACTTT		
pC0.071	$T_{ECK120030798}$	−5.9	42	AGAATAAATTCAACCGCCCGTCAGGGCGGTTGTCATATGGAG		
pC0.073	$T_{ECK120010869}$	−5.6	35	TAACGTAAAAACCCGCTTCGGCGGGTTTTTTTATG		
pC0.077	$T_{ECK120010841-R}$	−3.0	41	AAAAACAAAAACCCCGGACTCTCATCCAGGGTTCTCTGCTT		
pC0.308	$T_{ECK120033737}$	−8.0	57	GGAAACACAGAAAAAAGCCCGCACCTGACAGTGCGGGCTTTTTTTTTCGACCAAAGG		
pC0.309	$T_{ECK120033736}$	−8.7	53	AACGCATGAGAAAGCCCCCGGAAGATCACCTTCCGGGGGCTTTTTTATTGCGC		
pC0.310	$T_{ECK120010818}$	−10.8	54	CACCTGTTTTACGTAAAAACCCGCTTCGGCGGGTTTTTACTTTTGG		
pC0.311	$T_{ECK120015440}$	−6.4	49	TCCGGCAATTAAAAAAGCGGCTAACCACGCCGCTTTTTTTACGTCTGCA		
pC0.312	$T_{ECK120029600}$	−4.8	90	TTCAGCCAAAAAACTTAAGACCGCCGGTCTTGTCCACTACCTTGCAGTAATGCGGTGGACAGGATCGGCGGTTTTCTTTTCTCTTCTCAA		
pC0.313	$T_{ECK120010799}$	−10.6	60	TCAGGAAAAAAGGCGACAGAGTAATCTGTCGCCTTTTTTCTTTGC	*E. coli*	Chen et al., 2013
pC0.314	$T_{ECK120010876}$	−5.6	55	GAAAAATAAAAACGGGCGCTAAAAAGCGCCGTTTTTTTGACCGT		
pC0.315	$T_{ECK120015170}$	−8.5	47	TTTCGAAAAAACCCGCTTCGGCGGGTTTTTTTATAGC		
pC0.316	$T_{ECK120017009}$	−5.5	44	GATCTAACTAAAAAGGCCGCTCTGCGGCCTTTTTTCTTTTCACT		
pC0.317	$T_{ECK120051401}$	−7.4	47	ATAGCAAAAAAGCGCCTTTAGGGCGCTTTTTTACATTG		
pC0.318	$T_{ECK120010855}$	−5.7	42	AACAACGGAAACCGGCCATTGCGCCGGTTTTTTTGGCC		
pC0.082	T_{rrnB}	−12.2	123	CAAATAAAACGAAAGGCTCAGTCGAAAGACTGGGCCTTTCGTTTTATCTGTTGTTTGTCGGTGAACGCTCTCTACTAGAGTCACACTGGCTCACCTTCGGGTGGGCCTTTCTGCG	*E. coli/Viral*	Vasudevan et al., 2019
pC0.063	$T_{pSB1AK3}$	−11.8	44	ATTTCAGATAAAAAAAATCCTTAGCTTTCGCTAAGGATGATTTC	*E. coli*	
pC0.079	T_{psbA2}	−1.9	83	CCAACTGAATAATCTGCAAATTGCACTCTCCTTCAATGGGGGGTGCTTTTTGCTTGACTGAGTAATCTTCTGATTGCTGATCT	PCC 6803	
pC0.081	T_{psaB}	−10.6	53	TTAAGCTTGTCCCCTGCCCTCGTTGGTGGGGGATTTGCTTTAATTGGCTGATC		

*The sequences have been annotated with features common to intrinsic terminators, including the A-tract (black underlined), stem (blue), loop (red), and U-tract (green underlined) (see **Figure 1C**) as reported by Chen et al. (2013). The features for the additional terminators were predicted using ARNold (http://ma.igmors.u-psud.fr/toolbox/arnold), Kinefold (http://kinefold.curie.fr/), or FindTerm (http://www.softberry.com/) (Xayaphoummine et al., 2005; Naville et al., 2011). Gibbs free energy values for the extended hairpin formation (i.e., the A- and U-tract) (ΔG_A) were calculated according to the equation $\Delta G_A = \Delta G_{HA} - \Delta G_H$, where ΔG_{HA} is the free energy of the hairpin loop with the inclusion of eight nucleotides upstream and downstream, and ΔG_H is the free energy of the hairpin loop alone (for generation of ΔG_{HA} and ΔG_H values, see section "Materials and Methods"). Further free energy values are shown in **Supplementary Table S4**.*

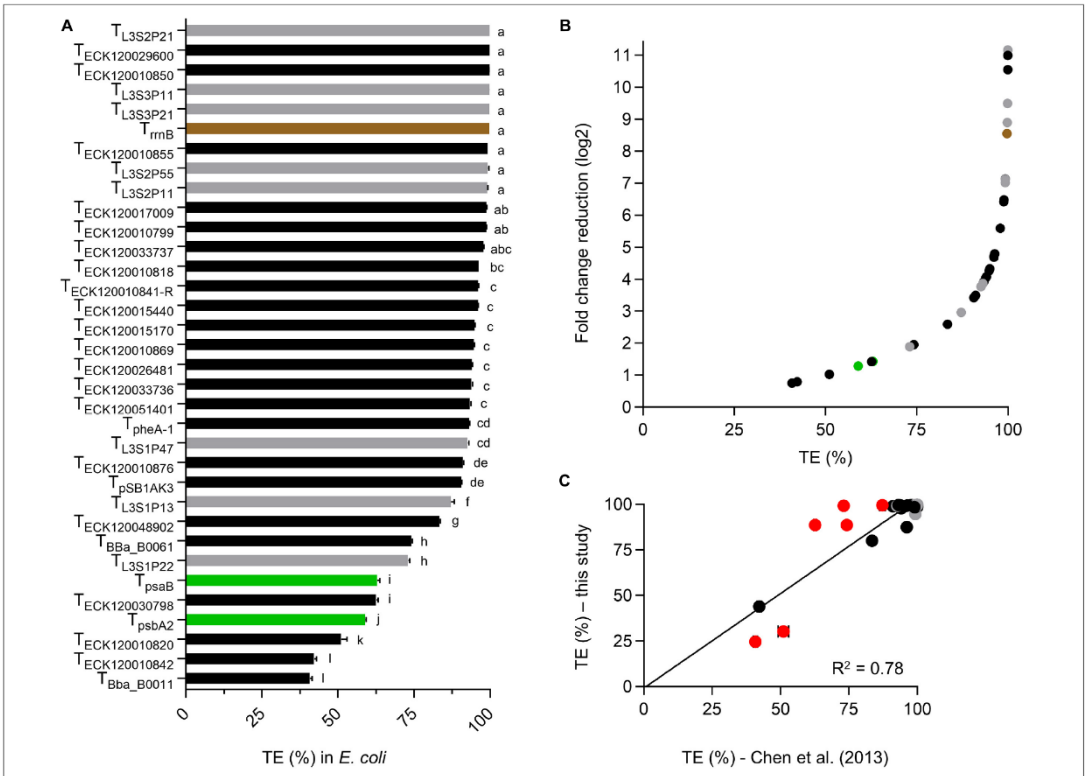

FIGURE 2 | Validation of the dual fluorescent reporter system in *E. coli*. **(A)** TE values for *E. coli* transformants at the early exponential phase of growth. Values are color coded for native *E. coli* (black), synthetic (gray) and native PCC 6803 terminators (green). T_{rrnB} is shown in brown. Error bars represent the ± standard error (SE) of the mean of >10,000 individual cells of four to eight biological replicates. Lowercase letters indicating significant difference ($P < 0.05$) are shown, as determined by ANOVA followed by Tukey's honestly significant difference test. **(B)** Comparison between TE and corresponding normalized fold change reduction in downstream reporter expression. An increase in one log2 value represents a 2-fold normalized change reduction. **(C)** Correlation analysis of TE values calculated from Chen et al. (2013) (**Supplementary Table S3**) and TE values determined in this study ($n = 30$). T_{rrnB}, $T_{pSB1AK3}$, T_{psbA2}, and T_{psaB} were excluded, as data was not available for comparison. The coefficient of determination (R^2) is shown. Terminator TE values marked in red ($T_{ECK120030798}$, $T_{ECK120010820}$, T_{Bba_B0011}, T_{Bba_B0061}, $T_{L3S1P22}$, and $T_{L3S1P13}$) differed from Chen et al. (2013) by more than 10%. Removal of these six terminator from the correlation analysis resulted in $R^2 = 0.9$).

point. The single exception was $T_{L3S2P21}$, which produced eYFP values consistently 2.5-fold higher than other strains. We are unsure why eYFP values were higher for $T_{L3S2P21}$, but we did re-confirm the terminator sequence in this strain by Sanger sequencing. In *E. coli* and bacteriophages, some intrinsic terminators can enhance upstream gene expression by enhancing the stability of the mRNA transcript via the hairpin loop (Abe and Aiba, 1996; Cisneros et al., 1996). Enhancement of mRNA stability by several putative intrinsic terminators has also been demonstrated for the marine species *Synechococcus* sp. PCC 7002, where transcripts with a canonical intrinsic terminator downstream were found to have a longer a half-life compared to transcripts without a downstream terminator (Gordon et al., 2020). However, $T_{L3S2P21}$ shares the same U-tract as both $T_{L3S2P11}$ and $T_{L3S2P55}$ but no increased eYFP expression was observed in the latter strains. mRNA transcript stability is a subject of ongoing research, but some examples of causative factors in heterotrophic bacteria include starvation in *E. coli* and *Lactococcus lactis* (Redon et al., 2005; Morin et al., 2020), and temperature induced stress in *Staphylococcus aureus* and *Mycobacterium tuberculosis* (Anderson et al., 2006; Rustad et al., 2013). mRNA concentration can influence mRNA stability, with increasing transcript concentration leading to decreased stability and mRNA turnover in *E. coli* and *L. lactis* (Nouaille et al., 2017). Similar examples have not been reported yet for PCC 6803.

Similarly to *E. coli*, PCC 6803 strains produced a wide range of mTagBFP fluorescence values at each time point (**Supplementary Figure S3B**), while the mTagBFP:eYFP ratio for the "no terminator" control pCA1.376 was also consistently higher by 21 ± 2% compared to pCA1.377. A strong correlation was shown between TE values measured at different time points with R^2 values ranging from 0.982 to 0.988 (**Supplementary Figure 3C**).

Comparison of TE values over the three time points were consistent for strong terminators (**Supplementary Table S3**). In contrast, weaker terminators tended to show a small decline in TE over time, although there was no significant change in the rankings observed. Overall, terminator behavior in PCC 6803 was consistent between on OD_{750} of 0.4 and 5.9 (**Supplementary Table S3**). Thus, we focused on reporting TE values at a single time point (48 h) below.

Thirteen terminators had TE values of >95% in PCC 6803 (**Figure 3A** and **Supplementary Table S3**), with $T_{L3S2P21}$ and $T_{ECK120029600}$ producing the highest value (99.5%) and $T_{ECK120010842}$ producing the lowest value (25.3%). Ten of the 13 strongest terminators in PCC 6803 also produced TE of >95% in *E. coli* (**Figure 2A**). Similarly, the two weakest terminators in PCC 6803 ($T_{ECK120010842}$ and T_{Bba_B0011}) were also the weakest in *E. coli*. Notably, $T_{L3S1P22}$ showed no detectable terminator activity in PCC 6803, but had a TE value of 73% in *E. coli*. Overall, the terminator library demonstrated a corresponding 8-fold change reduction in normalized downstream reporter expression in PCC 6803 (**Figure 3B**). The TE values of 10 terminators differed more widely from those in *E. coli* (i.e., by 12–46%). Thus, the correlation of TE values between *E. coli* and PCC 6803 was modest (R^2 = 0.46) (**Figure 3C**). Removal of $T_{L3S1P22}$ led to only a marginal improvement (R^2 = 0.53).

Performance of the Terminator Library in *Synechococcus elongatus* UTEX 2973 and Comparison Between Species

Lastly, we evaluated our terminator library in the high-light tolerant strain UTEX 2973. UTEX 2973 generally grew faster than PCC 6803, but showed more variability in growth rates (**Supplementary Figure S4A**). This was likely due to a greater relative difference in light distribution within the growth incubator under the higher light levels used for culturing UTEX 2973, as strains in the same plate showed more similar rates of growth compared to those located at different positions within the incubator. As for PCC 6803, we measured fluorescence

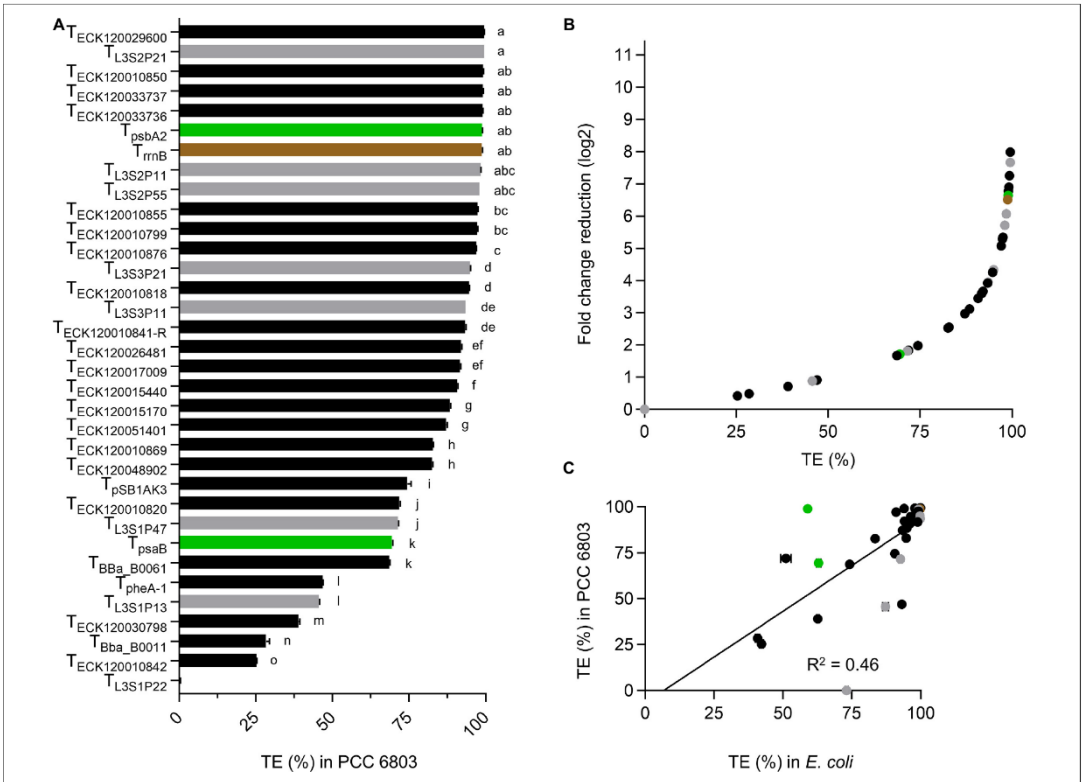

FIGURE 3 | Terminator performances in *Synechocystis* sp. PCC 6803. **(A)** TE values from PCC 6803 transconjugants after 48 h of growth. Color coding is as in **Figure 2**. Error bars represent the ±SE of the mean of >10,000 individual cells of four biological replicates. Lowercase letters indicating significant difference ($P < 0.05$) are shown, as determined by ANOVA followed by Tukey's honestly significant difference test. **(B)** Comparison between TE values and corresponding normalized fold change reduction in downstream reporter expression. **(C)** Correlation analysis of TE values between *E. coli* and PCC 6803 (n = 34).

levels for UTEX 2973 at 24, 48, and 72 h (**Supplementary Figure S4B**). Consistent with the observed differences in growth, the expression levels of eYFP were variable between strains at 24 hr. However, this variation decreased over time.

As for PCC 6803, mTagBFP fluorescence values for the UTEX 2973 strains showed a wide spread at each time point, while the mTagBFP:eYFP ratio for pCA1.376 was consistently higher by 20 ± 5% compared to pCA1.377. Furthermore, the expression levels of mTagBFP and eYFP for pCA1.337 were more variable over time in UTEX 2973, with large increases in both eYFP and mTagBFP fluorescence values observed at 48 h (**Supplementary Figure S4B**). The TE values over the three time points were similar for most strains, with R^2 values ranging from 0.964 to 0.978 (**Supplementary Figure 4C**), indicating that terminator behavior in UTEX 2973 was consistent between an OD_{750} of 0.4–11 (**Supplementary Table S3**). Thus, as for PCC 6803 we also focused on reporting TE values at 48 h below.

Eleven terminators had TE values of >95% in UTEX 2973 (**Figure 4A** and **Supplementary Table S3**), with $T_{ECK120029600}$ producing a very high value of 99.9% and T_{Bba_B0061} producing the lowest value (29.7%). Six of the 10 strongest terminators in UTEX 2973 produced TE values of >95% in *E. coli* (**Figure 2A**), while seven of these terminators also produced TE values of >95% in PCC 6803 (**Figure 3A**). The three weakest terminators in UTEX 2973 (T_{Bba_B0061}, $T_{ECK120030798}$, and $T_{ECK120010820}$) were among the bottom ten ranked terminators in PCC 6803 and *E. coli*. $T_{ECK120010820}$ achieved the same ranking (i.e., 3rd weakest terminator) in both UTEX 2973 and *E. coli*. Overall, the terminator library demonstrated a corresponding 10-fold change reduction of normalized downstream reporter expression in UTEX 2973 (**Figure 4B**). Similarly to PCC 6803, the correlation of TE values between UTEX 2973 and *E. coli* was low (R^2 = 0.35) (**Figure 4C**). More surprisingly, the correlation of TE values between UTEX 2973 and PCC 6803 was even lower (R^2 = 0.12) (**Figure 4D**).

We next compared the TE values for *E. coli*, PCC 6803 and UTEX 2973 to identify terminators that were consistently strong between different species (**Supplementary Table S3**). The overall strongest terminator was $T_{ECK120029600}$, which had TE values of >99.5% across all three species. A further four terminators ($T_{L3S2P21}$, $T_{ECK120010850}$, $T_{L3S2P11}$, and T_{rrnB}) also had consistent cross-species TE values of >96%. For the two cyanobacterial species alone, $T_{ECK120033736}$ and T_{psbA2} had TE values of >95.8%. The TE values for these seven strong terminators was also very consistent over time for PCC 6803 and UTEX 2973.

The Performance of the Seven Strongest Terminators Was Consistent Under Suboptimal Growth Conditions

To examine if terminator performance might be affected by the growth environment, we measured the TE values for the seven strongest terminators in PCC 6803 and UTEX 2973 grown under suboptimal conditions. Both species were cultured at 30°C in 300 μM photons m^{-2} s^{-1}, which is considered high light for PCC 6803 (typically grown at 100 μM photons m^{-2} s^{-1}) and a low temperature for UTEX 2973 (typically grown at 40°C) (Vasudevan et al., 2019).

Both PCC 6803 and UTEX 2973 grew at similar rates and reached an OD_{750} of 5.9 and 5.7 after 72 h, respectively (**Supplementary Figure S5A**). In higher light PCC 6803 grew faster than under typical conditions, while growth rates were reduced in UTEX 2973 due to the lower temperature. Fluorescence measurements for eYFP and mTagBFP in PCC 6803 were comparable to those under typical growth conditions (**Supplementary Figure S5B**). In contrast, fluorescence values were generally reduced at all time points in UTEX 2973 (**Supplementary Figure S5C**). TE values for each day were calculated as before (**Supplementary Table S3**), and the mean values for the three time points were compared (**Table 2**). Overall, all seven terminators retained TE values of >95.8% for both species under the suboptimal growth conditions, and $T_{ECK120029600}$ remained the strongest terminator. Overall, our results indicated that the performance of these terminators was generally consistent and robust between the two growth conditions.

DISCUSSION

Here, we adapted a dual reporter tool for the CyanoGate MoClo Assembly system that provides a normalized quantification of terminator efficiency within and between species. The pDUOTK1-L1 vector is compatible with several available libraries and thus facilitates easy adoption and sharing of parts with the community (Andreou and Nakayama, 2018; Lai et al., 2018; Valenzuela-Ortega and French, 2019; Vasudevan et al., 2019), and is accessible to any lab currently using Golden Gate cloning. The robustness of our system was validated by comparing results in *E. coli* against previously published data (Chen et al., 2013).

The pDUOTK1-L1 vector contains the broad host range replicative origin RSF1010, which has been shown to be functional in a wide diversity of prokaryotic species, including cyanobacteria from all five subsections (Mermet-Bouvier et al., 1993; Stucken et al., 2012; Bishé et al., 2019). Thus, pDUOTK1-L1 could help to make terminator characterization more accessible, as promising new strains are discovered (Włodarczyk et al., 2019; Jaiswal et al., 2020; Nies et al., 2020). To the best of our knowledge, this is the first study to compare the efficiencies of terminators between two different cyanobacterial species. We identified five strong terminators with consistent TE values in *E. coli*, PCC 6803 and UTEX 2973. These findings should help to inform future strategies for building gene expression systems or more advanced gene circuit designs.

Besides the double terminator T_{rrnB}, no unique features could be identified for any of the five strong terminators that behaved consistently between all three species (i.e., the hairpin loop length and GC content, and adenine and uracil content for the A-tract and U-tract, respectively). Overall, our results showed that terminator performances was highly reproducible at different growth points for the same strain but generally differed between the three species examined, and significant differences were observed between PCC 6803 and UTEX 2973 even though both are subsection I species (Castenholz et al., 2001). We also demonstrated that the performance of the seven strongest

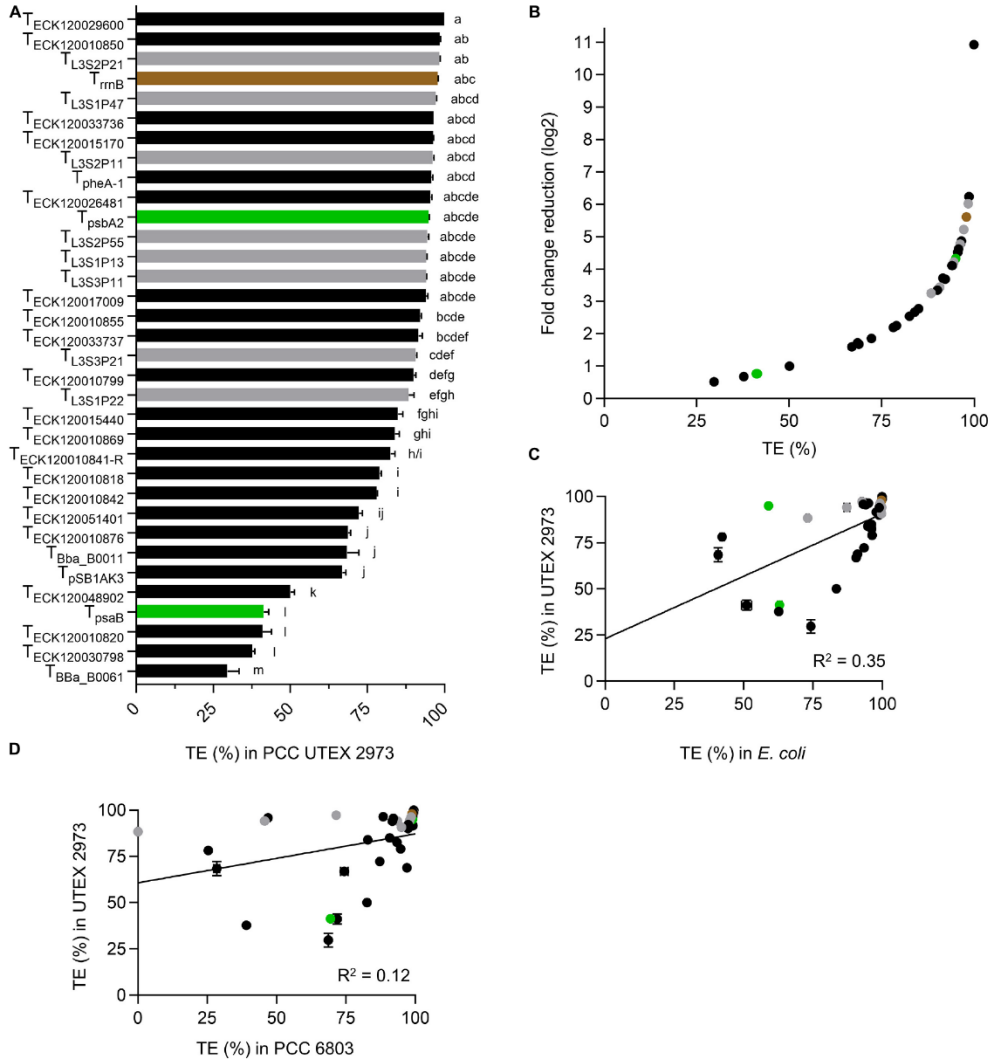

FIGURE 4 | Terminators performances in *Synechococcus elongatus* UTEX 2973. **(A)** TE value from UTEX 2973 after 48 h growth. Color coding is as in **Figure 2**. Error bars represent the ± SE of the mean of >10,000 individual cells of four biological replicates. Lowercase letters indicating significant difference ($P < 0.05$) are shown, as determined by ANOVA followed by Tukey's honestly significant difference test. **(B)** Comparison between TE values and corresponding normalized fold change reduction in downstream reporter expression. **(C)** Correlation analysis of TE values between *E. coli* and UTEX 2973 ($n = 34$). **(D)** Correlation analysis of TE values between PCC 6803 and UTEX 2973 ($n = 34$).

terminators was consistent in different growth conditions for PCC 6803 and UTEX 2793. Cyanobacterial RNAPs do differ in structure compared to other bacterial RNAPs [for a recent review see Stensjö et al. (2018)]. In addition, RNAP subunits also differ between cyanobacterial species [for a recent review see Srivastava et al. (2020)]. For example, the primary vegetative sigma factor (sigA) in PCC 6803 (srl0653) and UTEX 2973 (WP_071818124.1) have a shared identity and similarity of only 70.5 and 74.1%, respectively (**Supplementary Figure S7**). Furthermore, cyanobacteria lack transcription elongation factors commonly found in heterotrophic bacteria to restart elongation and for proofreading of transcripts. To compensate, cyanobacterial RNAPs have evolved additional proof-reading and elongation functionalities (Riaz-Bradley et al., 2020). These differences may

TABLE 2 | Terminator performances in *Synechocystis* sp. PCC 6803 and Synechococcus elongatus UTEX 2973 under suboptimal growth conditions.

	TE (%) in PCC 6803		TE (%) in UTEX 2973	
	30°C, 100 μM photons m^{-2} s^{-1}	30°C, 300 μM photons m^{-2} s^{-1}	40°C, 300 μM photons m^{-2} s^{-1}	30°C, 300 μM photons m^{-2} s^{-1}
$T_{L3S2P21}$	99.5 ± 0.1	99.6 ± 0.1	97.1 ± 2.2	98.1 ± 0.9
$T_{L3S2P11}$	98.3 ± 0.2	98.3 ± 0.6	95.9 ± 0.5	95.9 ± 1.0
$T_{ECK120010850}$	99.2 ± 0.2	99.4 ± 0.2	98.1 ± 0.6	98.5 ± 0.3
$T_{ECK120033736}$	99.0 ± 0.1	99.3 ± 0.3	97.0 ± 0.9	98.1 ± 1.3
$T_{ECK120029600}$	99.6 ± 0.3	99.7 ± 0.2	99.9 ± 0.1	99.9 ± 0.1
T_{rrnB}	98.4 ± 0.4	98.4 ± 0.9	98.5 ± 0.5	98.0 ± 0.7
T_{psbA2}	98.7 ± 0.2	98.8 ± 0.4	95.8 ± 0.9	96.9 ± 1.2

The mean TE values for PCC 6803 and UTEX 2973 at 24, 48, and 72 h are shown for typical and suboptimal growth conditions (see ***Supplementary Table S3*** *for daily values). The standard deviation represents four biological replicates from each time point (n = 12).*

account for the observed disparity in terminator performance between *E. coli* and cyanobacteria. However, the differences between PCC 6803 and UTEX 2973 were intriguing, and could suggest that RNAP activities differ between cyanobacterial species and/or that other unknown factors are involved.

Several methods and prediction tools exist for the identification and mapping of intrinsic terminators in different species (Carafa et al., 1990; de Hoon et al., 2005; Gardner et al., 2011; Naville et al., 2011; Fritsch et al., 2015; Millman et al., 2017). Traditionally, these approaches have relied on identifying sequence features associated with intrinsic terminators (e.g., the hairpin loop). Previous studies have suggested a relationship between terminator performance and the estimated Gibbs free energy of the extended hairpin (ΔG_A), the U-tract (ΔG_U) and to a lesser extent the hairpin loop (ΔG_H) (Cambray et al., 2013; Chen et al., 2013). In our study, we did not find a strong correlation between TE values and ΔG_A, ΔG_H or the estimated Gibbs free energy of the complete terminator sequence (**Supplementary Figure S6**). Although our terminator library was relatively small, the differences in terminator behavior within and between species indicated that there may be more factors involved in determining intrinsic termination than can be attributed to the properties of individual structural components. For example, the U-tract appears dispensable for intrinsic termination in mycobacteria (Ahmad et al., 2020). Cutting edge approaches utilizing RNA-seq methods have also been applied for the identification of previously unknown terminators in the *E. coli* genome, which go beyond that which has been achieved with previous structural identification models (Ju et al., 2019). In addition, recent work has shown that terminator sequences can be designed as tunable control elements that can be "turned on" to attenuate gene transcription at low temperatures (Roßmanith et al., 2018). With the growing evidence that the structural components of terminators may be malleable depending on species, future work should focus on understanding the combined contributions of terminator components, including those beyond transcriptional control (e.g., modulation of protein expression) for metabolic engineering (Curran et al., 2013; Ito et al., 2020). This may lead to better designs for strong synthetic terminators with consistent cross-species performance. As terminator research and cyanobacterial synthetic biology progresses, tools such as pDUOTK1-L1 will be useful for reliable and convenient determination of terminator efficiency across a broad-host range.

DATA AVAILABILITY STATEMENT

The original contributions presented in the study are included in the article/**Supplementary Material**, further inquiries can be directed to the corresponding author/s.

AUTHOR CONTRIBUTIONS

GG and AM: conceptualization and writing–original draft preparation. GG: performing the experiments. BW and AM: supervision. All authors: experimental design and writing–review and editing.

FUNDING

GG acknowledges funding support from the BBSRC EASTBIO CASE Ph.D. programme (BB/M010996/1). AM acknowledges funding from the UK Biotechnology and Biological Sciences Research Council (BBSRC) grant (BB/S020128/1). BW acknowledges funding support by the UK Research and Innovation Future Leaders Fellowship (MR/S018875/1) and the Leverhulme Trust research project grant (RPG-2020-241).

ACKNOWLEDGMENTS

Flow cytometry data were generated within the Flow Cytometry and Cell Sorting Facility in Ashworth, King's Buildings at the University of Edinburgh. The facility was supported by funding from Wellcome and the University of Edinburgh.

SUPPLEMENTARY MATERIAL

The Supplementary Material for this article can be found online at: https://www.frontiersin.org/articles/10.3389/fmicb.2020.624011/full#supplementary-material

REFERENCES

Abe, H., and Aiba, H. (1996). Differential contributions of two elements of rho-independent terminator to transcription termination and mRNA stabilization. *Biochimie* 78, 1035–1042. doi: 10.1016/S0300-9084(97)86727-2

Ahmad, E., Hegde, S. R., and Nagaraja, V. (2020). Revisiting intrinsic transcription termination in mycobacteria: u-tract downstream of secondary structure is dispensable for termination. *Biochem. Biophys. Res. Commun.* 522, 226–232. doi: 10.1016/j.bbrc.2019.11.062

Anderson, K. L., Roberts, C., Disz, T., Vonstein, V., Hwang, K., Overbeek, R., et al. (2006). Characterization of the Staphylococcus aureus heat shock, cold shock, stringent, and SOS responses and their effects on log-phase mRNA turnover. *J. Bacteriol.* 188, 6739–6756. doi: 10.1128/JB.00609-06

Andreou, A. I., and Nakayama, N. (2018). Mobius assembly: a versatile golden-gate framework towards universal DNA assembly. *PLoS One* 13:e0189892. doi: 10.1371/journal.pone.0189892

Behle, A., Saake, P., Germann, A. T., Dienst, D., and Axmann, I. M. (2020). Comparative dose–response analysis of inducible promoters in cyanobacteria. *ACS. Synth. Biol.* 9, 843–855. doi: 10.1021/acssynbio.9b00505

Bishé, B., Taton, A., and Golden, J. W. (2019). Modification of RSF1010-based broad-host-range plasmids for improved conjugation and cyanobacterial bioprospecting. *IScience* 20, 216–228. doi: 10.1016/J.ISCI.2019.09.002

Cambray, G., Guimaraes, J. C., Mutalik, V. K., Lam, C., Mai, Q. A., Thimmaiah, T., et al. (2013). Measurement and modeling of intrinsic transcription terminators. *Nucleic Acids Res.* 41, 5139–5148. doi: 10.1093/nar/gkt163

Camsund, D., Heidorn, T., and Lindblad, P. (2014). Design and analysis of LacI-repressed promoters and DNA-looping in a cyanobacterium. *J. Biol. Eng.* 8:4. doi: 10.1186/1754-1611-8-4

Carafa, Y. D. A., Brody, E., and Thermes, C. (1990). Prediction of rho-independent Escherichia coli transcription terminators. a statistical analysis of their RNA stem-loop structures. *J. Mol. Biol.* 216, 835–858. doi: 10.1016/S0022-2836(99)80005-9

Castenholz, R. W., Wilmotte, A., Herdman, M., Rippka, R., Waterbury, J. B., Iteman, I., et al. (2001). "Phylum BX. Cyanobacteria," in *Bergey's Manual® of Systematic Bacteriology: Volume One?: the Archaea and the Deeply Branching and Phototrophic Bacteria*, eds D. R. Boone, R. W. Castenholz, and G. M. Garrity (New York, NY: Springer), 473–599.

Chen, Y. J., Liu, P., Nielsen, A. A. K., Brophy, J. A. N., Clancy, K., Peterson, T., et al. (2013). Characterization of 582 natural and synthetic terminators and quantification of their design constraints. *Nat. Methods* 10, 659–664. doi: 10.1038/nmeth.2515

Cisneros, B., Court, D., Sanchez, A., and Montañez, C. (1996). Point mutations in a transcription terminator, λtI, that affect both transcription termination and RNA stability. *Gene* 181, 127–133. doi: 10.1016/S0378-1119(96)00492-1

Curran, K. A., Karim, A. S., Gupta, A., and Alper, H. S. (2013). Use of expression-enhancing terminators in Saccharomyces cerevisiae to increase mRNA half-life and improve gene expression control for metabolic engineering applications. *Metab. Eng.* 19, 88–97. doi: 10.1016/j.ymben.2013.07.001

de Hoon, M. J. L., Makita, Y., Nakai, K., and Miyano, S. (2005). Prediction of transcriptional terminators in bacillus subtilis and related species. *PLoS Comput. Biol.* 1:e25. doi: 10.1371/journal.pcbi.0010025

Engler, C., Youles, M., Gruetzner, R., Ehnert, T. M., Werner, S., Jones, J. D. G., et al. (2014). A golden gate modular cloning toolbox for plants. *ACS Synth. Biol.* 3, 839–843. doi: 10.1021/sb4001504

Englund, E., Liang, F., and Lindberg, P. (2016). Evaluation of promoters and ribosome binding sites for biotechnological applications in the unicellular cyanobacterium *Synechocystis sp*. PCC 6803. *Sci. Rep.* 6:36640. doi: 10.1038/srep36640

Eungrasamee, K., Miao, R., Incharoensakdi, A., Lindblad, P., and Jantaro, S. (2019). Improved lipid production via fatty acid biosynthesis and free fatty acid recycling in engineered *Synechocystis sp*. PCC 6803. *Biotechnol. Biofuels* 12:8. doi: 10.1186/s13068-018-1349-8

Ferreira, E. A., Pacheco, C. C., Pinto, F., Pereira, J., Lamosa, P., Oliveira, P., et al. (2018). Expanding the toolbox for *Synechocystis sp*. PCC 6803: validation of replicative vectors and characterization of a novel set of promoters. *Synth. Biol.* 3:ysy014. doi: 10.1093/synbio/ysy014

Fritsch, T. E., Siqueira, F. M., and Schrank, I. S. (2015). Intrinsic terminators in *Mycoplasma hyopneumoniae* transcription. *BMC Genomics* 16:273. doi: 10.1186/s12864-015-1468-6

Gale, G. A. R., Schiavon Osorio, A. A., Puzorjov, A., Wang, B., and McCormick, A. J. (2019). Genetic modification of cyanobacteria by conjugation using the cyanogate modular cloning toolkit. *J. Vis. Exp.* 152:e60451. doi: 10.3791/60451

Gardner, P. P., Barquist, L., Bateman, A., Nawrocki, E. P., and Weinberg, Z. (2011). RNIE: genome-wide prediction of bacterial intrinsic terminators. *Nucleic Acids Res.* 39, 5845–5852. doi: 10.1093/nar/gkr168

Gordon, G. C., Cameron, J. C., Gupta, S. T. P., Engstrom, M. D., Reed, J. L., and Pfleger, B. F. (2020). Genome-wide analysis of RNA decay in the cyanobacterium *Synechococcus sp*. Strain PCC 7002. *MSystems* 5:e00224–20 doi: 10.1128/msystems.00224-20

Herbert, K. M., Greenleaf, W. J., and Block, S. M. (2008). Single-molecule studies of RNA polymerase: motoring along. *Annu. Rev. Biochem.* 77, 149–176.

Hess, G. F., and Graham, R. S. (1990). Efficiency of transcriptional terminators in *Bacillus subtilis*. *Gene* 95, 137–141.

Huang, H. H., Lindblad, P. (2013). Wide-dynamic-range promoters engineered for cyanobacteria. *J. Biol. Eng.* 7:10. doi: 10.1186/1754-1611-7-10

Huang, H. H., Camsund, D., Lindblad, P., and Heidorn, T. (2010). Design and characterization of molecular tools for a synthetic biology approach towards developing cyanobacterial biotechnology. *Nucleic Acids Res.* 38, 2577–2593. doi: 10.1093/nar/gkq164

Huang, I.-S., and Zimba, P. V. (2019). Cyanobacterial bioactive metabolites—a review of their chemistry and biology. *Harmful Algae* 83, 42–94. doi: 10.1016/J.HAL.2018.11.008

Immethun, C. M., DeLorenzo, D. M., Focht, C. M., Gupta, D., Johnson, C. B., and Moon, T. S. (2017). Physical, chemical, and metabolic state sensors expand the synthetic biology toolbox for *Synechocystis sp*. PCC 6803. *Biotechnol. Bioeng.* 114, 1561–1569. doi: 10.1002/bit.26275

Ito, Y., Terai, G., Ishigami, M., Hashiba, N., Nakamura, Y., Bamba, T., et al. (2020). Exchange of endogenous and heterogeneous yeast terminators in *Pichia pastoris* to tune mRNA stability and gene expression. *Nucleic Acids Res.* 48, 13000–13012. doi: 10.1093/nar/gkaa1066

Jaiswal, D., Sengupta, A., Sengupta, S., Madhu, S., Pakrasi, H. B., and Wangikar, P. P. (2020). A novel cyanobacterium *Synechococcus elongatus* PCC 11802 has distinct genomic and metabolomic characteristics compared to its neighbor PCC 11801. *Sci. Rep.* 10:191. doi: 10.1038/s41598-019-57051-0

Ju, X., Li, D., and Liu, S. (2019). Full-length RNA profiling reveals pervasive bidirectional transcription terminators in bacteria. *Nat. Microbiol.* 4, 1907–1918. doi: 10.1038/s41564-019-0500-z

Kelly, C. L., Taylor, G. M., Hitchcock, A., Torres-Méndez, A., and Heap, J. T. (2018). A rhamnose-inducible system for precise and temporal control of gene expression in cyanobacteria. *ACS Synth. Biol.* 7, 1056–1066. doi: 10.1021/acssynbio.7b00435

Kelly, C. L., Taylor, G. M., Satkute, A., Dekker, L., and Heap, J. T. (2019). Transcriptional terminators allow leak-free chromosomal integration of genetic constructs in cyanobacteria. *BioRxiv [Preprint]* doi: 10.1101/689281

Kim, W. J., Lee, S.-M., Um, Y., Sim, S. J., and Woo, H. M. (2017). Development of synebrick vectors as a synthetic biology platform for gene expression in *Synechococcus elongatus* PCC 7942. *Front. Plant Sci.* 8:293. doi: 10.3389/fpls.2017.00293

Knoot, C. J., Ungerer, J., Wangikar, P. P., and Pakrasi, H. B. (2018). Cyanobacteria: promising biocatalysts for sustainable chemical production. *J. Biol. Chem.* 293, 5044–5052. doi: 10.1074/JBC.R117.815886

Lai, H. E., Moore, S., Polizzi, K., and Freemont, P. (2018). EcoFlex: a multifunctional moclo kit for E. coli synthetic biology. *Methods Mol. Biol.* 1772, 429–444. doi: 10.1007/978-1-4939-7795-6_25

Lea-Smith, D. J., Vasudevan, R., and Howe, C. J. (2016). Generation of marked and markerless mutants in model cyanobacterial species. *J. Vis. Exp.* 2016:54001. doi: 10.3791/54001

Lim, H. N., Lee, Y., and Hussein, R. (2011). Fundamental relationship between operon organization and gene expression. *Proc. Natl. Acad. Sci. USA* 108, 10626–10631. doi: 10.1073/pnas.1105692108

Lin, P. C., and Pakrasi, H. B. (2019). Engineering cyanobacteria for production of terpenoids. *Planta* 249, 145–154. doi: 10.1007/s00425-018-3047-y

Lin, P. C., Saha, R., Zhang, F., and Pakrasi, H. B. (2017). Metabolic engineering of the pentose phosphate pathway for enhanced limonene production in the cyanobacterium *Synechocysti s sp*. PCC. *Sci. Rep*. 7:17503. doi: 10.1038/s41598-017-17831-y

Liu, D., and Pakrasi, H. B. (2018). Exploring native genetic elements as plug-in tools for synthetic biology in the cyanobacterium *Synechocystis* sp. PCC 6803. *Microb. Cell. Fact.* 17, 1–8. doi: 10.1186/s12934-018-0897-8

Ma, A. T., Schmidt, C. M., and Golden, J. W. (2014). Regulation of gene expression in diverse cyanobacterial species by using theophylline-responsive riboswitches. *Appl. Environ. Microbiol.* 80, 6704–6713. doi: 10.1128/AEM.01697-14

Mairhofer, J., Wittwer, A., Cserjan-Puschmann, M., and Striedner, G. (2015). Preventing T7 RNA polymerase read-through transcription—a synthetic termination signal capable of improving bioprocess stability. *ACS Synth. Biol.* 4, 265–273. doi: 10.1021/sb5000115

Mermet-Bouvier, P., Cassier-Chauvat, C., Marraccini, P., and Chauvat, F. (1993). Transfer and replication of RSF1010-derived plasmids in several cyanobacteria of the genera *Synechocystis* and *Synechococcus*. *Curr. Microbiol.* 27, 323–327. doi: 10.1007/BF01568955

Millman, A., Dar, D., Shamir, M., and Sorek, R. (2017). Computational prediction of regulatory, premature transcription termination in bacteria. *Nucleic Acids Res.* 45, 886–893. doi: 10.1093/nar/gkw749

Morin, M., Enjalbert, B., Ropers, D., Girbal, L., and Cocaign-Bousquet, M. (2020). Genomewide stabilization of mRNA during a "Feast-To-Famine" growth transition in ⁢span class="named-content genus-species" id="named-content-1">*Escherichia coli*⁢/span&gt. *MSphere* 5, e276–e220. doi: 10.1128/mSphere.00276-20

Moser, F., Espah Borujeni, A., Ghodasara, A. N., Cameron, E., Park, Y., and Voigt, C. A. (2018). Dynamic control of endogenous metabolism with combinatorial logic circuits. *Mol. Syst. Biol.* 14:e8605. doi: 10.15252/msb.20188605

Naville, M., Ghuillot-Gaudeffroy, A., Marchais, A., and Gautheret, D. (2011). ARNold: a web tool for the prediction of Rho-independent transcription terminators. *RNA Biol.* 8, 11–13. doi: 10.4161/rna.8.1.13346

Nies, F., Mielke, M., Pochert, J., and Lamparter, T. (2020). Natural transformation of the filamentous cyanobacterium *Phormidium lacuna*. *PLoS One* 15:e023440. doi: 10.1371/journal.pone.0234440

Nouaille, S., Mondeil, S., Finoux, A. L., Moulis, C., Girbal, L., and Cocaign-Bousquet, M. (2017). The stability of an mRNA is influenced by its concentration: a potential physical mechanism to regulate gene expression. *Nucleic Acids Res.* 45, 11711–11724. doi: 10.1093/nar/gkx781

Peters, J. M., Mooney, R. A., Kuan, P. F., Rowland, J. L., Keleş, S., and Landick, R. (2009). Rho directs widespread termination of intragenic and stable RNA transcription. *Proc. Natl. Acad. Sci. U.S.A.* 106, 15406–15411. doi: 10.1073/pnas.0903846106

Peters, J. M., Vangeloff, A. D., and Landick, R. (2011). Bacterial transcription terminators: the RNA 3′-end chronicles. *J. Mol. Biol.* 412, 793–813. doi: 10.1016/j.jmb.2011.03.036

Redon, E., Loubiere, P., and Cocaign-Bousquet, M. (2005). Transcriptome analysis of the progressive adaptation of *Lactococcus lactis* to carbon starvation. *J. Bacteriol.* 187, 3589–3592. doi: 10.1128/JB.187.10.3589-3592.2005

Riaz-Bradley, A., James, K., and Yuzenkova, Y. (2020). High intrinsic hydrolytic activity of cyanobacterial RNA polymerase compensates for the absence of transcription proofreading factors. *Nucleic Acids Res.* 48, 1341–1352. doi: 10.1093/nar/gkz1130

Roßmanith, J., Weskamp, M., and Narberhaus, F. (2018). Design of a temperature-responsive transcription terminator. *ACS Synth. Biol.* 7, 613–621. doi: 10.1021/acssynbio.7b00356

Rustad, T. R., Minch, K. J., Brabant, W., Winkler, J. K., Reiss, D. J., Baliga, N. S., et al. (2013). Global analysis of mRNA stability in *Mycobacterium tuberculosis*. *Nucleic Acids Res.* 41, 509–517. doi: 10.1093/nar/gks1019

Shen, P., and Huang, H. V. (1986). Homologous recombination in *Escherichia coli*: dependence on substrate length and homology. *Genetics* 112, 441–457.

Sleight, S. C., Bartley, B. A., Lieviant, J. A., and Sauro, H. M. (2010). Designing and engineering evolutionary robust genetic circuits. *J. Biol. Eng.* 4:12. doi: 10.1186/1754-1611-4-12

Srivastava, A., Varshney, R. K., and Shukla, P. (2020). Sigma factor modulation for cyanobacterial metabolic engineering. *Trends Microbiol.* doi: 10.1016/j.tim.2020.10.012 Online ahead of print.

Stensjö, K., Vavitsas, K., and Tyystjärvi, T. (2018). Harnessing transcription for bioproduction in cyanobacteria. *Physiol. Plant.* 162, 148–155. doi: 10.1111/ppl.12606

Stucken, K., Ilhan, J., Roettger, M., Dagan, T., and Martin, W. F. (2012). Transformation and conjugal transfer of foreign genes into the filamentous multicellular cyanobacteria (subsection V) *Fischerella* and *Chlorogloeopsis*. *Curr. Microbiol.* 65, 552–560. doi: 10.1007/s00284-012-0193-5

Sun, T., Li, S., Song, X., Pei, G., Diao, J., Cui, J., et al. (2018). Re-direction of carbon flux to key precursor malonyl-CoA via artificial small RNAs in photosynthetic *Synechocystis sp*. PCC 6803. *Biotechnol. Biofuels* 11:26. doi: 10.1186/s13068-018-1032-0

Tsinoremas, N. F., Kutach, A. K., Strayer, C. A., and Golden, S. S. (1994). Efficient gene transfer in *Synechococcus sp*. strains PCC 7942 and PCC 6301 by interspecies conjugation and chromosomal recombination. *J. Bacteriol.* 176, 6764–6768. doi: 10.1128/jb.176.21.6764-6768.1994

Valenzuela-Ortega, M., and French, C. (2019). Joint universal modular plasmids (JUMP): a flexible and comprehensive platform for synthetic biology. *BioRxiv [Preprint]* doi: 10.1101/799585

Vasudevan, R., Gale, G. A. R., Schiavon, A. A., Puzorjov, A., Malin, J., Gillespie, M. D., et al. (2019). Cyanogate: a modular cloning suite for engineering cyanobacteria based on the plant moclo syntax. *Plant Physiol.* 180, 39–55. doi: 10.1104/pp.18.01401

Vijayan, V., Jain, I. H., and O'Shea, E. K. (2011). A high resolution map of a cyanobacterial transcriptome. *Genome Biol.* 12:R47. doi: 10.1186/gb-2011-12-5-r47

Williams, J. G. K. (1988). Methods in synechocystis 6803. *Methods Enzymol.* 167, 766–778.

Wilson, K. S., and Von Hippel, P. H. (1995). Transcription termination at intrinsic terminators: the role of the RNA hairpin. *Proc. Natl. Acad. Sci. USA* 92, 8793–8797. doi: 10.1073/pnas.92.19.8793

Włodarczyk, A., Selão, T. T., Norling, B., and Nixon, P. J. (2019). Unprecedented biomass and fatty acid production by the newly discovered cyanobacterium *Synechococcus sp*. PCC 11901. *BioRxiv [Preprint]* doi: 10.1101/684944

Xayaphoummine, A., Bucher, T., and Isambert, H. (2005). Kinefold web server for RNA/DNA folding path and structure prediction including pseudoknots and knots. *Nucleic Acids Res.* 33(Suppl. 2), 605–610. doi: 10.1093/nar/gki447

Yager, T. D., and von Hippel, P. H. (1991). A thermodynamic analysis of RNA transcript elongation and termination in *Escherichia coli*. *Biochemistry* 30, 1097–1118. doi: 10.1021/bi00218a032

Yao, L., Shabestary, K., Björk, S. M., Asplund-Samuelsson, J., Joensson, H. N., Jahn, M., et al. (2020). Pooled CRISPRi screening of the cyanobacterium *Synechocystis sp* PCC 6803 for enhanced industrial phenotypes. *Nat. Commun.* 11:1666. doi: 10.1038/s41467-020-15491-7

Yu, J., Liberton, M., Cliften, P. F., Head, R. D., Jacobs, J. M., Smith, R. D., et al. (2015). Synechococcus elongatus UTEX 2973, a fast growing cyanobacterial chassis for biosynthesis using light and CO_2. *Sci. Rep.* 5:8132. doi: 10.1038/srep08132

Zavřel, T., Očenášová, P., and Červený, J. (2017). Phenotypic characterization of *Synechocystis sp*. PCC 6803 substrains reveals differences in sensitivity to abiotic stress. *PLoS One* 12:e0189130. doi: 10.1371/journal.pone.0189130

Zuker, M. (2003). Mfold web server for nucleic acid folding and hybridization prediction. *Nucleic Acids Res.* 31, 3406–3415. doi: 10.1093/nar/gkg595

Conflict of Interest: The authors declare that the research was conducted in the absence of any commercial or financial relationships that could be construed as a potential conflict of interest.

5.3 Supplementary material

Evaluation and comparison of the efficiency of terminators in different cyanobacterial species

Grant A. R. Gale[1,2,3], Baojun Wang[2,3], Alistair J. McCormick[1,2*]

[1] Institute of Molecular Plant Sciences, School of Biological Sciences, University of Edinburgh, Edinburgh EH9 3BF, United Kingdom
[2] Centre for Synthetic and Systems Biology, University of Edinburgh, Edinburgh EH9 3BF, United Kingdom
[3] Institute of Quantitative Biology, Biochemistry and Biotechnology, School of Biological Sciences, University of Edinburgh, Edinburgh EH9 3FF, United Kingdom

Supplementary Material

Supplementary Information S1. Sequence maps (.gb files) of assembled level 0 vectors, 'no terminator' control vectors and pDUOTK1-L1. See .zip file.

Supplementary Table S1. List of primers used to generate level 0 terminator vectors and vector assemblies in this study.

Supplementary Table S2. List of level 1 terminator screening vectors used in this study.

Supplementary Table S3. The efficiency of terminators in *E. coli*, and *Synechocystis* sp. PCC 6803 and *Synechococcus* UTEX 2973 at three time points.

Supplementary Table S4. Gibbs free energy values for terminator sequences.

Supplementary Figure S1. Growth and fluorophore expression levels in *E. coli*.

Supplementary Figure S2. Representative distribution of fluorescence expression levels in *E. coli*, *Synechocystis* sp. PCC 6803 and *Synechococcus* UTEX 2973.

Supplementary Figure S3. Growth and fluorophore expression levels in *Synechocystis* sp. PCC 6803.

Supplementary Figure S4. Growth and fluorophore expression levels in *Synechococcus* UTEX 2973.

Supplementary Figure S5. Growth and fluorophore expression levels in *Synechocystis* sp. PCC 6803 and *Synechococcus* UTEX 2973 under suboptimal growth conditions.

Supplementary Figure S6. Gibbs free energy values for terminator sequences plotted against TE values for *E. coli*, *Synechocystis* sp. PCC 6803 and *Synechococcus* UTEX 2973.

Supplementary Figure S7. Amino acid alignment of primary vegetative sigma factors from *Synechocystis* sp. PCC 6803 and *Synechococcus* UTEX 2973.

Supplementary Table S1. List of primers used to generate level 0 terminator vectors and vector assemblies in this study. No terminator sequences required domestication (i.e. removal of *BsaI* or *BpiI* sites). All new terminator sequences (1-19) were from Chen et al. (2013). Sequence maps are provided in **Supplemental Information S1**.

Primers used to amplify terminator sequences for assembly into level 0

No.	Vector ID	Terminator	Amplicon length (bp)	Forward primer	Reverse primer
1	pC0.291	$T_{L3S2P21}$	93	GTACGAAGACTCGCTTCTCGGTACCAAATTCCAGAAAAGAGGCCTCCCGA	GTACGAAGACTCAGCGGGACCAAAACGAAAAAAGGCCCCCCTTTCGGGAGGCCT
2	pC0.292	$T_{L3S2P11}$	89	GTACGAAGACTCGCTTCTCGGTACCAAATTCCAGAAAAGAGACGCTT	GTACGAAGACTCAGCGGGACCAAAACGAAAAAAGACGCTCGAAAGCGTCTCTT
3	pC0.293	$T_{L3S2P55}$	89	GTACGAAGACTCGCTTCTCGGTACCAAAGACGAACAATAAGACGCTGAAAAG	GTACGAAGACTCAGCGGGACCAAAACGAAAAAAGACGCTTTTCAGCGTCT
4	pC0.294	$T_{L3S3P21}$	85	GTACGAAGACTCGCTTCCAATTATTGAAGGCCTCCCTAACGGGGGGCCTT	GTACGAAGACTCAGCGGGGAGACCAGAAACAAAAAAAGGCCCCCCGTT
5	pC0.295	$T_{L3S1P13}$	83	GTACGAAGACTCGCTTGACGAACAATAAGGCCTCCCTAACGGGGGGC	GTACGAAGACTCAGCGTTTTGTTATCAATAAAAAAGGCCCCCCGTTAGGG
6	pC0.296	$T_{L3S3P11}$	79	GTACGAAGACTCGCTTCCAATTATTGAACACCCTTCGGGGTGTTTT	GTACGAAGACTCAGCGGGGAGACCAGAAACAAAAAAACACCCCGAAG
7	pC0.306	$T_{L3S1P22}$	80	GTACGAAGACTCGCTTGACGAACAATAAGGCCGCAAATCGCGGC	GTACGAAGACTCAGCGTTTTGTTATCAATAAAAAAGGCCGCGATTTGCGG
8	pC0.307	$T_{L3S1P47}$	84	GTACGAAGACTCGCTTTTTTCGAAAAAAGGCCTCCCAAATCGGG	GTACGAAGACTCAGCGTTTTGTTGCTATAAAAAAAGGCCCCCCGATTTGG
9	pC0.308	$T_{ECK120033737}$	89	GTACGAAGACTCGCTTGGAAACACAGAAAAAAGCCCGCACCTGACAGTGC	GTACGAAGACTCAGCGCCTTTGGTCGAAAAAAAAAGCCCGCACTGTCAGGTGC
10	pC0.309	$T_{ECK120033736}$	85	GTACGAAGACTCGCTTAACGCATGAGAAAGCCCCCGGAAGATCACCTTCC	GTACGAAGACTCAGCGGCGCAATAAAAAAGCCCCCGGAAGGTGATCTT
11	pC0.310	$T_{ECK120010818}$	86	GTACGAAGACTCGCTTGTCAGTTTCACCTGTTTTACGTAAAAACCCGCTTCGGCG	GTACGAAGACTCAGCGCCAAAAGTAAAAACCCGCCGAAGC
12	pC0.311	$T_{ECK120015440}$	81	GTACGAAGACTCGCTTTCCGGCAATTAAAAAAGCGGCTAACCACGCCG	GTACGAAGACTCAGCGTGCAGACGTAAAAAAAGCGGCGTGGTTAG
13	pC0.312	$T_{ECK120029600}$	122	GTACGAAGACTCGCTTTTCAGCCAAAAAACTTAAGACCGCCGGTCTTGTCCACTACCTTGCAGTAATGCGGTGGACAGGA	GTACGAAGACTCAGCGTTGAGAAGAGAAAAGAAAACCGCCGATCCTGTCCACCGCATTACTGCAAGGTAGTGGACAAGAC
14	pC0.313	$T_{ECK120010799}$	92	GTACGAAGACTCGCTTGTTATGAGTCAGGAAAAAAGGCGACAGAGTAATCTGTCG	GTACGAAGACTCAGCGAAAGCAAGCAAAGAAAAAAGGCGACAGATTACTC
15	pC0.314	$T_{ECK120010876}$	87	GTACGAAGACTCGCTTTAAGGTTGAAAAATAAAAACGGCGCTAAAAAGCG	GTACGAAGACTCGCTTTAAGGTTGAAAAATAAAAACGGCGCTAAAAAGCG
16	pC0.315	$T_{ECK120015170}$	79	GTACGAAGACTCGCTTACAATTTTCGAAAAAACCCGCTTCGGCGG	GTACGAAGACTCAGCGTTTTAGCTATAAAAAAACCCGCCGAAGCGGGT

17	pC0.316	$T_{ECK120017009}$	76	GTACGAAGACTCGCTTGATCTAACTAAAAAGGCCGCTCTGCG	GTACGAAGACTCAGCGAGTGAAAAGAAAAAAGGCCGCAGAGCGGCCTTT
18	pC0.317	$T_{ECK120051401}$	79	GTACGAAGACTCGCTTCGCAGATAGCAAAAAAGCGCCTTTAGGG	GTACGAAGACTCAGCGCCACCAATGTAAAAAAGCGCCCTAAAGGCGCT
19	pC0.318	$T_{ECK120010855}$	74	GTACGAAGACTCGCTTGTAACAACGGAAACCGGCCATTGCGC	GTACGAAGACTCAGCGAGGCCAAAAAAAACCGGCGCAATGGCCG

Additional primers used for vector assembly

	Vector	Primer Name	Amplicon Length (bp)	Primer
20	pDUOTK1-L1	pCAT.262-F	995	GATCGAAGACTCACCGACATTTCCCCGAAAAGTGCCAC
21	pDUOTK1-L1	pCAT.262-R		GATCGAAGACTCGCTATTACTTGTACAGCTCGTCCATGC
22	pDUOTK1-L1	pICH47732_LacZ-F	610	GATCGAAGACTCCCGACTGGAAAGCGGGC
23	pDUOTK1-L1	pICH47732_LacZ-R		GATCGAAGACTCCTGCAGCGGCCGCTACAGCGGGAGACCGGATGCCGGGAGCAGACAA
24	pDUOTK1-L1	mTagBFP_RBS_Chen-F	871	GATCGAAGACTCGCAGAAAGAGGAGAAATACTAAATGAGCGAACTGATCAAAGAGAACAT
25	pDUOTK1-L1	mTagBFP-R		GATCGAAGACTCTCCCCGCAGAAAGGCCCACCC
26	pC1.376	pCAT.262-F	979	GATCGAAGACTCACCGACATTTCCCCGAAAAGTGCCAC
27	pC1.376	pCAT.262-NTC-R		GATCGAAGACTCGCTATTACTTGTACAGCTCGTCCATGC
28	pC1.376	mTagBFP-NTC-F	882	GATCGAAGACTCTAGCGGCCGCTGCAG
29	pC1.376	mTagBFP-R		GATCGAAGACTCTCCCCGCAGAAAGGCCCACCC
30	pC1.377	rd1.2-F	60	GATCGGTCTCAGCTTCGCCCCCGGAGGCTTTCCCGGG
31	pC1.377	rd1.2-R		GATGGGTCTCAAGCGTGATTTGCCCCGGGAAAGCC

Supplementary Table S2. List of level 1 terminator screening vectors assembled for this study. All level 0 terminator parts (see **Table 1**) were assembled into the level 1 acceptor vector pDUOTK1-L1.

Vector ID	Part name
pC1.342	pDUOTK1-L1-T_{pheA-1}
pC1.343	pDUOTK1-L1-$T_{ECK120010850}$
pC1.344	pDUOTK1-L1-$T_{ECK120026481}$
pC1.345	pDUOTK1-L1-$T_{ECK120010842}$
pC1.346	pDUOTK1-L1-$T_{ECK120048902}$
pC1.347	pDUOTK1-L1-T_{rrnB}
pC1.348	pDUOTK1-L1-$T_{L3S2P21}$
pC1.349	pDUOTK1-L1-$T_{L3S2P11}$
pC1.350	pDUOTK1-L1-$T_{L3S2P55}$
pC1.351	pDUOTK1-L1-$T_{L3S3P21}$
pC1.352	pDUOTK1-L1-$T_{L3S1P13}$
pC1.353	pDUOTK1-L1-$T_{L3S3P11}$
pC1.354	pDUOTK1-L1-$T_{L3S1P22}$
pC1.355	pDUOTK1-L1-$T_{L3S1P47}$
pC1.356	pDUOTK1-L1-$T_{ECK120033737}$
pC1.357	pDUOTK1-L1-$T_{ECK120033736}$
pC1.358	pDUOTK1-L1-$T_{ECK120010818}$
pC1.359	pDUOTK1-L1-$T_{ECK120015440}$
pC1.360	pDUOTK1-L1-$T_{ECK120029600}$
pC1.361	pDUOTK1-L1-$T_{ECK120010799}$
pC1.362	pDUOTK1-L1-$T_{ECK120010876}$
pC1.363	pDUOTK1-L1-$T_{ECK120015170}$
pC1.364	pDUOTK1-L1-$T_{ECK120017009}$
pC1.365	pDUOTK1-L1-$T_{ECK120051401}$
pC1.366	pDUOTK1-L1-$T_{ECK120010855}$
pC1.367	pDUOTK1-L1-T_{Bba_B0011}
pC1.368	pDUOTK1-L1- $T_{pSB1AK3}$
pC1.369	pDUOTK1-L1-$T_{ECK120010820}$
pC1.370	pDUOTK1-L1-T_{BBa_B0061}
pC1.371	pDUOTK1-L1-$T_{ECK120030798}$
pC1.372	pDUOTK1-L1-$T_{ECK120010869}$
pC1.373	pDUOTK1-L1-$T_{ECK120010841-R}$
pC1.374	pDUOTK1-L1-T_{psbA2}
pC1.375	pDUOTK1-L1-T_{psaB}
pC1.376	pDUOTK1-L1-No Term (Chen)
pC1.377	pDUOTK1-L1-No Term (Cambray spacer rd1.2)

Supplementary Table S3. The efficiency of terminators in *E. coli*, and *Synechocystis* sp. PCC 6803 and *Synechococcus* UTEX 2973 at three time points. To compare our measured TE values with data in Chen et al. (2013), we converted the reported terminator strength (TS) values to TE values to allow for meaningful comparison. TS is a non-linear derivative of TE, such that TS values tend to infinity as TE values approaches 100%. Thus, small increases when TE values are >95% result in large increases in TS values. We used the formula $TE = 100 \text{ x } 1 - \frac{1}{\text{TS}}$ to convert TS values to TE values, where TE is termination efficiency (%) and TS is termination strength (a.u.). Both TS values and calculated TE values are shown for Chen et al., (2013) below. TE values are shown for *E. coli*, PCC 6803 and UTEX 2973 measured under typical growth conditions (i.e. 37°C for *E. coli*, 30°C and 100 µM photons m^{-2} s^{-1} for PCC 6803, 40°C and 300 µM photons m^{-2} s^{-1} for UTEX 2973). A correlation matrix table is shown for PCC 6803 and UTEX 2973 at different time points under typical growth conditions. TE values are also shown for the suboptimal growth condition experiment (30°C and 300 µM photons m^{-2} s^{-1} for PCC 6803 and UTEX 2973) (**Supplementary Figure S5**).

Typical growth conditions		*E. coli* Chen et al., 2013		*E. coli* this study	PCC 6803			UTEX 2973		
Vector ID	Terminator	TS	TE (%)	TE (%)	24 hours TE (%)	48 hours TE (%)	72 hours TE (%)	24 hours TE (%)	48 hours TE (%)	72 hours TE (%)
pC0.291	$T_{L3S2P21}$	382.1	99.7	99.9	99.6	99.5	99.5	97.8	98.5	95.1
pC0.292	$T_{L3S2P11}$	261.5	99.6	99.2	98.1	98.5	98.2	95.9	96.2	95.6
pC0.293	$T_{L3S2P55}$	18.6	94.6	99.3	97.5	98.1	98.3	83.1	94.5	90.1
pC0.294	$T_{L3S3P21}$	246.6	99.6	99.8	95.7	95.0	95.1	83.5	90.7	87.4
pC0.295	$T_{L3S1P13}$	177.9	99.4	87.2	51.3	45.7	40.7	96.4	94.2	95.9
pC0.296	$T_{L3S3P11}$	172.6	99.4	99.9	93.6	93.5	92.6	97.3	94.2	97.6
pC0.306	$T_{L3S1P22}$	128.1	99.2	73.1	4.4	0.0	0.0	89.8	88.4	93.0
pC0.307	$T_{L3S1P47}$	123.4	99.2	92.7	74.2	71.5	68.2	95.4	97.2	96.7
pC0.066	T_{pheA-1}	243.5	99.6	93.1	49.8	47.0	40.2	96.5	95.8	96.7
pC0.068	$T_{ECK120010850}$	64.7	98.5	99.9	99.3	99.3	99.1	97.9	98.7	98.0
pC0.069	$T_{ECK120026481}$	45.9	97.8	94.1	92.8	92.1	87.1	93.9	95.6	93.9
pC0.072	$T_{ECK120010842}$	1.8	44.1	42.2	27.3	25.3	26.1	80.3	78.1	78.9
pC0.074	$T_{ECK120048902}$	5.0	80.0	83.4	84.2	82.6	81.1	55.6	50.1	53.0
pC0.062	T_{Bba_B0011}	1.3	24.7	40.8	34.0	28.5	19.7	69.7	68.5	66.9
pC0.064	$T_{ECK120010820}$	1.4	30.3	51.1	72.8	71.9	70.4	39.8	41.1	39.8

pC0.070	T_{BBa_B0061}	8.8	88.7	74.2	72.6	68.7	64.8	26.3	29.7	25.2
pC0.071	$T_{ECK120030798}$	8.8	88.7	62.6	43.7	39.1	43.5	39.7	37.7	28.5
pC0.073	$T_{ECK120010869}$	83.7	98.8	94.8	85.1	82.9	76.8	86.4	84.0	85.5
pC0.077	$T_{ECK120010841-R}$	8.0	87.5	96.2	93.7	93.4	91.8	85.3	82.6	85.1
pC0.308	$T_{ECK120033737}$	312.5	99.7	97.9	98.7	99.2	98.9	94.5	74.1	95.0
pC0.309	$T_{ECK120033736}$	164.6	99.4	94.0	98.8	99.1	99.1	98.2	96.6	96.2
pC0.310	$T_{ECK120010818}$	148.3	99.3	96.4	95.3	94.8	95.4	80.9	79.0	80.8
pC0.311	$T_{ECK120015440}$	119.2	99.2	96.1	92.2	90.8	90.5	82.7	85.0	82.4
pC0.312	$T_{ECK120029600}$	378.4	99.7	99.9	99.2	99.5	99.9	99.7	99.9	99.9
pC0.313	$T_{ECK120010799}$	101.0	99.0	98.8	97.8	97.4	97.1	93.3	90.1	93.6
pC0.314	$T_{ECK120010876}$	97.4	99.0	91.1	96.8	97.0	97.4	75.3	68.8	65.5
pC0.315	$T_{ECK120015170}$	85.8	98.8	95.0	90.8	88.5	85.5	98.1	96.4	95.7
pC0.316	$T_{ECK120017009}$	67.6	98.5	98.9	92.6	91.7	89.3	91.2	94.0	87.7
pC0.317	$T_{ECK120051401}$	67.2	98.5	93.4	88.7	87.2	83.1	68.4	72.2	64.9
pC0.318	$T_{ECK120010855}$	65.4	98.5	99.3	97.7	97.5	97.3	96.1	92.2	95.1
pC0.082	T_{rrnB}	N/A	N/A	99.7	97.9	98.8	98.4	99.0	97.9	98.6
pC0.063	$T_{pSB1AK3}$	N/A	N/A	90.7	78.7	74.4	65.8	62.3	66.9	50.9
pC0.079	T_{psbA2}	N/A	N/A	59.0	98.5	99.0	98.5	96.7	95.0	95.6
pC0.081	T_{psaB}	N/A	N/A	62.9	69.9	69.5	62.9	49.7	41.4	44.3

Correlation matrix table for PCC 6803

hours	24	48	72
24	1		
48	0.999	1	
72	0.991	0.994	1

Correlation matrix table for UTEX 2973

hours	24	48	72
24	1		
48	0.982	1	
72	0.988	0.982	1

Suboptimal growth conditions		PCC 6803			UTEX 2973		
Vector ID	Terminator	24 hours TE (%)	48 hours TE (%)	72 hours TE (%)	24 hours TE (%)	48 hours TE (%)	72 hours TE (%)
pC0.291	$T_{L3S2P21}$	99.5	99.7	99.7	99.2	97.4	97.6
pC0.292	$T_{L3S2P11}$	97.5	98.9	98.3	94.8	96.2	96.8
pC0.068	$T_{ECK120010850}$	99.2	99.5	99.5	98.6	98.3	98.5
pC0.309	$T_{ECK120033736}$	99.0	99.5	99.5	99.4	96.4	98.6
pC0.312	$T_{ECK120029600}$	99.5	99.8	99.9	99.9	99.9	99.9
pC0.082	T_{rrnB}	97.2	99.1	98.8	98.9	97.7	97.3
pC0.079	T_{psbA2}	98.3	98.8	99.3	98.0	95.5	97.2

Supplementary Table S4. Gibbs free energy values for terminator sequences. Free energy values are shown for the hairpin loop with the inclusion of the 8 nucleotides directly upstream and downstream (ΔG_{HA}), the hairpin loop alone (ΔG_H) and the complete terminator sequence (ΔG_{TERM}). Free energy values were calculated using mFold (http://unafold.rna.albany.edu/?q=mfold) and are given in kcal/mol (Zuker, 2003).

Terminator	ΔG_{HA}	ΔG_H	ΔG_{TERM}
$T_{L3S2P21}$	-30.8	-19.8	-37.9
$T_{L3S2P11}$	-18.4	-7.4	-25.5
$T_{L3S2P55}$	-12.6	-9.8	-25.8
$T_{L3S3P21}$	-22.1	-18.0	-23.3
$T_{L3S1P13}$	-20.8	-18.0	-22.5
$T_{L3S3P11}$	-14.3	-10.1	-15.5
$T_{L3S1P22}$	-14.5	-11.7	-16.2
$T_{L3S1P47}$	-24.5	-16.1	-24.5
T_{pheA-1}	-18.9	-16.1	-20.6
$T_{ECK120010850}$	-15.2	-10.8	-15.2
$T_{ECK120026481}$	-18.5	-12.2	-18.5
$T_{ECK120010842}$	-3.6	-1.1	-7.2
$T_{ECK120048902}$	-16.2	-8.3	-17.5
T_{Bba_B0011}	-10.0	-4.5	-11.2
$T_{ECK120010820}$	-11.4	-6.1	-11.4
T_{BBa_B0061}	-24.0	-10.9	-25.0
$T_{ECK120030798}$	-18.2	-12.3	-18.2
$T_{ECK120010869}$	-17.2	-11.6	-17.3
$T_{ECK120010841-R}$	-9.6	-6.6	-9.6
$T_{ECK120033737}$	-23.7	-15.7	-25.0
$T_{ECK120033736}$	-32.3	-23.6	-37.8
$T_{ECK120010818}$	-22.4	-11.6	-22.4
$T_{ECK120015440}$	-14.4	-8.0	-17.4
$T_{ECK120029600}$	-42.0	-37.2	-42.0
$T_{ECK120010799}$	-27.9	-17.3	-28.9
$T_{ECK120010876}$	-17.5	-11.9	-17.6
$T_{ECK120015170}$	-20.1	-11.6	-20.1
$T_{ECK120017009}$	-15.6	-10.1	-16.2
$T_{ECK120051401}$	-15.8	-8.4	-15.8
$T_{ECK120010855}$	-13.6	-7.9	-17.3
T_{rrnB}	-30.9	-18.7	-60.7
$T_{pSB1AK3}$	-23.2	-11.4	-30.5
T_{psbA2}	-12.9	-11.0	-22.7
T_{psaB}	-21.6	-11.0	-22.7

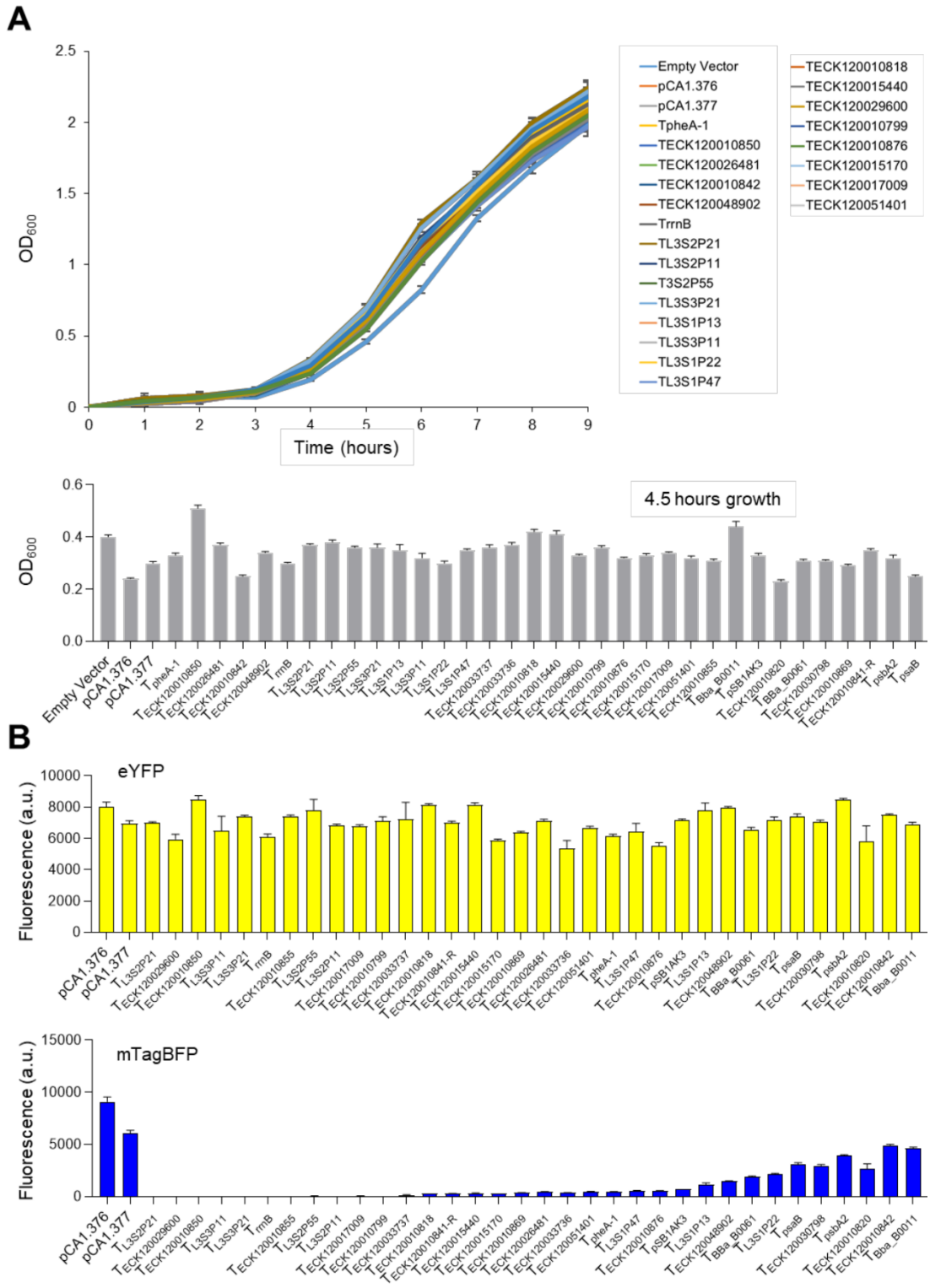

Supplementary Figure S1. Growth and fluorophore expression levels in *E. coli*. **(A)** Growth experiment conducted with a reduced number of transformants to identify the beginning of the exponential phase. Values are the means ± standard error (SE) of the mean from 4 biological replicates. OD_{600} values are shown at 4.5 hours growth for the full growth experiment. Average OD_{600} = 0.33±0.01 (n = 37). **(B)** Expression levels of eYFP and mBFP after 4.5 hours growth. Error bars represent the ±SE of the mean of 4-8 biological replicates, where each replicate represents the median measurement of at least 10,000 cells measured by flow cytometry.

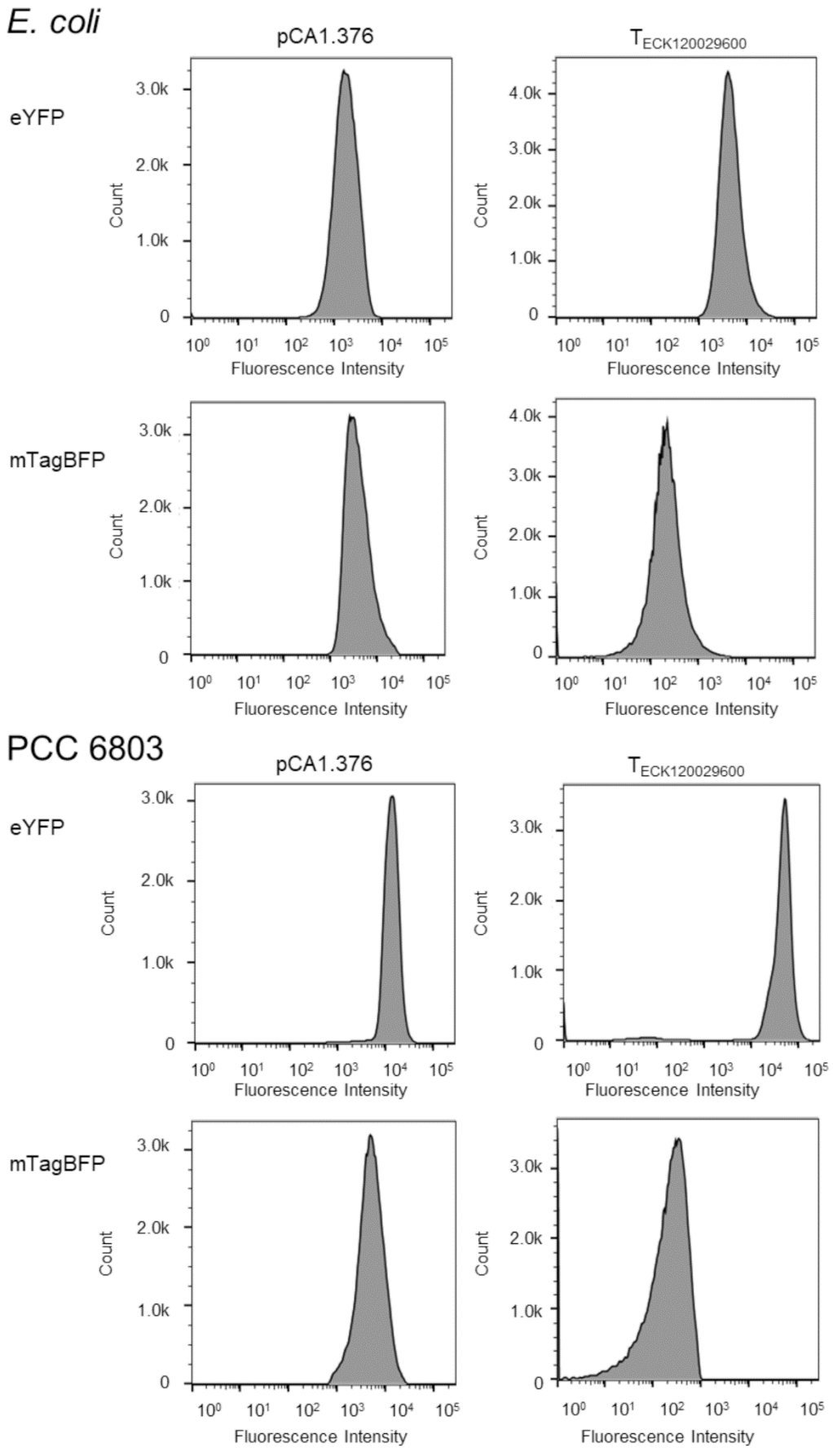
E. coli
pCA1.376
T ECK120029600
eYFP
mTagBFP
Count
Fluorescence Intensity
PCC 6803
pCA1.376
T ECK120029600
eYFP
mTagBFP
Count
Fluorescence Intensity

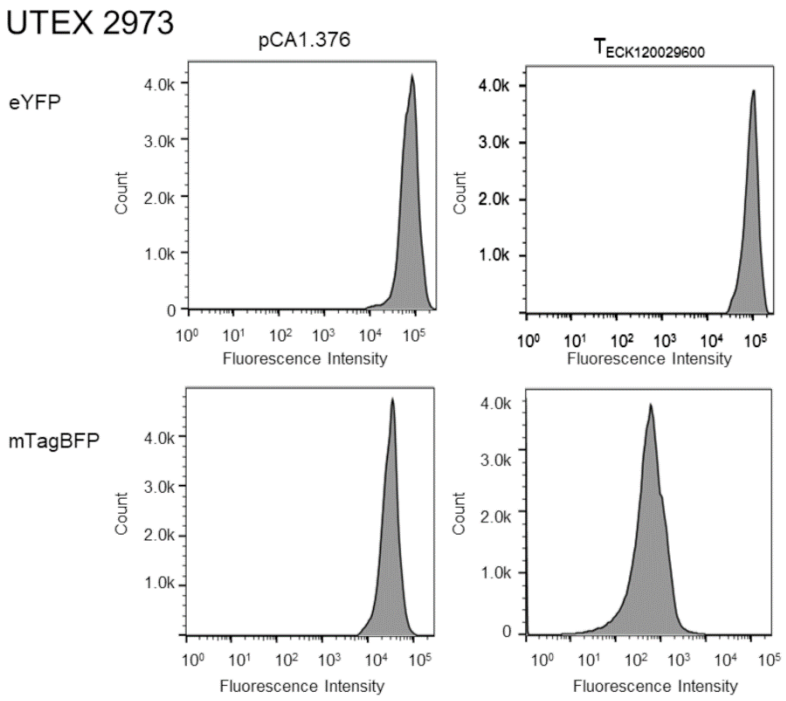

Supplementary Figure S2. Representative distribution of fluorescence expression levels in *E. coli*, *Synechocystis* sp. PCC 6803 and *Synechococcus* UTEX 2973. Populations of at least 10,000 cells were first gated by forward and side scatter (see Materials and Methods). Then histogram plots were generated, and the median fluorescence values extracted.

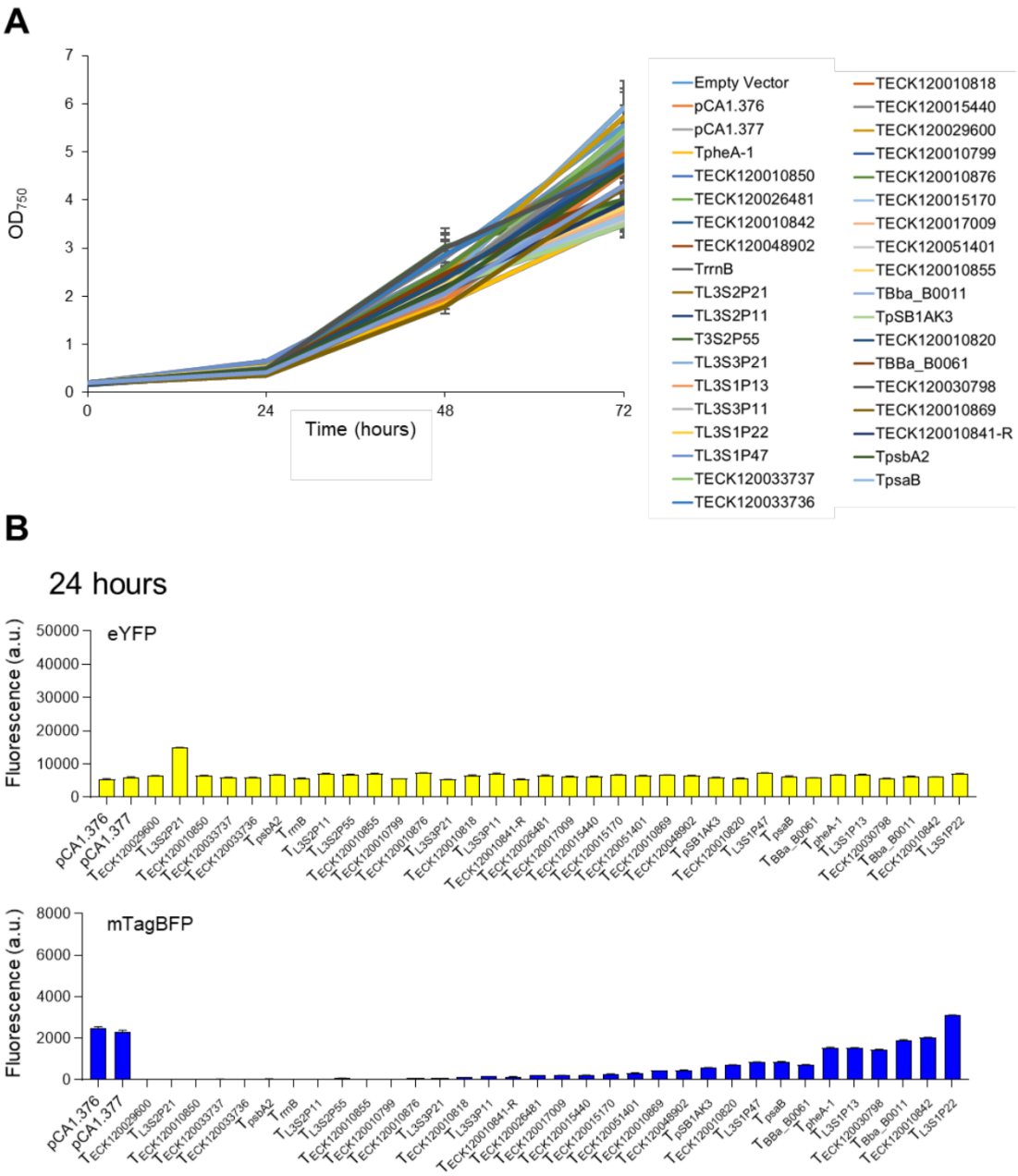
A
OD750
Time (hours)
Empty Vector
pCA1.376
pCA1.377
TpheA-1
TECK120010850
TECK120026481
TECK120010842
TECK120048902
TrrnB
TL3S2P21
TL3S2P11
T3S2P55
TL3S3P21
TL3S1P13
TL3S3P11
TL3S1P22
TL3S1P47
TECK120033737
TECK120033736
TECK120010818
TECK120015440
TECK120029600
TECK120010799
TECK120010876
TECK120015170
TECK120017009
TECK120051401
TECK120010855
TBba_B0011
TpSB1AK3
TECK120010820
TBBa_B0061
TECK120030798
TECK120010869
TECK120010841-R
TpsbA2
TpsaB
B
24 hours
eYFP
Fluorescence (a.u.)
mTagBFP
Fluorescence (a.u.)

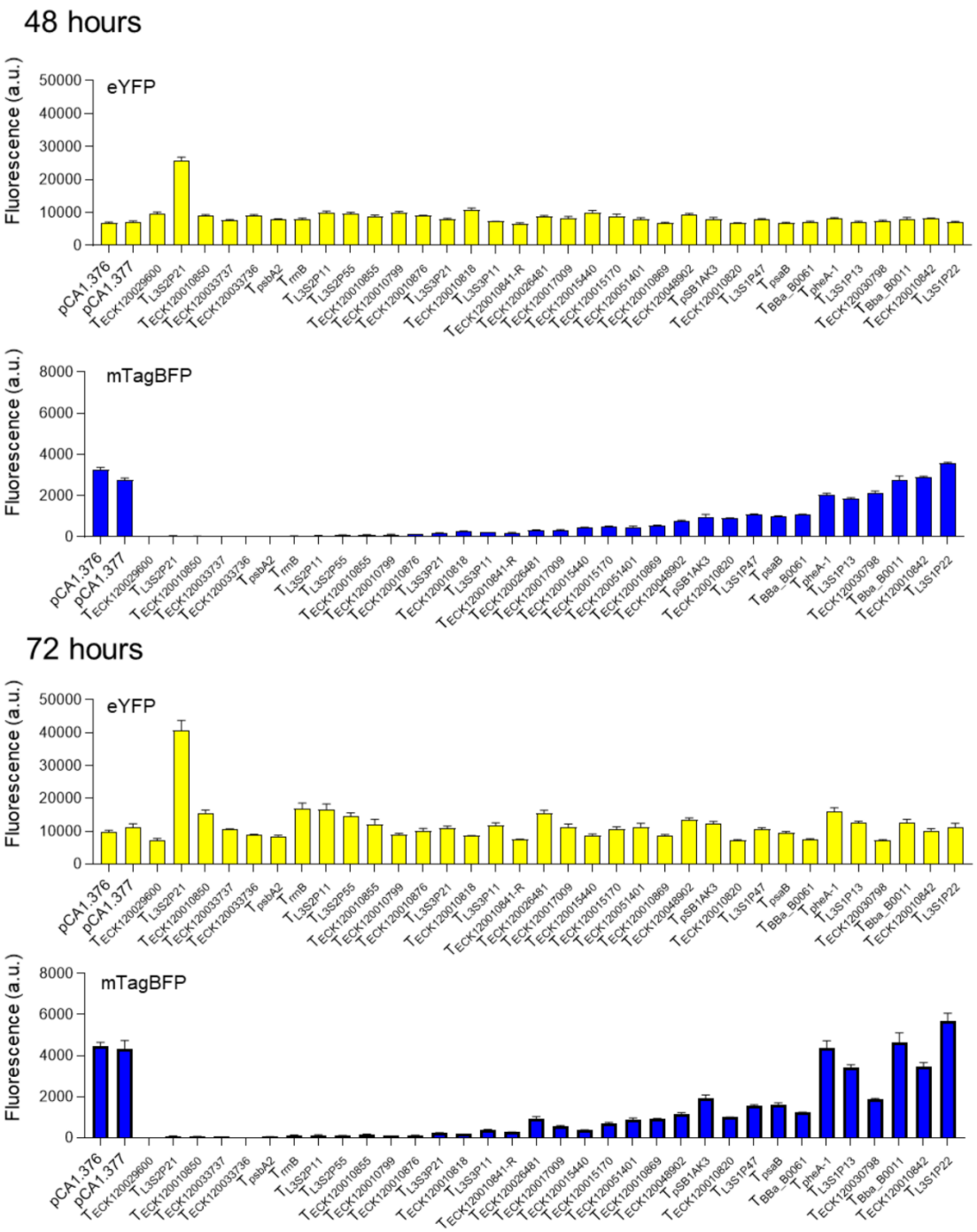
48 hours
eYFP
Fluorescence (a.u.)
50000
40000
30000
20000
10000
0
pCA1.376
pCA1.377
TECK120029600
TL3S2P21
TECK120010850
TECK120033737
TECK120033736
TpsbA2
TrnB
TL3S2P11
TL3S2P55
TECK120010855
TECK120010799
TECK120010876
TL3S3P21
TECK120010818
TL3S3P11
TECK120010841-R
TECK120026481
TECK120017009
TECK120015440
TECK120015170
TECK120051401
TECK120010869
TECK120048902
TpSB1AK3
TECK120010820
TL3S1P47
TpsaB
TBBa_B0061
TpheA-1
TL3S1P13
TECK120030798
TBba_B0011
TECK120010842
TL3S1P22
mTagBFP
Fluorescence (a.u.)
8000
6000
4000
2000
0
72 hours
eYFP
Fluorescence (a.u.)
50000
40000
30000
20000
10000
0
mTagBFP
Fluorescence (a.u.)
8000
6000
4000
2000
0

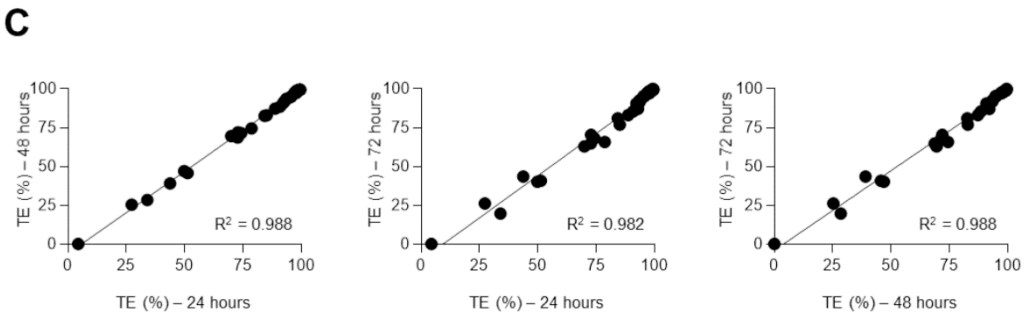

Supplementary Figure S3. Growth and fluorophore expression levels in *Synechocystis* sp. PCC 6803. **(A)** Cultures were grown for 72 hr at 30°C with continuous light (100 µmol photons m^{-2} s^{-1}). **(B)** Expression levels of eYFP and mTagBFP at three time points (24, 48 and 72 hr). Error bars represent the ±SE of the mean of four biological replicates, where each replicate represents the median measurement of at least 10,000 cells measured by flow cytometry. **(C)** Correlation analysis of TE values between the three different time points (n = 34). The coefficient of determination (R^2) is shown.

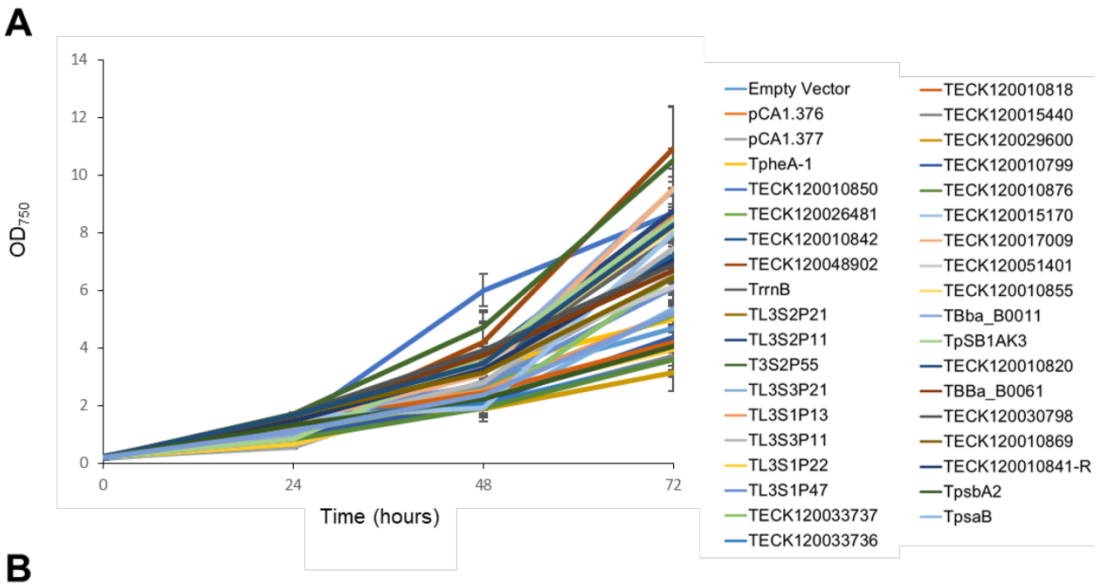
A
OD750
Time (hours)
Empty Vector
pCA1.376
pCA1.377
TpheA-1
TECK120010850
TECK120026481
TECK120010842
TECK120048902
TrrnB
TL3S2P21
TL3S2P11
T3S2P55
TL3S3P21
TL3S1P13
TL3S3P11
TL3S1P22
TL3S1P47
TECK120033737
TECK120033736
TECK120010818
TECK120015440
TECK120029600
TECK120010799
TECK120010876
TECK120015170
TECK120017009
TECK120051401
TECK120010855
TBba_B0011
TpSB1AK3
TECK120010820
TBBa_B0061
TECK120030798
TECK120010869
TECK120010841-R
TpsbA2
TpsaB

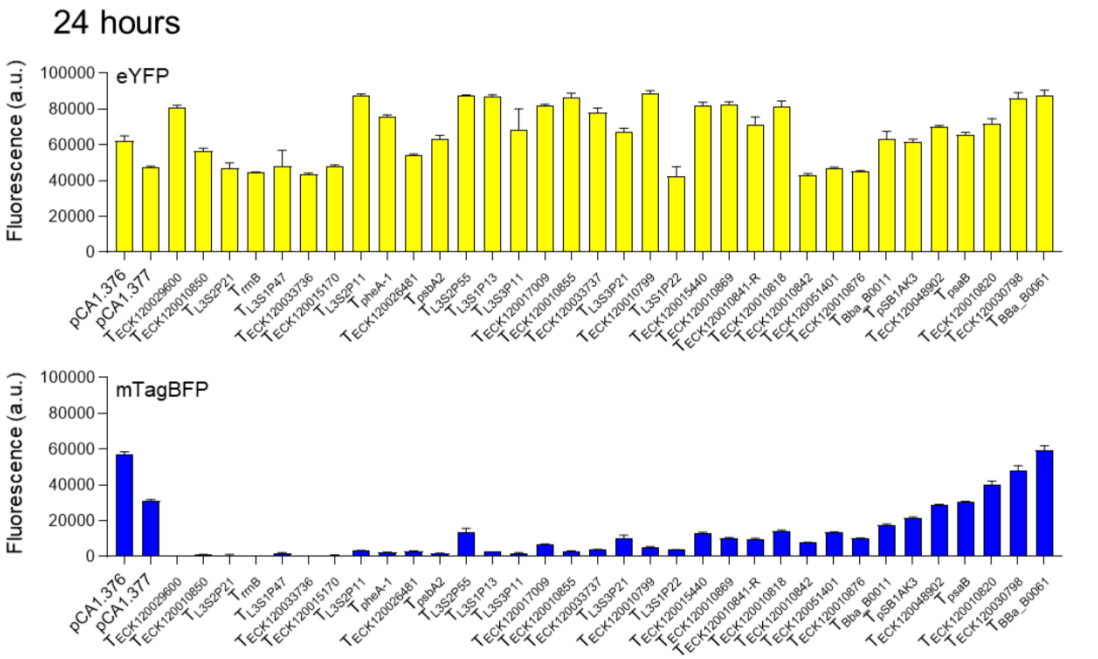
B
24 hours
eYFP
mTagBFP
Fluorescence (a.u.)

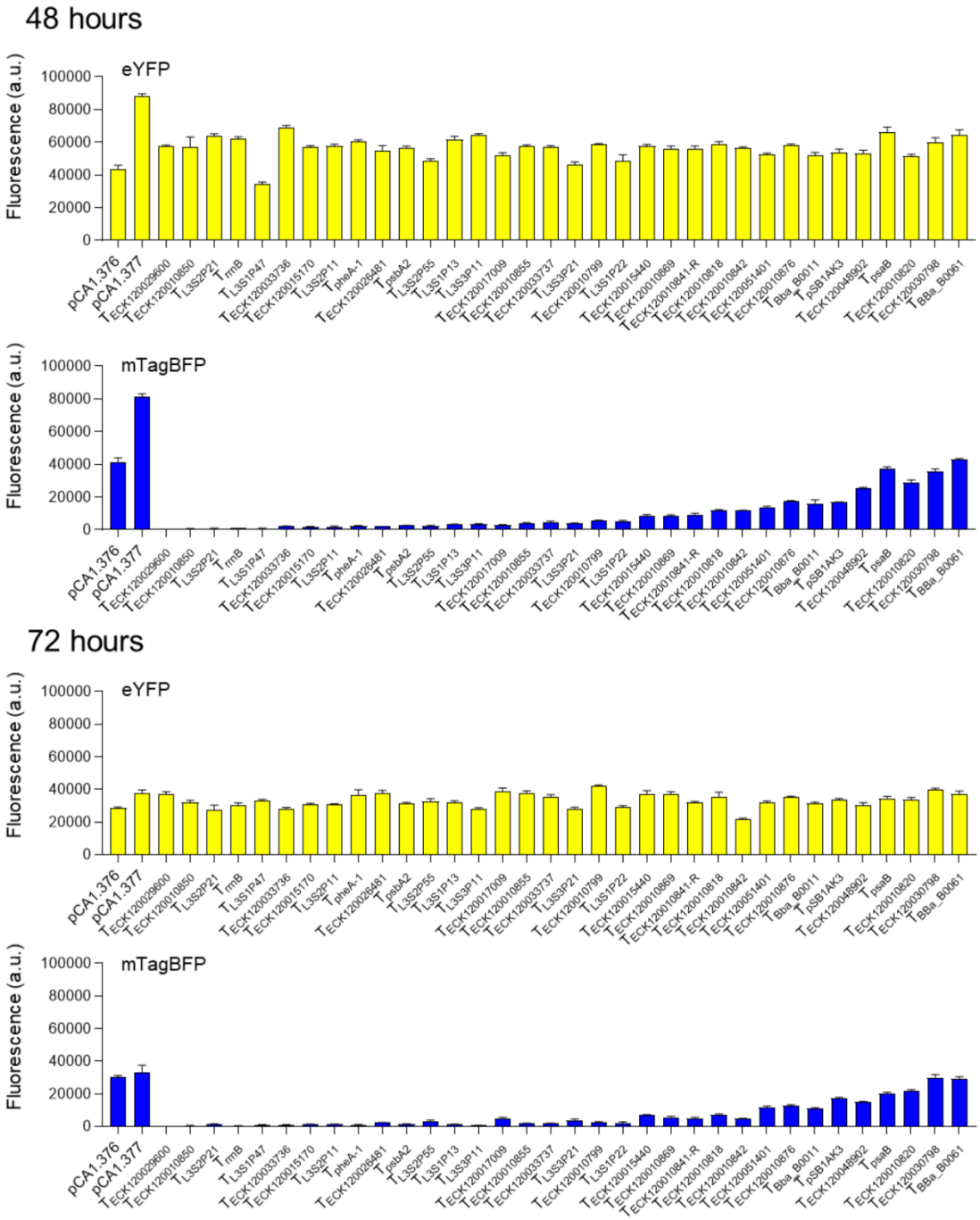
48 hours
eYFP
Fluorescence (a.u.)
100000
80000
60000
40000
20000
0
pCA1.376
pCA1.377
T ECK120029600
T ECK120010850
T L3S2P21
T rrnB
T L3S1P47
T ECK120033736
T ECK120015170
T L3S2P11
T pheA-1
T ECK120026481
T psbA2
T L3S2P55
T L3S1P13
T L3S3P11
T ECK120017009
T ECK120010855
T ECK120033737
T L3S3P21
T ECK120010799
T L3S1P22
T ECK120015440
T ECK120010869
T ECK120010841-R
T ECK120010818
T ECK120010842
T ECK120051401
T ECK120010876
T Bba_B0011
T pSB1AK3
T ECK120048902
T psaB
T ECK120010820
T ECK120030798
T BBa_B0061
mTagBFP
72 hours

C

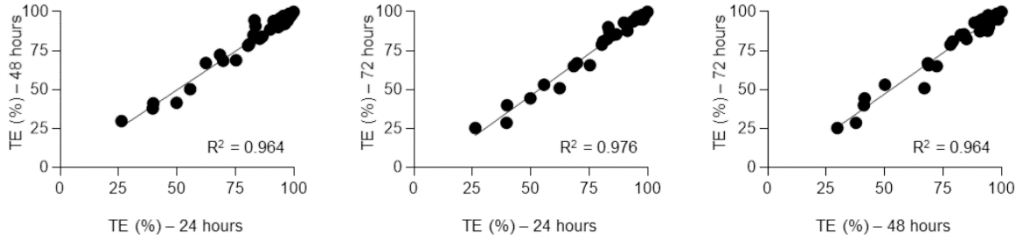

Supplementary Figure S4. Growth and fluorophore expression levels in *Synechococcus* UTEX 2973. **(A)** Cultures were grown for 72 hr at 40°C with continuous light (300 µmol photons m^{-2} s^{-1}). **(B)** Expression levels of eYFP and mTagBFP at three time points (24, 48 and 72 hr). Error bars represent the ±SE of the mean of four biological replicates, where each replicate represents the median measurement of at least 10,000 cells measured by flow cytometry. **(C)** Correlation analysis of TE values between the three different time points (n = 34). The coefficient of determination (R^2) is shown.

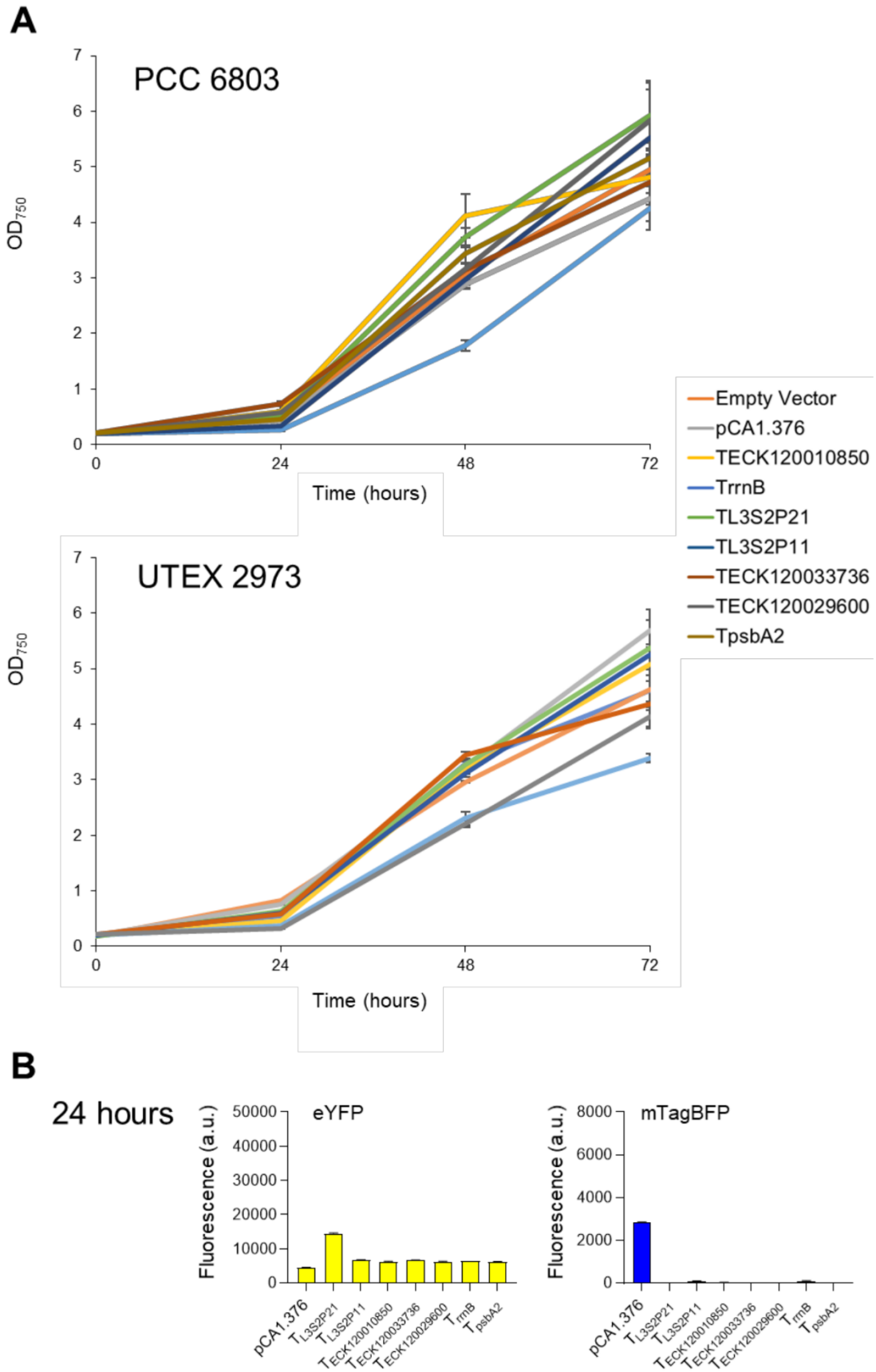
A
PCC 6803
OD750
Time (hours)
UTEX 2973
OD750
Time (hours)
Empty Vector
pCA1.376
TECK120010850
TrrnB
TL3S2P21
TL3S2P11
TECK120033736
TECK120029600
TpsbA2
B
24 hours
eYFP
Fluorescence (a.u.)
mTagBFP
Fluorescence (a.u.)
pCA1.376
TL3S2P21
TL3S2P11
TECK120010850
TECK120033736
TECK120029600
TrrnB
TpsbA2

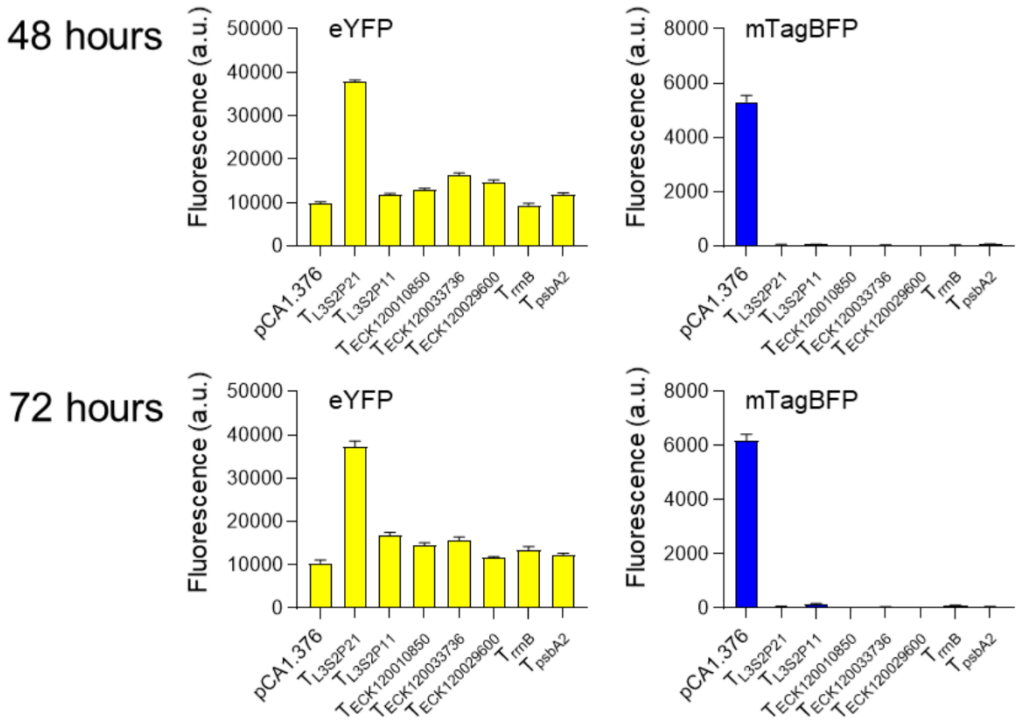
48 hours
eYFP
mTagBFP
Fluorescence (a.u.)
72 hours
eYFP
mTagBFP
Fluorescence (a.u.)
pCA1.376
TL3S2P21
TL3S2P11
TECK120010850
TECK120033736
TECK120029600
TrmB
TpsbA2

C

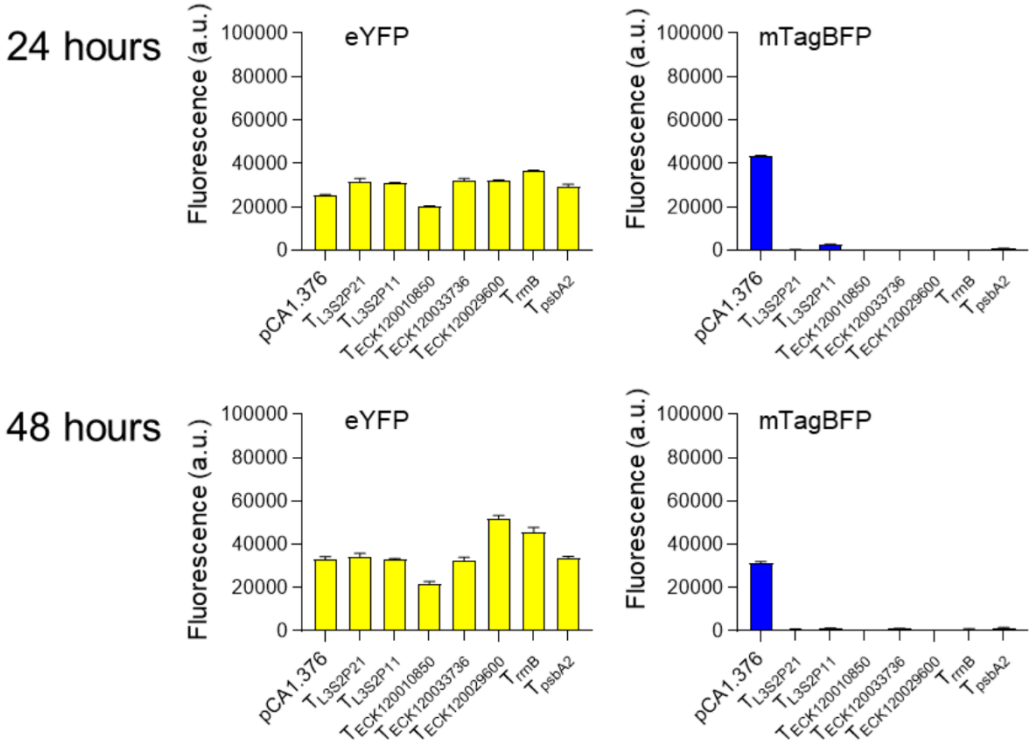
24 hours
eYFP
mTagBFP
Fluorescence (a.u.)
48 hours
eYFP
mTagBFP
Fluorescence (a.u.)
pCA1.376
TL3S2P21
TL3S2P11
TECK120010850
TECK120033736
TECK120029600
TrmB
TpsbA2

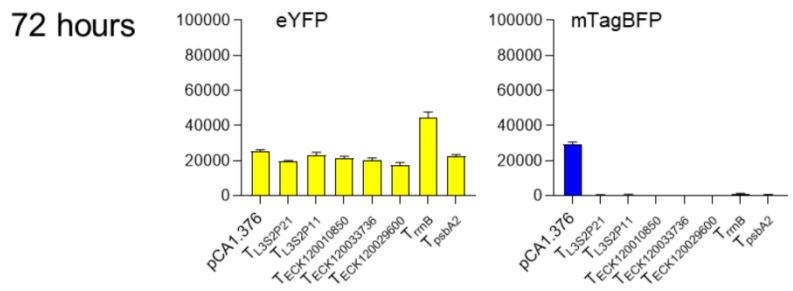

Supplementary Figure S5. Growth and fluorophore expression levels in *Synechocystis* sp. PCC 6803 and *Synechococcus* UTEX 2973 under suboptimal growth conditions. **(A)** Cultures were grown for 72 hr at 30°C with continuous high light (300 µmol photons m^{-2} s^{-1}). **(B)** Expression levels of eYFP and mTagBFP in PCC 6803 at three time points (24, 48 and 72 hr). **(C)** Expression levels of eYFP and mTagBFP in UTEX 2973 at three time points. Error bars represent the ±SE of the mean of four biological replicates, where each replicate represents the median measurement of at least 10,000 cells measured by flow cytometry.

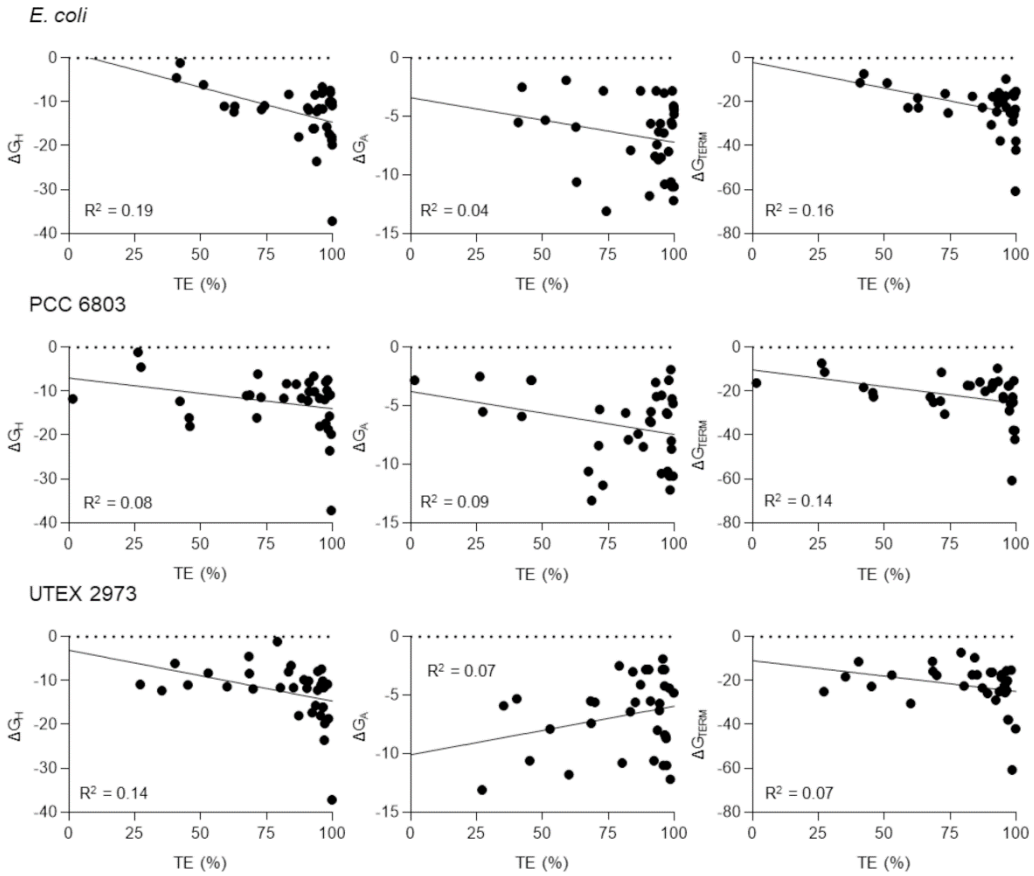

Supplementary Figure S6. Gibbs free energy values for terminator sequences plotted against TE values for *E. coli*, *Synechocystis* sp. PCC 6803 and *Synechococcus* UTEX 2973. Gibbs free energy values are taken from **Table 1** and **Supplementary Table S4**, TE values are from **Supplementary Table S3**.

```
slr0653             1 MTQTKEPL----------------TKAESAELEQEIELSQYINTDDIDDD
                      |||..|.|                .||.:|.:|....::...:.|.|||:
WP_071818124.1      1 MTQATELLDPALKPAETKAKRSSRKKATTAVVEPATTIAPTADVDAIDDE

slr0653            35 DIDVEDLEQEVAATEGKEKKVRKIRKDAVKKKPYTEDSIRIYLQEIGRIR
                      |...||   |.||.:.|.|          .:|.|||||||:|||||||||
WP_071818124.1     51 DSVGED---EDAAAKAKAK----------VRKTYTEDSIRLYLQEIGRIR

slr0653            85 LLRAEEEIELARQIADLLELELIRDNLTLQLERQPSELEWGKQVWKLETA
                      ||||:|||||||||||||.||.|||.|..||:|.||:.||...|
WP_071818124.1     88 LLRADEEIELARQIADLLALERIRDELLEQLDRLPSDAEWAAAV------

slr0653           135 KQRLVGDKKKEPKKKDIDSYLANPDNELSLENEWSQQPNKNFAAFRRRLF
                                  ||    |.:|                 ||||||
WP_071818124.1    132 -----------------DS----PLDE----------------FRRRLF

slr0653           185 LDRRAKDKMVQSNLRLVVSIAKKYMNRGLSFQDLIQEGSLGLIRAAEKFD
                      ..||||||||||||||||||||||||||||||||||||||||||||||||
WP_071818124.1    144 RGRRAKDKMVQSNLRLVVSIAKKYMNRGLSFQDLIQEGSLGLIRAAEKFD

slr0653           235 HEKGYKFSTYATWWIRQAITRAIADQSRTIRLPVHLYETISRIKKTTKLL
                      ||||||||||||||||||||||||||||||||||||||||||||||||||
WP_071818124.1    194 HEKGYKFSTYATWWIRQAITRAIADQSRTIRLPVHLYETISRIKKTTKLL

slr0653           285 SQEMRRKPTEEEIAEKMEMTIEKLRFIAKSAQLPISLETPIGKEEDSRLG
                      ||||.|||||||||.:||||||||||||||||||||||||||||||||||
WP_071818124.1    244 SQEMGRKPTEEEIATRMEMTIEKLRFIAKSAQLPISLETPIGKEEDSRLG

slr0653           335 DFIEADGETPEDEVSKNLLREDLENVLDTLSPRERDVLRLRYGLDDGRMK
                      |||||||||||||:|||||||||.||.||||||||||||||||||||||
WP_071818124.1    294 DFIEADGETPEDEVAKNLLREDLEGVLSTLSPRERDVLRLRYGLDDGRMK

slr0653           385 TLEEIGQIFNVTRERIRQIEAKALRKLRHPNRNSILKEYIR
                      |||||||:|||||||||||||||||||||||||||||||
WP_071818124.1    344 TLEEIGQLFNVTRERIRQIEAKALRKLRHPNRNSILKEYIR
```

Supplementary Figure S7. Sequence alignment of SigA isoforms in *Synechocystis* sp. PCC 6803 and *Synechococcus* UTEX 2973. SigA from PCC 6803 (srl0653) and SigA1 from UTEX 2973 (WP_071818124.1) was aligned using EMBOSS Needle (https://www.ebi.ac.uk/Tools/psa/emboss_needle), which produced a shared identity of 70.5% and similarity of 74.1%. The amino acid residues shown in blue and red highlight the conserved regions required for recognition of the -10 and -35 boxes for prokaryotic promoters, respectively (Lonetto et al., 1992; Panaghie et al., 2000; Srivastava et al., 2020).

Supplementary References

Chen, Y. J., Liu, P., Nielsen, A. A. K., Brophy, J. A. N., Clancy, K., Peterson, T., & Voigt, C. A. (2013). Characterization of 582 natural and synthetic terminators and quantification of their design constraints. *Nature Methods*, *10*(7), 659–664. https://doi.org/10.1038/nmeth.2515

Lonetto, M., Gribskov, M., & Gross, C. A. (1992). The sigma 70 family: sequence conservation and evolutionary relationships. *Journal of Bacteriology*, *174*(12), 3843–3849. https://doi.org/10.1128/JB.174.12.3843-3849.1992

Panaghie, G., Aiyar, S. E., Bobb, K. L., Hayward, R. S., & De Haseth, P. L. (2000). Aromatic amino acids in region 2.3 of Escherichia coli sigma 70 participate collectively in the formation of an RNA polymerase-Promoter open complex. *Journal of Molecular Biology*, *299*(5), 1217–1230. https://doi.org/10.1006/jmbi.2000.3808

Srivastava, A., Varshney, R. K., & Shukla, P. (2020). Sigma Factor Modulation for Cyanobacterial Metabolic Engineering. *Trends in Microbiology*, 1–12. https://doi.org/10.1016/j.tim.2020.10.012

5.4 Conclusion

This chapter expands on the capabilities of the CyanoGate kit. In this chapter, I have improved on an established strategy and created and validated a new molecular tool for calculation of transcription terminator efficiency. This tool can be used in a wide variety of cyanobacterial species and any other organisms compatible with the RSF1010 origin of replication. I demonstrated the high throughput capability of Golden Gate cloning and evaluated 34 terminators in *Synechocystis* sp. PCC 6803 and *Synechococcus elongatus* UTEX 2973. These results were compared to *Escherichia coli* and benchmarked to published data. We found that the library of terminators behaved differently between *E. coli* and the cyanobacterial species tested, but surprisingly, the termination efficiency was different between cyanobacterial strains. Our results indicated that there is likely more involved in the regulation of transcription termination than just the physicochemical properties of the RNA transcript, and further work will be required to elucidate.

Chapter 6 Designing and Characterising New Inducible Promoters and a Genetic Inverter in Cyanobacteria

6.1 Introduction

In this thesis so far, a large number of new tools for the control of gene expression in cyanobacteria have been described and characterised. Molecular parts for driving gene expression have thus far focused on constitutive promoters. To date, there have been a limited number of studies reporting heterologous transcription factor (TF) regulated expression systems (i.e. inducible promoters) in cyanobacteria, and even fewer that have demonstrated the desired attributes of an 'ideal' inducible expression system (see below). Inducible promoters that rely on expression of a heterologous TF have the advantage that the induction characteristics can be tuned by modulation of expression of the cognate TF (Merulla et al., 2013; Cameron & Collins, 2014; Wang et al., 2015; Fernandez-Rodriguez & Voigt, 2016). This is in contrast to the native *Synechocystis* inducible systems that rely on the respective cognate TF being expressed from the genome, where knockout lines would need to be generated for TF expression tuning to be possible (Peca et al., 2008; Blasi et al., 2012; Englund et al., 2016).

Inducible promoters allow flexible control over gene expression, usually in response to the addition of a small molecule inducer. In an ideal system, there should be no basal expression without inducer, expression should increase in a dose-dependent manner with increasing inducer concentration, and the inducer molecule should be stable at the experimental conditions, as well as non-toxic and not metabolised (Kelly et al., 2018). Generally, there are two modes of action for TF-regulated promoters – activation and repression. Transcriptional activators are TF proteins, which in the presence of the cognate inducer, will undergo a conformation change and bind the promoter region to facilitate transcription initiation (positive transcriptional regulation) (**Figure 6-1**). Transcriptional repressors are TF proteins, which without the presence of the inducer, will bind the promoter region and block transcription elongation. On the addition of inducer, the repressor will undergo a

conformation change, release from the promoter region and transcription elongation can proceed (**Figure 6-1**).

TF-regulated expression systems occur in nature and have evolved to allow organisms to respond to changes in environmental or metabolic state conditions. For example, L-rhamnose (P_{rhaBAD}) and L-arabinose (P_{BADWT}) induce TF-regulated expression in *E. coli* that, in the presence of these sugars, drive expression of the respective operons, expressing the enzymes required so that the cell may utilise these sugars as a carbon source (Casadaban, 1976; Ogden et al., 1980; Tobin & Schleif, 1987). Furthermore, several prokaryotes have developed resistance TF-regulated mechanisms that are induced when exposed to toxic metals (e.g. arsenic and mercury) (López-Maury et al., 2003; Silver & Phung, 2005; Boyd & Barkay, 2012). Many TF-regulated expression systems that respond to small molecule inducers have been ported into model species like *E. coli* and are now in common use as tools for conditional gene expression. Several strategies for the optimisation of these inducible promoters have been employed in *E. coli*. For instance, in *E. coli*, the P_{rhaBAD} expression system exhibits transient expression as induction with L-rhamnose induces native metabolism, so synthetic non-metabolisable analogues (e.g. L-mannose and L-lyxose) were identified that induced expression from P_{rhaBAD} (Kelly et al., 2016). Other strategies have sought to modify wild-type expression systems by using a rational design and directed evolution approach. This has resulted in optimisation of the promoter and TF sequences and subsequent improvement of the induction characteristics e.g. dynamic range, and reduction of cross-reactivity to other inducers. For example, Meyer et al. (2019) recently undertook this approach to optimise a set of 12 heterologous TF-regulated promoters for use in *E. coli* from various organisms including the promoter/repressor pairs P_{phlF}/PhlF and P_{van}/VanR from *Pseudomonas fluorescens* and *Corynebacter glutamicum*, respectively, and promoter/activator pairs P_{sal}/NahR and P_{Cin}/CinR from *Pseudomonas putida* and *Rhizobium leguminosarum,* respectively.

Thus far in cyanobacteria (i.e. *Synechocystis*), only P_{rhaBAD} has shown promising attributes as a TF-regulated inducible promoter. P_{rhaBAD} has been reported to have low leakiness and dose-dependent induction to L-rhamnose, which in turn is not metabolised by the cell or degraded at experimental growth conditions (Kelly et al., 2018). However, of the remaining inducible promoters tested thus far in *Synechocystis*, none have demonstrated ideal characteristics. Several metal ion inducible promoters have been reported, but in addition to the difficulties in tuning expression, these are difficult to work with as many of the inducers are present in the growth media (Peca et al., 2008; Blasi et al., 2012; Englund et al., 2016; Behle et al., 2020). The TetR repressible promoter P_{tet}, which is used commonly in *E. coli*, has been investigated in different cyanobacterial species (including *Synechocystis*, *Synechococcus elongatus* PCC 7942 (hereafter PCC 7942) and *Nostoc* PCC 7120). The P_{tet}/TetR system does demonstrate some desirable characteristics in cyanobacteria, such as low leakiness, tight repression and a high dynamic range. However, the inducer aTc (anhydrotetracycline) is photo-labile and as such, expression cannot be maintained for more than approximately 24 hours post induction in light grown cyanobacterial cultures (Huang & Lindblad, 2013; Huang et al., 2015; Zess et al., 2016; Behle et al., 2020). The vanillate-inducible promoter from *C. glutamicum* has recently been reported in *Synechocystis* in the form optimised for *E. coli* (P_{vanCC}/vanR), but suffers a similar issue to that of P_{tet}/TetR, with only transient expression reported (Meyer et al., 2019; Behle et al., 2020). Variants of the IPTG inducible promoter, derived from P_{lac} of the native lac operon from *E. coli*, have been tested in a number of cyanobacterial strains (including Synechocystis, PCC 7942 and *Synechococcus* sp. PCC 7002). However, due to low dynamic range and leakiness without the presence of inducer, use of this expression system in cyanobacteria is not ideal (Niederholtmeyer et al., 2010; Lan & Liao, 2011; Albers et al., 2015; Markley et al., 2015; Nozzi et al., 2017). Other TF regulated promoters have also been reported in *Synechocystis*, including P_{BADWT} from *E. coli* and λP_R of viral origin. However, reports between studies are conflicting; Immethun et al. (2017) reported that P_{BADWT} responded to induction with

L-arabinose in a dose-dependent manner, whereas Ferreira et al. (2018) could not replicate this behaviour. The lambda promoter was initially reported to have no measurable output in *Synechocystis* but a subsequent study demonstrated robust expression (Huang et al., 2010; Ferreira et al., 2018).

For the design and implementation of larger synthetic gene circuits, being able to regulate different promoters independently in the same cell is essential. For this, a series of orthogonal promoter systems are required. The lack of inducible expression systems that demonstrate ideal behaviours in cyanobacteria is a bottleneck to further synthetic gene circuit development.

6.1.1 Aims

In this chapter, I explored the use of four new heterologous TF-regulated promoters that have been well described in *E. coli* but are new to *Synechocystis*. I also attempted to re-characterise a selection of published TF-regulated promoters from the literature, to determine whether they might be useful for further consideration for synthetic gene circuit design.

6.2 Materials and Methods

6.2.1 Culture Conditions for *Synechocystis* sp. PCC 6803

The *Synechocystis* sp. PCC 6803 glucose tolerant (GT) strain (obtained from the Lea-Smith lab at the University of East-Anglia, UK) (Zavřel et al., 2017) was maintained on 1.5% (w/v) agar plates containing BG11 medium (Lea-Smith et al., 2016). Liquid cultures were grown in BG11 (supplemented with 10 mM $NaHCO_3$) in 100 ml Erlenmeyer flasks. Liquid cultures were shaken at 100 rpm and aerated with filter-sterilized, water-saturated air. *Synechocystis* transconjugants containing only pPMQAK1-T based vector were cultured in BG11 medium and on BG11 agar plates, supplemented with 50 µg/ml kanamycin (BG11+Kan50), media of transconjugants containing pSEVA421-T based vectors were supplemented with 10 µg/ml spectinomycin (BG11+Spec10), and media of co-conjugated strains containing both pPMQAK1-T and pSEVA421-T based vectors were supplemented with 50 µg/ml kanamycin and 10 µg/ml spectinomycin (BG11+Kan50+Spec10).

Strains were grown under continuous light at 30°C, 100 µmol photons m^{-2} s^{-1} in a Multitron Pro incubator supplied with warm white LED lighting (Infors HT).

6.2.2 Chemical Inducers

Master stocks of all chemical inducers were made in advance and stored at -20°C with the exception of vanillic acid, which was made fresh for each experiment. Serial dilution of the master stock was performed, to achieve the desired working stock solution concentration. To initiate induction, 50 µl of working inducer solution was added to 1950 µl *Synechocystis* culture.

Table 6-1: List of chemical inducers used in this study.

Inducer	Diluent	Master Stock Concentration	Source
Sodium arsenite solution (pre-made)	H_2O	50 mM	Sigma-Aldrich (1062771000)
DAPG (2,4-diacetylphloroglucinol)	DMSO	25 mM	Cambridge BioScience (16345-100 mg-CAY)
Sodium salicylate	H_2O	1 M	SIGMA-ALDRICH CO LTD (S3007-500G)
3-OH-C14:1-HSL	DMSO	10 mM	Sigma-Aldrich (51481)
L-rhamnose	H_2O	0.5 M	MP Biomedicals, LLC (210280910)
L-arabinose	H_2O	1 M	MP Biomedicals, LLC (0210070680)
Vanillic acid	EtOH	100 mM	Sigma-Aldrich (94770-10G)

6.2.3 Vector Construction and Parts Assembly

All cloning was performed in OneShot TOP10 *E. coli* cells. Transformed cells were cultured in LB medium and on 1.5% (w/v) LB agar plates supplemented with either 100 µg/ml spectinomycin, 100 µg/ml carbenicillin, or 50 µg/ml kanamycin as required. *E. coli* strain MC1061 was cultured in LB medium supplemented with 100 µg/ml ampicillin and 25 µg/ml chloramphenicol. All *E. coli* strains were grown at 37°C with shaking at 225 rpm. All PCR products were gel purified using a Monarch DNA Gel Extraction Kit (NEB) unless

otherwise stated. All PCR amplified sequences were verified with Sanger sequencing.

Promoter parts (except P_{BADWT}) were generated by overlap extension PCR (Q5 High-Fidelity DNA Polymerase (NEB)) using two synthesised oligonucleotides (Integrated DNA Technology) (**Appendix Table 8-4**) so that on digestion with *BsaI* (NEB), overhangs GGAG-TACT were generated. The sequence encoding *eYFP*-T_{rrnB} from the CyanoGate vector pCAT.262 was amplified using Q5 High-Fidelity DNA Polymerase (NEB) so that on digestion with *BsaI* (NEB), overhangs TACT-CGCT were generated. The promoter part (PCR product used without further purification) and *eYFP*-T_{rrnB} were then assembled together into Level 1 position 1 acceptor vector pICH47732 to form *Promoter-eYFP*-T_{rrnB} using Golden Gate assembly (Engler et al., 2014). The test construct for P_{BADWT} was assembled by amplification of the sequence encoding *araC*-P_{BADWT} (from DNA available in the Wang Lab) and ligating to *eYFP*-T_{rrnB} as above (see section 6.3.3.1.2).

The *Inducible Promoter x-eYFP*-T_{rrnB} assemblies were then used as templates and fused with a 'junction sequence' and cognate TF expression cassette, so that the TF expression cassette was in the reverse orientation relative to the cognate promoter to form *TF-Inducible-Promoter x-eYFP*-T_{rrnB}. Junction sequences were constructed that harboured a terminator, and promoter with RBS associated sequence in the reverse orientation to form the TF expression cassette. The junction sequences were generated by overlap extension PCR (Q5 High-Fidelity DNA Polymerase (NEB)) using four synthesised oligonucleotides (Integrated DNA Technology) (**Appendix Table 8-4**) and the PCR fragments were used without further purification. On digestion with *BpiI* (Thermo Fisher Scientific), overhangs GCTT-TACT and TACT-CGCT were generated and fragments were ligated into a holding vector (3U + Ter acceptor - pICH41276) for use as a template for subsequent assemblies. Sequences encoding *Inducible-Promoter x-eYFP*-T_{rrnB}, the 'junction sequence', and the respective TF coding sequence (from vectors available in the Wang Lab), were amplified using Q5 High-Fidelity DNA Polymerase (NEB)

(**Appendix Table 8-4**) and ligated into Level 1 position 1 acceptor vector pICH47732 using Golden Gate assembly (Engler et al., 2014). The level 1 assemblies were then assembled into pPMQAK1-T for conjugation into *Synechocystis* (Vasudevan et al., 2019).

To assemble the genetic inverter/NOT gates, the sequences encoding *rhaS*-P_{rhaBAD} and $phlF^{AM}$, and P_{phlF}-*eYFP*-T_{rrnB} were amplified using Q5 High-Fidelity DNA Polymerase (NEB) (**Appendix Table 8-4**) and ligated into Level 1 position 1 acceptor vector pICH47732 to form *rhaS*-P_{rhaBAD}-$phlF^{AM}$ and Level 1 position 2 acceptor vector pICH47742 respectively, using Golden Gate assembly (Engler et al., 2014). *rhaS*-P_{rhaBAD}-$phlF^{AM}$ and P_{phlF}-*eYFP*-T_{rrnB} were subsequently assembled into pPMQAK1-T for conjugation into *Synechocystis*. For the construction of the two vector NOT Gate/genetic inverter (NOT_Dual), *rhaS*-P_{rhaBAD}-$phlF^{AM}$ and P_{phlF}-*eYFP*-T_{rrnB} were assembled into pPMQAK1-T and pSEVA421-T, respectively.

For the degradation tag NOT gate variants, the tag coding sequences were added 3' to $phlF^{AM}$ using primers and Gibson-AQUA assembly (Beyer et al., 2015) (Sigma Aldrich) (**Appendix Table 8-4**). *rhaS*-P_{rhaBAD}-$phlF^{AM}$-*DT* and Level1 position 1 acceptor backbone were amplified using Q5 High-Fidelity DNA Polymerase (NEB). The fragment sizes were verified by running 5 µl on an electrophoresis gel, then the remainder of the PCR product was treated with DpnI (NEB) and incubated at 37°C for 1 hour followed by an inactivation step of 85°C for 20 minutes. The PCR products without any further treatment were combined in the ratio 3 µl backbone to 7 µl insert and incubated at room temperature for 1 hour after which 5 µl was transformed by heat shock into *E. coli* TOP10.

Five additional NOT gate variants were constructed by altering the RBS associated with $phlF^{AM}$. Using *rhaS*-P_{rhaBAD}-$phlF^{AM}$-T_{rrnB} as the template, two fragments *rhaS*-P_{rhaBAD}- and -$phlF^{AM}$-T_{rrnB} were amplified using Q5 High-Fidelity DNA Polymerase (NEB), and the RBSs was modified using (**Appendix Table 8-4**). The two fragments were assembled into Level 1

position 1 acceptor vector pICH47732 and assembled into pPMQAK1-T as above.

6.2.4 Cyanobacterial Conjugation

Genetic modification by conjugation in PCC 6803 was facilitated by *E. coli* strain MC1061 carrying the mobilizer vector pRK24 (www.addgene.org/51950) and helper vector pRL528 (www.addgene.org/58495) (Tsinoremas et al., 1994; Gale et al., 2019). Conjugal transfer was performed as in Gale et al. (2019). For co-conjugation, the pSEVA421-T based vector was transferred into a transconjugant strain already harbouring a pPMQAK1-T based vector that had been washed three times with fresh BG11 media.

6.2.5 Fluorescence Assays

To measure fluorescence in *Synechocystis*, transconjugants maintained on agar plates were first inoculated into 10 ml BG11 medium supplemented with appropriate antibiotic and grown for 2-3 days to OD_{750} ~1.0. To initiate the assay, the seed cultures were diluted to a starting OD_{750} of 0.2 in 24-well plates (Costar Corning Incorporated) containing fresh BG11 medium supplemented with appropriate antibiotic to a final volume of 2 ml. Cultures were grown for three days under culturing conditions and high humidity (95%) to avoid evaporation and OD_{750} was measured using a FLUOstar OMEGA microplate reader (BMG Labtech). eYFP fluorescence were measured by flow cytometry for individual cells (minimum 10,000 cells per culture) with an Attune NxT Flow Cytometer (Thermo Fisher Scientific). Cells were gated using forward and side scatter. Median eYFP fluorescence levels were calculated from excitation/emission wavelengths 488 nm/ 515-545 nm. An ‘empty’ pPMQAK1-T vector, or co-conjugated pPMQAK1-T and pSEVA421-T (i.e. with no eYFP expression cassettes) was included as a base line control. Fluorescence values for the latter control were subtracted from transconjugant strain measurements unless otherwise stated.

6.3 Results and Discussion

6.3.1 Generating vectors for screening and characterisation of inducible and repressible expression systems

To screen the heterologous TF-regulated expression systems in *Synechocystis*, I first assembled each promoter sequence with *eYFP* to generate an inducible promoter expression cassette (e.g. *inducible promoter X-eYFP*-T_{rrnB}). I subsequently assembled the latter cassette with the respective cognate TF expression cassette, to generate a pPMQAK1-T plasmid carrying both the TF cassette and inducible promoter cassette (**Figure 6-1A, Materials and Methods**) for conjugation into *Synechocystis* (Vasudevan et al., 2019). A set of TF-regulated promoters were chosen that were available in the Wang lab and also well described in *E. coli* (**Table 6-2**). For the promoters described by Meyer et al. (2019), the ribozyme-based insulator sequence RiboJ that is used in their promoter designs, was not included. There was limited information on the effect of RiboJ on expression in cyanobacteria, with one study reporting that expression was reduced with inclusion of RiboJ for one out of four species that they tested (Taton et al., 2014). The vanillate-inducible promoter was the only exception, as this had been characterised in *Synechocystis* with inclusion of RiboJ.

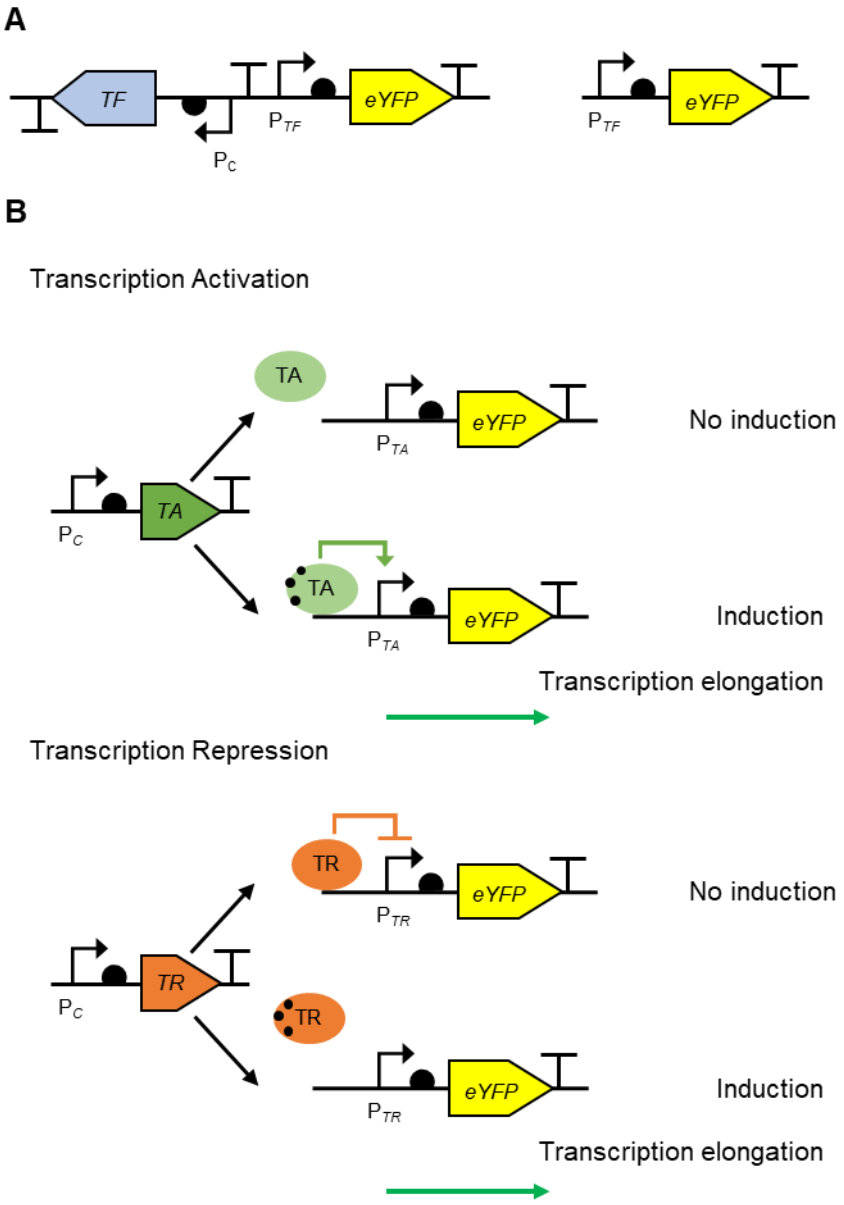

Figure 6-1: Test Constructs Used and Mode of Action of Transcription Activators and Repressors

(A) Two different construct design types were assembled for testing transcription factor (TF) regulated promoters (P_{TF}) in *Synechocystis* sp. PCC 6803. The left construct comprises P_{TF} driving reporter *eYFP*, with an expression cassette for the cognate TF driven by a constitutive promoter (P_C), in the reverse orientation and isolated by a junction terminator. The right comprises a test construct without co-expressed TF. (B) For transcription activation, the gene for the transcription activator (*TA*) is driven by P_C. Without addition of inducer (small black circles), expressed TA does not interact with the cognate promoter sequence (P_{TA}) and there is no transcription activation. On addition of inducer, TA undergoes a conformation change, which then interacts with P_{TA} and transcription is activated. For transcriptional repression, the

gene for the transcription repressor (*TR*) is driven by P_C. Without addition of inducer, expressed TR binds to the cognate promoter sequence (P_{TR}) and blocks transcription. On addition of inducer, TR undergoes a conformation change, which then releases P_{TR}, and transcription can occur (i.e. without co-expression of TR, P_{TR} is constitutive).

6.3.2 Investigation and characterisation of novel repression and activation expression systems in *Synechocystis* sp. PCC 6803

Four transcription factor regulated promoters new to cyanobacteria, consisting of two repressors and two activators, were chosen for testing that were available in the Wang Lab. During the initial experiments, unexpected growth defects were observed with the strains supplemented with inducer that had been prepared with DMF (dimethylformamide) as the solvent. From the literature, DAPG (2,4-diacetylphloroglucinol) and 3-OH-C14:1-HSL (N-(3-hydroxy-7-cis tetradecenoyl)-l-homoserine lactone) are reported to use DMF as the solvent for the master stock (Meyer et al., 2019). A growth experiment was conducted where *Synechocystis* harbouring an empty vector was subjected to varying concentrations of DMF, as well as ethanol (EtOH) and DMSO (dimethyl Sulfoxide). The growth experiment demonstrated that addition of DMF, even at the very low concentration of 0.25%, caused lack of growth in *Synechocystis,* whereas the strains exposed to either EtOH or DMSO grew similarly to the control culture (**Figure 6-2**). Therefore, DMSO was used in place of DMF, as it is commonly used and often interchanged with DMF.

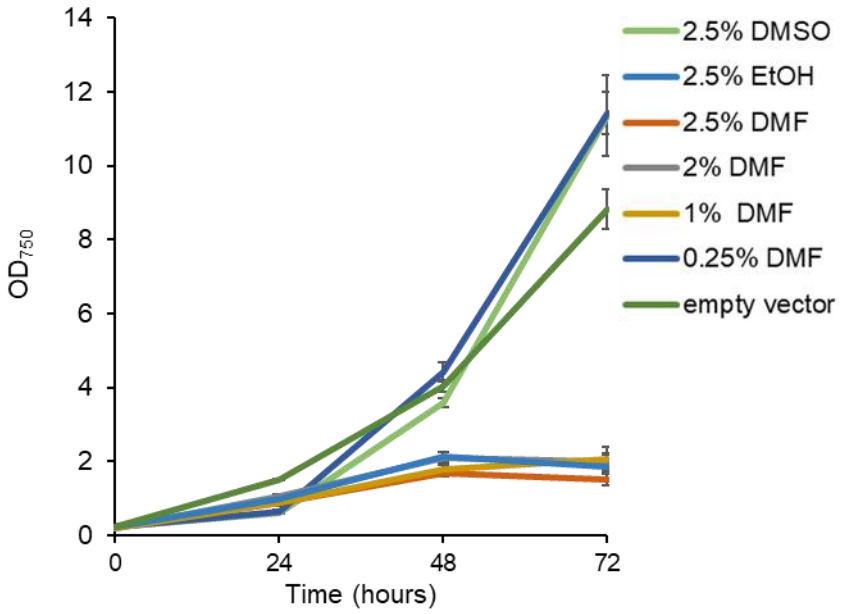

Figure 6-2: Growth of strains supplemented with DMF demonstrated severe growth defects.

Cultures were grown for 72 hr at 30°C with continuous light (100 µmol photons m^{-2}-s^{-1}). Cultures were supplemented with either varying concentration of DMF, or a single concentration of DMSO or ethanol (EtOH). Error bars represent ± standard error of the mean of four biological replicates.

Table 6-2: List of Promoter Variants Evaluated in This Study

All promoter variants were assembled into pPMQAK1-LT for evaluation in *Synechocystis* sp. PCC 6803 (**Materials and Methods**). All promoters, except P_{arsR}, were assembled with and without the respective cognate transcription factor (TF) (**Figure 6-1A**), the promoter and RBS for each TF expression cassette are listed, with expression system mode of action (**Figure 6-1B**) and organism the promoter originated. P_{BADWT} was assembled with the native constitutive promoter (P_C). P_{arsR} was not assembled with the cognate TF as no expression was observed (**see section 6.3.2.1.1**).

Name	Promoter + 5' UTR	Transcription Factor Expression Cassette	Transcription Factor	Inducer	Mode of Action	Origin	References
P_{arsR}_32 P_{arsR}_34	P_{arsR}_B0032 P_{arsR}_B0034	N/A	N/A (ArsR)	arsenic	repressor	*E. coli*	(Wan et al., 2019)
P_{phlF}(No_TF) P_{phlF}(114_TF)) P_{phlF}(101_TF)	P_{phlF}_B0034 P_{phlF}_B0034 P_{phlF}_B0034	N/A P_{J23114}_B0032-*phlF*^{AM} P_{J23101}_B0032-*phlF*^{AM}	N/A PhlF^{AM}	DAPG	repressor	*Pseudomonas fluorescens*	(Meyer et al., 2019)
P_{salTTC}(No_TF) P_{salTTC}(114_TF) P_{salTTC}(101_TF)	P_{salTTC}_B0034 P_{salTTC}_B0034 P_{salTTC}_B0034	N/A P_{J23114}_B0032-*nahR*^{AM} P_{J23101}_B0032-*nahR*^{AM}	N/A NahR^{AM}	sodium salicylate	activator	*Pseudomonas putida*	
P_{Cin}(No_TF) P_{Cin}(114_TF)) P_{Cin}(101_TF)	P_{Cin}_B0034 P_{Cin}_B0034 P_{Cin}_B0034	N/A P_{J23114}_B0032-*cinR*^{AM} P_{J23101}_B0032-*cinR*^{AM}	N/A CinR^{AM}	3-OH-C14:1-HSL	activator	*Rhizobium leguminosarum*	
P_{rhaBAD}	P_{rhaBAD}_B0034	P_{J23101}_B0032-*rhaS*	Rhas	L-rhamnose	activator	*E. coli*	(Kelly et al., 2018)
P_{BADWT}	PBAD_B0034	P_C_*araC*	AraC	L-arabinose	dual activity	*E. coli*	(Immethun et al., 2017)
P_{vanCC}	P_{vanCC}_RiboJ_RBS*	P_{J23100}_RBS_{Van3}-*vanR*	VanR	vanillate	repressor	*Corynebacter glutamicum*	(Meyer et al., 2019)
λP_R (No TF) λP_R (101_TF)	λP_R _B0034 λP_R _B0034	N/A P_{J23101}_B0032-*cI*	N/A CI	N/A	repressor	viral origin	(Ferreira et al., 2018)

6.3.2.1 Repressors

To screen the TF repressed promoters, the promoter cassette was first screened for fluorescence expression in the absence of the cognate TF cassette. In the latter expression system, the promoter should act constitutively (i.e., be 'continuously on') without co-expression of the TF (**Figure 6-1B**).

6.3.2.1.1 Arsenic-inducible promoter from E. coli

The arsenic responsive promoter, P_{arsR}, native to *E. coli* drives the *ars* operon, which is involved in arsenic resistance (Shi et al., 1996). In the absence of arsenic (i.e. arsenite [As^{III}]), a dimer of the cognate TF ArsR binds to a recognition site within the promoter region, thus blocking transcription. In the presence of arsenic, ArsR undergoes a conformational change, which releases the DNA thus lifting the transcription blockade allowing transcription elongation and expression to occur. Systems that confer arsenic resistance are present in other organisms including *Synechocystis*, but the native *arsBHC* operon from *Synechocystis* has been reported to be evolutionarily distinct from that of *E. coli* (López-Maury et al., 2003). On comparison of the ArsR homologues from *Synechocystis* and *E. coli*, these isoforms demonstrate low homology (**Figure 6-3A**). In addition to the non-homologous ArsR, the single operator site from *E. coli* 'ACTTACACATTCGTTAAGT' compared to tandem operator sites from *Synechocystis,* which are comprised of two identical sequences 'ATCAAGTTTTTTTGATG' separated by 12 bp (López-Maury et al., 2003), are also distinct and it is likely that P_{arsR} from these two organisms are orthogonal.

Two P_{arsR} constructs were tested, one with the relatively weak RBS BBa_B0032, and one with the strong RBS BBa_B0034 (**Table 6-2**) (Englund et al., 2016). Although orthogonality was assumed, I tested these constructs with and without arsenic induction to preclude any possibility of cross-talk between the native *Synechocystis* ArsR homologue and P_{arsR} from *E. coli*. Measurements from P_{arsR} strains showed a slight increase in fluorescence when compared to the empty vector negative control, but no significant difference in expression was observed (**Figure 6-3B**). An arsenite [As^{III}]

concentration of 500 µM was chosen, as this had previously been demonstrated to de-repress and induce transcription from the native P_{arsR} in *Synechocystis* and also cause no growth defects (López-Maury et al., 2003; Sure et al., 2016). Growth of the induced strains were comparable to the uninduced and empty vector strains (**Appendix Figure 8-3**). These constructs were tested in *E. coli* where fluorescence was observed (**Figure 6-3C**). The *E. coli* cultures were supplemented with arsenite [As^{III}] as TOP10 harbours *arsR* in the genome. These results indicate that P_{arsR} from *E. coli* does not drive sufficient transcription to be detected over background fluorescence in *Synechocystis*. I therefore did not test P_{arsR} with its cognate TF, ArsR (**Figure 6-1**) and removed P_{arsR} from further analyses.

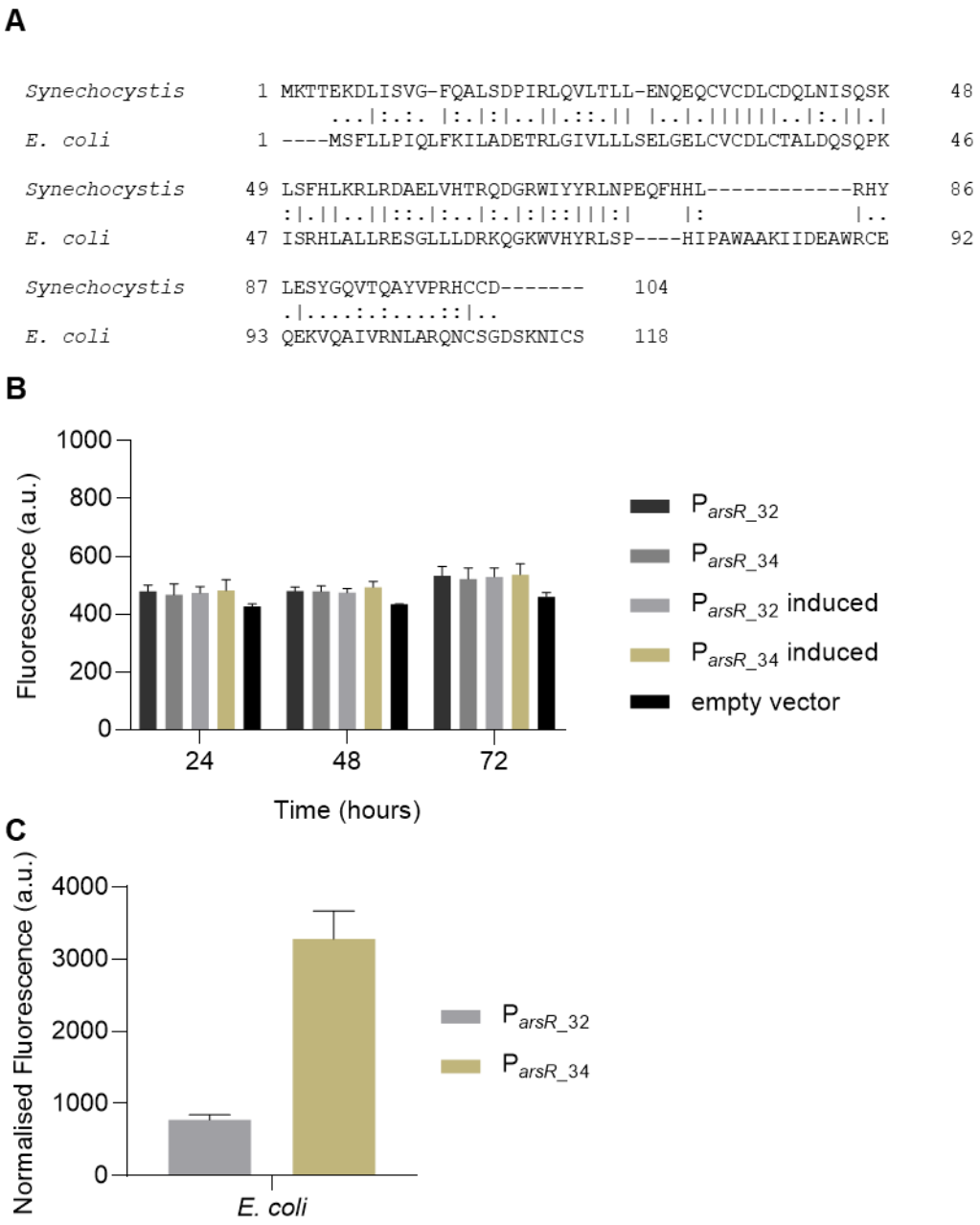

Figure 6-3: The arsenic-inducible promoter P_{arsR} from *E. coli* does not drive expression in *Synechocystis*.

(A) ArsR isoforms in *Synechocystis* and *E. coli*. were aligned using EMBOSS Needle (https://www.ebi.ac.uk/Tools/psa/emboss_needle/), which produced a shared identity of 29.4% and similarity of 46.0%. (B) Expression levels of eYFP at three time points (24, 48 and 72 hours). The induced strains are supplemented with 500 µM arsenite [As^{III}]. Autofluorescence from the empty vector is shown and has not been subtracted from fluorescence measurements from the other strains. Error bars represent the ± standard error (SE) of the mean of four biological replicates, where each replicate represents the median

measurement of at least 10,000 cells measured by flow cytometry. For each time point, ANOVA followed by Tukey's honestly significant difference test was performed and no significant difference was found between any strains and the empty vector at each time point ($P<0.05$). (C) Expression levels of eYFP in *E. coli* after ~7 hours growth. Cultures were supplemented with 1 µM arsenite [As^{III}]. Fluorescence was measured in a plate reader and normalised to OD_{600}. Error bars represent ± SE of four biological replicates.

6.3.2.1.2 DAPG-inducible promoter from Pseudomonas fluorescens

The DAPG-inducible promoter P_{phlF}, native to *Pseudomonas fluorescens*, drives expression of the operon *phlACBD*, which encodes the synthetic pathway for DAPG synthesis i.e. DAPG is a positive autoregulator for *phlACBD* and its own synthesis (Abbas et al., 2002). P_{phlF} is repressed by its cognate TF PhlF, which in the absence of DAPG, dimerises and binds to the operator site *ph0* and in turn blocks transcription. In the presence of DAPG, PhlF undergoes a conformational change, releasing the DNA, thus lifting the transcription blockade allowing transcription elongation and expression to occur. PhlF is a TetR family repressor, homologues of which have been identified in many prokaryotic species but not cyanobacteria (Ramos et al., 2005). Since initial identification and characterisation, the wild-type repressor PhlF has been further optimised for use in *E. coli*, yielding the promoter/repressor pair P_{phlF}/$PhlF^{AM}$ that demonstrated an increase in dynamic range and a reduction is cross-reactivity (Meyer et al., 2019).

First, the strain harbouring P_{phlF}-*eYFP*-T_{rrnB} was tested for fluorescence expression to determine whether the promoter without co-expression of $PhlF^{AM}$ would generate measurable fluorescence in *Synechocystis*. As fluorescence expression was observed, the strains harbouring *phlF*^{AM}-P_{phlF}-*eYFP*-T_{rrnB} were constructed and transferred by conjugation into *Synechocystis* for testing (**Table 6-2**). First, P_{phlF}(101_TF) was tested with addition of DAPG in the range 0 – 25 µM. Without addition of DAPG, fluorescence expression from P_{phlF}(101_TF) was reduced to undetectable levels, indicating that $PhlF^{AM}$ was being expressed, tightly repressing P_{phlF} and blocking transcription (**Figure 6-4A**). Induction with up to 25 µM DAPG did not produce any measurable fluorescence (**Figure 6-4A**), which is the maximum inducer concentration

reported for use in *E. coli* (Meyer et al., 2019). PhlF^{AM} is a strong repressor and high expression can lead to difficulties in de-repression, even with the addition of DAPG. Therefore P$_{phlF}$(114_TF) was tested, where *phlF^{AM}* is driven by the weak promoter P$_{J23114}$ (**Table 6-2**) (**Section 3.4.4.2**). DAPG concentration was increased up to 250 µM, which is 10 times the maximum level used in *E. coli* and no induction of fluorescence expression was observed (**Figure 6-4A**). Growth of all strains was comparable to the empty vector control (**Appendix Figure 8-4**). Without co-expression of PhlF^{AM}, P$_{phlF}$ has demonstrated robust expression at similar levels to P$_{J23111}$ and P$_{V02}$ (**Section 3.4.4.2**), and with co-expression of PhlF^{AM}, fluorescence expression was repressed to levels that were undetectable in *Synechocystis*. However, despite the robust expression and tight repression, on addition of DAPG, it was not possible to de-repress P$_{phlF}$. One possibly is that DAPG was not entering the cell at a sufficient concentration to cause the required confirmational change in PhlF^{AM}. These constructs were tested in *E. coli* where fluorescence was observed on induction with DAPG (**Figure 6-4B**). Nonetheless, there are a very limited number of tight repressors thus far reported in *Synechocystis* so the P$_{phlF}$/PhlF^{AM} promoter/repressor pair is potentially a valuable addition. If PhlF^{AM} is driven by an inducible expression system, this would create a trans-acting repressor, which are useful in the design of synthetic gene circuits (Stanton et al., 2014; Nielsen et al., 2016a).

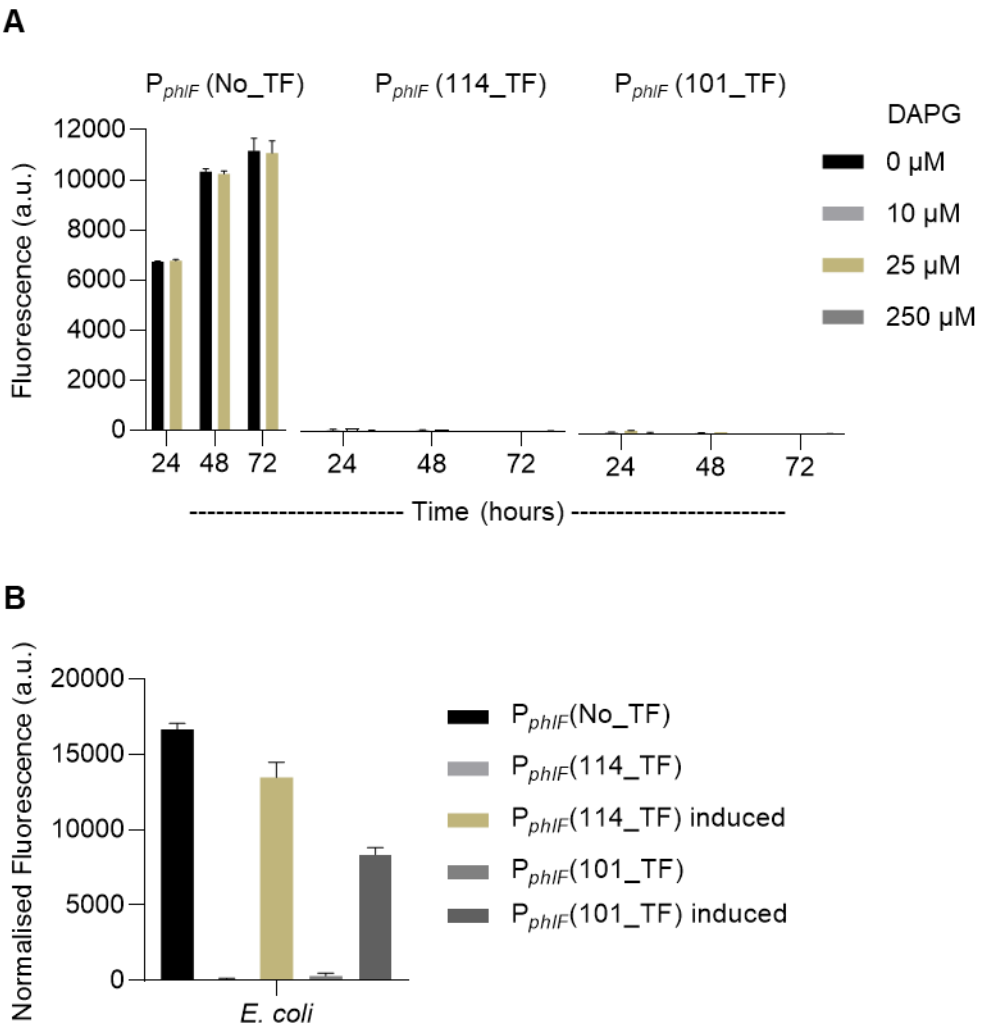

Figure 6-4: DAPG-inducible promoter P_{phlF} from *Pseudomonas fluorescens* drives expression and is tightly repressed in *Synechocystis*

(A) P_{phlF}(114_TF) and P_{phlF}(101_TF) represent P_{phlF}-eYFP-T_{rrnB} with co-expression of $PhlF^{AM}$ driven by P_{J23114} and P_{J23101}, respectively (**Table 6-2**). Expression levels of eYFP at three time points (24, 48 and 72 hours) with different concentrations of DAPG. Error bars represent ± SE of four biological replicates, where each replicate represents the median measurement of at least 10,000 cells measured by flow cytometry. (B) Expression levels of eYFP in *E. coli* after ~7 hours growth. Cultures were supplemented with 25 µM DAPG. Fluorescence was measured in a plate reader and normalised to OD_{600}. Error bars represent ± SE of four biological replicates.

6.3.2.2 Activators

Screening for inducible promoters where the mode of action is 'activation' is more challenging compared to repressible systems, as transcription should only be activated in the presence of both the cognate TF and inducer (**Figure 6-1B**). Therefore, induction requires both appropriate expression of the TF and efficient intracellular uptake of the inducer. To screen activators, variants of the *TF-Promoter-eYFP*-T_{rrnB} construct (**Figure 6-1A**) were tested with different promoters driving expression of the TF expression cassette (**Table 6-2**) with increasing inducer concentrations.

6.3.2.2.1 Salicylate-inducible promoter from Pseudomonas putida

The positive transcriptional regulator NahR was mined from *Pseudomonas putida*, where in the presence of salicylate, transcription is activated from promoters P_{nah} and P_{sal}. P_{nah} and P_{sal} drive the operons *nahA-F* and *nahG-M*, respectively. *nahA-F* encodes six enzymes that metabolise naphthalene into salicylate and pyruvate and *nahG-M* encodes eight enzymes that metabolise salicylate into intermediates of the Krebs cycle, allowing *P. putida* to utilise naphthalene as the sole carbon source (Dunn & Gunsalus, 1973; Schell, 1983). The wild-type promoter/activator pair P_{sal}/NahR has been further optimised for use in *E. coli* to form P_{salTTC}/$NahR^{AM}$ (Meyer et al., 2019). Before testing this promoter, I first searched the *Synechocystis* genome for homologues of $NahR^{AM}$ using BLASTP (Altschul et al., 1990, 1997). Only one protein was identified with any similarity (WP_010871778.1). However, with an E-value of 1×10^{-4}, similarity was low resulting in a score of 40 and maximum percentage identity of 23.25%.

Three different strains were tested, one without TF co-expression and two variants with either P_{J23114} or P_{J23101} driving expression of $NahR^{AM}$ (**Table 6-2**). Strains were grown for 72 hours and fluorescence and OD_{750} measurements were taken every 24 hours. Growth between strains, both induced and uninduced, was similar (**Figure 6-5**). Fluorescence measurements compared between strains were also similar, with the strain harbouring P_{salTTC}(No_TF)

showing similar expression to both P_{salTTC}(114_TF) and P_{salTTC}(101_TF) with or without the presence of inducer (**Figure 6-6A**).

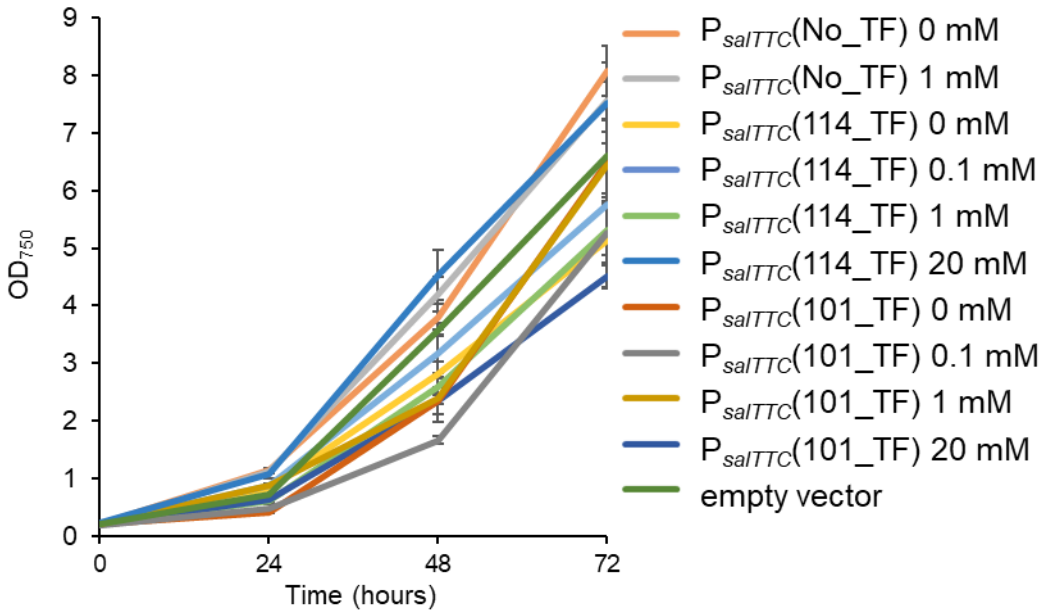

Figure 6-5: Growth of strains harbouring P_{salTTC} variants in *Synechocystis* sp. PCC 6803. Cultures were grown for 72 hr at 30°C with continuous light (100 µmol photons m^{-2}-s^{-1}). Error bars represent ± SE of the mean of four biological replicates. Induction was performed with varying concentration of salicylate (0 –20 mM).

These constructs were tested in *E. coli* where the strains without induction did demonstrate some fluorescence indicating the promoter is leaky. On induction, a four-fold change was observed for both variants (**Figure 6-6B**). $NahR^{AM}$ is a transcriptional activator, no expression should be observed from P_{salTTC}(No_TF). This indicates the possibility that P_{salTTC} has some cross-talk with native signalling pathways and thus lack of orthogonality in *Synechocystis.* These results suggested that P_{salTTC} was not useful for further consideration for use as an inducible expression system in *Synechocystis*.

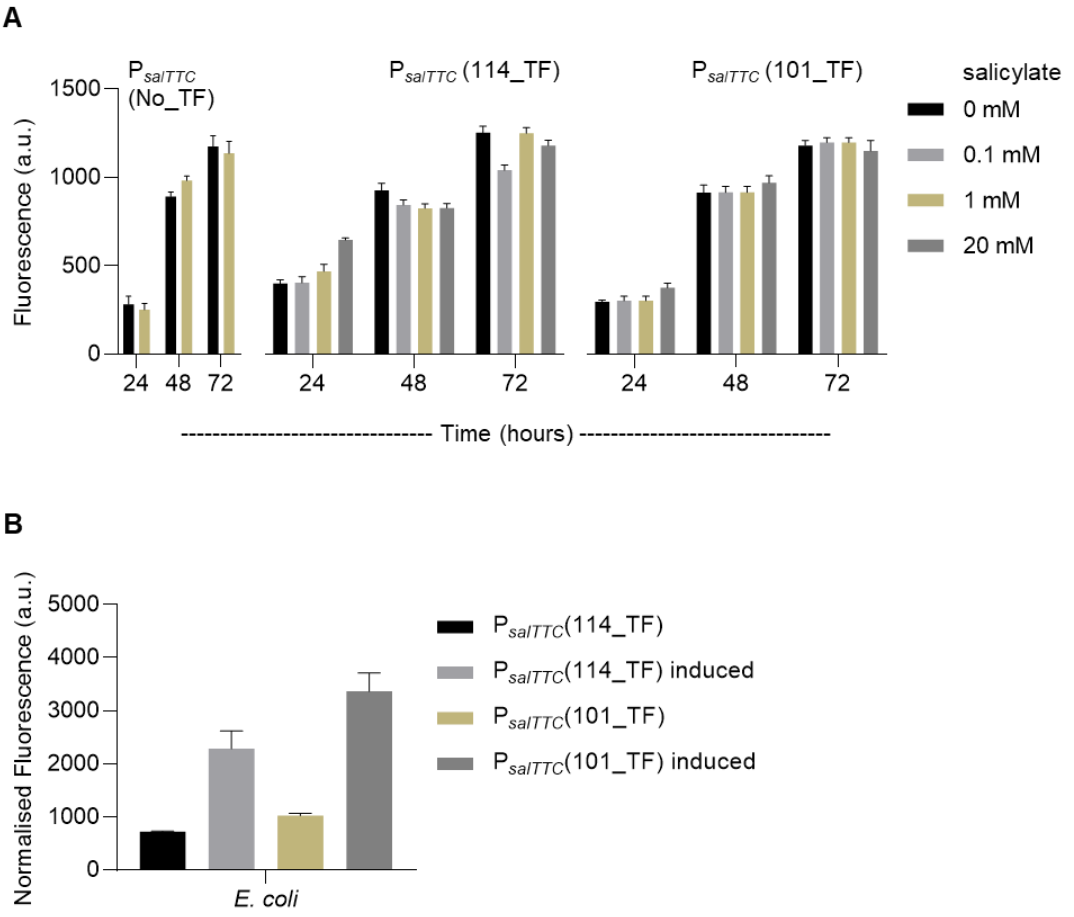

Figure 6-6: The salicylate-inducible promoter P_{salTTC} from *Pseudomonas putida* drives expression in *Synechocystis* irrespective of transcription factor or inducer.

(A) Expression levels of eYFP at three time points (24, 48 and 72 hours) with supplementation of different concentrations of sodium salicylate. Error bars represent ± SE of four biological replicates, where each replicate represents the median measurement of at least 10,000 cells measured by flow cytometry. (B) Expression levels of eYFP in *E. Coli* after ~7 hours growth. Cultures were supplemented with 100 µM sodium salicylate. Fluorescence was measured in a plate reader and normalised to OD_{600}. Error bars represent ± SE of four biological replicates.

6.3.2.2.2 Quorum sensing promoter P_{Cin} from Rhizobium leguminosarum

The positive transcriptional regulator CinR, from the *cinRI* gene cluster from *Rhizobium leguminosarum* was identified as being part of the innate quorum-sensing (QS) system that contains two genes, *cinI* and *cinR. R. leguminosarum* forms a symbiotic relationship with legumes and is involved in the formation of nitrogen-fixing root nodules (Allan Downie & González, 2014). QS systems have evolved to regulate these complex symbiotic interactions,

some of which respond to several derivates of N-acyl-homoserine lactone (AHL) (Wisniewski-Dyé & Downie, 2002). In the presence of the AHL derivative 3-OH-C14:1-HSL, CinR activates the expression of CinI, which in turn produces 3-OH-C14:1-HSL (Lithgow et al., 2000). The increase in AHL concentration that this positive feedback loop generates is sensed by the bacteria and subsequently regulates population growth. The CinR transcriptional activator has been optimised for *E. coli* to form P_{cin}/CinR^{AM} (Meyer et al., 2019). Before testing this promoter, I first searched the *Synechocystis* genome for homologies of CinR using BLASTP (using default settings) (Altschul et al., 1990, 1997), no proteins were identified with significant similarity. Three different strains were tested (**Table 6-2**), with OD_{750} and fluorescence measurements taken every 24 hours for 72 hours after induction. Growth between strains, both induced and uninduced was similar (**Appendix Figure 8-5**). When comparing fluorescence of the P_{Cin} containing strains to the empty vector, no expression above that of background autofluorescence was observed (**Figure 6-7A**). The maximum inducer concentration reported for used in *E. coli* is 10 µM (Meyer et al., 2019), inducer concentration was increased to 250 µM in *Synechocystis* with no resulting expression. As with P_{phlF}, one possibly is that 3-OH-C14:1-HSL does not enter the cell in sufficient concentrations to facilitate transcriptional activation by CinR^{AM}. These constructs were tested in *E. coli* where fluorescence was observed on induction with 3-OH-C14:1-HSL (**Figure 6-7B**). As no output was achieved with P_{Cin}/CinR^{AM}, this was not considered for further use in *Synechocystis*.

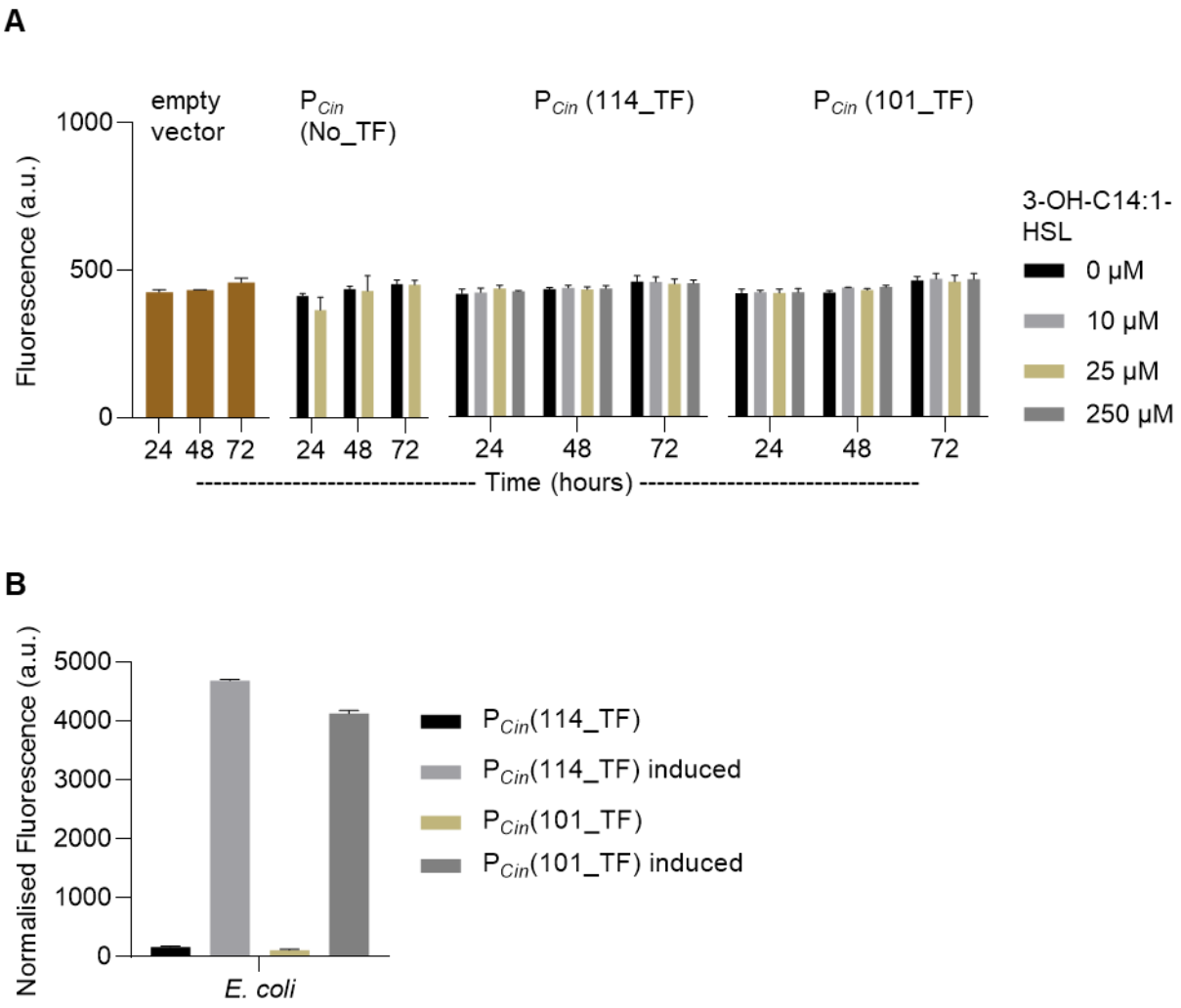

Figure 6-7: The quorum sensing promoter P_{cin} from *Rhizobium leguminosarum* does not drive expression in *Synechocystis*.

(A) Expression levels of eYFP at three time points (24, 48 and 72 hours) with different concentrations of 3-OH-C14:1-HSL. Dark brown bars represent autofluorescence from the empty vector and that has not been subtracted from the other strains. Error bars represent ± SE of four biological replicates, where each replicate represents the median measurement of at least 10,000 cells measured by flow cytometry. For each time point, ANOVA followed by Tukey's honestly significant difference test was performed and no significant difference was found between any strains and the empty vector ($P<0.05$). (B) Expression levels of eYFP in *E. Coli* after ~7 hours growth. Cultures were supplemented with 10 µM 3-OH-C14:1-HSL. Fluorescence was measured in a plate reader and normalised to OD_{600}. Error bars represent ± SE of four biological replicates.

6.3.3 Verification and characterisation of selected existing inducible promoters used in *Synechocystis* sp. PCC 6803

Of the four new inducible expression systems bested in *Synechocystis* (see section 6.3.2), none exhibited ideal behaviour. Accordingly, to progress synthetic gene circuit designs, selected inducible promoters from the literature were constructed and characterised.

6.3.3.1.1 L-rhamnose-inducible promoter from E. coli

The L-rhamnose inducible system from *E. coli* consists of the promoter P_{rhaBAD} and its transcriptional activator RhaS. P_{rhaBAD}/RhaS has been well characterised in *Synechocystis* (Kelly et al., 2018; Behle et al., 2020). To characterise this system, *rhaS*-P_{rhaBAD}-*eYFP*-T_{rrnB} was constructed with the low-medium strength constitutive promoter P_{J23101} driving expression of RhaS. To test the response to L-rhamnose induction, cultures were induced with varying concentration of L-rhamnose (0 – 3.8 mM) at the start of the experiment, and fluorescence and OD_{750} were measured every 24 hours for 96 hours. Without induction, very low expression was observed (405 ± 41 a.u.), indicating a very low level of leakiness. A maximum fluorescence expression of 59864 ± 886 a.u. was achieved at 96 hours following induction with 1.7 mM L-rhamnose. This represented a 160-fold induction and a similar output to the strong P_{cpc560} promoter (**see section 3.4.4.1**). These results are similar when compared to Behle et al. (2020) who reported a 143-fold or 165-fold induction when RhaS was expressed with P_{J23119} or P_{J23111}, respectively. In our hands, the L-rhamnose inducible expression system demonstrated a robust and reliable dose-response behaviour, with low leakiness and no observed negative effects on culture growth (**Appendix Figure 8-6**). Thus, the expression system was a good candidate for further synthetic gene circuit design.

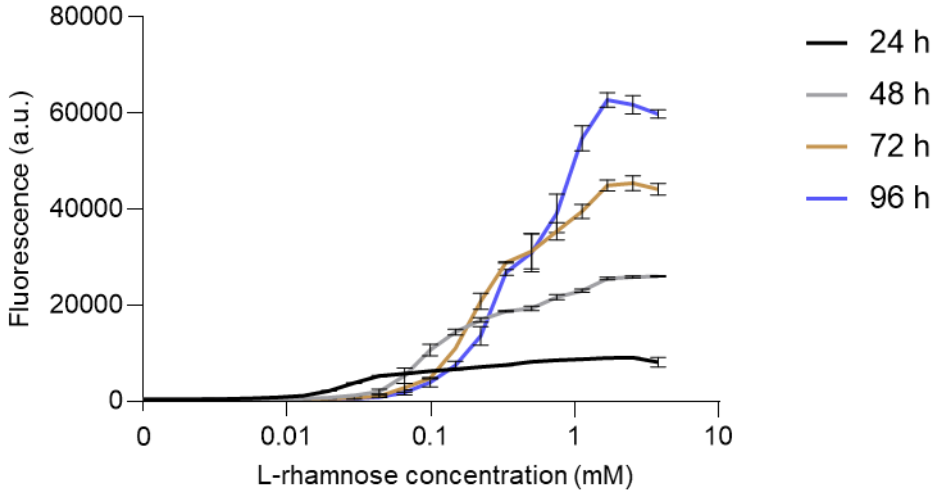

Figure 6-8: The L-rhamnose-inducible promoter from *E. coli* drives robust expression in *Synechocystis* in a dose-dependent manner.

Expression levels of eYFP at four time points (24, 48, 72 and 96 hours) with different concentrations of L-rhamnose (log_{10} scale). Error bars represent ± SE of four biological replicates, where each replicate represents the median measurement of at least 10,000 cells measured by flow cytometry.

6.3.3.1.2 L-arabinose-inducible promoter from E. coli

The L-arabinose-inducible promoter P_{BADWT} from *E. coli* is regulated by the cognate TF AraC. P_{BADWT} has been previously characterised in *Synechocystis* but with conflicting reports. Immethun et al. (2017) reported P_{BADWT} as a useful inducible expression system. Although weak output was demonstrated on addition of L-arabinose, induction was reliable and in a dose-dependent manner. In a subsequent study in *Synechocystis*, P_{BADWT} was shown to produce similar levels of expression with and without the addition of L-arabinose (Ferreira et al., 2018). The experimental design did vary between studies, with the former using *araC*-P_{BADWT} where AraC was expressed by the native constitutive promoter from the *E. coli* operon *araBAD* (P_C) (Casadaban, 1976), and the latter expressed AraC using the native P_{rrnB} from *Synechocystis*. To attempt to reproduce the former L-arabinose dose-dependent response, I used the wild-type P_{BADWT} promoter, where *araC* is under the control of the native constitutive promoter, P_C (Schleif, 2010), and where L-arabinose concentration of 5 mM produced the maximum

fluorescence signal after 72 hours growth (Immethun et al., 2017). L-arabinose concentrations up to 20 mM were added at the beginning of the experiment and fluorescence and OD_{750} measurements were taken at 24, 48 and 72 hours. Growth was similar between cultures (**Appendix Figure 8-7**) and weak fluorescence expression was observed at each time point independent of L-arabinose induction (**Figure 6-9A**). In contrast, the same construct tested in *E. coli* produced the expected behaviour, where fluorescence was only detected after induction with L-arabinose (**Figure 6-9B**). It is unclear why dose-dependent expression with L-arabinose cannot successfully be replicated in *Synechocystis* with P_{BADWT}, but one strategy to further explore would be to express AraC with a series of different strength constitutive promoters to determine whether this has any effect on the does-dependent response of P_{BADWT} to L-arabinose in *Synechocystis*. This strategy was not pursued here due to time constraints.

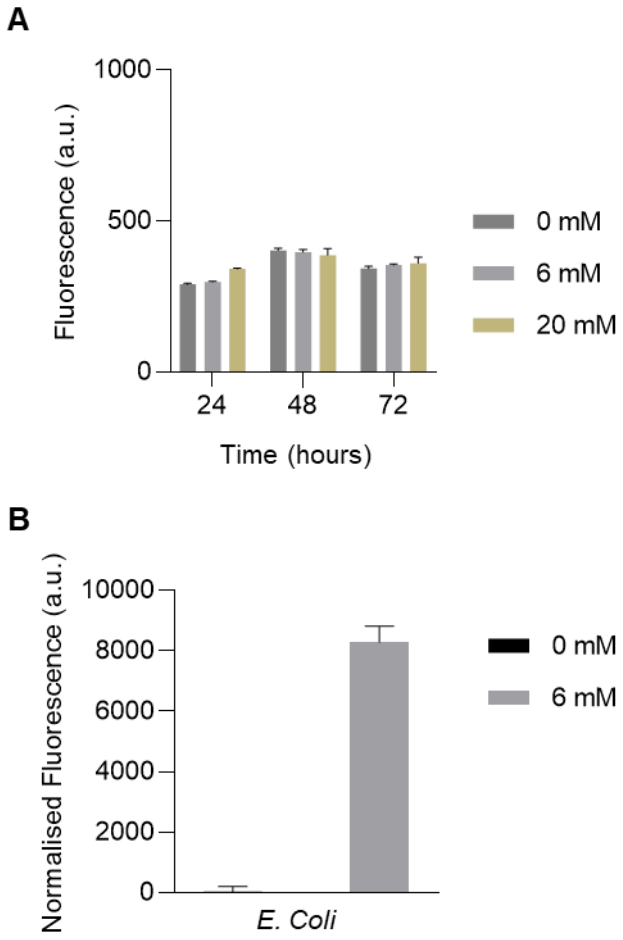

Figure 6-9: Dose-dependent expression of the P_{BADWT} promoter from *E. coli* cannot be replicated in *Synechocystis*

(A) Expression levels in *Synechocystis* of eYFP at three time points (24, 48 and 72 hours) with different concentrations of L-arabinose. Error bars represent ± SE of four biological replicates, where each replicate represents the median measurement of at least 10,000 cells measured by flow cytometry. (B) Expression levels of eYFP in *E. Coli* after induction with L-arabinose after ~7 hours growth. Fluorescence was measured in a plate reader and normalised to OD_{600}. Error bars represent ± SE of three biological replicates.

6.3.3.1.3 Vanillate-inducible promoter from Corynebacter glutamicum

The vanillate-inducible promoter from *Corynebacter glutamicum* is comprised of P_{van} and its cognate repressor VanR. This system has been optimised for use in *E. coli* to form P_{vanCC}/VanR (Meyer et al., 2019) and has recently been characterised in *Synechocystis*, where expression was reported to be dose-dependent but transient (Behle et al., 2020). To attempt to reproduce and confirm the previous vanillate dose-dependent response, the same sequences for the promoter and 5' UTR of P_{vanCC} and *vanR* was used. This includes the RiboJ and RSB* in the 5' UTR upstream of *eYFP*, and P_{J23100} with the designer RBS_{Van3} driving expression of VanR (**Table 6-2**) (Behle et al., 2020). To test the response to vanillate, cultures were induced with varying concentration (0 – 2000 µM) at the start of the experiment and fluorescence and OD_{750} were measured every 24 hours for 72 hours. All strains grew similarly irrespective of the presence of inducer (**Appendix Figure 8-8**). Without induction, no expression was observed, indicating that P_{vanCC} is tightly repressed by VanR in the absence of vanillate in *Synechocystis*. Maximum fluorescence expression of 948 ± 14 a.u. was observed at 24 hours after induction with 2000 µM vanillate, after 48 hours there was a marked reduction in expression for all cultures, with all expression returning to background levels by 72 hours (**Figure 6-10A**). These results follow a similar pattern to those reported in *Synechocystis* for the lower induction concentrations (100 – 500 µM), where a reduction in expression was reported between 24 and 48 hours after induction. However, this differs from the higher inducer concentrations (1000 – 2000 µM), where expression was reported to be maintained between 24 and 48 hours and declining at 72 hours (Behle et al., 2020). Their study also reported a 16-fold induction at 48 hours after the addition of 2000 µM vanillate, whereas I observed a 41-fold induction at 24 hours after the addition of 2000 µM vanillate. After induction, Behle et al. reported that all fluorescence reduced to background levels after a maximum of 90 hours, indicating that at best, P_{vanCC} expression is transient, and output is not maintained over time. The results here differ slightly in that expression peaked by 24 hours as opposed to 48 hours, with subsequent reduction to background levels ~24 hours earlier than

reported. There are some differences in experimental design, here cultures were grown at 100 µmol $m^{-2}s^{-1}$ of continuous light rather than 80 µmol $m^{-2}s^{-1}$ and our expression vector backbone contained a kanamycin resistance cassette rather than spectinomycin. Nonetheless, both characterisations demonstrated that the P_{vanCC}/VanR system did not maintain expression after induction at two different growth conditions in *Synechocystis*. I chose not to pursue further work with this promoter, as the transient nature of expression is less useful for synthetic gene circuit design.

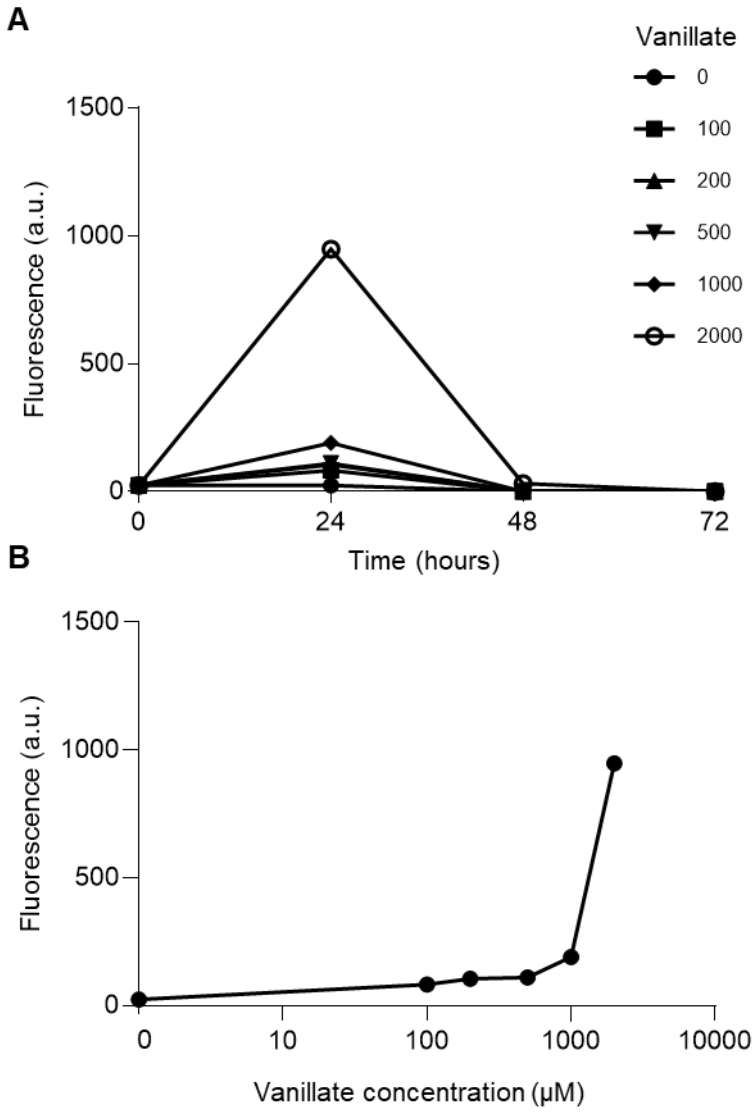

Figure 6-10: Expression from the vanillate-inducible promoter P_{vanCC} is not sustained in *Synechocystis*.

(A) Expression levels in *Synechocystis* of eYFP at three time points (24, 48, and 72hours) with different concentrations of vanillate (B) Vanillate dose-response at 24 hours (x-axis is shown as $\log_{10}$ scale). Error bars represent ± SE of four biological replicates, where each replicate represents the median measurement of at least 10,000 cells measured by flow cytometry.

6.3.3.1.4 The promoter λP_R from bacteriophage lambda

Lastly, the CI repressible promoter λP_R, from bacteriophage lambda was characterised. This promoter plays an important part in the life-cycle of the bacteriophage, with repression of λP_R establishing and maintaining latency. This is a repressible system only, with no small molecule inducer. Like P_{BADWT} above, the reports regarding the function of λP_R in *Synechocystis* are

conflicting with one study reporting no measurable unrepressed output (Huang et al., 2010), and another more recent study reporting robust expression 20-fold higher than the native P_{rnpB} without co-expression of CI, and 99% reduction with co-expression of CI (Ferreira et al., 2018). To test this promoter, λP_R was assembled with *eYFP*, with and without a *cI* expression cassette driven by P_{J23101} (**Figure 6-1A, Table 6-2**). Co-expression of CI did not affect growth, with all strains growing similarly (**Appendix Figure 8-9**). Fluorescence expression was robust, with levels similar to that of P_{J23111} (**Figure 6-11**, **Section 3.4.4.2**), and the relative values are similar with a ~22x higher expression from λP_R compared to P_{rrnB} at 48 hours (**Section 3.4.4.1**) (Ferreira et al., 2018). When compared to the strain co-expressing CI, fluorescence was repressed to below detectable levels. These results gave confidence that the λP_R promoter was functional, and that repression is tight and stable when CI is co-expressed in *Synechocystis*, making this a potentially useful promoter/repressor pair for future synthetic circuit design.

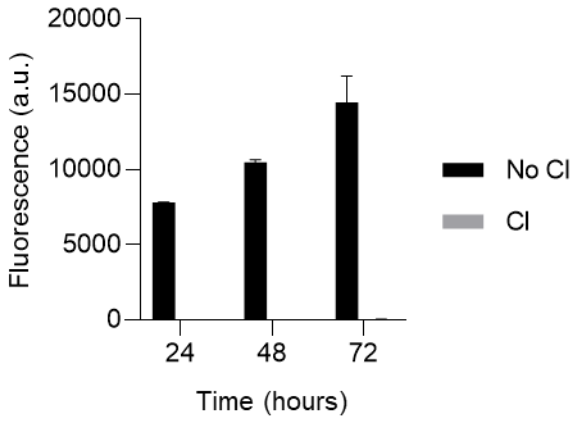

Figure 6-11: Promoter λP_R of viral origin demonstrates robust expression and tight and stable repression in the presence of the CI repressor in *Synechocystis*.

(A) Expression levels of eYFP at three time points (24, 48 and 72 hours) with and without co-expression of CI in *Synechocystis*. Error bars represent ± SE of four biological replicates, where each replicate represents the median measurement of at least 10,000 cells measured by flow cytometry.

6.3.4 Introducing an L-rhamnose powered genetic inverter to *Synechocystis* sp. PCC 6803

6.3.4.1 Generating and testing a genetic inverter circuit

A genetic inverter, or NOT gate, is a circuit that is comprised of one input and one output. The circuit inverts the input signal so that when the input is 'ON', the output is 'OFF', and vice versa (**Figure 6-12A**). Following on from the TF-regulated inducible promoter systems I screened in sections 6.3.2 and 6.3.3, I constructed a NOT gate with the input module based on the L-rhamnose inducible promoter system (*rhaS*-P_{rhaBAD}) and the output module based on the P_{phlF}/$PhlF^{AM}$ promoter/repressor pair. *rhaS*-P_{rhaBAD} was chosen as it demonstrated reliable induction coupled with sustained output over time and with very low measured leakiness (**Figure 6-8)**. The P_{phlF}/$PhlF^{AM}$ promoter/repressor pair was chosen because repression was robust with co-expression of $PhlF^{AM}$ leading to undetectable fluorescence levels (**Figure 6-4**). This robust repression in *Synechocystis* coupled with its use as a NOT gate output in *E. coli* (Stanton et al., 2014) made P_{phlF}/$PhlF^{AM}$ a promising candidate pair for the design and construction of a NOT gate in *Synechocystis*. For ease of detection, eYFP was chosen as the output signal for all NOT gate variants tested. Values are reported at 72 hours unless otherwise stated. This was to allo**w** P_{rhaBAD} to reach sufficient level of expression after induction **(Figure 6-8**).

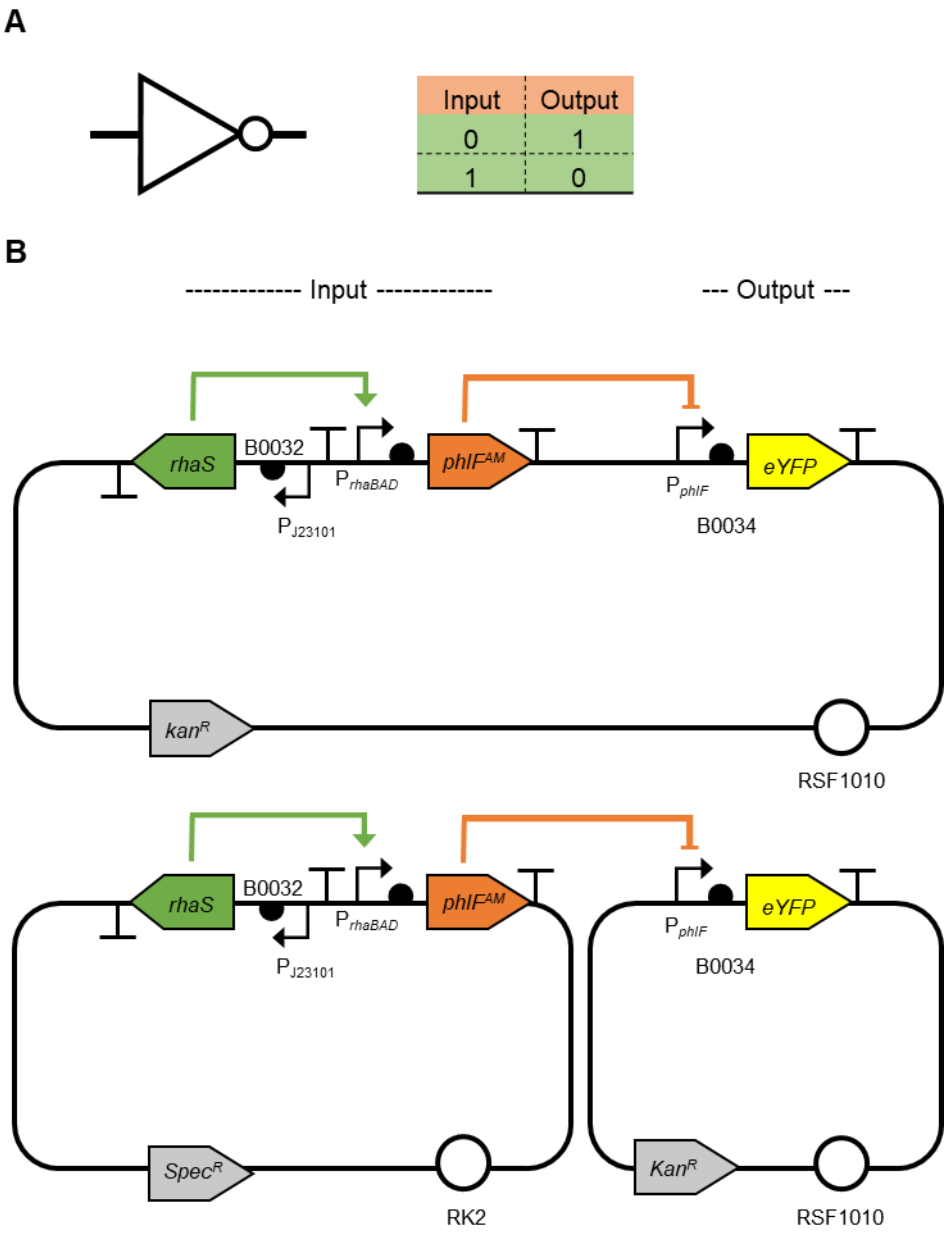

Figure 6-12: Schematic of the L-rhamnose powered NOT gate.

(A) The logical symbol for a NOT gate is shown, with the corresponding truth table. (B) Schematic of one and two vector NOT gates. The input comprises *rhaS*-P_{rhaBAD} driving expression of $PhlF^{AM}$. The output comprises P_{phlF} driving expression of the reporter eYFP. On induction with L-rhamnose, expressed $PhlF^{AM}$ will repress the P_{phlF} promoter, and stop eYFP expression. Without L-rhamnose induction, P_{phlF} will remain unrepressed and eYFP expression will occur. For the single vector NOT gate, both the input and output are encoded onto a single vector harbouring the RSF1010 origin of replication (ori). The two vector NOT gate splits the input and output modules, the former being encoded onto a vector harbouring RK2 ori, and the latter is encoded onto the RSF1010 based vector.

The input for the first NOT gate was constructed so that *phlF^{AM}* was assembled downstream of *rhaS*-P*$_{rhaBAD}$* fused with BBa_B0032 to form *rhaS*-P*$_{rhaBAD}$*-*phlF*. *eYFP* was assembled with P*$_{phlF}$* fused with BBa_B0034 to generate the output P*$_{phlF}$*-*eYFP* and both input and output modules were assembled into a single pPMQAK1-T vector to form NOT_Single (**Table 6-3**, **Figure 6-12B**) (**Materials and Methods**). The P*$_{phlF}$*(No_TF) strain was used as a control to represent the theoretical maximum NOT gate expression i.e. unrepressed P*$_{phlF}$*-*eYFP* without the presence of PhlF^{AM} (**Figure 6-4**).

Table 6-3: List of NOT Gate Input Modules Tested

List of NOT gate input module variants based on *rhas*-P*$_{rhaBAD}$*. DT1 and DT2 represent '*Synechocystis* 6803' and '*Synechocystis* 6803***' with amino acid sequences 'AANNIVSFKRVAIAA' and 'AANNIVSFKRVAGGG' respectively (Landry et al., 2013). * Designer RBS created by Alejandra A Schiavon.

Name	Promoter	RBS	Transcription Factor	Origin of Replication
NOT_Single	*rhaS*-P*$_{rhaBAD}$*	BBa_B0032	*phlF^{AM}*	RSF1010
NOT_Dual				RK2
NOT_DT1			*phlF$_{AM}$-DT1*	RSF1010
NOT_DT2			*phlF^{AM}-DT2*	
NOT_RBS0		RBS0*	*phlF^{AM}*	
NOT_RBS18		RBS18*		
NOT_RBS31		BBa_B0031		
NOT_RBS33		BBa_0033		
NOT_RBS35		BBa_B0035		

NOT_Single was induced with 1mM L-rhamnose and demonstrated the desired response with no detectable eYFP expression. Although the uninduced strain showed fluorescence levels that were reduced by ~90% when compared to the control (**Figure 6-13A**). This indicated that leakiness from the input module was expressing sufficient PhlF^{AM} in the absence of the inducer to significantly reduce the output. I then plotted the response function of NOT_Single with a range of L-rhamnose induction concentrations. At 24 hours, fluorescence expression compared to no L-rhamnose and increasing rhamnose concentrations was flat, with a constant expression of ~200 a.u. for

all inducer concentrations. Thus, no NOT gate function was observed at 24 hours (**Figure 6-13B**). This is likely because *rhaS*-P_{rhaBAD} had not started expressing sufficient $PhlF^{AM}$ to completely repress expression from the output. At 48 and 72 hours, NOT gate function was demonstrated, with the maximum expression observed without induction, then falling with increasing inducer concentration and reaching undetectable levels at 0.04 and 0.06 mM L-rhamnose respectively (**Figure 6-13B**). Although NOT gate function was observed, due to the poor uninduced output from NOT_Single, further optimisations were attempted to increase expression levels for the uninduced output.

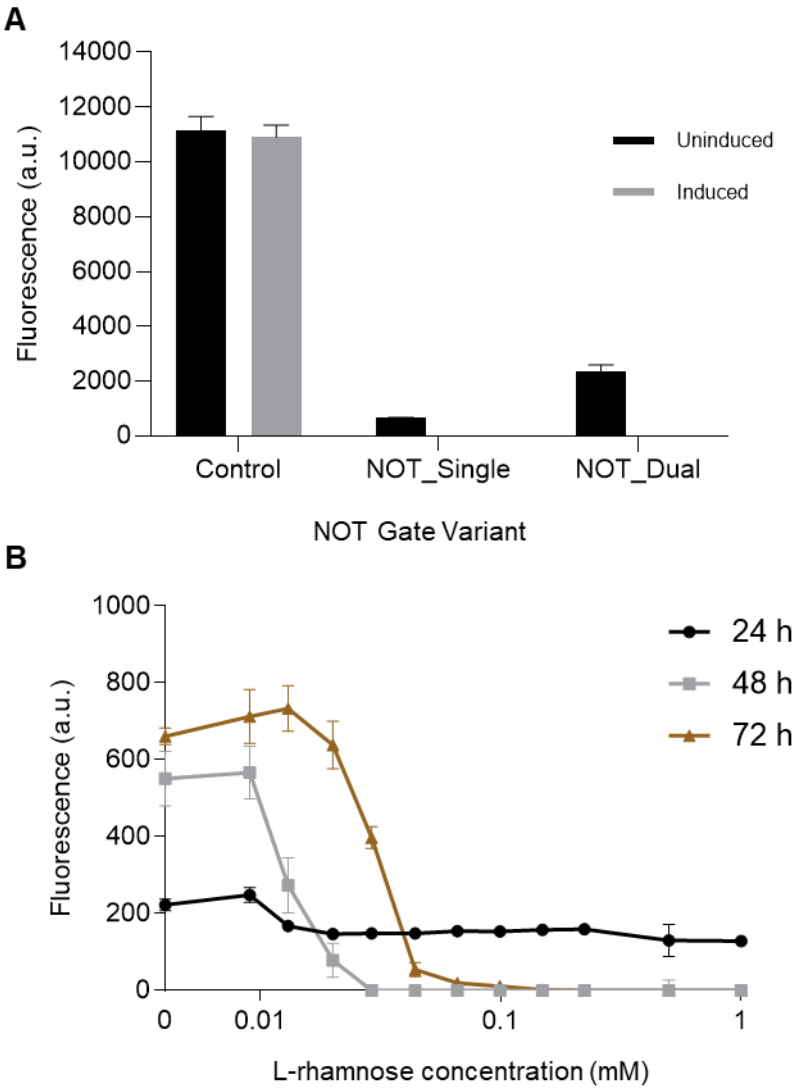

Figure 6-13: P_{rhaBAD} leakiness causes reduced output of NOT gates in *Synechocystis*
(A) Expression levels of eYFP at 72 hours after induction with 1 mM L-rhamnose of NOT gate variants compared to P_{phlF}(No_TF) control in *Synechocystis*. (B) Response function measured by eYFP fluorescence of NOT_Single at 24, 48 and 72 hours after induction of L-rhamnose 0-1 mM. Error bars represent ± SE of four biological replicates, where each replicate represents the median measurement of at least 10,000 cells measured by flow cytometry.

Two strategies for optimisation were pursued: the first was to lower the number of transcripts produced by *rhaS*-P_{rhaBAD} from the input in the uninduced state. The second targeted translation, either by adding a degradation tag (DT) to increase protein turnover and reduce accumulation, or changing the RBS associated with $PhlF^{AM}$ to tune protein expression down by attenuating the translation initiation rate (TIR). In cyanobacterial research, the most common means of tuning gene expression at the transcriptional level has been the use of different strength constitutive promoters. One common strategy for tuning gene expression at the transcriptional level used in *E. coli* relies on encoding modules of a gene circuit onto different plasmids with varying copy number. This allows the tuning of gene expression so a module that requires increased expression would be encoded in a higher copy number plasmid, and a module where decreased expression is desired, a lower copy number plasmid would be considered (Bradley et al., 2016). Up until recently, RSF1010 was the only heterologous origin of replication shown to self-replicate in cyanobacteria, that all non-native vectors were based (e.g. pPMQAK1-T) (Mermet-Bouvier et al., 1993; Vasudevan et al., 2019). In ***section 3.4.5***, I characterised the origin of replication RK2, which self-replicates in *Synechocystis* and has a lower copy number compared to RSF1010 of 9 ± 2 and 31 ± 5 per cell, respectively.

Here, the input and output modules were split so that the input was encoded on pSEVA421-T (harbouring RK2 ori), and the output was encoded onto pPMQAK1-T, to make NOT_Dual (**Table 6-3**, **Figure 6-12B**). On induction of NOT_Dual with 1mM L-rhamnose, there was no detectable eYFP expression and NOT gate behaviour was observed (**Figure 6-13A**). In contrast to NOT_Single, the uninduced strain showed an output that was reduced by ~80% when compared to the control. Thus the uninduced expression of NOT_Dual had shown a 100% improvement when compared to the NOT_Single. Nevertheless, the uninduced output was still significantly reduced compared to the control strain (**Figure 6-13A**).

6.3.4.2 NOT gate optimisation via protein expression modulation

Next, two new input modules were generated by fusing the coding sequences of two different DTs downstream of *phlF*^{AM} (**Table 6-3**). For NOT_DT1 and NOT_DT2, uninduced output was recovered to 100% and 90% compared to the control, whereas for the induced strains, fluorescence expression was reduced only by 28% and 35%, respectively (**Figure 6-14A**). This indicated that either PhlF^{AM} was being degraded too quickly leading to insufficient levels to repress P_{phlF} in the output, or that the addition of the DT fusion had effected the protein so that it no longer bound as efficiently to the P_{phlF} operator sites (**Figure 6-14A**). To test this, alternative DTs with lower activity could be tested. However, this was not pursued due to time constraints.

Lastly, five different variants of the input module were tested in the single vector configuration, varying the RBS associated with *phlF*^{AM} (**Table 6-3, Materials and Methods**). Previous work in the McCormick lab has demonstrated that these RBS variants produced reduced fluorescence levels that ranged from 8 to 48% compared to BBa_B0032 (Schiavon Osorio, unpublished). All NOT gates RBS variants were induced with 1 mM L-rhamnose. Remarkably, on induction, the fluorescence levels for NOT_RBS0 and NOT_RBS31 were reduced to below background levels and the uninduced expression was ~90% and 100%, respectively when compared to the control (**Figure 6-14B**). Thus, both NOT_RBS0 and NOT_RBS31 demonstrated robust NOT gate function, with NOT_RBS31 demonstrating 'perfect function', with no observed deficit in uninduced output. These results indicated that the leakiness of expression of PhlF^{AM} was at a sufficiently low level so as to not impair uninduced expression for OT_RBS31. The uninduced output of NOT_RBS0, was also considerably improved compared to NOT_Single and NOT Dual, with only ~10% reduction in fluorescence expression when compared to the control, indicating that PhlF^{AM} expression in the uninduced state had also been substantially reduced (**Figure 6-13A, Figure 6-14B**). NOT_RBS18 did demonstrate similar expression to the control in the uninduced state, but on induction, fluorescence expression was only reduced by ~15% suggesting that the levels of PhlF^{AM} were too low for

sufficient repression of the output to occur. Fluorescence levels of NOT_RBS33 were reduced by ~15% when compared to the control, but in both the induced and uninduced states, whereas NOT_RBS35 showed almost no expression in both the induced and uninduced states (**Figure 6-14B**). It is unclear why NOT_RBS33 demonstrated this behaviour. The behaviour of NOT_RBS35 suggests that fusing BBa_B0035 with $PhlF^{AM}$, leads to high expression of the transcriptional repressor and the output is repressed even without the presence of the inducer.

The NOT gate variants presented here based on the L-rhamnose inducible expression system and promoter/repressor pair P_{phlF}/$PhlF^{AM}$ have several advantages over other NOT gates reported in cyanobacteria. The existing NOT gates have outputs based on P_{van} and P_{trc2O} and inputs that are designed with a constitutive promoter driving the cognate TF (VanR and LacI, respectively), where TF expression is controlled by the inclusion of a theophylline-responsive riboswitch (Taton et al., 2017). The use of a theophylline-responsive riboswitch to control expression of the transacting TF allows only limited potential for expression modulation. If differential expression of the TF was required, new variants would need to be assembled. Whereas, expressing the TF-repressor with an inducible system such as *rhaS*-P_{rhaBAD}, allows for a large dynamic range with no additional cloning requirements (**See Figure 6-8;Figure 6-13B**). P_{van} is not an ideal promoter for construction of the output modules as P_{Van} has a low output when compared to P_{phlF} (**see Figure 6-4; Figure 6-10**). P_{trc2O} is also not ideal as despite robust expression in the absence of LacI, fluorescence was still detected with co-expression of the TF-repressor (Camsund et al., 2014). The leakiness of P_{trc2O}, even with co-expression of LacI, is likely the cause of detection of low levels of fluorescence, even when the NOT gate was supplemented with theophylline (Taton et al., 2017).

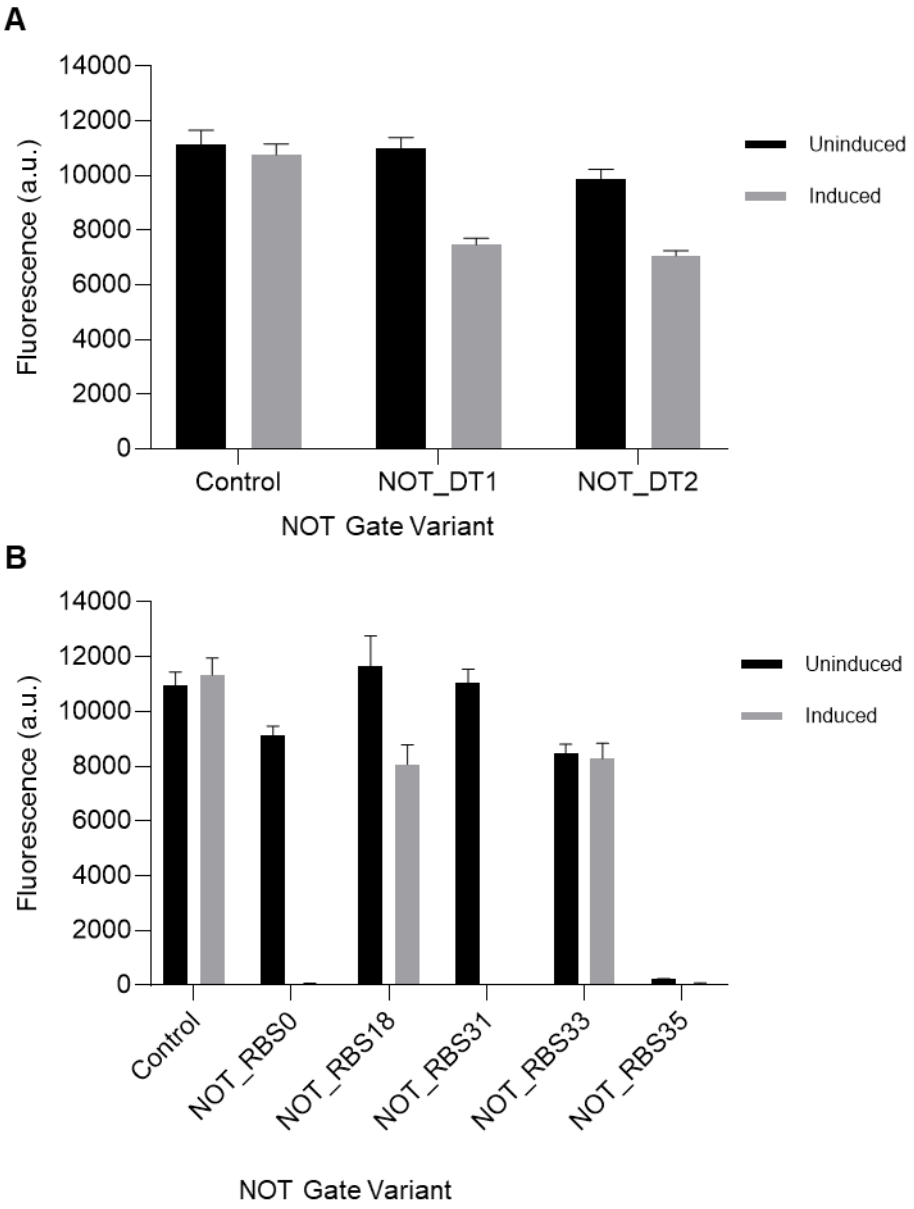

Figure 6-14: Modulation of transcription factor protein expression can rescue NOT gate function.

(A) Expression levels of eYFP at 72 hours after induction with 1 mM L-rhamnose of degradation tag NOT gate variants (**Table 6-3**) compared to P_{phlF}(No_TF) control (**see Figure 6-4**) in *Synechocystis* . (B) Expression levels of eYFP at 72 hours after induction with 1 mM L-rhamnose of the RBS NOT gate variants (**Table 6-3**) compared to P_{phlF}(No_TF) in *Synechocystis*. Error bars represent ± SE of four biological replicates, where each replicate represents the median measurement of at least 10,000 cells measured by flow cytometry.

6.4 Conclusion

The lack of reliable inducible expression systems is a substantial bottleneck in cyanobacterial synthetic biology and synthetic gene circuit research. In this chapter, four heterologous TF-regulated expression systems new to cyanobacteria and four existing systems from the literature have been evaluated in *Synechocystis*. The new promoter/repressor pair P_{phlF}PhlF^{AM} was identified that demonstrated robust expression, with corresponding tight repression when the TF-repressor was co-expressed.

The P_{phlF}/PhlF^{AM} expression system in *E. coli* is induced by the presence of DAPG (Meyer et al., 2019). However, despite induction with DAPG up to 10-times that used in *E. coli*, and modulation of intracellular PhlF^{AM} concentration, it was not possible to demonstrate fluorescence on induction with DAPG when PhlF^{AM} was co-expressed.

A series of genetic inverter NOT gates were constructed based on the reliable L-rhamnose inducible promoter *rhaS*-P_{rhaBAD}. Variants of the NOT gate input were constructed where *rhaS*-P_{rhaBAD} was used to express PhlF^{AM}. The output consisted of P_{phlF} driving expression of eYFP. Several methods were used to optimise NOT gate function including both transcriptional and translational modulation of PhlF^{AM} expression. I demonstrated that choice of RBS appears to have a large impact on NOT gate function and should be further explored. Additional RBS variants could lead to a suite of NOT gates with varying outputs, thus useful for differential expression of a target gene. The NOT gate described in this chapter, improved on those available from the literature, with higher maximum uninduced output, more tightly repressed induced output, and more flexibility for modulation of expression.

Chapter 7 Concluding Remarks

Cyanobacteria show great potential as a chassis for the production of high-value chemicals and the green biotechnology revolution. However, despite recent advances and the increase in molecular tool availability, this great potential is still to be fully realised. Several hurdles existed that needed to be overcome including the relative lack of 'off the shelf' molecular tools for modulation of gene expression compared to model heterotrophic chassis e.g. *Escherichia coli* and *Saccharomyces cerevisiae*. This is exacerbated by the fact that molecular tools do not behave in a predictable way when ported to cyanobacteria, and each part must first be characterised and evaluated in the cyanobacterial species in question. Core to synthetic biology is the paradigm of *design-build-test*; each of these steps has led to bottlenecks in cyanobacterial research. In this thesis, I have expanded the synthetic biology toolkit and optimised protocols for high-throughput testing in cyanobacteria.

Firstly, we designed and constructed CyanoGate, a large suite of well characterised molecular parts for the engineering of cyanobacteria. CyanoGate was designed to harness the power of the Golden Gate cloning syntax. Golden Gate methodology enables part sharing and reusability, ease of assembly and automation compatibility, helping to alleviate the bottlenecks associated with the build cycle. During our work building and testing CyanoGate, we had to design and optimise strategies for the high-throughput testing of many cyanobacterial strains in parallel, which we have shared with the community.

Secondly, building on CyanoGate, I adapted and improved an existing strategy for testing the efficiency of intrinsic transcription terminators and applied this to cyanobacteria. Transcription terminators are important control elements in the regulation of gene expression, with studies limited to the model specie *Synechocystis* sp. PCC 6803 only. Using high-throughput Golden Gate cloning and experimental testing strategies, we tested a set of heterologous and synthetic transcription terminators across three different species, which comprised the model heterotroph *E. coli*, and the two model cyanobacteria

Synechocystis and *Synechococcus elongatus* UTEX 2973. We discovered that transcription terminators do not only behave differently between heterotrophic *E. coli* and photosynthetic cyanobacteria, but the behaviour also differs between the two cyanobacterial strains.

Lastly, I investigated several heterologous transcription factor regulated expression systems new to cyanobacteria. If synthetic gene circuit research is to prosper in cyanobacteria, the identification and characterisation of novel conditional gene expression systems is essential. I identified the new repressor PhlF^{AM}, that tightly bound its cognate promoter sequence (P_{phlF}) so that expression was efficiently repressed when PhlF^{AM} was co-expressed. Combining P_{phlF}/PhlF^{AM} with the efficient L-rhamnose inducible expression system in *Synechocystis*, allowed me to construct a series of functional genetic inverter NOT gate variants, that can be used in basic and synthetic biology research.

Chapter 8 Appendices

8.1 Appendix I For Chapter 3

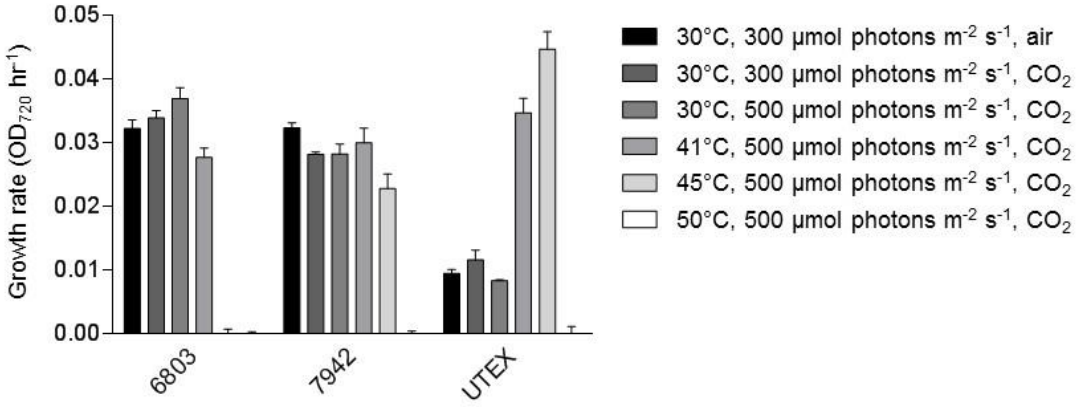

Appendix Figure 8-1: Comparison of growth for *Synechocystis*, PCC 7942 and UTEX 2973 under different culturing conditions.

Values are the means ± SE from at least five biological replicates from two independent experiments.

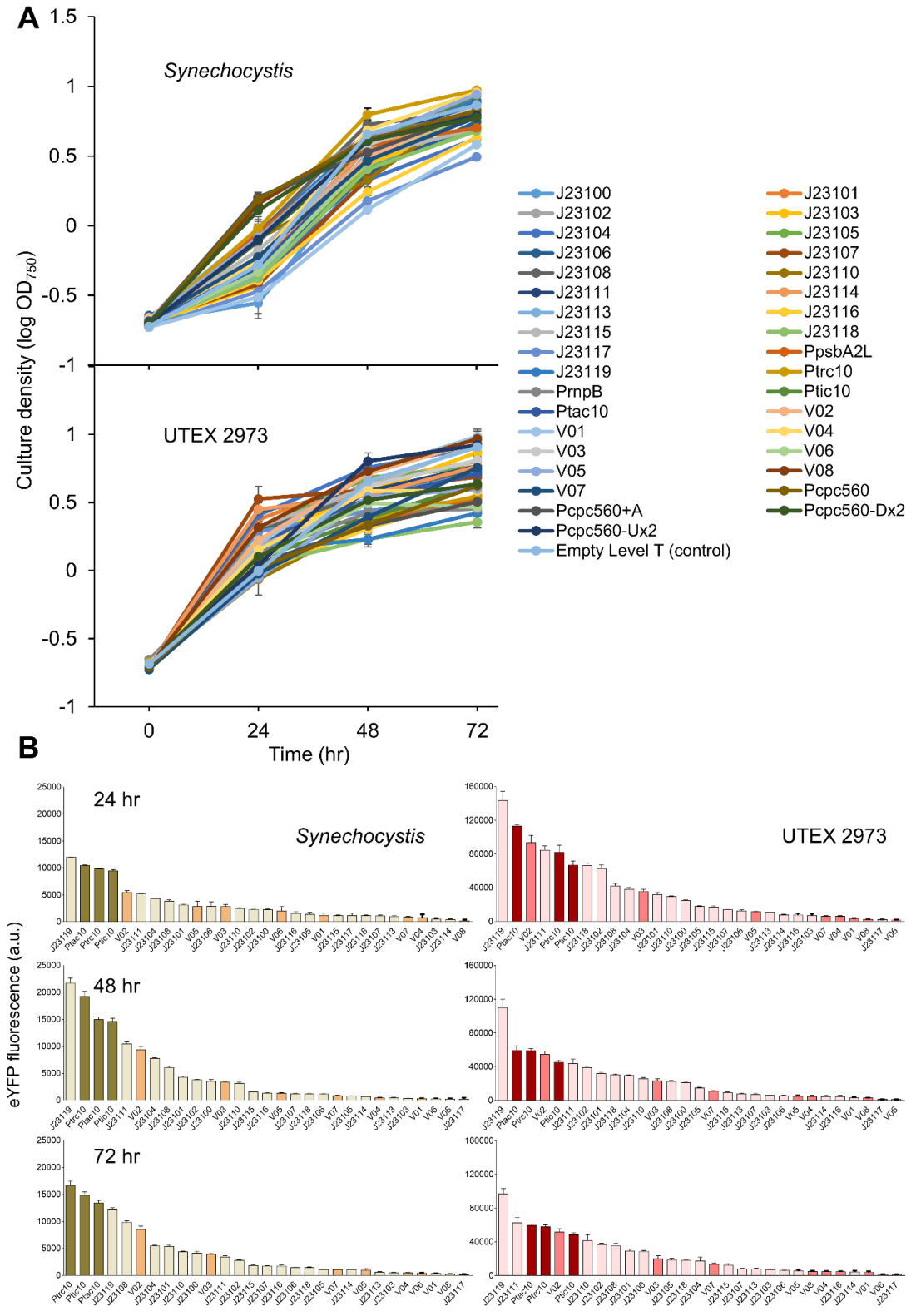

Appendix Figure 8-2: Growth and expression levels of heterologous and synthetic promoters in *Synechocystis* and UTEX 2973.

(A) *Synechocystis* and UTEX 2973 were cultured for 72 hr at 30°C with continuous light (100 µmol photons m^{-2} s^{-1}) and 40°C with 300 µmol photons m^{-2} s^{-1}, respectively

(see **Figure 3-6**). (B) Expression levels of eYFP are shown at three time points (24, 48 and 72 hr after inoculation). Values are the means ± SE from at least four biological replicates where each replicate represents the median measurements of 10,000 cells.

Appendix Table 8-1: Table of all parts from CyanoGate kit generated in this work.

Domestication refers to the removal of *BsaI* and/or *BsiI* sites (modifications are indicated in sequence maps provided in **Supplemental Information S4**).

No.	Vector ID	Part name	Level	5' overhang	3' overhang	Backbone	Domesticated	Selection	Notes	References
Acceptors										
Level T										
1	pCAT.000	pPMQAK1-T	T	TGCC	GGGA	pPMQAK1	yes	Amp^R, Kan^R	Modified BioBrick vector, RSF1010-derived ori.	Huang et al., 2010
2	pCAT.011	pSEVA421-T	T	TGCC	GGGA	pSEVA421	yes	$Spec^R$	Modified SEVA vector, RK2 ori vector.	Silva-Rocha et al., 2013
3	pCAT.015	pUC19A-T	T	TGCC	GGGA	pUC19	yes	Amp^R	Modified pUC19 vector.	Yanisch-Perron et al., 1985
4	pCAT.334	pUC19S-T	T	TGCC	GGGA	pUC19	yes	$Spec^R$	Modified pUC19 vector.	Yanisch-Perron et al., 1985
Level 0										
1	pCA0.001	Prom TSS acceptor	0	GGAG	TAGC	pICH41331	yes	$Spec^R$	Acceptor for promoters truncated to transcription start site.	*This study*
2	pCA0.002	pSB4K5 prom acceptor	0	GGAG	AATG	pSB4K5	yes	Kan^R	Acceptor for promoters, low copy number,pSC101 ori.	Shetty et al., 2008
Linkers										
1	pC0.116	Unmark LINKER	0	AATG	GCTT	pICH41308	no	$Spec^R$	See Fig. 1.	*This study*
2	pC0.117	UP FLANK LINKER	0	AATG	CGCT	pICH41331	no	$Spec^R$		
3	pC0.118	DOWN FLANK LINKER	0	GGAG	GCTT	pICH41331	no	$Spec^R$		
4	pC0.119	sacB UP LINKER	0	GGAG	AATG	pICH1295	no	$Spec^R$		
5	pC0.120	AbR DOWN LINKER	0	GCTT	CGCT	pICH1276	no	$Spec^R$		
6	pC0.121	AbR UP LINKER	0	GGAG	AGGT	pICH41331	no	$Spec^R$		
Parts										
1	pC0.008	eYFP	0	AATG	GCTT	pICH41308	yes	$Spec^R$	eYFP fluorescent marker (CDS).	Huang et al., 2010
2	pC0.009	eYFP+deg-tag	0	AATG	GCTT	pICH41308	yes	$Spec^R$	eYFP with a C-terminal protein degradation tag (CDS).	Huang et al., 2010; Landry et al., 2013

3	pC0.161	eYFP C-term tag	0	TTCG	GCTT	pAGM1301	yes	$Spec^R$	eYFP (-C terminal tag).	Huang et al., 2010
4	pC0.017	dCas9	0	AATG	GCTT	pICH41308	yes	$Spec^R$	Catalytically deactivated Cas9 (dCas9) (CDS). (www.addgene.org/44249)	Qi et al., 2013
5	pC0.018	dCas9+deg-tag	0	AATG	GCTT	pICH41308	yes	$Spec^R$	dCas9 with a C-terminal protein degradation tag (CDS).	Landry et al., 2013
6	pC0.026	sacB	0	AATG	AGGT	pICH41258	yes	$Spec^R$	Levansucrase expression cassette (CDS).	Lea-Smith et al., 2016
7	pC0.027	Ab^RKan	0	AGGT	GCTT	pICH41264	no	$Spec^R$	Antibiotic resistance (Ab^R) cassette for Kanamycin.	Lea-Smith et al., 2016
8	pC0.028	Ab^RSpec	0	AGGT	GCTT	pICH41264	no	$Spec^R$	Ab^R cassette for Spectinomycin.	Kulkarni and Golden 1997
9	pC0.029	Ab^REry	0	AGGT	GCTT	pICH41264	no	$Spec^R$	Ab^R cassette for Erythromycin.	Cai and Wolk, 1990
10	pC0.286	Ab^RChl	0	AGGT	GCTT	pICH41264	no	$Spec^R$	Ab^R cassette for Chloramphenicol	Dzelzkalns et al., 1984
11	pC0.265	lacI	0	AATG	GCTT	pICH41308	yes	$Spec^R$	LacI, for repression at lacO domains (CDS).	Polard and Chandler, 1995
12	pC0.122	sgRNA scaffold	0	GTTT	CGCT	pICH41331	no	$Spec^R$	sgRNA scaffold derived from *Streptococcus pyogenes* (see Fig. 1).	Qi et al., 2013; Yao et al., 2015
13	pC0.123	srRNA HFQ handle	0	GTTT	CGCT	pICH41331	no	$Spec^R$	HFQ handle based on sRNA MicC from *E. coli* (see Fig. 1).	Na et al., 2013
Insertion sites										
1	pC0.024	6803 cpcBAC1&C2 Up Flank	0	GGAG	AATG	pICH41295	no	$Spec^R$	Synechocystis sp. PCC 6803, sequence upstream of cpcBA operon.	Lea-Smith et al., 2014
2	pC0.025	6803 cpcBAC1&C2 Down Flank	0	GCTT	CGCT	pICH41276	no	$Spec^R$	Synechocystis sp. PCC 6803, sequence downstream of cpcBA operon.	Lea-Smith et al., 2014
3	pC0.165	6803 NS1 Up Flank	0	GGAG	AATG	pICH41295	no	$Spec^R$	Synechocystis sp. PCC 6803, sequence upstream of slr0573. N8 in Pinto et al., 2015.	Pinto et al., 2015
4	pC0.166	6803 NS1 Down Flank	0	GCTT	CGCT	pICH41276	no	$Spec^R$	Synechocystis sp. PCC 6803, sequence downstream of slr0573. N8 in Pinto et al., 2015.	Pinto et al., 2015
5	pC0.167	6803 NS2 Up Flank	0	GGAG	AATG	pICH41295	no	$Spec^R$	Synechocystis sp. PCC 6803, sequence upstream of slr1396. N10 in Pinto et al., 2015.	Pinto et al., 2015
6	pC0.168	6803 NS2 Down Flank	0	GCTT	CGCT	pICH41276	yes	$Spec^R$	Synechocystis sp. PCC 6803, sequence downstream of slr1396. N10 in Pinto et al., 2015.	Pinto et al., 2015
7	pC0.169	6803 NS3 Up Flank	0	GGAG	AATG	pICH41295	yes	$Spec^R$	Synechocystis sp. PCC 6803, sequence upstream of slr0271. N15 in Pinto et al., 2015.	Pinto et al., 2015
8	pC0.170	6803 NS3 Down Flank	0	GCTT	CGCT	pICH41276	no	$Spec^R$	Synechocystis sp. PCC 6803, sequence downstream of slr0271. N15 in Pinto et al., 2015.	Pinto et al., 2015
9	pC0.171	6803 NS4 Up Flank	0	GGAG	AATG	pICH41295	no	$Spec^R$	Synechocystis sp. PCC 6803, sequence upstream of slr0397. N16 in Pinto et al., 2015.	Pinto et al., 2015
10	pC0.172	6803 NS4 Down Flank	0	GCTT	CGCT	pICH41276	no	$Spec^R$	Synechocystis sp. PCC 6803, sequence downstream of slr0397. N16 in Pinto et al., 2015.	Pinto et al., 2015
11	pC0.173	7942 NS1 Up Flank	0	GGAG	AATG	pICH41295	no	$Spec^R$	Synechoccoccus elongatus PCC 7942, sequence upstream of Synpcc7942_2498.	Bustos and Golden, 1992; Kulkarni and Golden, 1997

12	pC0.174	7942 NS1 Down Flank	0	GCTT	CGCT	pICH41276	yes	SpecR	Synechoccoccus elongatus PCC 7942, sequence downstream of Synpcc7942_2498.	Bustos and Golden, 1992; Kulkarni and Golden, 1997
13	pC0.175	7942 NS2 Up Flank	0	GGAG	AATG	pICH41295	yes	SpecR	Synechoccoccus elongatus PCC 7942, sequence upstream of Synpcc7942_0085.	Andersson et al., 2000
14	pC0.176	7942 NS2 Down Flank	0	GCTT	CGCT	pICH41276	yes	SpecR	Synechoccoccus elongatus PCC 7942, sequence downstream of Synpcc7942_0085.	Andersson et al., 2000
15	pC0.177	7942 NS3 Up Flank	0	GGAG	AATG	pICH41295	no	SpecR	Synechoccoccus elongatus PCC 7942, sequence upstream of Synpcc7942_0739.	Niederholtmeyer et al., 2010
16	pC0.178	6803 NS4 Down Flank	0	GCTT	CGCT	pICH41276	no	SpecR	Synechocystis sp. PCC 6803, sequence downstream of slr0397. N16 in Pinto et al., 2015.	Niederholtmeyer et al., 2010
17	pC0.282	7002 NS1 Up Flank	0	GGAG	AATG	pICH41295	no	SpecR	Synechoccoccus sp. PCC 7002, upstream sequence for A0159.	Vogel et al., 2017
18	pC0.281	7002 NS1 Down Flank	0	GCTT	CGCT	pICH41276	no	SpecR	Synechoccoccus sp. PCC 7002, downstream sequence for A0159.	Vogel et al., 2017
19	pC0.284	7002 NS2 Up Flank	0	GGAG	AATG	pICH41295	no	SpecR	Synechoccoccus sp. PCC 7002, between SYNPCC7002_A0932 and SYNPCC7002_A0933.	Ruffing et al., 2016
20	pC0.283	7002 NS2 Down Flank	0	GCTT	CGCT	pICH41276	no	SpecR	Synechoccoccus sp. PCC 7002, between SYNPCC7002_A0932 and SYNPCC7002_A0933.	Ruffing et al., 2016
Promoters										
Native (*Synechocystis* sp. PCC 6803)										
1	pC0.057	P_{arsB}	0	GGAG	AATG	pSB4K5	yes	Kan^R	AsO_2^- inducible promoter from the *arsB* gene. RBS* added (22 bp) upstream of ATG.	Blasi et al., 2012; Englund et al., 2016
2	pC0.056	P_{coaT}	0	GGAG	AATG	pICH41295	no	$Spec^R$	Co_2^+ inducible promoter from the *coaT* gene. RBS* added (22 bp) upstream of ATG.	Guerrero et al., 2012; Englund et al., 2016
3	pC0.004	$P_{cpc560+A}$	0	GGAG	AATG	pICH41295	yes	$Spec^R$	cpc560 promoter with extended spacer region.	Zhou et al., 2014
4	pC0.005	P_{cpc560}	0	GGAG	AATG	pICH41295	yes	$Spec^R$	Strong, light responsive cpc560 (cpcBA) promoter.	Zhou et al., 2014
5	pC0.007	$P_{cpc560-Dx2}$	0	GGAG	AATG	pICH41295	yes	$Spec^R$	cpc560 promoter, extended spacer region, downstream TFB site region duplicated.	Zhou et al., 2014
6	pC0.006	$P_{cpc560-Ux2}$	0	GGAG	AATG	pICH41295	yes	$Spec^R$	cpc560 promoter, extended spacer region, upstream TFB site region duplicated.	Zhou et al., 2014
7	pC0.055	P_{isiAB}	0	GGAG	AATG	pSB4K5	yes	Kan^R	Fe_3^+ repressed promoter from the *isiAB* operon. RBS* added (22 bp) upstream of ATG.	Kunert et al., 2003
8	pC0.054	P_{petE}	0	GGAG	AATG	pICH41295	no	$Spec^R$	Cu_2^+ inducible promoter from the *PetE* gene. RBS* added (22 bp) upstream of ATG.	Guerrero et al., 2012; Englund et al., 2016
9	pC0.053	P_{nirA}	0	GGAG	AATG	pICH41295	no	$Spec^R$	NO_3^- inducible promoter from the *nir* operon. RBS* added by modifying the region upstream of ATG.	Qi et al., 2013; Englund et al., 2016
10	pC0.052	P_{nrsB}	0	GGAG	AATG	pICH41295	no	$Spec^R$	Ni_2^+ inducible promoter from the *nrsB* gene. RBS* added (22 bp) upstream of ATG.	Peca et al., 2007; 2008; Englund et al., 2016
11	pC0.051	P_{rnpB}	0	GGAG	AATG	pICH41295	no	$Spec^R$	RNase P subunit B promoter. RBS* added (22 bp) upstream of ATG.	Huang et al., 2010; Englund et al., 2016
12	pC0.050	P_{psbA2L}	0	GGAG	AATG	pICH41295	no	$Spec^R$	Light, Ni_2^+ and Co_2^+ inducible promoter for *psbA2* gene. RBS* added (22 bp) upstream of ATG.	Lindberg et al., 2010; Englund et al., 2016
Heterologous/synthetic										

1	pC0.049	BBa_J23119MH	0	GGAG	AATG	pSB4K5	no	Kan^R		
2	pC0.030	J23100MH	0	GGAG	AATG	pICH41295	no	$Spec^R$		
3	pC0.031	J23101MH	0	GGAG	AATG	pICH41295	no	$Spec^R$		
4	pC0.032	J23102MH	0	GGAG	AATG	pICH41295	no	$Spec^R$		
5	pC0.033	J23103MH	0	GGAG	AATG	pICH41295	no	$Spec^R$		
6	pC0.034	J23104MH	0	GGAG	AATG	pSB4K5	no	Kan^R		
7	pC0.035	J23105MH	0	GGAG	AATG	pICH41295	no	$Spec^R$		
8	pC0.036	J23106MH	0	GGAG	AATG	pICH41295	no	$Spec^R$		
9	pC0.037	J23107MH	0	GGAG	AATG	pICH41295	no	$Spec^R$		
10	pC0.038	J23108MH	0	GGAG	AATG	pICH41295	no	$Spec^R$	A subset of BioBrick promoters derived from promoter part BBa_J23119 (http://partsregistry.org/Part:BBa_J23119). Promoters contain a lacO repressor and the broad-range BBa_B0034 RBS.	Huang et al., 2010; Markley et al., 2015
11	pC0.039	J23109MH	0	GGAG	AATG	pICH41295	no	$Spec^R$		
12	pC0.040	J23110MH	0	GGAG	AATG	pICH41295	no	$Spec^R$		
13	pC0.041	J23111MH	0	GGAG	AATG	pSB4K5	no	Kan^R		
14	pC0.043	J23113MH	0	GGAG	AATG	pICH41295	no	$Spec^R$		
15	pC0.044	J23114MH	0	GGAG	AATG	pICH41295	no	$Spec^R$		
16	pC0.045	J23115MH	0	GGAG	AATG	pICH41295	no	$Spec^R$		
17	pC0.046	J23116MH	0	GGAG	AATG	pICH41295	no	$Spec^R$		
18	pC0.047	J23117MH	0	GGAG	AATG	pICH41295	no	$Spec^R$		
19	pC0.048	J23118MH	0	GGAG	AATG	pICH41295	no	$Spec^R$		
20	pC0.083	J23119MH_V01	0	GGAG	AATG	pICH41295	no	$Spec^R$		
21	pC0.084	J23119MH_V02	0	GGAG	AATG	pICH41295	no	$Spec^R$		
22	pC0.085	J23119MH_V03	0	GGAG	AATG	pICH41295	no	$Spec^R$	Modifications to CG_BBa_J23119MH made by Vasudevan.	*This study*
23	pC0.088	J23119MH_V04	0	GGAG	AATG	pICH41295	no	$Spec^R$		
24	pC0.089	J23119MH_V05	0	GGAG	AATG	pICH41295	no	$Spec^R$		

25	pC0.090	J23119MH_V06	0	GGAG	AATG	pICH41295	no	$Spec^R$		
26	pC0.091	J23119MH_V07	0	GGAG	AATG	pICH41295	no	$Spec^R$		
27	pC0.092	J23119MH_V08	0	GGAG	AATG	pICH41295	no	$Spec^R$		
28	pC0.093	P_{BAD}	0	GGAG	AATG	pICH41295	no	$Spec^R$	L-arabinose inducible promoter from the arabinose operon in *E. coli*.	Abe et al., 2014
29	pC0.285	P_{cat}	0	GGAG	AATG	pICH41295	no	$Spec^R$	Promoter for the chloramphenicol acetyl transferase (CAT) gene in *Salmonella enterica*.	Dzelzkalns et al., 1984
30	pC.264	P_{lacIQ}	0	GGAG	AATG	pICH41295	no	$Spec^R$	Promoter for LacI gene from *E. coli.*	Polard and Chandler, 1995
31	pC.060	P_{tac10}	0	GGAG	AATG	pSB4K5	no	Kan^R	Synthetic variant of the tac promoter from *E. coli.*	Albers et al., 2015
32	pC.061	P_{tic10}	0	GGAG	AATG	pSB4K5	no	Kan^R	Synthetic variant of the tic promoter from *E. coli*	Albers et al., 2015
33	pC.059	P_{trc10}	0	GGAG	AATG	pSB4K5	no	Kan^R	Synthetic variant of the trc promoter from *E. coli*	Geerts et al., 1995; Huang et al., 2010
Promoters (transcription start site only)										
1	pC0.219	BBa_J23119_TSS	0	GGAG	TAGC	pICH41295	no	$Spec^R$	BBa_J23119 promoter truncated to transcription start site.	
2	pC0.215	J23115_TSS	0	GGAG	TAGC	pICH41295	no	$Spec^R$	J23115 promoter truncated to transcription start site.	
3	pC0.208	J23108_TSS	0	GGAG	TAGC	pICH41295	no	$Spec^R$	J23108 promoter truncated to transcription start site.	*This study*
4	pC0.203	J23103_TSS	0	GGAG	TAGC	pICH41295	no	$Spec^R$	J23103 promoter truncated to transcription start site.	
5	pC0.220	P_{trc10_TSS}	0	GGAG	TAGC	pICH41295	no	$Spec^R$	trc promoter truncated to transcription start site.	
Terminators										
1	pC0.082	T_{rrnB}	0	GCTT	CGCT	pICH41276	no	$Spec^R$	Double terminator (BBa_B0015) from *E. coli*.	Liu and Pakrasi, 2018; Wang et al., 2018
2	pC0.062	Bba_B0011	0	GCTT	CGCT	pICH41276	no	$Spec^R$	Terminator for *luxICDABEG* operon from *Vibrio fischeri*.	Chen et al., 2013
3	pC0.070	BBa_B0061	0	GCTT	CGCT	pICH41276	no	$Spec^R$	Bi-directional terminator for *yciA*/*tonA* genes from *E. coli.*	Chen et al., 2013
4	pC0.067	BBa_J61053	0	GCTT	CGCT	pICH41276	no	$Spec^R$	Terminator for ribonuclease T1 (fmn T1) from *E. coli.*	Chen et al., 2013
5	pC0.075	ECK120010801	0	GCTT	CGCT	pICH41276	no	$Spec^R$	Terminator from *ars* operon from *E. coli*.	Chen et al., 2013
6	pC0.064	ECK120010820	0	GCTT	CGCT	pICH41276	no	$Spec^R$	Terminator from *hupB* gene from *E. coli*.	Chen et al., 2013
7	pC0.077	ECK120010841-R	0	GCTT	CGCT	pICH41276	no	$Spec^R$	Terminator from *rpoH* gene from *E. coli*.	Chen et al., 2013
8	pC0.072	ECK120010842	0	GCTT	CGCT	pICH41276	no	$Spec^R$	Terminator from *hyaABCDEF* operon from *E. coli*.	Chen et al., 2013
9	pC0.068	ECK120010850	0	GCTT	CGCT	pICH41276	no	$Spec^R$	Terminator for *clpPX* gene from *E. coli*.	Chen et al., 2013

10	pC0.065	ECK120010860	0	GCTT	CGCT	pICH41276	no	$Spec^R$	Terminator *araBAD* operon from *E. coli*.	Chen et al., 2013
11	pC0.073	ECK120010869	0	GCTT	CGCT	pICH41276	no	$Spec^R$	Terminator from *rplJL-rpoBC*,*rplKAJL-rpoBC*,*rpoBC* gene cluster from *E. coli*.	Chen et al., 2013
12	pC0.069	ECK120026481	0	GCTT	CGCT	pICH41276	no	$Spec^R$	Terminator from *arcA* gene from *E. coli*.	Chen et al., 2013
13	pC0.071	ECK120030798	0	GCTT	CGCT	pICH41276	no	$Spec^R$	Terminator from *tatABCD* operon from *E. coli*.	Chen et al., 2013
14	pC0.074	ECK120048902	0	GCTT	CGCT	pICH41276	no	$Spec^R$	Terminator from Cysteine synthase A gene (cysK) from *E. coli*.	Chen et al., 2013
15	pC0.063	pSB1AK3 terminator	0	GCTT	CGCT	pICH41276	no	$Spec^R$	Terminator derived from Biobricks plasmid pSB1AK3.	Shetty et al., 2008
16	pC0.078	T_{cpc_operon}	0	GCTT	CGCT	pICH41276	no	$Spec^R$	Terminator for the *cpc* operon *Synechocystis* sp. PCC 6803.	*This study*
17	pC0.080	T_{cpcG1}	0	GCTT	CGCT	pICH41276	no	$Spec^R$	Terminator for the *cpcG1* gene *Synechocystis* sp. PCC 6803.	*This study*
18	pC0.066	T_{pheA-1}	0	GCTT	CGCT	pICH41276	no	$Spec^R$	Terminator from pheA gene from *E. coli*.	Chen et al., 2013
19	pC0.081	T_{psaB}	0	GCTT	CGCT	pICH41276	no	$Spec^R$	Terminator for the *psaB* gene *Synechocystis* sp. PCC 6803.	*This study*
20	pC0.079	T_{psbA2}	0	GCTT	CGCT	pICH41276	no	$Spec^R$	Terminator for the *psbA2* gene *Synechocystis* sp. PCC 6803.	*This study*
21	pC0.076	T_{tetA}	0	GCTT	CGCT	pICH41276	no	$Spec^R$	Terminator from *tetA* gene from E. coli.	Chen et al., 2013

Additional references

Cai, Y.P, Wolk, C.P. (1990) Use of a conditionally lethal gene in Anabaena sp. strain PCC 7120 to select for double recombinants and to entrap insertion sequences. *J. Bacteriol.*, **172**, 3138–3145.

Chen, Y.J., Liu, P., Nielsen, A.A., Brophy, J.A., Clancy, K., Peterson, T., Voigt, C.A. (2013) Characterization of 582 natural and synthetic terminators and quantification of their design constraints. *Nat. Methods*, **10**, 659–664.

Dzelzkalns, V.A., Owens, G.C., Bogorad, L. (1984) Chloroplast promoter driven expression of the chloramphenicol acetyl transferase gene in a cyanobacterium. *Nucleic Acids Res.*, **12**, 8917–8925.

Geerts, D., Bovy, A., deVreize, G. Borrias, M., Weisbeek, P. (1995) Inducible expression of heterologous genes targeted to a chromosomal platform in the cyanobacterium *Synechococcus* sp. PCC 7942. *Microbiol.*, **141**, 831–841.

Landry, B.P., Stöckel, J., Pakrasi, H.B. (2013) Use of degradation tags to control protein levels in the cyanobacterium Synechocystis sp. strain PCC 6803. *Appl. Environ. Microbiol.*,**79**, 2833–2835.

Peca, L., Kós, P.B., Vass, I. (2007) Characterization of the activity of heavy metal-responsive promoters in the cyanobacterium Synechocystis PCC 6803. *Acta Biol. Hung.*, **58**, 11–22.

Polard, P., Chandler, M. (1995) An in vivo transposase-catalvzed single-stranded DNA circularization reaction. *Genes Dev.*, **9**, 2846–2858.

Ruffing, A.M., Jensen, T.J., Strickland, L.M. (2016) Genetic tools for advancement of Synechococcus sp. PCC 7002 as a cyanobacterial chassis. *Microb. Cell Fact.*, **15**, 190.

Shetty, R.P., Endy, D., Knight, T.F. (2008) Engineering BioBrick vectors from BioBrick parts. *J. Biol. Eng.*, **2**, 5.

Yanisch-Perron, C., Vieira, J., Messing, J. (1985) Improved M13 phage cloning vectors and host strains: nucleotide sequences of the M13mpl8 and pUC19 vectors. *Gene*, **33**, 103–119.

Appendix Table 8-2: List of level T vectors used in this study.

Vector ID	Part name	Acceptor backbone	Level 1 vectors	Selection	Notes
Assembled Level T vector (integrative)					
pCAT.336	pUC19A-T (cpcBA-M)	pUC19A-T	1	Amp^R	Generated a marked mutant in the cpcBA promoter and operon (Fig. 3).
pCAT.337	pUC19A-T (cpcBA-UM)		1		Generated an unmarked mutant in the cpcBA promoter and operon (Fig. 3).
pCAT.312	pUC19A-T (cpcBA-eYFP)		3		Introduced a eYFP expression cassette into the marked ΔcpcBA "Olive" mutant (Fig. 4).
Assembled Level T vector (replicative)					
pCAT.9	pSEVA431-T	pSEVA431 Level T	-	$Spec^R$	Level T Acceptor, pBBR1 replicative origin (50).
pCAT.13	pSEVA442-T	pSEVA442 Level T	-		Level T Acceptor, pRO1600/ColE1 replicative origin (50).
pCAT.163	pSEVA421-T (P_{cpc560}-eYFP-T_{rrnB})	pSEVA421-T	1		Level T assembly with eYFP expression cassette, RK2 replicative origin (Fig. 8) (50).
pCAT.214	pPMQAK1-T (J23100 MH-eYFP-T_{rrnB})	pPMQAK1-T	1	Amp^R, Kan^R	Level T assemblies with eYFP expression cassette (Fig. 5-7) (18), pPMQAK1-T replicative origin.
pCAT.235	pPMQAK1-T (J23101MH-eYFP-T_{rrnB})		1		
pCAT.236	pPMQAK1-T (J23102MH-eYFP-T_{rrnB})		1		
pCAT.237	pPMQAK1-T (J23103MH-eYFP-T_{rrnB})		1		
pCAT.238	pPMQAK1-T (J23104MH-eYFP-T_{rrnB})		1		
pCAT.239	pPMQAK1-T (J23105MH-eYFP-T_{rrnB})		1		
pCAT.240	pPMQAK1-T (J23106MH-eYFP-T_{rrnB})		1		
pCAT.241	pPMQAK1-T (J23107MH-eYFP-T_{rrnB})		1		
pCAT.242	pPMQAK1-T (J23108MH-eYFP-T_{rrnB})		1		

pCAT.243	pPMQAK1-T (J23109MH-eYFP-T_{rrnB})	1
pCAT.244	pPMQAK1-T (J23110MH-eYFP-T_{rrnB})	1
pCAT.245	pPMQAK1-T (J23111MH-eYFP-T_{rrnB})	1
pCAT.193	pPMQAK1-T (J23113MH-eYFP-T_{rrnB})	1
pCAT.247	pPMQAK1-T (J23114MH-eYFP-T_{rrnB})	1
pCAT.248	pPMQAK1-T (J23115MH-eYFP-T_{rrnB})	1
pCAT.249	pPMQAK1-T (J23116MH-eYFP-T_{rrnB})	1
pCAT.250	pPMQAK1-T (J23117MH-eYFP-T_{rrnB})	1
pCAT.251	pPMQAK1-T (J23118MH-eYFP-T_{rrnB})	1
pCAT.252	pPMQAK1-T (BBa_J23119MH-eYFP-T_{rrnB})	1
pCAT.253	pPMQAK1-T (P_{psbA2L}-eYFP-T_{rrnB})	1
pCAT.254	pPMQAK1-T (P_{rnpB}-eYFP-T_{rrnB})	1
pCAT.262	pPMQAK1-T (P_{trc10}-eYFP-T_{rrnB})	1
pCAT.263	pPMQAK1-T (P_{tac10}-eYFP-T_{rrnB})	1
pCAT.264	pPMQAK1-T (P_{tic10}-eYFP-T_{rrnB})	1
pCAT.267	pPMQAK1-T (J23119MH_V01-eYFP-T_{rrnB})	1
pCAT.268	pPMQAK1-T (J23119MH_V02-eYFP-T_{rrnB})	1
pCAT.269	pPMQAK1-T (J23119MH_V03-eYFP-T_{rrnB})	1
pCAT.272	pPMQAK1-T (J23119MH_V04-eYFP-T_{rrnB})	1
pCAT.273	pPMQAK1-T (J23119MH_V05-eYFP-T_{rrnB})	1
pCAT.274	pPMQAK1-T (J23119MH_V06-eYFP-T_{rrnB})	1

pCAT.265	pPMQAK1-T (J23119MH_V07-eYFP-T_{rrnB})		1		
pCAT.266	pPMQAK1-T (J23119MH_V08-eYFP-T_{rrnB})		1		
pCAT.278	pPMQAK1-T (P_{cpc560}+A-eYFP-T_{rrnB})		1		
pCAT.279	pPMQAK1-T (P_{cpc560}-eYFP-T_{rrnB})		1		
pCAT.280	pPMQAK1-T ($P_{cpc560-Ux2}$-eYFP-T_{rrnB})		1		
pCAT.281	pPMQAK1-T ($P_{cpc560-Dx2}$-eYFP-T_{rrnB})		1		
pCAT.314	pPMQAK1-T (P_{cpc560}-dCas9-T_{rrnB}) + (P_{trc10_TSS}-sgRNA+31-sgRNA scaffold)	pPMQAK1-T	2	AmpR, KanR	Level T assemblies for CRISPRi (Fig. 9) (81), pPMQAK1-T replicative origin.
pCAT.315	pPMQAK1-T (P_{cpc560}-dCas9-T_{rrnB}) + (P_{trc10_TSS}-sgRNA+118-sgRNA scaffold)		2		
pCAT.316	pPMQAK1-T (P_{cpc560}-dCas9-T_{rrnB}) + (P_{trc10_TSS}-sgRNA+171-sgRNA scaffold)		2		
pCAT.317	pPMQAK1-T (P_{cpc560}-dCas9-T_{rrnB}) + (P_{trc10_TSS}-sgRNA+233-sgRNA scaffold)		2		
pCAT.319	pPMQAK1-T (P_{trc10_TSS}-sgRNA+31-sgRNA scaffold)		1		
pCAT.320	pPMQAK1-T (P_{trc10_TSS}-sgRNA+118-sgRNA scaffold)		1		
pCAT.321	pPMQAK1-T (P_{trc10_TSS}-sgRNA+171-sgRNA scaffold)		1		
pCAT.322	pPMQAK1-T (P_{trc10_TSS}-sgRNA+233-sgRNA scaffold)		1		

Appendix Table 8-3: Sequences of synthetic oligonucleotides used to determine copy number.

Primers used for amplifying the *petB* locus were from Pinto et al. (2012).

Name	Locus	Amplicon length (bp)	Forward primer	Reverse primer
pPMQAK1-T (RSF1010)	-	245	AGTTAAGCCAGCCCCGACACC	TTGAGTGAGCTGATACCGCT
pSEVA421-T (RK2)	-	135	ACGACCAAGAAGCGAAAAACC	CCACGGCGCAATATCGAAC
petB locus	-	1000	ATAGTACGCTGATTATATGCGATTTTACGG	CATGTAAAGAATGTCGTTGGGCCA
petB	slr0342 (Chr:2647386-2650184)	179	CCTTCGCCTCTGTCCAATAC	TAGCATTACACCCACAACCC
secA locus	-	1000	CATAACCTTCTTGCTTATATTCAATCAAGGGA	AGCCAGGAAACGGAAGACTTAC
secA	sll0616 (Chr:2428010-2428678)	113	TTAAATCCAAACCTTCCAGCACCC	AACCTATTACTACGACATCCGTAAGC

Appendix Information 8-1: Comparison of Gibson Assembly and Golden Gate Assembly.

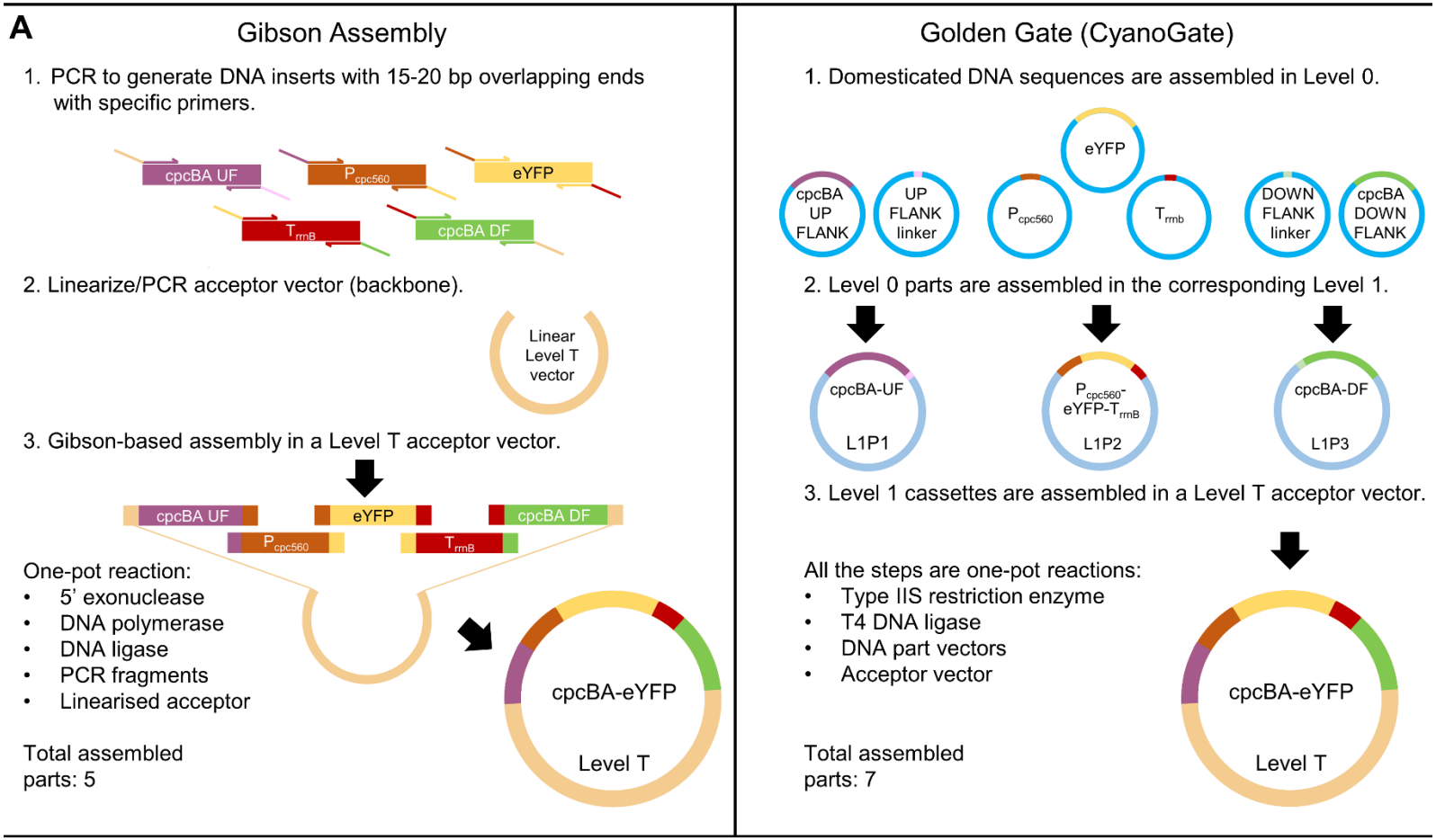

Description	**The Gibson Assembly (GA)** approach allows for the joining of two or more DNA fragments to generate plasmid vectors in a single isothermal reaction (Gibson et al., 2009, *Nat Methods*, 6:343-345).	**The Golden Gate (GG) Assembly** approaches (e.g. MoClo and GoldenBraid) use Type IIS restriction enzymes (REs) to generate standardised, non-palindromic overhangs that enable ordered assembly of multiple DNA parts in a single digestion-ligation reaction (Vazquez-Vilar et al., 2018).
Advantages	• Virtually any DNA fragments and any plasmid can be assembled together without prior modifications. • Allows seamless (scarless), directional cloning of multiple DNA fragments. • Can be used for cloning a wide range of DNA fragment sizes (i.e. 100-100,000 bp). • Depending on the number of fragments, GA can help to avoid multiple rounds of cloning (i.e. into different levels). • GA does not require DNA domestication (i.e. removal of incompatible restriction enzyme recognition sites). • Apart from vector assembly, GA can be used for numerous additional applications such, site-directed mutagenesis, library construction, shotgun cloning and the development of bacterial artificial chromosomes (BACs) (Li et al., 2018, *Methods Mol Biol*, 1671:203-209).	• Can re-use parts without modification in new assemblies. • Once parts are made, no subsequent PCR or clean-ups steps are required, and new assemblies do not require sequence checking. • GG only requires liquid handing (no columns or gels) so can be automated. Thus, GG is simple to scale for high-throughput protocols (e.g. assembly of combinatorial libraries). • GG allows for the standardisation of parts and vectors:- o Standard overhangs allow for directional and hierarchical assembly. o Assemblies are carried out with a common set of established acceptor vectors and a defined assembly protocol. o Standard antibiotic selection markers and visual colony screening (e.g. blue/white) at each assembly level to facilitate the detection of positive colonies. o Establishment of a common genetic syntax (i.e. the Phytobricks standard) has enabled

Advantages		broader exchange of parts and assemblies (Patron et al., 2015). ○ GG simplifies experimental replication, and comparable information is available for part performance and methods for reliable assembly. ○ The availability of libraries of standard exchangeable DNA parts (e.g. Phytobricks, MoClo).
Disadvantages	• Primers for each part are needed for every assembly. • Unique overlapping primer pairs are required to join two different DNA fragments. This can limit the ability to freely combine different parts (e.g. for promoter screening). • PCR can fail. • Secondary structures and/or repetitive sequences in the overlap region can limit the efficiency and accuracy of assembly. • Sequence verification of all regions that undergo PCR amplification is recommended. Some DNA regions are challenging to sequence (e.g. the pPMQAK1 backbone), which can increase the cost of sequencing.	• DNA parts and acceptor vectors require domestication to remove illegal Type IIS RE sites. • Some DNA sequences (e.g. promoters) may be challenging to domesticate due to the presence of RE sites in regulatory elements. • Assembly is quasi-seamless due to the use of standardised overhangs. • Initial setup can be time consuming, and purchase of Addgene kits could be a relatively costly starting investment.

Disadvantages	• Assembly efficiencies decline with six or more DNA fragments or with the use of fragments shorter than 100 bp. • • Very small parts have to be first assembled by extension/overlap PCR.	

Appendix Information 8-2: Detailed assembly strategies using the CyanoGate kit.

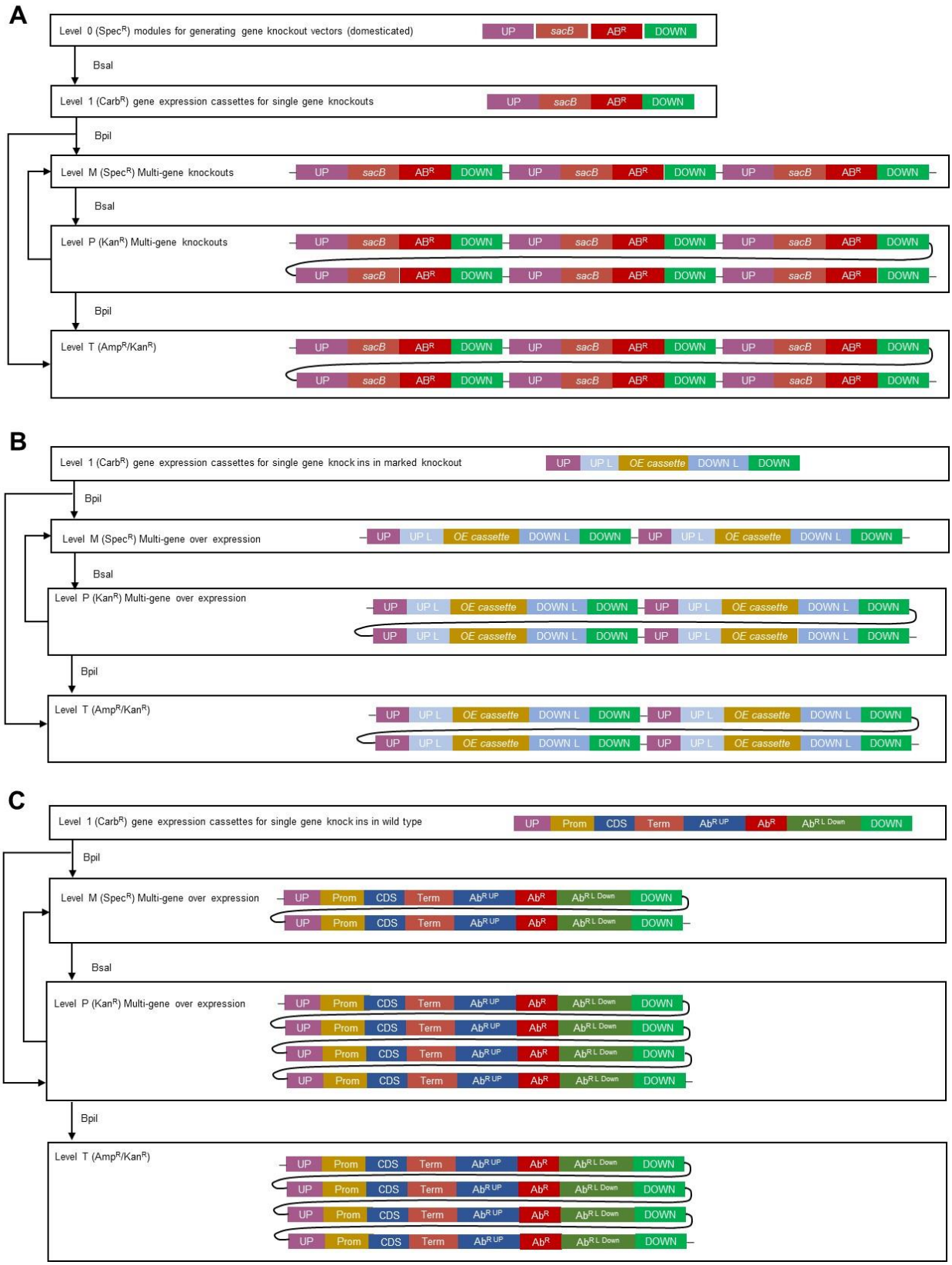

Appendix Information 8-3: Integrative engineering strategies using the CyanoGate kit.

(A) Marked mutants are generated using a level T marked knock out vector carrying DNA sequences flanking the target locus of the chromosome (~1 kb), an antibiotic resistance cassette (Ab^R) and a sucrose selection cassette (*sacB*) that produces the toxic compound levansucrase in the presence of sucrose (20). Several rounds of segregation are required to identify a marked mutant. (B) Marked mutants then can be unmarked with a level T unmarked knock out vector and selection on sucrose-containing agar plates. (C) Unmarked knock in mutants can also be generated from marked mutants using a level T unmarked knock in vector carrying a gene expression cassette (UP FLANK LINKER and DOWN FLANK LINKER are shown in pink and light green, respectively). (D) Alternatively marked knock in mutants can be engineered in a single step using a level T marked knock vector (Ab^R UP LINKER and DOWN LINKER are shown in blue and orange, respectively). See **Fig. 2** for abbreviations.

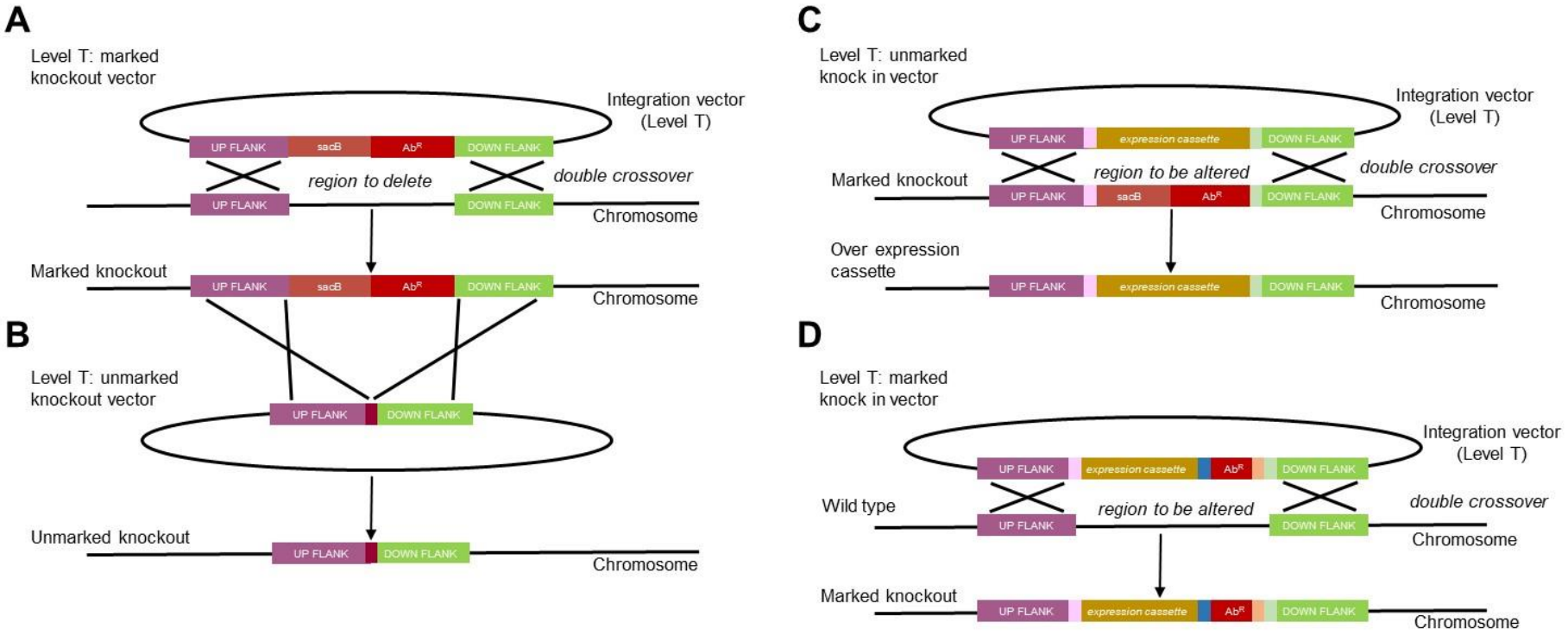

Appendix Information 8-4: Protocol and online interface for building CyanoGate vector assemblies.

A CyanoGate online vector assembly tool called Design and Build (DAB) from the Edinburgh Genome Foundry.

1. Site: dab.genomefoundry.org
2. Select "Home" and "Design New Assemblies".
3. Select "MoClo", then from the drop down list select "CyanoGate".
4. There are 3 options: a) L1-knockout, b) L1-knock in, and c) L1-standard.

a. L1-knockout
   - This is a level 1 assembly for generating a marked or unmarked knockout mutant (see **Fig. 2**). The level 1 module(s) then should be transferred to the integrative level T integrative vector (pCAT15.UC19) for chromosomal integration in species amenable to natural transformation (e.g. *Synechocystis* sp. PCC 6803) (20).
   - Example of level 1 assembly for generating a level T knockout vector: L1P1 acceptor (DOWN FLANK + *sacB* + Ab^{R}Kan + UP FLANK).

b. L1-knock in
   - This is a level 1 assembly for generating a knock in mutant (see **Fig. 3**). Each level 0 flanking region should be assembled into a specific level 1 position with gene expression cassettes (L1-standard) in between them.
   - The level 1 modules then should be transferred to the integrative level T integrative vector (pCAT15.UC19) for chromosomal integration in species amenable to natural transformation (e.g. *Synechocystis* sp. PCC 6803).
   - Example of 3 level 1 assemblies for generating a level T knock in vector: L1P1 acceptor (6803 NS1 Down Flank (slr0573) + DOWN FLANK), L1P2 acceptor (P_{trc10} + eYFP + T_{rrnB}), L1P3 acceptor (UP FLANK + 6803 NS1 Up Flank (slr0573)).

c. L1-standard.
   - This is a level 1 assembly for generating a standard gene expression cassette from level 0 parts.
   - These level 1 modules can be transferred to the integrative level T integrative vector (pCAT15.UC19) for chromosomal integration in species amenable to natural transformation (e.g. *Synechocystis* sp. PCC 6803).
   - Alternatively, the level 1 modules can be transferred to a replicative level T vector (e.g. pCAT0.PMQAK1) for transformation into cyanobacterial species amenable to conjugation or electroporation.
   - Example of a level 1 assembly for generating a level T expression vector: L1P1 acceptor (P_{trc10} + eYFP + T_{rrnB}).

Appendix Information 8-5: Protocols for MoClo assembly in level -1 through to level T.

Protocols for assembly in level 0, level M and level T acceptor vectors (restriction enzyme *Bpi*I required, left). Protocols for assembly in level -1, level 1 and level P backbone vectors (restriction enzyme *Bsa*I required, right). Adapted from "A quick guide to Type IIS cloning" (Patron Lab; patronlab.org). For troubleshooting Type IIS mediated assembly we recommend synbio.tsl.ac.uk/docs.

_Bpi_I protocol (in restriction buffer)

- 50-100 ng of acceptor vector.
- For each modular vector/part to insert, use a 2:1 ratio of insert: acceptor.
- 2 µl 10 mM ATP (not dATP).
- 2 µl Buffer G (Thermofisher).
- 2 µl BSA (10X).
- 10 units *Bpi*I (1 µl 10 U/µl *Bpi*I, ThermoFisher)
- 200 units T4 DNA ligase (1 µl 200U/µl, ThermoFisher)

37^0 C for 10 minutes
16^0 C for 10 minutes
} X5

37^0 C for 20 minutes

65^0 C for 10 minutes

16^0 C (hold)

_Bsa_I protocol (in restriction buffer)

- 50-100 ng of acceptor vector.
- For each modular vector/part to insert, use a 2:1 ratio of insert: acceptor.
- 2 µl 10 mM ATP (not dATP).
- 2 µl Buffer G (Thermofisher).
- 2 µl BSA (10X).
- 10 units *Bsa*I (1 µl 10 U/µl *Bsa*I, ThermoFisher)
- 200 units T4 DNA ligase (1 µl 200U/µl, ThermoFisher)

37^0 C for 10 minutes
16^0 C for 10 minutes
} X5

37^0 C for 20 minutes

65^0 C for 10 minutes

16^0 C (hold)

8.2 Appendix II for Chapter 6

Appendix Table 8-4: Primers used to PCR amplify genetic parts.

No sequences required domestication (i.e. removal of *BsaI* or *BpiI* sites).

No.	*Part*	*Forward primer*	*Reverse primer*
1	P_{arsR}	GATCGGTCTCTGGAGCCAACTCAAAATTCACACCTATTACCTTCC	GATCGGTCTCAAGTATTGCAGGTAGTGTCTCTCTTCGAAG
2	P_{phlF}	GATCGGTCTCTGGAGCGACGTACGGTGGAATCTGATTCGTTACCAATTGACATGATAC	GATCGGTCTCAAGTAACCTTAACGATACGGTACGTTTCGTATCATGTCAATTGGT
3	P_{SalTTC}	GATCGGTCTCTGGAGGGGGCCTCGCTTGGG	GATCGGTCTCAAGTAGTTAATAACGGTAACGGAGCAAACAATAT
4	P_{Cin}	GATCGGTCTCTGGAGCCCTTTGTGCGTCCAAACG	GATCGGTCTCAAGTAAGCGTTTTCAAGTTCGTGGAAAG
5	P_{rhaBAD}	GATCGGTCTCTGGAGTTATTGCAGAAAGCCATCCC	GATCGGTCTCAAGTATACGACCAGTCTAAAAAGCGC
6	$P_{araBADWT}$	GATCGGTCTCTGGAGAAGAAACCAATTGTCCATATTGCATCAG	GATCGGTCTCAAGTAATGGAGAAACAGTAGAGAGTTGCGA
7	P_{vanCC}	GATCGGTCTCTGGAGATTGGATCCAATTGACAGCTAGCTCAGTCCTAGGT	GATCGGTCTCAAGTAATTGGATCCAATGGTACCTAGGACTGAGCTAGCTG
8	P_{lambda}	GATCGGTCTCTGGAGTAACACCGTGCGTGTTGACTATTTTACCTCTGGCG	GATCGGTCTCAAGTAGCAACCATTATCACCGCCAGAGGTAAAA
9	$phlF^{AM}$	GATCGGTCTCTTACTAGAGTCACACAGGAAAGTACTAGATGG	GATCGGTCTCAAAGCTTATTAACACTGTGTACCCGGACAAAC
10	*nahR*	TCTGTGGTCTCAGGAGTTATTAATCCGTAAACAGGTCAAACATCAGTTG	CAGTGGTCTCAACTAGATGGAACTGCGTGACCT
11	*cinR*	TCTGTGGTCTCAGGAGTTATTACCAATTACGTCGCGTCATGC	CAGTGGTCTCAACTAGATGATTGAGAATACCTATAGCGAAAAGT
12	*rhaS*	TCTGTGGTCTCAGGAGTTATTGCAGAAAGCCATCCCGTCC	CAGTGGTCTCAACTAGATGACCGTATTACATAGTGTGGATTTTTTTCC
13	*vanR*	CTGTGAAGACAATGCCGAATTCG	CAGTGAAGACATAGCGCTTAAACTAACGAACGTAAATAAGGAGGATAGACATGGACATGCCTCGTATTAAACCG
14	*C1*	TCTGTGGTCTCAGGAGTTAACCAAAAGTCTCTTCAGGCCAC	CAGTGGTCTCAACTAGATGAGCACAAAAAAGAAACCATTAACACAAGAG
15	*Junction sequence (P_{J23101}) Frag 1*	TCTGTGGTCTCACATCTAGTACTTTCCTGTGTGACTCTAGTAGCTAGCAT	CAGTGGTCTCATTTACAGCTAGCTCAGTCCTAGGTATTATGCTAGCTACTAG
16	*Junction sequence (P_{J23101}) Frag 2*	CTGTGGTCTCATAAATACTAGAGCTCGGTACCAAATTCCAGAAAAGAGGCCTCCCGA	CAGTGGTCTCACTCTAGTAGGACCAAAACGAAAAAAGGCCCCCCTTTCGGGAGGCCTC
17	*eYFP-TrrnB*	GATCGGTCTCTTACTAGAGAAAGAGGAGAAATACTAAATGGTGAGC	GATCGGTCTCAAGCGCGCAGAAAGGCCCACCC

18	*phlF^{AM} for NOT_Single, NOT_Double*	AGACTGGTCGTATACTAGAGTCACACAGGAAAGTACTAaATGGCACGTACCCCGAG	CCTTTCGTTTTATTTGaagcTTATTAACACTGTGTACCCGGACAAACA
19	*PphlF-eYFjP-TrrnB*	TCTGTGGTCTCAGGAGCGACGTACGGTGGAATC	CAGTGGTCTCAAGCGCGCAGAAAGGC
20	*L1P1 for DT_AQUA*	GCTTCAAATAAAACGAAAGGCTCAGTCG	CTCTAGTATACGACCAGTCTAAAAAGCGC
21	*phlF^{AM}-DT1 for AQUA*	AGACTGGTCGTATACTAGAGTCACACAGGAAAGTACTAaATGGCACGTACCCCGAG	CCTTTCGTTTTATTTGaagcTTAGGCGGCAATGGCTACCCGCTTAAAGGAAACGATGTTATTGGCGGCACACTGTGTACCCGGACAAACA
22	*phlF^{AM}-DT2 for AQUA*	AGACTGGTCGTATACTAGAGTCACACAGGAAAGTACTAaATGGCACGTACCCCGAG	CCTTTCGTTTTATTTGaagcTTAGCCGCCGCCGGCTACCCGCTTAAAGGAAACGATGTTATTGGCGGCACACTGTGTACCCGGACAAACA
23	*rhaS PrhaBAD for NOT_RBS variants*	GATCGGTCTCTGGAGTTATTGCAGAAAGCCATCCC	GATCGGTCTCAAGTATACGACCAGTCTAAAAAGCGC
24	*phlF^{AM} for NOT_RBS0*	GATCGGTCTCTTACTCTAGAGAAAGAGGAGAATGGCACGTACCCCGAG	GATCGGTCTCAAGCGCGCAGAAAGGCCCACCC
25	*phlF^{AM} for NOT_RBS18*	GATCGGTCTCTTACTCTAGAGAAAGAGGAGAAATACTACTAGTGACAGAATGGCACGTACCCCGA	GATCGGTCTCAAGCGCGCAGAAAGGCCCACCC
26	*phlF^{AM} for NOT_RBS31*	GATCGGTCTCTTACTAGAGTCACACAGGAAACCTACTAGATGGCACGTACCCCG	GATCGGTCTCAAGCGCGCAGAAAGGCCCACCC
27	*phlF^{AM} for NOT_RBS33*	GATCGGTCTCTTACTAGAGTCACACAGGACTACTAAATGGCACGTACCCGAG	GATCGGTCTCAAGCGCGCAGAAAGGCCCACCC
28	*phlF^{AM} for NOT_RBS35*	GATCGGTCTCTTACTAGAGATTAAAGAGGAGAATACTAGATGGCACGTACCCCG	GATCGGTCTCAAGCGCGCAGAAAGGCCCACCC

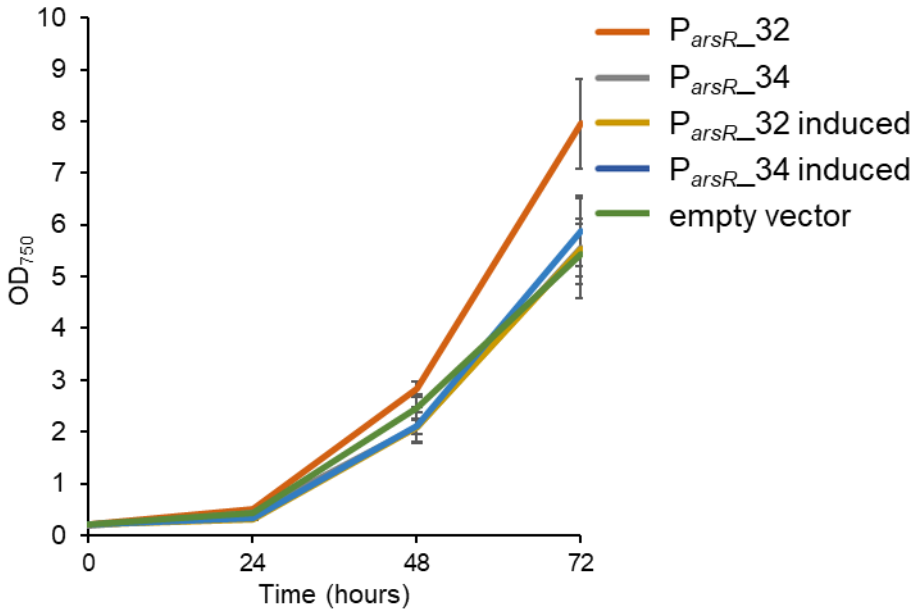

Appendix Figure 8-3: Growth of strains harbouring P_{arsR} variants in *Synechocystis* sp. PCC 6803.

Cultures were grown for 72 hr at 30°C with continuous light (100 µmol photons m^{-2}-s^{-1}). Error bars represent ± SE of the mean of four biological replicates. Induction was performed with arsenite [AsIII] 500µM where noted in the legend.

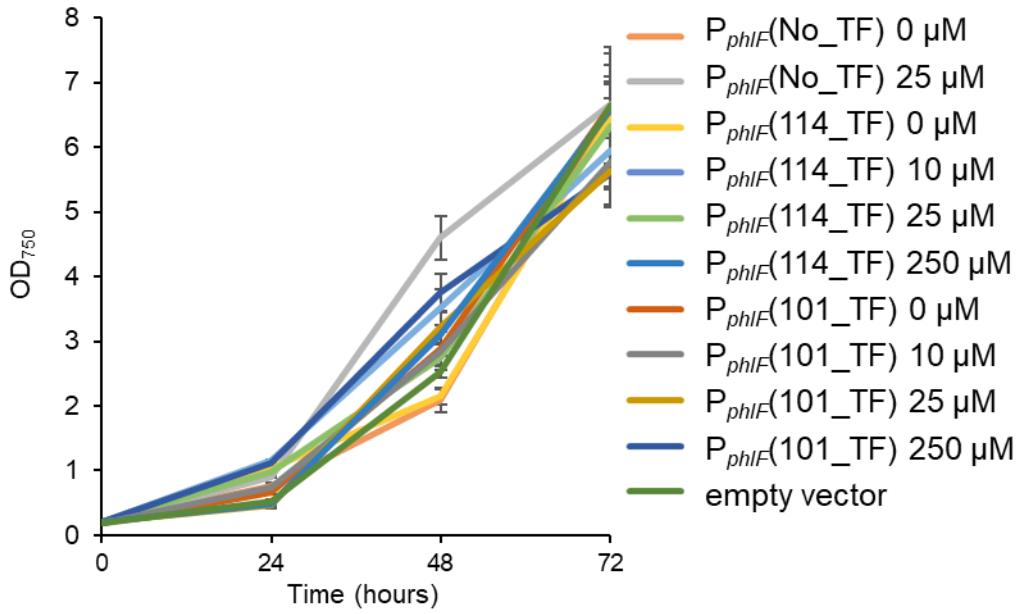

Appendix Figure 8-4: Growth of strains harbouring P_{phlF} variants in *Synechocystis* sp. PCC 6803.

Cultures were grown for 72 hr at 30°C with continuous light (100 µmol photons m^{-2}-s^{-1}). Error bars represent ± SE of the mean of four biological replicates. Induction was performed with varying concentration of DAPG (0 – 250 µM).

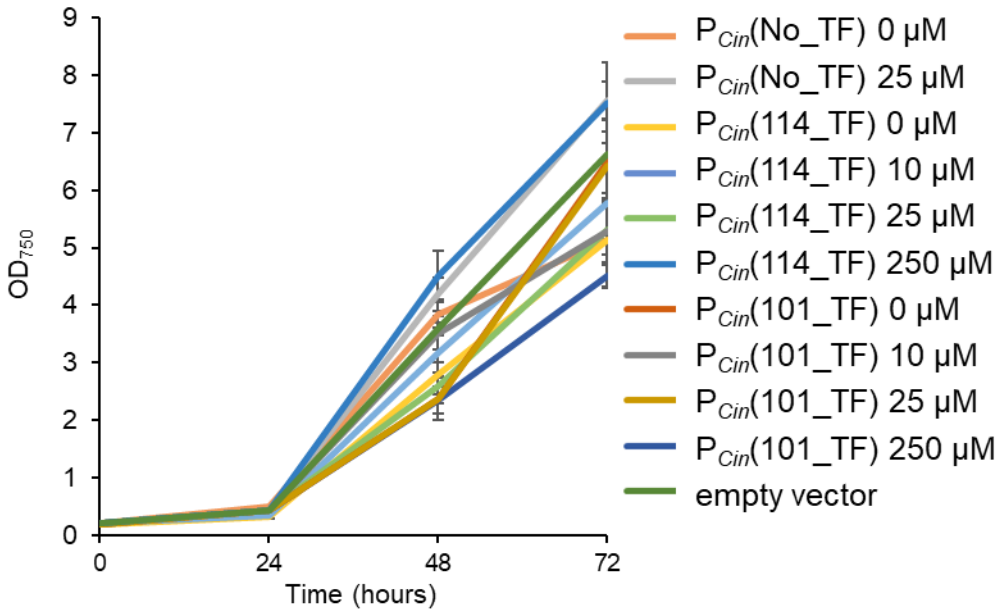

Appendix Figure 8-5: Growth of strains harbouring P_{Cin} variants in *Synechocystis* sp. PCC 6803.

Cultures were grown for 72 hr at 30°C with continuous light (100 µmol photons m^{-2}-s^{-1}). Error bars represent ± SE of the mean of four biological replicates. Induction was performed with varying concentration of salicylate (0 –250 µM).

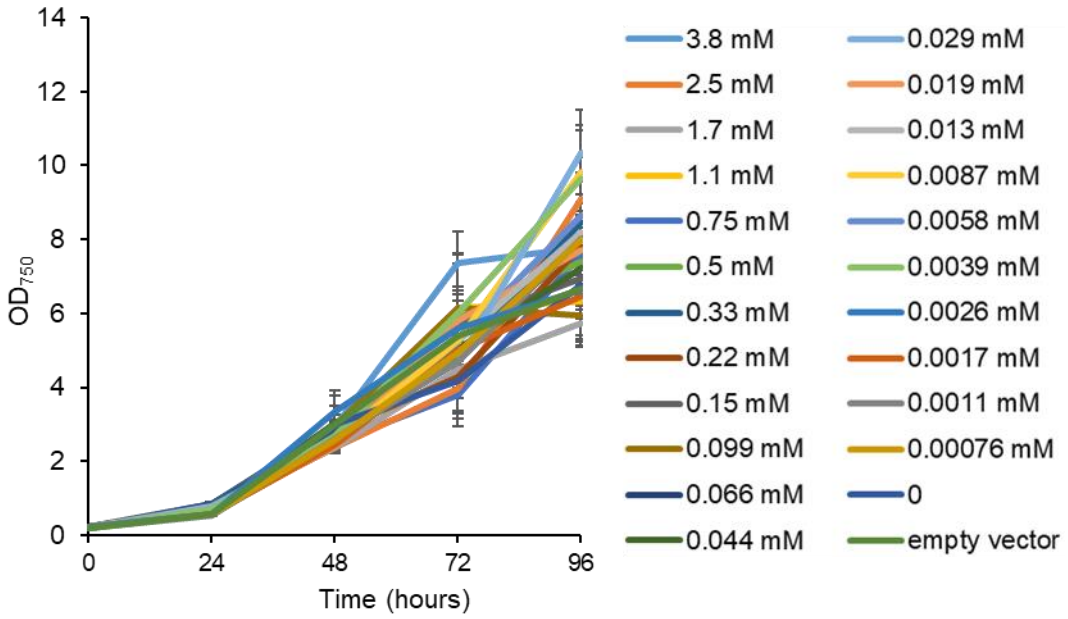

Appendix Figure 8-6: Growth of strains harbouring P_{rhaBAD} in *Synechocystis* sp. PCC 6803.

Cultures were grown for 72 hr at 30°C with continuous light (100 µmol photons m^{-2}-s^{-1}). Error bars represent ± SE of the mean of four biological replicates. Induction was performed with varying concentration of L-rhamnose (0 –3.8 mM).

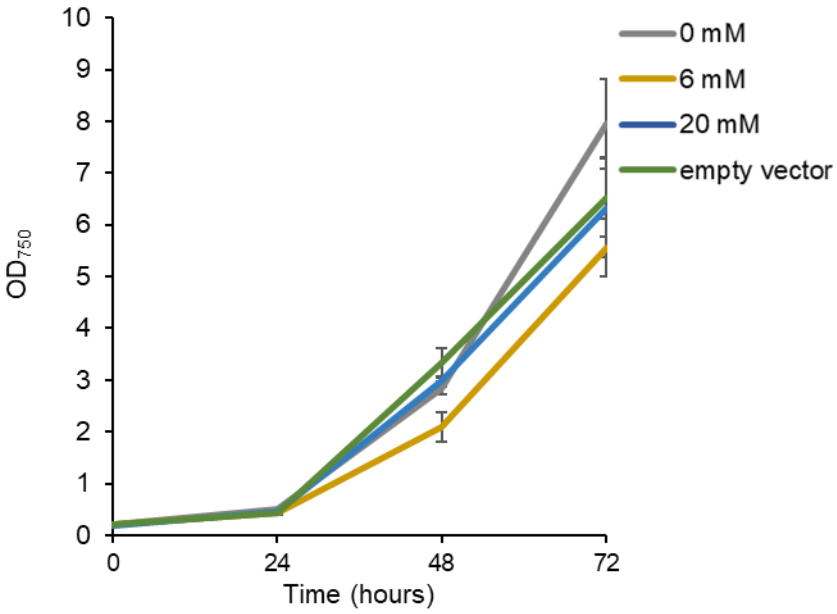

Appendix Figure 8-7: Growth of strains harbouring P_{BADWT} in *Synechocystis* sp. PCC 6803.

Cultures were grown for 72 hr at 30°C with continuous light (100 µmol photons m^{-2}-s^{-1}). Error bars represent ± SE of the mean of four biological replicates. Induction was performed with varying concentration of L-arabinose (0 –20 mM).

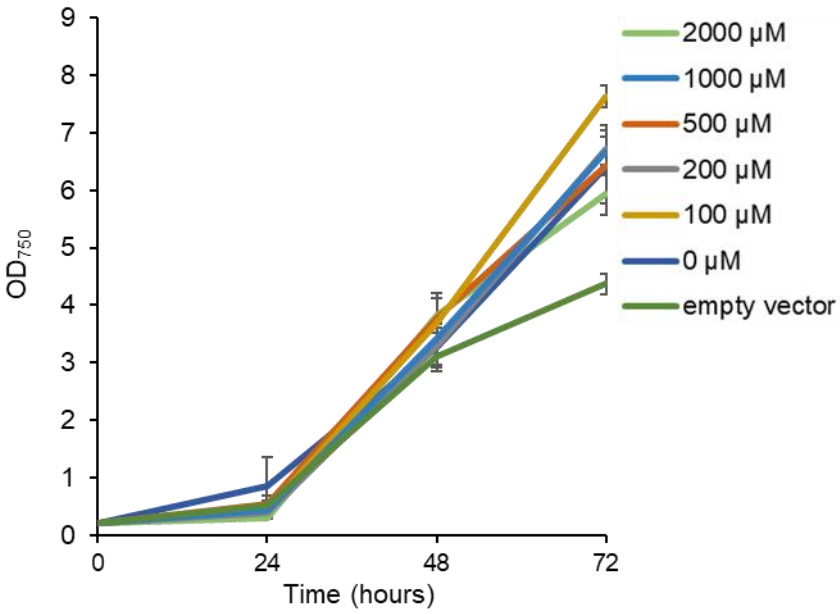

Appendix Figure 8-8: Growth of strains harbouring P_{VanCC} in *Synechocystis* sp. PCC 6803.

Cultures were grown for 72 hr at 30°C with continuous light (100 µmol photons m^{-2}-s^{-1}). Error bars represent ± SE of the mean of four biological replicates. Induction was performed with varying concentration of vanillate (0 –2000 µM).

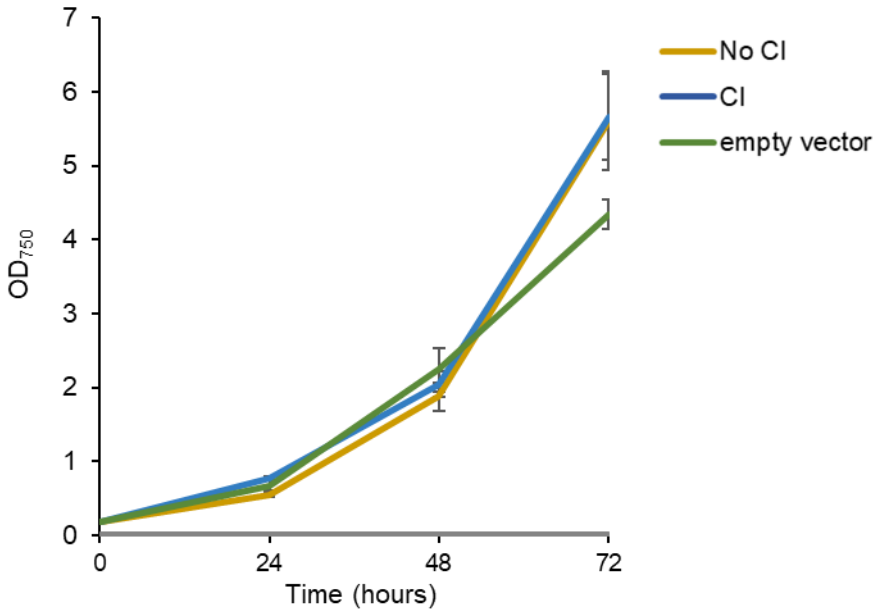

Appendix Figure 8-9: Growth of strains harbouring *λP*$_R$ variants in *Synechocystis* sp. PCC 6803.

Cultures were grown for 72 hr at 30°C with continuous light (100 µmol photons m^{-2}-s^{-1}). Error bars represent ± SE of the mean of four biological replicates.

8.3 Appendix III - Publications

8.3.1 List of publications

The articles listed below were published during my PhD and were presented wholly or as part of the following chapters:

Chapter 2

Gale, G. A. R., Schiavon, A. A.., Mills, L. A., Wang, B., Lea-Smith, D. J., & McCormick, A. J. (2019). Emerging species and genome editing tools: Future prospects in cyanobacterial synthetic biology. *Microorganisms*, *7*(10), 409. https://doi.org/10.3390/microorganisms7100409

Chapter 3

Vasudevan, R., **Gale, G. A. R**., Schiavon, A. A., Puzorjov, A., Malin, J., Gillespie, M. D., … Wang, B., Howe, C. J., Lea-Smith, D. J., McCormick, A. J. (2019). Cyanogate: A modular cloning suite for engineering cyanobacteria based on the plant moclo syntax. *Plant Physiology*, *180*(1), 39–55. https://doi.org/10.1104/pp.18.01401

Chapter 4

Gale, G. A. R., Schiavon, A. A., Puzorjov, A., Wang, B., & McCormick, A. J. (2019). Genetic Modification of Cyanobacteria by Conjugation Using the CyanoGate Modular Cloning Toolkit. *Journal of Visualized Experiments : JoVE*, (152), e60451. https://doi.org/10.3791/60451

Chapter 5

Gale, G. A. R., Wang, B., & McCormick, A. J. (2021). Evaluation and Comparison of the Efficiency of Transcription Terminators in Different Cyanobacterial Species. *Frontiers in Microbiology*, *11*, 3585. https://doi.org/10.3389/fmicb.2020.624011

8.3.2 Main text: CyanoGate: A Modular Cloning Suite for Engineering Cyanobacteria Based on the Plant MoClo Syntax

Breakthrough Technologies

CyanoGate: A Modular Cloning Suite for Engineering Cyanobacteria Based on the Plant MoClo Syntax[1][OPEN]

Ravendran Vasudevan,[a,b] Grant A.R. Gale,[a,b,c] Alejandra A. Schiavon,[a,b] Anton Puzorjov,[a,b] John Malin,[a,b] Michael D. Gillespie,[d] Konstantinos Vavitsas,[e,f] Valentin Zulkower,[b] Baojun Wang,[b,c] Christopher J. Howe,[g] David J. Lea-Smith,[d] and Alistair J. McCormick[a,b,2,3]

[a]Institute of Molecular Plant Sciences, School of Biological Sciences, University of Edinburgh, Edinburgh EH9 3BF, United Kingdom
[b]Centre for Synthetic and Systems Biology, University of Edinburgh, Edinburgh EH9 3BF, United Kingdom
[c]Institute of Quantitative Biology, Biochemistry and Biotechnology, School of Biological Sciences, University of Edinburgh, Edinburgh EH9 3FF, United Kingdom
[d]School of Biological Sciences, University of East Anglia, Norwich NR4 7TJ, United Kingdom
[e]Australian Institute of Bioengineering and Nanotechnology, The University of Queensland, Brisbane, Queensland 4072, Australia
[f]CSIRO, Synthetic Biology Future Science Platform, Brisbane, Queensland 4001, Australia
[g]Department of Biochemistry, University of Cambridge, Cambridge CB2 1QW, United Kingdom

ORCID IDs: 0000-0001-9195-1116 (R.V.); 0000-0002-1991-8693 (J.M.); 0000-0002-6828-1000 (K.V.); 0000-0002-4858-8937 (B.W.); 0000-0002-6975-8640 (C.J.H.); 0000-0003-2463-406X (D.J.L.); 0000-0002-7255-872X (A.J.M.).

Recent advances in synthetic biology research have been underpinned by an exponential increase in available genomic information and a proliferation of advanced DNA assembly tools. The adoption of plasmid vector assembly standards and parts libraries has greatly enhanced the reproducibility of research and the exchange of parts between different labs and biological systems. However, a standardized modular cloning (MoClo) system is not yet available for cyanobacteria, which lag behind other prokaryotes in synthetic biology despite their huge potential regarding biotechnological applications. By building on the assembly library and syntax of the Plant Golden Gate MoClo kit, we have developed a versatile system called CyanoGate that unites cyanobacteria with plant and algal systems. Here, we describe the generation of a suite of parts and acceptor vectors for making (1) marked/unmarked knock-outs or integrations using an integrative acceptor vector, and (2) transient multigene expression and repression systems using known and previously undescribed replicative vectors. We tested and compared the CyanoGate system in the established model cyanobacterium *Synechocystis* sp. PCC 6803 and the more recently described fast-growing strain *Synechococcus elongatus* UTEX 2973. The UTEX 2973 fast-growth phenotype was only evident under specific growth conditions; however, UTEX 2973 accumulated high levels of proteins with strong native or synthetic promoters. The system is publicly available and can be readily expanded to accommodate other standardized MoClo parts to accelerate the development of reliable synthetic biology tools for the cyanobacterial community.

Much work is focused on expanding synthetic biology approaches to engineer photosynthetic organisms, including cyanobacteria. Cyanobacteria are an evolutionarily ancient and diverse phylum of photosynthetic prokaryotic organisms that are ecologically important and are thought to contribute ~25% of the total oceanic net primary productivity (Castenholz, 2001; Flombaum et al., 2013). The chloroplasts of all photosynthetic eukaryotes, including plants, resulted from the endosymbiotic uptake of a cyanobacterium by a eukaryotic ancestor (Keeling, 2004). Therefore, cyanobacteria have proved useful as model organisms for the study of photosynthesis, electron transport, and associated biochemical pathways, many of which are conserved in eukaryotic algae and higher plants. Several unique aspects of cyanobacterial photosynthesis, such as the biophysical carbon concentrating mechanism, also show promise as a means for enhancing productivity in crop plants (Rae et al., 2017). Furthermore, cyanobacteria are increasingly recognized as valuable platforms for industrial biotechnology to convert CO_2 and water into valuable products using solar energy (Ducat et al., 2011; Tan et al., 2011; Ramey et al., 2015). They are metabolically diverse and encode many components (e.g. P450 cytochromes) necessary for generating high-value pharmaceutical products that can be challenging to produce in other systems (Nielsen et al., 2016; Wlodarczyk et al., 2016; Pye et al., 2017; Stensjö et al., 2018). Furthermore, cyanobacteria show significant promise in biophotovoltaic devices for generating electrical energy (McCormick et al., 2015; Saar et al., 2018).

Based on morphological complexity, cyanobacteria are classified into five subsections (I to V; Castenholz, 2001). Several members of the five subsections reportedly have been transformed (Vioque, 2007; Stucken et al., 2012), suggesting that many cyanobacterial species are amenable to genetic manipulation. Exogenous DNA can be integrated into or removed from the

genome through homologous recombination-based approaches using natural transformation, conjugation (triparental mating), or electroporation (Heidorn et al., 2011). Exogenous DNA can also be propagated by replicative vectors, although the latter are currently restricted to a single vector type based on the broad-host range RSF1010 origin (Mermet-Bouvier et al., 1993; Huang et al., 2010; Taton et al., 2014). Transformation tools have been developed for generating "unmarked" mutant strains (lacking an antibiotic resistance marker cassette) in several model species, such as *Synechocystis* sp. PCC 6803 (*Synechocystis* hereafter; Lea-Smith et al., 2016). More recently, markerless genome editing using clustered regularly interspaced short palindromic (CRISPR)-based approaches has been demonstrated to function in both unicellular and filamentous strains (Ungerer and Pakrasi, 2016; Wendt et al., 2016).

Although exciting progress is being made in developing effective transformation systems, cyanobacteria still lag behind in the field of synthetic biology compared to bacterial (heterotrophic), yeast, and mammalian systems. Relatively few broad host-range genetic parts have been characterized, but many libraries of parts for constructing regulatory modules and circuits are starting to become available, albeit using different standards, which makes them difficult to combine (Huang and Lindblad, 2013; Camsund et al., 2014; Albers et al., 2015; Markley et al., 2015; Englund et al., 2016; Immethun et al., 2017; Kim et al., 2017; Taton et al., 2017; Ferreira et al., 2018; Li et al., 2018; Liu and Pakrasi, 2018; Wang et al., 2018). One key challenge is clear: parts that are widely used in *Escherichia coli* behave very differently in model cyanobacterial species such as *Synechocystis* (Heidorn et al., 2011). Furthermore, different cyanobacterial strains generally show a wide variation regarding functionality and performance of different genetic parts (e.g. promoters, reporter genes, and antibiotic resistance markers; Taton et al., 2014, 2017; Englund et al., 2016; Kim et al., 2017). This suggests that parts need to be validated, calibrated, and perhaps modified for individual strains, including model species and strains that may be more commercially relevant. Rapid cloning and assembly methods are essential for accelerating the "design, build, test, and learn" cycle, which is a central tenet of synthetic biology (Nielsen and Keasling, 2016).

The adoption of new cloning and vector assembly methods (e.g. Isothermal [Gibson] Assembly and Modular Cloning [MoClo]), assembly standards, and part libraries has greatly enhanced the scalability of synthetic biology-based approaches in a range of biological systems (Moore et al., 2016; Vazquez-Vilar et al., 2018). Recent advances in synthetic biology have led to the development of standards for Type IIS restriction endonuclease-mediated assembly (commonly known as Golden Gate cloning) for several model systems, including plants (Sarrion-Perdigones et al., 2013; Engler et al., 2014; Andreou and Nakayama, 2018). Based on a common Golden Gate MoClo syntax, large libraries are now available for fusion of different genetic parts to assemble complex vectors cheaply and easily without proprietary tools and reagents (Patron et al., 2015). High-throughput and automated assembly are projected to be widely available soon through DNA synthesis and construction facilities, such as the United Kingdom DNA Synthesis Foundries, where MoClo is seen as the most suitable assembly standard (Chambers et al., 2016).

Here, we describe the development of an easy-to-use system called CyanoGate that unites cyanobacteria with plant and algal systems. This system builds on the established Golden Gate MoClo syntax and assembly library for plants (Engler et al., 2014) that has been adopted by the OpenPlant consortium (www.openplant.org), iGEM competitions as "Phytobricks," and the MoClo kit for the microalga *Chlamydomonas reinhardtii* (Crozet et al., 2018). First, we constructed and characterized a suite of known and new genetic parts (level 0) for use in cyanobacterial research, including promoters, terminators, antibiotic resistant markers, neutral sites (NS), and gene repression systems (Na et al., 2013; Yao et al., 2016; Sun et al., 2018). Second, we designed an additional level of acceptor vectors (level T) to facilitate integrative or replicative transformation. We characterized assembled level T vectors in *Synechocystis* and in *Synechococcus elongatus* UTEX 2973 (UTEX 2973 hereafter), which has a reported doubling time similar to that of *Saccharomyces cerevisiae* under specific growth conditions (Yu et al., 2015; Ungerer et al., 2018a, 2018b). Lastly, we developed an online tool for assembly of CyanoGate and Plant MoClo vectors to assist with the adoption of the CyanoGate system.

RESULTS AND DISCUSSION

Construction of the CyanoGate System

The CyanoGate system integrates with the two-part Golden Gate MoClo Plant Tool Kit, which can be

[1]This work was supported by the PHYCONET Biotechnology and Biological Sciences Research Council (BBSRC) Network in Industrial Biotechnology and Bioenergy (NIBB) and the Industrial Biotechnology Innovation Centre (IBioIC) (R.V., A.J.M., B.W., C.J.H.), a BBSRC EASTBIO CASE PhD studentship (BB/M010996/1 to G.A.R.G.), a United Kingdom BBSRC grant (BB/N007212/1 to B.W.), a Leverhulme Trust research grant (RPG-2015-445 to B.W.), a Consejo Nacional de Ciencia y Tecnología (CONACYT) PhD studentship (to A.A.S.), and a CSIRO Synthetic Biology Future Science Fellowship (to K.V.).

[2]Senior author.

[3]Author for contact: alistair.mccormick@ed.ac.uk.

The author responsible for distribution of materials integral to the findings presented in this article in accordance with the policy described in the Instructions for Authors (www.plantphysiol.org) is: Alistair J. McCormick (alistair.mccormick@ed.ac.uk).

R.V., G.A.R.G., A.A.S., and A.J.M. designed the study with input from B.W.; R.V., G.A.R.G., A.A.S., A.P., J.M., M.D.G., K.V. performed experiments; V.Z. designed online software; B.W. contributed research reagents and materials; and A.J.M. prepared the manuscript with input from experimentalists and B.W., C.J.H., and D.J.L.-S.

[OPEN] Articles can be viewed without a subscription.

www.plantphysiol.org/cgi/doi/10.1104/pp.18.01401

acquired from Addgene (standardized parts [Kit no. 1000000047] and backbone acceptor vectors [Kit no. 1000000044]; www.addgene.org; Engler et al., 2014). A comparison of the benefits of MoClo- and Gibson assembly-based cloning strategies is shown in Supplemental Information S1. The syntax for level 0 parts was adapted for prokaryotic cyanobacteria to address typical cloning requirements for cyanobacterial research (Fig. 1). New level 0 parts were assembled from a variety of sources (Supplemental Table S1). Level 1, M, and P acceptor vectors were adopted from the MoClo Plant Tool Kit, which facilitates assembly of level 0 parts in a level 1 vector, and subsequently up to seven level 1 modules in level M. Level M assemblies can be combined further into level P and cycled back into level M to produce larger multimodule vectors if required (Supplemental Information S2). Vectors >50 kb in size assembled by MoClo have been reported (Werner et al., 2012). Modules from level 1 or level P can be assembled in new level T vectors designed for cyanobacterial transformation (Fig. 2). We found that both UTEX 2973 and *Synechocystis* produced recombinants following electroporation or conjugation methods with level T vectors. For the majority of the work outlined below, we relied on the conjugation approach.

Integration—Generating Marked and Unmarked Knock-Out Mutants

A common method for engineering stable genomic knock-out and knock-in mutants in several cyanobacteria relies on homologous recombination via integrative (suicide) vectors using a two-step marked-unmarked strategy (Supplemental Information S3; Lea-Smith et al., 2016). Saar et al. (2018) recently used this approach to introduce up to five genomic alterations into a single *Synechocystis* strain. First, marked mutants are generated with an integrative vector carrying two sequences (~1 kb each) identical to the regions of the cyanobacterial chromosome flanking the deletion/insertion site. Two gene cassettes are inserted between these flanking sequences: a levansucrase expression cassette (*sacB*) that confers sensitivity to transgenic colonies grown on Suc and an antibiotic resistance cassette (Ab^R) of choice. Second, unmarked mutants (carrying no selection markers) are generated from fully segregated marked lines using a separate integrative vector carrying only the flanking sequences and selection on plates containing Suc.

We adapted this approach for the CyanoGate system (Fig. 1). To generate level 1 vectors for making knock-out mutants, sequences flanking the upstream (UP FLANK) and downstream (DOWN FLANK) sites of recombination were ligated into the plant MoClo Prom+5U (with overhangs GGAG-AATG) and 3U+Ter (GCTT-CGCT) positions, respectively, to generate new level 0 parts (Fig. 1B). In addition, full expression cassettes were made for Suc selection (*sacB*) and antibiotic resistance (Ab^RSpec, Ab^RKan, and Ab^REry) in level 0 that ligate into positions signal peptide (AATG-AGGT) and coding sequence 2 with stop codon (CDS2 [stop]; AGGT-GCTT), respectively. Marked level 1 modules can be assembled using UP FLANK, DOWN FLANK, *sacB*, and the required Ab^R level 0 part. For generating the corresponding unmarked level 1 module, a short 59-bp linker (UNMARK LINKER) can be ligated into the CDS1ns (no stop codon; AATG-GCTT) position for assembly with an UP FLANK and DOWN FLANK (Fig. 1D). Unmarked and marked level 1 modules can then be assembled into level T integrative vectors, with the potential capacity to include multiple knock-out modules in a single level T vector.

To validate our approach, we constructed the level 0 flanking vectors pC0.024 and pC0.025 and assembled two level T integrative vectors using pUC19-T (*cpcBA*-M and *cpcBA*-UM, with and without the *sacB* and Ab^R cassettes, respectively) to remove the *cpcBA* promoter and operon in *Synechocystis* and generate an "Olive" mutant unable to produce the phycobiliprotein C-phycocyanin (Fig. 3; Supplemental Table S1; Kirst et al., 2014; Lea-Smith et al., 2014). Following transformation with *cpcBA*-M, we successfully generated a marked Δ*cpcBA* mutant carrying the *sacB* and the Ab^RKan cassettes after selective segregation (~3 months; Fig. 3A). The unmarked Δ*cpcBA* mutant was then isolated following transformation of the marked Δ*cpcBA* mutant with *cpcBA*-UM and selection on Suc (~2 weeks; Fig. 3B). Absence of C-phycocyanin in the Olive mutant resulted in a characteristic drop in A_{625} (Fig. 3D) and a significant reduction in chlorophyll content compared to that in wild-type cells (28.4 ± 0.2 and 48.3 ± 0.2 amol chl $cell^{-1}$, respectively; Kirst et al., 2014; Lea-Smith et al., 2014).

Generating Knock-In Mutants

Flexibility in designing level 1 insertion cassettes is needed when making knock-in mutants. Thus, for knock-in mutants the upstream and downstream sequences flanking the insertion site, and any required expression or marker cassettes, are first assembled into separate level 1 modules from UP FLANK and DOWN FLANK level 0 parts (Fig. 1, E and F). Seven level 1 modules can be assembled directly into level T (Fig. 2). Therefore, with a single pair of flanking sequences, up to five level 1 expression cassettes could be included in a level T vector.

Linker parts (20 bp) UP FLANK LINKER and DOWN FLANK LINKER were generated to allow assembly of level 0 UP FLANK and DOWN FLANK parts into separate level 1 acceptor vectors. Similarly, level 0 linker parts were generated for *sacB* and Ab^R (Fig. 1, H and I). Level 1 vectors at different positions can then be assembled in level T (or M) containing one or more expression cassettes, an Ab^R of choice, or both *sacB* and Ab^R (Fig. 2).

Using this approach, CyanoGate can facilitate the generation of knock-in mutants using a variety of strategies. For example, if retention of a resistance

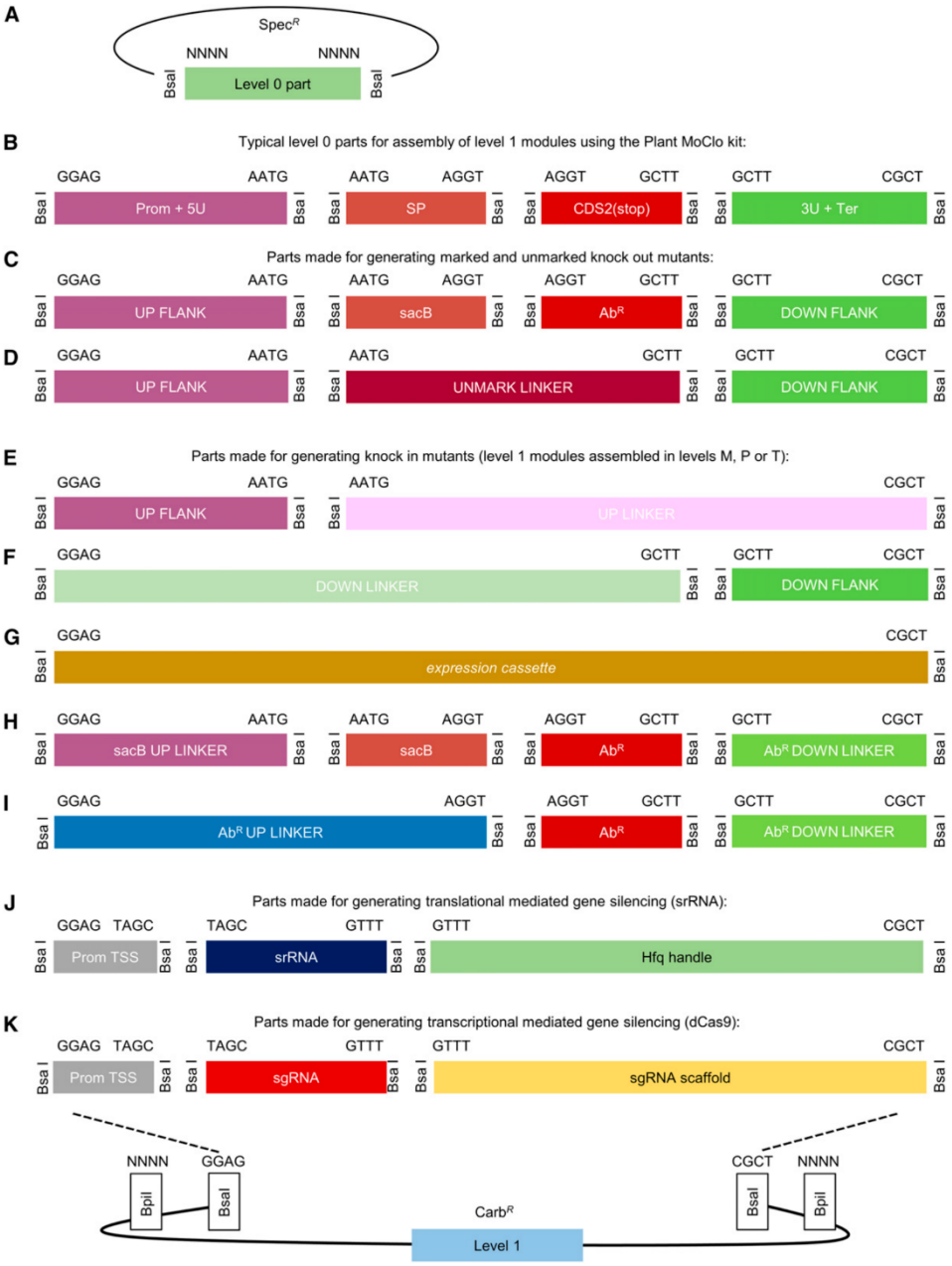

Figure 1. Adaptation of the Plant Golden Gate MoClo level 0 syntax for generating level 1 assemblies for transfer to level T. A, The format for a level 0 MoClo acceptor vector with the part bordered by two BsaI sites. B, Typical level 0 parts from the Plant MoClo kit (Engler et al., 2014), where parts of the same type are bordered by the same pair of fusion sites (for each fusion site, only the sequence of the top strand is shown). Note that the parts are not drawn to scale. C and D, The syntax of the Plant MoClo kit was adapted to generate level 0 parts for engineering marked and unmarked cyanobacterial mutant strains (Lea-Smith et al., 2016). E

marker is not an experimental requirement (e.g. Liberton et al., 2017), only a single antibiotic resistance cassette needs to be included in level T. Alternatively, a two-step marked-unmarked strategy could be followed, as for generating knock-out mutants.

Whereas knock-out strategies can target particular loci, knock-in approaches often rely on recombination at designated NS within the genome of interest that can be disrupted with no or minimal impact on the growth phenotype (Ng et al., 2015; Pinto et al., 2015). Based on loci reported in the literature, we have assembled a suite of flanking regions to target NS in *Synechocystis* (designated 6803 NS1–NS4; Pinto et al., 2015), *Synechococcus* sp. PCC 7002 (PCC 7002 hereafter; designated 7002 NS1 and NS2; Ruffing et al., 2016; Vogel et al., 2017), and NS common to UTEX 2973, PCC 7942 and *S. elongatus* PCC 6301 (designated 7942 NS1-3; Supplemental Table S1; Bustos and Golden, 1992; Kulkarni and Golden, 1997; Andersson et al., 2000; Niederholtmeyer et al., 2010). Pinto et al. (2015) have qualitatively compared the impact of the four *Synechocystis* NS assembled here under several different growth conditions, and observed that insertions at 6803 NS3 and NS4 had no significant effect on growth compared to that of wild-type cultures, whereas insertions at NS2 and NS1 had small but significant effects depending on the growth conditions. Several studies have used 6803 NS3, for example, to engineer a *Synechocystis* strain for the bioremediation of microcystins (Dexter et al., 2018) and the development of T7 polymerase-based synthetic promoter systems (Ferreira et al., 2018). For the two PCC 7002 NS, growth rates with insertions at 7002 NS1 were slightly reduced (Vogel et al., 2017), but not significantly affected with insertions at 7002 NS2 (Ruffing et al., 2016). Insertions at the three 7942 NS reportedly have no phenotypic effect on morphology or growth rate (Clerico et al., 2007; Niederholtmeyer et al., 2010) and have been used to study mRNA stability and translation (Kulkarni and Golden, 1997), circadian rhythms (Andersson et al., 2000), chromosome duplication (Watanabe et al., 2018) and to engineer PCC 7942 for synthesizing heterologous products (Niederholtmeyer et al., 2010; Gao et al., 2016). When using the NS supplied with CyanoGate (or others), we would still recommend a thorough growth analysis under the specific culturing conditions being tested to identify any potential impact of the inserted DNA on growth phenotype.

To validate our system, we generated a level T vector carrying the flanking regions for the *cpcBA* operon and an enhanced yellow fluorescent protein (eYFP) expression cassette (*cpcBA*-eYFP; Fig. 4, A and B; Supplemental Table S1). We successfully transformed this vector into our marked "Olive" *Synechocystis* mutant, and generated a stable olive mutant with constitutive expression of eYFP (Olive-eYFP; Fig. 4C).

Expression Comparison for Promoter Parts in *Synechocystis* and UTEX 2973

We constructed level 0 parts for a wide selection of synthetic promoters and promoters native to *Synechocystis*. Promoters were assembled as expression cassettes driving eYFP in replicative level T vector pPMQAK1-T to test for differences in expression when conjugated into *Synechocystis* or UTEX 2973. We first compared the growth rates of *Synechocystis*, UTEX, and PCC 7942 (a close relative of UTEX 2973 [Yu et al., 2015]) under a variety of different culturing conditions (Supplemental Fig. S1). We found that growth rates were comparable between *Synechocystis* and PCC 7942 at temperatures below 40°C regardless of light levels and supplementation with CO_2. In contrast, UTEX 2973 grew poorly under those conditions. UTEX 2973 only showed an enhanced growth rate at 45°C under the highest light tested (500 μmol photons m^{-2} s^{-1}) with CO_2, whereas all three strains failed to grow at 50°C. These results confirm that the enhanced growth phenotype reported for UTEX 2973 requires specific conditions as reported by Ungerer et al. (2018a, 2018b). Furthermore, they are consistent with recent reports that this phenotype is linked to an increased stress tolerance, which has been attributed to a small number of nucleotide polymorphisms (Lou et al., 2018; Ungerer et al., 2018b). We proceeded with CyanoGate part characterizations and comparisons under the best conditions achievable for *Synechocystis* and UTEX 2973 (see "Materials and Methods"; Supplemental Fig. S2A).

Promoters Native to Synechocystis

We assembled several previously reported promoters from *Synechocystis* in the CyanoGate kit. These include six inducible/repressible promoters (P_{nrsB}, P_{coaT}, P_{nirA}, P_{petE}, P_{isiAB}, and P_{arsB}), which were placed

Figure 1. (*Continued.*)
to l, To generate knock-in mutants, short linker parts (30 bp) were constructed to allow assembly of individual flanking sequences, or marker cassettes (Ab^R or *sacB*), in level 1 vectors for subsequent assembly in level T. J and K, Parts required for generating synthetic srRNA or CRISPRi level 1 constructs. See Supplemental Information S2 and S3 for workflows. 3U+Ter, 3′UTR and terminator; Ab^R, antibiotic resistance cassette; Ab^R DOWN LINKER, short sequence (~30 bp) to provide CGCT overhang; Ab^R UP LINKER, short sequence (~30 bp) to provide GAGG overhang; CDS2(stop), coding sequence with a stop codon; DOWN FLANK, flanking sequence downstream of target site; DOWN FLANK LINKER, short sequence (~30 bp) to provide GGAG overhang; Prom+5U, promoter and 5′ UTR; Prom TSS, promoter transcription start site; *sacB*, levansucrase expression cassette; *sacB* UP LINKER, short sequence (~30 bp) to provide GAGG overhang; sgRNA, single guide RNA; SP, signal peptide; srRNA, small regulatory RNA; UP FLANK, flanking sequence upstream of target site; UP FLANK LINKER, short sequence (~30 bp) to provide CGCT overhang; UNMARK LINKER, short sequence to bridge UP FLANK and DOWN FLANK.

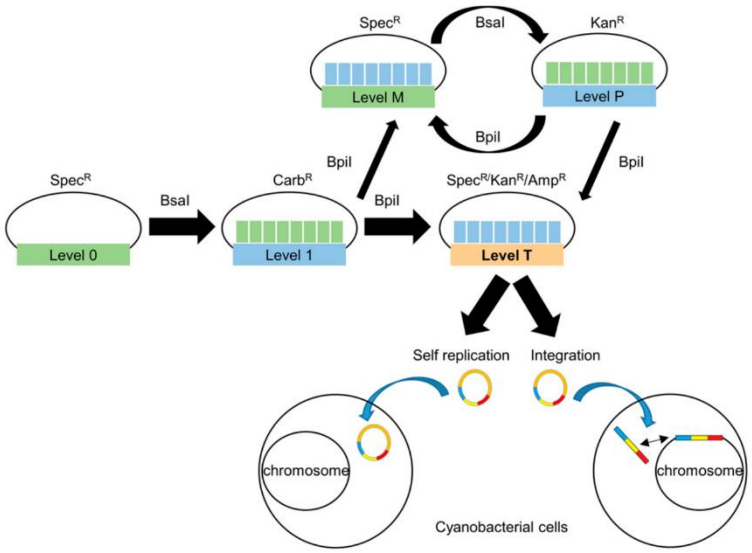

Figure 2. Extension of the Plant Golden Gate MoClo Assembly Standard for cyanobacterial transformation. Assembly relies on one of two Type IIS restriction endonuclease enzymes (*Bsa*I or *Bpi*I). Domesticated level 0 parts are assembled into level 1 vectors. Up to seven level 1 modules can be assembled directly into a level T cyanobacterial transformation vector, which consists of two subtypes (either a replicative or an integrative vector). Alternatively, larger vectors with more modules can be built by assembling level 1 modules into level M, then cycling assembly between level M and level P, and finally transferring from level P to level T. Antibiotic selection markers are shown for each level. Level T vectors are supplied with internal antibiotic selection markers (shown), but additional selection markers could be included from level 1 modules as required. See Supplemental Table S1 and Supplemental Information S4 for the full list and maps of level T acceptor vectors.

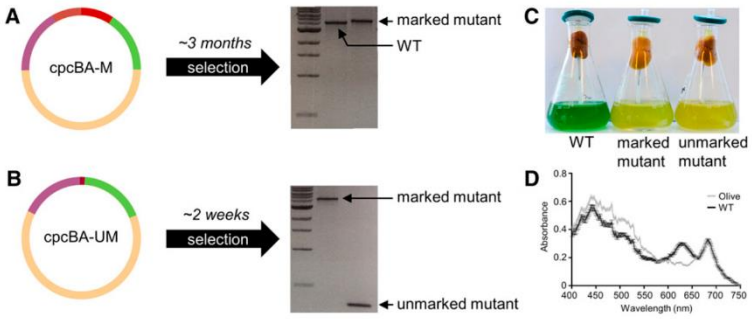

Figure 3. Generating knock-out mutants in cyanobacteria. A, Assembled level T vector *cpcBA*-M (see Fig. 1C) targeting the *cpcBA* promoter and operon (3,563 bp) to generate a marked Δ*cpcBA* "Olive" mutant in *Synechocystis* sp. PCC 6803. Following transformation and segregation on kanamycin (~3 months), a segregated marked mutant was isolated (wild-type [WT] band is 3,925 bp, marked mutant band is 5,503 bp, 1-kb DNA ladder [New England Biolabs] is shown). B, Assembled level T vector *cpcBA*-UM (see Fig. 1D) for generating an unmarked Δ*cpcBA* mutant. Following transformation and segregation on Suc (~2 weeks), an unmarked mutant was isolated (unmarked band is 425 bp). C, Liquid cultures of wild type and marked and unmarked Olive mutants. D, Spectrum showing the absorbance of the unmarked Olive mutant and wild-type cultures after 72 h of growth. Values are the average of four biological replicates ± SE and are standardized to 750 nm.

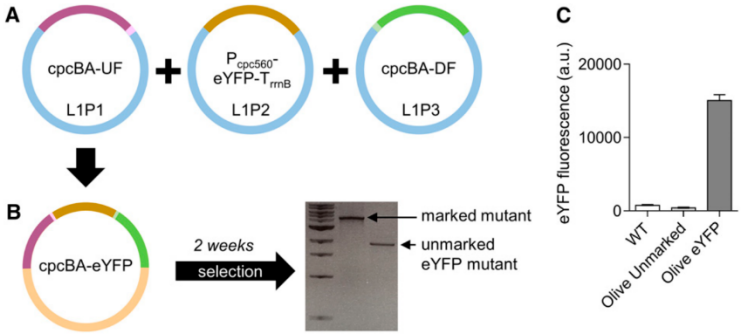

Figure 4. Generating knock-in mutants in cyanobacteria. A, Assembly of level 1 modules *cpcBA*-UF (see Fig. 1E) in the level 1, position 1 acceptor (L1P1), P_{cpc560}-eYFP-T_{rrnB} (see Fig. 1G) in L1P2, and *cpcBA*-DF (see Fig. 1F) in L1P3. B, Transfer of level 1 assemblies to level T vector *cpcBA*-eYFP for generating an unmarked Δ*cpcBA* mutant carrying an eYFP expression cassette. Following transformation and segregation on Suc (~3 weeks), an unmarked eYFP mutant was isolated (1,771 bp). C, Fluorescence values are the means ± SE of four biological replicates, where each replicate represents the median measurements of 10,000 cells.

in front of the strong, synthetic *Synechocystis* ribosomal binding site (RBS; Heidorn et al., 2011) as used in Englund et al. (2016; Supplemental Table S1; Supplemental Information S4). P_{nrsB} and P_{coaT} drive the expression of nickel and cobalt ion efflux pumps and are induced by Ni^{2+}, and Co^{2+} or Zn^{2+}, respectively (Peca et al., 2008; Blasi et al., 2012; Guerrero et al., 2012; Englund et al., 2016). P_{nirA}, from the nitrate assimilation operon, is induced by the presence of NO_3^- and/or NO_2^- (Kikuchi et al., 1996; Qi et al., 2005). P_{petE} drives the expression of plastocyanin and is induced by Cu^{2+}, which has previously been used for the expression of heterologous genes (Guerrero et al., 2012; Camsund et al., 2014). The promoter of the *isiAB* operon (P_{isiAB}) is repressed by Fe^{3+} and activated when the cell is under iron stress (Kunert et al., 2003). P_{arsB} drives the expression of a putative arsenite and antimonite carrier and is activated by AsO_2^- (Blasi et al., 2012).

We also cloned the *rnpB* promoter, P_{rnpB}, from the RNase P gene (Huang et al., 2010), a long version of the *psbA2* promoter, P_{psbA2L}, from the Photosystem II protein D1 gene (Lindberg et al., 2010; Englund et al., 2016) and the promoter of the C-phycocyanin operon, P_{cpc560} (also known as P_{cpcB} and P_{cpcBA}; Zhou et al., 2014). P_{rnpB} and P_{psbA2L} were placed in front of RBS (Fig. 5A; Heidorn et al., 2011). To build on a previous functional characterization of P_{cpc560} (Zhou et al., 2014), we assembled four variants of this strong promoter. First, $P_{cpc560+A}$ consisted of the promoter and the 4-bp MoClo overhang AATG. Second, P_{cpc560} was truncated by 1 bp (Fig. 5A, A), so that the start codon was aligned with the native P_{cpc560} RBS spacer region length. Zhou et al. (2014) identified 14 predicted transcription factor binding sites (TFBSs) in the upstream region of P_{cpc560} (−556 to −381 bp) and removal of this region resulted in a significant loss of promoter activity. However, alignment of the reported TFBSs showed that their locations are in the downstream region of the promoter (−180 to −5 bp). We identified 11 additional predicted TFBSs using Virtual Footprint (Münch et al., 2005) in the upstream region and hypothesized that the promoter activity may be modified by duplicating either of these regions. So, third, we generated P_{cpc560_Dx2} containing a duplicated downstream TFBS region. For P_{cpc560_Dx2}, only the region between −31 to −180 bp was duplicated to avoid repeating the Shine-Dalgarno sequence. Fourth, we duplicated the upstream region to generate P_{cpc560_Ux2}. We then assembled P_{rnpB}, P_{psbA2L}, and the four P_{cpc560} variants with eYFP and the *rrnB* terminator (T_{rrnB}) into a level 1 expression cassette, and subsequently into a level T replicative vector (pPMQAK1-T) for expression analysis (Supplemental Table S2).

In *Synechocystis* the highest-expressing promoter was P_{cpc560} (Fig. 5B), which indicated that maintaining the native RBS spacer region for P_{cpc560} is important for maximizing expression. Neither P_{cpc560_Dx2} nor P_{cpc560_Ux2} resulted in higher expression levels compared to that of P_{cpc560}. P_{cpc560_Dx2}–driven expression was strongly decreased compared to expression driven by P_{cpc560}, suggesting that promoter function is sensitive to modification of the downstream region and this region could be a useful target for modulating P_{cpc560} efficacy. Previous work in *Synechocystis* has suggested that modification of the middle region of P_{cpc560} (−380 to −181 bp) may also affect function (Lea-Smith et al., 2014). P_{psbA2L} produced lower expression levels than any variant of P_{cpc560} in *Synechocystis*, whereas P_{rnpB} produced the lowest expression levels. The observed differences in expression levels are consistent with those in other studies with *Synechocystis* (Camsund et al., 2014; Englund et al., 2016; Liu and Pakrasi, 2018).

In UTEX 2973, the trend in expression patterns was similar to that in *Synechocystis* (Fig. 5B). However, the overall expression levels of eYFP measured in UTEX 2973 were significantly higher than in *Synechocystis*. P_{cpc560} was increased by 30%, whereas P_{rnpB} showed a 20-fold increase in expression relative to *Synechocystis*.

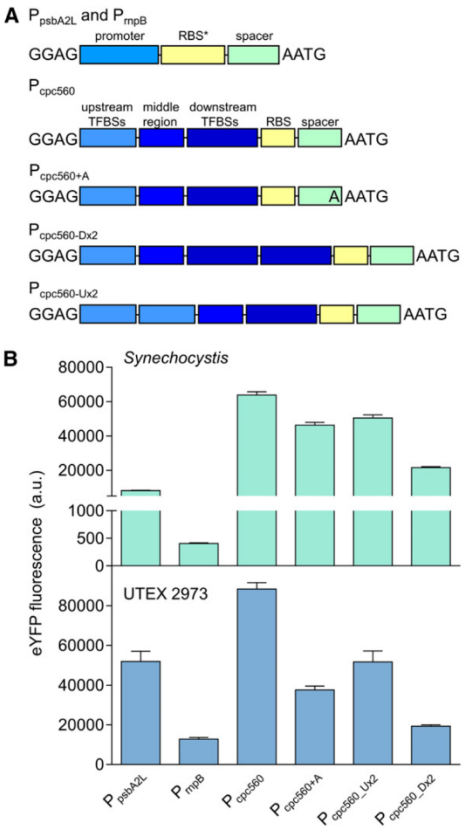

Figure 5. Expression levels of cyanobacterial promoters in *Synechocystis* and UTEX 2973. A, Structure of the cyanobacterial promoters adapted for the CyanoGate kit. Regions of P_{cpc560} shown are the TFBSs (−556 to −381 bp), middle region (−380 to −181 bp), and the downstream TFBSs, RBS, and spacer (−180 to −5 bp). B, Expression levels of eYFP driven by promoters in *Synechocystis* and UTEX 2973 calculated from measurements taken from 10,000 individual cells. Values are the means ± SE from at least four biological replicates after 48 h of growth (average OD_{750} values for *Synechocystis* and UTEX 2973 cultures were 3.5 ± 0.2 and 3.6 ± 0.2, respectively). See Supplemental Figure S2 for more info.

The relative expression strength of P_{psbA2L} was also higher than in *Synechocystis*, and second only to P_{cpc560} in UTEX 2973. As promoters derived from P_{psbA} are responsive to increasing light levels (Englund et al., 2016), the increased levels of expression for P_{psbA2L} may be associated with the higher light intensities used for growing UTEX 2973 compared to that used for growing *Synechocystis*. Background fluorescence levels were similar between UTEX 2973 and *Synechocystis* conjugated with an empty pPMQAK1-T vector (i.e. lacking an eYFP expression cassette), which suggested that the higher fluorescence values in UTEX 2973 were a direct result of increased levels of eYFP protein.

Heterologous and Synthetic Promoters

A suite of 20 constitutive synthetic promoters was assembled in level 0 based on the modified BioBricks BBa_J23119 library of promoters (Markley et al., 2015), and the synthetic P_{trc10}, P_{tic10}, and P_{tac10} promoters (Supplemental Table S1; Supplemental Information S4; Huang et al., 2010; Albers et al., 2015). We retained the broad-range BBa_B0034 RBS (AAAGAGGAGAAA) and *lac* operator (*lacO*) from Huang et al. (2010) for future *lacI*-based repression experiments (*lacI* and the P_{lacIQ} promoter are included in the CyanoGate kit; Bahl et al., 1977). We cloned eight new variants (J23119MH_V01-8) with mutations in the canonical BBa_J23119 promoter sequence (Fig. 6A). Additionally, we included the L-arabinose-inducible promoter from *E. coli* (P_{BAD}; Abe et al., 2014).

We encountered an unexpected challenge with random internal deletions in the −35 and −10 regions of some promoters of the BBa_J23119 library and *trc* promoter variants when cloning them into level 0 acceptors. Similar issues were reported previously for the *E. coli* EcoFlex kit (Moore et al., 2016) that may relate to the functionality of the promoters and the host vector copy number in *E. coli*, which consequently resulted in cell toxicity and selection for mutated promoter variants. To resolve this issue, we generated a low copy level 0 promoter acceptor vector compatible with CyanoGate (pSB4K5 acceptor) for cloning recalcitrant promoters (Supplemental Table S1; Supplemental Information S4). Subsequent assemblies in levels 1 and T showed no indication of further mutation.

We then tested the expression levels of eYFP driven by the synthetic promoters in *Synechocystis* and UTEX 2973 following assembly in pPMQAK1-T (Fig. 6B; Supplemental Table S2). The synthetic promoters showed a 120-fold dynamic range in both cyanobacterial strains. Furthermore, a similar trend in promoter expression strength was observed (R^2 = 0.84; Fig. 6C). However, eYFP expression levels were on average 8-fold higher in UTEX 2973 compared to that in *Synechocystis*. In *Synechocystis*, the highest expression levels were observed for J23119 and P_{trc10}, but these were still ~50% lower than values for the native P_{cpc560} promoters (Fig. 5B). The expression trends for the BBa_J23119 library were consistent with the subset reported by Camsund et al. (2014) in *Synechocystis*, whereas the observed differences between P_{trc10} and P_{cpc560} were similar to those reported by Liu and Pakrasi (2018).

In contrast, the expression levels in UTEX 2973 for J23119 were ~50% higher than that for P_{cpc560}. Several synthetic promoters showed expression levels in a similar range to those for the native P_{cpc560} promoter variants, including P_{trc10}, J23111, and the J23119 variant V02. V02 is identical to J23111 except for an additional "G" between the −35 and −10 motifs, suggesting that small changes in the length of this spacer region may not be critical for promoter strength (similar expression levels were also observed for these two promoters in *Synechocystis*). In contrast, a single bp difference

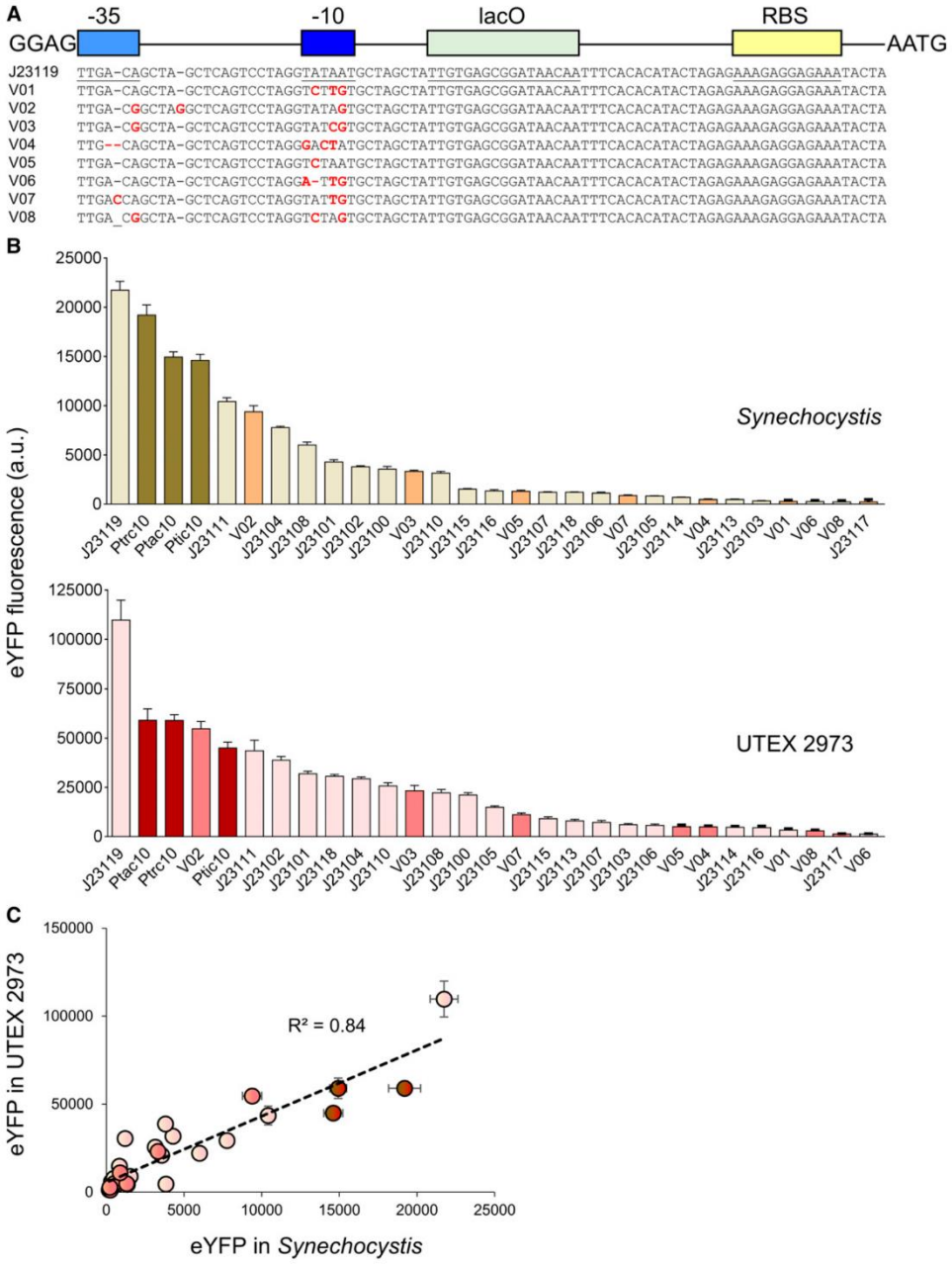

Figure 6. Expression levels of heterologous and synthetic promoters in *Synechocystis* and UTEX 2973. A, Structure and alignment of eight new synthetic promoters derived from the BioBricks BBa_J23119 library and P_{trc10} promoter design (Huang et al., 2010). B, Expression levels of eYFP driven by promoters in *Synechocystis* and UTEX 2973 calculated from measurements taken from 10,000 individual cells. C, Correlation analysis of expression levels of synthetic promoters tested in *Synechocystis* and UTEX 2973. The coefficient of determination (R^2) is shown for the J23119 library (red), new synthetic promoters (pink), and *trc* variants

between J23111 and J23106 in the −35 motif resulted in an 8- and 10-fold reduction in expression in *Synechocystis* and UTEX 2973, respectively. The results for UTEX 2973 were unexpected, and to our knowledge no studies to date have directly compared these promoters in this strain. Recent work has examined the expression of β-galactosidase using promoters such as P_{cpc560} and P_{trc} in UTEX 2973 (Li et al., 2018). Li et al. (2018) highlighted that different growth environments (e.g. light levels) can have significant effects on protein expression. Changes in culture density can also affect promoter activity, such that protein expression levels can change during the exponential and stationary growth stages depending on the promoter and expression vector used (Ng et al., 2015; Madsen et al., 2018). Here we tracked eYFP expression levels over time for 3 d during the early and late exponential growth phases for *Synechocystis* and UTEX 2973. Although expression levels for each promoter fluctuated over time, with peak expression levels at 24 h and 48 h in UTEX 2973 and *Synechocystis*, respectively, the overall expression trends were generally consistent for the two strains (Supplemental Fig. S2B).

Protein Expression Levels in *Synechocystis* and UTEX 2973

To investigate further the increased levels of eYFP expression observed in UTEX 2973 compared to that in *Synechocystis*, we examined cell morphology, protein content, and eYFP protein abundances in expression lines for each strain. Confocal image analysis confirmed the coccoid and rod shapes of *Synechocystis* and UTEX 2973, respectively, and the differences in cell size (Fig. 7A; van de Meene et al., 2006; Yu et al., 2015). Immunoblot analyses of eYFP from protein extracts of four eYFP-expressing strains correlated well with previous flow cytometry measurements (Figs. 5 and 6). eYFP driven by the J23119 promoter in UTEX 2973 produced the highest levels of eYFP protein (Fig. 7, B and C). Although the density of cells in culture was 2-fold higher in *Synechocystis* compared to that in UTEX 2973 (Fig. 7D), the protein content per cell was 6-fold lower (Fig. 7E). We then estimated the average cell volumes for *Synechocystis* and UTEX 2973 at 3.91 ± 0.106 μm^3 and 6.83 ± 0.166 μm^3 (n = 50 each), respectively, based on measurements from confocal microscopy images (Supplemental Fig. S3). Based on those estimates, we calculated that the density of soluble protein per cell was 4-fold higher in UTEX 2973 compared to that in *Synechocystis* (Fig. 7F). Thus, we hypothesized that the enhanced levels of eYFP observed in UTEX 2973 were a result of the expression system harnessing a larger available amino acid pool. Mueller et al. (2017) have reported that UTEX 2973 has an increased investment in amino acid content compared to that in PCC 7942, which may be linked to higher rates of translation in UTEX 2973. Therefore, UTEX 2973 continues to show promise as a bioplatform for generating heterologous protein products, although future work should study production rates under conditions optimal for faster growth (Lou et al., 2018; Ungerer et al., 2018a). Recent characterization of the UTEX 2973 transcriptome will also assist with native promoter characterizations (Tan et al., 2018).

The RK2 Origin of Replication Is Functional in *Synechocystis*

Synthetic biology tools (e.g. gene expression circuits, CRISPR/Cas-based systems) are often distributed between multiple plasmid vectors at different copy numbers in order to synthesize each component at the required concentration (Bradley et al., 2016). The large RSF1010 vector is able to replicate in a broad range of microbes including gram-negative bacteria such as *E. coli* and several cyanobacterial species. However, for 25 years it has remained the only nonnative vector reported to be able to self-replicate in cyanobacteria (Mermet-Bouvier et al., 1993). Recently, two small plasmids native to *Synechocystis*, pCA2.4 and pCB2.4, have been engineered for gene expression (Armshaw et al., 2015; Ng et al., 2015; Liu and Pakrasi, 2018). The pANS plasmid (native to PCC 7942) has also been adapted as a replicative vector, but so far it has been only shown to function in PCC 7942 and *Anabaena* PCC 7120 (Chen et al., 2016). Similarly, the high copy number plasmid pAQ1 (native to PCC 7002) has been engineered for heterologous expression, but up to now it has only been used in PCC 7002 (Xu et al., 2011). To expand the replication origins available for cyanobacterial research further we tested the capacity for vectors from the Standard European Vector Architecture (SEVA) library to replicate in *Synechocystis* (Silva-Rocha et al., 2013).

We acquired three vectors driven by three different replication origins (pSEVA421 [RK2], pSEVA431 [pBBR1], and pSEVA442 [pRO1600/ColE1]) and carrying a spectinomycin antibiotic resistance marker. These vectors were domesticated and modified as level T acceptor vectors, assembled, and then transformed into *Synechocystis* by electroporation or conjugation. Only *Synechocystis* strains conjugated with vectors carrying RK2 (pSEVA421-T) grew on spectinomycin-containing plates (Supplemental Table S1; Supplemental Information S4). To confirm that RSF1010 and RK2 replication origins can replicate autonomously in *Synechocystis*, we recovered the pPMQAK1-T or pSEVA421-T vector from lysates of axenic *Synechocystis* strains previously conjugated with each vector by

Figure 6. (*Continued.*)
(dark red). Values are the means ± SE from at least four biological replicates after 48 h of growth (average OD_{750} values for *Synechocystis* and UTEX 2973 cultures were 3.5 ± 0.2 and 3.6 ± 0.2, respectively). See Supplemental Figure S2 for more info.

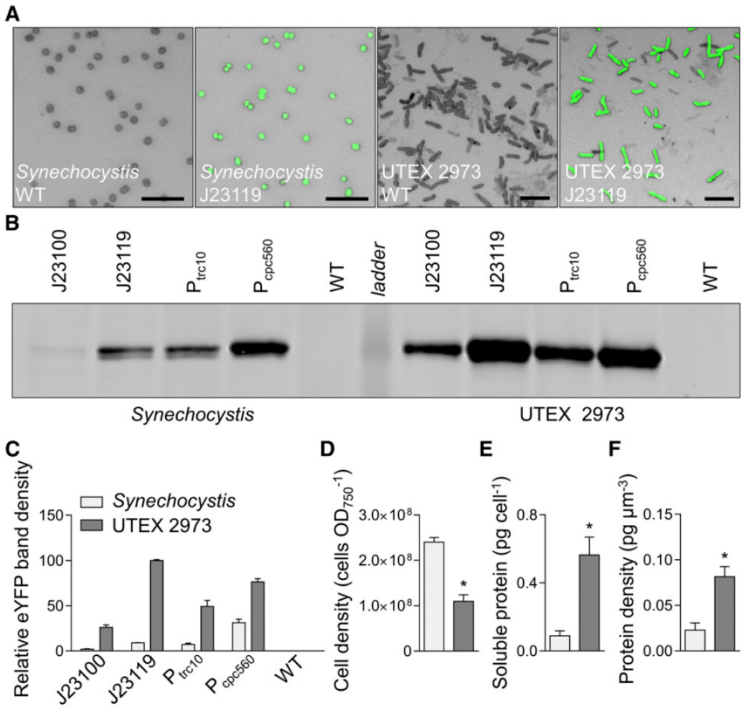

Figure 7. Protein expression levels in *Synechocystis* and UTEX 2973 cells. A, Confocal images of wild-type (WT) strains and mutants expressing eYFP (eYFP fluorescence shown in green on bright field images) driven by the J23119 promoter (bars = 10 μm). B, Representative immunoblot of protein extracts (3 μg protein) from mutants with different promoter expression cassettes (as in Fig. 6) probed with an antibody against eYFP. The protein ladder band corresponds to 30 kD. C, Relative eYFP protein abundance relative to that in UTEX 2973 mutants carrying the J23119 expression cassette. D to F, Cell density (D), protein content per cell (E), and protein density per estimated cell volume (F) for *Synechocystis* and UTEX 2973. Asterisks (*) indicate significant difference ($P < 0.05$) as determined by Student's *t* test. Values are the means ± SE of four biological replicates.

transformation into *E. coli*. The identity and integrity of pPMQAK1-T and pSEVA421-T extracted from transformed *E. coli* colonies were confirmed by restriction digest and Sanger sequencing.

We then assembled two level T vectors with an eYFP expression cassette (P_{cpc560}-eYFP-T_{rrnB}) to produce pPMQAK1-T-eYFP and pSEVA421-T-eYFP, which were conjugated into *Synechocystis* (Fig. 8; Supplemental Table S2). Both pPMQAK1-T-eYFP and pSEVA421-T-eYFP transconjugates grew at similar rates in 50 μg mL^{-1} kanamycin and 5 μg mL^{-1} spectinomycin, respectively (Fig. 8A). However, eYFP levels were 8-fold lower in pSEVA421-T-eYFP, suggesting that RK2 has a reduced copy number relative to RSF1010 in *Synechocystis* (Fig. 8B). We measured the heterologous plasmid vector copy number in strains expressing pSEVA421-T or pPMQAK1-T and estimated an average copy number per cell of 9 ± 2 and 31 ± 5, respectively (Fig. 8C). The copy number for pPMQAK1-T was similar to values reported previously for RSF1010-derived vectors in *Synechocystis* (~30; Ng et al., 2000). Our results are also consistent with the lower copy numbers in *E. coli* for vectors with RK2 (4 to 7 copies) compared to those with RSF1010 (10 to 12 copies) replication origins (Frey et al., 1992; Blasina et al., 1996). Furthermore, we compared the genome copies per cell between transformants and wild-type strains and found no significant differences—the average value was 11 ± 2, which is consistent with the typical range of genome copy numbers observed in *Synechocystis* cells (Zerulla et al., 2016).

Gene Repression Systems

CRISPR interference (CRISPRi) is a relatively new but well characterized tool for modulating gene expression at the transcription stage in a sequence-specific manner (Qi et al., 2013; Behler et al., 2018). CRISPRi typically uses a nuclease-deficient Cas9 from *Streptococcus pyogenes* (dCas9) and has been demonstrated to work in several cyanobacterial species, including *Synechocystis* (Yao et al., 2016), PCC 7002 (Gordon et al., 2016), PCC 7942 (Huang et al., 2016), and *Anabaena* sp. PCC 7120 (Higo et al., 2018). A second approach for gene repression uses rationally designed small regulatory RNAs (srRNAs) to regulate gene expression at the translation stage (Na et al., 2013; Higo et al., 2016). The synthetic srRNA is attached to a scaffold to recruit the Hfq protein, an RNA chaperone that is conserved in a wide range of bacteria and cyanobacteria, which facilitates the hybridization of srRNA and target mRNA, and directs mRNA for degradation. The role of cyanobacterial Hfq in interacting with synthetic srRNAs is still unclear (Zess et al., 2016). However, regulatory ability can be improved by

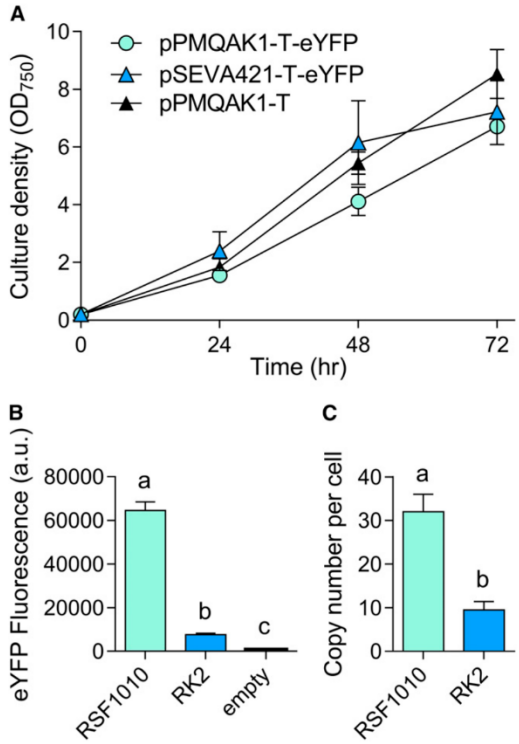

Figure 8. Cell growth and expression levels of eYFP with the RK2 replicative origin in *Synechocystis*. A, Growth of strains carrying RK2 (vector pSEVA421-T-eYFP), RSF1010 (pPMQAK1-T-eYFP), or empty pPMQAK1-T, with cultures containing appropriate antibiotic selection. Growth was measured as OD_{750} under a constant illumination of 100 μmol photons m^{-2} s^{-1} at 30°C. B, Expression levels of eYFP after 48 h of growth calculated from measurements taken from 10,000 individual cells. C, Plasmid copy numbers per cell after 48 h of growth. Lowercase letters indicating significant difference ($P < 0.05$) are shown, as determined by ANOVA followed by Tukey's honestly significant difference tests. Values are the means ± SE of four biological replicates.

introducing Hfq from *E. coli* into *Synechocystis* (Sakai et al., 2015). Both CRISPRi- and srRNA-based systems have potential advantages as they can be used to repress multiple genes simultaneously.

To validate the CRISPRi system, we assembled an expression cassette for dCas9 (P_{cpc560}-dCas9-T_{rrnB}) on the level 1 position 1 vector pICH47732, and four different sgRNA (single guide RNA) expression cassettes (P_{trc10_TSS}-sgRNA-sgRNA scaffold) targeting eYFP on the level 1 position 2 vector pICH47742 (Supplemental Table S2; Engler et al., 2014). For assembly of CRISPRi sgRNA expression cassettes in level 1, we targeted four 18- to 22-bp regions of the eYFP nontemplate strand with an adjacent 3′ protospacer adjacent motif of 5′-NGG-3′, as required by *S. pyogenes* dCas9 (Fig. 9A). The sgRNA sequences contained no off-target sites in the *Synechocystis* genome (confirmed by CasOT; Xiao et al., 2014). The sgRNAs were made by PCR using two complementary primers carrying the required overhangs and *Bsa*I sites, and were assembled with the P_{trc10_TSS} promoter (pC0.220) and the sgRNA scaffold (pC0.122). Level T vectors were assembled carrying dCas9 and a single sgRNA, or just the sgRNA alone. We subsequently conjugated the Olive-eYFP mutant and tracked eYFP expression.

Transconjugates carrying only the sgRNA showed no reduction in eYFP level compared to that in non-transconjugated Olive-eYFP (Fig. 9B). However, all strains carrying dCas9 and a sgRNA showed a decrease in eYFP that ranged from 40% to 90% depending on the sgRNA used. These reductions are similar to those observed previously in PCC 7002 and in *Synechocystis* (Gordon et al., 2016; Yao et al., 2016) and demonstrated that CRISPRi system is functional in the CyanoGate kit.

CONCLUSION

The CyanoGate kit was designed to increase the availability of well characterized libraries and standardized

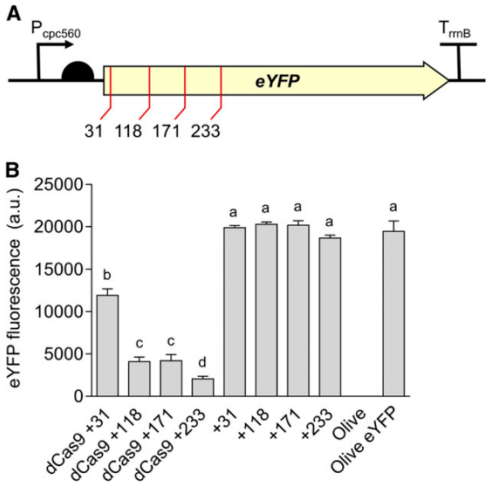

Figure 9. Gene regulation system using CRISPRi in *Synechocystis*. A, Four target regions were chosen as sgRNA protospacers to repress eYFP expression in Olive-eYFP (Fig. 4): "CCAGGATGGGCACCACCC" (+31), "ACTTCAGGGTCAGCTTGCCGT" (+118), "AGGTGGTCACGAGGG TGGGCCA" (+171), and "AGAAGTCGTGCTGCTTCATG" (+233). B, eYFP fluorescence of Olive-eYFP expressing constructs carrying sgRNAs with and without dCas9 (representative of 10,000 individual cells). Untransformed Olive-eYFP and the Olive mutant were used as controls. Lowercase letters indicating significant difference ($P < 0.05$) are shown, as determined by ANOVA followed by Tukey's honestly significant difference tests. Values are the means ± SE of four biological replicates.

modular parts in cyanobacteria (Sun et al., 2018). We aimed to simplify and accelerate modular cloning methods in cyanobacterial research and allow integration with the growing number of labs that rely on the established common plant and algal syntax for multipart DNA assembly (Patron et al., 2015; Crozet et al., 2018). Here, we have demonstrated the functionality of CyanoGate in sufficient detail to show that it is straightforward to adopt and functionally robust across two different cyanobacterial species. CyanoGate includes parts for usage in other cyanobacterial species and could likely be utilized also in noncyanobacterial microbes amenable to transformation (e.g. *Rhodopseudomonas* spp.) and adapted for use in subcellular eukaryotic compartments of prokaryote origin (e.g. chloroplasts; Economou et al., 2014; Doud et al., 2017; Leonard et al., 2018). In addition to the parts discussed, we have also assembled a suite of 21 terminators (Supplemental Table S1). To increase the accessibility and usability of the CyanoGate, we have included the vector maps for all parts and new acceptors (Supplemental Information S4), implemented support for Cyanogate assemblies in the online DNA "Design and Build" portal of the Edinburgh Genome Foundry (dab.genomefoundry.org; Supplemental Information S5), and submitted all vectors as a toolkit for order from Addgene (Addgene Kit #1000000146; www.addgene.org/kits/mccormick-cyanogate).

Standardization will help to accelerate the development of reliable synthetic biology tools for biotechnological applications and promote sharing and evaluation of genetic parts in different species and under different culturing conditions (Patron et al., 2015). Going forward, it will be important to test the performance of different parts with different components (e.g. gene expression cassettes) and in different assembly combinations. Several groups using plant MoClo assembly have reported differences in cassette expression and functionality depending on position and orientations (e.g. Ordon et al., 2017), which highlights a key synthetic biology crux—the performance of a system is not simply the sum of its components (Mutalik et al., 2013; Heyduk and Heyduk, 2018).

The increasing availability of genome-scale metabolic models for different cyanobacterial species and their utilization for guiding engineering strategies for producing heterologous high-value biochemicals has helped to reinvigorate interest in the industrial potential of cyanobacteria (Knoop et al., 2013; Hendry et al., 2016; Mohammadi et al., 2016; Shirai et al., 2016). Future efforts should focus on combining genome-scale metabolic models with synthetic biology approaches, which may help to overcome the production yield limitations observed for cyanobacterial cell factories (Nielsen et al., 2016), and will accelerate the development of more complex and precise gene control circuit systems that can better integrate with host metabolism and generate more robust strains (Bradley and Wang, 2015; Jusiak et al., 2016; Luan and Lu, 2018). The future development of truly "programmable" photosynthetic cells could provide significant advancements in addressing fundamental biological questions and tackling global challenges, including health and food security (Dobrin et al., 2016; Medford and Prasad, 2016; Smanski et al., 2016).

MATERIALS AND METHODS

Cyanobacterial Culture Conditions

Cyanobacterial strains of *Synechocystis*, UTEX 2973, and *Synechococcus elongatus* PCC 7942 (PCC 7942 hereafter) were maintained on 1.5% (w/v) agar plates containing BG11 (Blue-Green) medium. Liquid cultures were grown in Erlenmeyer flasks (100 mL) containing BG11 medium (Rippka et al., 1979) supplemented with 10 mM $NaHCO_3$, shaken at 100 rpm and aerated with filter-sterilized water-saturated atmospheric air. *Synechocystis* and PCC 7942 strains were grown at 30°C with continuous light (100 μmol photons m^{-2} s^{-1}) and UTEX 2793 strains were grown at 40°C with 300 μmol photons m^{-2} s^{-1} in an Infors Multitron-Pro supplied with warm white LED lighting (Infors HT).

Growth Analysis

Growth of *Synechocystis*, UTEX 2973, and PCC 7942 was measured in a Photon Systems Instrument Multicultivator MC 1000-OD (MC). Starter cultures were grown in a Photon Systems Instrument AlgaeTron AG 230 at 30°C under continuous warm-white light (100 μmol photons m^{-2} s^{-1}) with air bubbling and shaken at 160 rpm unless otherwise indicated. These were grown to an optical density at 750 nm (OD_{750}) of ~1.0 and used to seed 80-mL cultures for growth in the MC at a starting OD_{720} of ~0.2 (the MC measures culture growth at OD_{720}). Cultures were then grown under continuous warm-white light at 30°C (300 μmol photons m^{-2} s^{-1}) with air bubbling or 30°C (300 or 500 μmol photons m^{-2} s^{-1}) or 41°C, 45°C, and 50°C (500 μmol photons m^{-2} s^{-1}) with 5% CO_2 bubbling until the fastest grown strain was at OD_{720} = ~0.9, the maximum accurate OD that can be measured with this device. A total of five to six replicate experiments were performed over two separate runs (16 in total), each inoculated from a different starter culture.

Vector Construction

Level 0 Vectors

Native cyanobacterial genetic parts were amplified from genomic DNA using New England Biolabs Q5 High-Fidelity DNA Polymerase (Fig. 1; Supplemental Table S1). Where necessary, native genetic parts were domesticated (i.e. *Bsa*I and *Bpi*I sites were removed) using specific primers. Alternatively, parts were synthesized as Gblocks DNA fragments (Integrated DNA Technology) and cloned directly into an appropriate level 0 acceptor (see Supplemental Information S4 for vector maps; Engler et al., 2014).

Golden Gate assembly reactions were performed with restriction enzymes *Bsa*I (New England Biolabs) or *Bpi*I (Thermo Fisher Scientific), and T4 DNA ligase (Thermo Fisher Scientific; see Supplemental Information S2, S3, and S6 for detailed protocols). Vectors were transformed into One Shot TOP10 chemically competent *Escherichia coli* (Thermo Fisher Scientific) as per the manufacturer's instructions. Transformed cultures were grown at 37°C on 1.5% (w/v) LB agar plates or in liquid LB medium shaking at 260 rpm, with appropriate antibiotic selection for levels 0, 1, M and P vectors as outlined in Engler et al. (2014).

Level T Acceptor Vectors and New Level 0 Acceptors

A new level T vector system was designed that provides MoClo-compatible replicative vectors or integrative vectors for genomic modifications in cyanobacteria (Fig. 2; Supplemental Table S1; Supplemental Information S4; Heidorn et al., 2011). For replicative vectors, we modified the pPMQAK1 carrying an RSF1010 replicative origin (Huang et al., 2010) to make pPMQAK1-T, and vector pSEVA421 from the SEVA 2.0 database (seva.cnb.csic.es) carrying the RK2 replicative origin to make pSEVA421-T (Silva-Rocha et al., 2013). Replicative vector backbones were domesticated to remove native *Bsa*I and *Bpi*I sites

where appropriate. The region between the BioBrick's prefix and suffix was then replaced by a *lacZ* expression cassette flanked by two *Bpi*I sites that produce overhangs TGCC and GGGA, which are compatible with the plant Golden Gate MoClo assembly syntax for level 2 acceptors (e.g. pAGM4673; Engler et al., 2014). For integrative vectors, we domesticated a pUC19 vector backbone and introduced two *Bpi*I sites compatible with a level 2 acceptor (as above) to make pUC19A-T and pUC19S-T. In addition, we made a new low copy level 0 acceptor (pSC101 origin of replication) for promoter parts based on the BioBrick standard vector pSB4K5 (Liu et al., 2018). DNA was amplified using New England Biolabs Q5 High-Fidelity DNA Polymerase (New England Biolabs). All vectors were sequenced following assembly to confirm domestication and the integrity of the MoClo cloning site.

Level 0 Parts for CRISPRi and srRNA

A nuclease deficient Cas9 gene sequence sourced from Addgene (www.addgene.org/44249/) was domesticated and assembled as a level 0 CDS part (Supplemental Tables S1 and S2; Qi et al., 2013). Five promoters of different strengths were truncated to the transcriptional start site (TSS) and cloned into a new level 0 acceptor vector with the unique overhangs GGAG and TAGC (Fig. 1). Two new level 0 parts with the unique overhangs GTTT and CGCT were generated for the sgRNA scaffold and srRNA host factor-I protein handle (based on MicC; Na et al., 2013), respectively. Assembly of level 1 expression cassettes proceeded by combining appropriate level 0 parts with a PCR product for either a srRNA or sgRNA (Fig. 1).

Cyanobacterial Transformation and Conjugation

Transformation with integrative level T vectors was performed as in Lea-Smith et al. (2016). For transformation by electroporation, cultures were harvested during the exponential growth phase (OD_{750} of ~0.6) by centrifugation at 4,000 *g* for 10 min. The cell pellet was washed 3 times with 2 mL of sterile 1 mM HEPES buffer (pH 7.5), resuspended in water with 3–5 μg of level T vector DNA and transferred into a 0.1-cm electroporation cuvette (Scientific Laboratory Suppliers). Resuspended cells were electroporated using an Eppendorf 2510 electroporator (Eppendorf) set to 1200 V. Sterile BG11 (1 mL) was immediately added to the electroporated cells. Following a 1-h incubation at RT, the cells were plated on 1.5% (w/v) agar plates containing BG11 with antibiotics at standard working concentrations to select for transformed colonies. The plates were sealed with parafilm and placed under 15 μmol photons m^{-2} s^{-1} light at 30°C for 1 d. The plates were then moved to 30 μmol photons m^{-2} s^{-1} light until colonies appeared. After 15–20 d, putative transformants were recovered and streaked onto new plates with appropriate antibiotics for further study.

Genetic modification by conjugation in *Synechocystis* was facilitated by an *E. coli* strain (HB101) carrying both mobilizer and helper vectors pRK2013 (ATCC 37159) and pRL528 (www.addgene.org/58495/), respectively (Tsinoremas et al., 1994). For UTEX 2973, conjugation was facilitated by a MC1061 strain carrying mobilizer and helper vectors pRK24 (www.addgene.org/51950/) and pRL528, respectively. Cultures of HB101 and OneShot TOP10 *E. coli* strains carrying level T cargo vectors were grown for approximately 15 h with appropriate antibiotics. Cyanobacterial strains were grown to an OD_{750} of ~1. All bacterial cultures were washed three times with either fresh LB medium for *E. coli* or BG11 for cyanobacteria prior to use. *Synechocystis* cultures (100 μl, OD_{750} of 0.5–0.8) were conjugated by combining appropriate HB101 and the cargo strains (100 μL each) and plating onto HATF 0.45-μm transfer membranes (Merck Millipore) placed on LB:BG11 (1:19) agar plates. For UTEX 2973 conjugations, appropriate MC1061 and the cargo strains (100 μL each) were initially combined and incubated at 30°C for 30 min, then mixed with UTEX 2973 cultures (100 μL, OD_{750} of 0.5–0.8) and incubated at 30°C for 2 h, and then plated onto transfer membranes as above. *Synechocystis* and UTEX 2973 transconjugates were grown under culturing conditions outlined above. Following growth on nonselective media for 24 h, the membranes were transferred to BG11 agar plates supplemented with appropriate antibiotics. Colonies were observed within a week for both strains. Chlorophyll content of wild-type and mutant strains was calculated as in Lea-Smith et al. (2013).

Fluorescence Assays

Transgenic strains maintained on agar plates containing appropriate antibiotics were used to inoculate 10-mL seed cultures that were grown to an OD_{750} of ~1.0, as measured with a WPA Biowave II spectrometer (Biochrom). Seed cultures were diluted to an OD_{750} of 0.2, and 2-mL starting cultures were transferred to 24-well plates (Costar Corning Incorporated) for experiments. *Synechocystis* and UTEX 2973 strains were grown in an Infors Multitron-Pro in the same culturing conditions described above. OD_{750} was measured using a FLUOstar OMEGA microplate reader (BMG Labtech). Fluorescence of eYFP for individual cells (10,000 cells per culture) was measured by flow cytometry using an Attune NxT Flow Cytometer (Thermo Fisher Scientific). Cells were gated using forward and side scatter, and median eYFP fluorescence was calculated from excitation/emission wavelengths 488 nm/515–545 nm (Kelly et al., 2018) and reported at 48 h unless otherwise stated.

Cell Counts, Soluble Protein, and eYFP Quantification

Synechocystis and UTEX 2973 strains were cultured for 48 h as described above, counted using a hemocytometer, and then harvested for soluble protein extraction. Cells were pelleted by centrifugation at 4,000 *g* for 15 min, resuspended in lysis buffer (0.1 M potassium phosphate buffer [pH 7.0], 2 mM dithiothreitol, and one Roche cOmplete EDTA-free protease inhibitor tablet per 10 mL [Roche Diagnostics]) and lysed with 0.5 mm glass beads (Thistle Scientific) in a TissueLyser II (Qiagen). The cell lysate was centrifuged at 18,000 *g* for 30 min and the supernatant assayed for soluble protein content using Pierce 660nm Protein Assay Reagent against BSA standards (Thermo Fisher Scientific). Extracts were subjected to SDS-PAGE in a 4% to 12% (w/v) polyacrylamide gel (Bolt Bis-Tris Plus Gel; Thermo Fisher Scientific) alongside a SeeBlue Plus2 prestained protein ladder (Thermo Fisher Scientific), transferred to a polyvinylidene fluoride membrane, then probed with monoclonal anti-green fluorescent protein serum (AbCAM) at 1:1,000 dilution, followed by LI-COR IRDye 800CW goat anti-rabbit IgG (LI-COR Inc.) at 1:10,000 dilution, then viewed on an LI-COR Odyssey CLx Imager. eYFP protein content was estimated by immunoblotting using densitometry using LI-COR Lite Studio software v5.2 . Relative eYFP protein abundance was estimated by densitometry using LI-COR Lite Studio software v5.2.

Plasmid Vector and Genome Copy Number Determination

The genome copy number and copy number of heterologous self-replicating plasmid vectors in *Synechocystis* was estimated using a quantitative real-time PCR approach adapted from Zerulla et al. (2016). Cytoplasmic extracts containing total cellular DNA were harvested from *Synechocystis* cultures after 48 h growth (OD_{750} = ~5) according to Zerulla et al. (2016). Cells in 10 mL of culture were pelleted by centrifugation at 4,000 *g* for 15 min, disrupted by shaking at 30 Hz for 10 min in a TissueLyser II with a mixture of 0.2-mm and 0.5-mm acid washed glass beads (0.35 g each), and then resuspended in dH_2O. The culture cell count was determined prior to harvest using a hemocytometer and checked again after cell disruption to calculate the efficiency of cell disruption. A standard curve based on a dilution series of vector DNA was generated and used for a quantitative real-time PCR analysis in parallel with extracts carrying the same vector. Two DNA fragments (~1 kb) targeting two separate loci (*petB* and *secA*) were amplified from isolated genomic DNA from *Synechocystis* using standard PCR (Pinto et al., 2012). DNA mass concentrations were determined photometrically and the concentrations of DNA molecules were calculated from the known molecular mass. As above, a standard curve based on a dilution series of the two fragments was generated to estimate genome copy number in the extracts (Zerulla et al., 2016). The cycle threshold of the extracts were then plotted against the linear portion of the standard curves to estimate plasmid vector copy number and genome copy number per cell. Oligonucleotides used are summarized in Supplemental Table S3.

Confocal Laser Scanning Microscopy

Cultures were imaged using Leica TCS SP8 confocal microscopy (Leica Microsystems) with a water immersion objective lens (HCX APO L 20x/0.50 W). Excitation/emission wavelengths were 514 nm/527–546 nm for eYFP and 514 nm/605–710 nm for chlorophyll autofluorescence.

SUPPLEMENTAL DATA

The following supplemental materials are available:

Supplemental Figure S1. Comparison of growth for *Synechocystis*, PCC 7942 and UTEX 2973 under different culturing conditions.

Supplemental Figure S2. Growth and expression levels of heterologous and synthetic promoters in *Synechocystis* and UTEX 2973.

Supplemental Figure S3. Cell volume calculations for *Synechocystis* and UTEX 2973 from confocal microscopy images.

Supplemental Table S1. Table of all parts from CyanoGate kit generated in this work.

Supplemental Table S2. List of level T vectors used in this study.

Supplemental Table S3. Sequences of synthetic oligonucleotides used to determine copy number.

Supplemental Information S1. Comparison of Gibson Assembly and Golden Gate Assembly.

Supplemental Information S2. Detailed assembly strategies using the CyanoGate kit.

Supplemental Information S3. Integrative engineering strategies using the CyanoGate kit.

Supplemental Information S4. Sequence maps (.gb files) of the components of the CyanoGate kit.

Supplemental Information S5. Protocol and online interface for building CyanoGate vector assemblies.

Supplemental Information S6. Protocols for MoClo assembly in level −1 through to level T.

ACKNOWLEDGMENTS

We thank Conrad Mullineaux (Queen Mary University), Julie Zedler and Poul Erik Jensen (University of Copenhagen) for providing components for conjugation, and Eva Steel (University of Edinburgh) for assistance with assembling the CyanoGate kit.

Received November 8, 2018; accepted February 16, 2019; published February 28, 2019.

LITERATURE CITED

Abe K, Sakai Y, Nakashima S, Araki M, Yoshida W, Sode K, Ikebukuro K (2014) Design of riboregulators for control of cyanobacterial (*Synechocystis*) protein expression. Biotechnol Lett **36:** 287–294

Albers SC, Gallegos VA, Peebles CAM (2015) Engineering of genetic control tools in *Synechocystis* sp. PCC 6803 using rational design techniques. J Biotechnol **216:** 36–46

Andersson CR, Tsinoremas NF, Shelton J, Lebedeva NV, Yarrow J, Min H, Golden SS (2000) Application of bioluminescence to the study of circadian rhythms in cyanobacteria. Methods Enzymol **305:** 527–542

Andreou AI, Nakayama N (2018) Mobius Assembly: A versatile Golden-Gate framework towards universal DNA assembly. PLoS One **13:** e0189892

Armshaw P, Carey D, Sheahan C, Pembroke JT (2015) Utilising the native plasmid, pCA2.4, from the cyanobacterium *Synechocystis* sp. strain PCC6803 as a cloning site for enhanced product production. Biotechnol Biofuels **8:** 201

Bahl CP, Wu R, Stawinsky J, Narang SA (1977) Minimal length of the lactose operator sequence for the specific recognition by the lactose repressor. Proc Natl Acad Sci USA **74:** 966–970

Behler J, Vijay D, Hess WR, Akhtar MK (2018) CRISPR-based technologies for metabolic engineering in cyanobacteria. Trends Biotechnol. **36:** 996–1010.

Blasi B, Peca L, Vass I, Kós PB (2012) Characterization of stress responses of heavy metal and metalloid inducible promoters in *synechocystis* PCC6803. J Microbiol Biotechnol **22:** 166–169

Blasina A, Kittell BL, Toukdarian AE, Helinski DR (1996) Copy-up mutants of the plasmid RK2 replication initiation protein are defective in coupling RK2 replication origins. Proc Natl Acad Sci USA **93:** 3559–3564

Bradley RW, Wang B (2015) Designer cell signal processing circuits for biotechnology. N Biotechnol **32:** 635–643

Bradley RW, Buck M, Wang B (2016) Tools and principles for microbial gene circuit engineering. J Mol Biol **428**(5 Pt B): 862–888

Bustos SA, Golden SS (1992) Light-regulated expression of the psbD gene family in *Synechococcus* sp. strain PCC 7942: Evidence for the role of duplicated psbD genes in cyanobacteria. Mol Gen Genet **232:** 221–230

Camsund D, Heidorn T, Lindblad P (2014) Design and analysis of LacI-repressed promoters and DNA-looping in a cyanobacterium. J Biol Eng **8:** 4

Castenholz RW (2001) Phylum BX. Cyanobacteria. Oxygenic photosynthetic bacteria. *In* G Garrity, DR Boone, RW Castenholz, eds, Bergey's Manual of Systematic Bacteriology. Springer, New York, pp 473–599

Chambers S, Kitney R, Freemont P (2016) The Foundry: The DNA synthesis and construction Foundry at Imperial College. Biochem Soc Trans **44:** 687–688

Chen Y, Taton A, Go M, London RE, Pieper LM, Golden SS, Golden JW (2016) Self-replicating shuttle vectors based on pANS, a small endogenous plasmid of the unicellular cyanobacterium *Synechococcus elongatus* PCC 7942. Microbiology **162:** 2029–2041

Clerico EM, Ditty JL, Golden SS (2007) Specialized techniques for site-directed mutagenesis in cyanobacteria. Methods Mol Biol **362:** 155–171

Crozet P, Navarro FJ, Willmund F, Mehrshahi P, Bakowski K, Lauersen KJ, Pérez-Pérez ME, Auroy P, Gorchs Rovira A, Sauret-Gueto S, et al (2018) Birth of a photosynthetic chassis: A MoClo toolkit enabling synthetic biology in the microalga *Chlamydomonas reinhardtii*. ACS Synth Biol **7:** 2074–2086

Dexter J, Dziga D, Lv J, Zhu J, Strzalka W, Maksylewicz A, Maroszek M, Marek S, Fu P (2018) Heterologous expression of mlrA in a photoautotrophic host—Engineering cyanobacteria to degrade microcystins. Environ Pollut **237:** 926–935

Dobrin A, Saxena P, Fussenegger M (2016) Synthetic biology: Applying biological circuits beyond novel therapies. Integr Biol **8:** 409–430

Doud DFR, Holmes EC, Richter H, Molitor B, Jander G, Angenent LT (2017) Metabolic engineering of *Rhodopseudomonas palustris* for the obligate reduction of *n*-butyrate to *n*-butanol. Biotechnol Biofuels **10:** 178

Ducat DC, Way JC, Silver PA (2011) Engineering cyanobacteria to generate high-value products. Trends Biotechnol **29:** 95–103

Economou C, Wannathong T, Szaub J, Purton S (2014) A simple, low-cost method for chloroplast transformation of the green alga *Chlamydomonas reinhardtii*. Methods Mol Biol **1132:** 401–411

Engler C, Youles M, Gruetzner R, Ehnert T-M, Werner S, Jones JDG, Patron NJ, Marillonnet S (2014) A golden gate modular cloning toolbox for plants. ACS Synth Biol **3:** 839–843

Englund E, Liang F, Lindberg P (2016) Evaluation of promoters and ribosome binding sites for biotechnological applications in the unicellular cyanobacterium *Synechocystis* sp. PCC 6803. Sci Rep **6:** 36640

Ferreira EA, Pacheco CC, Pinot F, Pereira J, Lamosa P, Oliveira P, Kirov B, Jaramillo A, Tamagnini P (2018) Expanding the toolbox for *Synechocystis* sp. PCC 6803: Validation of replicative vectors and characterization of a novel set of promoters. Synth Biol **3:** ysy014.

Flombaum P, Gallegos JL, Gordillo RA, Rincón J, Zabala LL, Jiao N, Karl DM, Li WKW, Lomas MW, Veneziano D, et al (2013) Present and future global distributions of the marine Cyanobacteria *Prochlorococcus* and *Synechococcus*. Proc Natl Acad Sci USA **110:** 9824–9829

Frey J, Bagdasarian MM, Bagdasarian M (1992) Replication and copy number control of the broad-host-range plasmid RSF1010. Gene **113:** 101–106

Gao X, Gao F, Liu D, Zhang H, Nie X, Yang C (2016) Engineering the methylerythritol phosphate pathway in cyanobacteria for photosynthetic isoprene production from CO_2. Energy Environ Sci **9:** 1400–1411

Gordon GC, Korosh TC, Cameron JC, Markley AL, Begemann MB, Pfleger BF (2016) CRISPR interference as a titratable, trans-acting regulatory tool for metabolic engineering in the cyanobacterium *Synechococcus* sp. strain PCC 7002. Metab Eng **38:** 170–179

Guerrero F, Carbonell V, Cossu M, Correddu D, Jones PR (2012) Ethylene synthesis and regulated expression of recombinant protein in *Synechocystis* sp. PCC 6803. PLoS One **7:** e50470

Heidorn T, Camsund D, Huang HH, Lindberg P, Oliveira P, Stensjö K, Lindblad P (2011) Synthetic biology in cyanobacteria engineering and analyzing novel functions. Methods Enzymol **497:** 539–579

Hendry JI, Prasannan CB, Joshi A, Dasgupta S, Wangikar PP (2016) Metabolic model of *Synechococcus* sp. PCC 7002: Prediction of flux distribution and network modification for enhanced biofuel production. Bioresour Technol **213:** 190–197

Heyduk E, Heyduk T (2018) DNA template sequence control of bacterial RNA polymerase escape from the promoter. Nucleic Acids Res **46:** 4469–4486

Higo A, Isu A, Fukaya Y, Hisabori T (2016) Efficient gene induction and endogenous gene repression systems for the filamentous cyanobacterium *Anabaena* sp. PCC 7120. Plant Cell Physiol **57:** 387–396

Higo A, Isu A, Fukaya Y, Ehira S, Hisabori T (2018) Application of CRISPR interference for metabolic engineering of the heterocyst-forming multicellular cyanobacterium Anabaena sp. PCC 7120. Plant Cell Physiol **59:** 119–127

Huang HH, Lindblad P (2013) Wide-dynamic-range promoters engineered for cyanobacteria. J Biol Eng **7:** 10

Huang CH, Shen CR, Li H, Sung LY, Wu MY, Hu YC (2016) CRISPR interference (CRISPRi) for gene regulation and succinate production in cyanobacterium *S. elongatus* PCC 7942. Microb Cell Fact **15:** 196

Huang HH, Camsund D, Lindblad P, Heidorn T (2010) Design and characterization of molecular tools for a Synthetic Biology approach towards developing cyanobacterial biotechnology. Nucleic Acids Res **38:** 2577–2593

Immethun CM, DeLorenzo DM, Focht CM, Gupta D, Johnson CB, Moon TS (2017) Physical, chemical, and metabolic state sensors expand the synthetic biology toolbox for *Synechocystis* sp. PCC 6803. Biotechnol Bioeng **114:** 1561–1569

Jusiak B, Cleto S, Perez-Piñera P, Lu TK (2016) Engineering synthetic gene circuits in living cells with CRISPR technology. Trends Biotechnol **34:** 535–547

Keeling PJ (2004) Diversity and evolutionary history of plastids and their hosts. Am J Bot **91:** 1481–1493

Kelly CL, Taylor GM, Hitchcock A, Torres-Méndez A, Heap JT (2018) A rhamnose-inducible system for precise and temporal control of gene expression in cyanobacteria. ACS Synth Biol **7:** 1056–1066

Kikuchi H, Aichi M, Suzuki I, Omato T (1996) Positive regulation by nitrite of the nitrate assimilation operon in the cyanobacteria *Synechococcus* sp. strain PCC 7942 and *Plectonema boryanum*. J Bacteriol **178:** 5822–5825

Kim WJ, Lee SM, Um Y, Sim SJ, Woo HM (2017) Development of SyneBrick vectors as a synthetic biology platform for gene expression in *Synechococcus elongatus* PCC 7942. Front Plant Sci **8:** 293

Kirst H, Formighieri C, Melis A (2014) Maximizing photosynthetic efficiency and culture productivity in cyanobacteria upon minimizing the phycobilisome light-harvesting antenna size. Biochim Biophys Acta **1837:** 1653–1664

Knoop H, Gründel M, Zilliges Y, Lehmann R, Hoffmann S, Lockau W, Steuer R (2013) Flux balance analysis of cyanobacterial metabolism: the metabolic network of *Synechocystis* sp. PCC 6803. PLOS Comput Biol **9:** e1003081

Kulkarni RD, Golden SS (1997) mRNA stability is regulated by a coding-region element and the unique 5′ untranslated leader sequences of the three Synechococcus psbA transcripts. Mol Microbiol **24:** 1131–1142

Kunert A, Vinnemeier J, Erdmann N, Hagemann M (2003) Repression by Fur is not the main mechanism controlling the iron-inducible isiAB operon in the cyanobacterium *Synechocystis* sp. PCC 6803. FEMS Microbiol Lett **227:** 255–262

Lea-Smith DJ, Ross N, Zori M, Bendall DS, Dennis JS, Scott SA, Smith AG, Howe CJ (2013) Thylakoid terminal oxidases are essential for the cyanobacterium *Synechocystis* sp. PCC 6803 to survive rapidly changing light intensities. Plant Physiol **162:** 484–495

Lea-Smith DJ, Bombelli P, Dennis JS, Scott SA, Smith AG, Howe CJ (2014) Phycobilisome-deficient strains of *Synechocystis* sp. PCC 6803 have reduced size and require carbon-limiting conditions to exhibit enhanced productivity. Plant Physiol **165:** 705–714

Lea-Smith DJ, Vasudevan R, Howe CJ (2016) Generation of marked and markerless mutants in model cyanobacterial species. J Vis Exp **111:** e54001

Leonard SP, Perutka J, Powell JE, Geng P, Richhart DD, Byrom M, Kar S, Davies BW, Ellington AD, Moran NA, et al (2018) Genetic engineering of bee gut microbiome bacteria with a toolkit for modular assembly of broad-host-range plasmids. ACS Synth Biol **7:** 1279–1290

Li S, Sun T, Xu C, Chen L, Zhang W (2018) Development and optimization of genetic toolboxes for a fast-growing cyanobacterium *Synechococcus elongatus* UTEX 2973. Metab Eng **48:** 163–174

Liberton M, Chrisler WB, Nicora CD, Moore RJ, Smith RD, Koppenaal DW, Pakrasi HB, Jacobs JM (2017) Phycobilisome truncation causes widespread proteome changes in *Synechocystis* sp. PCC 6803. PLoS One **12:** e0173251

Lindberg P, Park S, Melis A (2010) Engineering a platform for photosynthetic isoprene production in cyanobacteria, using *Synechocystis* as the model organism. Metab Eng **12:** 70–79

Liu D, Pakrasi HB (2018) Exploring native genetic elements as plug-in tools for synthetic biology in the cyanobacterium *Synechocystis* sp. PCC 6803. Microb Cell Fact **17:** 48

Liu Q, Schumacher J, Wan X, Lou C, Wang B (2018) Orthogonality and burdens of heterologous AND Gate gene circuits in E. coli. ACS Synth Biol **7:** 553–564

Lou W, Tan X, Song K, Zhang S, Luan G, Li C, Lu X (2018) A specific single nucleotide polymorphism in the ATP synthase gene significantly improves environmental stress tolerance of *Synechococcus elongatus* PCC 7942. Appl Environ Microbiol **84:** e01222-18

Luan G, Lu X (2018) Tailoring cyanobacterial cell factory for improved industrial properties. Biotechnol Adv **36:** 430–442

Madsen MA, Semerdzhiev S, Amtmann A, Tonon T (2018) Engineering mannitol biosynthesis in *Escherichia coli* and *Synechococcus* sp. PCC 7002 using a green algal fusion protein. ACS Synth Biol **7:** 2833–2840

Markley AL, Begemann MB, Clarke RE, Gordon GC, Pfleger BF (2015) Synthetic biology toolbox for controlling gene expression in the cyanobacterium *Synechococcus* sp. strain PCC 7002. ACS Synth Biol **4:** 595–603

McCormick AJ, Bombelli P, Bradley RW, Thorne R, Wenzele T, Howe CJ (2015) Biophotovoltaics: oxygenic photosynthetic organisms in the world of bioelectrochemical systems. Energy Environ Sci **8:** 1092–1109

Medford JI, Prasad A (2016) Towards programmable plant genetic circuits. Plant J **87:** 139–148

Mermet-Bouvier P, Cassier-Chauvat C, Marraccini P, Chauvat F (1993) Transfer and replication of RSF1010-derived plasmids in several cyanobacteria of the general *Synechocystis* and *Synechococcus*. Curr Microbiol **27:** 323–327

Mohammadi R, Fallah-Mehrabadi J, Bidkhori G, Zahiri J, Javad Niroomand M, Masoudi-Nejad A (2016) A systems biology approach to reconcile metabolic network models with application to *Synechocystis* sp. PCC 6803 for biofuel production. Mol Biosyst **12:** 2552–2561

Moore SJ, Lai H-E, Kelwick RJR, Chee SM, Bell DJ, Polizzi KM, Freemont PS (2016) EcoFlex: a multifunctional MoClo kit for *E. coli* synthetic biology. ACS Synth Biol **5:** 1059–1069

Mueller TJ, Ungerer JL, Pakrasi HB, Maranas CD (2017) Identifying the metabolic differences of a fast-growth phenotype in Synechococcus UTEX 2973. Sci Rep **7:** 41569

Münch R, Hiller K, Grote A, Scheer M, Klein J, Schobert M, Jahn D (2005) Virtual Footprint and PRODORIC: an integrative framework for regulon prediction in prokaryotes. Bioinformatics **21:** 4187–4189

Mutalik VK, Guimaraes JC, Cambray G, Mai QA, Christoffersen MJ, Martin L, Yu A, Lam C, Rodriguez C, Bennett G, et al (2013) Quantitative estimation of activity and quality for collections of functional genetic elements. Nat Methods **10:** 347–353

Na D, Yoo SM, Chung H, Park H, Park JH, Lee SY (2013) Metabolic engineering of Escherichia coli using synthetic small regulatory RNAs. Nat Biotechnol **31:** 170–174

Ng AH, Berla BM, Pakrasi HB (2015) Fine-tuning of photoautotrophic protein production by combining promoters and neutral sites in the cyanobacterium *Synechocystis* sp. strain PCC 6803. Appl Environ Microbiol **81:** 6857–6863

Ng WO, Zentella R, Wang Y, Taylor JS, Pakrasi HB (2000) PhrA, the major photoreactivating factor in the cyanobacterium *Synechocystis* sp. strain PCC 6803 codes for a cyclobutane-pyrimidine-dimer-specific DNA photolyase. Arch Microbiol **173:** 412–417

Niederholtmeyer H, Wolfstädter BT, Savage DF, Silver PA, Way JC (2010) Engineering cyanobacteria to synthesize and export hydrophilic products. Appl Environ Microbiol **76:** 3462–3466

Nielsen J, Keasling JD (2016) Engineering cellular metabolism. Cell **164:** 1185–1197

Nielsen AZ, Mellor SB, Vavitsas K, Wlodarczyk AJ, Gnanasekaran T, Perestrello Ramos H de Jesus M, King BC, Bakowski K, Jensen PE (2016) Extending the biosynthetic repertoires of cyanobacteria and chloroplasts. Plant J **87:** 87–102

Ordon J, Gantner J, Kemna J, Schwalgun L, Reschke M, Streubel J, Boch J, Stuttmann J (2017) Generation of chromosomal deletions in dicotyledonous plants employing a user-friendly genome editing toolkit. Plant J **89:** 155–168

Patron NJ, Orzaez D, Marillonnet S, Warzecha H, Matthewman C, Youles M, Raitskin O, Leveau A, Farré G, Rogers C, et al (2015) Standards for plant synthetic biology: A common syntax for exchange of DNA parts. New Phytol **208:** 13–19

Peca L, Kós PB, Máté Z, Farsang A, Vass I (2008) Construction of bioluminescent cyanobacterial reporter strains for detection of nickel, cobalt and zinc. FEMS Microbiol Lett **289:** 258–264

Pinto F, Pacheco CC, Ferreira D, Moradas-Ferreira P, Tamagnini P (2012) Selection of suitable reference genes for RT-qPCR analyses in cyanobacteria. PLoS One **7:** e34983

Pinto F, Pacheco CC, Oliveira P, Montagud A, Landels A, Couto N, Wright PC, Urchueguía JF, Tamagnini P (2015) Improving a *Synechocystis*-based photoautotrophic chassis through systematic genome mapping and validation of neutral sites. DNA Res **22:** 425–437

Pye CR, Bertin MJ, Lokey RS, Gerwick WH, Linington RG (2017) Retrospective analysis of natural products provides insights for future discovery trends. Proc Natl Acad Sci USA **114:** 5601–5606

Qi LS, Larson MH, Gilbert LA, Doudna JA, Weissman JS, Arkin AP, Lim WA (2013) Repurposing CRISPR as an RNA-guided platform for sequence-specific control of gene expression. Cell **152:** 1173–1183

Qi Q, Hao M, Ng WO, Slater SC, Baszis SR, Weiss JD, Valentin HE (2005) Application of the *Synechococcus nirA* promoter to establish an inducible expression system for engineering the *Synechocystis* tocopherol pathway. Appl Environ Microbiol **71:** 5678–5684

Rae BD, Long BM, Förster B, Nguyen ND, Velanis CN, Atkinson N, Hee WY, Mukherjee B, Price GD, McCormick AJ (2017) Progress and challenges of engineering a biophysical CO2-concentrating mechanism into higher plants. J Exp Bot **68:** 3717–3737

Ramey CJ, Barón-Sola Á, Aucoin HR, Boyle NR (2015) Genome Engineering in Cyanobacteria: Where We Are and Where We Need To Go. ACS Synth Biol **4:** 1186–1196

Rippka R, Deruelles J, Waterbury JB, Herdman M, Stanier RY (1979) Generic assignments, strain histories and properties of pure cultures of cyanobacteria. Microbiology **111:** 1–61

Ruffing AM, Jensen TJ, Strickland LM (2016) Genetic tools for advancement of *Synechococcus* sp. PCC 7002 as a cyanobacterial chassis. Microb Cell Fact **15:** 190

Saar KL, Bombelli P, Lea-Smith DJ, Call T, Aro E-M, Müller T, Howe CJ, Knowles TPJ (2018) Enhancing power density of biophotovoltaics by decoupling storage and power delivery. Nat Energy **3:** 75–81

Sakai Y, Abe K, Nakashima S, Ellinger JJ, Ferri S, Sode K, Ikebukuro K (2015) Scaffold-fused riboregulators for enhanced gene activation in *Synechocystis* sp. PCC 6803. MicrobiologyOpen **4:** 533–540

Sarrion-Perdigones A, Vazquez-Vilar M, Palací J, Castelijns B, Forment J, Ziarsolo P, Blanca J, Granell A, Orzaez D (2013) GoldenBraid 2.0: A comprehensive DNA assembly framework for plant synthetic biology. Plant Physiol **162:** 1618–1631

Shirai T, Osanai T, Kondo A (2016) Designing intracellular metabolism for production of target compounds by introducing a heterologous metabolic reaction based on a Synechosystis sp. 6803 genome-scale model. Microb Cell Fact **15:** 13

Silva-Rocha R, Martínez-García E, Calles B, Chavarría M, Arce-Rodríguez A, de Las Heras A, Páez-Espino AD, Durante-Rodríguez G, Kim J, Nikel PI, et al (2013) The Standard European Vector Architecture (SEVA): A coherent platform for the analysis and deployment of complex prokaryotic phenotypes. Nucleic Acids Res **41:** D666–D675

Smanski MJ, Zhou H, Claesen J, Shen B, Fischbach MA, Voigt CA (2016) Synthetic biology to access and expand nature's chemical diversity. Nat Rev Microbiol **14:** 135–149

Stensjö K, Vavitsas K, Tyystjärvi T (2018) Harnessing transcription for bioproduction in cyanobacteria. Physiol Plant **162:** 148–155

Stucken K, Ilhan J, Roettger M, Dagan T, Martin WF (2012) Transformation and conjugal transfer of foreign genes into the filamentous multicellular cyanobacteria (subsection V) *Fischerella* and *Chlorogloeopsis*. Curr Microbiol **65:** 552–560

Sun T, Li S, Song X, Diao J, Chen L, Zhang W (2018) Toolboxes for cyanobacteria: Recent advances and future direction. Biotechnol Adv **36:** 1293–1307

Tan X, Yao L, Gao Q, Wang W, Qi F, Lu X (2011) Photosynthesis driven conversion of carbon dioxide to fatty alcohols and hydrocarbons in cyanobacteria. Metab Eng **13:** 169–176

Tan X, Hou S, Song K, Georg J, Klähn S, Lu X, Hess WR (2018) The primary transcriptome of the fast-growing cyanobacterium *Synechococcus elongatus* UTEX 2973. Biotechnol Biofuels **11:** 218

Taton A, Unglaub F, Wright NE, Zeng WY, Paz-Yepes J, Brahamsha B, Palenik B, Peterson TC, Haerizadeh F, Golden SS, et al (2014) Broad-host-range vector system for synthetic biology and biotechnology in cyanobacteria. Nucleic Acids Res **42:** e136

Taton A, Ma AT, Ota M, Golden SS, Golden JW (2017) NOT gate genetic circuits to control gene expression in cyanobacteria. ACS Synth Biol **6:** 2175–2182

Tsinoremas NF, Kutach AK, Strayer CA, Golden SS (1994) Efficient gene transfer in *Synechococcus* sp. strains PCC 7942 and PCC 6301 by interspecies conjugation and chromosomal recombination. J Bacteriol **176:** 6764–6768

Ungerer J, Pakrasi HB (2016) Cpf1 is a versatile tool for CRISPR genome editing across diverse species of cyanobacteria. Sci Rep **6:** 39681

Ungerer J, Lin P-C, Chen H-Y, Pakrasi HB (2018a) Adjustments to photosystem stoichiometry and electron transfer proteins are key to the remarkably fast growth of the cyanobacterium *Synechococcus elongatus* UTEX 2973. MBio **9:** e02327-17

Ungerer J, Wendt KE, Hendry JI, Marans CD, Pakrasi HB (2018b) Comparative genomics reveals the molecular determinants of rapid growth of the cyanobacterium Synechococcus elongatus UTEX 2973. Proc Natl Acad Sci USA **115:** E11761–E11770

van de Meene AM, Hohmann-Marriott MF, Vermaas WF, Roberson RW (2006) The three-dimensional structure of the cyanobacterium *Synechocystis* sp. PCC 6803. Arch Microbiol **184:** 259–270

Vazquez-Vilar M, Orzaez D, Patron N (2018) DNA assembly standards: Setting the low-level programming code for plant biotechnology. Plant Sci **273:** 33–41

Vioque A (2007) Transformation of Cyanobacteria. *In* R León, A Galván, E Fernández, eds, Transgenic Microalgae as Green Cell Factories. Advances in Experimental Medicine and Biology. **Vol 616**. Springer, New York, pp 12–22

Vogel AIM, Lale R, Hohmann-Marriott MF (2017) Streamlining recombination-mediated genetic engineering by validating three neutral integration sites in *Synechococcus* sp. PCC 7002. J Biol Eng **11:** 19

Wang B, Eckert C, Maness P-C, Yu J (2018) A genetic toolbox for modulating the expression of heterologous genes in the cyanobacterium *Synechocystis* sp. PCC 6803. ACS Synth Biol **7:** 276–286

Watanabe S, Noda A, Ohbayashi R, Uchioke K, Kurihara A, Nakatake S, Morioka S, Kanesaki Y, Chibazakura T, Yoshikawa H (2018) ParA-like protein influences the distribution of multi-copy chromosomes in cyanobacterium Synechococcus elongatus PCC 7942. Microbiology **164:** 45–56

Wendt KE, Ungerer J, Cobb RE, Zhao H, Pakrasi HB (2016) CRISPR/Cas9 mediated targeted mutagenesis of the fast growing cyanobacterium *Synechococcus elongatus* UTEX 2973. Microb Cell Fact **15:** 115

Werner S, Engler C, Weber E, Gruetzner R, Marillonnet S (2012) Fast track assembly of multigene constructs using Golden Gate cloning and the MoClo system. Bioeng Bugs **3:** 38–43

Wlodarczyk A, Gnanasekaran T, Nielsen AZ, Zulu NN, Mellor SB, Luckner M, Thøfner JFB, Olsen CE, Mottawie MS, Burow M, et al (2016) Metabolic engineering of light-driven cytochrome P450 dependent pathways into *Synechocystis* sp. PCC 6803. Metab Eng **33:** 1–11

Xiao A, Cheng Z, Kong L, Zhu Z, Lin S, Gao G, Zhang B (2014) CasOT: a genome-wide Cas9/gRNA off-target searching tool. Bioinformatics **30:** 1180–1182

Xu Y, Alvey RM, Byrne PO, Graham JE, Shen G, Bryant DA (2011) Expression of genes in cyanobacteria: adaptation of endogenous plasmids as platforms for high-level gene expression in *Synechococcus* sp. PCC 7002. Methods Mol Biol **684:** 273–293

Yao L, Cengic I, Anfelt J, Hudson EP (2016) Multiple gene repression in cyanobacteria using CRISPRi. ACS Synth Biol **5:** 207–212

Yu J, Liberton M, Cliften PF, Head RD, Jacobs JM, Smith RD, Koppenaal DW, Brand JJ, Pakrasi HB (2015) Synechococcus elongatus UTEX 2973, a fast growing cyanobacterial chassis for biosynthesis using light and CO_2. Sci Rep **5:** 8132

Zerulla K, Ludt K, Soppa J (2016) The ploidy level of *Synechocystis* sp. PCC 6803 is highly variable and is influenced by growth phase and by chemical and physical external parameters. Microbiology **162:** 730–739

Zess EK, Begemann MB, Pfleger BF (2016) Construction of new synthetic biology tools for the control of gene expression in the cyanobacterium Synechococcus sp. strain PCC 7002. Biotechnol Bioeng **113:** 424–432

Zhou J, Zhang H, Meng H, Zhu Y, Bao G, Zhang Y, Li Y, Ma Y (2014) Discovery of a super-strong promoter enables efficient production of heterologous proteins in cyanobacteria. Sci Rep **4:** 4500

References

Abbas, A., Morrissey, J. P., Carnicero Marquez, P., Sheehan, M. M., Delany, I. R., & O'Gara, F. (2002). Characterization of interactions between the transcriptional repressor PhlF and its binding site at the *phlA* promoter in *Pseudomonas fluorescens* F113. *Journal of Bacteriology*, 184(11), 3008–3016. https://doi.org/10.1128/JB.184.11.3008-3016.2002

Albers, S. C., Gallegos, V. A., & Peebles, C. A. M. (2015). Engineering of genetic control tools in *Synechocystis* sp. PCC 6803 using rational design techniques. *Journal of Biotechnology*, 216, 36–46. https://doi.org/10.1016/j.jbiotec.2015.09.042

Allan Downie, J., & González, J. E. (2014). Cell-to-Cell Communication in *Rhizobia*: Quorum Sensing and Plant Signaling. *Chemical Communication among Bacteria*, 213–232. https://doi.org/10.1128/9781555815578.ch14

Altschul, S. F., Gish, W., Miller, W., Myers, E. W., & Lipman, D. J. (1990). Basic local alignment search tool. *Journal of Molecular Biology*, 215(3), 403–410. https://doi.org/10.1016/S0022-2836(05)80360-2

Altschul, S. F., Madden, T. L., Schäffer, A. A., Zhang, J., Zhang, Z., Miller, W., & Lipman, D. J. (1997). Gapped BLAST and PSI-BLAST: A new generation of protein database search programs. Nucleic Acids Research, 25(17), 3389–3402. https://doi.org/10.1093/nar/25.17.3389

Andreou, A. I., & Nakayama, N. (2018). Mobius assembly: A versatile golden-gate framework towards universal DNA assembly. *PLoS ONE*, 13(1), 1–18. https://doi.org/10.1371/journal.pone.0189892

Armshaw, P., Carey, D., Sheahan, C., & Pembroke, J. T. (2015). Utilising the native plasmid, pCA2.4, from the cyanobacterium *Synechocystis* sp. strain PCC6803 as a cloning site for enhanced product production. *Biotechnology for Biofuels*, 8(1), 201. https://doi.org/10.1186/s13068-015-0385-x

Atsumi, S., Higashide, W., & Liao, J. C. (2009). Direct photosynthetic recycling of carbon dioxide to isobutyraldehyde. *Nature Biotechnology*, 27(12), 1177–1180. https://doi.org/10.1038/nbt.1586

Bahl, C. P., Wu, R., Stawinsky, J., & Narang, S. A. (1977). Minimal length of the lactose operator sequence for the specific recognition by the lactose repressor. *Proceedings of the National Academy of Sciences of the United States of America*, 74(3), 966–970. https://doi.org/10.1073/pnas.74.3.966

Behle, A., Saake, P., Germann, A. T., Dienst, D., & Axmann, I. M. (2020). Comparative Dose-Response Analysis of Inducible Promoters in Cyanobacteria. *ACS Synthetic Biology*, 9(4), 843–855. https://doi.org/10.1021/acssynbio.9b00505

Behler, J., Vijay, D., Hess, W. R., & Akhtar, M. K. (2018). CRISPR-Based Technologies for Metabolic Engineering in Cyanobacteria. *Trends in Biotechnology*, 36(10), 996–1010. https://doi.org/10.1016/j.tibtech.2018.05.011

Beyer, H. M., Gonschorek, P., Samodelov, S. L., Meier, M., Weber, W., & Zurbriggen, M. D. (2015). AQUA cloning: A versatile and simple enzyme-free cloning approach. *PLoS ONE*, 10(9), 1–20. https://doi.org/10.1371/journal.pone.0137652

Blasi, B., Peca, L., Vass, I., & Kós, P. B. (2012). Characterization of stress responses of heavy metal and metalloid inducible promoters in *Synechocystis* PCC 6803. *Journal of Microbiology and Biotechnology*, 22(2), 166–169. https://doi.org/10.4014/jmb.1106.06050

Blasina, A., Kittell, B. L., Toukdarian, A. E., & Helinski, D. R. (1996). Copy-up mutants of the plasmid RK2 replication initiation protein are defective in coupling RK2 replication origins. *Proceedings of the National Academy of Sciences of the United States of America*, 93(8), 3559–3564. https://doi.org/10.1073/pnas.93.8.3559

Boyd, E. S., & Barkay, T. (2012). The mercury resistance operon: From an origin in a geothermal environment to an efficient detoxification machine. *Frontiers in Microbiology*, 3(OCT), 1–13. https://doi.org/10.3389/fmicb.2012.00349

Bradley, R. W., Buck, M., & Wang, B. (2016). Tools and Principles for Microbial Gene Circuit Engineering. *Journal of Molecular Biology*, 428(5), 862–888. https://doi.org/10.1016/j.jmb.2015.10.004

Cameron, D. E., & Collins, J. J. (2014). Tunable protein degradation in bacteria. *Nature Biotechnology*, 32(12), 1276–1281. https://doi.org/10.1038/nbt.3053

Camsund, D., Heidorn, T., & Lindblad, P. (2014). Design and analysis of LacI-repressed promoters and DNA-looping in a cyanobacterium. *Journal of Biological Engineering*, 8(1), 1–23. https://doi.org/10.1186/1754-1611-8-4

Carbonell, V., Vuorio, E., Aro, E. M., & Kallio, P. (2019). Enhanced stable production of ethylene in photosynthetic cyanobacterium *Synechococcus elongatus* PCC 7942. *World Journal of Microbiology and Biotechnology*, 35(5), 1–9. https://doi.org/10.1007/s11274-019-2652-7

Casadaban, M. J. (1976). Regulation of the regulatory gene for the arabinose pathway, araC. *Journal of Molecular Biology*, 104(3), 557–566. https://doi.org/10.1016/0022-2836(76)90120-0

Castenholz, R. W., Wilmotte, A., Herdman, M., Rippka, R., Waterbury, J. B., Iteman, I., & Hoffmann, L. (2001). Phylum BX. Cyanobacteria. In D. R. Boone, R. W. Castenholz, & G. M. Garrity (Eds.), *Bergey's Manual® of Systematic Bacteriology* (pp. 473–599). New York, NY: Springer New York. https://doi.org/10.1007/978-0-387-21609-6_27

Chambers, S., Kitney, R., & Freemont, P. (2016). The Foundry: The DNA synthesis and construction Foundry at Imperial College. *Biochemical Society Transactions*, 44(3), 687–688. https://doi.org/10.1042/BST20160007

Chen, Y., Taton, A., Go, M., London, R. E., Pieper, L. M., Golden, S. S., & Golden, J. W. (2016). Self-replicating shuttle vectors based on pANS, a small endogenous plasmid of the unicellular cyanobacterium *Synechococcus elongatus* PCC 7942. *Microbiology* (United Kingdom), 162(12), 2029–2041. https://doi.org/10.1099/mic.0.000377

Cheng, A. A., & Lu, T. K. (2012). Synthetic Biology: An Emerging Engineering Discipline. *Annual Review of Biomedical Engineering*, 14(1), 155–178. https://doi.org/10.1146/annurev-bioeng-071811-150118

Crozet, P., Navarro, F. J., Willmund, F., Mehrshahi, P., Bakowski, K., Lauersen, K. J., … Lemaire, S. D. (2018). Birth of a Photosynthetic Chassis: A MoClo Toolkit Enabling Synthetic Biology in the Microalga *Chlamydomonas reinhardtii*. *ACS Synthetic Biology*, 7(9), 2074–2086. https://doi.org/10.1021/acssynbio.8b00251

Dexter, J., Dziga, D., Lv, J., Zhu, J., Strzalka, W., Maksylewicz, A., … Fu, P. (2018). Heterologous expression of *mlrA* in a photoautotrophic host – Engineering cyanobacteria to degrade microcystins. *Environmental Pollution*, 237, 926–935. https://doi.org/10.1016/j.envpol.2018.01.071

Doud, D. F. R., Holmes, E. C., Richter, H., Molitor, B., Jander, G., & Angenent, L. T. (2017). Metabolic engineering of *Rhodopseudomonas palustris* for the obligate reduction of n-butyrate to n-butanol. *Biotechnology for Biofuels*, 10(1), 1–11. https://doi.org/10.1186/s13068-017-0864-3

Ducat, D. C., Way, J. C., & Silver, P. A. (2011). Engineering cyanobacteria to generate high-value products. *Trends in Biotechnology*, 29(2), 95–103. https://doi.org/10.1016/j.tibtech.2010.12.003

Dunn, N. W., & Gunsalus, I. C. (1973). Transmissible plasmid coding early enzymes of naphthalene oxidation in Pseudomonas putida. *Journal of Bacteriology*, 114(3), 974–979. https://doi.org/10.1128/jb.114.3.974-979.1973

Durall, C., Lindberg, P., Yu, J., & Lindblad, P. (2020). Increased ethylene production by overexpressing phosphoenolpyruvate carboxylase in the cyanobacterium *Synechocystis* PCC 6803. *Biotechnology for Biofuels,* 13(1), 1–13. https://doi.org/10.1186/s13068-020-1653-y

Economou, C., Wannathong, T., Szaub, J., & Purton, S. (2014). A Simple, Low-Cost Method for Chloroplast Transformation of the Green Alga *Chlamydomonas reinhardtii*. In P. Maliga (Ed.), *Chloroplast Biotechnology: Methods and Protocols* (pp. 401–411). Totowa, NJ: Humana Press. https://doi.org/10.1007/978-1-62703-995-6_27

Engler, C., Youles, M., Gruetzner, R., Ehnert, T. M., Werner, S., Jones, J. D. G., … Marillonnet, S. (2014). A Golden Gate modular cloning toolbox for plants. *ACS Synthetic Biology*, 3(11), 839–843. https://doi.org/10.1021/sb4001504

Englund, E., Liang, F., & Lindberg, P. (2016). Evaluation of promoters and ribosome binding sites for biotechnological applications in the unicellular cyanobacterium *Synechocystis* sp. PCC 6803. *Scientific Reports*, 6(November), 1–12. https://doi.org/10.1038/srep36640

Englund, E., Shabestary, K., Hudson, E. P., & Lindberg, P. (2018). Systematic overexpression study to find target enzymes enhancing production of terpenes in *Synechocystis* PCC 6803, using isoprene as a model compound. *Metabolic Engineering*, 49(April), 164–177. https://doi.org/10.1016/j.ymben.2018.07.004

Fernandez-Rodriguez, J., & Voigt, C. A. (2016). Post-translational control of genetic circuits using Potyvirus proteases. *Nucleic Acids Research*, 44(13), 6493–6502. https://doi.org/10.1093/nar/gkw537

Fernández-Rojas, B., Hernández-Juárez, J., & Pedraza-Chaverri, J. (2014). Nutraceutical properties of phycocyanin. *Journal of Functional Foods*, 11(C), 375–392. https://doi.org/10.1016/j.jff.2014.10.011

Ferreira, E. A., Pacheco, C. C., Pinto, F., Pereira, J., Lamosa, P., Oliveira, P., … Tamagnini, P. (2018). Expanding the toolbox for *Synechocystis* sp. PCC 6803: Validation of replicative vectors and characterization of a novel set of promoters. *Synthetic Biology*, 3(1), 1–15. https://doi.org/10.1093/synbio/ysy014

Flombaum, P., Gallegos, J. L., Gordillo, R. A., Rincón, J., Zabala, L. L., Jiao, N., … Martiny, A. C. (2013). Present and future global distributions of the marine Cyanobacteria *Prochlorococcus* and *Synechococcus*. *Proceedings of the National Academy of Sciences of the United States of America*, 110(24), 9824–9829. https://doi.org/10.1073/pnas.1307701110

Fonfara, I., Richter, H., BratoviÄ, M., Le Rhun, A., & Charpentier, E. (2016). The CRISPR-associated DNA-cleaving enzyme Cpf1 also processes precursor CRISPR RNA. *Nature*, 532(7600), 517–521. https://doi.org/10.1038/nature17945

Frey, J., Bagdasarian, M. M., & Bagdasarian, M. (1992). Replication and copy number control of the broad-host-range plasmid RSF1010. *Gene*, 113(1), 101–106. https://doi.org/10.1016/0378-1119(92)90675-F

Gale, G. A. R., Osorio, A. A. S., Mills, L. A., Wang, B., Lea-Smith, D. J., & McCormick, A. J. (2019). Emerging species and genome editing tools: Future prospects in cyanobacterial synthetic biology. *Microorganisms*, 7(10), 409. https://doi.org/10.3390/microorganisms7100409

Gale, G. A. R., Schiavon Osorio, A. A., Puzorjov, A., Wang, B., & McCormick, A. J. (2019). Genetic Modification of Cyanobacteria by Conjugation Using the CyanoGate Modular Cloning Toolkit. *Journal of Visualized Experiments*, (152), e60451. https://doi.org/10.3791/60451

Gao, X., Gao, F., Liu, D., Zhang, H., Nie, X., & Yang, C. (2016). Engineering the methylerythritol phosphate pathway in cyanobacteria for photosynthetic isoprene production from CO_2. *Energy and Environmental Science*, 9(4), 1400–1411. https://doi.org/10.1039/c5ee03102h

Gibson, D. G., Young, L., Chuang, R. Y., Venter, J. C., Hutchison, C. A., & Smith, H. O. (2009). Enzymatic assembly of DNA molecules up to several hundred kilobases. *Nature Methods*, 6(5), 343–345. https://doi.org/10.1038/nmeth.1318

Glazer, A. N. (1994). Phycobiliproteins - a family of valuable, widely used fluorophores. *Journal of Applied Phycology*, 6(2), 105–112. https://doi.org/10.1007/BF02186064

Gordon, G. C., Korosh, T. C., Cameron, J. C., Markley, A. L., Begemann, M. B., & Pfleger, B. F. (2016). CRISPR interference as a titratable, trans-acting regulatory tool for metabolic engineering in the cyanobacterium *Synechococcus* sp. strain PCC 7002. *Metabolic Engineering*, 38, 170–179. https://doi.org/10.1016/j.ymben.2016.07.007

Heidorn, T., Camsund, D., Huang, H.-H., Lindberg, P., Oliveira, P., Stensjö, K., & Lindblad, P. (2011). Chapter Twenty-Four - Synthetic Biology in Cyanobacteria: Engineering and Analyzing Novel Functions. In C. Voigt (Ed.), *Methods in Enzymology* (Vol. 497, pp. 539–579). Academic Press. https://doi.org/https://doi.org/10.1016/B978-0-12-385075-1.00024-X

Henao, E., Rzymski, P., & Waters, M. (2019). A Review on the Study of Cyanotoxins in Paleolimnological Research: Current Knowledge and Future Needs. Toxins, 12(1), 6. https://doi.org/10.3390/toxins12010006

Heyduk, E., & Heyduk, T. (2018). DNA template sequence control of bacterial RNA polymerase escape from the promoter. *Nucleic Acids Research*, 46(9), 4469–4486. https://doi.org/10.1093/nar/gky172

Higo, A., Isu, A., Fukaya, Y., Ehira, S., & Hisabori, T. (2018). Application of CRISPR Interference for Metabolic Engineering of the Heterocyst-Forming Multicellular Cyanobacterium *Anabaena* sp. PCC 7120. *Plant & Cell Physiology*, 59(1), 119–127. https://doi.org/10.1093/pcp/pcx166

Huang, C. H., Shen, C. R., Li, H., Sung, L. Y., Wu, M. Y., & Hu, Y. C. (2016). CRISPR interference (CRISPRi) for gene regulation and succinate production in cyanobacterium *S. elongatus* PCC 7942. *Microbial Cell Factories*, 15(1), 1–11. https://doi.org/10.1186/s12934-016-0595-3

Huang, Hsin Ho & Lindblad, P. (2013). Wide-dynamic-range promoters engineered for cyanobacteria. *Journal of Biological Engineering*, 7(1), 10. https://doi.org/10.1186/1754-1611-7-10

Huang, Hsin Ho, Camsund, D., Lindblad, P., & Heidorn, T. (2010). Design and characterization of molecular tools for a synthetic biology approach towards developing cyanobacterial biotechnology. *Nucleic Acids Research*, 38(8), 2577–2593. https://doi.org/10.1093/nar/gkq164

Huang, Hsin Ho, Seeger, C., Danielson, U. H., Lindblad, P., Helena Danielson, U., & Lindblad, P. (2015). Analysis of the leakage of gene repression by an artificial TetR-regulated promoter in cyanobacteria Molecular Biology. *BMC Research Notes*, 8(1), 4–11. https://doi.org/10.1186/s13104-015-1425-0

Immethun, C. M., DeLorenzo, D. M., Focht, C. M., Gupta, D., Johnson, C. B., & Moon, T. S. (2017). Physical, chemical, and metabolic state sensors expand the synthetic biology toolbox for *Synechocystis* sp. PCC 6803. *Biotechnology and Bioengineering*, 114(7), 1561–1569. https://doi.org/10.1002/bit.26275

Jazmin, L. J., Xu, Y., Cheah, Y. E., Adebiyi, A. O., Johnson, C. H., & Young, J. D. (2017). Isotopically nonstationary 13C flux analysis of cyanobacterial isobutyraldehyde production. *Metabolic Engineering*, 42(May), 9–18. https://doi.org/10.1016/j.ymben.2017.05.001

Jones, M. R., Pinto, E., Torres, M. A., Dörr, F., Mazur-Marzec, H., Szubert, K., … Janssen, E. M. L. (2021). CyanoMetDB, a comprehensive public database of secondary metabolites from cyanobacteria. *Water Research*, 196, 117017. https://doi.org/10.1016/j.watres.2021.117017

Keeling, P. J. (2004). Diversity and evolutionary history of plastids and their hosts. *American Journal of Botany*, 91(10), 1481–1493. https://doi.org/10.3732/ajb.91.10.1481

Kelly, C. L., Taylor, G. M., Hitchcock, A., Torres-Méndez, A., & Heap, J. T. (2018). A Rhamnose-Inducible System for Precise and Temporal Control of Gene Expression in Cyanobacteria. *ACS Synthetic Biology*, 7(4), 1056–1066. https://doi.org/10.1021/acssynbio.7b00435

Kelly, L., Liu, Z., Yoshihara, A., Jenkinson, S. F., Wormald, M. R., Otero, J., … Heap, J. T. (2016). Synthetic Chemical Inducers and Genetic Decoupling Enable Orthogonal Control of the *rhaBAD* Promoter. *ACS Synthetic Biology*, 5(10), 1136–1145. https://doi.org/10.1021/acssynbio.6b00030

Kerfeld, C. A., & Melnicki, M. R. (2016). Assembly, function and evolution of cyanobacterial carboxysomes. *Current Opinion in Plant Biology*, 31, 66–75. https://doi.org/10.1016/j.pbi.2016.03.009

Kim, W. J., Lee, S.-M., Um, Y., Sim, S. J., & Woo, H. M. (2017). Development of SyneBrick Vectors As a Synthetic Biology Platform for Gene Expression in *Synechococcus elongatus* PCC 7942. *Frontiers in Plant Science*, 8(March), 1–9. https://doi.org/10.3389/fpls.2017.00293

Kirst, H., Formighieri, C., & Melis, A. (2014). Maximizing photosynthetic efficiency and culture productivity in cyanobacteria upon minimizing the phycobilisome light-harvesting antenna size. *Biochimica et Biophysica Acta - Bioenergetics*, 1837(10), 1653–1664. https://doi.org/10.1016/j.bbabio.2014.07.009

Knoot, C. J., Biswas, S., & Pakrasi, H. B. (2020). Tunable Repression of Key Photosynthetic Processes Using Cas12a CRISPR Interference in the Fast-Growing Cyanobacterium *Synechococcus* sp. UTEX 2973. *ACS Synthetic Biology*, 9(1), 132–143. https://doi.org/10.1021/acssynbio.9b00417

Korosh, T. C., Markley, A. L., Clark, R. L., McGinley, L. L., McMahon, K. D., & Pfleger, B. F. (2017). Engineering photosynthetic production of L-lysine. *Metabolic Engineering*, 44(October), 273–283. https://doi.org/10.1016/j.ymben.2017.10.010

Kubickova, B., Babica, P., Hilscherová, K., & Šindlerová, L. (2019). Effects of cyanobacterial toxins on the human gastrointestinal tract and the mucosal innate immune system. Environmental Sciences Europe, 31(1), 1–27. https://doi.org/10.1186/s12302-019-0212-2

Lan, E. I., & Liao, J. C. (2011). Metabolic engineering of cyanobacteria for 1-butanol production from carbon dioxide. *Metabolic Engineering*, 13(4), 353–363. https://doi.org/10.1016/j.ymben.2011.04.004

Landry, B. P., Stöckel, J., & Pakrasi, H. B. (2013). Use of degradation tags to control protein levels in the cyanobacterium *Synechocystis* sp. strain PCC 6803. *Applied and Environmental Microbiology*, 79(8), 2833–2835. https://doi.org/10.1128/AEM.03741-12

Lee, J., Lee, S., & Jiang, X. (2017). Cyanobacterial Toxins in Freshwater and Food: Important Sources of Exposure to Humans. Annual Review of Food Science and Technology, 8(1), 281–304. https://doi.org/10.1146/annurev-food-030216-030116

Lea-Smith, D. J., Bombelli, P., Dennis, J. S., Scott, S. A., Smith, A. G., & Howe, C. J. (2014). Phycobilisome-deficient strains of *Synechocystis* sp. PCC 6803 have reduced size and require carbon-limiting conditions to exhibit enhanced productivity. *Plant Physiology*, 165(2), 705–714. https://doi.org/10.1104/pp.114.237206

Lea-Smith, D. J., Vasudevan, R., & Howe, C. J. (2016). Generation of marked and markerless mutants in model cyanobacterial species. *Journal of Visualized Experiments*, 2016(111), 1–12. https://doi.org/10.3791/54001

Leonard, S. P., Perutka, J., Powell, J. E., Geng, P., Richhart, D. D., Byrom, M., … Barrick, J. E. (2018). Genetic Engineering of Bee Gut Microbiome Bacteria with a Toolkit for Modular Assembly of Broad-Host-Range Plasmids. *ACS Synthetic Biology*, 7(5), 1279–1290. https://doi.org/10.1021/acssynbio.7b00399

Li, L., Jiang, W., & Lu, Y. (2018). A Modified Gibson Assembly Method for Cloning Large DNA Fragments with High GC Contents. In M. K. Jensen & J. D. Keasling (Eds.), *Synthetic Metabolic Pathways: Methods and Protocols* (pp. 203–209). New York, NY: Springer New York. https://doi.org/10.1007/978-1-4939-7295-1_13

Liberton, M., Chrisler, W. B., Nicora, C. D., Moore, R. J., Smith, R. D., Koppenaal, D. W., … Jacobs, J. M. (2017). Phycobilisome truncation causes widespread proteome changes in *Synechocystis* sp. PCC 6803. *PLoS ONE*, 12(3), 1–18. https://doi.org/10.1371/journal.pone.0173251

Lin, P. C., Zhang, F., & Pakrasi, H. B. (2020). Enhanced production of sucrose in the fast-growing cyanobacterium *Synechococcus elongatus* UTEX 2973. *Scientific Reports*, 10(1), 1–8. https://doi.org/10.1038/s41598-019-57319-5

Lin, X., Yang, M., Liu, X., Cheng, Z., & Ge, F. (2020). Characterization of Lysine Monomethylome and Methyltransferase in Model Cyanobacterium *Synechocystis* sp. PCC 6803. *Genomics*, Proteomics and Bioinformatics, 18(3), 289–304. https://doi.org/10.1016/j.gpb.2019.04.005

Lindberg, P., Park, S., & Melis, A. (2010). Engineering a platform for photosynthetic isoprene production in cyanobacteria, using *Synechocystis* as the model organism. Metabolic Engineering, 12(1), 70–79. https://doi.org/10.1016/j.ymben.2009.10.001

Lithgow, J. K., Wilkinson, A., Hardman, A., Rodelas, B., Wisniewski-Dyé, F., Williams, P., & Downie, J. A. (2000). The regulatory locus *cinRI* in *Rhizobium leguminosarum* controls a network of quorum-sensing loci. Molecular Microbiology, 37(1), 81–97. https://doi.org/10.1046/j.1365-2958.2000.01960.x

Liu, D., Johnson, V. M., & Pakrasi, H. B. (2020a). A Reversibly Induced CRISPRi System Targeting Photosystem II in the Cyanobacterium *Synechocystis* sp. PCC 6803. *ACS Synthetic Biology*, 9(6), 1441–1449. https://doi.org/10.1021/acssynbio.0c00106

Liu, X., Zhu, X., Wang, H., Liu, T., Cheng, J., & Jiang, H. (2020b). Discovery and modification of cytochrome P450 for plant natural products biosynthesis. Synthetic and Systems Biotechnology, 5(3), 187–199. https://doi.org/10.1016/j.synbio.2020.06.008

Liu, D., & Pakrasi, H. B. (2018). Exploring native genetic elements as plug-in tools for synthetic biology in the cyanobacterium *Synechocystis* sp. PCC 6803. Microbial Cell Factories, 17(1), 1–8. https://doi.org/10.1186/s12934-018-0897-8

Liu, Q., Schumacher, J., Wan, X., Lou, C., & Wang, B. (2018). Orthogonality and Burdens of Heterologous and Gate Gene Circuits in *E. coli*. *ACS Synthetic Biology*, 7(2), 553–564. https://doi.org/10.1021/acssynbio.7b00328

Liu, Y., Wan, X., & Wang, B. (2019). Engineered CRISPRa enables programmable eukaryote-like gene activation in bacteria. *Nature Communications*, 10(1). https://doi.org/10.1038/s41467-019-11479-0

Long, B. M., Hee, W. Y., Sharwood, R. E., Rae, B. D., Kaines, S., Lim, Y. L., … Price, G. D. (2018). Carboxysome encapsulation of the CO2-fixing enzyme Rubisco in tobacco chloroplasts. *Nature Communications*, 9(1). https://doi.org/10.1038/s41467-018-06044-0

López-Maury, L., Florencio, F. J., & Reyes, J. C. (2003). Arsenic sensing and resistance system in the cyanobacterium *Synechocystis* sp. Strain PCC 6803. *Journal of Bacteriology*, 185(18), 5363–5371. https://doi.org/10.1128/JB.185.18.5363-5371.2003

Magnusson, J. P., Rios, A. R., Wu, L., & Qi, L. S. (2021). Enhanced Cas12a multi-gene regulation using a CRISPR array separator. BioRxiv, 2021.01.27.428408. Retrieved from https://doi.org/10.1101/2021.01.27.428408

Markley, A. L., Begemann, M. B., Clarke, R. E., Gordon, G. C., & Pfleger, B. F. (2015). Synthetic biology toolbox for controlling gene expression in the cyanobacterium *Synechococcus* sp. strain PCC 7002. *ACS Synthetic Biology*, 4(5), 595–603. https://doi.org/10.1021/sb500260k

McCormick, A. J., Bombelli, P., Bradley, R. W., Thorne, R., Wenzel, T., & Howe, C. J. (2015). Biophotovoltaics: Oxygenic photosynthetic organisms in the world of bioelectrochemical systems. *Energy and Environmental Science*, 8(4), 1092–1109. https://doi.org/10.1039/c4ee03875d

Mermet-Bouvier, P., Cassier-Chauvat, C., Marraccini, P., & Chauvat, F. (1993). Transfer and replication of RSF1010-derived plasmids in several cyanobacteria of the genera *Synechocystis* and *Synechococcus*. *Current Microbiology,* 27(6), 323–327. https://doi.org/10.1007/BF01568955

Merulla, D., Hatzimanikatis, V., & Van der Meer, J. R. (2013). Tunable reporter signal production in feedback-uncoupled arsenic bioreporters. *Microbial Biotechnology*, 6(5), 503–514. https://doi.org/10.1111/1751-7915.12031

Meyer, A. J., Segall-Shapiro, T. H., Glassey, E., Zhang, J., & Voigt, C. A. (2019). *Escherichia coli* "Marionette" strains with 12 highly optimized small-molecule sensors. *Nature Chemical Biology*, 15(2), 196–204. https://doi.org/10.1038/s41589-018-0168-3

Miao, R., Liu, X., Englund, E., Lindberg, P., & Lindblad, P. (2017). Isobutanol production in *Synechocystis* PCC 6803 using heterologous and endogenous alcohol dehydrogenases. *Metabolic Engineering Communications*, 5(July), 45–53. https://doi.org/10.1016/j.meteno.2017.07.003

Möllers, K., Cannella, D., Jørgensen, H., & Frigaard, N.-U. (2014). Cyanobacterial biomass as carbohydrate and nutrient feedstock for bioethanol production by yeast fermentation. *Biotechnology for Biofuels*, 7(1), 64. https://doi.org/10.1186/1754-6834-7-64

Moore, S. J., Lai, H. E., Kelwick, R. J. R., Chee, S. M., Bell, D. J., Polizzi, K. M., & Freemont, P. S. (2016). EcoFlex: A Multifunctional MoClo Kit for *E. coli* Synthetic Biology. *ACS Synthetic Biology*, 5(10), 1059–1069. https://doi.org/10.1021/acssynbio.6b00031

Münch, R., Hiller, K., Grote, A., Scheer, M., Klein, J., Schobert, M., & Jahn, D. (2005). Virtual Footprint and PRODORIC: An integrative framework for regulon prediction in prokaryotes. *Bioinformatics*, 21(22), 4187–4189. https://doi.org/10.1093/bioinformatics/bti635

Mutalik, V. K., Guimaraes, J. C., Cambray, G., Mai, Q. A., Christoffersen, M. J., Martin, L., … Arkin, A. P. (2013). Quantitative estimation of activity and quality for collections of functional genetic elements. *Nature Methods*, 10(4), 347–353. https://doi.org/10.1038/nmeth.2403

Na, D., Yoo, S. M., Chung, H., Park, H., Park, J. H., & Lee, S. Y. (2013). Metabolic engineering of *Escherichia coli* using synthetic small regulatory RNAs. *Nature Biotechnology*, 31(2), 170–174. https://doi.org/10.1038/nbt.2461

Nakashima, N., Tamura, T., & Good, L. (2006). Paired termini stabilize antisense RNAs and enhance conditional gene silencing in *Escherichia coli. Nucleic Acids Research*, 34(20), 1–10. https://doi.org/10.1093/nar/gkl697

Ng, A. H., Berla, B. M., & Pakrasi, H. B. (2015). Fine-tuning of photoautotrophic protein production by combining promoters and neutral sites in the cyanobacterium *Synechocystis* sp. strain PCC 6803. *Applied and Environmental Microbiology*, 81(19), 6857–6863. https://doi.org/10.1128/AEM.01349-15

Ng, W. O., Zentella, R., Wang, Y., Taylor, J. S. A., & Pakrasi, H. B. (2000). *phrA*, the major photoreactivating factor in the cyanobacterium *Synechocystis* sp. strain PCC 6803 codes for a cyclobutane-pyrimidine-dimer- specific DNA photolyase. *Archives of Microbiology*, 173(5–6), 412–417. https://doi.org/10.1007/s002030000164

Nicoletti, M. (2016). Microalgae Nutraceuticals. *Foods*, 5(3), 54. https://doi.org/10.3390/foods5030054

Niederholtmeyer, H., Wolfstädter, B. T., Savage, D. F., Silver, P. A., & Way, J. C. (2010). Engineering cyanobacteria to synthesize and export hydrophilic products. *Applied and Environmental Microbiology*, 76(11), 3462–3466. https://doi.org/10.1128/AEM.00202-10

Nielsen, A. A. K., Der, B. S., Shin, J., Vaidyanathan, P., Paralanov, V., Strychalski, E. A., … Voigt, C. A. (2016). Genetic circuit design automation. *Science*, 352(6281). https://doi.org/10.1126/science.aac7341

Nielsen, A. Z., Mellor, S. B., Vavitsas, K., Wlodarczyk, A. J., Gnanasekaran, T., Perestrello Ramos H de Jesus, M., … Jensen, P. E. (2016). Extending the biosynthetic repertoires of cyanobacteria and chloroplasts. *Plant Journal*, 87(1), 87–102. https://doi.org/10.1111/tpj.13173

Nielsen, J., & Keasling, J. D. (2016). Engineering Cellular Metabolism. *Cell*, 164(6), 1185–1197. https://doi.org/10.1016/j.cell.2016.02.004

Nozzi, N. E., Case, A. E., Carroll, A. L., & Atsumi, S. (2017). Systematic Approaches to Efficiently Produce 2,3-Butanediol in a Marine Cyanobacterium. *ACS Synthetic Biology*, 6(11), 2136–2144. https://doi.org/10.1021/acssynbio.7b00157

Ogden, S., Haggerty, D., Stoner, C. M., Kolodrubetz, D., & Schleif, R. (1980). The *Escherichia coli* L-arabinose operon: Binding sites of the regulatory proteins and a mechanism of positive and negative regulation. *Proceedings of the National Academy of Sciences of the United States of America*, 77(6 I), 3346–3350. https://doi.org/10.1073/pnas.77.6.3346

Ordon, J., Gantner, J., Kemna, J., Schwalgun, L., Reschke, M., Streubel, J., … Stuttmann, J. (2017). Generation of chromosomal deletions in dicotyledonous plants employing a user-friendly genome editing toolkit. *Plant Journal*, 89(1), 155–168. https://doi.org/10.1111/tpj.13319

Patron, N. J., Orzaez, D., Marillonnet, S., Warzecha, H., Matthewman, C., Youles, M., … Haseloff, J. (2015). Standards for plant synthetic biology: A common syntax for exchange of DNA parts. *New Phytologist*, 208(1), 13–19. https://doi.org/10.1111/nph.13532

Pattanaik, B., Englund, E., Nolte, N., & Lindberg, P. (2020). Introduction of a green algal squalene synthase enhances squalene accumulation in a strain of *Synechocystis* sp. PCC 6803. *Metabolic Engineering Communications,* 10(February), e00125. https://doi.org/10.1016/j.mec.2020.e00125

Peca, L., Kós, P. B., Máté, Z., Farsang, A., & Vass, I. (2008). Construction of bioluminescent cyanobacterial reporter strains for detection of nickel, cobalt and zinc. FEMS *Microbiology Letters*, 289(2), 258–264. https://doi.org/10.1111/j.1574-6968.2008.01393.x

Pedersen, D., & Miller, S. R. (2017). Photosynthetic temperature adaptation during niche diversification of the thermophilic cyanobacterium *Synechococcus* A/B clade. *ISME Journal,* 11(4), 1053–1057. https://doi.org/10.1038/ismej.2016.173

Pinto, F., Pacheco, C. C., Ferreira, D., Moradas-Ferreira, P., & Tamagnini, P. (2012). Selection of suitable reference genes for RT-qPCR analyses in cyanobacteria. *PLoS ONE*, 7(4), 1–9. https://doi.org/10.1371/journal.pone.0034983

Pinto, F., Pacheco, C. C., Oliveira, P., Montagud, A., Landels, A., Couto, N., … Tamagnini, P. (2015). Improving a *Synechocystis*-based photoautotrophic chassis through systematic genome mapping and validation of neutral sites. *DNA Research*, 22(6), 425–437. https://doi.org/10.1093/dnares/dsv024

Puente-Sánchez, F., Arce-Rodríguez, A., Oggerin, M., García-Villadangos, M., Moreno-Paz, M., Blanco, Y., … Parro, V. (2018). Viable cyanobacteria in the deep continental subsurface. *Proceedings of the National Academy of Sciences of the United States of America*, 115(42), 10702–10707. https://doi.org/10.1073/pnas.1808176115

Pye, C. R., Bertin, M. J., Lokey, R. S., Gerwick, W. H., & Linington, R. G. (2017). Retrospective analysis of natural products provides insights for future discovery trends. *Proceedings of the National Academy of Sciences*, 114(22), 5601–5606. https://doi.org/10.1073/pnas.1614680114

Qi, L. S., Larson, M. H., Gilbert, L. A., Doudna, J. A., Weissman, J. S., Arkin, A. P., & Lim, W. A. (2013). Repurposing CRISPR as an RNA-γuided platform for sequence-specific control of gene expression. *Cell*, 152(5), 1173–1183. https://doi.org/10.1016/j.cell.2013.02.022

Rae, B. D., Long, B. M., Badger, M. R., & Price, G. D. (2013). Functions, Compositions, and Evolution of the Two Types of Carboxysomes: Polyhedral Microcompartments That Facilitate CO_2 Fixation in Cyanobacteria and Some Proteobacteria. *Microbiology and Molecular Biology Reviews*, 77(3), 357–379. https://doi.org/10.1128/mmbr.00061-12

Rae, B. D., Long, B. M., Förster, B., Nguyen, N. D., Velanis, C. N., Atkinson, N., … McCormick, A. J. (2017). Progress and challenges of engineering a biophysical CO_2-concentrating mechanism into higher plants. *Journal of Experimental Botany,* 68(14), 3717–3737. https://doi.org/10.1093/jxb/erx133

Rae, B. D., Long, B. M., Whitehead, L. F., Förster, B., Badger, M. R., & Price, G. D. (2013). Cyanobacterial carboxysomes: Microcompartments that facilitate CO_2 fixation. *Journal of Molecular Microbiology and Biotechnology*, 23(4–5), 300–307. https://doi.org/10.1159/000351342

Ramey, C. J., Barón-Sola, Á., Aucoin, H. R., & Boyle, N. R. (2015). Genome Engineering in Cyanobacteria: Where We Are and Where We Need to Go. *ACS Synthetic Biology*, 4(11), 1186–1196. https://doi.org/10.1021/acssynbio.5b00043

Ramos, J. L., Martínez-Bueno, M., Molina-Henares, A. J., Terán, W., Watanabe, K., Zhang, X., … Tobes, R. (2005). The TetR Family of Transcriptional Repressors. *Microbiology and Molecular Biology Reviews*, 69(2), 326–356. https://doi.org/10.1128/mmbr.69.2.326-356.2005

Rampelotto, P. (2013). Extremophiles and Extreme Environments. *Life*, 3(3), 482–485. https://doi.org/10.3390/life3030482

Rippka, R., Deruelles, J., & Waterbury, J. B. (1979). Generic assignments, strain histories and properties of pure cultures of cyanobacteria. *Journal of General Microbiology*, 111(1), 1–61. https://doi.org/10.1099/00221287-111-1-1

Saar, K. L., Bombelli, P., Lea-Smith, D. J., Call, T., Aro, E. M., Müller, T., … Knowles, T. P. J. (2018). Enhancing power density of biophotovoltaics by decoupling storage and power delivery. *Nature Energy*, 3(1), 75–81. https://doi.org/10.1038/s41560-017-0073-0

Sakai, Y., Abe, K., Nakashima, S., Ellinger, J. J., Ferri, S., Sode, K., & Ikebukuro, K. (2015). Scaffold-fused riboregulators for enhanced gene activation in *Synechocystis* sp. PCC 6803. MicrobiologyOpen, 4(4), 533–540. https://doi.org/10.1002/mbo3.257

Sarrion-Perdigones, A., Vazquez-Vilar, M., Palací, J., Castelijns, B., Forment, J., Ziarsolo, P., … Orzaez, D. (2013). Goldenbraid 2.0: A comprehensive DNA assembly framework for plant synthetic biology. *Plant Physiology*, 162(3), 1618–1631. https://doi.org/10.1104/pp.113.217661

Sarsekeyeva, F., Zayadan, B. K., Usserbaeva, A., Bedbenov, V. S., Sinetova, M. A., & Los, D. A. (2015). Cyanofuels: Biofuels from cyanobacteria. Reality and perspectives. *Photosynthesis Research*, 125(1–2), 329–340. https://doi.org/10.1007/s11120-015-0103-3

Schell, M. A. (1983). Cloning and expression in *Escherichia coli* of the naphthalene degradation genes from plasmid NAH7. *Journal of Bacteriology*, 153(2), 822–829. https://doi.org/10.1128/jb.153.2.822-829.1983

Schleif, R. (2010). AraC protein, regulation of the l-arabinose operon in *Escherichia coli*, and the light switch mechanism of AraC action. *FEMS Microbiology Reviews*, 34(5), 779–796. https://doi.org/10.1111/j.1574-6976.2010.00226.x

Schopf, J. W., & Packer, B. M. (1987). Early archean (3.3-billion to 3.5-billion-year-old) microfossils from Warrawoona Group, Australia. Science, 237(4810), 70–73. https://doi.org/10.1126/science.11539686

Seckbach, J. (Ed.). (2007). Algae and Cyanobacteria in Extreme Environments (Vol. 11). *Dordrecht: Springer Netherlands*. https://doi.org/10.1007/978-1-4020-6112-7

Shi, W., Dong, J., Scott, R. A., Ksenzenko, M. Y., & Rosen, B. P. (1996). The role of arsenic-thiol interactions in metalloregulation of the *ars* operon. *Journal of Biological Chemistry,* 271(16), 9291–9297. https://doi.org/10.1074/jbc.271.16.9291

Silva-Rocha, R., Martínez-García, E., Calles, B., Chavarría, M., Arce-Rodríguez, A., De Las Heras, A., … De Lorenzo, V. (2013). The Standard European Vector Architecture (SEVA): A coherent platform for the analysis and deployment of complex prokaryotic phenotypes. *Nucleic Acids Research*, 41(D1), 666–675. https://doi.org/10.1093/nar/gks1119

Silver, S., & Phung, L. T. (2005). Genes and enzymes involved in bacterial oxidation and reduction of inorganic arsenic. *Applied and Environmental Microbiology*, 71(2), 599–608. https://doi.org/10.1128/AEM.71.2.599-608.2005

Singh, M. K., Rai, P. K., Rai, A., Singh, S., & Singh, J. S. (2019). Poly-β-hydroxybutyrate production by the cyanobacterium *scytonema geitleri bharadwaja* under varying environmental conditions. *Biomolecules*, 9(5). https://doi.org/10.3390/biom9050198

Skeie, R. B., Peters, G. P., Fuglestvedt, J., & Andrew, R. (2021). A future perspective of historical contributions to climate change. *Climatic Change*, 164(1–2), 1–13. https://doi.org/10.1007/s10584-021-02982-9

Stanton, B. C., Nielsen, A. A. K., Tamsir, A., Clancy, K., Peterson, T., & Voigt, C. A. (2014). Genomic mining of prokaryotic repressors for orthogonal logic gates. *Nature Chemical Biology*, 10(2), 99–105. https://doi.org/10.1038/nchembio.1411

Stensjö, K., Vavitsas, K., & Tyystjärvi, T. (2018). Harnessing transcription for bioproduction in cyanobacteria. *Physiologia Plantarum*, 162(2), 148–155. https://doi.org/10.1111/ppl.12606

Stucken, K., Ilhan, J., Roettger, M., Dagan, T., & Martin, W. F. (2012). Transformation and conjugal transfer of foreign genes into the filamentous multicellular cyanobacteria (subsection V) *Fischerella* and *Chlorogloeopsis*. *Current Microbiology*, 65(5), 552–560. https://doi.org/10.1007/s00284-012-0193-5

Stukenberg, D., Hensel, T., Hoff, J., Daniel, B., Inckemann, R., Tedeschi, J. N., … Fritz, G. (2021). The Marburg Collection: A Golden Gate DNA Assembly Framework for Synthetic Biology Applications in *Vibrio natriegens. BioRxiv*. https://doi.org/10.1101/2021.03.26.437105

Sun, T., Li, S., Song, X., Diao, J., Chen, L., & Zhang, W. (2018). Toolboxes for cyanobacteria: Recent advances and future direction. *Biotechnology Advances*, 36(4), 1293–1307. https://doi.org/10.1016/j.biotechadv.2018.04.007

Sun, T., Li, S., Song, X., Pei, G., Diao, J., Cui, J., … Zhang, W. (2018). Re-direction of carbon flux to key precursor malonyl-CoA via artificial small RNAs in photosynthetic *Synechocystis* sp. PCC 6803. *Biotechnology for Biofuels*, 11(1), 26. https://doi.org/10.1186/s13068-018-1032-0

Sure, S., Ackland, M. L., Gaur, A., Gupta, P., Adholeya, A., & Kochar, M. (2016). Probing *Synechocystis*-arsenic interactions through extracellular nanowires. *Frontiers in Microbiology*, 7(JUL), 1–12. https://doi.org/10.3389/fmicb.2016.01134

Tan, X., Yao, L., Gao, Q., Wang, W., Qi, F., & Lu, X. (2011). Photosynthesis driven conversion of carbon dioxide to fatty alcohols and hydrocarbons in cyanobacteria. *Metabolic Engineering*, 13(2), 169–176. https://doi.org/10.1016/j.ymben.2011.01.001

Taton, A., Ma, A. T., Ota, M., Golden, S. S., & Golden, J. W. (2017). NOT Gate Genetic Circuits to Control Gene Expression in Cyanobacteria. *ACS Synthetic Biology*, 6(12), 2175–2182. https://doi.org/10.1021/acssynbio.7b00203

Taton, A., Unglaub, F., Wright, N. E., Zeng, W. Y., Paz-Yepes, J., Brahamsha, B., … Golden, J. W. (2014). Broad-host-range vector system for synthetic biology and biotechnology in cyanobacteria. *Nucleic Acids Research*, 42(17), 1–16. https://doi.org/10.1093/nar/gku673

Taylor, G. M., Mordaka, P. M., & Heap, J. T. (2019). Start-Stop Assembly: A functionally scarless DNA assembly system optimized for metabolic engineering. *Nucleic Acids Research*, 47(3). https://doi.org/10.1093/nar/gky1182

Tobin, J. F., & Schleif, R. F. (1987). Positive regulation of the *Escherichia coli* L-rhamnose operon is mediated by the products of tandemly repeated regulatory genes. *Journal of Molecular Biology*, 196(4), 789–799. https://doi.org/10.1016/0022-2836(87)90405-0

Tsinoremas, N. F., Kutach, A. K., Strayer, C. A., & Golden, S. S. (1994). Efficient gene transfer in *Synechococcus* sp. strains PCC 7942 and PCC 6301 by interspecies conjugation and chromosomal recombination. *Journal of Bacteriology*, 176(21), 6764–6768. https://doi.org/10.1128/jb.176.21.6764-6768.1994

Ungerer, J., Lin, P. C., Chen, H. Y., & Pakrasi, H. B. (2018). Adjustments to photosystem stoichiometry and electron transfer proteins are key to the remarkably fast growth of the Cyanobacterium *Synechococcus elongatus* UTEX 2973. *MBio*, 9(1), 1–12. https://doi.org/10.1128/mBio.02327-17

Ungerer, J., & Pakrasi, H. B. (2016). Cpf1 Is A Versatile Tool for CRISPR Genome Editing Across Diverse Species of Cyanobacteria. *Scientific Reports,* 6(October), 1–9. https://doi.org/10.1038/srep39681

Ungerer, J., Wendt, K. E., Hendry, J. I., Maranas, C. D., & Pakrasi, H. B. (2018). Comparative genomics reveals the molecular determinants of rapid growth of the cyanobacterium *Synechococcus elongatus* UTEX 2973. *Proceedings of the National Academy of Sciences of the United States of America*, 115(50), E11761–E11770. https://doi.org/10.1073/pnas.1814912115

Valenzuela-Ortega, M., & French, C. (2021). Joint universal modular plasmids (JUMP): a flexible vector platform for synthetic biology. *Synthetic Biology*, 6(February), 1–11. https://doi.org/10.1093/synbio/ysab003

Vasudevan, R., Gale, G. A. R., Schiavon, A. A., Puzorjov, A., Malin, J., Gillespie, M. D., … McCormick, A. J. (2019). Cyanogate: A modular cloning suite for engineering cyanobacteria based on the plant moclo syntax. *Plant Physiology*, 180(1), 39–55. https://doi.org/10.1104/pp.18.01401

Vazquez-Vilar, M., Orzaez, D., & Patron, N. (2018). DNA assembly standards: Setting the low-level programming code for plant biotechnology. *Plant Science*, 273(December 2017), 33–41. https://doi.org/10.1016/j.plantsci.2018.02.024

Vioque, A. (2007). Transformation of Cyanobacteria. In R. León, A. Galván, & E. Fernández (Eds.), *Transgenic Microalgae as Green Cell Factories* (pp. 12–22). New York, NY: Springer New York. https://doi.org/10.1007/978-0-387-75532-8_2

Wan, X., Volpetti, F., Petrova, E., French, C., Maerkl, S. J., & Wang, B. (2019). Cascaded amplifying circuits enable ultrasensitive cellular sensors for toxic metals. *Nature Chemical Biology*, 15(5), 540–548. https://doi.org/10.1038/s41589-019-0244-3

Wang, Baojun, Barahona, M., & Buck, M. (2015). Amplification of small molecule-inducible gene expression via tuning of intracellular receptor densities. *Nucleic Acids Research*, 43(3), 1955–1964. https://doi.org/10.1093/nar/gku1388

Wang, Bo, Eckert, C., Maness, P. C., & Yu, J. (2018). A Genetic Toolbox for Modulating the Expression of Heterologous Genes in the Cyanobacterium *Synechocystis* sp. PCC 6803. *ACS Synthetic Biology*, 7(1), 276–286. https://doi.org/10.1021/acssynbio.7b00297

Wang, X., Liu, W., Xin, C., Zheng, Y., Cheng, Y., Sun, S., … Yuan, J. S. (2016). Enhanced limonene production in cyanobacteria reveals photosynthesis limitations. *Proceedings of the National Academy of Sciences of the United States of America*, 113(50), 14225–14230. https://doi.org/10.1073/pnas.1613340113

Wendt, K. E., Ungerer, J., Cobb, R. E., Zhao, H., & Pakrasi, H. B. (2016). CRISPR/Cas9 mediated targeted mutagenesis of the fast-growing cyanobacterium *Synechococcus elongatus* UTEX 2973. *Microbial Cell Factories*, 15(1), 1–8. https://doi.org/10.1186/s12934-016-0514-7

Werner, S., Engler, C., Weber, E., Gruetzner, R., & Marillonnet, S. (2012). Fast track assembly of multigene constructs using golden gate cloning and the MoClo system. *Bioengineered Bugs*, 3(1), 38–43. https://doi.org/10.4161/bbug.3.1.18223

Wisniewski-Dyé F, Downie JA. Quorum-sensing in *Rhizobium*. *Antonie Van Leeuwenhoek*. 2002 Aug;81(1-4):397-407. doi: 10.1023/a:1020501104051.

Wlodarczyk, A., Gnanasekaran, T., Nielsen, A. Z., Zulu, N. N., Mellor, S. B., Luckner, M., … Jensen, P. E. (2016). Metabolic engineering of light-driven cytochrome P450 dependent pathways into *Synechocystis* sp. PCC 6803. *Metabolic Engineering*, 33, 1–11. https://doi.org/10.1016/j.ymben.2015.10.009

Xiao, A., Cheng, Z., Kong, L., Zhu, Z., Lin, S., Gao, G., & Zhang, B. (2014). CasOT: A genome-wide Cas9/gRNA off-target searching tool. *Bioinformatics*, 30(8), 1180–1182. https://doi.org/10.1093/bioinformatics/btt764

Xu, Y., Alvey, R. M., Byrne, P. O., Graham, J. E., Shen, G., & Bryant, D. A. (2011). Expression of Genes in Cyanobacteria: Adaptation of Endogenous Plasmids as Platforms for High-Level Gene Expression in *Synechococcus* sp. PCC 7002. In R. Carpentier (Ed.), *Photosynthesis Research Protocols* (pp. 273–293). Totowa, NJ: Humana Press. https://doi.org/10.1007/978-1-60761-925-3_21

Yang, G., Cozad, M. A., Holland, D. A., Zhang, Y., Luesch, H., & Ding, Y. (2018). Photosynthetic Production of Sunscreen Shinorine Using an Engineered Cyanobacterium. *ACS Synthetic Biology*, 7(2), 664–671. https://doi.org/10.1021/acssynbio.7b00397

Yao, L., Cengic, I., Anfelt, J., & Hudson, E. P. (2016). Multiple Gene Repression in Cyanobacteria Using CRISPRi. *ACS Synthetic Biology*, 5(3), 207–212. https://doi.org/10.1021/acssynbio.5b00264

Yu, J., Liberton, M., Cliften, P. F., Head, R. D., Jacobs, J. M., Smith, R. D., … Pakrasi, H. B. (2015). *Synechococcus elongatus* UTEX 2973, a fast-growing cyanobacterial chassis for biosynthesis using light and CO_2. *Scientific Reports*, 5(1), 8132. https://doi.org/10.1038/srep08132

Zavřel, T., Očenášová, P., & Červený, J. (2017). Phenotypic characterization of *Synechocystis* sp. PCC 6803 substrains reveals differences in sensitivity to abiotic stress. *PLoS ONE*, 12(12), 1–21. https://doi.org/10.1371/journal.pone.0189130

Zerulla, K., Ludt, K., & Soppa, J. (2016). The ploidy level of *Synechocystis* sp. PCC 6803 is highly variable and is influenced by growth phase and by chemical and physical external parameters. *Microbiology* (United Kingdom), 162(5), 730–739. https://doi.org/10.1099/mic.0.000264

Zess, E. K., Begemann, M. B., & Pfleger, B. F. (2016). Construction of new synthetic biology tools for the control of gene expression in the cyanobacterium *Synechococcus* sp. strain PCC 7002. *Biotechnology and Bioengineering*, 113(2), 424–432. https://doi.org/10.1002/bit.25713

Zetsche, B., Gootenberg, J. S., Abudayyeh, O. O., Slaymaker, I. M., Makarova, K. S., Essletzbichler, P., … Zhang, F. (2015). Cpf1 Is a Single RNA-Guided Endonuclease of a Class 2 CRISPR-Cas System. Cell, 163(3), 759–771. https://doi.org/10.1016/j.cell.2015.09.038

Zhang, S., Liu, Y., & Bryant, D. A. (2015). Metabolic engineering of *Synechococcus* sp. PCC 7002 to produce poly-3-hydroxybutyrate and poly-3-hydroxybutyrate-co-4-hydroxybutyrate. *Metabolic Engineering*, 32, 174–183. https://doi.org/10.1016/j.ymben.2015.10.001

Zhang, X., Wang, J., Wang, J., Cheng, Q., Zheng, X., & Zhao, G. (2017). Multiplex gene regulation by CRISPR-ddCpf1. *Cell Discovery*, 3, 1–9. https://doi.org/10.1038/celldisc.2017.18

Zhou, J., Zhang, H., Meng, H., Zhu, Y., Bao, G., Zhang, Y., … Ma, Y. (2014). Discovery of a super-strong promoter enables efficient production of heterologous proteins in cyanobacteria. *Scientific Reports*, 4, 4500. https://doi.org/10.1038/srep04500